Influència de la disponibilitat i hormesi del ferro i la glucosa en l'autofàgia i la vida cronològica en *Saccharomyces cerevisiae*

Sandra Montellà Manuel

Universitat de Lleida

TESI DOCTORAL

Influència de la disponibilitat i hormesi del ferro i la glucosa en l'autofàgia i la vida cronològica en *Saccharomyces cerevisiae*

Sandra Montellà Manuel

Memòria presentada per optar al grau de Doctor per la Universitat de Lleida
Programa de Doctorat en Salut

Director/a
Maria Angeles de la Torre Ruiz

Tutor/a
Maria Angeles de la Torre Ruiz

2023

RESUM-RESUMEN-ABSTRACT

RESUM

El ferro és un metall essencial per a tots els tipus cel·lulars. Aquest metall participa en diversos processos metabòlics com en la respiració mitocondrial dins la cadena de transport electrònic, la síntesi de proteïnes, lípids i ribosomes, així com en la biosíntesi i reparació del DNA, entre altres. La falta de ferro provoca problemes de salut en éssers humans com l'anèmia ferropènica, malalties cardiovasculars i està relacionada amb alteracions neurològiques així com en el càncer de mamà, entre d'altres. En aquesta tesi es demostra que la manca de ferro causa en *Saccharomyces cerevisiae* la inactivació del complex TORC1 i indueix l'activació de la macroautofàgia, resposta que afavoreix al reciclatge d'aquest metall. Adicionalment es presenten evidències que demostren que el senyal de depleció de ferro requereix l'activitat de TORC2/Ypk1 (ortòlegs de mTORC2/Sgk1 en cèl·lules humanes) per aconseguir la subseqüent inactivació de TORC1 induint la defosforilació d'Atg13 i l'autofosforilació activatoria d'Atg1, activant així l'autofàgia generalitzada. El restabliment dels nivells de ferro intracel·lulars causa la reducció del flux autofàgic a través de l'AMPK Snf1 i la subseqüent activació del factor de transcripció del reguló del ferro, Aft1. Aquest senyal convergeix en la hiperfosforilació d'Atg13 mitjançada per TORC1. La limitació de ferro promou l'entrada de les cèl·lules en quiescència, que juntament amb l'activació de l'autofàgia, són dos mecanismes que contribueixen a l'extensió de la vida cronològica de les cèl·lules de S. cerevisiae.

Els resultats que es mostren en aquest estudi demostren que TORC2/Ypk1 són necessaris perquè Aft1 és transloqui al nucli com a resposta a la depleció de ferro. En aquesta senyalització intervé la ruta dels esfingolípids, concretament els esfingolípids complexos. Les nostres observacions atorguen un nou rol als esfingolípids que mitjançant la regulació de TORC2/Ypk1 garanteixen la correcta localització i activitat d'Aft1 en resposta a la manca de ferro.

Mtl1 és un receptor de la paret cel·lular que forma part de la via CWI i està involucrat en la recepció de la senyal de la concentració de glucosa i la seva transmissió a la via Ras2/Sch9 que repercuteix en l'activació de l'autofàgia generalitzada. La funció de Mtl1 en la repressió de Ras2 i Sch9 també és important en la senyalització de la degradació específica de les mitocòndries a través de mitofàgia durant la fase estacionària, d'una manera totalment dependent d'Atg33 i Atg11. Aquests resultats reforcen la importància del receptor Mtl1 en els processos de senyalització que responen al dèficit de glucosa en *S. cerevisiae.*

RESUMEN

El hierro es un metal esencial para todos los tipos celulares. Este metal participa en diversos procesos metabólicos, tales como la respiración mitocondrial, la síntesis de proteínas, lípidos y ribosomas, así como en la biosíntesis y reparación del DNA, entre otros. El déficit de hierro conlleva problemas de salud en los seres humanos, como es el caso de la anemia ferropénica, enfermedades cardiovasculares, alteraciones neurológicas, así como con el cáncer de mama, entre otros.

En esta tesis se demuestra que la falta de hierro induce, en *Saccharomyces cerevisiae,* la inactivación del complejo TORC1 y promueve la activación de la macroautofagia. Asimismo, se presentan evidencias que demuestran que la señal de depleción de hierro requiere la actividad de TORC2/Ypk1 (ortólogos de mTORC2/Sgk1 en células humanas) para lograr la inactivación de TORC1, induciendo asi la defosforilación de Atg13 y la autofosforilación de Atg1, lo que conduce a la activación de la autofagia. El restablecimiento de los niveles de hierro intracelular provoca la reducción del flujo autofágico a través de la AMPK Snf1 y la subsecuente activación del factor de transcripción del regulón del hierro, Aft1. Esta señal converge en la hiperfosforilación de Atg13 mediada por TORC1. La limitación de hierro promueve la entrada de las células en quiescencia, que,junto con la activación de la autofagia, contribuyen a la extensión de la vida cronológica de las células de *S. cerevisiae*.

Los resultados presentados en este estudio demuestran que TORC2/Ypk1 son necesarios para que Aft1 se localice en el núcleo en respuesta a la depleción de hierro. En este proceso de señalización interviene la vía de señalización de los esfingolípidos, concretamente los esfingolípidos complejos. Nuestras observaciones otorgan un nuevo rol a la via de los esfingolípidos como mediadora de la señal entre TORC2/Ypk1 y el mecanismo de homeostasis del hierro.

Mtl1 es un receptor de la pared celular que forma parte de la vía CWI y está relacionado con la señalización de la concentración de glucosa y el estrés oxidativo. El receptor Mtl1 es esencial para detectar la disminución en la concentración de glucosa y transmitir la señal hacia la represión de las actividades de Ras2 y Sch9, lo que repercute en la activación de la autofagia generalizada. La función de Mtl1 en la represión de Ras2 y Sch9 además es importante en la señalización de la degradación específica de las mitocondrias a través de mitofagia durante la fase estacionaria, de una manera totalmente dependiente de Atg33 y Atg11. Estos resultados refuerzan la importancia del receptor Mtl1 en los procesos de señalización que responden al déficit de glucosa en *S. cerevisiae*.

ABSTRACT

Iron is an essential metal for all cell types since participates in various metabolic processes such as mitochondrial respiration, protein, lipid, and ribosome synthesis, as well as DNA biosynthesis and repair, among others. Iron deficiency leads to health problems in humans, including iron-deficiency anemia, and cardiovascular diseases, and it is associated with neurological disorders as well as breast cancer, among others. We have demonstrated that iron deficiency in *Saccharomyces cerevisiae* leads to the inactivation of the TORC1 complex and concomitantly induces the activation of macroautophagy. This work also presents evidence that the iron depletion signal requires the activity of TORC2/Ypk1 (orthologs of mTORC2/Sgk1 in human cells) to subsequently inactivate TORC1 complex thus inducing both, the dephosphorylation of Atg13 and also the activating autophosphorylation of Atg1, leading the activation of bulk autophagy. Restoring intracellular iron levels reduces autophagic flux through the AMPK Snf1 and the subsequent activation of the iron regulon mediated by the transcription factor Aft1. This signal converges in the hyperphosphorylation of Atg13 mediated by TORC1. Iron limitation promotes cell entry into quiescence, which, together with autophagy activation, both contribute to the extension of the chronological life in the budding yeast.

The results presented in this study demonstrate that TORC2/Ypk1 are necessary to promote Aft1 nuclear localization upon iron depletion. Sphingolipids are required for this signaling, specifically complex sphingolipids. These results give a new role to the sphingolipids pathway as a mediator of the signal between TORC2/Ypk1 and the iron homeostasis mechanism.

Mtl1 is a cell wall receptor that is part of the CWI pathway and is involved in receiving the glucose concentration signal to transmit it to Ras/Sch9 pathways. The repression of these pathways in response to the descent in glucose availability results in the activation of generalized autophagy. Mtl1 function in the repression of both Ras2 and Sch9 is also important in signaling the specific degradation of mitochondria through mitophagy during the stationary phase, dependent on Atg33 and Atg11. These results reinforce the importance of the Mtl1 receptor in the signaling processes that respond to glucose deficiency in *S. cerevisiae.*

ABREVIACIONS

AC: Adenylate cyclase
AIM: Atg8-Interacting Motif
AMP: Adenosine MonoPhosphate
AMPK: AMP- activated Kinase
Ams1: Alpha-MannoSidase 1
Ape1: AminoPEptidase 1
ATG: AuTophagyc related Gene
ATP: Adenosine TriPhosphate
cAMP: Cyclic AMP
CDS: CoDing Sequence
Cer: Ceramide
CFUs: Colony Forming Units
CFW: CalcoFluor White
CK2: Casein Kinase 2
CLS: Chronological Life Span
CMA: Chaperone-Mediated Autophagy
CO_2: Carbon dioxide
CoA: Coenzyme A
CR: Caloric Restriction
Cvt: cytoplasm to Vacuole Targeting
CWI: Cell-Wall Integrity
DHC: DiHydroCeramide
DHS: DiHydroSphingosine
DNA: Deoxyribonucleic Acid
EGOC: Ego Complex
eIF-2: Eukaryotic translations Initiation Factor 2
ER: Endoplasmic Reticulum
ERCs: Extrachromosomal rDNA Circles
EST: Ever Shorter Telomeres
Fe: Iron
FeRe: Iron Regulatory Element
FRB: FKBP12-Rapamycin-Binding
G_0: Quiescence
G_1: Gap 1
G_2: Gap 2
GAAC: General Amino Acid Control
GAP: GTPase-Activating Protein
GDP: Guanosine DiPhosphate
GEF: GDP/GTP Exchange Factor
GPCR: G-Protein-Coupled Receptor
GRAS: Generally Regarded As Safe
GRO: Genomic Run-On
GSH: Glutathione
GTP: Guanosine TriPhosphate
HA: HemAgglutinin
HisRS: Histidyl-tRNA Synthetase
HOG: High-Osmolarity Glycerol
HXK2: HeXoKinase PII
HXT: Hexose Transporters
IPC: Inositol PhosphoCeramide
IRC: Index of Respiratory Competence
LCB: Long-Chain Base
M: Mitosis
MAPK: Mitogen-Activated Protein Kinase
MAPKK: MAPK Kinase
MAPKKK: MAPKK Kinase
MIPC: Mannose-Inositol-PhosphoCeramide
$M(IP)_2C$: Mannose-$(Inositol\text{-}P)_2$-PhosphoCeramide
miRNA: micro Ribonucleic Acid
mRNA: messenger Ribonucleic Acid
NADH: Nicotinamide Adenine Dinucleotide

NCR: Nitrogen Catabolic Repression
ORFs: Open Reading Frames
PAS: Pre-Autophagosomal Site
PE: PhosphatidylEthanolamine
PHC: PhytoCeramide
PHS: PhytoSphingosine
PKA: Protein Kinase A
PM: Plasmatic Membrane
PtdIns3K: PhosphaTiDylINOsitol-3-kinase
RA: mRNA Amounts
rDNA: recombinant Deoxyribonucleic Acid
RiBi: Ribosomal Biogenesis
RP: Ribosomal Protein
RLS: Replicative Life Span
RNA: Ribonucleic Acid
ROS: Reactive Oxygen Species
rRNA: Ribosomal RNA
RTG: ReTrograde response Genes
S: Sulfur
S: Synthesis
S. cerevisiae: *Saccharomyces cerevisiae*
SD: Standard Deviation
SIR: Silent Information Regulator
SNF: Sucrose Non Fermenting
SPT: Serine Palmmitoyl Transferase
STRE: STress Responsive Elements
TCA: TriCarboxylic Acid
TOR: Target of Rapamycin
TORC1: TOR Complex 1
TORC2: TOR complex 2
TR: Transcription Rate
tRNAs: Transfer RNA
uORFs: Upstream ORFs
UPR: Unfolded Protein Response
wt: Wild-Type

AGRAÏMENTS

AGRAÏMENTS

Inicialment, voldria agrair a la Dra. Maria Angeles de la Torre, la directora i tutora d'aquesta tesi, qui ha estat el meu referent durant els cinc anys que he estat en el seu laboratori i m'ha donat l'oportunitat de realitzar la meva tesi doctoral amb el seu grup d'investigació. La Dra. De la Torre m'ha ajudat a desenvolupar la meva identitat investigadora, fomentat el meu pensament crític i guiat el meu camí en el desenvolupament de la present tesi. Valoro molt les discussió diàries amb ella, així com la seva ajuda en el disseny experimental i supervisió diària. També voldria destacar la seva implicació i entusiasme amb els diferents projectes que desenvolupa en el laboratori.

En segon lloc, també volia agrair a la Dra. Núria Pujol, codirectora de la tesi. La Núria ha estat present durant el dia a dia en el laboratori, ajudant-me en tots els problemes i dubtes que podien sorgir durant l'execució dels experiments, així com participant en els processos de discussió. La Dra. Pujol ha estat un exemple de dedicació en el treball i la millor companyia que podria tenir dins el laboratori.

En tercer lloc, mostrar la meva gratitud al Dr. Ted Powers de la Universitat de Davis, Califòrnia, per obrir-me les portes del seu laboratori durant una tres mesos i mostrar-me una mica de Califòrnia. Les discussions dels resultats amb ell m'han ofert un nou punt de vista crític sobre els meus resultats i han fomentat noves inquietuds.

No voldria oblidar donar les gràcies al Dr. Jeremy Thorner, el qual em va rebre durant la meva estança a Califòrnia per comentar els meus resultats i expressar el seu punt de vista, establint un ambient de discussió molt enriquidor.

Les dos tècnics que han estat en el laboratori, la Inma Montoliu i la Roser Pané. Elles han estat de gran ajuda per desenvolupar aquest projecte i són persones excepcionals que m'han animat a continuar endavant.

Durant aquests anys al laboratori de Senyalització Cel·lular en Llevats, han passat diversos estudiants de Grau, Màster i Erasmus. Entre ells m'agradaria destacar el Joan i l'Alma. El Joan va ser dels primers estudiants que va estar al laboratori en els meus inicis del doctorat, i va fomentar un molt bon ambient en el laboratori. Quan vaig conèixer a l'Alma va ser durant les seves pràctiques de Tècniques Instrumentals del grau de Biomedicina, i des de llavors va estar en el laboratori durant el seu treball final de Grau Pràcticum del Màster. Des del primer

moment l'Alma es va convertir en una de les meves millors amigues i un gran suport al laboratori. Amb l'Alma he compartit els millors i pitjors moments del doctorat, i ella sempre ha estat al meu costat donant-me suport. Tot i que ara mateix, a causa dels quilòmetres que ens separen, hem perdut el contacte diari que teníem. Ella és per mi una gran amiga i sé que sempre podré comptar amb ella i ella amb mi.

També voldria destacar i mostrar el meu agraïment als companys i companyes de l'IRB amb els quals hem compartit cafès, inquietuds i riures, com l'Arabela una de les millors persones que he conegut mai, sempre disposada a ajudar-te i animar-te. També la Júlia, amb qui comparteixo amistat des del Grau en Biotecnologia fins a l'actualitat i espero que la nostra amistat continuï sempre. També la Marta, l'Elena, la Gisela, l'Alba i la Sandra per haver fet més fàcil aquesta etapa.

Ja fora de l'àmbit laboral, en primer lloc, vull mostrar el meu agraïment a la meva família, als meus pares Marta i Antonio, la meva germana Laia i a la meva padrina Rosario, la qual ens va deixar aquest any després del meu retorn de l'estada a Davis. Sense ells la realització d'aquesta tesi i estar escrivint aquests agraïments hauria estat impossible. Ells sempre han estat els meus pilars i els que m'han permès i facilitat tenir una bona formació acadèmica. Als meus pares per donar-me suport i estar al meu costat tant en els moments bons de la tesi com en els dolents i a la meva germana per haver d'aguantar els meus monòlegs, segons ella, fent ús de massa paraules.

Finalment, donar les gràcies als meus amics de tota la vida de Tremp. La Marta, que no només ha estat amb mi durant tota la vida, ajudant-me, preocupant-se per mi i fent-me passar bons moments, sinó que també m'ha hagut d'aguantar com a companya de pis des de segon de carrera, tot i que podríem dir que a primer també pràcticament vivíem juntes. Ella ha fet que estar lluny de casa fos més fàcil. A l'Anna una persona com poques queden, tothom hauria de tenir una amiga com l'Anna. Ella es preocupa sempre per tots nosaltres per sobre de tot, una amiga amb qui sempre pots comptar, no importa la situació ni el moment, ella sempre està present per recolzar-te i transmetre't energia positiva animant-te a continuar endavant i assolir els teus objectius. La Judith, una persona que tot i conèixer-la de tota la vida per ser veïnes de pobles, ella de Gavet i jo de Fontsagrada, en els últims anys ha passat a formar part del meu cercle més propè d'amics, i un gran suport durant el període en què he estat fent el doctorat. La

Sandra una amiga amb una personalitat molt positiva i alegre que et contagia. D'ella vull destacar la seva desimboltura i entusiasme i les hores que hem estat al telèfon compartint inquietuds, històries personals i anècdotes. L'Albert, el noi del grup, tot i que a vegades ideològicament tenim pensaments oposats ell sempre està disposat a anar a fer un cafè i escoltar als altres. Sense tots ells hauria estat molt difícil arribar al punt que estic avui. Per acabar esmentar al Jaume amb qui hem compartit experiències de doctorat, i actualment ja el podem anomenar doctor, tot i que aviat deixarà de ser l'únic Doctor.

Dedico la meva tesi doctoral a la meva família i en especial a la meva padrina Rosario.

INDEX

1. INTRODUCCIÓ GENERAL

1.1 *Saccharomyces cerevisiae* com organisme model en la recerca biomèdica

Saccharomyces cerevisiae és un llevat que des d'un punt de vista filogenètic es pot classicar dins el regne Fungi, filum *Ascomycota,* classe *Saccharomycetes,* ordre *Saccharomycetales,* família *Saccharomycetacea,* gènere *Saccharomyces* i espècie *cerevisiae.* Aquesta cèl·lula eucariota és divideix per gemmació i presenta dues fases biològiques estables, una haploide i una diploide. La transició entre les dues fases és regulada a través de canvis ambientals, la disponibilitat de nutrients i la presència d'altres cèl·lules. Aquest llevat, també conegut com llevat de gemmació, llevat de la cervesa o llevat del pa, ocupa una posició important en la taxonomia dels fongs, ja que és un dels llevats més rellevants i estudiats en biologia cel·lular i molecular, recerca genètica, la indústria i la biotecnologia (Carvelli and Galli 2021; Ariño 2011). L'any 1996 el genoma de *S. cerevisiae* va ser el primer genoma eucariota completament seqüenciat. És un genoma relativament petit, compacte i senzill de manipular, amb 6275 gens distribuïts en 16 cromosomes (Goffeau et al. 1996).

Tot i la seva simple estructura unicel·lular, les diferències morfològiques i cel·lulars, i els bilions d'anys evolució separada amb organismes eucariotes superiors, molts processos cel·lulars essencials com són la replicació del DNA, la transcripció i traducció, la glicòlisi, la divisió cel·lular, la resposta a l'estrès, l'autofàgia, entre d'altres, s'han conservat (Kachroo et al. 2022). Convertint al llevat en una eina molt potent per a elucidar gran part de la biologia bàsica i caracteritzar rutes de senyalització comunes amb les cèl·lules humanes (Carvelli and Galli 2021). Aquesta afirmació es ratifica amb els 5 Premis Nobel en Fisiologia o Medicina atorgats fins al present moment, en estudis realitzats utilitzant el llevat com a organisme model: i) Premi Nobel del 2001 a Leland H. Hartwell, Tim Hunt i Sir Paul M. Nurse, pels seus descobriments en reguladors claus del cicle cel·lular; ii) Premi Nobel del 2006 atorgat a Andrew Z. Fire i Craig C. Mello per la seva investigació en el RNA d'interferència; iii) Premi Nobel del 2009 d'Elizabeth H. Blackburn, Carol W. Greider i Jack W. Szostak, gràcies a la descoberta de com els cromosomes estan protegits per telòmers i l'enzim telomerasa; iv) Premi Nobel del 2013 guanyat per James E. Rothman, Randy W. Schekman i Thomas C. Südhof per les seves investigacions en la maquinaria reguladora del tràfic vesicular; i finalment, el v) Premi Nobel del 2016 atorgat a Yoshinori Ohsumi per al descobriment del mecanisme de l'autofàgia

(Prize n.d.).

S. cerevisiae, com en la investigació bàsica, té una gran importància en la investigació aplicada i biotecnològica. Aquest llevat és utilitzat per a la producció de proteïnes recombinants, la investigació genètica, l'estudi de malalties, la recerca farmacològica, la biologia sintètica, l'optimització de processos fermentatius, entre d'altres. El llevat del pa, és una eina molt versàtil en la investigació aplicada que contribueix a moltes àrees de coneixement, des de la comprensió de la biologia a la producció de medicaments. Un clar exemple d'aquesta versatilitat l'ús dels llevats com a plataformes per a la producció de proteïnes humanes (Pujol-carrion et al. 2022) i la investigació de malalties a través de la humanització del llevat. Aquesta tècnica, es va començar a utilitzar als anys 90, i fa referència a un procés en que es modifiquen llevats, com *S. cerevisiae,* per incorporar-hi gens (Mechoud et al. 2020) o característiques pròpies de cèl·lules humanes (Kachroo et al. 2022). En l'àmbit biomèdic, existeixen models en llevat de diverses malalties, incloent-hi: i) malalties neurodegeneratives, ii) desordres mitocondrials, iii) malalties de prions, iv) desordres metabòlics i v) càncer. Modelitzar aquestes malalties en llevat és possible, ja que, tot i els milions d'anys d'evolució que els separa amb els humans, hi ha entre un 20% i 60% d'homologia genètica en els gens que tenen funcions bàsiques, com són els de les rutes metabòliques, el cicle cel·lular i la regulació gènica (Kaminska et al. 2022). No existeix un percentatge global únic d'homologia genètica entre humans i el llevat de gemmació, ja que varia segons el gen o la regió especifica del genoma que es consideri.

S. cerevisiae és considerat un organisme GRAS (Generally Regarded As Safe) que pot ser manipulat sense precaucions especials. El seu ús com a organisme model en el laboratori presenta alguns avantatges: i) creix ràpidament (~90 min) en medis de cultiu simples i econòmics, ii) és estable i es pot treballar amb ell en forma haploide o diploide, iii) existeixen un gran nombre de mutants per a qualsevol mecanisme cel·lular i iv) els coneixements adquirits gràcies a l'estudi en aquest organisme tenen transferència i aplicació en organismes superiors (Ariño 2011). En definitiva, la recerca en el llevat *S. cerevisiae,* s'ha convertit en un els pilars fonamentals per a l'adquisició de coneixement en les àrees de la bioquímica, biologia cel·lular, genètica i biologia molecular.

L'ús del llevat com a organisme model també comporta algunes limitacions: i) algunes proteïnes humanes expressades en el llevat no presentaran la mateixa funcionalitat que en el

seu ambient endogen, ii) algunes interaccions proteiques poden estar alterades, a causa de la mancà de la proteïna d'interacció o de la divergència d'aquestes en les cèl·lules humanes, iii) hi ha condicions de "*splicing*" del transcrit, llocs d'unió de miRNA (MIcro RiboNucleic Acid) o proteïnes d'unió de mRNA (Messenger RNA), que no es poden reproduir en una cèl·lula de llevat, iv) al ser un organisme unicel·lular, també existeix una limitació en la reproducció de fenotips resultants de la interacció cel·lular, fet que no permet l'estudi de processos de desenvolupament (Kaminska et al. 2022; Carvelli and Galli 2021). En resum, tot i que el llevat no permet la investigació de l'impacte d'una malaltia a nivell sistèmic, sí que possibilita l'estudi molecular d'una patologia de manera simple, ràpida i econòmica.

1.2 Creixement cel·lular del llevat de *S. cerevisiae*

S. cerevisiae presenta cinc fases de creixement cel·lular (Figura 1), les quals estan definides pels factors de creixement i la disponibilitat nutricional:

i) **Fase de latència.** És el període inicial en què les cèl·lules de llevat s'adapten a un nou entorn. En aquesta etapa, el llevat no experimenta un creixement actiu com a resposta al canvi de la font de carboni emprada, generalment, d'etanol a glucosa. L'exposició de les cèl·lules a nous medis enriquits dona lloc a una imminent activació de rutes bioquímiques i una alta expressió gènica (Brejning and Jespersen 2002).

ii) **Fase exponencial o logarítmica**. Un cop les cèl·lules del llevat s'han adaptat a l'entorn, es comencen a dividir de forma activa produint un ràpid augment de la població (Busti et al. 2010). Durant aquesta fase el llevat del pa presenta l'habilitat de fermentar ràpidament els sucres transformant-los en etanol i diòxid de carboni (CO_2), tant en condicions aeròbiques com anaeròbiques. Aquest procés es coneix amb el nom d'efecte Crabtree (Dashko et al. 2014). La capacitat fermentativa dels llevats, ha esdevingut una de les tecnologies més antigues emprades pels éssers humans, els seus orígens es remunten al període Neolític. Els primers estudis de les característiques químiques, fisiològiques i microbiològiques de les fermentacions daten del segle XVIII. Antoine Lavoiser l'any 1789, va presentar dades on es descrivien els canvis químics que succeïen durant la conversió del sucre en alcohol i CO_2, en el procés de fermentació vinícola. Posteriorment, Louis Pasteur, a finals de la dècada del 1850, va desenvolupar

estudis fisiològics que demostraven el rol del llevat en les fermentacions alcohòliques i va determinar diferències quantitatives entre la conversió aeròbica i anaeròbica del sucre (Barnett 2003). La fermentació dels sucres, com la glucosa i la fructosa, proporciona l'energia necessària a la cèl·lula per créixer i mantenir les seves funcions biològiques.

El llevat és capaç de detectar la disponibilitat de glucosa en el medi, i expressar els transportadors d'hexosa (*HXT)*, per tal d'internalitzar-la, a través de difusió facilitada. Un cop internalitzada, la glucosa, és dona la glicòlisi, que és el procés inicial d'oxidació dels sucres, permeten la conversió de la glucosa en dues molècules de piruvat i alliberant ATP (Adenosine TriPhosphate) i NADH (reduced Nicotinamide Adenine Dinucleotide), sense la necessitat d'oxigen. El piruvat citoplasmàtic és fermentat alcohòlicament donant lloc a etanol i CO_2. El piruvat també pot ser convertit en acetil-CoA, a escala citoplasmàtica, a través del bypass de la piruvat deshidrogenasa. Aquesta via involucra la conversió de l'acetaldehid a àcid acètic, el qual es converteix en acetil-CoA. La ruta de bypass és essencial per a *S. cerevisiae,* ja que és l'única manera d'obtenir acetil-CoA citoplasmàtic, a través de la glucosa, necessari per a la biosíntesi de lípids (Piškur and Compagno 2014).

iii) **Fase de transició o "*shift*" diauxic**. Aquesta fase fa referència a un canvi en el metabolisme i creixement del llevat *S. cerevisiae* en resposta a l'esgotament de la font de carboni fermentable que utilitza per créixer. En aquesta situació, el llevat ajusta la seva maquinària metabòlica i genètica per poder emprar altres fonts de carboni disponible. El metabolisme passa de ser fermentatiu a respiratori. L'etanol generat durant la fermentació, és oxidat a les mitocòndries generant acetil-CoA. Finalment, les reaccions del cicle de Krebs i la cadena de transport electrònic, generen a partir de l'acetil-CoA una gran quantitat d'ATP que proveeix d'energia les cèl·lules (Gray et al. 2004).

iv) **Fase post-diauxica.** Durant aquesta etapa un alt nombre gens presenten canvis en la seva expressió, les cèl·lules creixent molt lentament (una o dues divisions) i minva la síntesi proteica. L'exhauriment de la font de carboni respiratòria marca el final d'aquesta fase (Stahl et al. 2004).

v) **Fase estacionària.** L'esgotament de totes les fonts de carboni del medi indueix una sèrie de canvis que de forma conjunta defineixen la fase estacionària. Aquests canvis són: a) reducció dramàtica del creixement, b) inducció de l'emmagatzematge de glicogen, c) increment a la resistència d'estrès mediambiental, d) augment del cos de la paret cel·lular, e) disminució severa de la transcripció gènica, traducció i síntesi proteica, i f) augment de la supervivència davant la inanició. (Herman 2002; Busti et al. 2010; Gray et al. 2004).

L'entrada en fase estacionària està regulada per la inactivació d'alguna de les vies de senyalització de Ras o Tor (posteriorment descrites), totes dues són crítiques per modular el creixement cel·lular. Aquestes rutes regulen positivament processos com la traducció de proteïnes, la qual és essencial per al creixement cel·lular, i inhibeixen activitats contràries a la proliferació cel·lular (Herman 2002).

En cultius que es troben en fase estacionària, es poden distingir dues fraccions cel·lulars, cèl·lules quiescents i cèl·lules no-quiescents. La fracció majoritària és la de cèl·lules quiescents (Breitenbach, Jazwinski, and Laun 2012).

a) **Quiescència (G_0).** La quiescència en la cèl·lula de llevat, és definida per Gray et al, com a un estat on la cèl·lula creix en un cultiu líquid fins a obtenir la saturació del medi (Gray et al. 2004). Un alt nombre de cèl·lules passen la major part de la seva vida en quiescència. En la natura els organismes unicel·lulars, majoritàriament, estan quiescents (Sagot and Laporte 2019). En el laboratori, es poden aconseguir cèl·lules quiescents, a partir d'un cultiu líquid en medi ric a 30ºC, creixent durant un període de 5 a 7 dies.

Les cèl·lules quiescents presenten un seguit de característiques que divergeixen de les cèl·lules proliferatives: 1) no proliferen, 2) no acumulen massa ni volum, 3) es troben en un estat de repòs i sense gemmes, 4) la taxa de transcripció és entre 3 i 5 vegades inferior respecte la fase exponencial, 5) hi ha repressió genètica, com per exemple de gens codificants per a proteïnes ribosomals, 6) s'inhibeix la degradació del mRNA, 7) la síntesi proteica es redueix fins a un 0,3% comparada amb la de la fase logarítmica de creixement, 8) els cromosomes es condensen, 9) les cèl·lules presenten parets cel·lulars més consistents i menys poroses, 10) s'indueix

l'autofàgia, 11) s'incrementa la termotolerància i l'osmotolerància, 12) disminueix la quantitat de ROS (Reactive Oxygen Species) i 13) augmenta la supervivència (Gray et al. 2004; Breitenbach, Jazwinski, and Laun 2012; Werner-Washburne et al. 1993).

En la bibliografia es presenta l'estat de quiescència com una reacció reversible. L'entrada en quiescència s'assoleix quan les cèl·lules proliferants censen una disminució del carboni; i la sortida de la quiescència es veu marcada per la resposta a la presència d'una font de carboni (Gray et al. 2004).

Les cèl·lules de llevat quiescents i les de mamífer comparteixen les mateixes característiques (Gray et al. 2004). Fet que permet transferir el coneixement adquirit en les cèl·lules de llevat a cèl·lules d'organismes superiors, com poden ser les cèl·lules humanes.

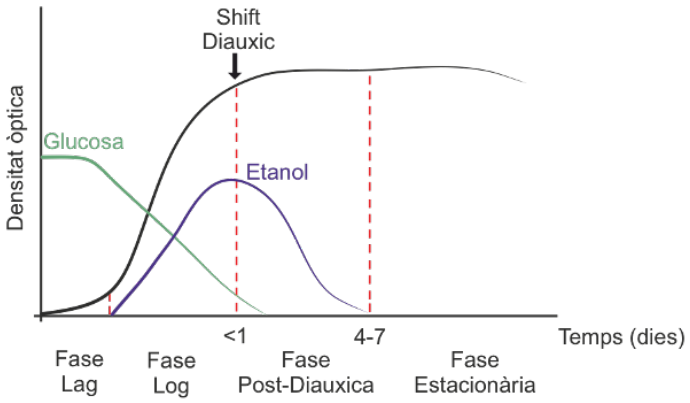

Figura 1. Corba de creixement de *S. cerevisiae*. Fases de creixement del llevat en un medi ric on la font fermentable de carboni és la glucosa a 30ºC. La inoculació de cèl·lules en fase estacionària en un medi de cultiu fresc provoca una fase inicial de latència de temps variable. Posteriorment, les cèl·lules comencen a fermentar la glucosa a etanol i la proliferació cel·lular incrementa exponencialment durant la fase logarítmica (Log) o també anomenada fase exponencial. L'escassetat de la glucosa, provoca una disminució del creixement cel·lular i un canvi del metabolisme fermentatiu a metabolisme respiratori, aquest moment es coneix com a "*shift*" diauxic. Durant la fase post-diauxica, les cèl·lules creixen

lentament consumint l'etanol produït durant la fermentació. L'exhauriment de l'etanol provoca una aturada en el creixement del cultiu i entrada en fase estacionària. En la fase estacionària les cèl·lules poden adoptar un estat de quiescència durant llargs períodes de temps.

1.3 Metabolisme del ferro en *S. cerevisiae*

El ferro és un nutrient essencial per a tots els organismes vius (Jing et al. 2022). És un element amb un paper clau en el metabolisme cel·lular. Una de les seves funcions és ser emprat com a cofactor redox en diversos processos: i) la respiració cel·lular (X. Jin et al. 2021), ii) el metabolisme dels lípids (Venkataramani 2021), iii) la biogènesi d'aminoàcids (Qian et al. 2017), iv) la replicació i reparació del DNA (C. Zhang 2014), v) el transport d'oxigen (Sanders-Loehr 1988), vi) la fotosíntesi (Castell et al. 2022) i vii) la fixació del nitrogen (Yu et al. 2021). Tot i que el ferro és essencial, quantitats excessives poden ser perjudicials, ja que, el Fe^{2+} lliure, és capaç de reduir el peròxid d'hidrogen generant radicals lliures hidroxils a través de la reacció de Fenton, els quals són perjudicials (Martins, Costa, and Pereira 2018). El dany cel·lular que es pot desencadenar té lloc a diversos nivells: i) sobre els àcids nucleics, ii) a les proteïnes, iii) a escala lipídica i iv) sobre el DNA (Martínez-Pastor, Perea-García, and Puig 2017). Aquestes descompensacions acceleren el dany cel·lular i desencadenen l'aparició de malalties i envelliment (Martins, Costa, and Pereira 2018). Algunes malalties humanes provocades per alteracions en l'homeòstasi del ferro són: i) l'anèmia (Newhall, Oliver, and Lugthart 2020), ii) l'hemocromatosi hereditària (Murphree et al. 2020), iii) l'atàxia de Friedrich (Cook and Giunti 2017), iv) l'aceruloplasminèmia (Vroegindeweij et al. 2021) i v) incrementa el risc d'infeccions i de càncer (Camiolo et al. 2020). De manera que els organismes per protegir-se de la toxicitat del ferro, han desenvolupat mecanismes de regulació del metabolisme del ferro.

L'estudi del metabolisme del ferro és un altre exemple de la importància del llevat *S. cerevisiae* com a model, ja que ha permès establir els mecanismes de transport, distribució i regulació del ferro i descobrir les bases moleculars de malalties relacionades amb el ferro ja mencionades anteriorment.

1.3.1 Regulació de l'homeòstasi del ferro

En aquest llevat existeixen diferents mecanismes de captar ferro. Presenta dos mecanismes de

baixa afinitat i un sistema d'alta afinitat mediat per sideròfors. Tots aquests mecanismes es regulen a nivell transcripcional (Martins, Costa, and Pereira 2018). Els nivells de ferro cel·lular són detectats a través de la síntesi i biodisponibilitat de clústers Fe/S, no a través de la concentració de ferro lliure. La formació de clústers Fe/S és un procés que es troba conservat durant l'evolució. La membrana de la mitocòndria presenta dos transportadors, Mrs3 i Mrs4, els quals regulen l'import de ferro a l'interior de la mitocòndria. Un cop el ferro és dins la mitocòndria el complex format per Nfs1-Isd11 juntament amb la frataxina, Yfh1, faciliten la unió del clúster [2Fe-2S] a una proteïna "*scaffold"* Isu1. Posteriorment, el clúster es transfereix a través d'un sistema de xaperones format per Ssq1-Jac1-Mge1 a un dímer format per la glutaredoxina monotiol, Grx5. Finalment, els clústers Fe/S són exportats de la mitocòndria al citoplasma a través del transportador Atm1 (Figura 2) (Lill, Srinivasan, and Mühlenhoff 2014). Un cop al citoplasma, els clústers Fe/S es converteixen en clústers $[2Fe\text{-}2S]^{2+}$, els quals s'uneixen amb dues glutaredoxines monotiol, Grx3 i Grx4. Grx3 i Grx4 formen part de la família de glutaredoxines monotiol de multidomini, formades per un domini tioredoxina a l'extrem N-terminal i un domini glutaredoxina en el C-terminal. També presenten dos llocs actius de cisteïnes, anomenats CGFS, que coordinen els clústers Fe/S (H. Li et al. 2009). Grx3 i Grx4 són homòlogues, però no totalment redundants (Pujol-Carrion et al. 2006). Aquestes glutaredoxines tenen un paper en la distribució i detecció del ferro (Pujol-Carrion et al. 2006). Les dues glutaredoxines s'uneixen com a monodímers amb el clúster $[2Fe\text{-}2S]^{2+}$ juntament amb dues molècules de glutatió (GSH) (Mühlenhoff et al. 2010). El clúster Fe/S forma homodímers amb Grx3/4 que interaccionen amb una proteïna tipus Bol-1, Fra2, per formar el complex [2Fe-2S]Fra2-Grx3/4. Els clústers Fe/S dins el complex format amb Grx3/4 poden ser emprats per a la biogènesi de proteïnes Fe/S citosòliques i nuclears (H. Li et al. 2009).

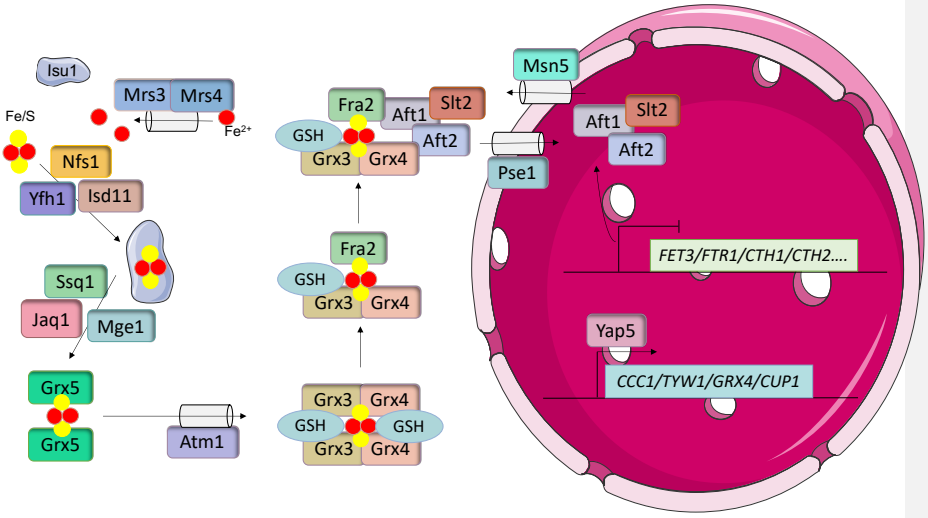

Figura 2. Regulació intracel·lular del metabolisme del ferro. El ferro del citoplasma és internalitzat a la mitocòndria a través dels transportadors Mrs3/Mrs4. Un cop dins la mitocòndria s'uneix amb el sofre per formar clústers Fe/S. Els clústers s'uneixen a la proteïna Isu1 a través del complex Nfs1-Isd11 juntament amb Yfh1. Posteriorment, són transferits a un dímer format per la proteïna Grx5, a través del complex Ssq1-Jaq1-Mge1. Finalment, els clústers Fe/S són exportats de la mitocòndria a través d'Atm1. Un cop al citoplasma, s'uneixen a monodímers de les glutaredoxines Grx3 i Grx4 i a dues molècules de glutatió (GSH). Seguidament, un homodímer de les glutaredoxines i una molècula de GSH són intercanviades per la proteïna Fra2. En aquestes condicions els factors de transcripció Aft1/Aft2, que són exportats del nucli a través de Msn5, s'uneixen als clústers Fe/S del citoplasma impedint la seva internalització al nucli, a través del seu transportador específic, Pse1. Aft1/Aft2 quan es troben al citoplasma no es poden unir als promotors de gens relacionats amb la captació del ferro inhibint així la seva transcripció. A més a més, quan hi ha un excés de ferro el factor transcripcional Yap5, promou la transcripció de gens que ajuden la cèl·lula a protegir-se dels efectes perjudicials de l'excés de ferro. Aft1, independentment de la localització subcel·lular i de la concentració de ferro es troba unit a la quinasa Slt2. En condicions d'escassetat de ferro, la quinasa Slt2 fosforila i regula negativament a Aft1, per tal d'impedir una captació excessiva del metall.

En condicions de suficiència de ferro, els clústers Fe/S es transfereixen del complex que formen amb Fra2 i Grx3/4 als factors de transcripció Aft1/Aft2, formant un homodímer amb els clústers. Aft1 i Aft2 són dos factors transcripcionals que coordinen la transcripció d'un grup de gens que formen part del reguló del ferro (Philpott, Leidgens, and Frey 2012). El reguló del

ferro està format aproximadament per 30 gens. Aquests gens s'agrupen segons la seva funció: i) gens relacionats amb l'adquisició de ferro d'alta afinitat a la membrana plasmàtica, ii) gens involucrats en el transport de ferro intracel·lular, iii) gens responsables del reciclatge del ferro i iv) gens encarregats de la remodelació metabòlica per l'optimització de l'ús del ferro. Els gens que formen part del reguló del ferro, en la seva regió promotora presenten un element regulador del ferro (FeRE), el qual és reconegut per Aft1 o Aft2 (Kaplan and Kaplan 2009). La unió d'Aft1/2 als clústers Fe/S provoca que disminueix la seva afinitat pel DNA promovent la seva dissociació dels elements FeRE i, per tant, la transcripció dels gens del reguló del ferro disminueix (Ueta et al. 2012). En aquestes condicions Aft1/2 són exportats al citoplasma, mitjançant l'exportador Msn5 (Yamaguchi-Iwai et al. 2002; Ueta et al. 2007). Si durant aquest període on no hi ha mancà de ferro, hi ha un procés cel·lular que necessita ferro, el metall és captat a través d'un sistema de baixa afinitat format per Smf1 i Fet4, els quals es troben constitutivament activats (Dix et al. 1994).

Quan es detecta una disminució del ferro disponible s'activa un grup de gens que formen part del transport d'alta afinitat del ferro. L'activació d'aquests gens es dona a través del factor de transcripció Aft1 i el seu homòleg Aft2 (Kaplan and Kaplan 2009). L'escassetat de ferro fa que disminueixin els clústers Fe/S als que s'uneixen, pel que Aft1/2 queden lliures al citoplasma i són translocats al nucli a través de Pse1 (Ueta, Fukunaka, and Yamaguchi-Iwai 2003). Aft1/2 dins el nucli s'uneixen a les regions FeRE activant la transcripció de gens involucrats en la captació de ferro (Yamaguchi-Iwai et al. 2002). La captació de ferro pel sistema d'alta afinitat pot estar associada a una via reductora o no (Martins, Costa, and Pereira 2018). En la via reductora, les molècules de Fe^{3+} es redueixen a Fe^{2+} a la superfície cel·lular a través de les metal·loreductases Fre1 i Fre2, un cop reduïdes són transportades al citosol a través d'un complex format per Fet3 i Ftr1 (Stearman et al. 1996). La via no reductora s'associa amb sideròfors i els complexos sideròfor-Fe^{3+} són transportats a través de la membrana plasmàtica per Arn1, Arn2, Arn3 i Arn4 (Lesuisse, Simon-Casteras, and Labbe 1999). El ferro unit a sideròfors també pot ser reduït per les reductases fèrriques Fre1-Fre4 i transportat per Fet3/Ftre1 (Martins, Costa, and Pereira 2018). Les proteïnes associades a la paret cel·lular, Fit1 i Fit2 també formen part del reguló del ferro i estan involucrades en la retenció dels complexos sideròfor-Fe^{3+} a la paret cel·lular facilitant la captació de ferro (Protchenko et al. 2001). En presència d'estrès oxidatiu la captació de ferro es dona per les vies no reductores per minimitzar el dany oxidatiu dels ions ferrosos (Castells-Roca et al. 2011).

Recentment, un estudi dut a terme pel grup de la Dra. de la Torre, ha demostrat que en condicions d'escassetat de ferro, Slt2 fosforila i regula negativament l'activitat d'Aft1 quan es troba dins el nucli. Això suggereix un mecanisme de regulació directe de l'expressió del reguló del ferro, ja que, Slt2 sempre està unit a Aft1. Aquesta regulació és crucial per a la supervivència pel fet que els mutants *slt2,* presenten disfuncions en Aft1, les quals repercuteixen en una disminució de la CLS (Pujol-Carrion et al. 2021).

L'activació del reguló del ferro també dona lloc a la transcripció de *CTH1* i *CTH2*. Cth1/2 són proteïnes que s'uneixen al mRNA de proteïnes involucrades en processos que tenen una alta demanda de ferro, per facilitar la seva desintegració (Puig, Askeland, and Thiele 2005). Un dels mRNAs dels que promou la seva degradació és el de *CCC1,* el qual codifica per una proteïna que facilita l'import de ferro al vacúol, disminuït així l'emmagatzematge del ferro al vacúol (Martínez-Pastor et al. 2013). Els fongs i les plantes guarden el ferro dins el vacúol per protegir-se de la toxicitat, ja que no expressen la proteïna d'unió de ferro citosòlica ferritina (L. Li and Ward 2018a).

En condicions d'excés de ferro les cèl·lules del llevat presenten diversos mecanismes per protegir-se dels efectes perjudicials de la sobrecàrrega de ferro. El factor de transcripció Yap5 coordina la resposta enfront elevats nivells de ferro activant l'expressió de dianes gèniques (Pimentel et al. 2012). Yap5 es localitza al nucli independentment dels nivells de ferro (L. Li et al. 2008). Aquesta proteïna, igual que Aft1/2, no censa el nivell de ferro citosòlic, es regula a través dels clústers Fe/S que sintetitza la mitocòndria (L. Li et al. 2012). El primer gen regulat per Yap5 que es va descriure va ser *CCC1* (L. Li and Ward 2018a). Yap5 es troba constitutivament unit al promotor de *CCC1* independentment dels nivells de ferro. L'activació de transcripció de *CCC1* es a través de la unió de dos clústers Fe/S en un domini ric en cisteïnes de Yap5, induint un canvi conformacional que permet la transcripció de *CCC1* (Rietzschel et al. 2015). Yap5 també regula l'expressió gènica de *GRX4, TYW1* i *CUP1* (Pimentel et al. 2012). L'activació de *GRX4,* serveix per inhibir la funció d'Aft1/2 en resposta a l'increment dels nivells de ferro (Pimentel et al. 2012). Tyw1 codifica per un enzim que protegeix les cèl·lules de la toxicitat de ferro segrestant a molècules de ferro lliures del citoplasma i unint-les als clústers Fe/S (A. Li et al. 2011). Cup1 és una metal·loproteïna d'unió a coure citosòlica que limita el coure disponible per Fet2 i protegeix a les cèl·lules del estrès oxidatiu (X. D. Liu and Thiele 1996).

1.4 Vies de senyalització cel·lular de *S. cerevisiae*

En tots els organismes vius, les rutes de senyalització són mecanismes intracel·lulars que regulen una àmplia gamma de processos biològics. Alteracions en la senyalització cel·lular poden donar lloc a malalties com el càncer (Wu et al. 2021) o la neurodegeneració (Woodbury and Ikezu 2014; Jęśko et al. 2019). Les vies de senyalització cel·lular s'han conservat durant l'evolució, des dels llevats fins a organismes superiors. Gràcies a aquest fet, el llevat de gemmació ha esdevingut una eina molt potent per a l'estudi dels mecanismes de senyalització.

En aquest apartat de la introducció es mostraran algunes de les rutes de senyalització cel·lular del llevat més importants.

1.4.1 Ruta de senyalització de la integritat de paret cel·lular (CWI)

La via de senyalització d'integritat de paret cel·lular (CWI) és una de les principals cascades de senyalització en el llevat. Aquesta s'activa en resposta a estrès mediambiental i processos morfològics que alteren la superfície cel·lular (Jiménez-Gutiérrez, Alegría-Carrasco, Sellers-Moya, et al. 2020). Les seves funcions principals són: i) controlar la biosíntesi de paret cel·lular (Klis, Boorsma, and De Groot 2006), ii) mantenir l'estabilitat de la cèl·lula enfront d'agressions a l'estructura superficial (Mishra et al. 2017; Verna et al. 1997; Vilella et al. 2005; Quilis, Gomar-Alba, and Igual 2021) i iii) regular la dinàmica del citoesquelet d'actina (Qadota et al. 1996).

La paret cel·lular del llevat és un complex macromolecular, format majoritàriament (80-90%) per β-1,3-glucà, β-1,6-glucà (8-18%) i minoritàriament (1-2%) per xitina i mannoproteïnes (Levin 2011; Jendretzki et al. 2011). Les propietats i dinàmica de la paret cel·lular varien constantment, a causa de la divisió i proliferació cel·lular i de les diferents condicions d'estrès ambiental que afecten la integritat de la paret, com són la font de carboni, la biodisponibilitat d'oxigen, la temperatura o el pH extern (A. B. Sanz et al. 2018). La paret cel·lular del llevat és una estructura essencial que envolta la cèl·lula i és necessària per mantenir la morfologia i la viabilitat (A. B. Sanz et al. 2022).

Alteracions en la paret cel·lular són detectades per cinc mecanosensors de membrana els quals

connecten la paret cel·lular amb la membrana plasmàtica (Dunayevich et al. 2018). Aquests es divideixen en dues subfamílies, els sensors tipus Wsc (Wsc1, Wsc2, Wsc3) (Verna et al. 1997; Jacoby, Nilius, and Heinisch 1998) i Mid2 (Ketela, Green, and Bussey 1999) i Mtl1 (Rajavel et al. 1999), els quals tot i tenir una estructura global compartida, presenten una petita seqüència primària diferent (Jendretzki et al. 2011). Tots ells contenen un domini transmembrana, el qual connecta amb una petita cua citoplasmàtica i una regió extracel·lular rica en Serines i Treonines altament O-mannosilades (Rajavel et al. 1999; Petkova, Pujol-Carrion, and de la Torre-Ruiz 2012). Els mecanosensors, mitjançant els factors d'intercanvi de GDP/GTP (GEFs), Rom1, Rom2 i Tus1, activen a la GTPasa Rho1 (Ozaki et al. 1996; Schmelzle, Helliwell, and Hall 2002). Rho1 un cop és activada interacciona amb Pkc1, per activar la cascada de fosforilació formada per les MAPKs (Mitogen-Activated Protein Kinases) (Kamada et al. 1996).

Les rutes de senyalització MAPK tenen una estructura comuna en totes les cèl·lules eucariotes (González-Rubio et al. 2021). Estan formades per un mòdul de tres proteïnes quinasa que actuen com una cascada de fosforilació, MAPKKK (MAPK Kinase Kinase), MAPKK (MAPK Kinase) i MAPK (Jiménez-Gutiérrez, Alegría-Carrasco, Alonso-Rodríguez, et al. 2020). La cascada de MAPKs que activa la ruta CWI a través de Pkc1 està formada per la MAPKKK, Bck1 (Kyung S Lee and Levin 1992), dues MAPKK, Mkk1 i Mkk2 (Irie et al. 1993) i finalment, la MAPK Slt2 o també anomenada Mpk1 (K S Lee et al. 1993). La fosforilació de Slt2 indueix al factor de transcripció Rlm1 i el complex SBF. Els quals regulen l'expressió d'un conjunt de gens (entre 100 i 200) involucrats en la construcció de la paret cel·lular, per tal de reparar el dany causat (Figura 3) (A. B. Sanz et al. 2018; Jiménez-Gutiérrez, Alegría-Carrasco, Alonso-Rodríguez, et al. 2020).

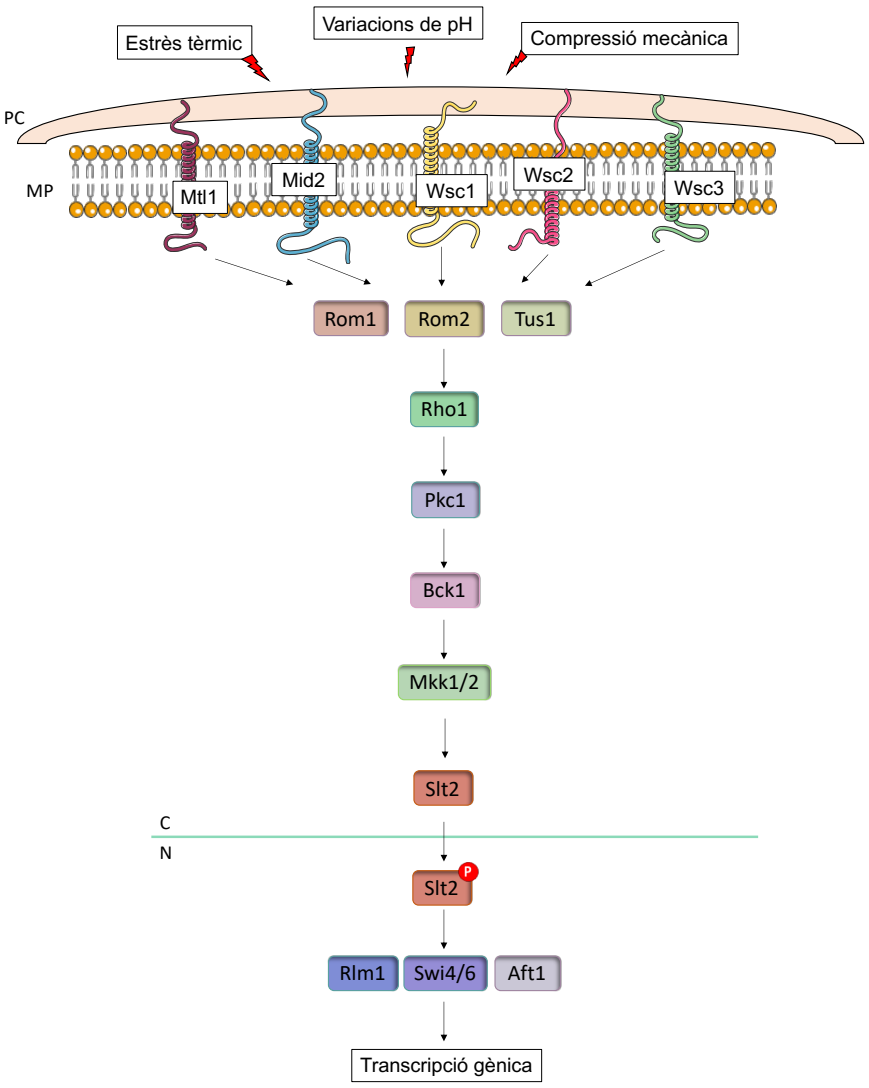

Figura 3. Ruta de senyalització de la integritat de paret. Estímuls directes o indirectes sobre el llevat com l'estrès tèrmic, canvis en el pH extern, compressió mecànica de la cèl·lula, entre altres, alteren l'estructura de la paret cel·lular (PC) del llevat. Aquests estímuls són detectats per cinc sensors (Mtl1, Mid2, Wsc1/2/3) localitzats en la membrana plasmàtica (MP), els quals a través de Rom1, Rom2 i Tus1 transmeten el senyal a la GTPasa Rho1. Rho1 interacciona amb Pkc1 induint la cascada de senyalització de les MAPKs Bck1, Mkk1/2 i Slt2. Finalment, Slt2 és fosforilada i translocada del citoplasma (C) al

nucli (N) permeten la transcripció de Rlm1, Swi4/6 i Aft1; factors de transcripció de gens de remodelació de la paret cel·lular, cicle cel·lular i de l'homeòstasi del ferro respectivament.

Rlm1 és el responsable de l'expressió de la majoria dels gens (aproximadament el 90%) que s'indueixen a través de la resposta d'estrès de paret cel·lular. Slt2 és l'encarregada de regular l'activitat transcripcional de Rlm1 fosforilant-lo en dos residus (Ser427 i Thr439) (Jung et al. 2002). *SLT2* i *RLM1* presenten un mecanisme de feedback positiu, necessari per obtenir una activació transcripcional completa (A. B. Sanz et al. 2022). Per al contrari, SBF principalment està involucrat en la regulació de gens durat la transició G_1/S (A. B. Sanz et al. 2018), tot i que també s'ha vist la seva participació en la regulació de l'expressió d'un petit grup de gens en resposta a l'estrès de paret per altes temperatures (K.-Y. Kim, Truman, and Levin 2008). El complex SBF està format per dues proteïnes, Swi4 i Swi6. Swi4 és l'encarregat d'unir-se al DNA a través d'una seqüència específica anomenada SCB (CA/GGGAAA) i activar la transcripció (Taylor et al. 2000). Aquesta unió és possible gràcies a Swi6, la qual s'uneix a l'extrem C-terminal de Swi4, incrementant l'estabilitat del complex i l'afinitat de Swi4 per la seqüència SCB (Andrews and Moore 1992).

Una activació errònia de la cascada de senyalització MAPK compromet la integritat de la paret cel·lular donant lloc a la lisi cel·lular en els llocs de creixement polaritzat (Levin 2011). Aquest fet és degut a Rho1, que integra la senyalització de la superfície cel·lular i del cicle de divisió cel·lular, a la vegada que regula una gran varietat d'estímuls involucrats en la biogènesi de la paret cel·lular, l'organització de l'actina i la secreció polaritzada (Qadota et al. 1996).

1.4.1.1 Estímuls activadors de la CWI

La ruta d'integritat de paret cel·lular és activada per una àmplia varietat d'estímuls, directes o indirectes, que alteren l'estructura de la paret cel·lular, alguns dels quals ja mencionats anteriorment:

i) **Canvis en el pH extern**. *S. cerevisiae* creix en un ambient una mica àcid, el seu pH òptim es troba entre 5 i 6, sent capaç de créixer fins a pH 3. Mid2 activa la CWI en resposta a pH àcid. El senyal es pot detectar amb la fosforilació Slt2 al cap de 20 minuts (Claret et al. 2005). Contràriament, és Wsc1 l'encarregat d'activar la via

CWI enfront de pH alcalí. L'activació de Slt2 en resposta a pHs alts, és ràpida, s'observa entre els 5 i 15 minuts (Serrano et al. 2006).

ii) **Estrès de membrana plasmàtica**. Alteracions en la membrana plasmàtica de la cèl·lula, ja sigui per el tractament amb reactius químics com el SDS (Igual, Johnson, and Johnston 1996), o per processos físics com per exemple l'estrès tèrmic desencadenen la cascada de senyalització de la CWI (Delley and Hall 1999), fosforilant Slt2.

a) **Estrès per compressió mecànica**. Pressions extracel·lulars afecten la paret cel·lular i a la integritat de la membrana plasmàtica donant lloc a la lisi cel·lular. Aquest estímul és detectat per Mid2, activant la CWI. Paral·lelament, la pressió extracel·lular activa la senyalització del calci a través de la calcineurina, pel que Mishra et al. suggereixen una actuació conjunta de les dues vies, CWI i Calci en resposta a l'estrès mecànic (Mishra et al. 2017).

b) **Canvis tèrmics**. Les temperatures elevades incrementen la fluïdesa de la membrana i es dona una alteració de la turgència a causa de la producció de trehalosa. Els mecanosensors que detecten un augment de la temperatura són Wsc1 (Verna et al. 1997) i Mid2 (Ketela, Green, and Bussey 1999) activant la cascada de fosforilació de Slt2 i la transcripció de Rlm1 i Swi4/6. Wsc1 també detecta les temperatures baixes, Slt2 rep el senyal, tot i que en aquest cas s'activa la ruta TORC1-cAMP-PKA (Córcoles-Sáez et al. 2012). L'activació de la via per estrès tèrmic és detectada després de 20 min de l'aplicació de l'estímul (Kamada et al. 1995).

c) **Xoc osmòtic**. Alteracions en l'osmolaritat del medi donen lloc a modificacions en l'abundància de soluts intracel·lulars (Jiménez-Gutiérrez, Alegría-Carrasco, Alonso-Rodríguez, et al. 2020). La resistència a estrès osmòtic s'assoleix a través de la sobreexpressió d'enzims de remodelació de la paret cel·lular reduint l'elasticitat d'aquesta (A. B. Sanz et al. 2018).

1) **Xoc hipoosmòtic.** Actualment, no es coneix com el senyal és censat per la cèl·lula, però el xoc hipoosmòtic, activa la via CWI i fosforila

Slt2, permeten l'obertura de l'aquagliceroporina Fsp1 de la membrana plasmàtica, alliberant glicerol des de l'interior de la cèl·lula a l'exterior i així, restaurant l'equilibri osmòtic i impedint que la cèl·lula exploti. La resposta s'activa 15 segons després i al cap de 30 minuts es recuperen els nivells basals (Davenport et al. 1995).

2) **Xoc hiperosmòtic.** La CWI és la cascada de senyalització principal necessària per a controlar les respostes d'estrès de paret cel·lular, però existeixen altres vies de senyalització que regulen l'expressió de gens diana de la CWI, com és el cas de la ruta HOG (High-Osmolarity Glycerol). HOG engloba dues branques de senyalització principals, SLN1 i SHO1. La branca SLN1 és controlada per l'osmosensor Sln1. La branca SHO1 està formada per dos osmosensors transmembrana Hkr1 i Msb2, i una proteïna "*scaffold*", Sho1 (Udom et al. 2019). En resposta a estrès hiperosmòtic s'activa un primer senyal ràpid a través de les dues branques d'HOG, les quals convergeixen en Pbs2, que fosforila a la MAPK Hog1. Hog1 és desplaçada al nucli per tal d'activar diferents factors de transcripció, entre ells Hot1, Smp1, Msn2 i Msn4, induint l'activació de gens de síntesi i captació de glicerol i inhibint a Fsp1, per tant, incrementant el glicerol intracel·lular (A. B. Sanz et al. 2018). A conseqüència de l'increment de glicerol intracel·lular, s'indueix una resposta tardana, al cap de 45-60 minuts del xoc hiperosmòtic, a través de la CWI, on la fosforilació de Slt2 es produeix a través de Sho1 de la via HOG i de Pkc1, Bck1 i Mkk1/2 de la CWI, però és independent de Rho1 (García-Rodríguez et al. 2005).

iii) **Estrès oxidatiu**. Les ROS intracel·lulars causen danys en diferents compartiments cel·lulars i alteren la integritat de paret cel·lular. La resposta que desencadena l'estrès oxidatiu és complexa, una de les rutes de senyalització que s'activen és la CWI. L'estrès oxidatiu pot ser causat per una gran varietat d'estressos o per diferents agents oxidants, activant la ruta d'una forma diferent. La diamida oxida les proteïnes de la paret cel·lular, alteració que és detectada per Mtl1 i es transmet a través dels elements reguladors de la ruta induint la transcripció de Rlm1 (Vilella

et al. 2005). D'altra banda, el peròxid d'hidrogen és censat per Mid2 i Mtl1, els quals per un costat activen la ruta CWI i Mtl1, a més, és necessari inactivar Tor1 i Ras2 per tal de mantenir la viabilitat cel·lular (Petkova et al. 2010). El sensor Wsc1 s'ha vist implicat en la senyalització d'estrès oxidatiu induït per altres estressos com són la cloroquina (Baranwal et al. 2014) o les nanopartícules d'òxid de zinc (Babele et al. 2018).

iv) **Estrès genotòxic**. El material genètic es troba constantment exposat a alteracions a causa dels processos fisiològics, com defectes en la replicació, activitats errònies d'enzims, ROS o agents externs físics o químics (Quilis, Gomar-Alba, and Igual 2021). Dany en el DNA pot donar lloc a alteracions en les funcions cel·lulars i induir la mort cel·lular, de manera que és essencial disposar de sistemes de reparació del DNA i mantenir l'estabilitat genòmica (Jiménez-Gutiérrez, Alegría-Carrasco, Sellers-Moya, et al. 2020). Diferents treballs connecten la CWI amb la resposta de dany a DNA (Queralt and Igual 2005; Dardalhon et al. 2009). Slt2 i Bck1 interaccionen genèticament amb diferents "*check-points*" de dany en DNA i Slt2 és fosforilat en resposta a dany en DNA. Swe1 és una de les proteïnes que es proposa com a regulador de la resposta de Slt2 enfront de l'estrès genotòxic (Quilis, Gomar-Alba, and Igual 2021).

v) **Alteracions en el citoesquelet d'actina**. La despolarització del citoesquelet d'actina activa la CWI per tal de tornar a polaritzar-lo. L'actina es pot despolaritzar després d'estrès tèrmic, oxidatiu o acidesa del pH (Jiménez-Gutiérrez, Alegría-Carrasco, Alonso-Rodríguez, et al. 2020). El complex de dinactina té funcions específiques en el "*check-point*" d'integritat de paret cel·lular. Els autors Sukegawa et al. demostren que la MAPK de la CWI té un paper rellevant en aquest "*check-point*" (Sukegawa et al. 2018). De fet, l'organització de l'actina està controlada per Rho1 a través de les proteïnes Bni1 i Bnr1 (Levin 2011).

vi) **Estrès de reticle endoplasmàtic (ER).** L'augment de proteïnes mal plegades dins l'ER activa la resposta de proteïnes no plegades, UPR. Aquesta via connecta l'ER amb el nucli i és essencial per al control de la qualitat proteic durant la secreció de proteïnes. L'acumulació de proteïnes mal plegades comporta, indirectament, estrès de paret cel·lular, que és sensat per Mid2, desencadenant la fosforilació de Slt2 per

tal d'obtenir una resposta transcripcional a l'estrès de ER a través de Swi6, el qual indueix l'activitat basal de la UPR (Chen et al. 2005; Scrimale et al. 2009).

vii) **Altres substàncies que activen la CWI**. Existeixen altres compostos que activen la CWI, com són la rapamicina (Torres et al. 2002), l'etanol (Udom et al. 2019), la manca de glucosa (Petkova et al. 2010), el blanc de calcofluor (CFW) (Ketela, Green, and Bussey 1999), el congo red (Bermejo et al. 2010), la tunicamicina (Bonilla and Cunningham 2003) i la cafeïna (Martín et al. 2000), entre d'altres.

1.4.1.2 Inhibició de la ruta CWI

La inhibició de la via CWI es pot donar a varis nivells. A l'inici de la via, Rho1 és regulada negativament a través de 4 proteïnes activadores de GTPasa (GAPs): Bem2 (Peterson et al. 1994), Sac7 (A. Schmidt, Schmelzle, and Hall 2002), Bag7 (A. Schmidt, Schmelzle, and Hall 2002) i Lrg1 (Roumanie et al. 2001). Bem2 i Sac7 són específiques de la inhibició de la ruta CWI en resposta a estrès de paret, mentre que Bag7 i Sac7 controlen el citoesquelet d'actina i Lrg1 la síntesi de β-1,3-glucà (Watanabe, Abe, and Ohya 2001; Levin 2011).

Al final de la cascada de senyalització, l'activitat de Slt2 pot ser inhibida a través de diferents fosfatases, Ptp2, Ptp3 (Mattison et al. 1999), Ptc1 (Tatjer et al. 2016), Msg5 (Marín et al. 2009) i Sdp1 (Hahn and Thiele 2002); sent Ptp2 i Msg5 estimulades transcripcionalment per Slt2, mostrant un feedback negatiu de regulació de la ruta. Slt2 també participa en altres bucles negatius de regulació de la ruta CWI, com per exemple, en la disminució de l'activitat de Rom2 a través d'una retrofosforilació de la cascada MAPK (A. B. Sanz et al. 2018). Mgs5 és una fosfatasa que manté a Slt2 defosforilada durant estats d'absència d'estrès i en resposta a dany en DNA Msg5 és degradada permeten l'activació de Slt2 (L. Liu and Levin 2018).

1.4.1.3 Altres substrats de Slt2

Slt2 pot senyalitzar a altres dianes que no siguin els factors de transcripció Rlm1 i SBF, com per exemple Sir3 (Ray et al. 2003), Bcy1 (Soulard et al. 2010), els reguladors del cicle cel·lular, Sic1 i Ciclina C (C. Jin, Strich, and Cooper 2014), el regulador de la calcineurina Rcn2, el

repressor de la traducció Caf20 i la proteïna de Golgi, Gga1 (Alonso-Rodríguez et al. 2016). Addicionalment, Slt2 participa en vies alternatives a la remodelació de la paret cel·lular, com per exemple, la regulació de la homeòstasi del ferro, on fosforila i regula negativament l'activitat d'Aft1 en condicions de falta de ferro (Pujol-Carrion et al. 2021); la pexofàgia i la mitofàgia on té un paper en les etapes inicials del procés durant la unió de la mitocòndria amb el PAS (Pre-Autophagosomal Site) (Mao and Klionsky 2011).

1.4.2 Senyalització cel·lular a través de la via Ras/cAMP/PKA

La via de senyalització Ras/cAMP/PKA és indispensable per la regulació del creixement i el metabolisme cel·lular i la resistència a estrès (A. Zhang et al. 2011). La glucosa del medi, és la responsable d'activar aquesta ruta de senyalització, induint la síntesi d'AMP cíclic (cAMP) (Rolland, Winderickx, and Thevelein 2002). La detecció de la glucosa té lloc a través de dos sistemes (Figura 4): i) un sistema de receptors format per proteïnes G (GPCR) (Colombo et al. 1998) i ii) un sistema de fosforilació dependent de la glucosa a través de les proteïnes Ras (Rolland et al. 2000).

El sistema GPCR consisteix en dues proteïnes G (proteïnes que poden unir nucleòtids de guanina), Gpr1 i Gpa2, les quals censen la glucosa extracel·lular. El gen *GPR1* codifica per un receptor de glucosa localitzat a la superfície cel·lular i format per set regions transmembrana. Gpr1 interacciona físicament amb Gpa2 a través del seu domini C-terminal (A. Zhang et al. 2011). Gpa2 és l'encarregada de transmetre el senyal de la glucosa i induir la síntesi de cAMP (Colombo et al. 1998). Rgs2 és la proteïna encarregada d'inhibir aquest senyal activant l'activitat GTPasa de Gpa2 (Versele, De Winde, and Thevelein 1999). El sistema GPCR requereix l'activitat basal de Ras per tal d'induir la producció de cAMP, per ell sol és incapaç; a més a més els estudis mostren que la seva funció és necessària en la resposta a llarg termini i no en la resposta ràpida a la biodisponibilitat de la glucosa (Ying Wang et al. 2004; Tisi, Belotti, and Martegani 2014).

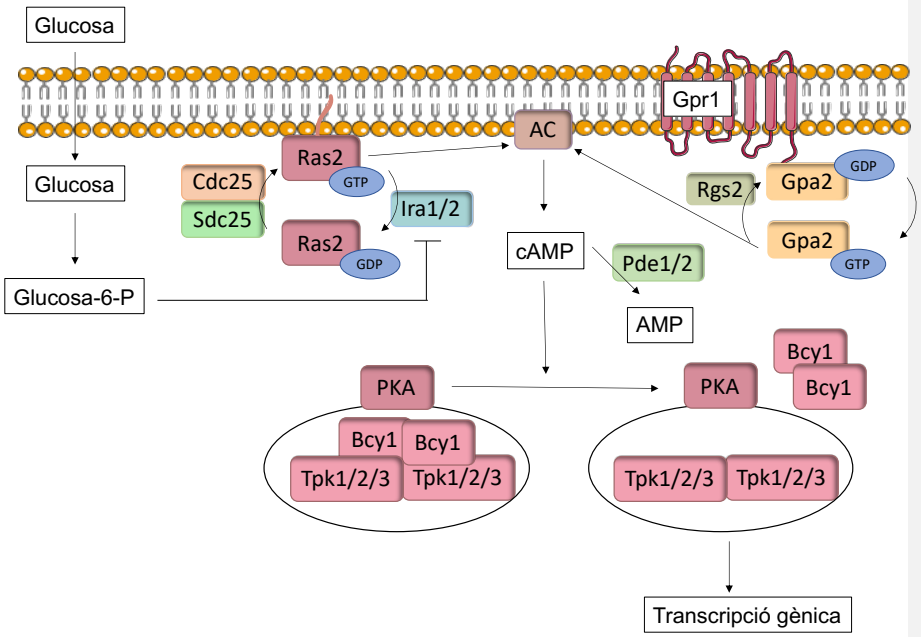

Figura 4. Ruta de senyalització mitjançada per Ras/cAMP/PKA. En presència de glucosa en el medi, aquesta és internalitzada dins la cèl·lula i fosforilada a Glucosa-6-P. La Glucosa-6-P permet la càrrega de Ras2 amb GTP a través de les GEFs Cdc25 i Sdc25, inhibint les GAPs Ira1 i Ira2. Ras2-GTP activa l'adenilat ciclasa (AC) estimulant la producció de cAMP. L'AC també pot ser activada pel sistema GPCR, format per Gpr1 i Gpa2. AMP cíclic, senyalitza a PKA, permeten la dissociació de les subunitats catalítiques (Tpk1/2/3), de les dues subunitats reguladores (Bcy1), de manera que PKA esdevé activa regulant diversos processos cel·lulars. Els nivells de cAMP cel·lulars es regulen a través de les fosfodiesterases Pde1 i Pde2.

El llevat *S. cerevisiae* conté dos gens *RAS*, *RAS1* i *RAS2,* els quals codifiquen per les proteïnes Ras, altament homologues amb les de mamífer i essencials per al creixement (S. Powers et al. 1984; Kataoka, Broek, and Wigler 1985). Aquestes proteïnes es troben alterades en moltes cèl·lules tumorals de mamífer (Capon et al. 1983; Nakhaei-Rad et al. 2023). Les proteïnes Ras són GTPases monomèriques, que es troben inactives quan estan unides a GDP i actives en unir-se a GTP (Santangelo 2006). Són sintetitzades com a precursors en el citosol, posteriorment sofreixen diverses modificacions postranscripcionals: i) eliminació de l'extrem C-teminal per farnesilació, ii) acetilització dels àcids grassos, iii) palmitosilació i iv) carboximetilació; i finalment, a través d'un mecanisme de transport específic, són dipositades a la superfície de la

membrana plasmàtica on desenvolupen la seva senyalització (Tamanoi 1988; Tisi, Belotti, and Martegani 2014).

Els mecanismes de regulació són diferents en els dos gens *RAS*, el mRNA de *RAS1* es reprimeix en els cultius que creixen sota una font de carboni no-fermentable com són l'etanol o l'acetat, a través de Tup1, proteïna que s'uneix a la regió promotora del gen de *RAS1*. Pel contrari, *RAS2,* s'expressa amb eficiència en qualsevol font de carboni, presentant un pic durant la fase exponencial (Tamanoi 1988). Les dianes d'acció també són diferents pels dos gens, *RAS1* regula els fosfolípids d'inositol (Kaibuchi et al. 1986), mentre que *RAS2* està involucrat en la producció del cAMP (Toda et al. 1985). L'activitat de les proteïnes Ras és controlada per dues proteïnes reguladores, Cdc25 i Sdc25, són dos GEFs, les quals estimulen l'intercanvi de GDP/GTP de Ras (Camonis et al. 1986). Contràriament, les proteïnes Ira1 i Ira2, són GAPs, que promouen la hidròlisi del GTP a GDP (Tanaka et al. 1990; A. Zhang et al. 2011; Tisi, Belotti, and Martegani 2014). Els primers activadors fisiològics de Ras2, identificats en el llevat, són els sucres fermentables, com la glucosa (J. M. Thevelein 1991). En presència de glucosa en el medi, aquesta s'internalitza dins la cèl·lula i és fosforilada mitjançant tres enzims, Hxk1, Hxk2 i Glk1. La glucosa fosforilada estimula l'increment de la càrrega GTP a Ras2, a través de la inhibició de les proteïnes Ira (Colombo et al. 2004; Santangelo 2006; Tisi, Belotti, and Martegani 2014). Paral·lelament, la glucosa intracel·lular causa acidificació citoplasmàtica que també contribueix a un ràpid increment de GTP en les proteïnes Ras (Caspani et al. 1985; Lastauskiene, Zinkevičiene, and Čitavičius 2014). La càrrega de Ras amb GTP no necessita l'activitat del sistema GPCR (Tisi, Belotti, and Martegani 2014).

Ras2 i Gpa2 estimulen la producció de cAMP a través de la adenilat ciclasa (AC) codificada pel gen *CYR1* (Kataoka, Broek, and Wigler 1985; Conrad et al. 2014). Les condicions nutricionals influeixen en els nivells cel·lulars de cAMP, els quals es regulen a través de l'estimulació de la seva síntesi o degradació. Les cèl·lules de llevat presenten un nivell basal de cAMP, sent estimulada la seva síntesi en presència de fonts de carboni fermentables (Park, Grant, and Dawes 2005) i el cAMP és degradat a AMP per les fosfodiesterases de baixa i alta afinitat, Pde1 i Pde2, respectivament (Nikawa, Sass, and Wigler 1987; Sass et al. 1986), on Pde1 només sembla ser necessària en absència de Pde2 (Park, Grant, and Dawes 2005).

El senyal es transmet des del cAMP fins a PKA, un tetràmer format per dues subunitats reguladores codificades pel gen *BCY1* (Toda, Cameron, Sass, Zoller, Scott, et al. 1987) i dues

subunitats catalítiques, codificades pels gens *TPK1, TPK2* i *TPK3* (Toda, Cameron, Sass, Zoller, and Wigler 1987). La font de carboni condiciona la localització de Bcy1, i el cAMP és qui controla la localització de Tpk1. Quan la font de carboni és la glucosa, Bcy1 i Tpk2 es localitzen en el nucli, i Tpk1 i Tpk3 presenten un patró difús entre el nucli i el citoplasma, pel contrari, quan la font de carboni és el glicerol o les cèl·lules es troben en fase estacionaria les diferents subunitats de PKA es localitzen al citoplasma, aquestes variacions en la localització subcel·lular són importants per la senyalització, de la mateixa manera que les diferents subunitats catalítiques donen lloc a diferents expressions gèniques (A. Zhang et al. 2011; Santangelo 2006). PKA s'activa quan el cAMP s'uneix a les subunitats reguladores induint la dissociació de les subunitats catalítiques (Schmelzle et al. 2004; Park, Grant, and Dawes 2005). A més a més, PKA presenta un feedback de regulació negatiu de la ruta mitjançant diferents dianes: i) fosforila a Cdc25 a través de Tpk2, disminuït la seva activitat GEF (A. Zhang et al. 2011); ii) regula Pde1, per tal d'inhibir la senyalització de cAMP (Ma et al. 1999); iii) influint en la localització i concentració de Pde2 (Hu et al. 2010).

PKA regula diferents processos cel·lulars i fisiològics: i) el metabolisme del carboni i l'acumulació de glicogen i trehalosa (W. Schepers et al. 2012; Rittenhouse, Moberly, and Marcus 1987; Smith, Ward, and Garrett 1998; Rolland et al. 2000); ii) el control de la biogènesi dels ribosomes, mitjançada pels nutrients, principalment activant el factor de transcripció Rap1 i regulant la localització subcel·lular del major regulador de la biogènesi de ribosomes (RiBi) i de gens i proteïnes ribosomals (RP) (Klein and Struhl 1994; Neuman-Silberberg, Bhattacharya, and Broach 1995); (iii) la progressió del cicle cel·lular, a través de la fosforilació de la proteïna Whi3, inhibint la seva interacció amb la Ciclina 3, Cln3, necessària per promoure la transició de la fase G_1/S (Johan M. Thevelein and De Winde 1999; Mizunuma et al. 2013); iv) la quiescència, inhibint l'activitat de Rim15, una proteïna necessària per entrar en quiescència (Pedruzzi et al. 2003); v) tolerància a l'estrès a través de la fosforilació de Msn2-Msn4, els quals s'uneixen a elements de resposta a estrès (STRE) (Görner, Durchschlag, Martinez-pastor, et al. 1998); vi) el canvi del creixement d'esporulació a filamentós (Johan M. Thevelein and De Winde 1999); vii) l'autofàgia, inhibint els seus passos inicials (Budovskaya et al. 2004); viii) l'envelliment i la supervivència (Budovskaya et al. 2004; Longo 2003); ix) la repolarització de l'actina (Gourlay and Ayscough 2006) i x) l'apoptosi del llevat en resposta a l'acidificació del medi (Lastauskiene, Zinkevičiene, and Čitavičius 2014).

1.4.3 Senyalització i regulació de l'expressió gènica a través del complex SNF1

Snf1 (Sucrose Non-Fermenting 1) és una proteïna quinasa que forma part de la família de les quinases serina/treonina; aquestes proteïnes estan conservades evolutivament en tots els eucariotes, en mamífers s'anomena AMPK (AMP-activated Kinase). Snf1 té un paper important en la resposta a l'estrès nutricional i ambiental (Celenza and Carlson 1984; X. Lin 2021). La proteïna Snf1 de llevat, és l'ortòloga de la subunitat α catalítica del complex AMPK en mamífers (Grahame, Carling, and Carlson 1998). Snf1 forma part d'un complex heterotrimèric juntament amb la subunitat reguladora γ, Snf4, i la subunitat β, una proteïna "*scaffold"*, que pot ser una d'aquestes tres: Sip1, Sip2 o Gal83 (Figura 5). Les tres isoformes β determinen la localització subcel·lular del complex i la seva diana d'acció (P. Sanz, Viana, and Garcia-Gimeno 2016). Sip1 dirigeix al complex al vacúol (Hedbacker, Townley, and Carlson 2004) i li proporciona una baixa activitat quinasa (Nath, McCartney, and Schmidt 2002). Sip2 manté el complex SNF1 al citoplasma (Vincent et al. 2001) i se li ha descrit un paper en l'envelliment (Ashrafi et al. 2000). Gal83 és la isoforma més important per regular el creixement de la cèl·lula en presència d'una font de carboni no fermentable. Snf1 unida a Gal83 es localitza majoritàriament al nucli (Vincent et al. 2001). D'ara endavant quan es parla de tot el complex s'utilitza la forma SNF1.

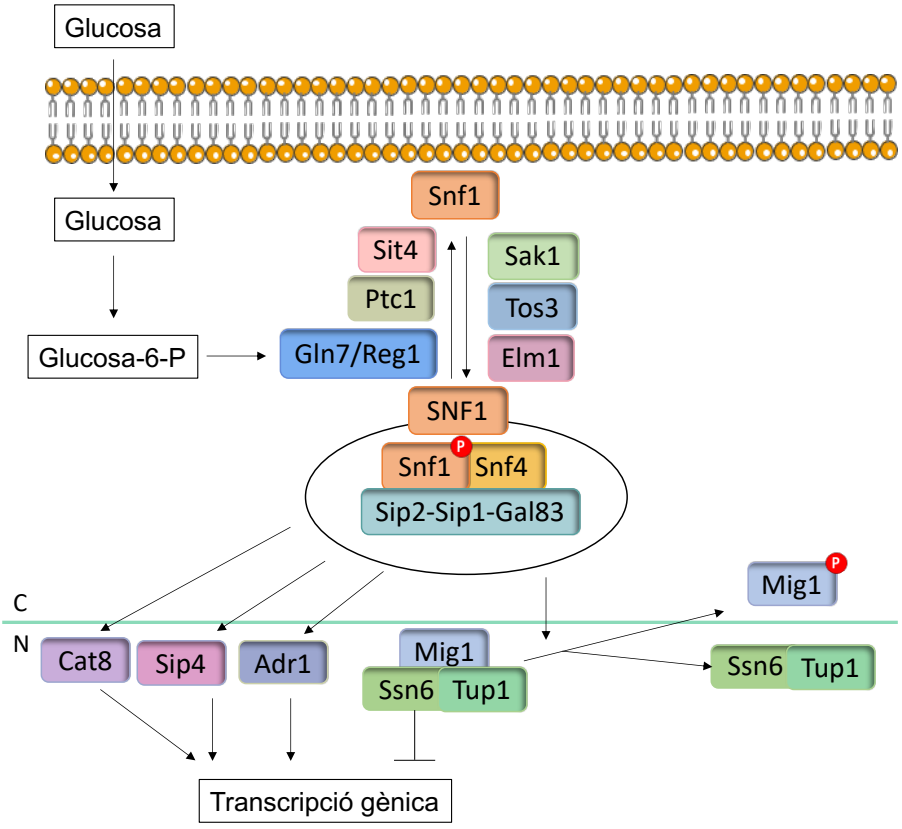

Figura 5. Mecanisme de senyalització del complex SNF1. La presència de glucosa en el medi de cultiu del llevat de gemmació estimula la defosforilació de la proteïna Snf1 a través de les fosfatases Gln7/Reg1, Ptc1 o Sit4 impedint la formació del complex SNF1. Quan la glucosa s'exhaureix Snf1 és fosforilada a través de les quinases Sak1, Tos3 i Elm1 en el seu "*loop*" del domini quinasa. Snf1 fosforilada s'uneix a la subunitat reguladora, Snf4, i a una de les tres possibles proteïnes, Sip2, Sip1 o Gal83, les quals actuen de proteïna "*scaffold*". Aquest complex heterotrimèric s'anomena complex SNF1 i és actiu. SNF1 indueix la fosforilació del repressor Mig1 translocant-lo del citoplasma al nucli, provocant la dissociació de la seva unió amb els correpressors Ssn6 i Tup1. D'aquesta forma s'indueix la transcripció de gens involucrats en la gluconeogènesi, entre d'altres. A més a més, SNF1 estimula a les proteïnes reguladores d'expressió gènica Cat8 i Sip4 i al factor transcripcional Adr1.

SNF1 s'activa o inactiva, principalment, en resposta a la concentració de glucosa del medi, tot i que, l'estrès ambiental també el pot activar. Baixes concentracions de glucosa, inferiors a

l'1%, indueixen la fosforilació de Snf1 en el seu "*loop*" d'activació del domini quinasa, concretament en la Treonina 210 (Thr-210), permetent l'activació del complex com a resposta de l'increment cel·lular de la ràtio AMP/ATP. Les quinases d'estrès Sak1, Tos3 i Elm1 són les encarregades de fosforilar a Snf1 (Hong et al. 2003; Wilson, Hawley, and Hardie 1996; Willis et al. 2018). En el llevat, aquestes tres quinases es troben actives constitutivament, per tant, la regulació de l'activitat de Snf1 es dona a través de la defosforilació del residu Thr-210, mitjançant la fosfatasa del llevat tipus 1, Glc7, i la seva subunitat reguladora, Reg1. Glc7/Reg1 defosforilen a Snf1 en resposta a l'addició de glucosa al medi (Ludin, Jiang, and Carlson 1998; P. Sanz et al. 2000). Posteriorment, s'han descrit altres mecanismes d'inhibició de l'activitat de SNF1. Les fosfatases Sit4 i Ptc1 s'han descrit com fosfatases alternatives a Glc7 (Ruiz, Xu, and Carlson 2011, 2013). A més, la via Ras/cAMP/PKA controla negativament a Snf1 a través de la fosforilació de Sak1 i de la localització subcel·lular de la subunitat β, Sip1 (Barrett et al. 2012; X. Lin 2021). Aquestes dues vies de senyalització, Ras/cAMP/PKA i SNF1, estan altament connectades, ja que no només s'ha demostrat la regulació de la primera sobre la segona, sinó que també s'ha descrit una regulació des de Snf1 cap a PKA a través la interacció física de Snf1 amb AC, provocant una disminució dels nivells intracel·lulars de cAMP i, per tant, en l'activitat de PKA (Nicastro et al. 2015). Finalment, es coneix un altre residu de fosforilació de Snf1, el qual també es troba en el seu "*loop*" d'activació del domini quinasa, la serina 214 (Ser-214), important per a la regulació del complex, ja que la seva fosforilació l'inactiva (McCartney et al. 2016).

La fosforilació de Snf1 no és suficient per activar a SNF1, es requereix l'associació entre la subunitat α i γ, per tal d'estabilitzar la conformació activa de la quinasa (Jiang and Carlson 1996). Les modificacions postraducionals d'alguna de les subunitats del complex també regulen la seva activitat. Sip1 és miristoilada per tal de localitzar-la a la membrana vacuolar en resposta a la depleció de glucosa, permeten l'orientació de l'activitat catalítica de Snf1 a substrats localitzats a la membrana vacuolar (Hedbacker, Townley, and Carlson 2004). Sip2 pot ser acetilada per estabilitzar la interacció amb la subunitat catalítica de Snf1, inhibint l'activitat del complex (Y. yi Lin et al. 2009); a més pot ser miristoilada, localitzant-se a la membrana plasmàtica, segrestant Snf4 i, per tant, inhibint SNF1 (S. S. Lin, Manchester, and Gordon 2003). La quinasa Snf1 també és modificada en presència de glucosa. La lligasa E3-SUMO, Mms21, catalitza la unió de SUMO a l'extrem C-terminal de Snf1, inhibint l'activitat del complex i marcant a la proteïna per ser ubiquitinitzada a través de les proteïnes Slx5-Slx8

i posteriorment, degradada. Aquesta modificació és reversible a través de la proteasa-SUMO Ulp1 (Simpson-Lavy and Johnston 2013).

SNF1 actiu fosforila al repressor Mig1, desplaçant-lo del nucli al citoplasma, i inhibint així la seva interacció amb els correpressors Ssn6-Tup1, permetent la transcripció dels gens inhibits per la glucosa (Östling and Ronne 1998; Papamichos-Chronakis, Gligoris, and Tzamarias 2004). Mig1 dins el nucli també interactua amb l'hexoquinasa PII (Hxk2), enzim que desenvolupa un paper en la glicòlisi i en la regulació de la transcripció de gens inhibits per la glucosa (Ahuatzi et al. 2007; Palomino, Herrero, and Moreno 2006). Addicionalment, SNF1 activa a Cat8 i Sip4, reguladors de l'expressió de gens gluconeogènics i de l'activador transcripcional Adr1, el qual regula l'expressió de gens involucrats en l'ús d'etanol com a font de carboni (Tripodi et al. 2018).

SNF1 regula molts processos metabòlics i fisiològics, segons la biodisponibilitat de la glucosa: i) l'expressió de gens necessaris per la gluconeogènesi (Soontorngun et al. 2007), ii) la transcripció dels gens que formen part del cicle del glioxilat (Soontorngun et al. 2007), iii) el control de l'expressió gènica del procés de la β-oxidació dels àcids grassos, a través de diversos factors de transcripció (Soontorngun et al. 2007), iv) reprimeix la biosíntesi lipídica inhibint la carboxiacetilasa d'Acetil-CoA (Acc1) (Woods et al. 1994), v) té un paper en la biosíntesi d'aminoàcids i l'assimilació d'amoni a través de la interacció amb Gcn2, activant-la i estimulant la síntesi de Gcn4 (J. Zhang et al. 2011; Shirra et al. 2008), vi) controla l'ús de fons de carboni alternatives a la glucosa com la sucrosa, galactosa, maltosa i etanol (Hong and Carlson 2007), vii) influeix en la respiració mitocondrial i l'entrada en quiescència (Miyata et al. 2022) viii) durant el "*shift*" diauxic contribueix a la inducció de gens relacionats amb l'homeòstasi del ferro a través del factor transcripcional Aft1 (Haurie, Boucherie, and Sagliocco 2003), ix) regula la resposta general d'estrès (Alepuz, Cunningham, and Estruch 1997; Hong and Carlson 2007), x) el creixement pseudofilial (Kuchin, Vyas, and Carlson 2002; Orlova et al. 2006), xi) l'envelliment (Ashrafi et al. 2000; Y. Yao et al. 2015), xii) l'homeòstasi dels ions (Portillo, Mulet, and Serrano 2005; Ye, Elbing, and Hohmann 2008), xiii) l'autofàgia generalitzada, juntament amb TORC1, a través de la fosforilació d'Atg1 i Atg13 (Z. Wang et al. 2001), i l'autofàgia especialitzada de reticle a través de la transcripció d'*ATG39,* gen inhibit per Mig1 (Mizuno, Muroi, and Irie 2020), xiv) l'estrès oxidatiu (Willis et al. 2018), xv) és important per emmagatzemar els proteosomes en forma de gràmuls a causa de disfuncions

mitocondrials (Waite and Roelofs 2022), xvi) promou l'orientació del fus mitòtic durant la divisió cel·lular (Tripodi et al. 2018), xvii) és important per la formació d'espores (Honigberg and Lee 1998) i xviii) a través de la remodelació de la cromatina pot controlar l'expressió gènica, interaccionant i fosforilant a la histona acetiltransferasa, Gcn5 (Abate et al. 2012).

1.4.4 Ruta de senyalització encarregada del control general d'aminoàcids (GAAC)

Els aminoàcids són essencials per la síntesi proteica, la qual té un paper important en l'eficiència i eficàcia de l'expressió gènica de les cèl·lules (Magazinnik et al. 2005). La mancà nutricional d'un o més aminoàcids indueix la cascada de senyalització del control general d'aminoàcids, GAAC (Conrad et al. 2014). L'activació de la ruta GAAC (General Amino Acid Control) desencadena el bloqueig de la traducció gènica i permet l'expressió del factor transcripcional Gcn4, el qual activa a més de 50 gens relacionats amb la biosíntesi d'aminoàcids, l'ús del nitrogen i la senyalització i expressió gènica (Alan G. Hinnebusch 1986; Staschke et al. 2010).

La cèl·lula percep la falta d'aminoàcids a través de l'acumulació de tRNAs (Transfer RNAs) no carregats, els quals són detectats per la proteïna quinasa Gcn2. Aquesta proteïna, en condicions normals es troba inactiva a través d'interaccions moleculars autoinhibitories, que fan que la proteïna es mantingui en un estat latent i exposat a el senyal d'activació (Castilho et al. 2014). Gcn2 presenta un domini homòleg a l'enzim Histidil-tRNA sintasa (HisRS); enzim responsable de la síntesi d'histidil-tRNA, que és essencial per incorporar la histidina a les proteïnes (Freist et al. 1999). Els tRNA no carregats s'uneixen directament a aquest domini tipus-HisRS (Yang, Wek, and Wek 2000). Aquest fet provoca reorganitzacions al·lostèriques, les quals permeten que Gcn2 s'autofosforili en dos aminoàcids específics del seu "*loop*" d'activació, en les treonines 882 i 887 (Thr-882 i Thr-887). Provocant l'estimulació del domini catalític de Gcn2, i induint que la quinasa fosforili la subunitat α del factor d'iniciació eucariota 2 (eIF-2α) en la serina 51 (Ser-51) (Figura 6) (Castilho et al. 2014; Yang, Wek, and Wek 2000). Perquè l'activació de Gcn2 i fosforilació d'eIF-2α siguin possibles és necessària la interacció de Gcn2 amb Gcn1 (Gottfried et al. 2022).

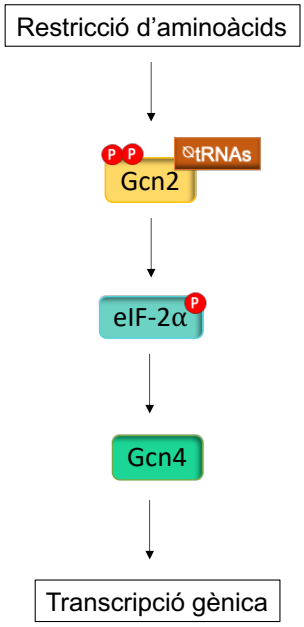

Figura 6. Ruta de senyalització GAAC. En resposta a la restricció d'aminoàcids els tRNA no carregats s'uneixen a la quinasa Gcn2, provocant la seva autofosforilació en dos residus activant la seva activitat quinasa per a fosforilar la subunitat α d'eIF-2. eIF-2α fosforilat incrementa l'expressió del gen *GCN4,* el producte d'aquest gen, la proteïna Gcn4, estimula la transcripció de gens relacionats amb la biosíntesi d'aminoàcids, entre d'altres.

En condicions òptimes de creixement, eIF-2 es troba en la seva forma activa unit a GTP, transportant els tRNAs d'iniciació, carregats amb metionina (^{Met}tRNA), als ribosomes per tal d'iniciar la síntesi de proteïnes (Kimball 1999; Castilho et al. 2014). La fosforilació de la subunitat α d'eIF-2, a causa de la no biodisponibilitat d'aminoàcids dins la cèl·lula, indueix l'intercanvi de GTP a GDP, reduint l'eficiència dels ribosomes per reiniciar la traducció dels mRNA i s'incrementa l'expressió de *GCN4* (Yang, Wek, and Wek 2000; Conrad et al. 2014).

La regulació de l'expressió de *GCN4* es dona a través de quatre petites uORFs (Upstream Open Reading Frames) situades a l'extrem 5' de la seqüència no codificant del mRNA de *GCN4* (A. G. Hinnebusch 1984). Davant la biodisponibilitat d'aminoàcids, aquestes uORFs bloquegen la transcripció de la seqüència codificant (CDS) de *GCN4*. En aquestes condicions els ribosomes

tradueixen la uORF1, posteriorment, a causa de l'alta abundància d'eIF-2-GTP-^{x}tRNA, els ribosomes poden traduir les altres tres uORFs. Després de traduir aquestes 4 uORF la majoria dels ribosomes es dissocien el mRNA obtenint una baixa taxa de traducció de la CDS de *GCN4*. La fosforilació de l'eIF-2α, converteix a eIF2 en un inhibidor competitiu del GEF eIF2B, provocant una disminució en els nivells d'eIF-2-GTP-^{x}tRNA. Conseqüentment, després de traduir la uORF1 els ribosomes no tenen eIF-2-GTP-^{x}tRNA disponibles per a traduir les uORF2,3 i 4, però sí per reiniciar a lectura en l'ORF de *GCN4*, permeten un increment de la transcripció de *GCN4* (Dever et al. 1992, 1995; Magazinnik et al. 2005). Els alts nivells de la proteïna Gcn4 resultants, estimulen l'expressió de gens d'enzims i transportadors necessaris per a la síntesi d'aminoàcids (Vazquez de Aldana et al. 1994).

Tot i que la transcripció de *GCN4* s'associa amb falta d'aminoàcids, hi ha altres estressos que poden induir la fosforilació d'eIF-2α, a través de Gcn2, i per tant la transcripció de *GCN4*. Aquests estressos són: i) l'escassetat de glucosa, on Gcn2 incrementa l'acumulació d'aminoàcids al vacúol i contribueix en mantenir els nivells de glicogen (Yang, Wek, and Wek 2000); ii) la mancà de purines, també incrementa l'expressió de *GCN4* a través de Gcn2, indicant una regulació coordinada entre les rutes de biosíntesi de nucleòtids i d'aminoàcids (Rolfes and Hinnebusch 1993), iii) la radiació UV, provoca l'activació de Gcn4 a través de la cooperació de les rutes de senyalització Gcn2 i Ras/cAMP (Marbach et al. 2001).

1.4.5 Senyalització mitjançada pels complexes TOR

A conseqüència de canvis ambientals, les cèl·lules activen un conjunt de senyals transcripcionals que permeten regular el creixement i metabolisme cel·lular, per tal d'adaptar-se. Els complexos TOR (Target Of Rapamycin) tenen un paper central en aquesta regulació (Deprez et al. 2018). La ruta TOR va ser originalment caracteritzada en *S. cerevisiae* (Heitman, Movva, and Hall 1991) i es troba funcionalment i estructuralment preservada en l'evolució (Conrad et al. 2014).

A diferència de la majoria de les cèl·lules eucariotes que només posseeixen un gen *TOR*, el genoma del llevat de gemmació, codifica per a dos gens *TOR*, *TOR1* i *TOR2*. Les proteïnes Tor són quinases del tipus serina/treonina que pertanyen a la família de les quinases fosfatidil-inositol (PI). Un tret característic d'aquestes proteïnes és que actuen en forma de complex amb

altres proteïnes, les quals els hi proporcionen versatilitat funcional (Helliwell et al. 1994). Totes les proteïnes Tor presenten els mateixos components essencials en la seva estructura, des de l'extrem N-terminal al C-terminal estan formats per: i) repeticions HEAT, que són les regions d'unió de les diferents subunitats del complex Tor; ii) un domini FAT, altament conservat, iii) domini FRB (FKBP12-Rapamycin-Binding), és el domini responsable d'unió a rapamicina; iv) el domini quinasa i v) el domini FATC (FAT C-terminous) (Schmelzle and Hall 2000; Wullschleger, Loewith, and Hall 2006; Loewith and Hall 2011).

La purificació de les proteïnes Tor1 i Tor2 del llevat, va portar a la identificació de dos complexos TOR diferents, complex 1 de TOR (TORC1) i el complex 2 de TOR (TORC2) (Loewith et al. 2002). La proteïna Tor és la subunitat catalítica d'aquests complexos i es troba unida a subunitats específiques de cada complex. TORC1 està compost per: Kog1, Tco89, Lst8 i una de les proteïnes Tor, Tor1 o Tor2, a diferència de TORC2 que està format per Avo1, Avo2, Avo3, Bit61, Lst8 i Tor2 (Reinke et al. 2004; Wullschleger, Loewith, and Hall 2006).

La rapamicina és una petita molècula hidrofòbica produïda per un bacteri del sòl *Streptomyces hygroscopicus* descoberta a l'illa de Rapa Nui (Ted Powers 2022). El complex TORC1 és sensible a la droga, gràcies al domini FRB que permet la seva unió, pel contrari TORC2 és insensible a la rapamicina, ja que el domini d'unió al macròlid està protegit per Avo1, impedint la seva unió (Wullschleger et al. 2005); tot i que en mamífers una exposició prolongada en el temps a la rapamicina pot impedir la unió del complex TORC2 i, per tant, indirectament inhibir a TORC2 en alguns tipus cel·lulars (Sarbassov et al. 2006). Com el complex TORC2 exclusivament està format per Tor2, fa que *TOR2* sigui un gen essencial. L'any 2005, estudis d'organització molecular, van revelar que TORC2 és un supercomplex oligomèric, que es troba en forma de dímer TORC2-TORC2, associat a través de la interacció Tor2-Tor2 (Wullschleger et al. 2005).

1.4.5.1 TORC1

El complex PI quinasa TORC1 (Figura 7) és regulat positivament pels nutrients intracel·lulars (González and Hall 2017a), els nivells d'energia i factors de creixement extracel·lulars; afavorint l'increment de massa cel·lular, estimulant la síntesi de proteïnes, lípids i nucleòtids (Caligaris et al. 2023), l'homeòstasi dels esfingolípids (Swinnen et al. 2014a), inhibint

l'autofàgia i modulant la viabilitat (Sampaio-Marques et al. 2011).

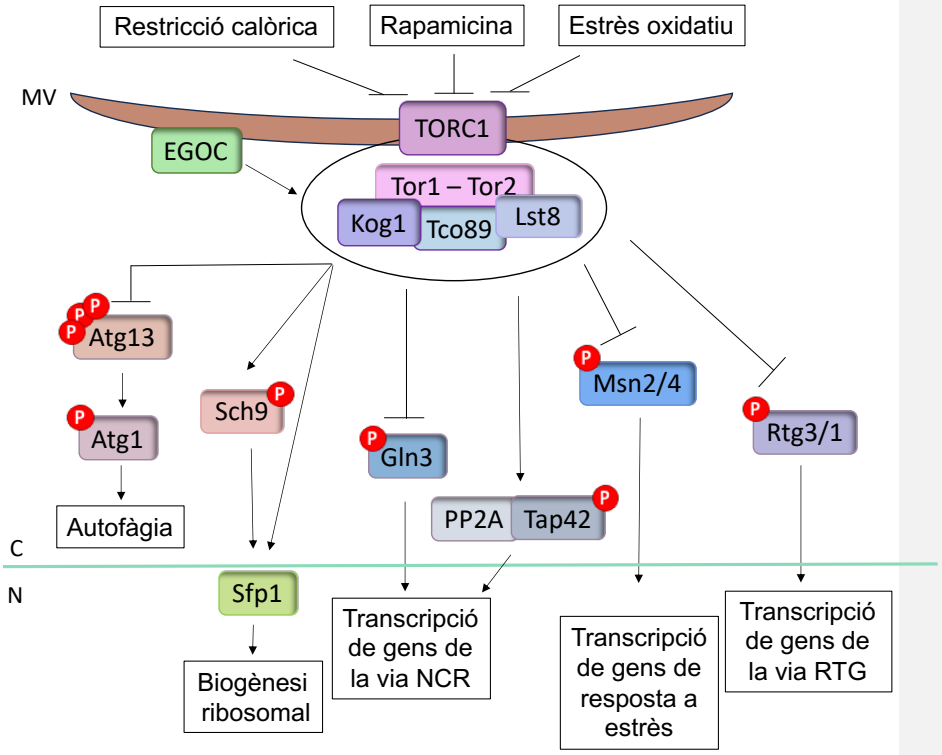

Figura 7. Senyalització i regulació transcripcional del complex 1 de TOR. El complex TORC1 és localitza a la membrana vacuolar (MV) i està format per les proteïnes Kog1, Tco89, Lst8 i Tor1 o Tor2. L'activitat del complex és regulada a través del complex EGO. La restricció calòrica, l'estrès oxidatiu o la rapamicina actuen bloquejant l'activitat del complex. TORC1 té activitat quinasa i a través de la fosforilació de diferents substrats controla diferents processos cel·lulars com són el creixement cel·lular, síntesi de proteïnes i l'autofàgia entre d'altres. Alguns exemples dels processos cel·lulars més rellevants que controla TORC1 són: i) l'autofàgia, fosforilant a Atg13; ii) la biogènesi ribosomal, mitjançant l'activació de la quinasa Sch9 i el factor transcripcional Sfp1; iii) la transcripció de gens de la via NCR a través de la proteïna Gln3 i el complex PP2A unit a Tap42; iv) la regulació de gens de resposta a estrès mitjançant la fosforilació i localització subcel·lular dels factors transcripcionals Msn2/4; i v) la transcripció de gens de la via de resposta retrograda (RTG) mitjançant a les proteïnes Rtg3 i Rtg1.

L'activitat de TORC1 es regula a la membrana vacuolar, on es localitza principalment, a través de 4 proteïnes, Ego1, Ego3, Gtr1 i Gtr2, les quals formen el complex EGO (EGOC) (Dubouloz et al. 2005). EGOC pot regular positivament o negativament al complex Tor, a través d'interaccions físiques amb les diferents subunitats del complex (Conrad et al. 2014). Gtr1 i Gtr2 són dos Rag GTPases, les quals presenten dues conformacions estables, l'activadora de TORC1, on Gtr1 es troba unida a GTP i Gtr2 a GDP i la conformació inhibitòria, es dona quan la càrrega de GTP/GDP és l'oposada (Gtr1-GDP i Gtr2-GTP). Aquestes dues conformacions estan regulades per les seves GAPs, SEAIT i SEACT, en resposta al nivell d'aminoàcids (González and Hall 2017a). El senyal de TORC1 es transmet majoritàriament per dues branques, a través de la quinada Sch9 i del complex Tap42-PP2A (Loewith and Hall 2011).

La proteïna quinasa Sch9 coordina els processos relacionats amb la biodisponibilitat nutricional (Roosen et al. 2005), la progressió del cicle cel·lular (Y. Jin and Weisman 2015), la mida de la cèl·lula (Jorgensen et al. 2004), l'autofàgia (Yorimitsu et al. 2007), resistència a estrès i la síntesi de ribosomes i síntesi proteica (Huber et al. 2011). L'activitat de Sch9 es controla a través de la fosforilació. Aquesta quinasa pot ser fosforilada per: i) TORC1 en sis residus serina i treonina de l'extrem C-terminal, (Urban et al. 2007) ii) Pkh1 i Pkh2 en diferents residus del extrem C-terminal (Roelants, Torrance, and Thorner 2004) i iii) Snf1, en residus completament diferents dels anteriors (Lu et al. 2011). En resposta a la manca de carboni, nitrogen, fosfat i aminoàcids Sch9 es defosforila ràpidament en resposta a la inhibició de TORC1; conseqüentment, els factors de transcripció Stb3 i Dot6/Tod6, juntament amb el complex histona deacetilasa Rpd3L reprimeixen la transcripció de gens ribosomals i RiBi (Urban et al. 2007; Binda et al. 2009).

La segona branca controlada per TORC1 a través de l'activitat de PP2A i la proteïna tipus PP2A és l'encarregada de controlar el metabolisme del nitrogen i aminoàcids (Weisman 2016), la resposta a estrès ambiental (Düvel et al. 2003) o l'autofàgia en resposta a condicions adverses com l'estrès tèrmic, dany en paret cel·lular i la falta de nitrogen (Yorimitsu, Ke Wang, and Klionsky 2009). PP2A és un complex heterotrimèric format per una subunitat "*scaffold*", Tpd3, una subunitat catalítica que pot ser, Pph21, Pph22 o Pph3 i una subunitat reguladora, Cdc55 o Rts1. El complex tipus PP2A està format per una subunitat catalítica, que pot ser Sit4 o Ppg1 i acompanyat per una subunitat reguladora. Ambdós complexos poden interaccionar amb Tap42, que és la proteïna reguladora que controla la seva activitat i localització (Weisman 2016). TORC1 fosforila a Tap42 permeten la seva unió amb la subunitat catalítica dels complexos

PP2A i tipus PP2A, associant-los a la membrana vacuolar i inactivant-los (Deprez et al. 2018). De manera que en resposta a la manca de nitrogen o la davallada en la qualitat d'aquest s'indueix la inhibició de TORC1, el qual a través de l'activació de Rho1 altera la interacció del complex PP2A amb Tap42 promovent la seva dissociació i activació de les fosfatases (Crespo and Hall 2002). Addicionalment, es defosforila la proteïna Ure2, alliberant i permeten la desfosforilació de Gln3 i Gat1, les quals són translocades al nucli per tal d'activar la transcripció de gens que tenen un paper crític en la regulació de la repressió catabòlica del nitrogen (NCR), el procés pel que les fonts de carboni d'alta qualitat són importades i assimilades en preferència a les de baixa qualitat (Weisman 2016). Maf1 i Rrn3, són reguladors de la biogènesi ribosomal, és una altra diana d'aquesta branca de senyalització. PP2A estimula la ràpida defosforilació de Maf1 en resposta a la falta de nutrients o al tractament per rapamicina i inhibeix la degradació de Rrn3 (Rohde et al. 2008).

El complex 1 de TOR també regula l'activitat d'altres proteïnes i factors transcripcionals, sigui de manera dependent o independent de les dues vies de senyalització anteriorment descrites. En condicions d'estrès les cèl·lules necessiten ajustar els nivells de transcripció de gens per tal de mantenir l'homeòstasi cel·lular. Msn2/4 i Gis1, són factors de transcripció importants per a la regulació de l'expressió gènica en resposta a estrès. TORC1, a través de Sch9 i Tap42, pot modular la fosforilació d'aquests factors de transcripció i mediar la seva translocació al nucli (Yuhua Wang et al. 2023).

Una altra funció de TORC1 es regula a diferents nivells la biosíntesi de ribosomes: i) a través de la inducció transcripcional del RNA ribosomal (rRNA), ii) activant la transcripció de proteïnes ribosomals o iii) regulant el reguló de biogènesi de ribosomes (Weisman 2016). La quinasa Sch9, pot regular la transcripció dels gens RP i RiBi, tot i que existeix un factor de transcripció, Sfp1, que de manera independent a Sch9 i específica regula la transcripció d'aquests gens. Sfp1 és fosforilat per TORC1 promovent la seva localització nuclear i unió a promotors de gens RP, activant la seva transcripció (Wei and Zheng 2011). En condicions d'escassetat nutricional, la cèl·lula redueix la biogènesi de ribosomes i degrada els ribosomes a través de l'autofàgia o el proteosoma (Kraft et al. 2008), tot i que una degradació excessiva elimina els ribosomes impedeix la reactivació del creixement en restablir els nivells nutricionals. Per evitar la degradació excessiva, hi ha un petit "*pool*" de ribosomes que es protegeixen de la degradació gràcies a Slm1, un factor de preservació dels ribosomes. Quan les condicions nutricionals tornen a ser favorables TORC1 fosforila i inhibeix a Slm1 estimulant

la iniciació de la transcripció (Shetty et al. 2023). La regulació de la biosíntesi de ribosomes serveix per a controlar els nivells de síntesi de proteïna, a més a més, TORC1, té altres mecanismes per regular la síntesi proteica, a través de la fosforilació de Gcn2 i regulació del factor eIF2α (Weisman 2016).

Dins les múltiples funcions de TORC1, s'engloba la inhibició de l'autofàgia, en condicions de creixement favorable, mitjançant la fosforilació d'Atg13 i així, impedint la formació del complex quinasa Atg1, clau per a la inducció de l'autofàgia. En resposta a la inhibició de TORC1, Atg13 es defosforila incrementant la seva interacció amb Atg1 (Weisman 2016).

Un altre grup de gens que responen a la repressió per glutamina, anomenats *RTG*, són necessaris per a biosíntesi "*de novo"* del glutamat i la glutamina (T. Powers et al. 2004). Aquests gens inclouen enzims involucrats en el cicle del TCA (TriCarboxilic Acid) i del glioxilat, com Cit2, Cit1, Aco1, Idh1 i Idh2, que són regulats pels factors de transcripció Rtg1 i Rtg3 (Z. Liu and Butow 1999). L'expressió dels gens *RTG* proveeix de nivells de α-cetoglutarat per a la producció de glutamat, que a la vegada són necessaris per a la síntesi de glutamina. L'activitat TOR és necessària per mantenir el complex format per Rtg1/Rtg3 al citoplasma quan les cèl·lules creixen en presència de glutamina o glutamat, pel contrari quan les cèl·lules creixen en un medi ric en nitrogen i es tracten amb Rapamicina, el complex es trasllada del citoplasma al nucli per activar als seus gens diana (Komeili et al. 2000a).

Finalment, es coneix que la reducció de l'activitat TORC1 incrementa la CLS, a través de la defosforilació Sch9 en un procés que involucra l'activació de l'autofàgia i gens de resposta a estrès (Weisman 2016).

1.4.5.2 TORC2

El complex TORC2, es troba majoritàriament en la membrana plasmàtica tot i que també s'ha identificat en el citoplasma. Actualment, no es coneixen inhibidors específics de TORC2, fet que fa més complicat l'estudi de les seves funcions. Tot i aquest fet se sap que l'activitat de TORC2 és regulada positivament davant la inhibició de la síntesi d'esfingolípids (Roelants et al. 2011a), condicions hipotòniques (Niles et al. 2011), estrès tèrmic (Y. Sun et al. 2012) i l'exposició a altes concentracions exògenes d'un àcid orgànic feble (Guerreiro et al. 2016). Les

activitats que regula TORC2 són, l'organització del citoesquelet d'actina, l'endocitosi, síntesi lipídica i la supervivència cel·lular (Conrad et al. 2014).

El principal substrat de TORC2 són les proteïnes que formen part de la família de proteïnes quinasa AGC, Ypk1 i el seu paràleg Ypk2 (Figura 8) (Thorner 2022). Tot i que no són l'únic substrat de TORC2, existeixen evidències que Pkc1 és substrat de TORC2 (Wullschleger, Loewith, and Hall 2006). Perquè Ypk1 esdevingui activa i mantingui la seva activitat basal, necessita ser fosforilada en el seu "*loop*" d'activació, concretament, en el residu treonina 504 (Thr-504), per les proteïnes quinasa Pkh1 i Pkh2, que són components associats als eisosomes. TORC2, en condicions d'estrès, incrementa l'activitat de Ypk1 fosforilant-lo en quatre residus més del seu extrem C-terminal, entre ells la treonina 662 (Thr-662) (Locke and Thorner 2019). Ypk1 controla la composició lipídica de la membrana plasmàtica, l'endocitosi, la biosíntesi d'esfingolípids i la concentració intracel·lular de glicerol.

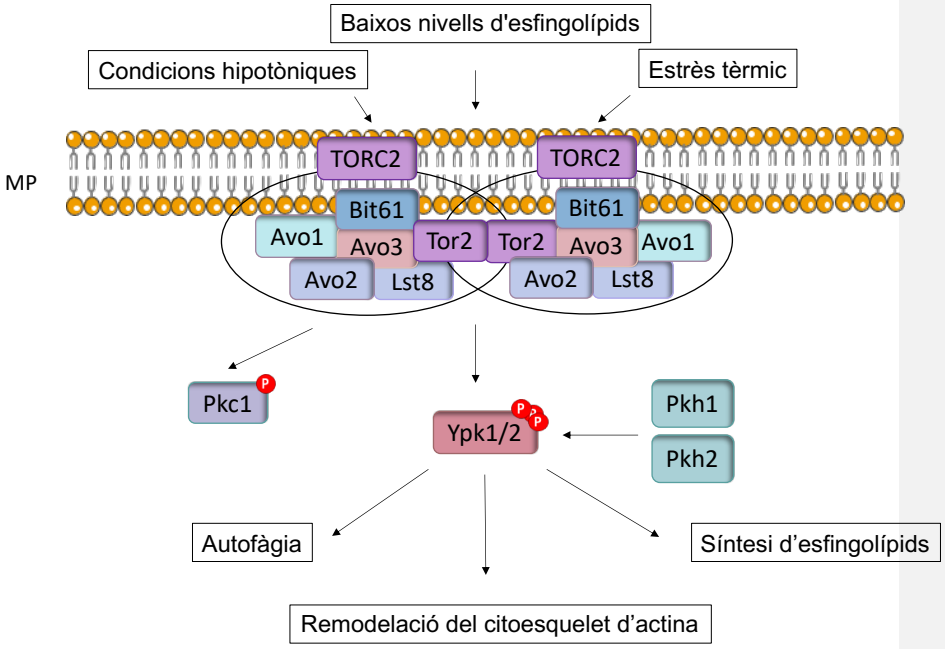

Figura 8. Funcions cel·lulars de TORC2. A la membrana plasmàtica s'hi localitza el complex TORC2 en forma de dímer. El complex TORC2 engloba les proteïnes: Avo1, Avo2, Avo3, Bit61, Lst8 i Tor2. L'activitat del complex és induïda en resposta a baixos nivells d'esfingolípids, a l'estrès tèrmic i condicions cel·lulars hipotòniques. TORC2 té dues dianes Pkc1 i Ypk1/2, a les quals regula la seva activitat a través de la fosforilació. Les quinases Ypk1/2 són el major efector de TORC2, aquestes quinases són fosforilades per TORC2, però per tal d'aconseguir una activitat completa requereixen la fosforilació de les proteïnes Pkh1 i Pkh2. L'activitat d'Ypk1/2 controla positivament els processos d'autofàgia, la remodelació del citoesquelet d'actina i la síntesi d'esfingolípids.

En el llevat de gemmació un gran percentatge del creixement es produeix en la gemma, i per assolir aquesta fita, el llevat polaritza els seus cables d'actina cap a la gemma, facilitant el tràfic de macromolècules de la cèl·lula mare a la gemma. L'activitat del complex 2 de TOR regula aquest procés (Wullschleger, Loewith, and Hall 2006). La senyalització de TORC2 sobre el citoesquelet d'actina és a través de l'activació de la GTPasa Rho1, la qual interacciona amb Pkc1, senyalitzant a través de la via MAPK al citoesquelet d'actina (Wullschleger, Loewith, and Hall 2006).

Alteracions en la membrana plasmàtica, també activen a TORC2, les proteïnes Slm actuen per sobre del complex promovent l'activació del complex en resposta a estrès de membrana plasmàtica (Weisman 2016). Aquestes dues proteïnes també poden regular l'organització del citoesquelet d'actina independentment de Ypk1/2 (Fadri et al. 2005).TORC2 no només actua enfront de l'estrès de la membrana plasmàtica, sinó que Shmidt et al., van descriure la seva implicació en el manteniment de la integritat de la membrana plasmàtica (O. Schmidt et al. 2020).
Dins de les funcions descrites en la literatura de TORC2, una d'elles és el control de la ruta de biosíntesi d'esfingolípids, a través d'Ypk1/2 mediant la biosíntesi "*de novo"* de la ceramida (posteriorment s'explica amb més detall) (Aronova et al. 2008).

Per concloure, Vlahakis et al. l'any 2014, van demostrar la implicació de TORC2-Ypk1 en la inducció de l'autofàgia en resposta a la falta d'aminoàcids (Vlahakis et al. 2014).

1.5 Biosíntesi i senyalització d'esfingolípids en *S. cerevisiae*

Els esfingolípids són components essencials de les membranes de tots els organismes

eucariotes i la seva estructura bàsica consisteix en un esquelet format per una base de cadena llarga (LCB) (Spincemaille et al. 2014). Aquests lípids actuen com una part estructural important de la membrana i, a més a més, tenen un paper com a molècules de senyalització cel·lular (Dickson, Nagiec, Skrzypek, et al. 1997) en processos de divisió cel·lular (Spiegel and Merrill 1996), mort cel·lular (Spiegel et al. 1998) i autofàgia (S. Liu et al. 2023). La seva diversitat funcional és deguda a les modificacions que pateixen, com la fosforilació, hidroxilació i dessaturació, les quals canvien les seves propietats bioquímiques i biofísiques (Megyeri et al. 2016). La via de síntesi d'esfingolípids es troba altament conservada entre els humans i els llevats (Spincemaille et al. 2014). L'alteració del seu metabolisme provoca desordres cel·lulars; s'ha descrit el seu paper en càncers (Muthusamy et al. 2020), malalties com la diabetis (Roszczyc-Owsiejczuk and Zabielski 2021), patologies cardiovasculars (Levade et al. 2001), infeccions microbianes (McQuiston, Haller, and Poeta 2006), desordres neurològics com l'Alzheimer (Czubowicz et al. 2019) i disfuncions immunològiques (Schirmer et al. 2019), per tant, les cèl·lules posseeixen mecanismes de resposta enfront del metabolisme aberrant dels esfingolípids (Dickson 2008; Tani and Funato 2018). El mecanisme més caracteritzat és el de regulació per TORC2 (Roelants et al. 2011b), tot i que també s'ha identificat un paper de la ruta HOG (Urita et al. 2022).

1.5.1 Biosíntesi d'esfingolípids

La biosíntesi "*de novo"* dels esfingolípids (Figura 9) s'inicia amb la condensació d'una serina i un àcid acil-CoA grassós, típicament un palmitoil-CoA, per generar 3-quetodihidrosfingosina (Dickson 2010). Aquesta conversió es dona a través de l'enzim palmitoiltransferasa (SPT), format per tres subunitats, Lcb1, Lcb2 (Pinto et al. 1992) i Tsc3 (Gable et al. 2000). L'enzim SPT és regulat negativament per les proteïnes Orm, Orm1 i Orm2 (Breslow et al. 2010). L'activitat de les proteïnes Orm es regula a través de fosforilació (Roelants et al. 2011b). Posteriorment, la 3-quetodihidrosfingosina es redueix a dihidroesfingosina (DHS), mitjançant la 3-queto reductasa, Tsc10, codificada per un gen essencial (Beeler et al. 1998). Després, la DHS és acetilada per les ceramides sintases, Lag1, Lac1 i Lip1 per a formar dihidroceramida (DHC) (Guillas et al. 2001; Vallée and Riezman 2005). DHS i DHC poden ser hidroxilades a través de l'enzim Sur2 per generar fitoesfingosina (PHS) i fitoceramida (PHC), respectivament (Haak et al. 1997; Montefusco, Matmati, and Hannun 2014). Addicionalment, DHC i PHC poden ser degradades per Ydc1 i Ypc1, respectivament per tornar a donar DHS i PHS (Megyeri

et al. 2016). Seguidament, les DHC i PHC són hidroxilades per l'enzim Scs7 resultant en hidroxil-dihidroceramida (Megyeri et al. 2016). Fins aquest estadi, totes les reaccions tenen lloc al reticle endoplasmàtic. Finalment, es formen els esfingolípids complexos a través de l'addició de grups polars en la posició 1-OH de la ceramida. Aquest procés té lloc en l'aparell de Golgi (Obeid, Okamoto, and Mao 2002). El llevat té tres tipus d'esfingolípids complexos: i) inositolfosfoceramida (IPC), obtinguda a través de l'addició de fosfo-inositol, mitjançant l'IPC sintasa, composta per Aur1 i Kei1 (Nagiec et al. 1997; Sato, Noda, and Yoda 2009); ii) manosa-inositolfosfoceramida (MIPC), la qual es genera a partir d'incorporar una manosa a l'IPC, gràcies a l'acció de la MIPC sintasa, formada per les subunitats Csg1, Csg2 i Csh1 (Uemura et al. 2003); i iii) manosa-diinositolfosfoceramida ($M(IP)_2C$) catalitzat per la inositolfosfotransferasa, Ipt1, que afegeix un inositolfosfat a MIPC (Dickson, Nagiec, Wells, et al. 1997).

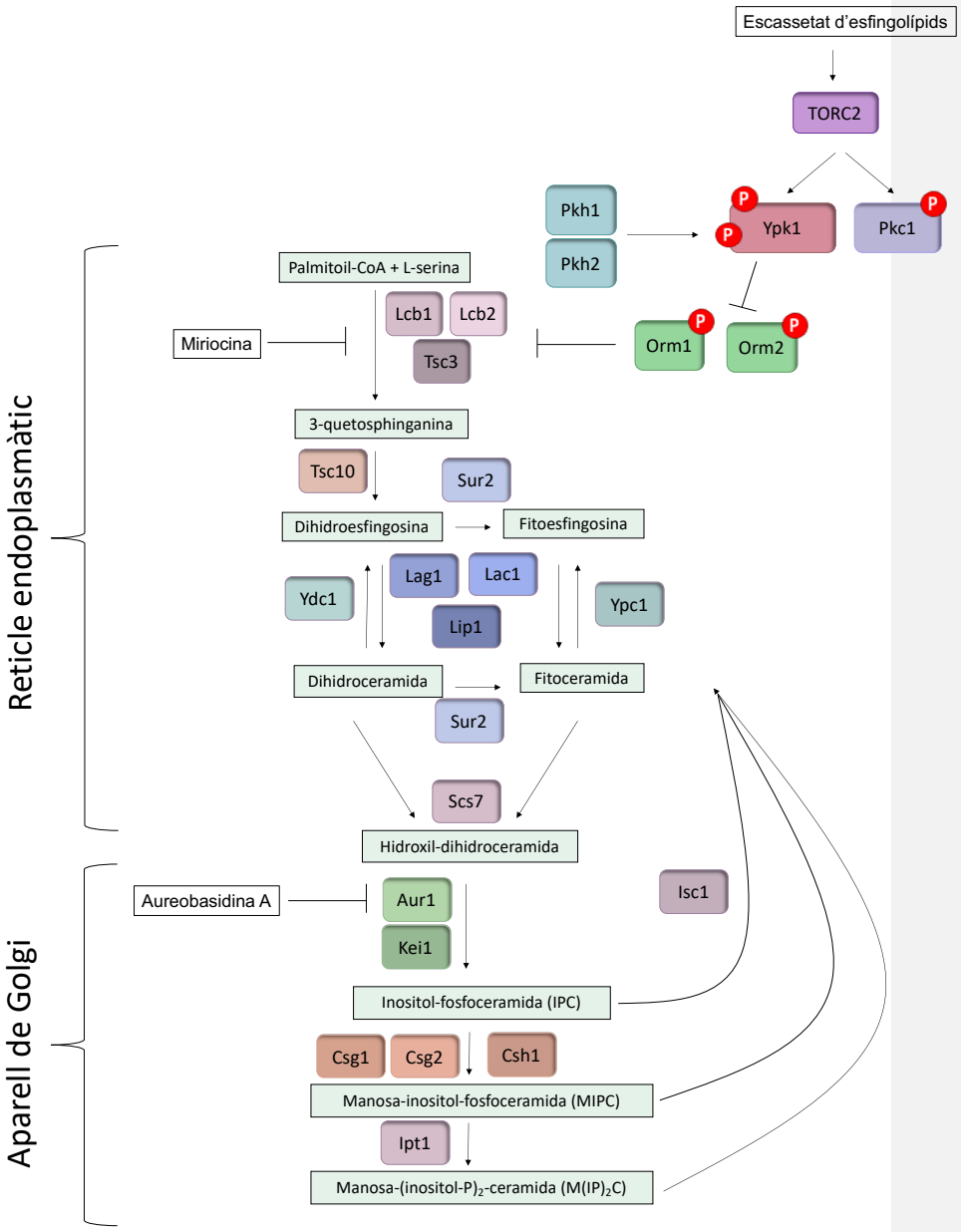

Figura 9. Ruta de la biosíntesi d'esfingolípids. L'escassetat d'esfingolípids és detectada per TORC2, fosforilant i activant a Ypk1. Ypk1 actiu fosforila a les proteïnes Orm1 i Orm2, inhibidores de la SPT, activant la biosíntesi "*de novo*" dels esfingolípids. La síntesi comença amb la condensació d'una serina

i un palmitoil-CoA per format 3-quetoesfingosina. Posteriorment, a través de l'enzim Tsc10 la 3-quetoesfingosina es transforma en dihidroesfingosina, que pot convertir-se en fitoesfingosina a través de Sur2 o en dihidroceramida a través de les ceramida sintases. L'enzim Scs7 catalitza la formació d'hidroxil-dihidroceramida. Totes aquestes reaccions tenen lloc al reticle endoplasmàtic. La ceramida es transporta a l'aparell de Golgi per ser modificada a través de l'addició de caps polars, formant els esfingolípids complexes, IPC, MIPC i $M(IP)_2C$. Si és necessari en resposta a la falta d'esfingolípids, els esfingolípids complexos poden ser processats per l'enzim Isc1 per donar fitoceramida. La miriocina i l'aureobasidina A són drogues que inhibeixen la ruta de síntesi en diferents etapes. La miriocina bloqueja a l'enzim SPT, per tant, inhibeix les etapes inicials. Pel contrari, l'aureobasidina A impedeix la formació dels esfingolípids complexos bloquejant l'acció de l'enzim Aur1 i, a conseqüència, la formació del primer dels esfingolípids complexos.

Dins les cèl·lules, existeix un altre mecanisme per obtenir esfingolípids, a través del reciclatge d'una proporció significant d'esfingolípids complexos. Aquest reciclatge consisteix amb la hidròlisi dels esfingolípids complexos, a través de l'enzim inositol fosfoesfingolípid-fosfolipasa C, Isc1, per obtenir PHC (Sawai et al. 2000). Aquest enzim també és essencial per a la coordinació de la morfologia cel·lular i el cicle cel·lular (Matmati et al. 2020), i està involucrat en la tolerància o sensibilitat agents tòxics, com són el sodi, liti, peròxid, àcid acètic i hidroxiurea, entre altres (Spincemaille et al. 2014).

Els passos inicials de la biosíntesi d'esfingolípids tenen lloc en el reticle endoplasmàtic, i s'han de transportar a l'aparell de Golgi per a sintetitzar esfingolípids complexos, els quals posteriorment es traslladen a les seves destinacions finals. El moviment dels lípids entre els orgànuls està regulat i es fa a través de mecanismes específics (Funato, Vallée, and Riezman 2002). Les ceramides es poden transportar del reticle endoplasmàtic al Golgi a través de transport vesicular i no vesicular. El transport no vesicular requereix el contacte entre les membranes dels orgànuls per facilitar la transferència. Per altra banda el transport dels esfingolípids complexos a les membranes és a través de vesícules secretores (Hechtberger and Daum 1995).

La importància fisiològica de la biosíntesi d'esfingolípids ha portat al descobriment de drogues que inhibeixen enzims específics de la via. Les millor caracteritzades i més utilitzades als laboratoris són: i) la miriocina, isolada de *Myriociccum albomyces* i *Mycelia setrilla*; la seva diana és l'enzim SPT (Miyake et al. 1995), ii) l'aureobasidina A, produïda per *Aureobasidum*

pullulans; efectuant la seva acció sobre la proteïna Aur1 (Kuroda et al. 1999) i iii) la fumosina B1, provinent de *Fusarium monoliforme;* que inhibeix la ceramida sintasa (Riley and Merrill 2019).

1.5.2 Regulació cel·lular de la síntesi d'esfingolípids

Fisiològicament, TORC2 regula la síntesi d'esfingolípids. En resposta a l'escassetat d'esfingolípids o al tractament amb miriocina, les proteïnes Slm1 i Slm2 és dissocien dels eisosomes activant a TORC2 (Berchtold et al. 2012). Posteriorment, TORC2 fosforila a Ypk1 en el residu Thr-662, activant-la (Aronova et al. 2008). Ypk1 activa fosforila a les proteïnes inhibidores de la SPT, Orm1 i Orm2, inhibint-les i permetent l'activació de l'enzim per iniciar la síntesi *de novo* d'esfingolípids (Roelants et al. 2011b). Addicionalment, Ypk1 controla l'activitat enzimàtica de les ceramida sintases Lag1 i Lac1, estimulant la biosíntesi de Cer (Muir et al. 2014).

La ruta de senyalització TORC2 no és l'única amb capacitat de regular la síntesi d'esfingolípids. La quinasa Sch9, a través del control de l'expressió dels gens *LAG1, LAC1, YCP1* i *YDC1* i la localització subcel·lular d'Isc1, pot controlar la biosíntesi d'esfingolípids (Swinnen et al. 2014b). Les quinases Pkh1/Pkh2 s'activen en resposta a l'increment dels nivells d'esfingolípids. Aquestes quinases regulen la transcripció del gen *CHA1,* que codifica per una serina/diamida dehidratasa que participa en la degradació de la serina intracel·lular limitant la seva biodisponibilitat i així impedint l'inici de la biosíntesi d'esfingolípids (Montefusco et al. 2012).

Alteracions en el metabolisme dels esfingolípids comporten desordres cel·lulars. L'acumulació de ceramida és tòxica per a les cèl·lules del llevat. En les cèl·lules els nivells de ceramida han de ser inferiors als dels esfingolípids complexos, i si aquesta ràtio s'altera, les cèl·lules pateixen un defecte en el creixement (Nagiec et al. 1997). Les disfuncions mitocondrials també s'han descrit com conseqüència d'alteracions en el metabolisme d'esfingolípids, tant en llevats com en cèl·lules de mamífer (Spincemaille, Cammue, and Thevissen 2014). Isc1 té un paper en la coordinació de la funció mitocondrial. Aquest enzim es troba en el RE, però durant el "*shift*" diauxic i la post-diauxia es localitza en la membrana exterior de la mitocòndria. Les cèl·lules que no expressen l'enzim, presenten major estrès oxidatiu, apoptosi i decreix la seva CLS,

indicadors de disfunció mitocondrial (Spincemaille et al. 2014).

L'any 2012 es va demostrar la relació entre la senyalització mitjançant esfingolípids amb l'estrès causat per la toxicitat del ferro (Spincemaille, Cammue, and Thevissen 2014). Els resultats que presenten Lee et. al. en el seu treball demostren que una disminució en la síntesi i senyalització d'esfingolípids, permet a les cèl·lules el llevat créixer en condicions de toxicitat per ferro, demostrant que la senyalització per esfingolípids contribueix a regular la toxicitat per ferro (Y. J. Lee et al. 2012).

1.6 Mecanisme autofàgic en *S. cerevisiae*

La paraula autofàgia deriva del grec i està formada per *"auto"* (jo mateix) i *"phagy"* (menjar) (W. Li et al. 2020). L'autofàgia és una ruta essencial involucrada en l'homeòstasi cel·lular a través de la degradació i el reciclatge de tots els components cel·lulars, des de proteïnes a lípids i orgànuls, en el vacúol en els llevats i al lisosoma en mamífers, per retornar els blocs de construcció, com els aminoàcids al citoplasma i així suplir les demandes metabòliques (Abeliovich 2015).

El llevat ha estat un model crucial en l'estudi i regulació de l'autofàgia, d'acord amb el premi Nobel de Fisiologia o Medicina de l'any 2016 a Yoshinori Ohsumi pels seus treballs en les bases de l'autofàgia utilitzant principalment el llevat *S. cerevisiae* com a model. L'ús del llevat, entre altres coses, ha permès el descobriment dels més de 30 gens relacionats amb l'autofàgia (*ATGs)* gràcies al fet que l'autofàgia s'ha conservat durant l'evolució, tal com es pot observar en l'homologia entre el llevat i els mamífers en les proteïnes Atg i la seva funció en el procés entre els llevats i els mamífers (Taula 1) (Meijer et al. 2007; J. Schepers and Behl 2021).

Taula 1. Funció de les proteïnes autofàgiques en llevats i els seus homòlegs en mamífer. (Part 1 de 2)

Proteïna en Llevat	Homòleg en mamífer	Funció
Atg1	ULK1/ULK2	Formació del PAS
Atg13	ATG13	Formació del PAS
Atg17	FIP200	Formació del PAS
Atg29	ATG101	Formació del PAS
Atg31	ATG101	Formació del PAS
Vps15	p150	Nucleació del PAS
Vps34	VPS34	Nucleació del PAS
Atg6	BECN1	Nucleació del PA
Atg14	ATG14L	Nucleació del PAS
Atg2	ATG2/ATG28	Transferència de lípids al PAS
Atg9	ATG9A	Transferència de lípids al PAS
Atg18	WIPI1/WIPI2/WIPI3/WIPI4	Transferència de lípids al PAS
Atg23	-	Transport d'Atg9 al PAS
Atg27	-	Transport d'Atg9 al PAS
Atg5	ATG5	Formació del autofagosoma
Atg12	ATG12	Formació del autofagosoma
Atg16	ATG16L1	Formació del autofagosoma
Atg3	ATG3	Enzim tipus E2
Atg7	ATG7	Enzim tipus E1
Atg10	ATG10	Enzim tipus E2
Atg4	ATG4A/ATG4B/ATG4C/ATG4D	Modificar Atg8
Atg8	LC3A/LC3B/LC3C/GABARAP/ GABARAPL/GABARAPL2	Formació del autofagosoma
Ccz1	-	Fusió del autofagosoma amb el vacúol
Mon1	MON1A/MON1B	Fusió del autofagosoma amb el vacúol
Vam3	-	Fusió del autofagosoma amb el vacúol
Vam7	STX8	Fusió del autofagosoma amb el vacúol
Vti1	VTI1A	Fusió del autofagosoma amb el vacúol
Ykt6	YKT6	Fusió del autofagosoma amb el

Taula 1. Funció de les proteïnes autofàgiques en llevats i els seus homòlegs en mamífer. (Part 2 de 2)

		vacúol
Ypt7	RAB7A	Fusió del autofagosoma amb el vacúol
Atg15	-	Degradació del autofagosoma
Atg22	-	Exportació d'aminoàcids del vacúol
Atg11	FIP200	Autofàgia selectiva
Atg19	-	Receptor de Cvt
Atg32	-	Receptor de mitofàgia
Atg33	-	Receptor de mitofàgia
Atg44	-	Fissió de mitocòndries per la mitofàgia

El reciclatge selectiu dels orgànuls o components cel·lulars a través de l'autofàgia és crític per mantenir l'homeòstasi de les cèl·lules eucariòtiques. L'autofàgia protegeix les cèl·lules de productes tòxics i permet el reciclatge i reutilització de les biomolècules bàsiques per la síntesi de noves macromolècules i components dels orgànuls. Les anteriors afirmacions fan que l'autofàgia sigui un procés essencial i la seva desregulació s'ha relacionat amb diverses malalties com: i) la neurodegeneració (He and Klionsky 2006; Sarkar et al. 2020), ii) el càncer (Gao et al. 2022; Bankov et al. 2023), iii) malalties metabòliques (S. Wang et al. 2020; Chua et al. 2022), iv) cardiopaties (Dong et al. 2019; Du, Li, and Zhao 2020), v) malalties inflamatòries (M. Jin and Zhang 2020; Deretic 2021) i vi) l'envelliment (Ren and Zhang 2018; Aman et al. 2021).

Actualment, es coneixen 3 tipus d'autofàgia: i) la macroautofàgia, ii) la microautofàgia i iii) l'autofàgia mitjançada per xaperones (CMA) (Figura 10) (Kirchner et al. 2019).

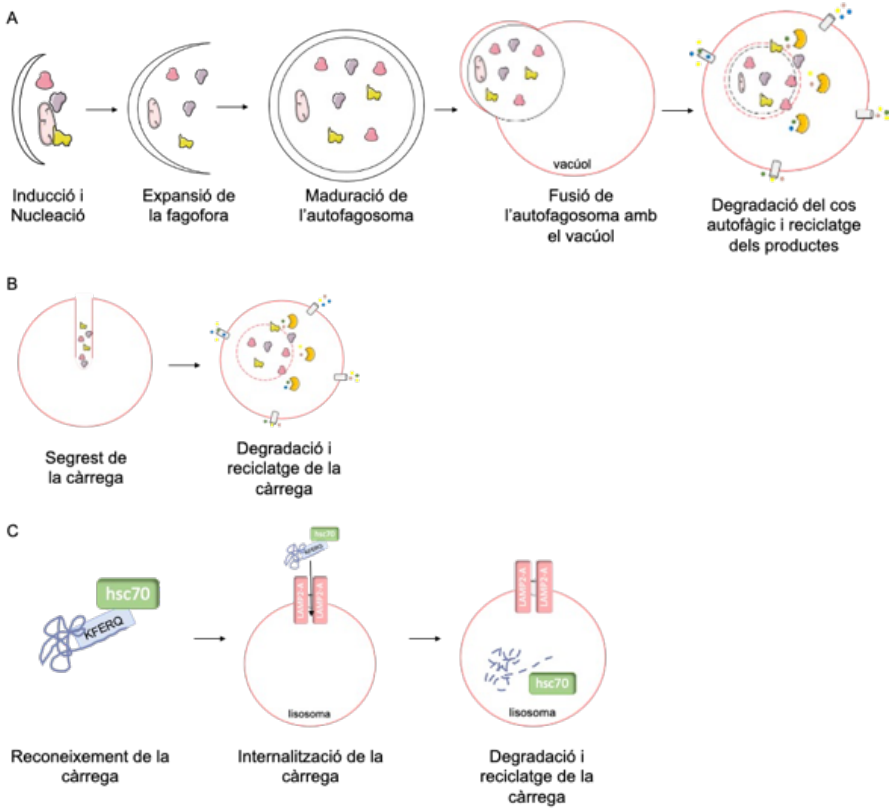

Figura 10. Diferents tipus d'autofàgia. A) Macroautofàgia. L'autofàgia s'inicia amb la inducció i nucleació de la membrana de la fagofora. Seguidament, la fagofora s'expandeix envoltant el substrat, que pot ser porcions citoplasmàtics o orgànuls específics com les mitocòndries. L'autofagosoma madur s'aconsegueix un com s'ha tancat l'estructura de doble membrana. L'autofagosoma madur es fusiona amb el vacúol alliberant el cos autofàgic. Finalment, el cos autofàgic és degradat i el seu contingut reciclat i alliberat a l'exterior per poder ser emprat en noves reaccions anabòliques. B) Microautofàgia. Invaginacions de la membrana vacuolar segresten porcions properes del citoplasma, les quals són degradades a l'interior del vacúol sense haver de formar un autofagosoma. C) Autofàgia mitjançada per xaperones (CMA). Les proteïnes danyades que específicament expressen el motiu KFERQ són reconegudes per la xaperona hsc70. Aquesta xaperona dirigeix a les proteïnes al lisosoma on seran internalitzades a través d'un canal format per quatre molècules de LAMP2-A. Un cop dins el lisosoma la carrega és degradada.

1.6.1 Macroautofàgia

La macroautofàgia és el procés de degradació autofàgic majoritari, usualment anomenat com autofàgia (Kiššova et al. 2007). Consisteix amb la captura de porcions del citoplasma, mitjançant una estructura de doble membrana, anomenada autofagosoma. L'autofagosoma madur és fusionat amb el compartiment lític, on les hidrolases vacuolars desintegraran la membrana exposant el contingut per a la seva degradació (J. Li and Hochstrasser 2020; Abeliovich 2015). Aquest procés involucra el catabolisme de molècules cel·lulars, orgànuls i agregats de proteïnes. La formació de l'autofagosoma es pot dividir en 5 passos: i) inducció i nucleació de la membrana de la fagofora, ii) expansió de la fagofora, iii) tancament i maduració de la fagofora per formar l'autofagosoma, iv) fusió de l'autofagosoma amb el vacúol i v) degradació i retorn dels productes al citoplasma (Figura 10A) (Delorme-Axford and Klionsky 2018).

L'autofàgia s'indueix en períodes d'inanició (Qin 2019). Es coneix que en períodes de dèficit nutricional TORC1 és inactivat per desencadenar una resposta cel·lular. L'any 1998 Noda i Ohsumi demostraren la implicació de TORC1 en la regulació de l'autofàgia (Noda and Ohsumi 1998). Paral·lelament a TORC1, PKA i Snf1 també regulen la resposta autofàgica, negativament i positivament, respectivament (Lynch-Day and Klionsky 2010; Nakatogawa 2020). L'activitat de TORC1 hiperfosforila a la proteïna Atg13 en condicions de riquesa nutricional (Figura 11). En resposta a la deprivació nutricional TORC1 és inhibit donant lloc a la defosforilació d'Atg13 a través de les fosfatases 2A i 2C (Yeasmin et al. 2016; Nakatogawa 2020). Atg13 té 51 residus de fosforilació, 6 dels quals són llocs d'unió a Atg1, per la qual cosa la defosforilació d'Atg13 afavoreix la seva associació amb la quinasa Atg1 incrementant l'activitat quinasa (Lynch-Day and Klionsky 2010). Addicionalment, en resposta a la inanició Atg17, Atg29 i Atg31 formen un complex ternari el qual s'uneix amb Atg1-Atg13, incrementant l'activitat quinasa d'Atg1. Aquest complex format per Atg1-Atg13-Atg17-Atg29-Atg31 es coneix com a Complex Atg1 (Kabeya et al. 2005). Múltiples còpies del complex Atg1 s'uneixen per formar unes estructures en forma de punts anomenades estructures preautofagosomals (PAS) (Tyler and Johnson 2018a).

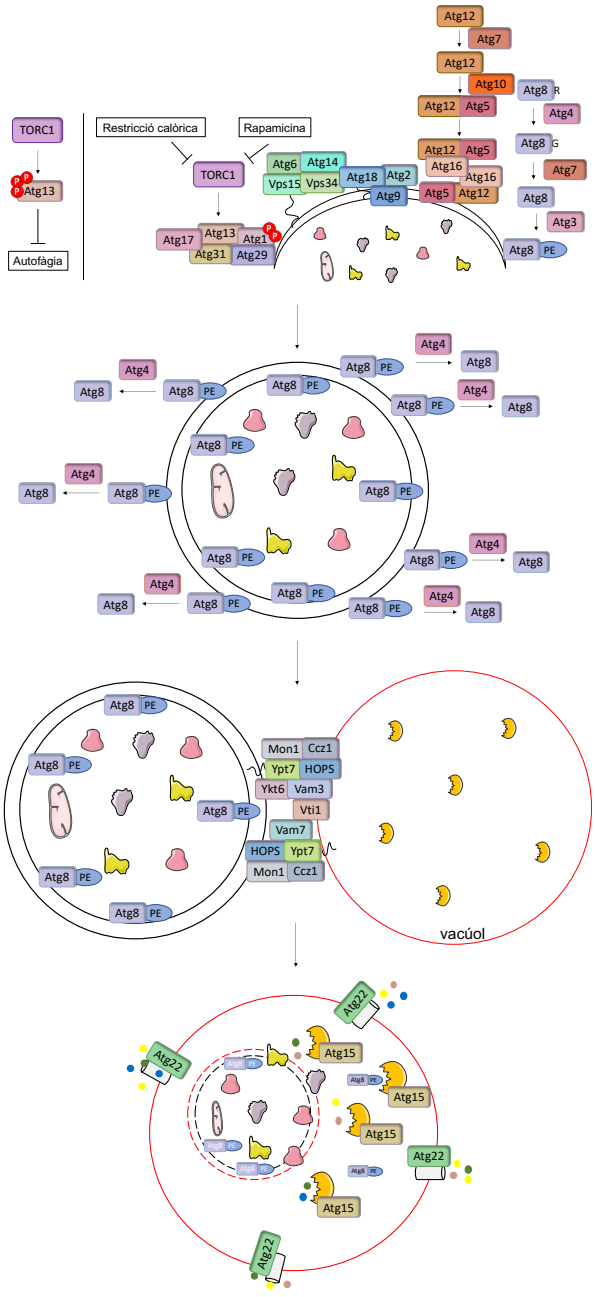

Inducció, nucleació i expansió de la fagofora

Maduració de l'autofagosoma

Fusió de l'autofagosoma amb el vacúol

Degradació del cos autofàgic i reciclatge dels productes

Figura 11. Esquema de la Macroautofàgia. En condicions normals TORC1 es troba actiu i inhibint a Atg13. En resposta a la restricció calòrica o la rapamicina TORC1 s'inhibeix permeten la defosforilació d'Atg13 i la seva unió amb Atg1. Atg1 s'autofosforila i forma un complex juntament amb Atg13, Atg17, Atg31 i Atg29. El complex Atg1 se situa al PAS. L'etapa de nucleació del PAS necessita l'associació de Vps34 amb Vps15, Atg6 i Atg14, els quals permeten la unió del complex Atg18-Atg2-Atg9. Aquest complex regula la transferència de lípids i membranes perquè es pugui expandir la fagofora. Posteriorment, dues rutes de conjugació tipus ubiquitina són necessàries per formar l'autofagosoma. La primera consisteix amb Atg12, Atg7, Atg10, Atg5 i Atg16; i la segona està formada per Atg8, Atg4, Atg7 i Atg3. El resultat és la conjugació d'Atg8 amb un grup fosfatidiletanolamina, el qual dirigeix l'expansió de la vesícula de doble membrana. L'Atg8-PE unit a la membrana externa de l'autofagosoma madur és processat per Atg4 sent així reciclat i utilitzat per la formació de nous autofagosomes. Finalment, la membrana interna de l'autofagosoma madur es fusiona amb el vacúol a través d'un complex de receptors format per Ykt6, Vam6, Vam3 i Vti1 juntament amb el complex HOPS i les proteïnes Mon1, Ccz1 i Ypt7. Un cop l'autofagosoma és fusionat amb el vacúol s'allibera el cos autofàgic al lumen vacuolar on la seva membrana és degradada per la lipasa Atg15, exposant la càrrega a les hidrolases vacuolars. Les petites molècules com els aminoàcids, resultants de la digestió del cos autofàgic són alliberats a l'exterior gràcies a la permeasa de la membrana vacuolar Atg22.

La fosfatidilinositol 3-quinasa de classe III (PtdIns3K), Vps34, controla la nucleació del PAS. Vps34 s'associa amb dos complexos diferents, un d'ells necessari per a l'autofàgia. El complex està format per Vps34, Vps15, Atg6 i Atg14 i s'anomena complex PI3K I (Tyler and Johnson 2018b). Atg14 és la proteïna responsable de localitzar el complex al PAS i unir-lo amb la proteïna Atg18. Atg18 forma un complex amb Atg2 per transportar a Atg9 al PAS (Lynch-Day and Klionsky 2010). Atg9 és una proteïna integral de membrana que es mou entre el PAS i llocs perifèrics com l'aparell de Golgi i els endosomes. Tot i que la majoria d'Atg9 es localitza en vesícules mòbils del citoplasma, anomenades vesícules d'Atg9 o en clústers tubulars de vesícules anomenats reservoris d'Atg9. La transferència d'Atg9 dels reservoris al PAS és dependent d'Atg23 i Atg27 (Nakatogawa 2020). Atg9 és la proteïna més rellevant per ser la font de transferència de membranes per l'expansió de la fagofora (Y. Inoue and Klionsky 2010). A més, Atg2 transfereix lípids del RE a la membrana en formació. La transferència d'aquests lípids alliberats per Atg2 de la membrana externa a la interna de la fagofora en formació és a través d'Atg9 (Matoba et al. 2020).

L'any 1998, el grup liderat per Ohsumi va descobrir la ruta de conjugació tipus ubiquitina, necessària per al procés d'expansió de la fagofora (N Mizushima et al. 1998). La ubiquitina és

caracteritzada per ser unida reversiblement a altres proteïnes a través d'un sistema enzimàtic de tres passos: i) enzim d'activació (E1), ii) enzim de conjugació (E2) i iii) enzim de lligació (E3) (Kirkin 2020). El sistema de conjugació consisteix en la formació del complex Atg12-Atg5. Atg12 és activat per Atg7, un enzim tipus E1 i conjugat per Atg10, un enzim tipus E2, la conjugació es dona entre un residu glicina de l'extrem C-terminal d'Atg12 amb una lisina interna d'Atg5 (Noboru Mizushima, Noda, and Ohsumi 1999). Finalment Atg12-Atg5 s'associen amb la proteïna Atg16 per formar el complex Atg12-Atg5-Atg16. Atg16 oligomeritza per formar un dímer i és el responsable de portar el complex multimèric al PAS. Aquest complex un cop l'autofagosoma és completat s'allibera de la seva superfície i les proteïnes són reutilitzades (Fujioka et al. 2010; Y. Inoue and Klionsky 2010).

Posteriorment, l'any 2000 Ohsumi va descriure un segon sistema de conjugació tipus ubiquitina essencial per a la formació de l'autofagosoma (Kirisako et al. 2000). Aquest segon sistema conjuga a Atg8 amb un grup fosfatidiletanolamina (PE) per a ser associat a la membrana de la fagofora i autofagosoma (Lynch-Day and Klionsky 2010). Atg8 és sintetitzat com a precursor amb una arginina a l'extrem C-terminal, que és eliminada per la proteasa Atg4 exposant un residu de glicina (Y. Inoue and Klionsky 2010). Seguidament, Atg8 és activat per Atg7 i conjugat per Atg3, un enzim tipus E2, amb el cap hidrofílic de PE per tal d'acorar a Atg8 a la doble membrana en formació (Xie, Nair, and Klionsky 2008). El complex format pel primer sistema de conjugació, Atg12-Atg5-Atg16 actua com a enzim tipus E3 amb Atg3 per incrementar la seva activitat (Lynch-Day and Klionsky 2010). Aquests dos sistemes de conjugació són necessaris per completar la formació de l'autofagosoma. Un cop l'autofagosoma és completat, Atg4 també actua com a enzim de deconjugació per remoure el PE d'Atg8 de la membrana externa de l'autofagosoma per ser reutilitzat. L'Atg8-PE de la membrana interna de l'autofagosoma es manté unit a ella i és degradat dins el vacúol (Tyler and Johnson 2018b).

Finalment, l'autofagosoma madur es fusiona amb el vacúol a través d'un complex de receptors SNARE. Ykt6, Vam3, Vti1 i Vam7 formen part d'un paquet de 4 hèlixs que juntament amb el complex HOPS, Mon1, Ccz1 i Ypt7, fusionen la membrana exterior de l'autofagosoma amb el vacúol, alliberant la membrana interna de l'autofagosoma, ara anomenada cos autofàgic, al lumen vacuolar acídic (Y. J. Huang and Klionsky 2022). La membrana del cos autofàgic és degradada per la lipasa Atg15 exposant el seu contingut a les hidrolases vacuolars (Y. J. Huang and Klionsky 2022). Els aminoàcids i petites molècules alliberades són transportades per

Atg22, una permeasa de la membrana vacuolar, i alliberades al citoplasma per a ser reutilitzades en reaccions anabòliques (Lynch-Day and Klionsky 2010).

La degradació de porcions no especifiques del citoplasma es classifica com a autofàgia no-selectiva, però també existeixen formes d'autofàgia selectiva.

1.6.1.1 Autofàgia selectiva

L'autofàgia selectiva es caracteritza per la necessitat de receptors autofàgics que s'uneixen a la carrega per a que sigui degradada dins el vacúol. Els receptors de l'autofàgia especifica presenten un motiu d'interacció amb Atg8 (AIM), el qual els i proporciona la característica de la seva unió selectiva amb Atg8. Atg8 no només contribueix a la maduració i biogènesi del autofagosoma, sinó que també funciona com pont entre la carrega específica i la maquinaria autofàgica permeten el reconeixement i segrest de la carrega (W. Li et al. 2020).

Les autofàgies selectives que es descriuen en la literatura són: i) mitofàgia, autofàgia de les mitocòndries (Bhatia-Kissova and Camougrand 2021), ii) proteofàgia, autofàgia del proteosoma (Waite et al. 2022), iii) ribofàgia, autofàgia dels ribosomes (Waliullah et al. 2017), iv) pexofàgia, autofàgia dels peroxisomes (Sakai et al. 2006), v) ER-fàgia, autofàgia del reticle endoplasmàtic (Gubas and Dikic 2022), vi) lipofàgia, autofàgia de lípids (Shin 2020) i vii) nucleofàgia, autofàgia del nucli (Mijaljica and Devenish 2013).

Dins l'autofàgia selectiva també s'engloba el que es coneix com la via Cvt (Cytoplasm to Vacuole Targeting). Aquest tipus d'autofàgia emprà el receptor Atg19 i incorpora dins una estructura de doble membrana anomenada vesícula Cvt, les formes precursores dels enzims aminopeptidasa 1 (ApeI) o α-manosidasa (Ams1) per ser transportades al vacúol, on les hidrolases vacuolars les activaran (Meijer et al. 2007; Lynch-Day and Klionsky 2010). La Cvt requereix la proteïna Atg11, una proteïna que és necessària en totes les autofàgies selectives, per aquest motiu la Cvt es classifica dins l'autofàgia selectiva (Lynch-Day and Klionsky 2010). Una característica especifica de la Cvt és que es tracta d'una via biosintètica que té lloc durant el creixement vegetatiu, a diferència de l'autofàgia que s'indueix en resposta a la inanició (J. Kim and Klionsky 2000).

1.6.1.1.1 Mitofàgia

La mitocòndria és la base d'obtenció d'energia cel·lular, i contribueix a la regulació de l'homeòstasi de la cèl·lula, i per això la regulació i el control de qualitat d'aquests orgànuls és indispensable. L'homeòstasi de la mitocòndria s'assoleix a través d'un conjunt de vies de senyalització involucrades en la reorganització del contingut mitocondrial en resposta a diferents estressos mitocondrials que impliquen els processos de divisió, fusió i mitofàgia (Bhatia-Kissova and Camougrand 2021).

La mitofàgia es pot produir per micromitofàgia o macromitofàgia (Bhatia-Kissova and Camougrand 2021). La micromitofàgia és induïda quan les cèl·lules creixen en lactat i la macromitofàgia en glucosa (Kiššova et al. 2007).

Durant la micromitofàgia les mitocòndries són capturades per invaginacions o pertorbacions de la membrana vacuolar. La proteïna Uth1 és essencial per a la micromitofàgia (Welter et al. 2013). Durant la macromitofàgia les mitocòndries són segrestades per membranes de nova formació. Les mitocòndries són englobades dins els autofagosomes i després es fusionen amb el vacúol per alliberar el seu contingut (Bhatia-Kissova and Camougrand 2021). La macromitofàgia, a diferència de la macroautofàgia requereix dos passos addicionals: i) la selecció de regions mitocondrials determinades i ii) la modificació de la morfologia de la mitocòndria per a poder ser incorporada dins l'autofagosoma (Fukuda et al. 2023).

L'any 2009, paral·lelament Okamoto et. al. i Kanki et. al. van identificar el primer receptor de la mitofàgia, la proteïna Atg32 la qual es troba ancorada a la membrana externa de la mitocòndria i pot interaccionar amb Atg11 i Atg8 (Okamoto, Kondo-Okamoto, and Ohsumi 2009; Kanki, Wang, Cao, et al. 2009). Atg33 és un altre receptor de la mitofàgia de fase estacionaria (Bhatia-Kissova and Camougrand 2021). Un cop s'indueix la mitofàgia, Atg32 és fosforilada en dos residus, permeten la seva unió amb la proteïna citosòlica Atg11 (Innokentev and Kanki 2021). Posteriorment, Atg11 interacciona amb el complex Atg1 per iniciar la formació de la fagofora (Figura 12). Les mitocòndries tenen una mida superior al de l'autofagosoma, pel que abans de ser incorporades en aquest, les mitocòndries es fissionen per a generar fragments de la mida adequada. Atg44 és una proteïna de l'espai intermembranal de la mitocòndria que proporciona fragilitat lipídica a les membranes de la mitocòndria facilitant

la fissió de la membrana de la mitocòndria. Un cop les mitocòndries són capturades dins l'autofagosoma aquest es fusiona amb el vacúol per a reciclar el seu contingut (Fukuda et al. 2023).

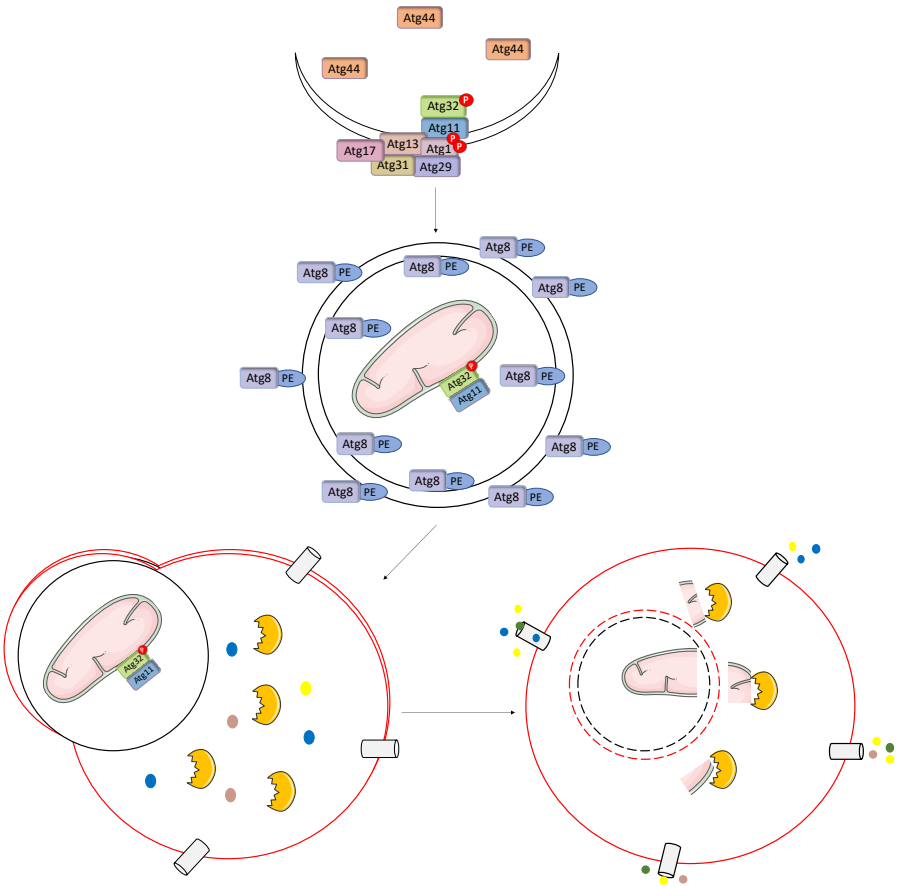

Figura 12. Macromitofàgia. Les mitocòndries expressen la proteïna Atg32, que es fosforila en resposta a alteracions mitocondrials. Atg32 fosforilada interacciona amb Atg11 que actua com a proteïna d'unió entre les mitocòndries disfuncionals i el complex Atg1 del PAS. Les mitocòndries són uns orgànuls molt grans i per poder ser encabits dins un autofagosoma requereixen l'acció d'Atg44. Atg44 és una proteïna de la membrana mitocondrial que proporciona fragilitat lipídica permeten la fissió mitocondrial i així que les mitocòndries puguin ser encapsulades dins l'autofagosoma. Un cop format l'autofagosoma aquest es fusiona amb el vacúol alliberant el cos autofàgic i promovent la degradació de les mitocòndries

disfuncionals.

La importància de la mitocòndria com a orgànul cel·lular fa que la mitofàgia estigui altament regulada. La regulació es dona a nivell transcripcional i posttranscripcional. La proteïna d'unió al DNA Ume6 i el complex d'histona deacetilasa Sin3-Rpd3 interaccionen directament amb el promotor d'*ATG32* per bloquejar la seva transcripció. La inhibició de TORC1 permet que aquestes proteïnes es desuneixin permeten la transcripció del gen. Per altra banda, l'estrès oxidatiu també contribueix a la inducció de la transcripció *d'ATG32* (Innokentev and Kanki 2021). Posttraduccionalment, Atg32 és processada en el seu extrem C-terminal per la proteasa Yme1, proporcionant una major afinitat entre Atg32 i Atg11 per tal d'induir la mitofàgia (K. Wang et al. 2013). Atg32 també és modificada a través de la fosforilació dues serines, la 114 i la 119; concretament la fosforilació de la Ser-114 incrementa l'afinitat d'Atg32 amb Atg11 (Aoki et al. 2011; Okamoto, Kondo-Okamoto, and Ohsumi 2009). La caseïna quinasa 2 (CK2) és la responsable d'aquesta fosforilació. CK2 s'expressa en les cèl·lules de manera constitutiva, per evitar la constant fosforilació d'Atg32, el complex Far interacciona amb Atg32 reclutant a Ppg1 per a impedir la fosforilació d'Atg32. Quan la mitofàgia s'indueix, el complex Far es dissocia d'Atg32, permeten la seva fosforilació (Innokentev and Kanki 2021).

La mitofàgia s'ha relacionat amb diverses malalties com: i) fetge gras (Zhou et al. 2019), ii) tumorogènesi (Deng et al. 2021), iii) malalties neurodegeneratives com el Parkinson (Malpartida et al. 2021) i l'Alzheimer (Sorrentino et al. 2017), iv) també té un paper en la resposta immunitària (Angajala et al. 2018) i v) en l'envelliment (J. Guo and Chiang 2022). La modulació de la mitofàgia pot esdevenir una manera prometedora de tractar aquestes malalties associades amb disfuncions mitocondrials.

1.7 *S. cerevisiae* com a model d'envelliment

L'envelliment és un procés que es dona en tots els organismes vius, des d'organismes més simples unicel·lulars, fins a organismes complexos pluricel·lulars. Els estudis d'envelliment en organismes superiors, com els mamífers són limitats degut a la seva llarga esperança de vida. Actualment, existeixen estudis d'envelliment en rosegadors, tot i que per tal d'accelerar el procés s'empren cultius primaris de cèl·lules humanes o de ratolí (Steinkraus, Kaeberlein, and Kennedy 2008). Una segona aproximació, i la més utilitzada, és l'ús d'organismes model

invertebrats com la mosca de la fruita (*Drosophila melanogaster)* (S. Li et al. 2020), els cucs (*Caenorhabditis elegants)* (Kenyon et al. 1993) o el llevat (*Saccharomyces cerevisiae)* (Sundaram et al. 2015). A priori, estudiar el procés d'envelliment en un organisme unicel·lular, pot semblar una decisió errònia, però fins al present moment, centenars d'estudis d'envelliment s'han realitzat en *S. cerevisiae*, gràcies al fet que el procés d'envelliment entre els llevats i les eucariotes superiors està altament conservat (Steinkraus, Kaeberlein, and Kennedy 2008). La recerca de l'envelliment en *S. cerevisiae* ha permès el descobriment de gens, rutes de senyalització i petites molècules, que també estan involucrades en el procés d'envelliment en organismes eucariotes pluricel·lulars (Mohammad et al. 2018). S'han identificat més de 200 gens involucrats en la regulació de l'envelliment i associat diferents esdeveniments que hi contribueixen: i) inestabilitat genòmica del DNA ribosomal, ii) disfunció mitocondrial, iii) acumulació de proteïnes danyades, iv) disminució del nombre d'histones, v) pèrdua de cromatina en els telòmers i vi) errors en l'homeòstasi del vacúol (Crane et al. 2020). Fets que proven l'ús del llevat *S. cerevisiae* com una eina única per a l'estudi del procés d'envelliment.

El llevat presenta dos tipus d'aproximacions per estudiar el procés d'envelliment, l'envelliment replicatiu (RLS) i l'envelliment cronològic (CLS). El nombre de divisions que una cèl·lula pot tenir és el que es coneix com a RLS (Replicative Life Span), a diferència de la CLS (Chronological Life Span), que es defineix com l'esperança de vida d'una cèl·lula (Galdieri et al. 2010). Els dos processos d'envelliment tenen lloc durant la fase estacionària del creixement (Herman 2002).

1.7.1 Envelliment cronològic (CLS)

L'envelliment cronològic és defineix com el temps que una cèl·lula, que no es divideix, pot ser viable (Steinkraus, Kaeberlein, and Kennedy 2008). La CLS pot servir com a sistema model de l'envelliment de les cèl·lules postmitòtiques de mamífer, concretament de l'envelliment de les neurones del sistema nerviós central (Breitenbach, Jazwinski, and Laun 2012), pel que destaca la rellevància de *S. cerevisiae* com a model d'estudi de malalties relacionades amb l'envelliment com són el càncer i la neurodegeneració (Steinkraus, Kaeberlein, and Kennedy 2008).

El mètode per monitoritzar la CLS es va desenvolupar als anys noranta (Longo, Gralla, and

Valentine 1996) i actualment és molt utilitzat en laboratoris de tot el món. L'assaig per mesurar la CLS es du a terme quan les cèl·lules es troben en un estat d'inanició i la supervivència depèn de la resposta cel·lular i dels canvis morfològics i fisiològics que comporta la mancà nutricional (Breitenbach, Jazwinski, and Laun 2012). La supervivència és valorada fins que el 99% de les cèl·lules moren, i s'expressa amb la mitja i màxima supervivència cel·lular, calculada a partir del nombre de cèl·lules amb capacitat de formar colònies, CFUs (Colony Forming Units), en un medi de cultiu ric (Fabrizio and Longo 2008; Mohammad et al. 2020). Aquesta aproximació és possible, ja que en els cultius estacionaris del llevat es distingeixen dues poblacions: i) cèl·lules mare que es moren per apoptosi i ii) cèl·lules joves (filles) amb una baixa activitat metabòlica que es divideixen molt lentament, aquesta fracció representa entre un 3 i 8% del cultiu (Breitenbach, Jazwinski, and Laun 2012).

Els estudis de CLS han portat al descobriment de dues vies de senyalització que modulen l'extensió de la vida cronològica, les dues censen la biodisponibilitat de nutrients i controlen el seu ús: i) Tor/Sch9 i ii) Ras/PKA (Figura 13). Aquestes rutes de senyalització estan conservades evolutivament i formen part del procés d'envelliment d'organismes eucariotes superiors (Fabrizio and Longo 2008). La inhibició d'aquestes rutes de senyalització convergeix en l'activació del reguló de residència a estrès, a través de Rim15, el qual promou la translocació al nucli dels factors de transcripció Msn2/Msn4 i Gis1 induint la transcripció de gens proCLS (Fabrizio and Longo 2008; Longo et al. 2012).

La CLS no està només regulada a través de les rutes de senyalització mencionades anteriorment, és un procés multifactorial, la disfunció mitocondrial, l'estrès oxidatiu i les ROS, el dany i mutagènesi del DNA, alteracions metabòliques, disminució de l'autofàgia, escurçament dels telòmers, són alguns dels factors que influeixen la CLS (Figura 13) (Longo et al. 2012). La disminució de la senyalització de Tor/Sch9 incrementa la CLS, però també indueix l'activitat mitocondrial, fet que indueix una major producció de ROS mitocondrials. El paper de les ROS en la CLS és complex, ja que la producció de ROS durant la fase exponencial contribueixen a l'extensió de la CLS, mentre que les ROS durant la fase estacionària tenen un paper negatiu en l'extensió de la vida cronològica del llevat (Bonawitz et al. 2007). Un dels gens de resistència a estrès, que els factors de transcripció Msn2/4 i Gis1 regulen, és *SOD2.* Sod2 és una superòxid dismutasa mitocondrial, la qual protegeix a la cèl·lula enfront l'estrès oxidatiu i les espècies reactives d'oxigen. La sobreexpressió de Sod2 incrementa la CLS de la cèl·lula bloquejant la producció de ROS (Fabrizio et al. 2003).

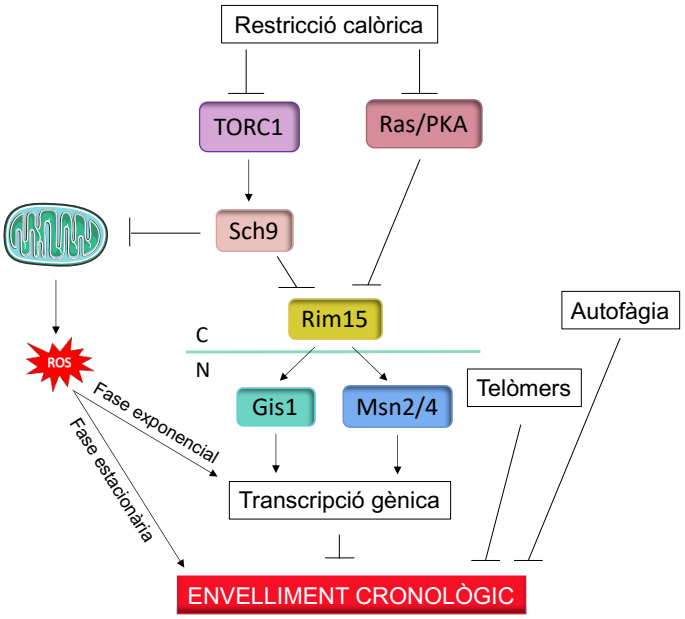

Figura 13. Factors que impacten en l'envelliment cronològic del llevat. La restricció calòrica inhibeix l'activitat de les vies de senyalització Tor/Sch9 i Ras/PKA, permeten la translocació dels factors de transcripció Gis1 i Msn2/4 al nucli (N) a través de la proteïna Rim15. Gis1 i Msn2/4 indueixen la transcripció gènica de proteïnes implicades en la resposta a estrès, incrementant la CLS. Sch9 té un paper dual, a més a més, bloqueja l'activitat mitocondrial impedint la generació de ROS, les quals si apareixen durant la fase exponencial del creixement, tenen un paper positiu sobre la CLS i si la seva producció es dona en la fase estacionària, repercuteixen negativament a la CLS. Els telòmers i l'autofàgia també s'han descrit com a extensors de la vida cronològica del llevat i d'altres organismes.

Els telòmers estan directament relacionats amb l'envelliment. El descobriment dels telòmers en *S. cerevisiae* va ser reconegut l'any 2009 atorgant un Premi Nobel a Elizabeth H. Blackburn,

Carol W. Greider i Jack W. Szostak. Els telòmers es troben en tots els cromosomes lineals eucariotes, i són unes estructures formades per repeticions de DNA i proteïnes específiques d'aquestes regions. Les estructures telomèriques varien entre els organismes, la seqüència concreta i la llargària és diversa, però en tots els casos una de les cadenes és rica en guanines i l'altra en cisteïnes, i les bases de la seva regulació estan conservades. Els telòmers són essencials per mantenir l'estabilitat genòmica, serveixen per distingir entre els cromosomes i els trencaments de doble cadena de DNA que es donen accidentalment en la cèl·lula. Els telòmers també tenen una funció important durant la replicació, ja que l'asimetria en què és replicat el DNA i la direcció de la síntesi del DNA, fa que en cada divisió cel·lular l'últim nucleòtid del cromosoma no es dupliqui, de manera que els extrems dels cromosomes s'escurcen en cada divisió (Harari et al. 2020). Els organismes que presenten una divisió constant, com els fongs, codifiquen per un enzim específic dels telòmers, la telomerasa, la qual actua com a transcriptasa inversa estenent els telòmers. La telomerasa va ser descoberta en el llevat del pa, un dels gens que codifica per la telomerasa és *EST1* (Ever Shorter Telomeres). En llevat, els mutants *est1* són viables, però tenen una entrada en senescència anticipada i els telòmers s'escurcen. Quan els telòmers són críticament curts, les cèl·lules entren en senescència i es dona una parada del cicle cel·lular. Restablir la telomersa incrementa la CLS (J. Liu et al. 2019). En els humans, la llargària dels telòmers decreix amb l'edat correlacionant l'envelliment i els telòmers (Aubert and Lansdorp 2008).

Un altre modulador de la CLS és l'autofàgia. L'autofàgia és induïble, i en la majoria de les cèl·lules, presenten nivells basals d'activitat. L'autofàgia degrada components cel·lulars per a ser reciclats, per exemple orgànuls danyats com poden ser les mitocòndries, les quals poden contribuir a l'envelliment cel·lular, tal com s'ha esmentat anteriorment. Mutants en gens autofàgics com *ATG1, ATG2, ATG7* i *ATG8* presenten una CLS inferior a la de cèl·lules wt (Matecic et al. 2010; Tyler and Johnson 2018a). Concloent que en *S. cerevisiae* l'autofàgia és necessària per a la CLS. Aquesta afirmació és certa en altres espècies com *C. elegants* i *D. melanogaster* (Alvers et al. 2009). En mamífers, el bloqueig de l'autofàgia en alguns teixits incrementa les malalties neurodegeneratives, cardiovasculars, defectes metabòlics i càncers, entre altres (X. J. Zhang et al. 2013). En essència, l'autofàgia és considerada com una via protectora enfront l'envelliment.

2. OBJECTIUS

1. Analitzar la connexió entre la via TORC1 i el metabolisme del ferro.

2. Establir la relació entre la depleció de ferro, l'autofàgia i les rutes de senyalització involucrades en aquest procés, determinant-ne la seva importància biològica.

3. Explicar la correlació entre l'autofàgia, depenent de la biodisponibilitat de glucosa, i el receptor de la via de senyalització d'integritat de la paret cel·lular, Mtl1, així com el seu paper en el reciclatge de les mitocòndries durant el procés d'envelliment.

4. Elucidar la connexió entre TORC2/Ypk1, la ruta dels esfingolípids i el metabolisme del ferro.

3. METODOLOGIA

3.1 Soques de llevat utilitzades en l'estudi

Les soques de llevat *S. cerevisiae* utilitzades en aquesta tesi estan enumerades en la Taula 2, la qual inclou el genotip i la font d'obtenció.

Per a la disrupció genètica per tal d'obtenir mutants es van substituir les ORFs corresponents pels cassets *Kan*Mx4, *Nat*Mx4 o *HIS3*Mx6 emprant tècniques de recombinació homòloga descrites per Goldstein i McCusker l'any 1999 (Goldstein and McCusker 1999). Les soques obtingudes mitjançant aquesta tècnica són: GSL218, 222, 238, 293, 296, 324, 364, 384, 394, 420, 430, 431, 435, 436, 437, 447, 448, 404, *rpd3*Δ, *dot6*Δ*tod6*Δ i *pub1*Δ.

Les soques GSL 197, 198, 199, 200, 201, 202, 226, 265, 279, 297, 313, 325, 352, 370, 371, 374, 382, 414 i 415 s'han assolit a través de la integració del plàsmid pGFP-Atg8 , digerit prèviament amb StuI, en el locus *URA3* (el nom original d'aquest plàsmid és pHab142). A través de la integració del plàsmid pAtg1-HA, prèviament digerit amb BstEII, s'han assolit les soques GSL 372, 389, 390, 393, 395, 398, 399, 401 i 416. La soca GSL421 s'ha obtingut a través de la integració del plàsmid pAft1C291F-HA prèviament digerit amb EcoRV. La integració del plàsmid pYpk1-HA, prèviament digerit amb BstEII, s'ha utilitzat per a la construcció de les soques GSL454 i 455. Finalment, la soca GSL451, s'ha aconseguit a través de la integració del plàsmid pYpk1$^{S644A/T662A}$, prèviament digerit amb BstEII.

Taula 2. Soques de llevat. Part 1 de 4.

Soca	Genotip	Font/Referència
CML128	*MAT**a** leu2-3,112, ura3-52, trp1, his4*	(Gallego et al. 1997)
GSL011	CML128 background, *mtl1::NatMx4*	(Petkova, Pujol-Carrion, and de la Torre-Ruiz 2010)
GSL034	CML128 background, *tor1::KanMx4*	(Petkova, Pujol-Carrion, and de la Torre-Ruiz 2010)
GSL053	CML128 background, *ras2::Leu2MX5*	(Petkova, Pujol-Carrion, and de la

Taula 2. Soques de llevat. Part 2 de 4.

		Torre-Ruiz 2010)
GSL054	CML128 background, *mtl1::KanMx4 ras2::LEU2Mx5*	(Petkova, Pujol-Carrion, and de la Torre-Ruiz 2010)
GSL190	CML128 background, *slt2::KanMx4*	(Sundaram et al. 2015)
GSL197	CML128 background, *GFP-ATG8::URA3*	Aquest treball
GSL198	CML128 background, *mtl1::NatMx4 GFP-ATG8::URA3*	Aquest treball
GSL199	CML128 background, *tor1::KanMx4 GFP-ATG8::URA3*	Aquest treball
GSL200	CML128 background, *mtl1::NatMx4 tor1::LEU2 GFP-ATG8::URA3*	Aquest treball
GSL201	CML128 background, *ras2::Leu2MX5 GFP-ATG8::URA3*	Aquest treball
GSL202	CML128 background, *mtl1::KanMx4 ras2::LEU2Mx5 GFP-ATG8::URA3*	Aquest treball
GSL205	CML128 background, *sch9::NatMx4*	(Sundaram et al. 2015)
GSL206	CML128 background, *sch9::NatMx4 mtl1::KanMx4*	(Sundaram et al. 2015)
GSL218	CML128 background, *atg7::NatMx4*	Aquest treball
GSL222	CML128 background, *atg13::NatMx4*	Aquest treball
GSL226	CML128 background, *atg7::NatMx4 GFP-ATG8::URA3*	Aquest treball
GSL238	CML128 background, *atg17::NatMx4*	Aquest treball
GSL265	CML128 background, *slt2::NatMx4 GFP-ATG8::URA3*	Aquest treball
GSL279	CML128 background, *sch9::NatMx4 GFP-ATG8::URA3*	Aquest treball
GSL280	CML128 background, *tetO$_7$AFT1C291F-HA::LEU2*	(Pujol-Carrion et al. 2021)
GSL284	CML128 background, *aft1::KanMx4*	(Pujol-Carrion et al. 2013)
GSL293	CML128 background, *atg11::NatMx4*	Aquest treball
GSL296	CML128 background, *atg33::NatMX4*	Aquest treball
GSL297	CML128 background, *atg11::NatMx4 GFP-ATG8::URA3*	Aquest treball
GSL308	CML128 background, *tetO$_7$Aft1-HA::LEU2*	(Pujol-Carrion et al. 2021)
GSL313	CML128 background, *aft1::KanMx4 GFP-ATG8::URA3*	Aquest treball
GSL324	CML128 background, *atg1::NatMx4*	Aquest treball

Taula 2. Soques de llevat. Part 3 de 4.

GSL325	CML128 background, *atg1::NatMx4 GFP-ATG8::URA3*	Aquest treball
GSL350	CML128 background, *gcn2::KanMx4*	(Mechoud et al. 2020)
GSL352	CML128 background, *gcn2::KanMx4 GFP-ATG8::URA3*	Aquest treball
GSL364	CML128 background, *atg32::KanMx4*	Aquest treball
GSL370	CML128 background, *rho0 GFP-ATG8::URA3*	Aquest treball
GSL371	CML128 background, *atg32::KanMx4 GFP-ATG8::URA3*	Aquest treball
GSL372	CML128 background, *ATG1-HA::LEU2*	Aquest treball
GSL374	CML128 background, *ypk1::KanMx4 GFP-ATG8::URA3*	Aquest treball
GSL382	CML128 background, *snf1:KanMx4 GFP-ATG8::URA3*	Aquest treball
GSL384	CML128 background, *ypk1::KanMx4*	Aquest treball
GSL385	CML128 background, *ypk1::KanMx4 tetO$_7$Aft1-HA::LEU2*	(Pujol-Carrion et al. 2021)
GSL389	CML128 background, *tor1::KanMx4 ATG1-HA::LEU2*	Aquest treball
GSL390	CML128 background, *aft1::KanMx4 ATG1-HA::LEU2*	Aquest treball
GSL393	CML128 background, *ypk1::KanMx4 ATG1-HA::LEU2*	Aquest treball
GSL394	CML128 background, *snf1:KanMx4*	Aquest treball
GSL395	CML128 background, *snf1:KanMx4 ATG1-HA::LEU2*	Aquest treball
GSL398	CML128 background, *atg1::NatMx4 ATG1-HA::LEU2*	Aquest treball
GSL399	CML128 background, *atg7::NatMx4 ATG1-HA::LEU2*	Aquest treball
GSL401	CML128 background, *gcn2::KanMx4 ATG1-HA::LEU2*	Aquest treball
GSL410	CML128 background, *pkc1::LEU2*	(Mitjana, Petkova, and Pujol-carrion 2011)
GSL414	CML128 background, *mtl1::KanMX4 sch9::NatMx4 GFP-ATG8::URA3*	Aquest treball
GSL415	CML128 background, *mtl1::KanMx4 slt2::NatMx4 GFP-ATG8::URA3*	Aquest treball
GSL416	CML128 background, *mtl1:NatMx4 ATG1-HA::LEU2*	Aquest treball
GSL420	CML128 background, *ypk1::KanMx4 atg7::NatMx4*	Aquest treball
GSL421	CML128, *ypk1::KanMx4 tetO$_7$AFT1C291F-HA::LEU2*	Aquest treball
GSL430	CML128 background, *lac1::KanMx4*	Aquest treball
GSL431	CML128 background, *lag1::KanMx4*	Aquest treball
GSL435	CML128 background, *fet3::KanMx4*	Aquest treball
GSL436	CML128 background, *ccc1::KanMx4*	Aquest treball
GSL437	CML128 background, *mrs3::KanMx4*	Aquest treball

Taula 2. Soques de llevat. Part 4 de 4.

GSL447	CML128 background, *fet5::KanMx4*	Aquest treball
GSL448	CML128 background, *atm1::KanMx4*	Aquest treball
GSL451	CML128 background, *ypk1::KanMx4 YPK1^{S644AT662A}-HA::LEU2*	Aquest treball
GSL454	CML128 background, *YPK1-HA::LEU2*	Aquest treball
GSL455	CML128 background, *ypk1::KanMx4 YPK1-HA::LEU2*	Aquest treball
R43	CML128 background, *rho0*	Aquest treball
BY4741	*MAT**a** his3-1, leu2, met15, ura3*	(Niles et al. 2011)
pho8Δ	BY4741 background, *pho8::HPH*	(Guedes, Ludovico, and Sampaio-Marques 2016)
GSL404	BY4741 background, *ypk1::KanMx4*	Aquest treball
FY250	*MATα his3-200, leu2-1, trp1-63, ura3-52*	(Mayordomo, Estruch, and Sanz 2002)
SEY6210	*MAT**a** his3-200, leu2-3, lys2-801, trp1-901, ura3-52, suc2-9 GAL*	(Tomotake and Daniel 2008)
W303	*MAT**a** ade2-1, trp1-1, leu2-3,2-111, his3-11,75, ura3*	(Niles et al. 2011)
GSL417	W303 background, *tor2^{ts}::LEU2*	(Costanzo et al. 2010)
*pub1*Δ	W303 background, *pub1::KanMx4*	Aquest treball
LHY291	*MAT**a** his3, trp1, lys2, ura3, leu2, bar1*	(Fresques et al. 2015)
PLY979	LHY291 background, *cka2::TRP1*	(Fresques et al. 2015)

3.2 Plàsmids utilitzats en aquest l'estudi

Els plàsmids emprats en aquest estudi es descriuen en la Taula 3.

El plàsmid pMM351 és un vector integratiu que expressa 3 còpies de l'epítop hemaglutinina (HA) en l'extrem C-terminal i el promotor $tetO_7$ en l'extrem N-terminal. Aquest plàsmid es va fer servir com a vector per construir els plàsmids: i) pAtg1-HA, clonant la seqüència d'*ATG1* entre els llocs de restricció de PmeI i PstI; ii) pYpk1-HA, amplificant la seqüència d'*YPK1* entre els llocs de restricció dels enzims PmeI i NotI; i iii) pPkc1*, a partir de l'amplificació la seqüència de *PKC1* del plàsmid pGALPkc1* (proporcionat per la Dra. Maria Molina), el qual expressa un al·lel constitutivament actiu del gen *PKC1,* entre els llocs de restricció dels enzims

PmeI i NotI.

El vector pUG35 expressa la proteïna verda yGRP3 en el seu extrem C-terminal sota el control del promotor regulable MET25. Els plàsmids que es van construir utilitzant aquest vector són: i) pSfp1-GFP, a partir de l'amplificació de la seqüència del gen *SFP1,* entre els llocs de restricció dels enzims SalI i SmaI; ii) pAtg13-GFP, amplificant l'ORF d'*ATG13,* flanquejada per les seqüències de restricció dels enzims XbaI i SalI; i iii) pPse1-GFP, gràcies a la clonació de la seqüència del gen *PSE1,* entre els llocs de restricció dels enzims BamHI i SalI.

El vector pCM64, el qual conté el promotor LacZ es va utilitzar per a construir el plàsmid pCM64-p_{ACO1}-lacZ, a través de la inserció d'un fragment del promotor d'ACO1 en els llocs de restricció de BglII i BamHI.

Finalment, el vector pCM265, el qual conté el promotor ADH1 i 3 còpies d'HA en l'extrem C-terminal, va ser usat per a la construcció del plàsmid pAtg13-HA a partir de l'amplificació de la seqüència d'*ATG13* entre els llocs de restricció dels enzims NotI i PstI.

Cada ORF particular es va amplificar per PCR a partir de DNA genòmic per ser direccionalment clonat en el plàsmid específic. Excepte l'ORF de *PKC1* constitutivament actiu que es va utilitzar com a DNA motlle el plàsmid original pGALPkc1*.

Taula 3. Plàsmids emprats. Part1 de 2.

Plàsmid	Marcador	Promotor	Epítop	Font/Referència
pSfp1-GFP	*URA3*	MET25	GFP	Aquest treball
pGFP-Atg8	*URA3*	ATG8	GFP	(Ecker et al. 2010)
pAtg13-HA	*URA3*	ADH1	HA	Aquest treball
pYX242-cytPho8	*LEU2*	PHO8		(Guedes, Ludovico, and Sampaio-Marques 2016)
pAdh1-Msn2-GFP	*LEU2*	ADH1	GFP	(Görner, Durchschlag, Martinez-Pastor, et al. 1998)

Taula 3. Plàsmids emprats. Part 2 de 2.

pAtg13-GFP	*URA3*	MET25	GFP	Aquest treball
pAtg1-HA	*LEU2*	$tetO_7$	HA	Aquest treball
pRtg1-GFP	*URA3*	RTG1	GFP	(Komeili et al. 2000b)
pAMS363	*URA3*	2xCDRE:lacZ		(Vlahakis et al. 2014)
pIdp1-GFP	*URA3*	IDP1	GFP	(Hagai et al. 2017)
pBcy1-HA	*HIS3*	ADH1	HA	(Sundaram et al. 2015)
pPkc1*	*LEU2*	$tetO_7$	HA	Aquest treball
pBck1-*20*	*TRP1*	LAC		(Petkova et al. 2010)
pAft1-GFP	*URA3*	MET25		(Pujol-Carrion et al. 2006)
p$tetO_7$Aft1-HA	*LEU2*	$tetO_7$	HA	(Pujol-Carrion et al. 2006)
pAft1C291F-HA	*LEU2*	$tetO_7$	HA	(Pujol-Carrion et al. 2021)
pFet3-LacZ	*URA3*	LacZ		(Jordá, Rozès, and Puig 2021)
pPse1-GFP	*URA3*	MET25	GFP	Aquest treball
pYpk1-HA	*LEU2*	$tetO_7$	HA	Aquest treball
p$Ypk1^{S644A/T662A}$	*LEU2*	ADH1	HA	(Niles et al. 2014)
pC-terminal3-HA	*UAR3*	ADH1	HA	(Niles et al. 2014)
pUG35	*URA3*	MET25	GFP	(Pujol-carrion et al. 2022)
pCM265	*URA3*	ADH1	HA	(Petkova, Pujol-carrion, and Torre-ruiz 2012)
pMM351	*LEU2*	$tetO_7$	HA	(Pujol-Carrion et al. 2006)

3.3 Medis de cultiu, condicions de creixement i reactius

Els medis de cultius utilitzats en l'elaboració d'aquesta recerca han estat:

i) YPD, és un medi ric que conté glucosa (Serva, 22720.02) al 2%, peptona (Quimega, 1616.00) al 2% i extracte de llevat (Quimega, 1702.00) al 1%.

ii) SC, és un medi definit que conté 0,67% de base nitrogenada de llevat (BD, 291940), 2% de glucosa (Serva, 22720.02) i 0,2% de "*drop out*" (Formedium; DCS1389). El "*drop out"* és una combinació de bases nitrogenades i aminoàcids els quals es detallen en la Taula 4.

iii) SD, és un medi definit a base del 0,67% de base nitrogenada de llevat (BD, 291940) i 2% de glucosa (Serva, 22720.02).

iv) SD-Glucosa, medi definit sense glucosa obtingut a partir del 0,67% de base nitrogenada de llevat (BD, 291940).

v) SD-Nitrogen, medi definit sense nitrogen elaborat amb el 2% de glucosa (Serva, 22720.02).

vi) SD-Ferro, és un medi definit sense ferro que conté 0,67% de base nitrogenada de llevat que no conté ferro (US Biological, Y2037), 2% de glucosa (Serva, 22720.02) i 80 μM de BPS (4,7-diphenyl-1,10-phenanthrolinedisulfonic acid) (Sigma, 146617), un quelant de ferro extracel·lular.

vii) SGlicerol, és un medi definit a base del 0,67% de base nitrogenada de llevat (BD, 291940) i 3% de glicerol (Fisher scientific, 800689).

viii) SSucrosa, medi definit a base de 0,67% de base nitrogenada de llevat (BD, 291940) i 2% de sucrosa (Sigma, S0389).

ix) SFructosa, medi definit elaborat al 0,67% de base nitrogenada de llevat (BD, 291940) i 2% de fructosa (Sigma, 47740).

x) LB, medi ric per al cultiu de bacteri que conté triptona (Pronadisa, 1612.00) l'1%, NaCl (Serva, 170081) l'1% i extracte de llevat al 0,5% (Quimega, 1702.00). Aquest medi s'ajusta a pH 7,5 amb NaOH (Scharlau, 1839).

Taula 4. Composició del "*drop out"*

Component	**mg/l**	**Component**	**mg/l**	**Component**	**mg/l**
Adenina	20	Glutamina	20	Fenilalanina	50
Alanina	20	Àcid glutàmic	100	Prolina	20
Arginina	20	Glicina	20	Serina	400
Asparagina	20	Isoleucina	30	Treonina	200
Àcid aspàrtic	100	Lisina	30	Tirosina	30
Cisteïna	20	Metionina	20	Valina	150

A excepció dels medis rics, els medis de cultius es complementen amb els requisits auxotròfics necessaris.

Per als medis de cultiu sòlid, en tots els casos, s'afegeix el 2% d'agar a la composició descrita anteriorment.

Les cèl·lules en placa s'han crescut a l'incubador (Memmert) i els cultius líquids en agitació a 170 rpm. Els cultius bacterians s'han incubat a 37ºC , mentre que els de llevat a 30ºC. En els casos en què s'han utilitzat mutants termosensibles, els cultius s'han incubat a 25ºC i posteriorment es realitza un canvi a 37ºC durant dues hores per inactivar la proteïna mutada. En aquesta tesi es considera cultius en fase exponencial els que es troben a absorbància òptica a 600nm ($O.D_{600}$):0,6, en els casos que ha estat necessari l'ús de poblacions en una etapa de creixement diferent, s'ha detallat i justificat degudament al text.

A continuació es mostra una llista dels agents químics que s'afegeixen als medis de cultiu per dur a terme els diferents assaigs on es detalla la concentració final en què s'utilitzen i la casa comercial on s'han adquirit: àcid 4,7-difenil-1,10-fenanthrolidisulfonic (BPS) 80 µM (Sigma, 146617); N-Acetil cisteina (NAC) 5 mM (Sigma, A9165); Rapamicina (Rapa) 200 ng/ml (Sigma, R0395); Cicloheximida (CHX) 150 mg/ml (Sigma, C4859); DAPI 2 mg/ml (Sigma, D9541); (N-(3-trietilammonipropil)-4-(p-dietilaminofenilhexatrienil)) piridinum dibromur (FM464) 30 µg/µl (Invitrogen, T-3166); Miriocina (Myr) 2 mM (Sigma, M1177); D-eritro-

Dihidrosfingosina (DHS) 20 µM (Sigma, D3314); Aureobasidina A (Aur) 250 ng/ml (MedChem Express, HY-P1975); SUlfat d'amoni de ferro (III) hexacahidrat [$NH_4Fe(SO_4)_2 \cdot 6H_2O$] (Fe) 10 mM (Sigma, F1543); Fosfatasa alcalina (PA) (Roche, 105677520001); Clorur de calci dihidrat [$CaCl_2 \cdot 2H_2O$] 100mM (Serva, 15587); peròxid d'hidrogen [H_2O_2] 0,5 mM (Sigma, H1009); Sorbitol 0,8 M (Sigma, S6021); Dihidroetidi (DHE) 50 µM (Sigma, D7008); Eritromicina 0,5 mM (Sigma, E6376); ATP 200 mM (Sigma, A1852); Glicerol 3% (Fisher scientific, 800689); Sucrosa 2% (Sigma, S0389); Fructosa 2% (Sigma, 47740).

3.4 Determinació de la concentració glucosa, trehalosa i etanol

Per tal de determinar la glucosa i la trehalosa es va seguir el protocol descrit anteriorment en (Hernandez-Lopez, Prieto, and Randez-Gil 2003).

La concentració d'etanol en el sobrenedant es va determinar a través de la tècnica HPLC en el cromatògraf "*Surveyor Plus"* (Thermo Fisher Scientific), equipat amb un detector d'índex de refracció, un mostrejador automàtic i un detector UV-visible. Cada mostra es va analitzar per duplicat.

3.5 Determinació de l'activitat Calcineurina

Per determinar l'activitat de la calcineurina es va emprar un reporter lacZ d'un element de resposta dependent de la calcineurina (CDRE) (Stathopoulos and Cyert 1997), facilitat pel Dr. Ted Powers, i seguidament es va procedir a elaborar un assaig β-galactosidasa, explicat posteriorment en aquest apartat de material i mètodes.

3.6 Tinció cel·lular

Per establir les localitzacions subcel·lulars es va fer ús de diferents compostos que tenyeixen components cel·lulars específics:

i) Tinció de la membrana vacuolar amb FM4-64.

ii) Tinció del material genètic del nucli i mitocòndries amb DAPI.

iii) Tinció cel·lular per determinar oxidació cel·lular amb DHE.

Alíquotes d'1 mL de cultiu, van ser recol·lectades, centrifugades durant 5 minuts a 3000 rpm i resuspeses en 50 µl de medi fresc. Posteriorment, les mostres s'incubaren amb 5 µl de FM4-64 (Invitrogen, T-3166), 0,5 µl de DAPI (Sigma, D9541) o 1 µl de DHE (Sigma, D7008), durant 1 hora a 30ªC. Finalment, abans de l'observació de les mostres, es van efectuar tres rentats amb aigua MiliQ estèril i es van resuspendre en 50 µl de medi de cultiu fresc.

3.7 Determinació del índex de competència respiratòria (IRC) i freqüència de mutacions mitocondrials

El IRC es va calcular a través de la ràtio del nombre de CFUs observades en plaques de medi no fermentable YPEG (Glicerol) i les observades en plaques de medi fermentable YPD (Glucosa).

L'assaig de freqüència de mutacions mitocondrials es va determinar entre la ràtio de CFUs contades en plaques YPEG amb eritromicina (Sigma, E6376) i el nombre de CFUs contades en plaques de YPD.

Ambdós protocols es van portar a terme segons les directrius descrites en (Parrella and Longo 2008).

3.8 Supervivència cel·lular i CLS

Per tal de determinar la supervivència cel·lular, les cèl·lules es van créixer fins a OD_{600}: 0,6 en el medi de cultiu descrit per a cada experiment. La viabilitat es va calcular a través de dilucions seriades del cultiu plaquejades per triplicat en plaques de YPD i crescudes a 30ºC durant 3 dies. La CLS es va determinar a través de poblacions de cèl·lules que no estan en divisió tal com s'indica en (Sundaram et al. 2015). És calcula contant el nombre de cèl·lules que poden formar colònies. Els cultius es van iniciar a OD_{600}: 0,6. El mateix nombre de cèl·lules eren recollides

de cada cultiu i plaquejades per triplicat en plaques de YPD, les quals es van deixar créixer a 30ºC durant 3-4 dies. La representació dels resultats es mostra en forma de gràfica a partir de les mitges i desviacions estàndard corresponents de tres experiments independents. La mesura comença al dia 3 de cultiu fins als 15 dies.

3.9 Extracció de proteïna i anàlisi per immunodetecció en "*western blot*"

Per aquesta tècnica se segueix el mateix protocol que està descrit en (Pujol-carrion et al. 2022). Els extractes de proteïna s'obtenen a partir de mostres de cèl·lules equivalents a 15 mL de cultiu a OD_{600}: 0,6. Les cèl·lules de llevat són escalfades a 95ºC durant 2 minuts amb 15 µl d'urea 5M (Serva, 24524). Les cèl·lules són llisades amb un volum equivalent de boles de vidre (Sigma, G9268) al "*Ribolyser*" (5,5 m/s, 5-7 vegades a 4ºC). Els lisats cel·lulars es desnaturalitzen a 95ºC durant 2 minuts amb 50 µl de SDS (Affymetrix, 75819) al 10%. Posteriorment, es centrifuga i separa el sobrenedant del pellet. El sobrenedant conté les proteïnes desnaturalitzades, les quals, es quantifiquen a través de l'assaig de proteïnes Micro DC (Bio-Rad, 5000111). Quantitats iguals de proteïna total es carreguen i separen en gels de SDS-poliacrilamida al 10%. Els gels corren amb presència de "*Running Buffer"* (Tris 0,25 M (Sigma, 37190); Glicina 1,92 M (Fisher, BP381-1); SDS 1% (Affymetrix, 75819) a pH 8,4-8,9). Seguidament, les proteïnes es transfereixen del gel a una membrana de PVDF (Millipore, IPVH00010) amb presència de buffer de transferència (Glicina 39 mM (Fisher, BP381-1); Tris 48 mM (Sigma, 37190); SDS 0,0375% (Affymetrix, 75819); Metanol 20% (Fisher, 10675112). Un cop les proteïnes s'han transferit a la membrana, aquesta és bloquejada amb buffer B (5% de llet desnatada, dissolta en TBS-T (Tris 20 mM (Sigma, 37190); NaCl 150 mM (Sigma, 30183); i Tween 20 al 0,1% (Fisher, 11417160)) durant 1 hora. Posteriorment, es renten les membranes amb TBS-T i s'incuba tota la nit amb l'anticòs primari. Després, les membranes es netegen per eliminar l'excés d'anticòs amb TBS-T i s'incuben amb l'anticòs secundari durant 1 hora a temperatura ambient. Finalment, les membranes es netegen amb TBS-T.

La detecció dels complexes proteïna-anticòs es realitza mitjançant el kit "*Clarity™ Western ECL Substarte*" (Bio-Rad, 170-5060) i l'equip de detecció "*Chemidoc™-MP Imaging System*" (Bio-Rad). L'adquisició de les imatges i processament es fa en el programa "*Image Lab*" (Bio-Rad).Els anticossos emprats en els "*western blots*" es detallen en la Taula 5.

Taula 5. Anticossos utilitzats per la detecció de proteïnes en "*western blot"*.

Anticòs Primari	**Productor i Referència**	**Dilució**	**Anticòs Secundari**	**Productor i Referència**	**Dilució**
anti-GFP	Living Colours, 632381	1:2000	anti-Mouse	GE Healthcare, LNA931v/AG	1:10000
anti-HA (3F10)	Roche, 12158167001	1:2000	anti-Rat	Millipore, AP136P	1:10000
anti-PGK1	Invitrogen, 459250	1:12000	anti-Mouse	GE Healthcare, LNA931v/AG	1:10000
anti-phospho-eIF2α	Cell Signalling, 3597S	1:1000	anti-Rabbit	GE Healthcare, LNA934v/AG	1:10000
anti-phospho-AMPKα	Cell Signalling, 167253S	1:1000	anti-Rabbit	GE Healthcare, LNA934v/AG	1:10000
anti-phospho-Ypk1	Dr. Ted Powers	1:20000	anti-Rabbit	GE Healthcare, LNA934v/AG	1:10000

3.10 Detecció de l'autofàgia

La progressió de l'autofàgia es va monitoritzar a través de diferents aproximacions: i) detecció immunològica de l'acumulació de GFP lliure procedent de la fusió genòmica GFP-Atg8, la qual s'allibera dins el vacúol com a resultat de la formació del cos autofàgic (Takahiro Shintani and Daniel J. Klionsky 2004); ii) l'observació microscòpica de l'acumulació de GFP dins el vacúol. En general aquestes dues aproximacions són suficients per determinar l'activitat autofàgica. En algunes ocasions especials també es va utilitzar un assaig enzimàtic per determinat l'autofàgia no específica mitjançat l'activitat enzimàtica de *pho8*□60, tal com van descriure Noda i Klionsky (Noda and Klionsky 2009), i van modificar Guedes i els seus Companys (Guedes, Ludovico, and Sampaio-Marques 2016).

3.11 Detecció de ferro endogen

Per detectar el ferro endogen es va emprar un assaig colorimètric descrit per Jordi Tamarit l'any 2006 (Tamarit et al. 2006).

3.12 Activitat β-galactosidasa

L'activitat β-galactosidasa es va determinar tal com es descriu en (Mónica A. Mechoud, Nuria Pujol-Carrion, Sandra Montella-Manuel 2020), amb algunes modificacions. Es recol·lecta 1ml de cultiu cel·lular a OD600 0,6 i se centrifuga 5 minuts a 3000rpm. Els pelletes es suspenen en 50µL de buffer Z (Na_2HPO_4 60 mM (Serva, 30200.01); NaH_2PO_4 40 mM (Serva, 13472-35-0); KCl 10 mM (Serva, 26868); $MgSO_4$ 1mM (Sigma, M7634-100G); β-mercaptoetanol 50 mM (BioRad, 161-0710)) més 2,5 µl de sarcosil 10% (Sigma, T4376) i 0,5 µl de toluè (Merck, 244511). Posteriorment, s'afegeixen 150 µl de buffer Z i 50 µl d' *o*-nitrofenil-β-D-galactopiranòsid (ONPG) 4 mg/ml (Sigma, N1127) i s'incuba a 28ºC durant 5 minuts. Finalment, s'afegeixen 500 µl de Na_2CO_3 1 M (Sigma, S7795-500G) per parar la reacció. La descomposició del substrat produeix un canvi de color que es mesura a absorbància 420nm.

3.13 Microscopi de Fluorescència

Les cèl·lules s'observen al microscopi de fluorescència (Olympus BX-51) utilitzant l'objectiu d'augment 60X. Les localitzacions cel·lulars són efectuades als temps indicats en els resultats sota les condicions descrites per a cada experiment.

3.14 Anàlisi estadística

Les barres d'error en els histogrames representen la desviació estàndard (SD) calculada a partir d'experiments independents. La significança dels resultats es determina a través del *P-valor* de la prova t de Student, seguint el següent criteri: *=0,05>P>0,01; **=0,01>P>0,001; ***=0,001>P>0,0001; ****=P>0,0001.

4. ARTICLES PUBLICATS

4.1 PRIMER ARTICLE

A yeast genome-wide transcriptional study reveals that iron deficiency inhibits protein translation via the TORC1 pathway

Antonia María Romero[1], Lucía Ramos-Alonso[1], Sandra Montellá-Manuel[2], José García-Martínez[3,5], María Ángeles de la Torre-Ruiz[2], José Enrique Pérez-Ortín[4,5], María Teresa Martínez-Pastor[4]* and Sergi Puig[1]*

[1] Departamento de Biotecnología, Instituto de Agroquímica y Tecnología de Alimentos (IATA), Consejo Superior de Investigaciones Científicas (CSIC), Catedrático Agustín Escardino 7, Paterna, Valencia, E-46980, Spain.

[2] Department of Basic Medical Sciences, IRB-Lleida. University of Lleida, Alcalde Rovira Roure 80, Lleida, E-25198. Spain

[3] Departamento de Genética, [4]Departamento de Bioquímica y Biología Molecular, and [5]ERI Biotecmed, Universitat de València, Doctor Moliner 50, E-Burjassot, Valencia, 46100, Spain.

* To whom correspondence should be addressed. Tel: (+34) 963 900 022; Fax: (+34) 963 636 301; Email: spuig@iata.csic.es and

maria.teresa.martinez@uv.es

ABSTRACT

Iron is an essential micronutrient that participates as a protein cofactor in a broad range of metabolic processes. The yeast *Saccharomyces cerevisiae* has been widely used to characterize the responses of eukaryotic cells to iron depletion. Here, we used a genomic approach to investigate the contribution of transcription rates (TR) and mRNA stabilities to the modulation of mRNA amount (RA) during yeast adaptation to iron starvation. We show that iron deficiency causes an overall decrease in the TR, which effect on RA is partially compensated by a global mRNA stabilization. Genes from the iron regulon, mitochondrial retrograde pathway and general stress response display a remarkable increase in both TR and RA upon iron limitation, whereas genes encoding ribosomal proteins or ribosome biogenesis factors exhibit a pronounced fall. This expression profile is consistent with a slow but irreversible activation of the environmental stress response. Specific molecular markers including the phosphorylation status of Sch9, Dot6, Rps6, Maf1 and eIF2α suggest that the conserved TORC1 signaling pathway is inhibited during iron deficiency leading to a general repression of protein translation. These results uncover an intricate crosstalk between iron metabolism and the TORC1 pathway that should be considered in many pathological situations.

INTRODUCTION

Iron is an essential micronutrient for all eukaryotes because it participates as a redox cofactor in fundamental cellular processes including DNA replication and repair, translation and cellular respiration. Although iron is quite abundant, its bioavailability is very restricted under aerobic conditions because of the insolubility of ferric iron at physiological pH. Thus, the acquisition and maintenance of sufficient iron levels suppose a challenge for living organisms, which have evolved sophisticated mechanisms to modulate iron homeostasis. Indeed, iron deficiency anemia is the most widespread nutritional disorder in humans, estimated to affect more than two billion people with a high prevalence in children and women of childbearing age (1). The budding yeast *Saccharomyces cerevisiae* has proved to be a reliable model to identify and characterize mechanisms of adaptation to iron deficiency in humans and plants. *S. cerevisiae* responds to the scarcity of iron through two complementary strategies, which occur at the transcriptional and post-transcriptional level, respectively. First, the transcription factors Aft1 and Aft2 accumulate into the nucleus, bind to iron responsive elements (FeREs), and activate the expression of ~35 genes known as the iron regulon, which are mainly involved in the acquisition of extracellular iron and the mobilization and recycling of intracellular iron (reviewed in (2)). Second, two mRNA-binding proteins denoted Cth1 and Cth2, which are part of the iron regulon, specifically bind to AU-rich elements within the 3'untranslated region of many mRNAs, and stimulate their turnover and translational inhibition (3-6). This post-transcriptional regulation promotes a metabolic remodeling that limits the utilization of the scarce iron in non-essential processes, such as respiration, and optimizes its utilization in indispensable pathways such as DNA synthesis.

The conserved target of rapamycin (TOR) serine/threonine kinase and its namesake pathway, which were first discovered in yeast, control cell growth and metabolism in response to environmental cues such as nutrient levels, cell integrity, stress or energy status ((reviewed in (7-9)). The TOR kinase can function in two different multiproteic complexes, TORC1 and TORC2, which are conserved from yeast to mammals. The yeast TORC1 complex is composed of Tor1 or Tor2 kinase, and the Lst8, Kog1 and Tco89 proteins. The two major downstream effectors of the TORC1 complex are the Sch9 kinase and the phosphatase complex Tap42-PP2A. When the environmental conditions are favorable, the TORC1 pathway promotes ribosome biogenesis and protein translation by favoring the expression of ribosomal proteins (RPs), ribosome biogenesis (RiBi) factors, rRNAs and tRNAs at multiple levels (7). Under nutrient limitation, or in the presence of the lipophilic drug rapamycin, the inactivation of TORC1 provokes a decrease in the phosphorylation of Sch9, and subsequently of Stb3 and Dot6/Tod6 transcription factors, which, together with the Rpd3L histone deacetylase complex, repress the transcription of RP and

RiBi genes (7,10). Under these conditions, Sfp1, an activator of RP and RiBi genes and a direct target of TORC1, is inactivated by dephosphorylation and exported to the cytoplasm (reviewed in (7)). Under optimal conditions, TORC1 enhances rRNA expression by inhibiting the proteasome-dependent degradation of Rrn3, the activating factor of the RNA polymerase I (RNA Pol I) (11), and tRNA transcription by regulating the phosphorylation stage of the RNA polymerase III (RNA Pol III) repressor Maf1. TORC1 also regulates the initiation of translation through eIF2α. Under amino acid starvation or rapamycin treatment, eIF2α is phosphorylated by the protein kinase Gcn2, which is previously activated by Tap42-PP2A-dependent dephosphorylation. The phosphorylation of eIF2α causes a block in global 5' cap-dependent translation initiation, while permitting the translation of genes containing upstream ORFs, such as *GCN4*, the transcriptional activator of amino acid biosynthetic genes.

The retrograde response is a signaling pathway that communicates mitochondria with the nucleus, activating the expression of several nuclear genes that are necessary for the synthesis of glutamate and other anabolic precursors of amino acids through anaplerotic reactions. These genes include *CIT2*, the peroxisomal isoform of citrate synthase that produces citrate as part of the glyoxylate cycle, and the genes encoding the enzymes of the three first steps in the tricarboxylic acid (TCA) cycle: *CIT1*, coding for the mitochondrial isoform of citrate synthase; *ACO1*, aconitase, and *IDH1/2*, encoding NAD^+-dependent isocitrate dehydrogenase (reviewed in (12)), which enable cells to maintain glutamate and glutamine supplies when mitochondria are dysfunctional and cells are respiratory deficient through the synthesis of α-ketoglutarate. The retrograde signaling requires the nuclear translocation of a heterodimeric transcription factor constituted by Rtg1 and Rtg3 proteins, which occurs after the Rtg2-dependent partial dephosphorylation of Rtg3. The TORC1 complex negatively regulates retrograde signaling through its component Lst8, acting both upstream and downstream of Rtg2 (reviewed in (12,13)).

Previous global studies have analyzed the changes in mRNA levels that *S. cerevisiae* undergoes in response to iron deficiency (3,14,15). The information obtained from these transcriptomic analyses is nonetheless limited, as it involves the measurement of steady-state mRNA amounts (RA), and does not take into account that RA is the result of the coordinated balance between mRNA synthesis and decay. In order to assess the relative contribution of transcriptional and post-transcriptional strategies to the adaptation to iron limitation, we have used the genomic run-on (GRO) technique (16) to determine the TR and RA for the entire yeast transcriptome during the progress from mild to severe iron deficiency, and we have calculated the mRNA decay rates from the TR and RA experimental data. Our data uncover new insights onto the molecular mechanisms involved in the adaptation to iron deprivation, including changes in mRNA stability, an activation of the environmental stress response

(ESR), a TOR-mediated down-regulation of protein translation, and the activation of the mitochondrial retrograde response.

MATERIALS AND METHODS

Yeast strains, plasmids and growth conditions. The yeast strains used in this study are listed in the Supplementary Table S1. The pCM64-P_{ACO1}-lacZ reporter plasmid was made by the insertion of a 613-bp PCR amplified fragment from the *ACO1* promoter region into the BglII-BamHI sites of pCM64 vector (from Charles Moehle). The Sfp1-GFP plasmid was constructed by amplifying *SFP1* sequence flanked by SalI and SmaI restriction sites, digestion and cloned into pUG35 plasmid. Yeast W303 cells were cultivated in SC medium for at least 15 hours to reach early exponential phase (OD_{600} = 0.2). Then, 100 µM of the Fe^{2+}-specific chelator bathophenanthroline disulfonic acid (BPS; Sigma) was added, and aliquots were isolated at 0, 10, 30, 90, 180 and 360 minutes after iron limitation. In the case of yeast cells from the BY4741 background, an overnight preculture was used to inoculate SC (+Fe) or SC + 100 µM BPS cultures (-Fe), and aliquots were taken at the specified times. For mRNA half-life measurements, yeast cells were cultivated in SC or SC + 100 µM BPS for 3 hours to exponential phase. Then, thiolutin was added to a final concentration of 3 µg/mL to inhibit RNA polymerase II (RNA Pol II) transcription, and aliquots were isolated at successive times (0, 5, 10, 15, 20, 35 and 70 min). For microscopy, cultures were grown at 30ºC in SC to OD_{600} = 0.6. Then, yeast cells were washed four times in either SD or SD + 10 µM BPS. Half of the cells were transferred to fresh SD medium or alternatively to SD + 10 µM BPS (-Fe) at OD_{600} = 0.2. Cultures were grown for 8 hours in continuous shaking. Samples were taken for observation in an Olympus Bx51 fluorescence microscope.

Determination and analyses of transcription rates and mRNA levels. To determine the transcription rates (TR) and RA of each gene on a genome-wide scale, we followed the GRO and mRNA measurement protocols previously described (16), except that cells were frozen and the reverse transcription of mRNA was carried out using an oligo-d$(T)_{15}$VN instead of random primers. Quantification and normalization of the data were performed as reported (16). Changes in the normalized median values of TR and RA were evaluated by cluster analysis with WebMeV (Multiple Experiment Viewer). Finally, we used the Gene Ontology enRIchment anaLysis and visuaLizAtion tool (http://cbl-gorilla.cs.technion.ac.il) to ascertain the enrichment of clusters in specific gene ontology (GO) categories. Three biologically independent replicates were performed for each experiment.

Total poly(A) RNA measurements. We used a dot-blot procedure to determine the poly(A) mRNA/cell as previously described (16).

Messenger RNA decay rate calculations. The decay rate constant (k_D) was calculated from the TR and RA mean value from three biological replicates. We assumed steady-state conditions for time zero and 180 min of BPS, whereas

non-steady state conditions were considered for 10, 30 and 90 min of BPS. The k_D at steady-state decay conditions was calculated as the TR/RA ratio (16).

A k_D value for the time interval between t_1 and t_2 was obtained and assigned to a time point in the middle of both experimental times (17).

RNA analyses. Total yeast RNA isolation, reverse transcription and quantitative PCR (RT-qPCR) were performed as previously described (5). An oligo-dT primer was used for reverse transcription, except in mRNA half-life measurements, where random primers were used. Specific primer pairs were used for the qPCR (listed in Supplementary Table S2). The data and error bars represent the relative average and standard deviations of three independent biological samples.

Protein analyses. Yeast proteins were extracted and analyzed by Western blot as previously reported (5), except in the case of Sch9 and Maf1 protein phosphorylations, which were studied with specific procedures (18-20). Chromatin immunoprecipitation (ChIP) assays were performed to determine RNA pol II binding to Rtg1-regulated gene promoters as described (21). Cell extracts for ChIP were incubated with Dynabeads Pan Mouse IgG (Invitrogen), previously bound to a monoclonal mouse anti-Rpb1 antibody (clone 8WG16, Covance), and DNA was purified with the High Pure PCR Product Purification Kit (Roche). The primers used for the RT-qPCR analyses are listed in Supplementary Table S2. The primary antibodies used in this study included anti-Rpb1 (clone 8WG16, Covance), anti-Rpb1-Ser2-Phosphorylated (Abcam), anti-HA (3F10; Sigma), anti-Rpa190A (from Olga Calvo), anti-GFP (Roche), anti-Rps6 (Cell Signaling Technology), anti-Rps6-Ser235/Ser236 (Cell Signaling Technology), anti-eIF2α (from John M. Zaborske), anti-eIF2α-Ser51/Ser52 (Cell Signaling Technology), anti-Maf1 (from Olivier Lefebvre) and anti-Pgk1 (22C5D8; Invitrogen).

Determination of glucose and ethanol concentrations. Glucose and ethanol concentrations in all the supernatant samples were determined by HPLC in a Surveyor Plus Chromatograph (Thermo Fisher Scientific, Waltham, MA) equipped with a refraction index detector, an autosampler and a UV-Visible detector. Each sample was analyzed in duplicate.

Miscellaneous. Polyribosome profile analyses were performed as previously described (5). Cell median volumes were determined with a Coulter Counter Z (Beckman Coulter, USA). Rrp12-GFP expressing cells were stained with 4',6-diamidino-2-phenylindole (DAPI) and visualized in an Axioskop 2 fluorescence

microscope (Zeiss), and images were captured with a SPOT camera (Diagnostic Instruments). β-Galactosidase activity was measured as previously described (21). Tailed t-student tests were applied to evaluate statistical significance.

Accession numbers. The Gene Expression Omnibus (GEO) accession number for the whole experiment is GSE127875.

RESULTS

General responses during the adaptation to iron deficiency

Various studies have shown that the yeast *S. cerevisiae* alters the steady-state levels of many transcripts in response to nutritional or genetic iron deficiencies (3,14,15). However, little is known about the relative contribution of transcriptional and post-transcriptional regulatory mechanisms to the abundance of specific mRNAs upon iron scarcity. To address this question, we determined the TR and the RA per cell of the entire yeast genome during the progress of iron deficiency. We cultivated a haploid prototroph W303 yeast strain to early exponential phase (A_{600} = 0.3; $7 \cdot 10^6$ cells/mL), and then we added 100 μM of bathophenanthroline disulfonate (BPS), a widely used Fe^{2+}-specific chelator that limits extracellular iron bioavailability. With the aim of deciphering both early and late responses to iron deprivation, aliquots were collected up to six hours after iron limitation. Growth rate slightly decreased after 6 hours of iron depletion, but cells continued duplicating up to 24 hours under these conditions (Supplementary Figure S1A and S1B). Metabolite analyses showed a mild decrease in glucose concentration and increase in ethanol levels (Supplementary Figure S1C). No important changes were observed in cellular volume during the progress of the experiment (Supplementary Figure S1D). To quantify the RNA polymerase II (RNA Pol II) TR of each yeast gene, we used the GRO method (16) (Materials and Methods). The whole RNA Pol II TR was obtained from the median of the TR corresponding to all the yeast protein-coding genes, whereas the total RA was determined by hybridization with labeled oligo(dT) (16) (Materials and Methods).

The profile of total RA and TR distinguished three different stages along the iron deficiency (Figure 1A). First, cells experienced an early response to low iron (from 0 to 30 min), in which both total RA and TR decreased. Following this initial stage, the TR and RA increased to reach their maximum levels between 90 and 180 min. By using these experimental data, we calculated the predicted global mRNA degradation constant (k_D) (Materials and Methods). We obtained k_D values below 1.0 during the second and third hour of the iron limitation, which are indicative of mRNA stabilization (Supplementary Figure S2). Finally, both TR and RA fell and achieved their minimal value after 6 hours of iron depletion (Figure 1A). To obtain some insight into the molecular reasons for these changes in TR, we determined the mRNA and protein levels of the largest subunit of the RNA Pol II complex, Rpb1. Consistently with a decrease in the RNA Pol II TR, both Rpb1 mRNA and protein levels slightly decreased as the iron deficiency advanced (Figure 1B and 1C). Remarkably, the levels of elongating Rpb1, which is transiently phosphorylated at the second serine of the heptapeptide repeat within its carboxy-terminal domain (Rpb1-S_2-P), further diminished (Figure 1B), indicating a stronger defect in elongating RNA Pol II at longer times. Collectively, these results indicate that yeast cells experience

important changes in both transcription and mRNA stability during the adaptation to iron deficiency. Broadly, we observe a decrease in global TR that is partially compensated by mRNA stabilization during the first stages of iron starvation.

Identification of gene clusters with coordinated changes in transcription rates, mRNA levels and mRNA stabilities during iron depletion

To identify sets of genes coordinately regulated at the transcriptional or post-transcriptional levels along the iron deficiency kinetics, we performed gene clustering analyses according to the experimental TR and RA profiles on one side (Supplementary Data S1 and S2), and to the calculated k_D pattern on the other side (Supplementary Data S3 and S4). The individual RA values after 6 hours of iron deficiency were not included in these analyses because we obtained no detectable signal. By this method, we classified 4389 genes into 8 TR+RA different clusters and 4255 genes in 18 k_D clusters, which were statistically enriched in specific functional categories (Supplementary Figures S3 and S4; Supplementary Data S2 and S4; $p \leq 10^{-4}$). The profile for each cluster was represented (Figure 2; Supplementary Figure S5). Consistent with the activation of the iron regulon by the Aft1 and Aft2 transcription factors previously reported (3,14,15), the gene ontology (GO) category "iron ion homeostasis" was over-represented in the TR+RA cluster 1 ($p = 7.4 \cdot 10^{-17}$), which TR and RA gradually augmented during the time-course of iron deficiency (Figure 2; Supplementary Figure S3). Cluster 1 also contained the Mga2-dependent transcriptional induction reported for the *OLE1* fatty acid desaturase in response to iron limitation (21). Regarding the k_D clustering, we observed that the k_D cluster 2 was enriched in targets for the Cth1 and Cth2 RNA-binding proteins (3,4), which promote the mRNA turnover of many transcripts in response to iron depletion, especially those involved in mitochondrial respiration (Supplementary Figure S4; Supplementary Data S4; $p = 1.8 \cdot 10^{-15}$). In particular, the k_D values for this cluster 2 are always above one, which is indicative of mRNA destabilization (Supplementary Figure S5). Taken together, these results validated our experimental conditions and, from here onwards, we focused on identifying new functional categories coordinately regulated in response to iron depletion.

We first focused on analyzing the TR+RA clustering (Figure 2; Supplementary Figure S3). Clusters 2-4 displayed a global increase in RA, although milder than the one observed in cluster 1. Interestingly, the higher RA obtained in cluster 2 was not explained by a parallel elevation in the TR, indicating that mRNA stabilization contributes to the RA augment as seen by the median k_D profile calculated for this cluster (Figure 2; Supplementary Figure S6). Cluster 5 exhibited a remarkable increase in TR at 6 hours of iron

depletion, and was enriched with the functional categories “redox processes” ($p = 4.0 \cdot 10^{-9}$) and “tricarboxylic acid cycle” ($p = 4.5 \cdot 10^{-9}$) (Figure 2; Supplementary Figure S3). The rest of genes (clusters 6-8) did not increase their RA during iron limitation. Our data suggested an important contribution for mRNA stabilization in genes from cluster 6, while genes in cluster 8 were probably greatly destabilized (Supplementary Figure S6). The largest cluster 7 (containing 2164 out of 4389 genes) exhibited an early decrease in both TR and RA followed by a stabilization of the RA, as shown for the global TR, RA and k_D patterns (Figure 2; Supplementary Figure S3 and S6). Importantly, this profile was shared by highly expressed genes including the GO categories “RNA processing” ($p = 9.3 \cdot 10^{-22}$), “ribosome biogenesis” ($p = 1.3 \cdot 10^{-13}$), and “translation” ($p = 1.2 \cdot 10^{-15}$) (Figure 2; Supplementary Figures S3 and S6). Collectively these results strongly suggest that transcription, but also mRNA stability, contributes to the response of yeast cells to iron deficiency.

To study the contribution of mRNA stability in more detail, we further analyzed the data that resulted from a more discriminating gene clustering made directly by their k_D profile up to 3 hours of iron deficiency (Supplementary Figures S4 and S5; Supplementary Data S4). In addition to the enrichment of k_D cluster 2 with Cth1 and Cth2 target genes and members of the respiratory electron transport chain highlighted above, we observed that members of the GO “mitochondrial respiratory chain complex IV assembly” ($p = 4.5 \cdot 10^{-7}$) grouped separately in cluster 15 (Supplementary Figure S4). Interestingly these transcripts were stabilized at both short and long term iron deficiency (Supplementary Figure S5). A similar k_D pattern was observed for the GO category “negative regulation of cell cycle”, which was present in the k_D cluster 14 ($p = 6.4 \cdot 10^{-7}$). Finally, the GO category “cytoplasmic translation” ($p < 10^{-10}$) was significantly represented in k_D clusters 3 and 5 mostly due to RP gene contribution (Supplementary Figure S4). The k_D profile for RP genes showed a transient destabilization at very short times followed by mRNA stabilization (Supplementary Figure S5). These data indicate that mRNA stability contributes to the expression profile of genes implicated in mitochondrial respiration, protein translation and cell cycle during the progress of iron starvation.

Previous studies have demonstrated that yeast cells initiate a common gene expression program called the environmental stress response (ESR) to acclimate to multiple suboptimal conditions (22-24). The ESR set of genes is comprised of ~300 induced mRNAs (iESR), which encompass genes involved in protecting cells against stress conditions, and ~600 repressed transcripts (rESR) encoding RPs, RiBis and other proteins implicated in translation (22). Since a notable conclusion of our TR+RA clustering was the down-regulation of genes involved in ribosome biogenesis and translation ($p < 10^{-12}$), we decided to explore whether the ESR program was initiated in response to iron depletion. For this purpose, we represented the median TR and RA profiles of the iESR

and rESR genes referred to a normalized global TR and RA pattern, respectively, during the progress of the iron limitation. Consistent with an activation of the ESR program, we observed an up-regulation of the iESR and a down-regulation of the rESR set of genes for both the TR and RA profiles in response to iron deficiency (Figure 3A). This result suggests that transcriptional mechanisms activate the ESR program upon iron depletion. To compare the ESR response initiated upon iron depletion to the one activated by other stresses, we represented the ESR genes described for the oxidative stress achieved by the addition of 0.1 mM *ter*-butyl hydroperoxide (25) (Figure 3). The iron deficiency ESR response was milder and slower than the one commonly observed in response to oxidative and other stresses (ESR RA-ox)(22,24).

Previous studies had demonstrated that the general stress transcription factors Msn2 and Msn4 contribute to the activation of a set of the iESR genes in response to various stresses (22). To ascertain the potential relevance of the iESR signature and the Msn2 and Msn4 transcription factors to the adaptation to iron depletion, we assayed the growth of an *msn2*Δ*msn4*Δ yeast mutant in iron-deficient conditions and observed a significant decrease in growth as compared to wild-type cells (Figure 3B). These results support a role for the Msn2 and Msn4 transcription factors and the iESR genes in the response to iron deficiency.

Next, we focused our interest on genes contained in the TR+RA cluster 7, which include highly expressed genes encoding ribosomal proteins (RP) and proteins implicated in ribosome biogenesis (RiBi), due to their large contribution to the global expression profile. Our GRO measurements during the first 3 hours of iron deficiency revealed that the TR of RP and RiBi genes declined when iron bioavailability was limited (Figure 4A; Supplementary Figure S7A). These experimental data supported that the RA of RP and RiBi genes was maintained in response to iron scarcity as a consequence of an increase in its stability (Figures 4B; Supplementary Figure S7B). To directly address it, we determined the half-life of three representative RP mRNAs (*RPL27A*, *RPL8B* and *RPS16B*) that exhibited a TR pattern below their RA profile, which was indicative of mRNA stabilization (Supplementary Figure S7C-E). Consistent with our genomic data, the mRNA half-life measurements of *RPL27A*, *RPL8B* and *RPS16B* mRNAs showed an important stabilization in iron-deficient conditions (Figure 4C-D). The Pub1 mRNA-binding protein has been implicated in the stabilization of RP mRNAs (26). Indeed, we observed a destabilization of the RP mRNAs *RPS16B* and *RPL8B* in *pub1*Δ as compared to wild-type cells (Supplementary Figure S8). Upon iron depletion, both wild-type and *pub1*Δ cells increased the mRNA half-life of the RP mRNAs analyzed, although the stabilization was less pronounced in the *pub1*Δ mutant (Supplementary Figure S8). These results indicate that the TR of RP genes diminishes during the initial stages of iron limitation, but their mRNA levels are partially compensated

through specific mRNA stabilization by Pub1 and other unknown regulatory factors.

Iron limitation inhibits Sfp1 and the Sch9 branch of the TORC1 pathway

We noticed that the median TR of genes included in the TR+RA cluster 7, and specifically the RP and RiBi genes, further decreased when the iron deficiency persisted (360 min; Figure 2; Supplementary Data S1). To ascertain whether this drop in TR had a consequence in the RA, we determined the mRNA levels of specific RP and RiBi genes by RT-qPCR in two different yeast backgrounds, W303 and BY4741. All the RP and RiBi genes tested diminished their RA when the iron deficiency period was extended (Figure 5A and 5B; Supplementary Figure S9). In the case of the W303 strain, 6 hours of iron depletion were sufficient to observe the down-regulation of RP and RiBi mRNAs (Figure 5A and 5B), whereas 9 hours were necessary for the BY4741 strain (BY4741 background) (Supplementary Figure S9). These results suggest that the stabilization of RP and RiBi genes cannot overcome the decrease in TR that occurs when the iron defect persists.

Multiple pathways regulate the transcription of RP and RiBi genes. One mechanism involves the transcription factor Sfp1 that, in response to stress or low nutrient availability, exits the nucleus, and RP and RiBi expression decreases (reviewed in (7)). To investigate the implication of Sfp1 in the response to iron starvation, we studied its subcellular localization under both iron-sufficient and deficient conditions. As expected, Sfp1 localized to the nucleus under iron-replete conditions (Figure 5C and 5D). Consistent with a decrease in RP and RiBi gene expression, Sfp1 exited the nucleus when iron was depleted (Figure 5C and 5D). These results demonstrate that Sfp1 subcellular localization responds to iron bioavailability, and probably alters RP and RiBi gene expression. Another mechanism that regulates RP and RiBi gene expression involves Stb3 and the paralog proteins Dot6 and Tod6, which recruit the RPD3L histone deacetylase complex to RP and RiBi promoters to repress transcription when growth conditions are not favorable (10). To test the involvement of these regulatory factors in iron-deficient conditions, we determined the fold change of multiple RP and RiBi mRNAs in *dot6*Δ*tod6*Δ, *stb3*Δ, and *rpd3*Δ mutants as compared to wild-type cells (BY4741 background). The RA of the RP genes tested decreased in the iron-deficient wild-type strain, whereas no decline was observed for the *stb3*Δ and *rpd3*Δ mutants (Figure 5E). Moreover, the RiBi RA down-regulation caused by iron depletion was disrupted in the *dot6*Δ*tod6*Δ and *rpd3*Δ mutants (Figure 5F). These results strongly suggest that Stb3 and Dot6-Tod6 repress the expression of RP and RiBi genes respectively in response to iron deficiency, via the Rpd3 histone deacetylase.

Under optimal growth conditions, the TORC1 kinase complex directly phosphorylates and activates Sfp1 transcription factor and Sch9 kinase (reviewed in (7)). Then, Sch9 phosphorylates Stb3 and Dot6-Tod6 proteins, inhibiting their function and facilitating the transcription of RP and RiBi genes to promote ribosome biogenesis and protein translation (10). Upon TORC1 inhibition, Sch9 is dephosphorylated and deactivated, and accordingly the downstream Stb3 and Dot6-Tod6 proteins are also dephosphorylated and become active in the repression of RP and RiBi genes. The Stb3 and Dot6-Tod6 dependent down-regulation of RP and RiBi genes promoted by the depletion of iron predicted a dephosphorylation of these regulatory factors. We observed that iron deficiency promoted an increase in the electrophoretic mobility of Dot6 protein and a decrease in its abundance similar to the one obtained by the addition of the TORC1 inhibitor rapamycin (Figure 5G). These results suggested that Dot6 protein is dephosphorylated in response to iron limitation. Then, we determined the phosphorylation state of the key TORC1-dependent kinase Sch9. We observed that Sch9 protein was gradually dephosphorylated and its abundance diminished during the advance of the iron deficiency to reach a stage similar to that obtained with the rapamycin treatment (Figure 5H). Collectively, these results strongly suggest that the dephosphorylation of the TORC1-dependent kinase Sch9 limits the expression of RP and RiBi genes in response to iron starvation via Stb3, Dot6-Tod6 and Rpd3.

Iron starvation limits the transcription of all RNA polymerases

The TORC1 pathway coordinates the expression of RP and RiBi genes to rRNA and tRNA synthesis in response to different environmental conditions. Specifically, TORC1 regulates at different stages the activity of RNA Pol I, which is responsible for the transcription of the 35S precursor of the mature 25S, 18S and 5.8S rRNAs, and RNA Pol III, which transcribes tRNA genes and the 5S rRNA (reviewed in (7)). Therefore, we explored whether the deprivation of iron altered the synthesis of rRNA. We first observed that the RA, which mostly (~80%) corresponds to rRNA, was fairly constant up to three hours of iron deficiency, but dropped to 50% after 6 hours (Figure 6A). Consistent with a drop in the RA, we observed both a decrease in the RNA Pol I TR and a down-regulation of *25S* and *18S* RNA levels along the iron starvation period (Figures 6B and 6C). Different mechanisms could account for the decrease in RNA Pol I activity. We observed that the protein levels of the largest subunit of the RNA Pol I complex, A190 (Rpa190), strongly diminished after 6 hours of iron deficiency, when the decrease in RNA Pol I TR is more severe (Figures 6B and 6D). Furthermore, the abundance of the RNA Pol I activating protein Rrn3, which is degraded in response to TORC1 inactivation (11), decreased at severe iron deficiency (Figure 6E; cells from BY4741 background). These results

demonstrate that the transcription of rRNAs by the RNA Pol I diminish in response to a prolonged iron deficiency.

The TORC1-dependent kinase Sch9 also regulates the RNA Pol III inhibitor protein Maf1. Under conditions favorable for growth, Sch9 phosphorylates Maf1, leading to its retention in the cytoplasm. On the contrary, TORC1 inactivation leads to the dephosphorylation of Maf1 and its accumulation in the nucleus where it binds to the RNA Pol III blocking tRNA synthesis (19). To investigate whether this branch of the TORC1 pathway was also altered by changes in iron availability, we determined the phosphorylation state of Maf1 protein under iron-deficient conditions. Similarly to the rapamycin treatment, the depletion of iron led to Maf1 dephosphorylation (Figure 6F; Supplementary Figure S10). Moreover, as shown for the biggest subunit of RNA Pol I and II (Figures 1B and 6D), the protein levels of the largest RNA Pol III subunit C160 (Rpc160) also diminished in response to low iron levels (Figure 6F). Consistent with defects in RNA Pol III activity, the levels of multiple tRNAs decreased in iron-deficient conditions (Figure 6G). The decrease in total and elongating RNA Pol II shown above (Figure 1C) matches with the pattern exhibited by the other two RNA Pol (Figure 6D and 6F). Thus, these results strongly suggest that the activity of all RNA polymerases decreases in response to iron deficiency via TORC1-dependent and probably independent mechanisms.

The efficiency of protein translation decreases in response to iron limitation

In addition to the regulation of RP and RiBi gene transcription, the inhibition of the TORC1 cascade promotes a decrease in the levels of newly synthesized ribosomal subunits that causes the nucleolar entrapment of specific ribosomal biogenesis factors (27). To address if this was the case of iron deficiency, we determined the subcellular localization of the Rrp12-GFP protein, which is trapped in the nucleolus upon TOR inactivation (27). We observed that the Rrp12-GFP protein did not properly distribute all over the cell when iron was scarce, but instead it was trapped in the nucleus (Supplementary Figure S11). We also determined the phosphorylation state of the small ribosomal subunit Rps6, which is phosphorylated by the Ypk3 kinase in a TORC1-dependent manner (28,29). By using an antibody specific for its phosphorylated form, we could state that Rps6 dephosphorylates upon iron depletion, whereas no changes were observed for the levels of total Rps6 protein (Figure 7A). Both Rrp12 mislocalization and Rps6 dephosphorylation support the inactivation of the TORC1 pathway by iron scarcity.

The drop of rRNA, tRNA, RP and RiBi mRNA levels suggested that protein translation could be defective during the advance of iron limitation due

to TORC1-mediated inhibition. To ascertain the efficiency of global protein translation, we determined the polysome profiles of wild-type W303 cells cultivated in iron-sufficient conditions or subjected to iron starvation. Only a slight decrease in polysome abundance was observed after three hours of iron deficiency (from 80% to 72%; Figure 7B and 7C). However, after six hours of depletion, we observed a significant increase of the monosomal ribosome peak and an important decrease in polysome abundance (from 80% to 44%), both indicative of a general repression of translation (Figure 7D). The TORC1 complex regulates the translation initiation factor eIF2α via both the Sch9 and the Tap42-PPase branches (18,30). Under optimal growth conditions, eIF2α properly initiates protein translation. However, upon amino acid starvation or TORC1-inhibition, the Gcn2 kinase is activated and phosphorylates eIF2α, which interferes with 5'cap-dependent mRNA translation. By using a specific antibody that only recognizes the phosphorylated form of eIF2α, we could determine that iron depletion promotes eIF2α phosphorylation without substantially altering its protein levels (Figure 7E). This result suggested that Gcn2 represses protein translation in response to iron deficiency. To test this hypothesis, we determined the polysome profile of wild-type and *gcn2*Δ cells under both iron-sufficient and deficient conditions, and observed that the deletion of *GCN2* partially rescued the repression of global translation caused by the depletion of iron (Supplementary Figure S12). Opposite to the global pattern, the translation of *GCN4*, which encodes for a transcriptional regulator of amino acid biosynthetic genes, is specifically favored when translation initiation is repressed by eIF2α phosphorylation due to the presence of short upstream open reading frames (31). To determine the translational state of the *GCN4* transcript in iron-deficient cells, we extracted RNA from the different polysomal fractions, and determined *GCN4* mRNA levels. Consistent with an activation of Gcn2 kinase at severe iron deficiency, we observed accumulation of the *GCN4* transcript in the monosomal fractions of cells in iron sufficiency, which was still maintained during mild iron deficiency (3 hours; Figure 7F). However, after 6 hours of iron deprivation, the *GCN4* mRNA shifted to the polysomal fractions, which evidenced ribosome enrichment and suggested an enhancement in its translation (Figure 7F). Collectively, these results strongly suggest that the inactivation of the TORC1 cascade during the progress of iron deficiency inhibits the general initiation of translation via Gcn2 and eIF2α factors.

Iron deficiency activates the mitochondrial retrograde pathway

The Lst8 integral component of the TORC1 kinase complex negatively regulates the mitochondrial retrograde (RTG) pathway. Therefore, TORC1 inhibition activates the RTG signaling. To address whether this was the case in iron deficiency, we paid attention to the TR of the RTG genes *IDH1*, *IDH2*,

CIT1, *CIT2* and *ACO1*, which were included in the TR+RA cluster 5. Remarkably, the TR of all of them augmented at severe iron depletion (Figure 8A). This TR up-regulation correlated with an increase in mRNA levels, except for the *ACO1* transcript (Figure 8B). Previous studies had shown that, in response to iron depletion, the mRNA-binding proteins Cth1 and Cth2 promote the degradation of multiple mRNAs including *ACO1* (3,4). Consistent with a simultaneous post-transcriptional decay by Cth1 and Cth2, we observed an increase in *ACO1* mRNA levels in iron-deficient *cth1*Δ*cth2*Δ cells (Supplementary Figure S13A). The Rtg1-Rtg3 transcription factors and the Rtg2 regulatory protein activate the RTG pathway in response to mitochondrial defects (12,13). Various observations indicated that they were also required for the activation of the RTG pathway when iron was scarce. First, no up-regulation in the mRNA levels of the different *RTG* genes was observed in iron-deficient *rtg1*Δ, *rtg2*Δ and *rtg3*Δ cells (Figure 8C). Second, a fusion of the *ACO1* promoter to *lacZ* caused an increase in β-galactosidase activity when iron was depleted, which did not occur in *rtg1*Δ, *rtg2*Δ and *rtg3*Δ cells (Supplementary Figure S13B). Third, RNA Pol II was recruited to the promoter of *RTG* genes in response to iron depletion in wild-type cells but not in *rtg1*Δ mutants (Figure 8D). And fourth, Rtg1 transcription factor moved to the nucleus upon iron deficiency (Figure 8E and 8F). Taken together, these results demonstrate that the mitochondrial RTG response is activated in response to iron depletion.

DISCUSSION

Both transcriptional and post-transcriptional mechanisms regulate the adaptation of yeast cells to iron deficiency

Gene expression studies on the yeast *S. cerevisiae* have focused on the alterations in steady-state mRNA levels that occur when iron is scarce. However, regardless of Aft1-Aft2 and Cth1-Cth2 mediated regulation, few studies have assessed whether the changes in mRNA levels in response to low iron conditions are under transcriptional or post-transcriptional control (32). The simultaneous determination of TR and RA performed here enables the indirect assessment of transcript decay rates and allows the identification of novel regulatory mechanisms otherwise hidden (17,24,25). For instance, the pronounced drop in TR observed for RP genes during the initial 3 hours of iron depletion did not turn into a parallel decrease in RA due to transcript stabilization partially mediated by the mRNA-binding protein Pub1 (Figure 4, Supplementary Figure S8). The transient mRNA stabilization of RP genes upon iron deficiency is a distinct effect from that observed in response to other stresses, such as heat shock, oxidative and osmotic stress, where RP genes exhibit a decrease in both TR and RA; but similar to what is observed under other nutritional stresses such as glucose deprivation (16,17,22,24,25,33). Moreover, the TR and RA profile displayed by the iron regulon (TR+RA cluster 1) suggests that mRNA stabilization also contributes to its up-regulation (Figure 2; Supplementary Figure S6). In fact, previous data had shown that multiple surveillance pathways, including RNase III, post-transcriptionally limit the expression of a subset of the iron regulon genes in iron-replete conditions (34). A decrease in the activity of these mRNA degradative pathways during the response to iron deficiency could account for the predicted up-regulation in transcript stability. The direct clustering of genes according to their k_D pattern also points out that, in addition to Cth1, Cth2 and Pub1, other post-transcriptional factors could be regulating genes that participate in mitochondrial respiration, protein synthesis and cell cycle control when iron is scarce. In the end, this global approach suggests that multiple transcriptional and post-transcriptional mechanisms to be explored regulate the response of yeast cells to iron deficiency.

Similarly to other stresses (22,24), iron depletion activates the yeast ESR program including the up-regulation of stress-related genes and the down-regulation of genes implicated in protein translation (Figure 3). The analysis of both RA and TR profiles for the ESR also suggests that this regulation is exerted at the level of transcription probably via Msn2/Msn4 for the iESR, and Sfp1, Dot6-Tod6 and Stb3 for the rESR. A recent study has demonstrated that the initiation of the ESR is not simply the consequence of changes in the growth

rate or the cell-cycle phase (23). Instead, failure to down-regulate the rESR genes leads to a defect in polysome association and translation of the iESR transcripts (23). These data strongly suggest that yeast stressed cells redirect its translational capacity toward the synthesis of the induced transcripts (23), which in the case of iron depletion would presumably include the machinery for iron uptake and mobilization, the RTG response, some stress-related genes, and essential iron-containing proteins such as Ole1 fatty acid desaturase. An important difference between the ESR signature observed in response to multiple non-lethal stresses and the profile observed in response to iron deficiency is that in the former case the ESR response is faster but transient (22,24), probably due to a recovery from the stress, whereas Iron deficiency, which is a nutritional defect, is irreversible and the ESR remains activated at an intermediate levels unless iron bioavailability resumes (Figure 3A).

Activation of the mitochondrial retrograde signaling in response to iron depletion

Despite the global decrease in TR that occurs in response to iron limitation, yeast cells remarkably activate the transcription of genes from the mitochondrial RTG via the Rtg1/Rtg3 and Rtg2 regulatory factors (Figure 8). The physiological significance of RTG activation by iron depletion could be to ensure the supply of sufficient α-ketoglutarate, which is the source of glutamate, required as a nitrogen donor for biosynthetic processes. This is especially important under iron-deficient conditions because the iron-requiring pathway for glutamate synthesis that depends on the iron sulfur cluster-containing enzyme glutamate synthase Glt1 is repressed, and all glutamate biosynthesis relies on glutamate dehydrogenases Gdh1 and Gdh3 (14). Several factors could contribute to the initiation of the mitochondrial RTG signaling in response to iron depletion. Iron deficiency limits the expression of multiple components of the TCA cycle and the electron transport chain, which compromises mitochondrial respiration and eventually could decrease ATP concentration and mitochondrial membrane potential, which is a signal to activate the retrograde response (35). Therefore, mitochondrial malfunctions would be the main candidate to trigger RTG activation when iron is scarce. However, other factors could participate in this regulation. For instance, the E3 ubiquitin ligase complex SCF^{Grr1}, which positively regulates RTG signaling by promoting the ubiquitination and degradation of the Rtg1/Rtg3-inhibitor protein Mks1, has been recently implicated in the degradation of the iron-regulated protein Cth2, and *grr1*Δ cells are unable to grow in iron-deficient conditions (36). Importantly, the integral component of the TORC1 complex Lst8 negatively regulates the RTG signaling pathway acting both upstream and downstream of Rtg2 (reviewed in (12,13)). The connection between the RTG and the TORC1 kinase pathway is

bidirectional, since mitochondrial dysfunctions also lead to a decrease in the phosphorylation state and activity of the Sch9 kinase (37).

The nutrient sensing TORC1 pathway is inactivated during the adaptation to iron deficiency

Studies in different organisms have suggested that TOR signaling influences iron metabolism (reviewed in (38)). Mammalian TOR (mTOR) modulates the expression of iron transporters and the cellular flux of iron via tristetraprolin, the mammalian Cth2 homologue (39). Consistent with this, an additional study showed that the disturbance of the mTORC1 pathway in red blood cells resulted in anemia (40). A proteomic study has also shown that TOR gene silencing deregulates the import of proteins into the mitochondria and the adaptation to iron starvation of the human pathogenic fungus *Aspergillus fumigatus* (41). In yeast, the inhibition of TOR pathway by Torin2, a potent inhibitor of both TORC1 and TORC2 has been recently shown to increase the expression of metalloreductases involved in iron uptake leading to excess iron sensitivity (42). The influence of cellular and systemic iron status on mTOR signaling has also been explored (38). To this end, the expression or phosphorylation status of either the mTOR kinase, its upstream regulators Akt, TSC2 or REDD1, or its downstream target ribosomal protein S6, have been determined. However, the conclusions obtained with these studies are contradictory. On one side, data with iron-deficient rats, murine red blood cells, human myeloid leukemia and intestinal epithelia cells suggest that iron depletion could inactivate mTOR signaling (40,43-45). On the other side, two genetic mouse models that cause neuronal-specific iron deficiency support the opposite conclusion (46). TORC1 studies in yeast have enormously increased our current understanding of the contribution of this pathway to nutrient signaling and growth control (7,8). By using a yeast genome-wide approach, we have shown here that iron deficiency inhibits protein synthesis via the TORC1 pathway. Multiple specific molecular markers including Sch9, Dot6, Rps6 and Maf1 dephosphorylation, eIF2α phosphorylation, nuclear retention of Rrp12, activation of the RTG pathway, decreased expression of RP, RiBi, rRNA and tRNA genes, and global repression of translation, are consistent with TORC1 inhibition when iron bioavailability decreases (Figure 9).

TORC1 constitutes a major hub to sense and respond to nutrients, in particular to amino acid and glucose levels (20). At the molecular level, TORC1 activity is regulated by different signaling pathways, which could be directly or indirectly influenced by iron depletion. Yeast TORC1 activity is controlled by two major mechanisms that depend on the conserved Gtr1 and Gtr2 GTPases and the aggregation of TORC1 into inactive vacuolar-associated aggregates called TOROIDs (TORC1 organized in inhibited domain) (47). A recent report has

described that both regulatory pathways are tightly coupled by a multilayered set of proteins including Gcn2 (48). In yeast, the biosynthesis of multiple amino acids including leucine, lysine, methionine and glutamate depends on iron-requiring enzymes. In fact, the biosynthesis of leucine, and probably lysine and methionine, decreases in response to iron depletion via specific Cth2-mediated degradation and metabolite-dependent decrease in the transcription of crucial iron-dependent enzymes (32). Therefore, despite that the synthetic complete medium used in these experiments is highly rich in amino acids and other nutrients, we cannot discard that a decrease in amino acid levels could facilitate the down-regulation of translation observed upon iron depletion via Gcn2-eIF2α or TORC1. Furthermore, recent studies suggest that Gcn4, which expression is activated upon phosphorylation and inhibition of eIF2α, can work as a repressor of protein synthesis under different stress conditions (49). A thorough and systematic study including multiple regulatory factors and the global metabolic adaptations that occur during the progress of iron deficiency would provide some insight onto the underlying molecular mechanisms. The alteration of cellular and systemic iron homeostasis is on the basis of many disorders including chronic anemia, hemochromatosis, thalassemia, aceruloplasminemia, various neurodegenerative diseases and cancer (50). TORC1 is also implicated in aging, cancer, cardiovascular diseases, and autoimmune and metabolic disorders such as diabetes and obesity (7,9). A better comprehension of the crosstalk between eukaryotic iron metabolism and TOR signaling in both yeast and mammals is necessary to understand the impact of current treatments and to develop novel therapeutic strategies for both iron and TOR related diseases in a selective manner.

SUPPLEMENTARY DATA

Supplementary Data are available at NAR online.

ACKNOWLEDGEMENT

We thank the members of the "Iron Homeostasis" and "Yeast Functional Genomics" laboratories for scientific comments and technical assistance, especially Dr. Paula Alepuz, Dr. Daniel Medina, and Pilar Miró. We are also grateful to Drs. Emilia Matallana, Olga Calvo, Francisco Navarro, Francisco Estruch, John Zaborske, Olivier Lefebvre, Fred Cross, Andrew Capaldi, Joachim Griesenbeck, Charles Moehle, and Ted Powers for providing yeast strains, plasmids or antibodies used in this study.

FUNDING

This work was supported by predoctoral contracts from the Spanish Ministry of Science, Innovation and Universities (MICINN) to AMR and LRA; a fellowship from the "Generalitat de Catalunya" (Spain) to SMM; European Union Funds (FEDER) and MICINN grants BIO2017-87828-C2-1-P to SP, BIO2017-87828-C2-2-P to MATR, BFU2016-77728-C3-3-P to JEPO, and BFU2015-71978-REDT to SP and JEPO; and Regional Government of Valencia PROMETEOII 2015/006 grant to JEPO.

CONFLICT OF INTEREST

The authors declare no conflict of interest associated with this manuscript.

FIGURE LEGENDS

Figure 1. Changes in RNA polymerase II during the progress of iron deficiency.

(A) RNA Pol II transcription rate (TR) and total poly(A) mRNA (RA) per cell. At time zero, 100 µM BPS was added to W303 cells exponentially growing in SC at 30°C. Aliquots were processed to measure total RA per cell and RNA Pol II TR per cell at the indicated times, (Materials and Methods). The values were referred to their respective values at time zero. The standard deviation of at least three biologically independent replicates is shown. **(B)** *RPB1* mRNA levels were determined by RT-qPCR using specific primers. Average values and standard deviations from at least two independent experiments are shown and referred to those in time zero. **(C)** The levels of total and elongating RNA pol II were determined by Western blot analyses using the anti-Rpb1 antibody that recognizes all the RNA pol II molecules and the anti-Ser2-phosphorylated antibody that measures elongating RNA pol II. A representative experiment of three independent biological replicates is shown.

Figure 2. Global changes in TR and RA during the progress in iron deficiency corresponding to each cluster.

The graphs represent the median TR and RA for all genes included in each group. The values are referred to time zero. Clusters are defined in Supplementary Figure S3.

Figure 3. Activation of the ESR in response to iron depletion. (A) The

median TR and RA corresponding to the genes classified as iESR and rESR was represented during the progress of the iron deficiency and referred to the normalized global patterns of TR and RA, respectively. The median RA pattern of the iESR and rESR genes in response to the oxidative stress achieved by addition of 0.1 mM *ter*-butyl hydroperoxide previously reported (25) is also represented as ESR-ox (circles). **(B)** Msn2 and Msn4 transcription factors are required for growth in iron-deficient conditions. Wild-type BY4741 and *msn2*Δ*msn4*Δ double mutant were grown in SC (+Fe) and SC with 600 µM Ferrozine (-Fe).

Figure 4. The stability of the RP mRNAs increases in response to iron scarcity.

(A) TR and RA profiles for RP mRNAs during the first three hours in iron deficiency. **(B)** Representation of the median of the k_D values corresponding to the RP mRNAs. The values are referred to value 1 at time zero. **(C, D, E)** Experimental determination of mRNA half-life. W303 cells were grown at 30 °C for 3 hours in SC (+Fe) or in SC with 100 µM BPS (-Fe). Then,

thiolutin (3 µg/mL) was added to stop transcription. *RPL27A*, *RPL8B* and *RPS16B* mRNA levels were determined by RT-qPCR using random primers for reverse transcription and specific primers for qPCR. *SCR1* levels were used as a loading control. Mean values of mRNA half-lives were calculated on the basis of at least three independent experiments and standard deviation is represented.

Figure 5. Regulation of Sfp1, Sch9, Dot6, Stb3, Rpd3, RP and RiBi genes in **response to iron deficiency. (A, B)** Determination of specific RP and RiBi mRNA levels during the progress of iron deficiency by RT-qPCR. W303 cells were grown as indicated in Figure 1A (GRO experiment). *ACT1* mRNA levels were used to normalize. Mean values and standard deviations from at least two independent experiments are shown and referred to time zero. **(C, D)** Sfp1 relocalizes to the cytoplasm in response to iron deficiency. Wild type yeast cells transformed with the SFP1-GFP plasmid were grown at 30 °C in SD (+Fe) and SD with 10 µM BPS (-Fe) for 8 hours. Sfp1-GFP subcellular localization was determined by fluorescence microscopy. Representative images are shown (panel C). The white bar represents 10 µm. The percentage of cells with either predominantly cytoplasmic or nuclear GFP signal was determined by triplicate. The average and the standard deviation are represented (Panel D). **(E, F)** Fold change in RP and RiBi mRNA levels. Wild type BY4741, *dot6Δtod6Δ*, *stb3Δ* y *rpd3Δ* yeast strains were grown at 30 °C in SC (+Fe) and SC with 100 µM BPS (-Fe) for 9 hours. Specific mRNA levels of RP and RiBi genes were determined as mentioned above. Mean values of fold induction in iron deficiency and standard deviations from at least two independent experiments are shown. **(G)** Dot6 protein levels. Yeast cells expressing *DOT6-HA* were grown at 30 °C in SC (+Fe), SC with 100 µM BPS (-Fe) for 9 hours and in the presence of rapamycin (200 ng/ml) for 30 minutes. Dot6-HA and Pgk1 protein levels were analyzed by western blot with anti-HA and anti-Pgk1 antibodies, respectively. **(H)** Determination of Sch9 protein levels and phosphorylation state. Yeast cells expressing *SCH9-HA* were grown as in panel E and NTCB-treated protein extracts were analyzed as described in Materials and methods.

Figure 6. The activities of RNA polymerase I and III are inhibited in iron **scarcity. (A)** Total RNA per cell during the iron deficiency kinetics. W303 cells were grown as in Figure 1A and total RNA per cell determined. **(B)** The RNA Pol I transcription rate was determined by summing up the specific probes for *18S* and *25S* in every time point of the GRO experiment. **(C)** The *18S* and *25S* RNA levels were analyzed by RT-qPCR using specific primers. *ACT1* was used to normalize. **(D)** The protein levels of the largest RNA Pol I subunit Rpa190 and Pgk1 were determined by Western Blot using the anti-Rpa190 and anti-

Pgk1 antibodies, respectively. **(E)** Determination of Rrn3 protein levels. Yeast BY4741 cells expressing *RRN3-GFP* were grown at 30 °C in SC (+Fe) and SC with 100 µM BPS (-Fe) for 9 hours. Rrn3-GFP and Pgk1 protein levels were analyzed with anti-GFP and anti-Pgk1 antibodies, respectively. **(F)** Yeast BY4741 cells expressing RPC160-HA were grown at 30 °C in SC (+Fe), SC with 100 µM BPS (-Fe) for 11 hours and in presence of rapamycin (200 ng/ml) for 30 minutes. Rpc160-HA, Maf1 and Pgk1 protein levels were analyzed by Western blot with anti-HA, anti-Maf1 and anti-Pgk1 antibodies, respectively. **(G)** Determination of specific tRNA levels. The level of some tRNAs was determined in the same conditions as mentioned to develop the GRO by RT-qPCR using specific primers. *ACT1* was used to normalize.

Figure 7. A general repression of protein translation occurs in response

iron deficiency. (A) Determination of Rps6 protein levels and phosphorylation state. W303 cells were grown as described in Figure 1A. The levels of total Rps6 and phosphorylated Rps6 protein were determined by Western blot analyses using the anti-Rps6 and anti-Rps6-Ser235/236 antibodies, respectively. A representative experiment of three independent biological replicates is shown. **(B, C, D)** Polysome profiles. W303 cells were grown in SC (+Fe) and SC with 100 µM BPS (-Fe) for 3 and 6 hours. Polysomal fractionations were obtained as described in Materials and Methods. The A_{260nm} profiles after gradient fractionation are shown and the ribosomal subunits (40S and 60S), monosomes (80S) and polysomes are indicated. The percentage of polysomes and the polysomes/monosomes (P/M) ratio are represented in each condition. **(E)** Determination of eIF2α protein levels and phosphorylation state. The levels of total eIF2α and phosphorylated eIF2α protein were determined by Western blot analyses using the anti-eIF2α and anti-eIF2α-Ser51/52 antibodies, respectively. A representative experiment of three independent biological replicates is shown. **(F)** Pattern of the *GCN4* mRNA in the polysome profile. The RNA from individual fractions of the polyribosome profiles was extracted and *GCN4* mRNA levels were analyzed by RT-qPCR as described in Materials and Methods.

Figure 8. The retrograde pathway is transcriptionally activated upon iron

depletion. (A) Transcription rates of *RTG* genes during the response to iron deficiency obtained from the GRO experiment. **(B)** Fold induction of *RTG* mRNA levels in response to low iron. W303 cells were grown as described in Figure 1A, and RNA extracted and analyzed at six hours of iron deficiency by RT-qPCR using specific primers. **(C)** Wild type BY4741, *rtg1Δ, rtg2Δ and rtg3Δ* strains were grown at 30 °C in SC (+Fe) and SC with 100 µM BPS (-Fe) for 9 hours. The mRNA levels of specific *RTG* genes were determined by RT-qPCR

using specific primers. *ACT1* was used as a loading control. Mean values of fold induction in iron deficiency and standard deviations from at least two independent experiments are shown. **(D)** RNA Pol II chromatin immunoprecipitation. The wild-type BY4741 and *rtg1Δ* cells were grown as described in panel B. Proteins were extracted and immunoprecipitated with anti-RNA Pol II monoclonal antibody. DNA was extracted and binding to *RTG* promoter regions was determined by RT-qPCR. The results were normalized to *FUS1* promoter. Mean values of fold induction in iron deficiency and standard deviations from at least two independent experiments are shown. **(E, F)** Rtg1 moves to the nucleus in response to iron deficiency. Wild type yeast cells transformed with the RTG1-GFP plasmid were grown at 30 °C in SD (+Fe) and SD with 10 µM BPS (-Fe) for 8 hours. Rtg1-GFP subcellular localization was determined by fluorescence microscopy. Representative images are shown (panel E). The white bar represents 10 µm. The percentage of cells with either predominantly cytoplasmic or nuclear GFP signal was determined by triplicate. The average and the standard deviation are represented (Panel F).

Figure 9. A model for TORC1 regulation in response to iron depletion.

TORC1 regulates protein and ribosome synthesis, as well as metabolic pathways including the retrograde response mostly via Sch9 kinase and Tap42-PP2A protein phosphatases. Upon iron deficiency, yeast cells inhibit the TORC1 pathway, and consequently yeast cells repress the transcription of RP and RiBi genes, translational initiation, and the activity of the RNA Pol I and III. Moreover, the ESR and RTG pathways are transcriptionally activated in response to iron scarcity.

SUPPLEMENTARY FIGURE LEGENDS

Supplementary Figure S1. Determination of specific parameters during the iron deficiency experiment.

(A) W303 cells were grown in SC (+Fe) and SC with 100 µM BPS (-Fe). The OD_{600nm} was measured to compare growth in both conditions. The values were referred to their respective values at time zero. **(B)** Yeast W303 and BY4741 cells were grown in SC with 100 µM BPS (-Fe). The OD_{600nm} was measured to compare growth in both strains during the advance of iron deficiency. **(C)** Changes in glucose and ethanol levels were obtained by HPLC analysis during the progress of iron starvation. **(D)** Cell volume was determined during the growth in iron-deficient conditions as described in Materials and Methods. The standard deviation of at least three biologically independent replicates is shown.

Supplementary Figure S2. Changes in global k_D values in response to iron deficiency.

The graph represents the median k_D value for all genes at each indicated time referred to time zero. The values were calculated as described in Materials and Methods.

Supplemental Figure S3. Clustering of genes according to their TR and RA profiles.

Time course profiles for both parameters were considered for clustering. Dataset series are referred to their respective time zero in logarithm scale. Relative repression is shown in green and relative induction in red. The most significant GO categories (p value $\leq 10^{-4}$) are indicated with their respective p values. The individual data for each gene and the list of genes in each cluster are listed in Supplementary Data S1 and S2, respectively.

Supplemental Figure S4. Clustering of genes according to their k_D profile.

The time course profile for k_D was considered for clustering. The dataset is referred to its time zero in logarithm scale. Relative decrease in k_D is shown in green and relative increase in red. The most significant GO categories (p value $\leq 10^{-4}$) are indicated with their respective p values. The individual data for each gene and the list of genes in each cluster are listed in Supplementary Data S4.

Supplementary Figure S5. Clustering of genes according to their k_D profiles in response to iron depletion.

Representation of the mean k_D value corresponding to all the genes in each cluster relative to time zero as a function of time.

Supplementary Figure S6. Predicted stability of mRNAs corresponding to **the different TR+RA gene clusters after iron depletion.** Representation of the mean k_D value corresponding to all the genes in each TR+RA cluster relative to time zero in function of time.

Supplementary Figure S7. Expression of RiBi genes in response to iron **deficiency. (A)** TR and RA profiles for RiBi mRNAs during the first three hours in iron deficiency. **(B)** Representation of the median of the k_D values corresponding to the RiBi mRNAs. All values are referred to time zero. **(C-E)** TR and RA profiles for *RPL27A*, *RPL8B* and *RPS16B* mRNAs during the iron limitation progress.

Supplementary Figure S8. Role of Pub1 in the stability of RP mRNAs. W303 and *pub1Δ* cells were grown at 30°C for 3 hours in SC (+Fe) or in SC with 100 µM BPS (-Fe). Then, thiolutin (3 µg/mL) was added to stop transcription. *RPL27A*, *RPL8B* and *RPS16B* mRNA levels were determined by RT-qPCR using random primers for reverse transcription and specific primers for qPCR. *SCR1* was used to normalize. Mean values of mRNA half-lives (calculated on the basis of at least three independent experiments) and standard deviation are represented.

Supplementary Figure S9. RP and RiBi mRNA levels decrease in response **to severe iron deficiency. (A, B)** Wild type BY4741 strain was grown at 30°C in SC with 100 µM BPS (-Fe) for 9 hours. The levels of specific RP and RiBi genes were determined by RT-qPCR using specific primers. *ACT1* was used to normalize. Mean values and standard deviations from at least two independent experiments are shown and referred to time zero.

Supplementary Figure S10. Maf1 is dephosphorylated during the iron **deficiency progress.** W303 cells were grown as described in Figure 1A. The phosphorylation state of Maf1 protein was analyzed by immunoblotting using an anti-Maf1 antibody. Pgk1 protein levels were used as a loading control.

Supplementary Figure S11. Rrp12 is anchored in the nucleolus in iron- **deficient conditions.** Yeast cells expressing *RRP12-GFP* were grown in SC (+Fe) and SC with 100 µM BPS (-Fe) and were visualized after 9 hours of

growth. DIC, differential interference microscopy. DAPI, 4',6-diamidino-2-phenylindole.

Supplementary Figure S12. *GCN2* deletion improves translation during the **growth in iron scarcity.** Wild type BY4741 and *gcn2Δ* strains were grown in SC (+Fe) and SC with 100 µM BPS (-Fe) for 9 hours. Polysome fractionation was carried out as described in Materials and Methods. The A_{260nm} profiles after gradient fractionation are shown and the ribosomal subunits (40S and 60S), monosomes (80S) and polysomes are indicated. The percentage of polysomes and the P/M ratio are represented in each condition.

Supplementary Figure S13. *ACO1* is transcriptionally and post-**transcriptionally regulated in response to iron deficiency. (A)** Wild type BY4741 and *cth1Δcth2Δ* strains were grown in SC (+Fe) and SC with 100 µM BPS (-Fe) for 9 hours. *ACO1* mRNA levels were determined by RT-qPCR. Mean values of fold induction in iron deficiency and standard deviations from at least two independent experiments are shown. **(B)** Wild type BY4741, *rtg1Δ, rtg2Δ and rtg3Δ* strains transformed with the plasmid P_{ACO1}-lacZ were grown at 30 °C in SC-ura (+Fe) and SC-ura with 100 µM BPS (-Fe) for 9 hours. β-Galactosidase assays were carried out as described in Materials and Methods. Mean values of fold induction in iron scarcity and standard deviations from at least two independent experiments are shown.

SUPPLEMENTARY TABLES

Supplementary Table S1. List of *Saccharomyces cerevisiae* strains used in this work.

Strain	Description	Source
W303a	HTLU-2832-1B: *HIS3, TRP1, LEU2, URA3, ADE2, can1*	Fred Cross
pub1Δ	*W303a pub1::KanMX4*	This work
BY4741	*MATa, his3Δ1, leu2Δ0, met15Δ0, ura3Δ0*	Research Genetics
rpd3Δ	*BY4741 rpd3::KanMX4*	This work
dot6Δtod6Δ	*BY4741 dot6::KanMX4, tod6::HIS3MX6*	This work
stb3Δ	*BY4741 stb3::KanMX4*	Research Genetics
Sch9-HA	ACY359: *Sch9-HA (TRP1)*	Andrew Capaldi
Dot6-HA	ACY322: *Dot6-HA (KanMX)*	Andrew Capaldi
Rrp12-GFP	*BY4741 RRP12-GFP-HIS3MX6*	Joachim Griesenbeck
Rrn3-GFP	OCG0150	Olga Calvo
HA-RPC160	MW671: *MATα, ade2-101, ade2-101, lys2-801, leu2-delta1, his3delta200, ura3-52, trp1-delta63, rpc160-1::HIS3, pC160-240[TRP1 HA-RPC160]*	Francisco Navarro
rtg1Δ	*BY4741 rtg1::KanMX4*	Research Genetics
rtg2Δ	*BY4741 rtg2::KanMX4*	Research Genetics
rtg3Δ	*BY4741 rtg3::KanMX4*	Research Genetics
msn2Δmsn4Δ	*MATa, ade2-101, trp1Δ, msn4-Δ2::URA3, msn2-Δ3::HIS3*	Francisco Estruch

Supplementary Table S2. List of oligonucleotides used for RT-qPCR and ChIP in this work.

Name	*Sequence (from 5' to 3')*
ACO1-613-BglII-F	GGAAGATCTTATACTTCGCACTTTACATAT
ACO1:6-BamHI-R	CGCGGATCCCAGCATTGTATATCTATAGTA
ACT1-qPCR-F	TCGTTCCAATTTACGCTGGTT
ACT1-qPCR-R	CGGCCAAATCGATTCTCAA
SCR1-qPCR-F	TATCCAGCGTCAGCAAAGGT
SCR1-qPCR-R	CCAAATTAAACCGCCGAAG
RPB1-qPCR-F	CCAGAAGTGGTCACACCATATAA
RPB1-qPCR-R	GGTCTCCGCTATCACGAATG
RPL17A-qPCR-F	TCTTCTCCATCCCACATTGA
RPL17A-qPCR-R	GCGGCGATTCTACCTCTTT
RPL8B-qPCR-F	GGGTGTTCCATACGCCATT
RPL8B-qPCR-R	TTCGTCTTCGGCTCTGACTT
RPS16B-qPCR-F	GACGAACAATCCAAGAACGA
RPS16B-qPCR-R	AGAACGAGCACCCTTACCAC
RPL27A-qPCR-F	AGTTGCTGTCGTTGTCCGTG
RPL27A-qPCR-R	ATGGGTGAGACTTGGAACCT
18S-qPCR-F	CATGGCCGTTCTTAGTTGGT
18S-qPCR-R	ATTGCCTCAAACTTCCATCG
25S-qPCR-F	ATTGTCAGGTGGGGAGTTTG
25S-qPCR-R	GGGGCTTTTACCCTTTTGTT
tL(UAA)-qPCR-F	CTGTGGGAATACTCAGGTATCGT
tL(UAA)-qPCR-R	TTTCTCGTCTTTAGTCGGCTTC
tV(UAC)-qPCR-F	TCCTAAGCTGTCATCCGTAA
tV(UAC)-qPCR-R	ATCGAACTCGGGACCTTTG
tS(AGA)J-qPCR-F	CGAGTGGTTAAGGCGAAAGA
tS(AGA)J-qPCR-R	GGCAAAGCCCAAAAGATTTC
tK(CUU)C-qPCR-F	AATCGGTAGCGCGTATGACT
tK(CUU)C-qPCR-R	GCTCGAACCCCTAACCTTAT
LTV1-qPCR-F	CGTTTTGGTTCCTGTCTCCA
LTV1-qPCR-R	CCCTCCTACCCTTTGGTTTT
SRO9-qPCR-F	GAATCGGCAGTAGGTGAGGA
SRO9-qPCR-R	AGGTGGTTGTTGCTGTTGTG
GUA1-qPCR-F	ACTTCGCCGTTGATTTGTGT
GUA1-qPCR-R	GGACCGACCAGTTTTCTGATT
NOP14-qPCR-F	GAAGAAGGCGAAGAAAGAGGA
NOP14-qPCR-R	CAGAATCAGCAATACCGTCA
BRX1-qPCR-F	TGAAGATGGCGAAGAAGACA
BRX1-qPCR-R	GGACCACCAAATGAACC
GCN4-qPCR-F	GACAACTTCATTCTTACCCACTCC

GCN4-qPCR-R	GATTCGTCATCCTTTCCAACA
CIT1-qPCR-F	GGTCGTGCCAATCAAGAAGT
CIT1-qPCR-R	TGCGTTCAAAGTATCCCACA
CIT2-qPCR-F	GATTTCGTGGACTTGATGAGAC
CIT2-qPCR-R	GGGACAGATAAGGTGATGATAGTG
IDH1-qPCR-F	GAGAAAACACGGAGGGTGAG
IDH1-qPCR-R	GGCGAAGTCAAAGGCAAATC
IDH2-qPCR-F	CGAGGAGGTTTTTGGCTACT
IDH2-qPCR-R	TCAGGTCCGATACCATCACC
DLD3-qPCR-F	AGGACTTGCCTTTCCCTCTG
DLD3-qPCR-R	GCTTCTCATCGTCGTGTCTCT
ACO1-qPCR-F	GCCATCAAGAGACCCATTGT
ACO1-qPCR-R	ATCCAGCGTTTCCACATTCT
DLD3-ChIP-prom-183F	GGATGACACCACTTGCCACA
DLD3-ChIP-prom-57R	GCATTTTGGCACCCTGTTCT
IDH1-ChIP-prom-150F	CCGCTTCATTGGCTTATTCTTG
IDH1-ChIP-prom-25R	AGGGAGAAGAATGAGGATAGGG
CIT2-ChIP-prom-159F	GGCCCATTATTCTCGACGTT
CIT2-ChIP-prom-85R	TGAGGAACGAACACCATATC
ACO1-ChIP-prom-186F	GAAAGGCAAGCACAAAAAGG
ACO1-ChIP-prom-64R	GAGTGAACAGAACAAGGGACAA
FUS1-ChIP-prom-F	CATGTGGACCCTTTCAAAAC
FUS1-ChIP-prom-R	AGACAGCGCGAAAAGTGACA

REFERENCES

1. Zimmermann, M.B. and Hurrell, R.F. (2007) Nutritional iron deficiency. *Lancet*, **370**, 511-520.
2. Philpott, C.C. and Protchenko, O. (2008) Response to iron deprivation in Saccharomyces cerevisiae. *Eukaryot Cell*, **7**, 20-27.
3. Puig, S., Askeland, E. and Thiele, D.J. (2005) Coordinated remodeling of cellular metabolism during iron deficiency through targeted mRNA degradation. *Cell*, **120**, 99-110.
4. Puig, S., Vergara, S.V. and Thiele, D.J. (2008) Cooperation of two mRNA-binding proteins drives metabolic adaptation to iron deficiency. *Cell Metab*, **7**, 555-564.
5. Ramos-Alonso, L., Romero, A.M., Soler, M.A., Perea-Garcia, A., Alepuz, P., Puig, S. and Martinez-Pastor, M.T. (2018) Yeast Cth2 protein represses the translation of ARE-containing mRNAs in response to iron deficiency. *PLoS Genet*, **14**, e1007476.
6. Prouteau, M., Daugeron, M.C. and Seraphin, B. (2008) Regulation of ARE transcript 3' end processing by the yeast Cth2 mRNA decay factor. *EMBO J*, **27**, 2966-2976.
7. Loewith, R. and Hall, M.N. (2011) Target of rapamycin (TOR) in nutrient signaling and growth control. *Genetics*, **189**, 1177-1201.
8. Gonzalez, A. and Hall, M.N. (2017) Nutrient sensing and TOR signaling in yeast and mammals. *EMBO J*, **36**, 397-408.
9. Wullschleger, S., Loewith, R. and Hall, M.N. (2006) TOR signaling in growth and metabolism. *Cell*, **124**, 471-484.
10. Huber, A., French, S.L., Tekotte, H., Yerlikaya, S., Stahl, M., Perepelkina, M.P., Tyers, M., Rougemont, J., Beyer, A.L. and Loewith, R. (2011) Sch9 regulates ribosome biogenesis via Stb3, Dot6 and Tod6 and the histone deacetylase complex RPD3L. *EMBO J*, **30**, 3052-3064.
11. Philippi, A., Steinbauer, R., Reiter, A., Fath, S., Leger-Silvestre, I., Milkereit, P., Griesenbeck, J. and Tschochner, H. (2010) TOR-dependent reduction in the expression level of Rrn3p lowers the activity of the yeast RNA Pol I machinery, but does not account for the strong inhibition of rRNA production. *Nucleic Acids Res*, **38**, 5315-5326.
12. Jazwinski, S.M. (2014) The retrograde response: a conserved compensatory reaction to damage from within and from without. *Prog Mol Biol Transl Sci*, **127**, 133-154.
13. Liu, Z. and Butow, R.A. (2006) Mitochondrial retrograde signaling. *Annu Rev Genet*, **40**, 159-185.
14. Shakoury-Elizeh, M., Tiedeman, J., Rashford, J., Ferea, T., Demeter, J., Garcia, E., Rolfes, R., Brown, P.O., Botstein, D. and Philpott, C.C. (2004) Transcriptional remodeling in response to iron deprivation in Saccharomyces cerevisiae. *Mol Biol Cell*, **15**, 1233-1243.
15. Hausmann, A., Samans, B., Lill, R. and Muhlenhoff, U. (2008) Cellular and mitochondrial remodeling upon defects in iron-sulfur protein biogenesis. *J Biol Chem*, **283**, 8318-8330.

16. Garcia-Martinez, J., Aranda, A. and Perez-Ortin, J.E. (2004) Genomic run-on evaluates transcription rates for all yeast genes and identifies gene regulatory mechanisms. *Mol Cell*, **15**, 303-313.
17. Romero-Santacreu, L., Moreno, J., Perez-Ortin, J.E. and Alepuz, P. (2009) Specific and global regulation of mRNA stability during osmotic stress in Saccharomyces cerevisiae. *RNA*, **15**, 1110-1120.
18. Urban, J., Soulard, A., Huber, A., Lippman, S., Mukhopadhyay, D., Deloche, O., Wanke, V., Anrather, D., Ammerer, G., Riezman, H. *et al.* (2007) Sch9 is a major target of TORC1 in Saccharomyces cerevisiae. *Mol Cell*, **26**, 663-674.
19. Oficjalska-Pham, D., Harismendy, O., Smagowicz, W.J., Gonzalez de Peredo, A., Boguta, M., Sentenac, A. and Lefebvre, O. (2006) General repression of RNA polymerase III transcription is triggered by protein phosphatase type 2A-mediated dephosphorylation of Maf1. *Mol Cell*, **22**, 623-632.
20. Hughes Hallett, J.E., Luo, X. and Capaldi, A.P. (2014) State transitions in the TORC1 signaling pathway and information processing in Saccharomyces cerevisiae. *Genetics*, **198**, 773-786.
21. Romero, A.M., Jorda, T., Rozes, N., Martinez-Pastor, M.T. and Puig, S. (2018) Regulation of yeast fatty acid desaturase in response to iron deficiency. *Biochim Biophys Acta Mol Cell Biol Lipids*, **1863**, 657-668.
22. Gasch, A.P., Spellman, P.T., Kao, C.M., Carmel-Harel, O., Eisen, M.B., Storz, G., Botstein, D. and Brown, P.O. (2000) Genomic expression programs in the response of yeast cells to environmental changes. *Mol Biol Cell*, **11**, 4241-4257.
23. Ho, Y.H., Shishkova, E., Hose, J., Coon, J.J. and Gasch, A.P. (2018) Decoupling Yeast Cell Division and Stress Defense Implicates mRNA Repression in Translational Reallocation during Stress. *Curr Biol*, **28**, 2673-2680 e2674.
24. Canadell, D., Garcia-Martinez, J., Alepuz, P., Perez-Ortin, J.E. and Arino, J. (2015) Impact of high pH stress on yeast gene expression: A comprehensive analysis of mRNA turnover during stress responses. *Biochim Biophys Acta*, **1849**, 653-664.
25. Molina-Navarro, M.M., Castells-Roca, L., Belli, G., Garcia-Martinez, J., Marin-Navarro, J., Moreno, J., Perez-Ortin, J.E. and Herrero, E. (2008) Comprehensive transcriptional analysis of the oxidative response in yeast. *J Biol Chem*, **283**, 17908-17918.
26. Grigull, J., Mnaimneh, S., Pootoolal, J., Robinson, M.D. and Hughes, T.R. (2004) Genome-wide analysis of mRNA stability using transcription inhibitors and microarrays reveals posttranscriptional control of ribosome biogenesis factors. *Mol Cell Biol*, **24**, 5534-5547.
27. Reiter, A., Steinbauer, R., Philippi, A., Gerber, J., Tschochner, H., Milkereit, P. and Griesenbeck, J. (2011) Reduction in ribosomal protein synthesis is sufficient to explain major effects on ribosome production after short-term TOR inactivation in Saccharomyces cerevisiae. *Mol Cell Biol*, **31**, 803-817.
28. Yerlikaya, S., Meusburger, M., Kumari, R., Huber, A., Anrather, D., Costanzo, M., Boone, C., Ammerer, G., Baranov, P.V. and Loewith, R. (2016) TORC1 and TORC2 work together to regulate ribosomal protein S6 phosphorylation in Saccharomyces cerevisiae. *Mol Biol Cell*, **27**, 397-409.
29. Gonzalez, A., Shimobayashi, M., Eisenberg, T., Merle, D.A., Pendl, T., Hall, M.N. and Moustafa, T. (2015) TORC1 promotes phosphorylation of

ribosomal protein S6 via the AGC kinase Ypk3 in Saccharomyces cerevisiae. *PLoS One*, **10**, e0120250.

30. Cherkasova, V.A. and Hinnebusch, A.G. (2003) Translational control by TOR and TAP42 through dephosphorylation of eIF2alpha kinase GCN2. *Genes Dev*, **17**, 859-872.
31. Hinnebusch, A.G. (2005) Translational regulation of GCN4 and the general amino acid control of yeast. *Annu Rev Microbiol*, **59**, 407-450.
32. Ihrig, J., Hausmann, A., Hain, A., Richter, N., Hamza, I., Lill, R. and Muhlenhoff, U. (2010) Iron regulation through the back door: iron-dependent metabolite levels contribute to transcriptional adaptation to iron deprivation in *Saccharomyces cerevisiae*. *Eukaryot Cell*, **9**, 460-471.
33. Castells-Roca, L., Pijuan, J., Ferrezuelo, F., Belli, G. and Herrero, E. (2016) Cth2 Protein Mediates Early Adaptation of Yeast Cells to Oxidative Stress Conditions. *PLoS One*, **11**, e0148204.
34. Lee, A., Henras, A.K. and Chanfreau, G. (2005) Multiple RNA surveillance pathways limit aberrant expression of iron uptake mRNAs and prevent iron toxicity in S. cerevisiae. *Mol Cell*, **19**, 39-51.
35. Miceli, M.V., Jiang, J.C., Tiwari, A., Rodriguez-Quinones, J.F. and Jazwinski, S.M. (2011) Loss of mitochondrial membrane potential triggers the retrograde response extending yeast replicative lifespan. *Front Genet*, **2**, 102.
36. Romero, A.M., Martinez-Pastor, M., Du, G., Sole, C., Carlos, M., Vergara, S.V., Sanvisens, N., Wohlschlegel, J.A., Toczyski, D.P., Posas, F. *et al.* (2018) Phosphorylation and Proteasome Recognition of the mRNA-Binding Protein Cth2 Facilitates Yeast Adaptation to Iron Deficiency. *MBio*, **9**.
37. Kawai, S., Urban, J., Piccolis, M., Panchaud, N., De Virgilio, C. and Loewith, R. (2011) Mitochondrial genomic dysfunction causes dephosphorylation of Sch9 in the yeast Saccharomyces cerevisiae. *Eukaryot Cell*, **10**, 1367-1369.
38. Guan, P. and Wang, N. (2014) Mammalian target of rapamycin coordinates iron metabolism with iron-sulfur cluster assembly enzyme and tristetraprolin. *Nutrition*, **30**, 968-974.
39. Bayeva, M., Khechaduri, A., Puig, S., Chang, H.C., Patial, S., Blackshear, P.J. and Ardehali, H. (2012) mTOR regulates cellular iron homeostasis through tristetraprolin. *Cell Metab*, **16**, 645-657.
40. Knight, Z.A., Schmidt, S.F., Birsoy, K., Tan, K. and Friedman, J.M. (2014) A critical role for mTORC1 in erythropoiesis and anemia. *Elife*, **3**, e01913.
41. Baldin, C., Valiante, V., Kruger, T., Schafferer, L., Haas, H., Kniemeyer, O. and Brakhage, A.A. (2015) Comparative proteomics of a tor inducible Aspergillus fumigatus mutant reveals involvement of the Tor kinase in iron regulation. *Proteomics*, **15**, 2230-2243.
42. Kumar, P., Awasthi, A., Nain, V., Issac, B. and Puria, R. (2018) Novel insights into TOR signalling in Saccharomyces cerevisiae through Torin2. *Gene*, **669**, 15-27.
43. Ohyashiki, J.H., Kobayashi, C., Hamamura, R., Okabe, S., Tauchi, T. and Ohyashiki, K. (2009) The oral iron chelator deferasirox represses signaling through the mTOR in myeloid leukemia cells by enhancing expression of REDD1. *Cancer Sci*, **100**, 970-977.
44. Ndong, M., Kazami, M., Suzuki, T., Uehara, M., Katsumata, S., Inoue, H., Kobayashi, K., Tadokoro, T., Suzuki, K. and Yamamoto, Y. (2009) Iron

deficiency down-regulates the Akt/TSC1-TSC2/mammalian Target of Rapamycin signaling pathway in rats and in COS-1 cells. *Nutr Res*, **29**, 640-647.

45. Watson, A., Lipina, C., McArdle, H.J., Taylor, P.M. and Hundal, H.S. (2016) Iron depletion suppresses mTORC1-directed signalling in intestinal Caco-2 cells via induction of REDD1. *Cell Signal*, **28**, 412-424.
46. Fretham, S.J., Carlson, E.S. and Georgieff, M.K. (2013) Neuronal-specific iron deficiency dysregulates mammalian target of rapamycin signaling during hippocampal development in nonanemic genetic mouse models. *J Nutr*, **143**, 260-266.
47. Prouteau, M., Desfosses, A., Sieben, C., Bourgoint, C., Lydia Mozaffari, N., Demurtas, D., Mitra, A.K., Guichard, P., Manley, S. and Loewith, R. (2017) TORC1 organized in inhibited domains (TOROIDs) regulate TORC1 activity. *Nature*, **550**, 265-269.
48. Sullivan, A., Wallace, R.L., Wellington, R., Luo, X. and Capaldi, A.P. (2019) Multilayered regulation of TORC1-body formation in budding yeast. *Mol Biol Cell*, **30**, 400-410.
49. Mittal, N., Guimaraes, J.C., Gross, T., Schmidt, A., Vina-Vilaseca, A., Nedialkova, D.D., Aeschimann, F., Leidel, S.A., Spang, A. and Zavolan, M. (2017) The Gcn4 transcription factor reduces protein synthesis capacity and extends yeast lifespan. *Nat Commun*, **8**, 457.
50. Muckenthaler, M.U., Rivella, S., Hentze, M.W. and Galy, B. (2017) A Red Carpet for Iron Metabolism. *Cell*, **168**, 344-361.

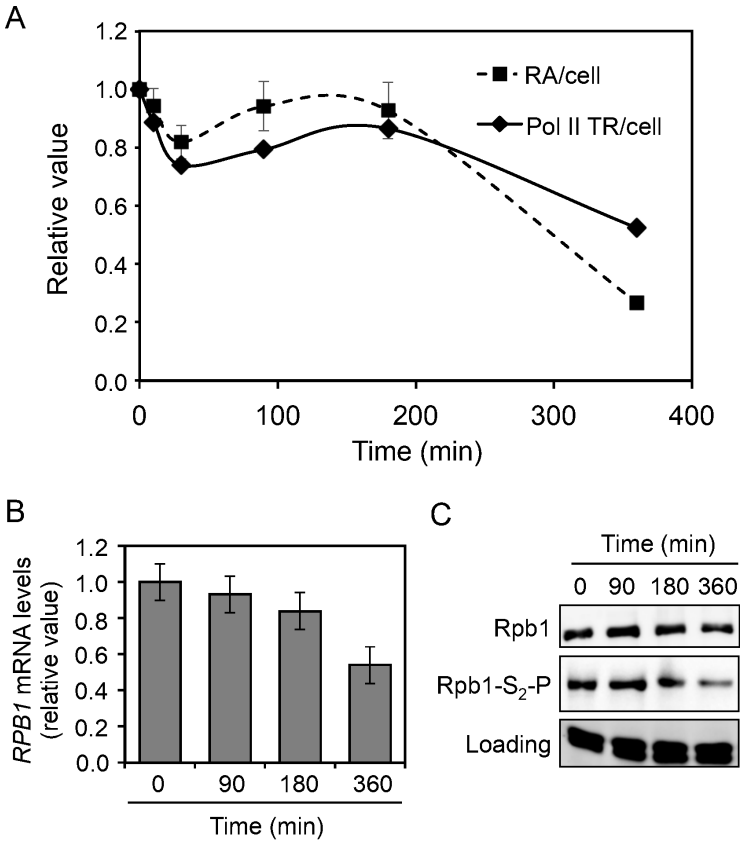
A
1.2
1.0
0.8
0.6
0.4
0.2
0.0
Relative value
RA/cell
Pol II TR/cell
0
100
200
300
400
Time (min)
B
RPB1 mRNA levels (relative value)
1.2
1.0
0.8
0.6
0.4
0.2
0.0
0
90
180
360
Time (min)
C
Time (min)
0 90 180 360
Rpb1
Rpb1-S2-P
Loading

Figure 1

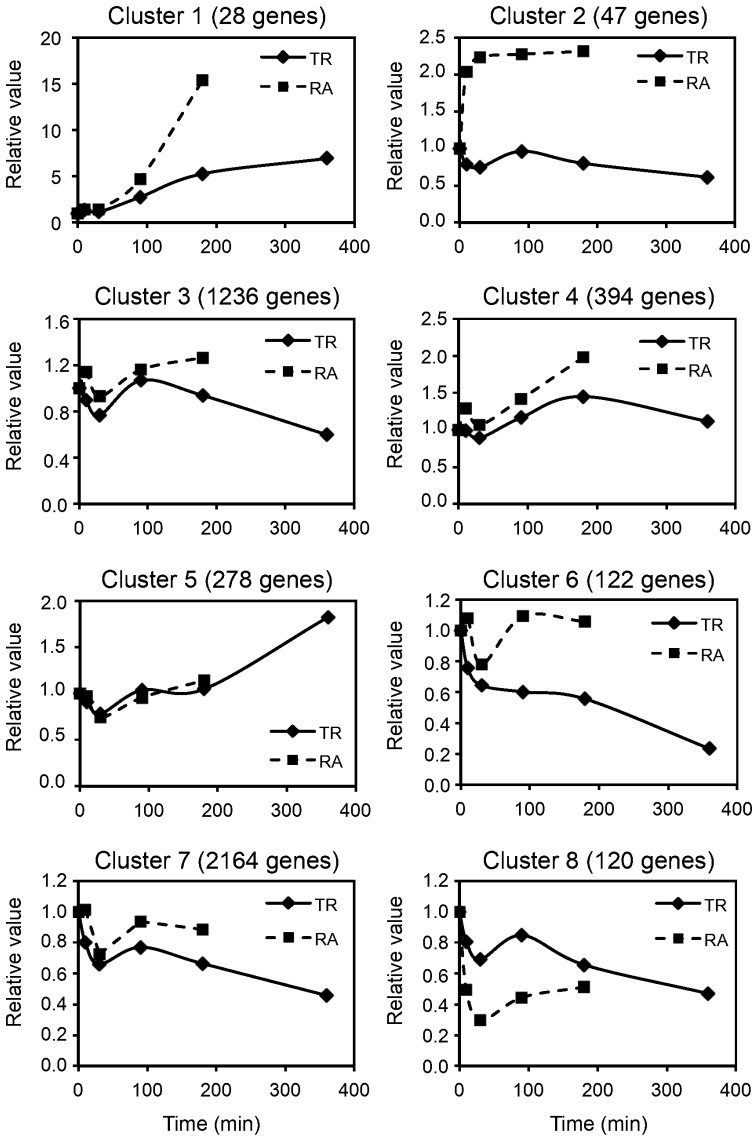
Cluster 1 (28 genes)
Cluster 2 (47 genes)
Cluster 3 (1236 genes)
Cluster 4 (394 genes)
Cluster 5 (278 genes)
Cluster 6 (122 genes)
Cluster 7 (2164 genes)
Cluster 8 (120 genes)
Relative value
Time (min)
TR
RA

Figure 2

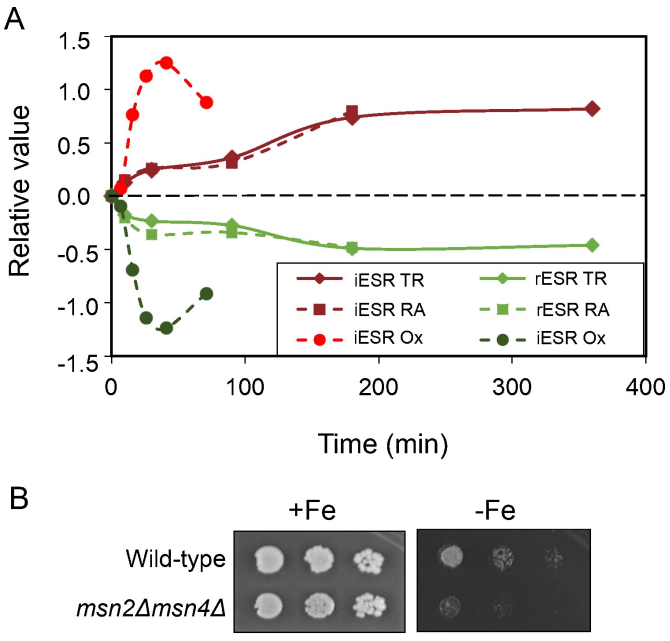
A
1.5
1.0
0.5
0.0
-0.5
-1.0
-1.5
Relative value
0
100
200
300
400
Time (min)
iESR TR
iESR RA
iESR Ox
rESR TR
rESR RA
iESR Ox
B
+Fe
-Fe
Wild-type
msn2Δmsn4Δ

Figure 3

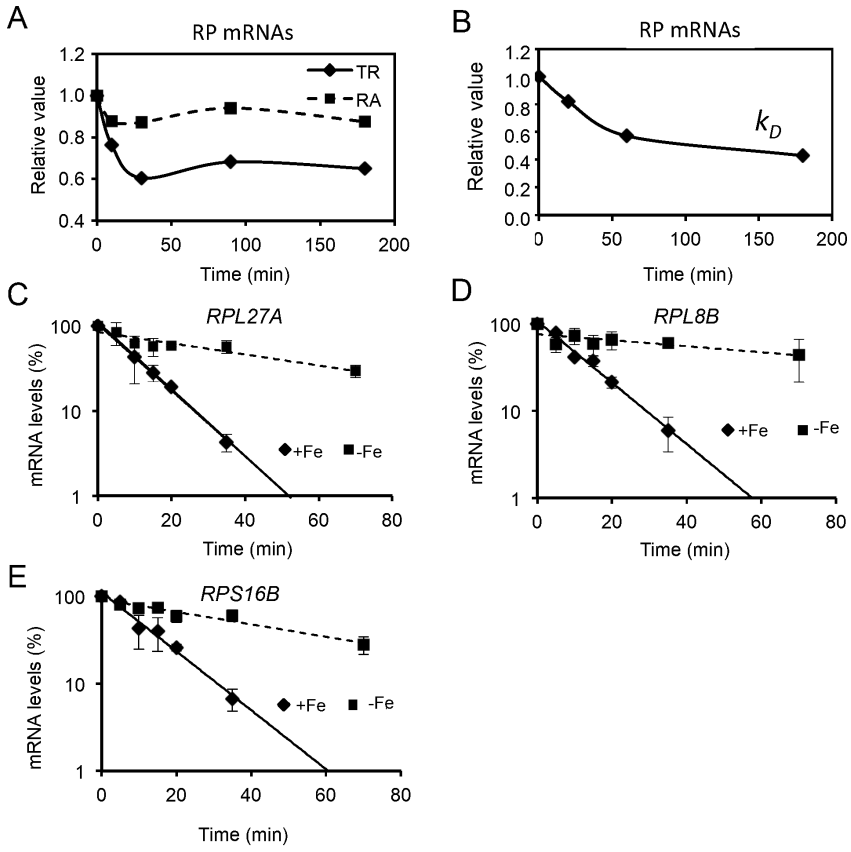
A
RP mRNAs
Relative value
TR
RA
Time (min)
B
RP mRNAs
Relative value
k_D
Time (min)
C
RPL27A
mRNA levels (%)
+Fe
-Fe
Time (min)
D
RPL8B
mRNA levels (%)
+Fe
-Fe
Time (min)
E
RPS16B
mRNA levels (%)
+Fe
-Fe
Time (min)

Figure 4

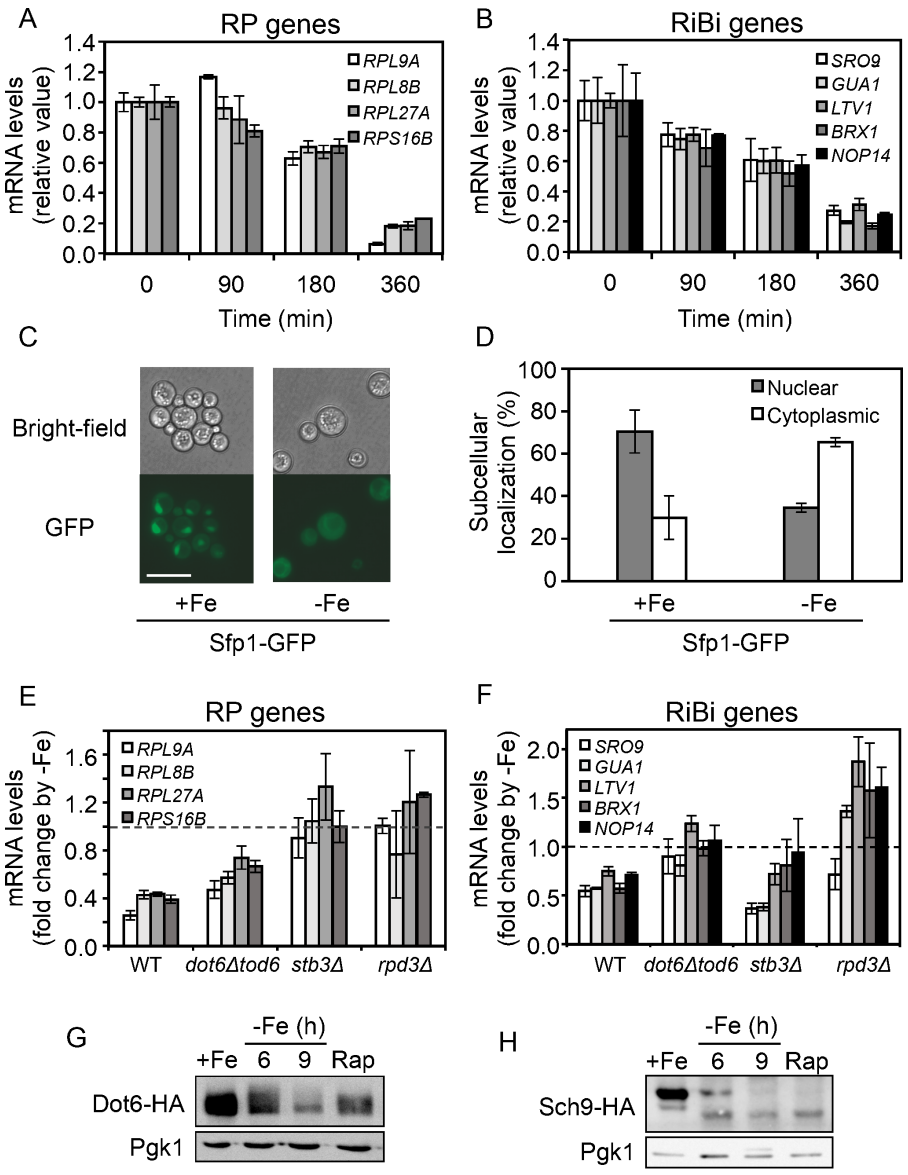
A
RP genes
mRNA levels (relative value)
RPL9A
RPL8B
RPL27A
RPS16B
Time (min)
B
RiBi genes
SRO9
GUA1
LTV1
BRX1
NOP14
C
Bright-field
GFP
+Fe
-Fe
Sfp1-GFP
D
Subcellular localization (%)
Nuclear
Cytoplasmic
E
RP genes
(fold change by -Fe)
WT
dot6Δtod6
stb3Δ
rpd3Δ
F
RiBi genes
G
-Fe (h)
Rap
Dot6-HA
Pgk1
H
Sch9-HA

Figure 5

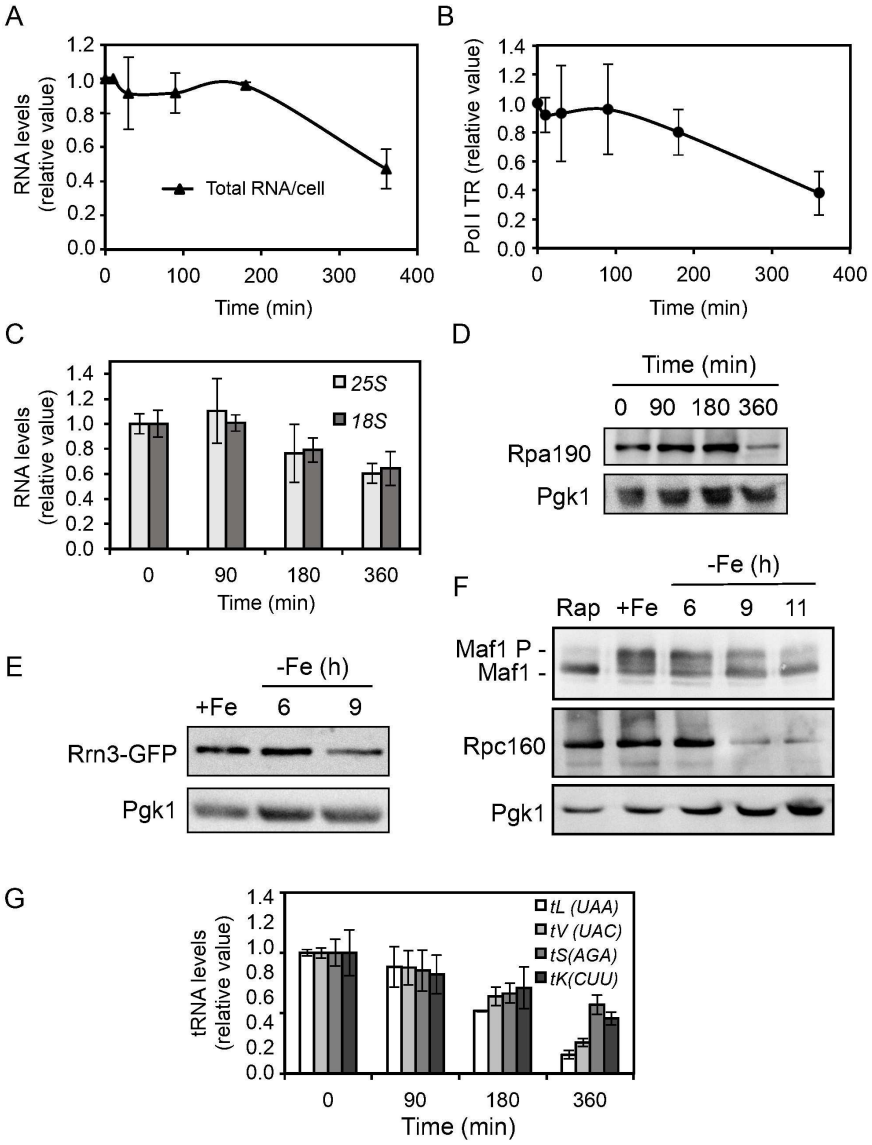
A
RNA levels (relative value)
Total RNA/cell
Time (min)
B
Pol I TR (relative value)
Time (min)
C
RNA levels (relative value)
25S
18S
Time (min)
D
Time (min)
0 90 180 360
Rpa190
Pgk1
E
-Fe (h)
+Fe 6 9
Rrn3-GFP
Pgk1
F
-Fe (h)
Rap +Fe 6 9 11
Maf1 P -
Maf1 -
Rpc160
Pgk1
G
tRNA levels (relative value)
tL (UAA)
tV (UAC)
tS(AGA)
tK(CUU)
Time (min)

Figure 6

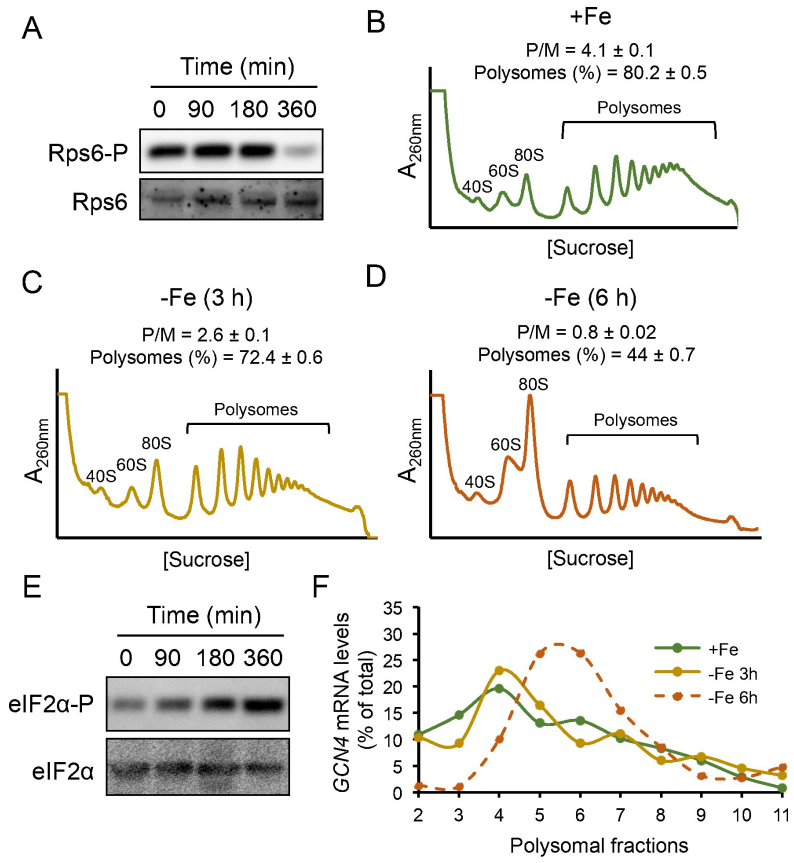
A
Time (min)
0 90 180 360
Rps6-P
Rps6
B
+Fe
P/M = 4.1 ± 0.1
Polysomes (%) = 80.2 ± 0.5
Polysomes
A260nm
40S
60S
80S
[Sucrose]
C
-Fe (3 h)
P/M = 2.6 ± 0.1
Polysomes (%) = 72.4 ± 0.6
Polysomes
A260nm
40S
60S
80S
[Sucrose]
D
-Fe (6 h)
P/M = 0.8 ± 0.02
Polysomes (%) = 44 ± 0.7
80S
Polysomes
60S
A260nm
40S
[Sucrose]
E
Time (min)
0 90 180 360
eIF2α-P
eIF2α
F
GCN4 mRNA levels (% of total)
35
30
25
20
15
10
5
0
+Fe
-Fe 3h
-Fe 6h
2 3 4 5 6 7 8 9 10 11
Polysomal fractions

Figure 7

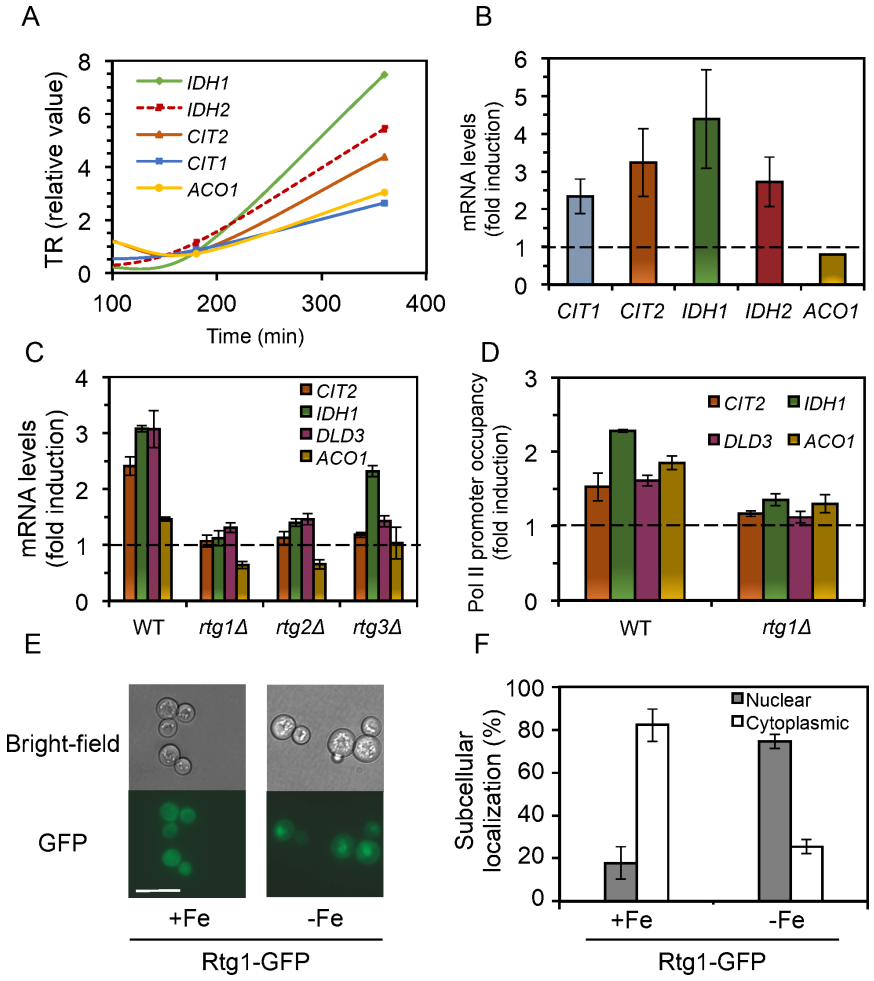
A
TR (relative value)
Time (min)
IDH1
IDH2
CIT2
CIT1
ACO1
B
mRNA levels (fold induction)
CIT1
CIT2
IDH1
IDH2
ACO1
C
mRNA levels (fold induction)
CIT2
IDH1
DLD3
ACO1
WT
rtg1Δ
rtg2Δ
rtg3Δ
D
Pol II promoter occupancy (fold induction)
CIT2
IDH1
DLD3
ACO1
WT
rtg1Δ
E
Bright-field
GFP
+Fe
-Fe
Rtg1-GFP
F
Subcellular localization (%)
Nuclear
Cytoplasmic
+Fe
-Fe
Rtg1-GFP

Figure 8

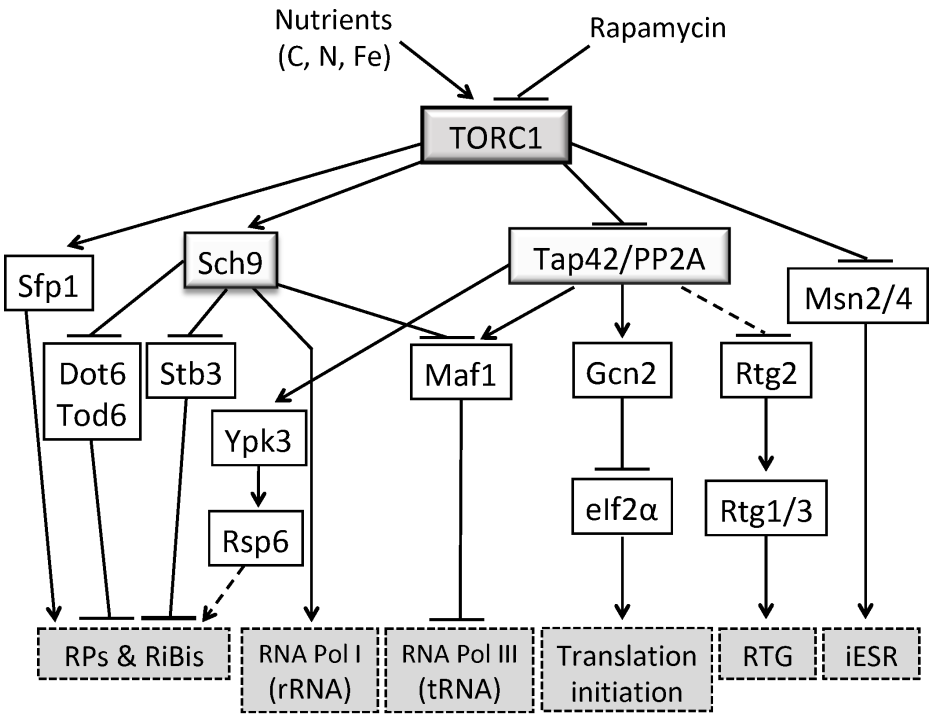
Nutrients
(C, N, Fe)
Rapamycin
TORC1
Sfp1
Sch9
Tap42/PP2A
Msn2/4
Dot6
Tod6
Stb3
Maf1
Gcn2
Rtg2
Ypk3
eIf2α
Rtg1/3
Rsp6
RPs & RiBis
RNA Pol I
(rRNA)
RNA Pol III
(tRNA)
Translation
initiation
RTG
iESR

Figure 9

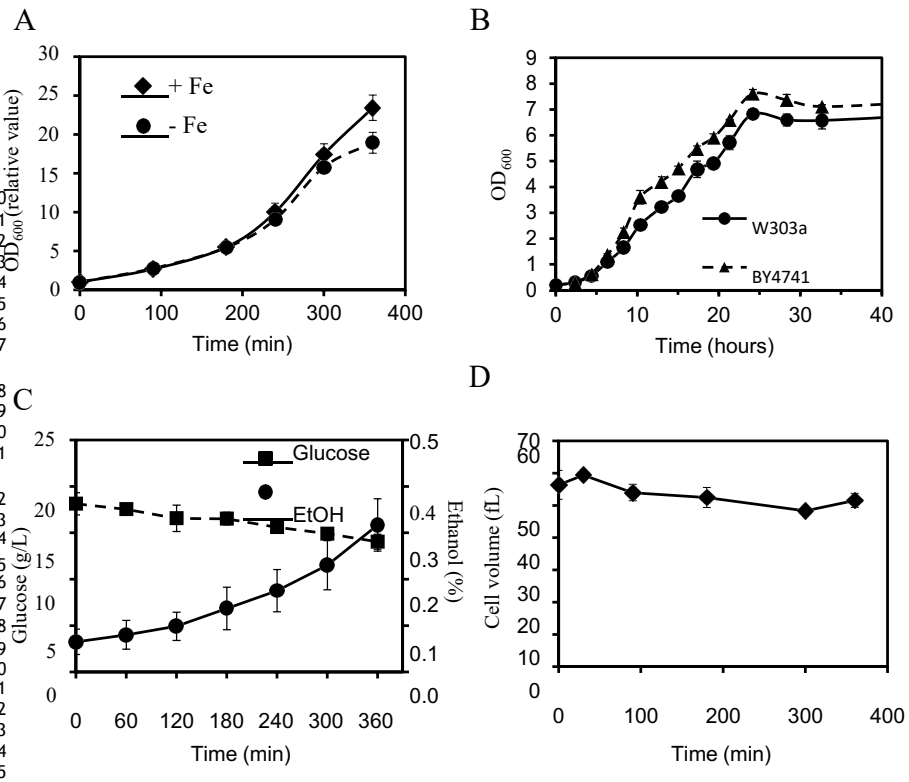
A
+ Fe
- Fe
OD600 (relative value)
Time (min)
B
OD600
W303a
BY4741
Time (hours)
C
Glucose
EtOH
Glucose (g/L)
Ethanol (%)
Time (min)
D
Cell volume (fL)
Time (min)

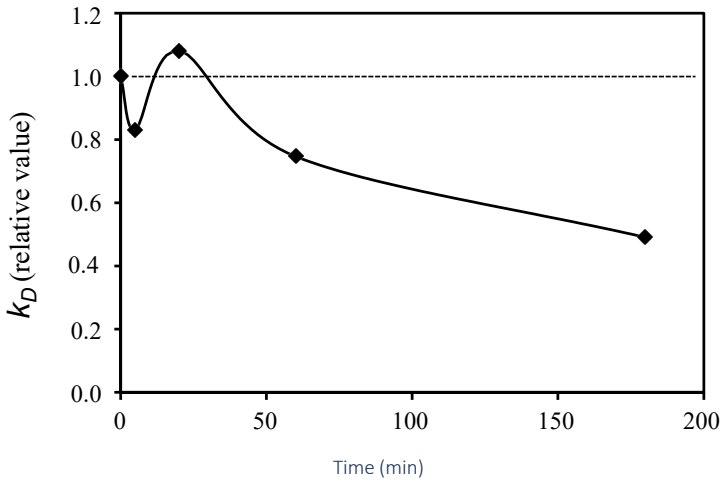
1.2
1.0
0.8
0.6
0.4
0.2
0.0
k_D (relative value)
0
50
100
150
200
Time (min)

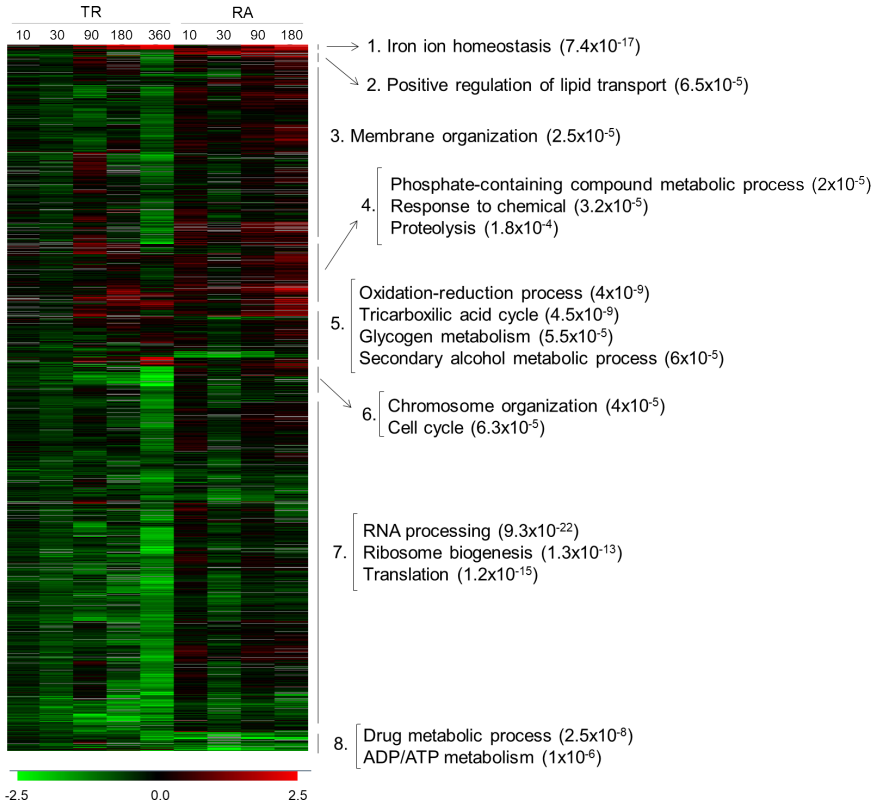
TR
RA
10 30 90 180 360 10 30 90 180
-2.5 0.0 2.5
1. Iron ion homeostasis (7.4x10-17)
2. Positive regulation of lipid transport (6.5x10-5)
3. Membrane organization (2.5x10-5)
4. Phosphate-containing compound metabolic process (2x10-5)
Response to chemical (3.2x10-5)
Proteolysis (1.8x10-4)
5. Oxidation-reduction process (4x10-9)
Tricarboxilic acid cycle (4.5x10-9)
Glycogen metabolism (5.5x10-5)
Secondary alcohol metabolic process (6x10-5)
6. Chromosome organization (4x10-5)
Cell cycle (6.3x10-5)
7. RNA processing (9.3x10-22)
Ribosome biogenesis (1.3x10-13)
Translation (1.2x10-15)
8. Drug metabolic process (2.5x10-8)
ADP/ATP metabolism (1x10-6)

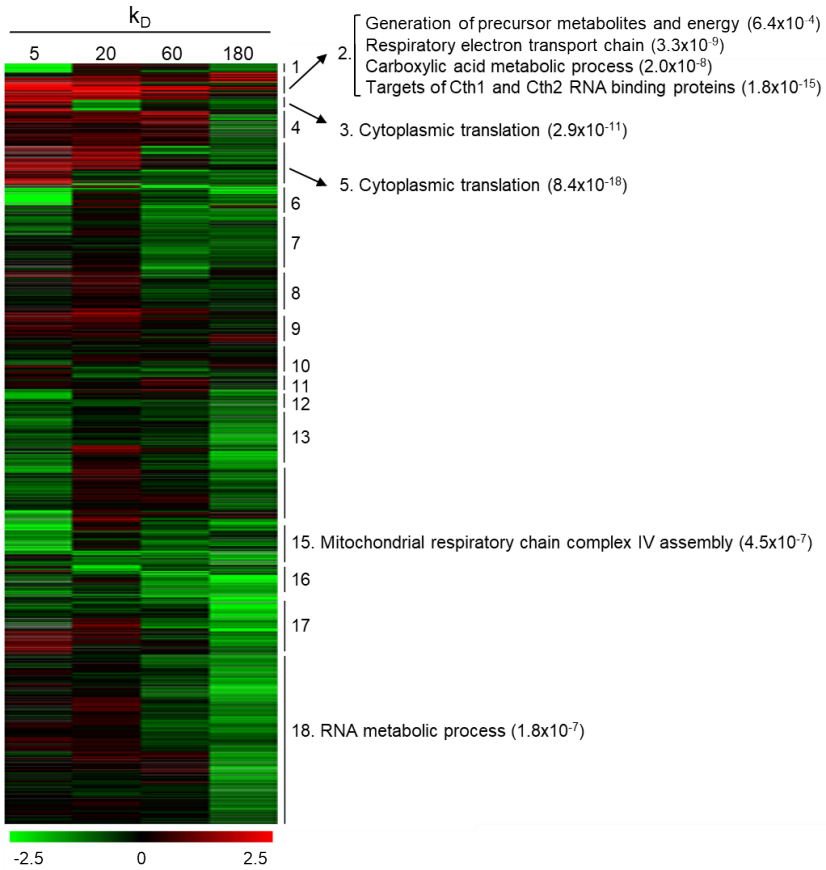
k_D
5
20
60
180
1
2. Generation of precursor metabolites and energy (6.4x10^{-4})
Respiratory electron transport chain (3.3x10^{-9})
Carboxylic acid metabolic process (2.0x10^{-8})
Targets of Cth1 and Cth2 RNA binding proteins (1.8x10^{-15})
4
3. Cytoplasmic translation (2.9x10^{-11})
5. Cytoplasmic translation (8.4x10^{-18})
6
7
8
9
10
11
12
13
15. Mitochondrial respiratory chain complex IV assembly (4.5x10^{-7})
16
17
18. RNA metabolic process (1.8x10^{-7})
-2.5
0
2.5

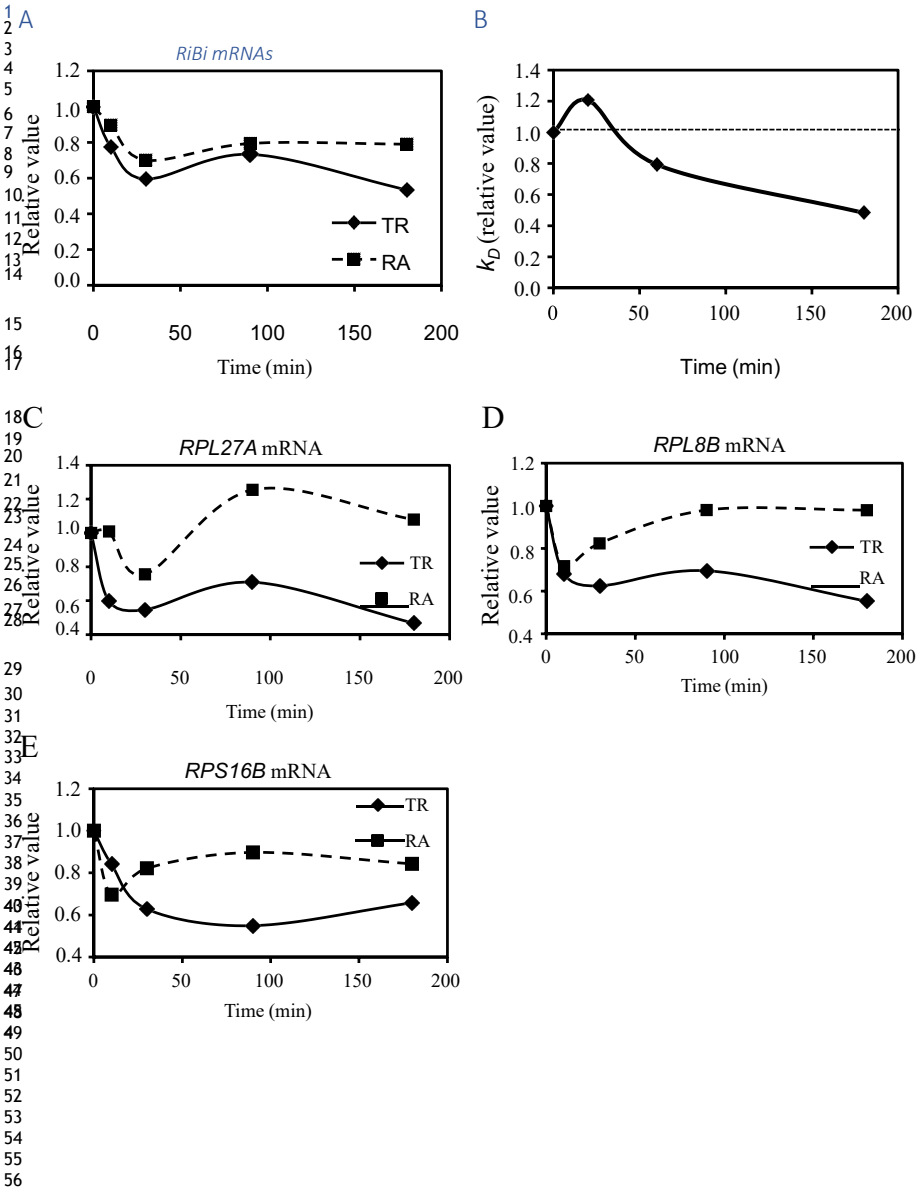
A
RiBi mRNAs
Relative value
TR
RA
Time (min)
B
k_D (relative value)
Time (min)
C
RPL27A mRNA
Relative value
TR
RA
Time (min)
D
RPL8B mRNA
Relative value
TR
RA
Time (min)
E
RPS16B mRNA
Relative value
TR
RA
Time (min)

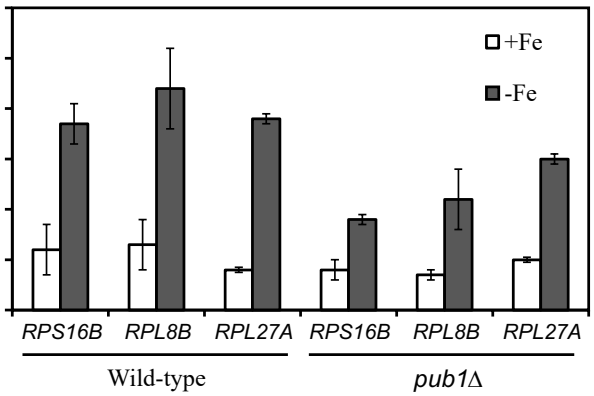

Supplementary Figure S8

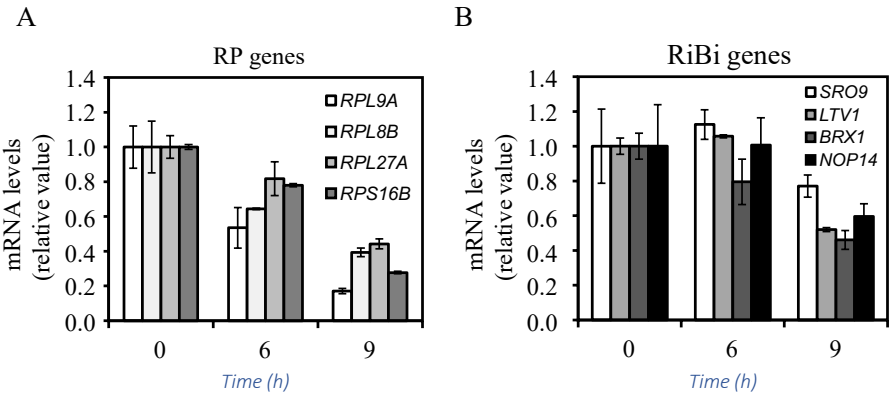

Supplementary Figure S9

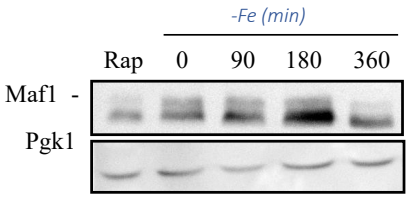
-Fe (min)
Rap
0
90
180
360
Maf1 -
Pgk1

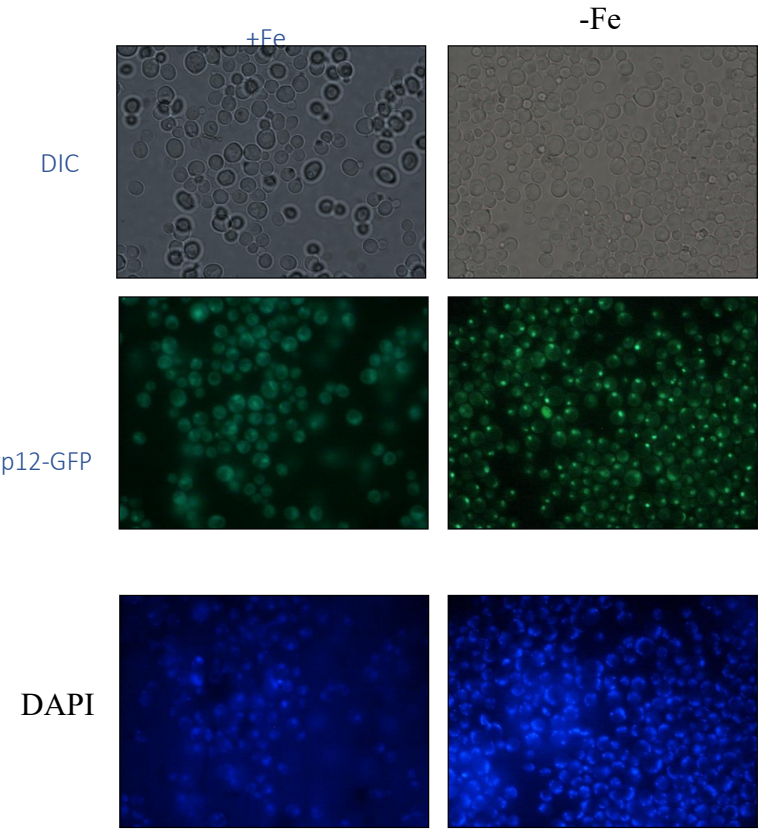
+Fe
-Fe
DIC
Rrp12-GFP
DAPI

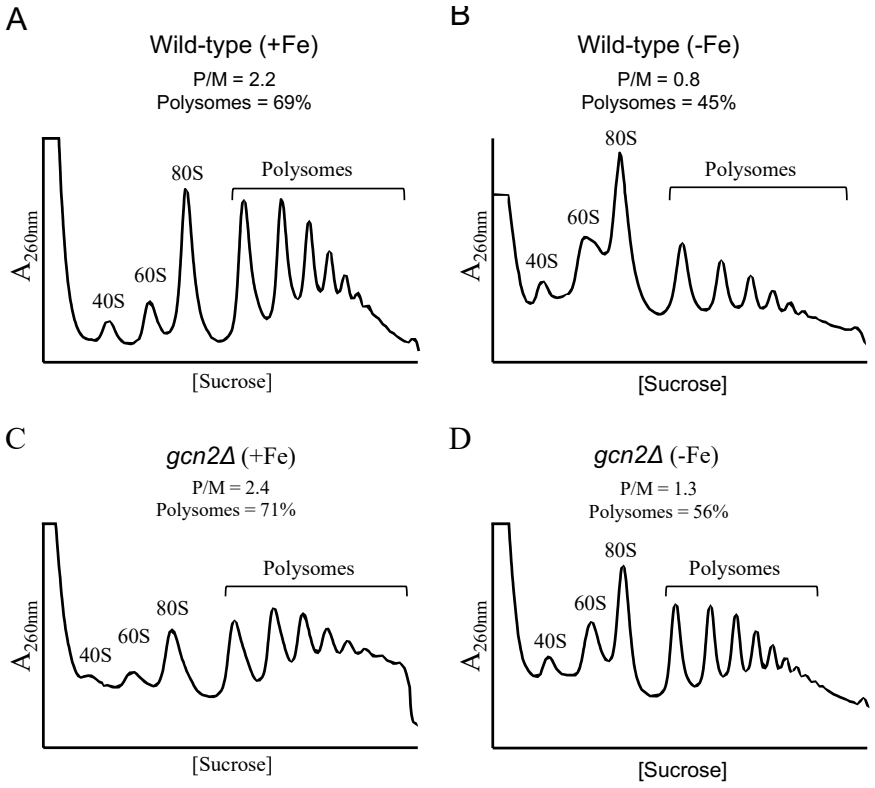
A
Wild-type (+Fe)
P/M = 2.2
Polysomes = 69%
40S
60S
80S
Polysomes
A260nm
[Sucrose]
B
Wild-type (-Fe)
P/M = 0.8
Polysomes = 45%
40S
60S
80S
Polysomes
A260nm
[Sucrose]
C
gcn2Δ (+Fe)
P/M = 2.4
Polysomes = 71%
40S
60S
80S
Polysomes
A260nm
[Sucrose]
D
gcn2Δ (-Fe)
P/M = 1.3
Polysomes = 56%
40S
60S
80S
Polysomes
A260nm
[Sucrose]

4.2 SEGON ARTICLE

Bulk autophagy induction and life extension is achieved when iron is the only limited nutrient in *Saccharomyces cerevisiae*

Sandra Montella-Manuel, Nuria Pujol-Carrion, Mónica A. Mechoud and Maria Angeles de la Torre-Ruiz.

[1]Cell Signalling in Yeast Unit, Department of Basic Medical Sciences, Institut de Recerca Biomèdica de Lleida (IRBLleida), University of Lleida, 25198, Lleida, Spain.

Corresponding autor: Maria Angeles de la Torre-Ruiz: mariaangeles.delatorre@udl.cat Tel. +34973702410

Abstract

We have investigated the effects that iron limitation provokes in *Saccharomyces cerevisiae* exponential cultures. We have demonstrated that one primary response is the induction of bulk autophagy mediated by TORC1. Coherently, Atg13 became dephosphorylated whereas Atg1 appeared phosphorylated. The signal of iron deprivation requires Tor2/Ypk1 activity and the inactivation of Tor1 leading to Atg13 dephosphorylation, thus triggering the autophagy process. Iron replenishment in its turn, reduces autophagy flux through the AMPK Snf1 and the subsequent activity of the iron responsive transcription factor, Aft1. This signaling converges in Atg13 phosphorylation mediated by Tor1. Iron limitation promotes accumulation of trehalose and the increase in stress resistance leading to a quiescent state in cells. All these effects contribute to the extension of the chronological life, in a manner totally dependent on autophagy activation.

Introduction

Iron is an essential metal for the majority of cellular types. It is required for a number of metabolic processes such as respiration, proteins, lipids or ribosome metabolism, DNA biosynthesis and repair and others [1, 2]. Since iron can be potentially toxic for cells, mechanisms tightly controlling its homeostasis are required. In budding yeast, Yap5, Aft1 and Aft2 are the classical iron regulators. Yap5 is a transcriptional factor responding to high levels of cytosolic iron [3] whereas Aft1 and its paralogue Aft2 mediate the responses to iron starvation [4, 5, 6]. Aft1 localization is determinant for its transcriptional function being localized in the nucleus when iron is scarce and translocate to the cytoplasm when iron is repleted [7]. Iron depletion causes health problems in humans such as cardiovascular diseases or anemia. Some researchers have described the activation of autophagy in response to iron deprivation as a positive mechanism to recirculate iron [8, 9]. Sensing and transducing the signal of the iron status to different cellular targets is essential to achieve a correct cellular homeostasis, hence, Hog1, Snf1, Ras2/PKA and Pkc1 signalling pathways have been directly or indirectly related to iron homeostasis (Reviewed in 10). The stress-activated protein kinase (SAPK) Hog1 (p38 in humans) phosphorylates and regulate Aft1 activity [10].

The kinase Snf1 belongs to the AMPK family, it has been demonstrated its participation

in the regulation of the iron regulon during diauxia through Aft1 [11] and also a role for Snf1 in iron resistance has been reported [12]. Our group has demonstrated that Slt2 the MAP kinase of the PKC1-MAPK pathway, also regulates Aft1 under iron deprivation conditions (submitted). Mitochondria and vacuole are both organelles in which iron is accumulated; this localisation probably contributes to the cellular sensing of iron. TOR is a known regulator of cellular metabolism and proliferation in all the known eukaryotic models.

Nutrient starvation provokes changes in the metabolism and cell cycle and under certain circumstances causes a G1 arrest and entrance in a long-lived quiescent state [13, 14] When cells are deprived of several biomolecules autophagy activation contributes to recycle nutrients (reviewed in: [15, 16] Many autophagy mutants exhibit a reduction in their chronological life span [17]. These findings have led to several studies demonstrating that autophagy can play a positive role in longevity (For reviews: [18, 19, 20].

TORC2 exerces a control in mitochondrial respiratory function, affecting calcineurin [21]. During amino acid starvation, TORC2 positively regulates autophagy by inhibiting the activity of the calcium-regulated phosphatase calcineurin and activating the general amino acid control (GAAC) [22]. In addition, TORC2, controls *ATG8* expression upon repression of the heterodimeric Zinc-finger transcription factors Msn2 and Msn4 [23] (Vlahakis et al., 2017b).

TORC1 is down regulated in conditions of iron limitation [24].The inactivation of the complex retards aging in *Saccharomyces cerevisiae* [25]; interestingly this mechanism has been demonstrated to be evolutionary conserved in many eukaryotic models and human cells (for a review [26]. TOR plays a crucial role in regulating autophagy in all eukaryotic models [27]. TORC1 is a negative regulator of autophagy [28]. Mild inactivation of TORC1 stimulates macroautophagy and extends life span [17]. TORC1 activity is registered through its multiple downstream effectors [29]. Sfp1, one of the downstream effectors of TORC1, is a transcriptional factor that regulates both RP and RiBi genes [30, 31]. When TORC1 is active, Sfp1 has a nuclear localisation whereas in conditions of TORC1 inactivation, Sfp1 is translocated to the cytoplasm. Non starved cells sequester Msn2/Msn4 in the cytoplasm upon their hyperphosphorylation mediated by TORC1 and cAMP-PKA. Nutritional starvation causes inactivation of both pathways leading to Msn2/Msn4 dephosphorylation and nuclear translocation, leading to the induction of the expression of a wide number of genes by the heterodimeric

transcription factor [32, 33]. Rtg1 is a basic helix–loop–helix/Zip transcription factor that along with Rtg3 and Rtg2 integrates the pathway termed retrograde regulation [34, 35]. Rtg1 is localized to the cytoplasm when cells grow in the presence of all the required nutrients in logarithmic phase. Several stimuli such as TORC1 inactivation, nutrient deprivation or mitochondrial dysfunction provoke Rtg1 translocation to the nucleus (reviewed in [36]. When active, TORC1 hyperphosphorylates Atg13, thus inhibiting autophagy [28]. TORC1 inactivation leads to Atg13 dephosphorylation that triggers Atg1 kinase activity then leading to the formation of the complex Atg13/Atg1/Atg17/Atg29/Atg31 activating the autophagy process [37, 38].

In this study, we demonstrate that iron deprivation activates macroautophagy in growth conditions in which iron is the only limiting nutrient. Tor2-Ypk1 is required to detect and transmit the signal of iron deprivation allowing Tor1 to dephosphorylate Atg13 and induce the autophagy mechanism. Snf1 and Aft1 participate in detecting the signal of iron repletion leading to Tor1 induction and the consequent repression of autophagy.

Iron limitation causes an early entrance in quiescence and extension of chronological life, conditioned to the simultaneous activation of the autophagy machinery. The results presented here suggest a coordinate linkage between nutritional signalling pathways, iron homeostasis and autophagy that favors life extension.

Materials and methods

Yeast strains and plasmids

Saccharomyces cerevisiae strains are listed in Table 1. All the strains named GSL are derivatives of the CML128 background. New null mutants described in this study were obtained by a one-step disruption method that uses the NatMx4 or KanMx4 cassettes [51]. Strains GSL199, 226, 297, 313, 325, 352, 374 and 382 were constructed upon integration of plasmid pGFP-Atg8 (original name: pHab142), previously digested with Stu1, in the *URA2* locus. Strains, GSL395, 398, 399 and 401 were constructed upon integration of plasmid pAtg1-HA previously digested with BstEII. The plasmid pAtg1- HA was obtained upon Atg1 cloning into the Pme1 and PstI sites of the integrative vector pMM351 [48].

Plasmid descriptions are listed in Table 2. Each particular ORF was amplified by PCR from genomic DNA to be directionally cloned in the specific plasmid.

Media, growth conditions and reagents

Yeasts were grown at 30ºC in SD medium (2% glucose, 0.67% yeast nitrogen base that lacked the corresponding amino acids for plasmid maintenance) plus amino acids [52]. Iron depletion conditions (-Fe) consisted on SD medium whose nitrogen base component was free of iron plus the addition of 80 μM of 4,7-diphenyl-1,10-phenanthrolinedisulfonic acid (BPS) (Sigma,146617) [42]. Iron was added as ammonium iron (III) sulfate hexacahydrate [$NH_4Fe(SO_4)_2$•$6H_2O$] (+Fe; F1543; Sigma) at a final concentration of 10mM.

We present a list of reagents detailing final concentrations in culture media and from which company they were purchased: Cycloheximide 150mg/ml (SIGMA, C4859); Rapid alkaline phosphatase (Roche, 105677520001). N-acetylcysteine: NAC 5 mM (Sigma, A9165); FM464 30 μg/μL (Invitrogen, T-3166); Rapamycin 200 ng/ml (Sigma, R0395); $CaCl_2 \cdot 2H_20$ 100 mM (SERVA 15587); H_2O_2 0.5 mM (Sigma, H1009); Sorbitol 0.8 M (Sigma, S6021); Dihydroethidium DHE 50 μM (Sigma, D7008); DAPI 2 mg/mL (Sigma, D9541); Eritromycin 0.5 mM (Sigma, E6376); Glicerol 3% (Fisher scientific, 800689). Cell cultures were exponentially grown at 600 nm [OD600] of 0.6.

Calcineurin activity

To determine calcineurin activity we used a calcineurin-dependent response element (CDRE) lacZ reporter described in [53] and β-galactosidase assay was determined according to the protocol previously publish by our group in [42].

Vacuole and dihydroethidium staining

For vacuole visualization, cells were stained with FM4-64 (N-(3-triethylammoniumpropyl)-4-(p-diethylaminophenylhexatrienyl) pyridinium dibromide, and to determine cellular oxidation we used dihydroethidium. Both protocols were previously described by our group in [41].

Glucose and trehalose determinations

We followed the directions detailed in [54].

The index of respiratory competence (IRC) and mitochondria mutation frequency assay

The IRC value was calculated as the ratio between the number of colony-forming units (CFUs) observed on plates containing a non-fermentable medium YPEG (glycerol) vs a fermentable medium YPD (glucose). Mitochondria mutation frequency assay was determined as the ratio between de CFUs counted on YPEG plates plus erythromycin vs the number el CFUs counted in YPD plates. Both protocols were carried out according to [55].

Cell survival and chronological life span

To assay cell viability cells were grown to mid log phase $O.D._{600}$: 0.6 in SD medium supplemented with the required amino acids. Viability was registered through serial dilutions and plated by triplicate onto YPD plates.

We measured the chronological life span (CLS) in the different strains based on the survival of populations of non-dividing yeast cells according to [42]. The viability was scored by counting the number of cells able to form colonies, CFU (colony-forming units). Cultures were started at an $O.D_{600}$: 0.6. The same number of cells collected from each culture were plated in triplicated into YPD plates and allowed to grow at 30ºC for 3-4 days. CLS curves were plotted with the corresponding averages and standard deviations from three independent experiments.

Protein extraction and immuno blot analyses

Total yeast protein extracts were prepared as previously described in [42]. The antibodies for western blotting were as follows: anti-HA 3F10 (no. 12158167001; Roche Applied Science), was used at a dilution of 1:2,000 in 0.25% non-fat milk and the corresponding secondary was goat anti-rat IgG horseradish peroxidase conjugate (no. AP136P, Millipore). Anti-GFP (no. 632381; Living Colours) was used at a dilution of 1:2,000 and anti-Phospho-glycerate kinase (459250, Invitrogen) used at a dilution 1:1,200, both with the secondary antibody anti-Mouse (LNA931v/AG, GE Healthcare). Anti- Phospho-eIF2α (Ser51) (3597S, Cell Signalling) at a dilution 1:1,000 and anti-Phospho-AMPKα (Thr172) (167253S, Cell Signalling) at a dilution of 1:1,000 both with the secondary antibody anti-Rabbit (LNA934v/AG, GE Healthcare). They were used as indicated by the manufacturers.

The protein-antibody complexes were visualized by enhanced chemiluminescence, using the Supersignal substrate (Pierce) in a Chemidoc (Roche Applied Science).

Autophagy activity

For monitoring autophagy, we used the protocol described by [56] and modified by [43].

Results

Iron deprivation activates autophagy flux in conditions in which the only limiting nutrient is iron.

Iron is an essential element for eukaryotic cells. In a previous study we have demonstrated that iron deprivation provoked a descent in TORC1 activity [24], therefore we wondered whether iron availability also determined the onset of autophagy, in conditions in which iron is the only nutritional restriction imposed during exponential phase.

We decided to analyze autophagy progression through the immunological detection of free GFP from GFP-Atg8 genomic fusion [57]. GFP accumulation was only clearly detected in wt cells depleted for iron in exponential conditions; however, the free GFP band was undetectable in *atg7* and *atg1* mutants (Fig. 1A). As expected, GFP moiety was undetectable in cells growing exponentially in control SD medium not depleted for iron in all the strains tested (Fig1A). The increase in autophagy flux [58] detected in iron depletion conditions (Fig 1B) was indicative of induction of bulk autophagy.

Moreover, total Atg8 also experienced an increase in wt cells growing in iron depletion conditions (Fig 1C). These results were confirmed upon the microscopical observation of GFP accumulation in vacuoles (the dye FM4-64 accumulates in the vacuolar membranes) in wt cells growing exponentially in iron starved medium (Fig 1D), as opposed to *atg7* and *atg1* mutants in which GFP-Atg8 showed a disperse location through the cytoplasm and occasionally as punctate location to the PAS (Fig 1D and E). In order to discard that this would be a specific effect of the background we used different backgrounds and observed that in all of them iron deprivation induced autophagy flux in exponentially growing cells (not shown). We also observed the appearance of PAS (preautophagosome sites) detected upon GFPAtg8 (Fig 1D white arrows and E) and Atg13GFP (Fig 1F) microscopical observation, indicative of activation of autophagy flux. We discarded the contribution of specialized autophagy in the vacuolar accumulation of GFP derived from GFP-Atg8 by analyzing *atg11* and *atg32* mutants (Supplementary Material)

We used the enzymatic *pho8*Δ60 assay [59, 56] to quantify autophagy and confirmed that iron deprivation provoked an increment of autophagy in cultures not limited for nutrients other than iron, as compared to SD control cultures (Fig 1G).

Tor1 and Tor2 regulate autophagy in response to iron availability during exponential phase.

To elucidate whether the signal of iron deprivation flows from TORC1 inhibition to the different read-outs and to the machinery of autophagy we have analyzed several TORC1 substrates in wt and *atg7* mutant deficient in autophagy (since we observed the same results in *atg7* and in *atg1* mutants we do not show the results corresponding to the later): Msn2/4 [47, 60, 32, 33], Rtg1 [34, 35] Sfp1[30, 31] GCN2/eIF2α [61, 62].

Under optimal growth conditions Rtg1 and Msn2/Msn4 are localized to the cytoplasm, whereas Sfp1 is located in the nucleus. Iron starvation provoked Rtg1 translocation to the nucleus and Sfp1 localisation to the cytoplasm (Fig 2A), however Msn2 was not affected by the scarcity of this metal in neither wt nor *atg7* strains and remained localized in the cytoplasm (Fig 2A). Rtg1 localisation upon iron deprivation was not a consequence of mitochondrial dysfunction leading to oxidative stress since treatment with the oxidant N-Acetyl cysteine was unable to induce the translocation of the transcription factor from the cytoplasm to the nucleus (Fig 2 B). TORC1 and a variety of stresses cause an increased abundance of uncharged tRNAs that activate the kinase Gcn2, which in turns phosphorylates eIF2α to globally attenuate the protein synthesis. Our data indicate that TORC1 inactivation caused by iron depletion did not provoke eIF2α phosphorylation when no other nutrient was limiting (Fig 2C).

Atg13 phosphorylation by TORC1 inhibits autophagy [63].

TORC1 inactivation leads to Atg13 dephosphorylation which provokes detachment and activation of Atg1 by phosphorylation with the subsequent activation of autophagy. We observed Atg13 dephosphorylated whereas Atg1 became phosphorylated upon iron depletion in wt cells and also in the autophagy mutants *atg1* and *atg7* (Fig 2D), suggesting that in conditions of iron depletion with no other nutrient limitation, TORC1 is correctly inactivated and this inactivation is an event previous to the transmission of the signal to Atg13 and Atg1 proteins to activate the autophagy machinery.

Consequently, in the absence of either Atg1 or Atg7, even when TORC1 is inactivated and Atg13 dephosphorylated the autophagy does not take place.

With the aim of completely inactivate TORC1 complex we treated control cultures growing exponentially with rapamycin and provoked both TORC1 inactivation and bulk autophagy and autophagy flux induction. However, in iron depleted cultures rapamycin did not cause any significant additional change taking into consideration that the starvation for this nutrient had previously caused the inactivation of TORC1 (Fig 2E).

The autophagy analysis of *pho8*Δ60 delivery to the vacuole confirmed our conclusions since rapamycin provoked an expected induction of autophagy in control conditions, but was unable to alter the already induced autophagy in iron starved conditions (Fig 2F).

Our results support the hypothesis that iron deprivation leads to TORC1 inactivation during logarithmic phase, however this signal flows only to specific read-outs.

We decided to test other possible signalling pathways related to nutritional responses that could be related to detection and transduction of the iron starvation signalling, these are, TOR2/Ypk1, Ras2, Gcn2 and Snf1. TOR2 signals to the mitochondrial function to positively regulate autophagy [50]. Ypk1 is the most relevant target of TORC2 for this mechanism, therefore we deleted *YPK1* as a surrogate for TORC2 disruption, as wisely indicated in [50]. We could observe that the absence of Ypk1 abrogated the autophagy flux induced by iron starvation in exponentially growing cells (Fig 3A, B). In addition, from the observation of TORC1 substrates upon iron deprivation, we concluded that in *ypk1* strain Tor1 activity was reduced only for some substrates, Rtg1 and Sfp1 (Fig 3C) but contrary to that observed in wild type cells, neither Atg1 became phosphorylated nor Atg13 became dephosphorylated (Fig 3D). We discarded the possibility that iron deprivation would be provoking mitochondrial damage since in both a *rho0* strain and upon antymicine treatment (not shown) activation of the autophagy flux was clearly detected (Fig 3E and F). Consequently, we do not believe that the absence of autophagy activity detected in *ypk1* mutant upon iron deprivation is due to mitochondrial damage. Consequently, our results are consistent with the absence of autophagy flux observed in *ypk1* mutant (Fig 3A) and indicate that in the absence of TOR2/Ypk1 the iron starvation signal cannot be transmitted to Atg13 and Atg1 to activate the autophagy machinery through Tor1. We added rapamycine to both wt and *ypk1* cultures to fully inactivate TORC1 complex in both wt and *ypk1* strains. Upon TORC1 inactivation with rapamycin, we observed autophagy activation in *ypk1* strain, both in conditions of iron deprivation or not. In accordance with these observations Atg13 became dephosphorylated and Atg1 phosphorylated in all the samples treated with rapamycin (Fig 4A). These results suggest that in conditions of iron deprivation, TORC1 is active

for specific substrates in the absence of Ypk1, nevertheless, TORC1 is inhibible upon treatment with the macrolide rapamyin which functions independently of iron signaling. Concerning TORC1 read-outs, we observed that Rtg1 was localized in the cytoplasm and Sfp1 was localized to the nucleus in 100% of the cells of both strains, indicating that TORC1 complex was completely inactivated (Fig 4B). Taking altogether our results we can conclude that Ypk1 is required to transmit the iron starvation signaling to the autophagy machinery through Tor1.

Ypk1 function has been associated to Gcn2 activation with the subsequent induction of autophagy in conditions of amino acids starvation [50]. We could determine that autophagy regulation upon iron deprivation when amino acids are not limiting does not involve Gcn2 activity since no eIF2alfa phosphorylation was detected (Fig 4C). Ypk1 signalling regulates autophagy by repressing the activity of calcineurin and thus inducing Gcn2 activity [50]. Calcineurin activity was measured using a CDRE-driven lacZ reporter, as described previously [53, 50]. Calcineurin activity was not reduced in iron starvation conditions, moreover, it was even higher than the activity quantified in SD control conditions, although much lower than that determined in *ypk1* mutant cells (Fig 4D). Moreover, *gcn2* mutant did not present any defect in autophagy activation in iron limiting conditions (Fig 4E). Taking into consideration that Msn2 is not translocate to the nucleus upon iron starvation (Fig 2A), we discard the possibility that neither Msn2/Msn4 [23] nor calcineurin/Gcn2 could be the Tor2 targets that govern autophagy induction when iron is limited in the cultures. Our results suggest that Tor2 activity is required in order to transmit the signal to the autophagy machinery through Tor1 when iron is limiting, suggesting that Tor1 inactivation as a consequence of iron depletion does not activate bulk autophagy without Tor2 activity. The absence of Ras2 kinase also presented results related to GFP accumulation from GFPAtg8 and Atg13 and Atg1 phosphorylation similar to those observed in wt cells (Fig 4E) 1). A certain level of autophagy was already detected in the mutant *tor1* growing in control SD medium that was significantly increased when cultures were grown in iron starvation conditions (Fig 4E). In addition, the absence of Snf1 caused a significant increase in Atg8 expression upon iron deprivation (Fig 4E) suggesting that the AMPK is playing a negative role with respect to the synthesis of Atg8.

Aft1 is the transcriptional factor involved in regulating iron homeostasis [5]. We observed that *aft1* deletion did not substantially differ from those results obtained with the wt strain with respect to the autophagy activation in response to iron depletion, since

autophagy flux, GFP accumulation in the vacuoles, Atg13 and Atg1 phosphorylation patterns were similar to that detected in wt cells upon iron starvation (Fig 4F). However, upon iron depletion the levels of total protein Atg8 suffered a significant increase in the absence of Aft1, suggesting that under this nutritional circumstances Aft1 negatively affects Atg8 synthesis (Fig 4F).

Taken altogether these results we conclude that when iron is the only scarce nutrient in the culture medium Tor2 activity is required in order to induce bulk autophagy through Tor1 inactivation.

Snf1 through Aft1 are both involved in signal detection of iron availability to down regulate autophagy through Tor1

Iron replenishment to exponential growing cultures previously grown without iron, caused a remarkable and gradual reduction in the autophagy and autophagy flux, evidenced upon identification of Pho8 activity (Fig 5A), GFP accumulation from GFP-Atg8 (Fig 5B), GFP-Atg8 localisation (Fig 5C), and both Atg13HA and Atg1HA phosphorylation (Fig 5D). Moreover, iron addition to wt cultures caused the activation of TORC1 through the induction of Atg13 phosphorylation (Fig 5D) and the relocalization of Sfp1to the nucleus (Fig 5E). In addition, when we tested mutants in several signalling pathways related to nutritional sensing *tor1*, *snf1, ypk1*, *ras2*, *gcn2* and (not shown), only *tor1* and *snf1* showed a clear impairment in signalling the autophagy down regulation upon iron refeeding given that we did not observe the descent in the autophagy flux, GFP-Atg8 translocation to the cytoplasm nor Atg13 phosphorylation as it did occurred in wt cultures (Fig 5B to E).

Given that Aft1 is involved in iron homeostasis and that is responsive to iron availability, we decided to investigate the potential contribution of the transcription factor in the detection and transmission of the iron availability and the transmission to the autophagy machinery. The absence of Aft1 prevented the down regulation of autophagy when iron was added to the culture medium (Fig 5B to E). These results suggest that Snf1, Aft1 and Tor1 are involved in the down regulation of autophagy upon iron refeeding.

We discard the possibility that Snf1 or Aft1 act as Tor1 functional regulators upon iron refeeding since Sfp1 translocated to the nucleus in both *snf1* and *aft1* mutant as occurred in wt cells (Fig 5E) suggesting that the signal of iron repletion flows from Snf1 to Aft1 and Tor1 only to specific substrates such is the case of Atg13.

In order to ascertain whether Snf1 kinase activity is responsive to iron signalling, we chose wt and *aft1* posdiauxic cultures because upon 2 days of growth in SD minimum medium, glucose levels are undetectable (data not shown). At the same time, Snf1 reached a maximum kinase activity (Fig 5F). Addition of iron to the culture medium provoked a fast inhibition of autophagy flux in wt cells growing in the presence or absence of Fe (Fig 5G). However, neither *snf1* nor *aft1* mutants experienced any reduction in autophagy flux (Fig 5G), on despite that the in *aft1* mutant Snf1 kinase activity was induced in SD medium equivalent to that detected in wt control cultures (Fig 5F and G). As expected, iron repletion did not repress Snf1 activity neither in wt nor in aft1 cultures (Fig 5F). In conclusion, since in a situation in which Snf1 is active, iron addition is not capable to inactivate autophagy in the absence of Aft1, we speculate that Snf1 might signal to Aft1 to inhibit autophagy upon Atg13 phosphorylation through Tor1. Taking together our results we conclude that iron excess actively represses autophagy through Snf1, Aft1 and Tor1-Atg13 signalling. Iron availability is a determinant factor to regulate autophagy and autophagy flux in optimal nutrient conditions when cells are not exposed to any other nutritional stress.

Iron scarcity promotes trehalose accumulation and resistance to several stresses resembling a quiescent state that is independent of bulk autophagy.

Iron deprivation caused an early entrance in diauxic shift and stationary phase (Fig 6A) already reported by [64]. Our data are in agreement with these observations but, in addition, we also observed a cell cycle blockade in G0, as evidenced by the accumulation of unbudded rounded and big cells, suggestive of quiescence (Fig 6B). To check this we determined in cells depleted or not for iron, both the accumulation of trehalose (Fig 6C) and the resistance to different stresses in stationary cells (Fig 6D) since quiescent cells are more resistant to different environmental stresses [65]. Iron deprivation induced trehalose accumulation and certain increase in the resistance to oxidative stress, high temperature and osmolality during stationary phase (Fig6C and D). The mutants *atg7* and *atg17* also accumulated trehalose as a response to iron deprivation, suggesting that this mechanism is independent of the autophagy machinery (Fig 6C). Calculation of the index of respiratory competence (IRC) indicated that iron deprivation did not reduce the respiratory capacity of the cells during exponential or

stationary phase (Fig 6E). In addition, mitochondria mutation frequency was null in cells growing in iron depleted media during 15 days of observation. However in control cultures growing in SD minimum medium, non-depleted for iron upon 6 days of growth some colonies erythromycin resistant were detected, and the number was sequentially increasing until the end of the experiment, indicating that mitochondrial mutations accumulate during aging when iron is not limited in the growth medium (Fig 6F).

Taking altogether these results, our hypothesis is that iron depletion causes a premature entrance into a quiescent like state that has a positive effect in the mitochondrial function

Iron depletion contributes to extend life conditioned to autophagy flux activation whereas iron overload shortens CLS

In view of the clear involvement that autophagy flux and activation of quiescence have in the response to iron depletion, we decided to analyze the possible biological role that iron starvation and the concomitant activation of autophagy flux could be playing in the chronological life span. First, we carried out experiments of chronological life span (CLS) up to 15 days in 3 different wt backgrounds (Fig 7A). Iron depletion caused a significant life extension in the three backgrounds tested as compared to their corresponding control cultures not starved for iron (Fig 7A). This result demonstrates that iron starvation causes a genuine effect expanding chronological life. We observed that cells starved for iron presented a clear tendency to become rounded unbudded and presented a healthier aspect during all the CLS experiment than wt cells growing in SD medium, consequence of the entrance in quiescent state, as described in the previous section (Fig 6B). Iron deprivation did not preclude mitochondrial function since cell survival was equivalent in glucose and in glycerol during the CLS experiment (Fig 7B). Mutants in different stages of autophagy: *atg7*, *atg13* and *atg17* already experienced a significant reduction in their CLS as previously reported for *atg7* in [17]. Interestingly, iron deprivation cultures experienced an additional reduction in their CLSs (Fig 7C). In conclusion, our results demonstrate that in *S. cerevisiae*, iron homeostasis is particularly relevant in aging associated and conditioned to the regulation of autophagy and autophagy flux.

Discussion

Results shown here indicate that iron depletion is itself a signal to activate autophagy when it is the only limiting nutrient in the culture medium. The observation that this response also occurs in rho0 strain suggest that the reservoir of iron in the mitochondria is not the source of the main signal to activate the autophagy machinery.

Some authors have reported that activation of the autophagy when iron is scarce could be a response to overcome the deleterious effects in the cells in human cells, however the molecular mechanism is poorly understood [8, 66]. According to the elegant studies of [21, 22, 23, 57] our results could indicate that an intact *TOR2* function might be required to maintain a correct mitochondrial function in order to activate autophagy flux when iron is the only limiting nutrient. Or alternatively that Tor2 would induce autophagy through Msn2/Msn4 [50, 21, 23]. However, the observation that a *rho0* mutant induced autophagy upon iron starvation suggested that mitochondrial function turned out to be dispensable for this response in the conditions established in this study. In addition, the observation that Msn2 did not translocate to the nucleus in response to iron deprivation also discarded the possibility that Ypk1 would be signalling to the activation of this transcription factor. Iron scarcity reveals the requirement for a *TOR2* activity as a positive regulator of autophagy through *YPK1* when any other nutrient is limiting. Our results suggest that iron starvation induces *TOR1* inactivation to dephosphorylate Atg13 and consequently to induce the autophagy machinery only when TOR2/YPK1 is active, meaning that these proteins are relevant to sense iron scarcity and to transmit de signal to the autophagy machinery for the adaptive response to iron deprivation specifically. Iron deficient cells exhibit alterations in the properties and functions of membranes [67]. A recent review by [68] updates the evidences that connect TOR2 to membrane homeostasis. Therefore we could speculate that TOR2 might play a role as membrane vigilant when iron is scarce and that one of the mechanisms to overcome this deficiency would be the activation of autophagy, although this hypothesis requires further research. Intriguingly, the transmission of the signal of iron deficiently from Ypk1 to TORC1 only occurs to certain substrates such is the case of Atg13 and Atg1. At the same time, the signal of iron deprivation influences TORC1 regulation on Sfp1 and Rtg1 substrates independently of Tor2/Ypk1. Further investigation in this mechanism will be required. Nevertheless, other nutritional limitations such as nitrogen [69] or even metals such as zinc [70] have been reported to also provoke the inactivation of TORC1. Nitrogen starvation, in particular signals only to specific TORC1 substrates, such as Sfp1

coincidentally, leading to autophagy activation. An elevated autophagy flux ensures iron availability for essential functions such as mitochondrial functioning and synthesis of iron-sulphur clusters, DNA repair, amino acid synthesis and others. In line with this, our results suggest that in conditions of serious iron limitation the requirements for a high autophagy flux to efficiently recycle the metal will preserve life extension.

Respiratory function is essential for standard CLS [71]. Iron depletion not only did not curtail CLS but notably extended it, respiration capacity was not negatively affected by low iron levels, meaning that mitochondrial function was potentially optimal. In accordance with other authors, our results support the hypothesis that iron limitation during aging requires an optimal mitochondrial function that is relevant for the modulation of autophagy flux [58] and life extension [72].

Iron hormesis is another possible explanation to the notable increase in life extension that cells experience in conditions of iron deprivation since the beginning of the experiment. This limitation forces cells to recycle iron from cellular components through autophagy and, in addition, it avoids an excess of iron circulation in the cell, provided that unnecessary vacuolar accumulation of the metal as a result of Aft1 and Aft2 activation, would be prone to cause oxidative stress.

Several studies have shown that quiescence [14] and autophagy contribute to life extension [74, 19, 73]. In this study we show that quiescent cells caused by iron deprivation conferred beneficial consequences for life extension. Iron limitation is another example of treatment intervention to extend life that requires the autophagy machinery since he CLS of *atg1* and *atg7* mutants were severely impaired as compared to cultures not starved for iron, on despite of having activated the quiescent program The observation that iron refeeding can provoke a dramatic descent in CLS and autophagy flux reinforce the idea that the entry in this quiescent state accompanied of autophagy flux induction is essential to extend life when iron is scarce, being any additional metabolic activity detrimental.

In our study we observed that iron limitation caused a mild shift in Snf1 kinase activity as reported in rat esqueletal muscle [75] apparently because in this metabolic condition there is a higher dependence on the glucose metabolism [67]. However, Snf1 is not directly involved in signalling autophagy induction, on the opposite its role is involved in down regulating autophagy flux once iron is refeeded. And it does so through Aft1. The Aft1 transcription factor, whose known function is to regulate iron homeostasis in *S. cerevisiae* is not required to induce autophagy in conditions of iron deficiency, as

previously reported by [64]. However, and interestingly, Aft1 participates in the transmision of the iron repletion signal to inactivate autophagy through Tor1 and Atg13 phosphorylation. This is not the first time in which an association between Snf1 and Aft1 has been reported. [11] already described that both proteins were related in order to induce certain genes from de iron regulon during diauxic shift.

Although autophagy is important for maintaining cellular viability during nutrient stress, excessive autophagy can be deleterious to cells and lead to apoptosis or necrosis [76]. As such, autophagy paradoxically serves as a mechanism for the suppression as well as the proliferation and survival of tumor cells [77]. Iron limitation in the time requires a fine tuning in nutrient recycling and metabolism and signalling activation, a further increase in any of these mechanisms disables the hormetic mechanism leading to early aging and cell death.

Acknowledgements

We want to thank Dr D. Abeliovitch (The Hebrew University of Jerusalem
Cell Biology, Freiburg, Germany) for kindly sending us the plasmid pGFP-Atg8 and to Dr T. Powers (Department of Molecular and Cellular Biology, College of Biological Sciences, UC Davis, USA) for sending us the plasmid pAMS363 and to Dr M. Cyerts (Department of Biology, Stanford, California, USA) for her permission. We want to acknowledge Ms Inmaculada Montoliu for her technical support. The research described in this publication was partly supported by the Plan Nacional de I+D+I of the Spanish Ministry of Economy, Industry and Competitiveness (BIO2017-87828-C2-2-P). Sandra Montella is funded by a fellowship from the Catalan Government (Spain).

Conflict of Interests

The authors declare no conflict of interests

References

1 Mühlenhoff, U. and Lill, R. (2000) Biogenesis of iron-sulfur proteins in eukaryotes: a novel task of mitochondria that is inherited from bacteria. Biochim Biophys Acta. **1459**, 370-382 https://doi.org/10.1016/s0005-2728(00)00174-2

2 Lill R. (2009) Function and biogenesis of iron-sulphur proteins. Nature. **460**, 831-838 https://doi.org/10.1038/nature08301

3 Li L., Jia X., Ward D.M. and Kaplan J. (2011) Yap5 protein-regulated transcription of the TYW1 gene protects yeast from high iron toxicity. J Biol Chem. **286**, 38488-38497 https://doi.org/10.1074/jbc.M111.286666

4 Philpott C.C. and Protchenko O. (2008) Response to iron deprivation in Saccharomyces cerevisiae. Eukaryot Cell. **7**, 20-27 https://doi.org/10.1128/EC.00354-07

5 Kaplan C.D. and Kaplan J. (2009) Iron acquisition and transcriptional regulation. Chem Rev. **109**, 4536-52 https://doi.org/10.1021/cr9001676

6 Yamaguchi-Iwai Y., Stearman R., Dancis A. and Klausner R.D. (1996) Iron-regulated DNA binding by the AFT1 protein controls the iron regulon in yeast. The EMBO Journal **15**, 3377-3384 https://doi.org/10.1002/j.1460-2075.1996.tb00703.x

7 Ueta R., Fujiwara N., Iwai K. and Yamaguchi-Iwai Y. (2007) Mechanism underlying the iron-dependent nuclear export of the iron-responsive transcription factor Aft1p in Saccharomyces cerevisiae. Mol. Biol. Cell. **18**, 2980-2990 https://doi.org/10.1091/mbc.e06-11-1054

8 Inoue H., Kobayashi K., Ndong M., et al. (2015) Activation of Nrf2/Keap1 signaling and autophagy induction against oxidative stress in heart in iron deficiency. Biosci Biotechnol Biochem. **79**, 1366-1368 https://doi.org/10.1080/09168451.2015.1018125

9 Inoue H., Hanawa N., Katsumata S.I., Katsumata-Tsuboi R., Takahashi N. and Uehara M. (2017) Iron deficiency induces autophagy and activates Nrf2 signal through modulating p62/SQSTM. Biomed Res. **38**, 343-350 https://doi.org/10.2220/biomedres.38.343

10 Martins T.S., Costa V. and Pereira C. (2018) Signaling pathways governing iron homeostasis in budding yeast. Mol Microbiol. **109**, 422-432 https://doi.org/10.1111/mmi.14009

11 Haurie V., Boucherie H. and Sagliocco F. (2003) The Snf1 protein kinase controls the induction of genes of the iron uptake pathway at the diauxic shift in Saccharomyces cerevisiae. J Biol Chem. **278**, 45391-45396 https://doi.org/10.1074/jbc.M307447200

12 Li L., Kaplan J. and Ward D.M. (2017) The glucose sensor Snf1 and the transcription factors Msn2 and Msn4 regulate transcription of the vacuolar iron importer gene CCC1 and iron resistance in yeast. J Biol Chem. **292**, 15577- 15586 https://doi.org/10.1074/jbc.M117.802504

13 An Z., Tassa A., Thomas C., et al. (2014) Autophagy is required for G_1/G_0 quiescence in response to nitrogen starvation in Saccharomyces cerevisiae. Autophagy. **10,** 1702-1711 https://doi.org/10.4161/auto.32122

14 Sagot I. and Laporte D. (2019) The cell biology of quiescent yeast - a diversity of individual scenarios. J Cell Sci. **132**, jcs213025 https://doi.org/10.1242/jcs.213025

15 Wen X. and Klionsky D.J. (2016) An overview of macroautophagy in yeast. J Mol Biol. **428**, 1681-1699 https://doi.org/10.1016/j.jmb.2016.02.021

16 Gross A.S. and Graef M. (2020) Mechanisms of Autophagy in Metabolic Stress Response. J Mol Biol. **432**, 28-52 https://doi.org/10.1016/j.jmb.2019.09.005

17 Alvers A.L., Wood M.S., Hu D., Kaywell A.C., Dunn W.A. Jr. and Aris J.P. (2009) Autophagy is required for extension of yeast chronological life span by rapamycin. Autophagy. **5**, 847-849 https://doi.org/10.4161/auto.8824

18 Rubinsztein D.C., Mariño G. and Kroemer G. (2011) Autophagy and aging. Cell. **146**, 682-695 https://doi.org/10.1016/j.cell.2011.07.030

19 Madeo F., Zimmermann A., Maiuri M.C. and Kroemer G. (2015) Essential role for autophagy in life span extension. J Clin Invest. **125**, 85–93 https://doi.org/10.1172/JCI73946

20 Luo L. and Qin Z.H. (2019) Autophagy, Aging, and Longevity. Adv Exp Med Biol. **1206**, 509-525 https://doi.org/10.1007/978-981-15-0602-4_24

21 Vlahakis A., Lopez Muniozguren N. and Powers T. (2016) Calcium channel regulator Mid1 links TORC2-mediated changes in mitochondrial respiration to autophagy. J Cell Biol. **215**, 779–788 https://doi.org/10.1083/jcb.201605030

22 Vlahakis A., Lopez Muniozguren N. and Powers T. (2017) Mitochondrial respiration links TOR complex 2 signaling to calcium regulation and autophagy. Autophagy. **13**, 1256-1257 https://doi.org/10.1080/15548627.2017.1299314

23 Vlahakis A., Lopez Muniozguren N. and Powers T. (2017b) Stress-response transcription factors Msn2 and Msn4 couple TORC2-Ypk1 signaling and mitochondrial respiration to ATG8 gene expression and autophagy. Autophagy. **13**, 1804-1812 https://doi.org/10.1080/15548627.2017.1356949

24 Romero A.M., Ramos-Alonso L., Montellá-Manuel S., García-Martínez J., de la Torre-Ruiz M.Á., Pérez-Ortín J.E., Martínez-Pastor M.T. and Puig S. (2019) A genome-wide transcriptional study reveals that iron deficiency inhibits the yeast TORC1 pathway. Biochim Biophys Acta Gene Regul Mech. **1862**, 194414 https://doi.org/10.1016/j.bbagrm.2019.194414

25 Powers R.W. 3rd, Kaeberlein M., Caldwell S.D., Kennedy B.K. and Fields S. (2006) Extension of chronological life span in yeast by decreased TOR pathway signaling. Genes Dev. **20**, 174-84 https://doi.org/10.1101/gad.1381406

26 Weichhart T. mTOR as Regulator of Lifespan, Aging, and Cellular Senescence: A Mini-Review. (2018) Gerontology. **64**, 127-134 https://doi.org/10.1159/000484629

27 Kim Y.C. and Guan K.L. (2015) mTOR: a pharmacologic target for autophagy regulation. J Clin Invest. **125**, 25-32 https://doi.org/10.1172/JCI73939

28 Kamada Y., Funakoshi T., Shintani T., Nagano K., Ohsumi M. and Ohsumi Y. (2000) Tor-mediated induction of autophagy via an Apg1 protein kinase complex. J Cell Biol **150**, 1507–1513 https://doi.org/10.1083/jcb.150.6.1507

29 Hughes Hallett J.E., Luo X. and Capaldi A.P. (2014) State transitions in the TORC1 signaling pathway and information processing in Saccharomyces cerevisiae. Genetics. **198**, 773-786 https://doi.org/10.1534/genetics.114.168369

30 Marion R.M., Regev A., Segal E., Barash Y., Koller D., Friedman N. and O'Shea E.K. (2004) Sfp1 is a stress- and nutrient-sensitive regulator of ribosomal protein gene expression. Proc Natl Acad Sci U S A **101**, 14315-22 https://doi.org/10.1073/pnas.0405353101

31 Lempiäinen H., Uotila A., Urban J., Dohnal I., Ammerer G., Loewith R. And Shore D. (2009) Sfp1 interaction with TORC1 and Mrs6 reveals feedback regulation on TOR signaling. Mol Cell **33**, 704-16 https://doi.org/10.1016/j.molcel.2009.01.034

32 Gorner W., Durchschlag E., Wolf J., Brown E.L., Ammerer G., Ruis H. and Schuller C. (2002) Acute glucose starvation activates the nuclear localization signal of a stress-specific yeast transcription factor. EMBO J. **21**, 135-144 https://doi.org/10.1093/emboj/21.1.135

33 De Wever V., Reiter W., Ballarini A., Ammerer G. and Brocard C. (2005) A dual role for PP1 in shaping the Msn2-dependent transcriptional response to

glucose starvation. EMBO J. **24**, 4115-4123 https://doi.org/10.1038/sj.emboj.7600871

34 Liao X. and Butow R.A. (1993) RTG1 and RTG2: two yeast genes required for a novel path of communication from mitochondria to the nucleus. Cell **72**, 61–71 https://doi.org/10.1016/0092-8674(93)90050-z

35 Crespo J.L., Powers T., Fowler B. and Michael N. Hall. (2002) The TOR-controlled transcription activators GLN3, RTG1, and RTG3 are regulated in response to intracellular levels of glutamine. Proc Natl Acad Sci U S A. **99**, 6784–6789 https://doi.org/10.1073/pnas.102687599

36 Guaragnella N., Coyne L.P., Chen X.J. and Giannattasio S. (2018) Mitochondria–cytosol–nucleus crosstalk: learning from Saccharomyces cerevisiae. FEMS Yeast Research. **18** https://doi.org/10.1093/femsyr/foy088

37 Fujioka Y., Suzuki S.W., Yamamoto H., et al. (2014) Structural basis of starvation-induced assembly of the autophagy initiation complex. Nat Struct Mol Biol. **21**, 513-521 https://doi.org/10.1038/nsmb.2822

38 Yamamoto H., Fujioka Y., Suzuki S.W., et al. (2016) The Intrinsically Disordered Protein Atg13 Mediates Supramolecular Assembly of Autophagy Initiation Complexes. Dev Cell. **38**, 86-99 https://doi.org/10.1016/j.devcel.2016.06.015

39 Gallego C., Garí E., Colomina N., Herrero E. and Aldea M. (1997) The Cln3 Cyclin Is Down-Regulated by Translational Repression and Degradation during the G1 Arrest Caused by Nitrogen Deprivation in Budding Yeast. The EMBO Journal **16**, 7196–7206 https://doi.org/10.1093/emboj/16.23.7196

40 Petkova M.I., Pujol-Carrion N. and De La Torre-Ruiz M.A. (2010) Signal Flow between CWI/TOR and CWI/RAS in Budding Yeast under Conditions of Oxidative Stress and Glucose Starvation. Communicative & Integrative Biology **3**, 555–57 https://doi.org/10.4161/cib.3.6.12974

41 Pujol-Carrion N., Petkova M.I., Serrano L. and De La Torre-Ruiz M.A. (2013) The MAP kinase Slt2 is involved in vacuolar function and actin remodeling in Saccharomyces cerevisiae mutants affected by endogenous oxidative stress. Appl. Environ. Microbiol. **79**, 6459–6471 http://doi.org/10.1128/AEM.01692-13

42 Mechoud M.A., Pujol-Carrion N., Montella-Manuel S. and De La Torre-Ruiz M.A. (2020) Interactions of GMP with Human Glrx3 and with Saccharomyces

cerevisiae Grx3 and Grx4 Converge in the Regulation of the Gcn2 Pathway. Appl. Environ. Microbiol. **86**, e00221-20 http://doi.org/10.1128/AEM.00221-20

43 Guedes A., Ludovico P. and Sampaio-Marques B. (2016) Caloric restriction alleviates alpha-synuclein toxicity in aged yeast cells by controlling the opposite roles of Tor1 and Sir2 on autophagy. Mech. Ageing. Dev. **161**, 270-276 http://dx.doi.org/10.1016/j.mad.2016.04.006

44 Mayordomo I., Estruch F. and Sanz P. (2002) Convergence of the Target of Rapamycin and the Snf1 Protein Kinase Pathways in the Regulation of the Subcellular Localization of Msn2, a Transcriptional Activator of STRE (Stress Response Element)-Regulated Genes. J. Biol. Chem. **277**, 35650–56 https://doi.org/10.1074/jbc.M204198200

45 Kanki T. and Klionsky D.J. (2008) Mitophagy in yeast occurs through a selective mechanism. J. Biol. Chem. **283**, 32386-93 https://doi.org/10.1074/jbc.M802403200

46 Nitai E., Mor A., Journo D. and Abeliovich H. (2010) Deprivation Is Distinct from Nitrogen Starvation- Induced Macroautophagy Induction of Autophagic Flux by Amino Acid Deprivation Is Distinct from Nitrogen Starvation-Induced Macroautophagy. Autophagy. **6**, 879-90. https://doi.org/10.4161/auto.6.7.12753

47 Gorner W., Durchschlag E., Martinez-Pastor M.T., Estruch F., Ammerer G., Hamilton B., Ruis H. and Schuller C. (1998) Nuclear localization of the C2H2 zinc finger protein Msn2p is regulated by stress and protein kinase A activity. Genes Dev. **12**, 586-597 http://doi.org/10.1101/gad.12.4.586

48 Pujol-Carrion N., Belli G., Herrero E., Nogues A. and De La Torre-Ruiz M.A. (2006) Glutaredoxins Grx3 and Grx4 regulate nuclear localisation of Aft1 and the oxidative stress response in Saccharomyces cerevisiae. J. Cell. Sci. **119**, 4554-4564 http://doi.org/10.1242/jcs.03229

49 Komeili, A., Wedaman K.P., O'Shea E.K. and Powers T. (2000) Mechanism of Metabolic Control: Target of Rapamycin Signaling Links Nitrogen Quality to the Activity of the Rtg1 and Rtg3 Transcription Factors. J. Cell Biol. **151**, 863– 78 https://doi.org/10.1083/jcb.151.4.863

50 Vlahakis A., Graef M., Nunnari J. and Powers T. (2014) TOR complex 2-Ypk1 signaling is an essential positive regulator of the general amino acid control response and autophagy. Proc. Natl. Acad. Sci. U S A. **111**, 10586–10591 http://doi.org/10.1073/pnas.1406305111

51 Wach M.P., Brachat A., Pohlmann R. and Philippsen P. (1994) New heterologous modules for classical or PCR-based gene disruptions in Saccharomyces cerevisiae. Yeast. **10**, 1793–1808 http://doi.org/10.1002/yea.320101310.

52 Kaiser C., Michaelis S. and Mitchell A. (1994) Methods in yeast genetics. NewYork Cold Spring Harbor Laboratory Press Ltd. **1994,** pp.107–121 ISBN:0-87969-451-3

53 Stathopoulos A.M. and Cyert M.S. (1997) Calcineurin acts through the CRZ1/TCN1-encoded transcription factor to regulate gene expression in yeast.
a. Genes Dev. **11**, 3432–3444. http://dx.doi.org/10.1101/gad.11.24.3432

54 Hernandez-Lopez M., Prieto J. and Randez-Gil F. (2003) Osmotolerance and leavening ability in sweet and frozen sweet dough. Comparative analysis between Torulaspora delbrueckii and Saccharomyces cerevisiae baker's yeast strains. Antonie van Leeuwenhoek. **84**, 125–34 http://doi.org/10.1023/a:1025413520192

55 Parrella, E. and Longo, V. D. (2008) The chronological life span of Saccharomyces cerevisiae to study mitochondrial dysfunction and disease. Methods. **46**, 256–262 http://doi.org/10.1016/j.ymeth.2008.10.004

56 Noda T. and Klionsky D.J. (2008) The Quantitative Pho8D60 Assay of Nonspecific Autophagy. Methods in Enzymology, **451**, 33-42 http://doi.org/10.1016/S0076-6879(08)03203-5

57 Shintani T. and Klionsky D.J. (2004) Cargo proteins facilitate the formation of transport vesicles in the cytoplasm to vacuole targeting pathway. J. Biol. Chem. **279**, 29889-94 http://doi.org/10.1074/jbc.M404399200

58 Graef M. and Nunnari J. (2011) Mitochondria regulate autophagy by conserved signalling pathways. EMBO J. **30,** 2101-14 http://doi.org/10.1038/emboj.2011.104

59 Noda T., Matsuura A., Wada Y. and Ohsumi, Y. (1995). Novel system for monitoring autophagy in the yeast Saccharomyces cerevisiae. Biochem. Biophys. Res. Commun. **210**, 126–132 http://doi.org/10.1006/bbrc.1995.1636

60 Beck T. and Hall M.N. (1999) The TOR signalling pathway controls nuclear localization of nutrient-regulated transcription factors. Nature. **402**, 689-692 http://doi.org/10.1038/45287

61 Cherkasova V.A. and Hinnebusch A.G. (2003) Translational control by TOR and TAP42 through dephosphorylation of eIF2alpha kinase GCN2. Genes Dev. **17**, 859-872 http://doi.org/10.1101/gad.1069003

62 Kubota H., Obata T., Ota K., Sasaki T. and Ito T. (2003) Rapamycin induced translational derepression of GCN4 mRNA involves a novel mechanism for activation of the eIF2 alpha kinase GCN2. J. Biol. Chem. **278**, 20457-20460 http://doi.org/10.1074/jcb.C300133200

63 Kamada Y., Yoshino K., Kondo C., et al. (2010) Tor directly controls the Atg1 kinase complex to regulate autophagy. Mol. Cell. Biol. **30**, 1049-1058 http://doi.org/10.1128/MCB.01344-09

64 Horie T., Kawamata T., Matsunami M. and Ohsumi Y. (2017) Recycling of iron via autophagy is critical for the transition from glycolytic to respiratory growth. J. Biol. Chem. **292**, 8533-8543 http://doi.org/10.1074/jbc.M116.762963

65 Goldberg A.A., Bourque S.D., Kyryakov P., Gregg C., Boukh-Viner T., Beach A., Burstein M.T., Machkalyan G., Richard V., Rampersad S., Cyr D., Milijevic S. and Titorenko V.I. (2009) Effect of calorie restriction on the metabolic history of chronologically aging yeast. Exp. Gerontol. **44**, 555-71. http://doi.org/10.1016/j.exger.2009.06.001

66 Krishan S., Jansson P.J., Gutierrez E., Lane D.J., Richardson D. and Sahni S. (2015) Iron metabolism and autophagy: a poorly explored relationship that has important consequences for health and disease. Nagoya. J. Med. Sci. **77**, 1-6

67 Shakoury-Elizeh M., Protchenko O., Berger A., et al. (2010) Metabolic response to iron deficiency in Saccharomyces cerevisiae. J. Biol. Chem. **285**, 14823- 14833 http://doi.org/10.1074/jbc.M109.091710

68 Riggi M., Niewola-Staszkowska K., Chiaruttini N., Colom A., Kusmider B., Mercier V., Soleimanpour S., Stahl M., Matile S., Roux A. and Loewith R. (2018) Decrease in plasma membrane tension triggers PtdIns(4,5)P2 phase separation to inactivate TORC2. Nat. Cell. Biol. **20**, 1043-1051 http://doi.org/10.1038/s41556-018-0150-z

69 Shin C.S. and Huh W.K. (2011) Bidirectional regulation between TORC1 and autophagy in Saccharomyces cerevisiae. Autophagy. **7**, 854-862 http://doi.org/10.4161/auto.7.8.15696

70 Kawamata T., Horie T., Matsunami M., Sasaki M. and Ohsumi Y. (2017) Zinc starvation induces autophagy in yeast. J. Biol. Chem. **292**, 8520-8530 http://doi.org/10.1074/jbc.M116.762948

71 Ocampo A., Liu J., Schroeder E.A., Shadel G.S. and Barrientos A. (2012) Mitochondrial respiratory thresholds regulate yeast chronological life span and its extension by caloric restriction. Cell Metab. **16**, 55-67 http://doi.org/10.1016/j.cmet.2012.05.013

72 Fabrizio P., Liou L.L-, Moy V.N., Diaspro A., Valentine J.S., Gralla E.B. and Longo V.D. (2003) SOD2 functions downstream of Sch9 to extend longevity in yeast. Genetics. **163**, 35-46

73 Tyler J.K. , Johnson J.E. (2019). The role of autophagy in the regulation of yeast life span. Ann. N. Y. Acad. Sci. **1418**, 31–43 http://doi.org/10.1111/nyas.13549

74 Eisenberg T., Knauer H., Schauer A., Büttner S., Ruckenstuhl C., Carmona-Gutierrez D., Ring J., Schroeder S., Magnes C., Antonacci L., Fussi H., Deszcz L., Hartl R., Schraml E., Criollo A., MegalouE., Weiskopf D., Laun P., Heeren G., Breitenbach M., Grubeck-Loebenstein B., Herker E., Fahrenkrog B., Fröhlich K.U., Sinner F., Tavernarakis N., Minois N., Kroemer G. and Madeo F. (2009) Induction of autophagy by spermidine promotes longevity. Nat. Cell Biol. **11**, 1305–1314 http://doi.org/10.1038/ncb1975

75 Merrill J.F., Thomson D.M., Hardman S.E., Hepworth S.D., Willie S. and Hancock C.R. (2012) Iron deficiency causes a shift in AMP-activated protein kinase (AMPK) subunit composition in rat skeletal muscle. Nutr. Metab. (Lond). **9**, 104. http://doi.org/10.1186/1743-7075-9-104

76 Maiuri M.C., Zalckvar E., Kimchi A. and Kroemer G. (2007) Self-eating and self-killing: Crosstalk between autophagy and apoptosis. Nat. Rev. Mol. Cell. Biol. **8**, 741–752 http://doi.org/10.1038/nrm2239

77 Yang Z.J., Chee C.E., Huang S. and Sinicrope F.A. (2011) The role of autophagy in cancer: Therapeutic implications. Mol. Cancer .Ther. **10**, 1533– 1541 http://doi.org/10.1158/1535-7163:MCT-11-0047

Figure 1. Iron deprivation as the only nutrient restriction induces bulk autophagy and increases the accumulation of both Atg8 and Atg13 foci. A) wt, *atg7* and *atg1* cultures in which the fusion protein GFP-Atg8 was integrated (strains GSL197, 226 and 325, respectively), were grown to log phase (OD_{600}: 0.6) in SD and SD-Fe medium at 30ºC. Aliquots were collected for total protein extraction and western blot. GFP-Atg8 was monitored using an anti-GFP antibody. As loading control we used anti-Pgk1 to detect Pgk1. B) Autophagic flux was calculated as the ratio between free GFP and total GFP-Atg8 detected in A. Total GFP-Atg8 was determined as the addition of the high mobility band corresponding to the form GFP-Atg8 and the slow mobility band corresponding to GFP, as a result of Atg8 vacuolar degradation. C) Total Atg8 was determined as the ratio between total GFP-Atg8 and Pgk1 expression. D) *In vivo* observation in the fluorescence microscope of a sample obtained from the experiment described in A. E) Percentage of Atg8 foci quantified in the experiment described in D was calculated upon microscopic observation of 1,000 cells. F) wt, *atg7* and *atg1* strains were transformed with plasmid pATG13-GFP. Culture conditions were identical as those described in A. Atg13 foci were counted from a total of 1,000 cells observed in the fluorescence microscopy. G) Autophagy activity was measured in exponential cultures limited or nor for iron by using the alkaline phosphatase assay in the strain BY4741*pho8*Δ expressing a plasmid with the inactive Pho8 proenzyme targeted to the cytosol.
For all the figures: We used anti-Pgk1 to detect Pgk1, selected as a loading control in all the western blots shown in this study. For western blot and microscopy images in this paper, we have selected representative samples. Error bars in the histograms represent the standard deviation (SD) calculated from 3 independent experiments. Significance of the data was determined by P-values from a Student unpaired t-test denoted as follows: *=0.05>P>0.01; **=0.01>P>0.001; ***=0.001>P>0.0001; ****=P>0.0001

Figure 2. Tor1 inhibition to specific substrates mediates the induction of bulk autophagy in response to iron deprivation. A) Strains wt and *atg7* were each transformed with the plasmids Sfp1GFP, Rtg1GFP or Msn2GFP, respectively, to be subsequently exponentially grown at 30ºC in SD and SD-Fe media. Aliquots were collected for in vivo observation in the fluorescence microscope. Histograms represent percentages of *in vivo* nuclear or cytoplasmic localization out of 1000 cells. B) Cultures of wt and *atg7* strains were transformed with a plasmid bearing Rtg1GFP to be subsequently grown at

30ºC to log phase in both SD and SD-Fe media, cultures were treated with N-Acetyl cysteine (NAC) 5mM for 2 hours. C) Strains wt and *atg7* were exponentially grown in both SD and SD-Fe and samples were collected for total protein extraction and western blot analysis. The phosphorylated form of eIF2α was detected by using and anti-eIF2α-P antibody. A 2 days culture of wt strain in SD medium, was included as a control to detect eIF2α phosphorylation. Histogram represents the values of phosphorylated eIF2α normalized with respect to values determined with the loading control. D) wt, *atg7* and *atg1* strains were transformed with plasmids bearing Atg13HA or Atg1HA, respectively. Cultures were exponentially grown in either SD or SD-Fe. Values of Atg13 or Atg1 proteins were determined upon western blot analysis by adding anti-HA antibody. Samples were collected and each of them was split into two parts, one part was treated 1h at 37ºC with alkaline phosphatase and the other remained untreated. E) wt and *atg7* bearing GFP-Atg8 were exponentially grown at 30ºC in SD and SD-Fe media. Rapamycin was added to the cultures at 200 ng/ml and samples were collected upon 2 hours of exposure to the drug for total protein extraction and western blot. GFP- Atg8 monitoring in microscope images and histograms were performed as described in Fig 1. F) Autophagic activity was determined through the alkaline phosphatase assay as in Fig 1G. Rapamycin treatment conditions were as described in Fig 2E.

Figure 3. TOR2/Ypk1 activity is required to transmit the iron starvation signal to the autophagy machinery. A) wt and *ypk1* strains in which the fusion protein GFP-Atg8 was integrated, were grown and GFP-Atg8 or GFP were detected as in Fig 1A. Autophagy flux and total Atg8 were determined as in Fig 1B and C, respectively. B) Microscopic observation of GFP-Atg8 was carried out as in Fig 1D. C) wt and *ypk1* strains were transformed with the plasmids Sfp1GFP, Rtg1GFP or Msn2GFP to be subsequently grown at 30ºC in SD and SD-Fe, respectively, until OD_{600}: 0.6. Aliquots were collected to be in vivo observed in the fluorescence microscope as in Fig 2A. Histograms represent percentages of *in vivo* nuclear or cytoplasmic localization. D) Atg13HA and Atg1HA phosphorylation and treatment with alkaline phosphatase were determined in wt and *ypk1* strains as described in Fig 2D. E) Autophagy determination in wt and *rho0* strains was performed as in A. F) Microscope images from samples collected in E.

Figure 4. Atg13 dephosphorylation dependent of TORC1 inactivation, requires a previous signalling by TOR2/Ypk1 upon iron starvation in order to initiate bulk

autophagy. A) wt and *ypk1* expressing either GFP-Atg8, Atg13HA or Atg1HA were exponentially grown at 30ºC in SD and SD-Fe media to OD_{600}: 0.6. Rapamycin was added to half of the cultures at 200ng/ml and samples were taken upon 2 hours for western blot analysis. Protein detection, autophagy flux, total Atg8 and *in vivo* observation in the fluorescence microscope was performed as described in Fig1A-D and 2D. B) wt and *ypk1* strains transformed with the plasmids Rtg1GFP, Sfp1GFP and Msn2GFP were treated as in A. Aliquots were collected for *in vivo* observation in the fluorescence microscope. C) wt and *ypk1* strains were exponentially grown in SD and SD-Fe media at 30ºC. Samples were collected for total protein extraction and western blot to analyze the phosphorylated form of eIF2α as in Fig 2C. D) wt and *ypk1* cells containing plasmid pAMS363 expressing a 2xCDRE:lacZ fusion were at 30ºC. Samples were harvested at OD600: 0.6 to determine β-galactosidase activity as described in Material and Methods. E) wt, *tor1, ras2, gcn2* and *snf1* strains expressing GFP-Atg8, Atg13HA or Atg1HA, respectively, were grown at 30ºC in SD and SD-Fe media.
Protein detection, treatment with alkaline phosphatase and *in vivo* observation in the fluorescence microscope was performed as described in Fig1A-D and 2D. F) wt and *aft1* transformed with GFP-Atg8, Atg13HA and Atg1HA, respectively were exponentially grown at 30ºC in SD and SD-Fe conditions. Protein detection, autophagy flux, total Atg8 calculations and in vivo observation in the fluorescence microscope was performed as described in Fig 1A-D and 2D.

Figure 5. Snf1, Aft1 and Tor1 are required to inactivate autophagy upon iron refeeding.
A) Autophagy activity was measured by means of the alkaline phosphatase assay as explained in Fig 1G. Iron was added to wt cultures at OD_{600}: 0.6, and samples were taken upon 2 hours of addition. B) Strains wt, *tor1, aft1* and *snf1* bearing GFP-Atg8 in the genome, were grown to OD_{600}: 0.6 at 30ºC in SD and SD-Fe media. Iron was added to the cultures as in A, and samples were collected upon 2 and 6 hours to detect GFP-Atg8 and C) cellular localization of GFP-Atg8. Autophagy flux and GFP-Atg8 total expression were determined as in Fig1. D) wt, *tor1, aft1* and *snf1* transformed either with Atg13HA or Atg1HA plasmids and subsequently treated as in B. Samples were processed for western blot assay by using anti-HA antibody. E) Localisation of Sfp1 was determined microscopically upon transformation of the strains wt, *tor1, aft1* and *snf1* with plasmid bearing the protein fused to GFP as described in the former figures. Cultures were carried out as described in B). F) wt and *aft1* strains were cultured in SD

and SD-Fe medium during 2 days, iron was added and samples were collected upon the times indicated in the Figure for western blot analysis. AMPK1 was detected using an anti-AMPK1-P. G) wt, *aft1* and *snf1* expressing the fusion protein GFP-Atg8, were cultured in SD and SD-Fe medium during 2 days. Iron was added to the cultures and aliquots were collected as indicated in the Figure for protein extraction and western blot analysis and for microscopical observation to detect GFP-Atg8 protein. Autophagic flux and total Atg8 expression were determined as in Fig 1.

Figure 6. Iron deprivation induces an early entrance into quiescence independent of bulk autophagy. A) wt cells were grown in each SD or SD-Fe media at 30ºC for 15 days in continuous shacking. Samples were taken daily to monitor the absorbance at 600nm to build the growth curves. Average values from three independent experiments were represented along with the corresponding error bars. B) The number of budded or unbudded cells was counted in a sample of 1,000 cells collected from wt cultures grown at OD_{600}: 0.6 in both SD or in SD-Fe. C) Trehalose concentration [μg/μL] was referred to the total protein determined in cultures from wt, atg7 and atg17 strains growing exponentially in either SD and SD-Fe media at 30ºC. D) Samples from wt cultures growing exponentially in SD or SD-Fe media were collected and the same number of cells was plated onto YPD plates to be incubated at 30ºC, 39ºC or 41ºC or alternative, cells were plated onto media containing H_2O_2 or sorbitol. Cell survival was determined as the ratio between the number of colonies isolated from the treatment plates and the number of colonies isolated in control YPD plates incubated at 30ºC. E) The index of respiratory competence (IRC) in wt cells and F) mitochondria mutation frequency, were both determined as described in Materials and Methods.

Figure 7. Iron starvation prolongs life span in a manner dependent of the activation of bulk autophagy. Cultures were exponentially grown either in SD, SD-Fe, SGly (containing glycerol as unique carbon source) or SGly-Fe media plus amino acids at 30°C. Samples were taken at the indicated times to determine CLS, as described in Materials and Methods. Numerical data regarding maximum life span (the day when cultures reach 10% survival) and average life span (the day at which 50% survival was recorded) for each strain is depicted.

Chronological life span curves for A) wt CML128, wt SEY6210 and wt FY250 in SD and SD-Fe media, respectively. B) wt cells growing in SD, SGly, SD-Fe and SGly-Fe media. C) wt, *atg7, atg13* and *atg17* strains cultured in SD and SD-Fe, respectively.

Table 1. Yeast strains used in this study

Strain	Genotype	Source
CML128	*MAT**a** leu2-3,112, ura3-52, trp1, his4*	[39]
GSL034	*MAT**a** tor1::KanMx4*	[40]
GSL053	*MAT**a** ras2::Leu2MX5*	[40]
GSL197	*MAT**a** leu2-3,112, uras3-52, trp1, his4 GFP-ATG8::URA3*	This work
GS199	*MAT**a** tor1::KanMx4 GFP-ATG8::URA3*	This work
GSL201	*MAT**a** ras2::Leu2MX5 GFP-ATG8::URA3*	This work
GSL218	*MAT**a** atg7::NatMx4*	This work
GSL222	*MAT**a** atg13::NatMx4*	This work
GSL226	*MAT**a** atg7::NatMx4 GFP-ATG8::URA3*	This work
GSL238	*MAT**a** atg17::NatMx4*	This work
GSL284	*MAT**a** aft1::KanMx4*	[41]
GSL293	*MAT**a** atg11:NatMx4*	This work
GSL297	*MAT**a** atg11:NatMx4 GFP-ATG8::URA3*	This work
GSL313	*MAT**a** aft1::KanMx4 GFP-ATG8::URA3*	This work
GSL324	*MAT**a** atg1::NatMx4*	This work
GSL325	*MAT**a** atg1::NatMx4 GFP-ATG8::URA3*	This work
GSL350	*MAT**a** gcn2::KanMx4*	[42]
GSL352	*MAT**a** gcn2::KanMx4 GFP-ATG8::URA3*	This work
GSL364	*MAT**a** atg32::KanMx4 GFP-ATG8::URA3*	This work
GSL370	*MAT**a** rho0 GFP-ATG8::URA3*	This work
GSL371	*MAT**a** atg32::KanMx4 GFP-ATG8::URA3*	This work
GSL372	*MAT**a** leu2-3,112, uras3-52, trp1, his4 ATG1-HA::LEU2*	This work
GSL374	*MAT**a** ypk1::KanMx4 GFP-*	This work

	ATG8::URA3	
GSL382	*MAT**a** snf1:KanMx4 GFP-ATG8::URA3*	This work
GSL384	*MAT**a** ypk1::KanMx4*	This work
GSL389	*MAT**a** tor1::KanMx4 ATG1-HA::LEU2*	This work
GSL390	*MAT**a** aft1::KanMx4 ATG1-HA::LEU2*	This work
GSL393	*MAT**a** ypk1::KanMx4 ATG1-HA::LEU2*	This work
GSL394	*MAT**a** snf1::KanMx4*	This work
GSL395	*MAT**a** snf1::KanMx4 ATG1-HA::LEU2*	This work
GSL398	*MAT**a** atg1::NatMx4 ATG1-HA::LEU2*	This work
GSL399	*MAT**a** atg7::NatMx4 ATG1-HA::LEU2*	This work
GSL401	*MAT**a** gcn2::KanMx4 ATG1-HA::LEU2*	This work
BY4741 *pho8Δ*	*MAT**a** pho8 his3D1, leu2D0, met15D0, ura3D0*	[43]
FY250	*MAT**α** his3-200, leu2-1, trp1-63, ura3-52*	[44]
SEY6210	*MAT**a** his3-200, leu2-3, lys2-801, trp1-901, ura3-52, suc2-9 GAL*	[45]

Table 2. Plasmids used in this study

Plasmid	Restriction sites to clone the ORF	Marker	Promoter	Epitope	Source
pSfp1-GFP	SalI, SmaI	*URA3*	MET25	GFP	This work
pGFP-Atg8	EcoRI, XhoI	*URA3*	ATG8	GFP	[46]
pAtg13-HA	NotI, PstI	*URA3*	ADH1	HA	This work
pYX242-cytPho8	AvrII, MluI	*LEU2*	PHO8		[43]
pAdh1-Msn2-GFP	KspI, SalI	*LEU2*	ADH1	GFP	[47]
pAtg13-GFP	XbaI, SalI	*URA3*	MET25	GFP	This work
pMM351	PstI, HindIII	*LEU2*	ADH1	HA	[48]
pAtg1-HA	PmeI, PstI	*LEU2*	ADH1	HA	This work
pRtg1-GFP	XhoI, EcoRI	*URA3*	RTG1	GFP	[49]
pAMS363	XhoI, SalI	*URA3*	2xCDRE:lacZ		[50]

Figure 1

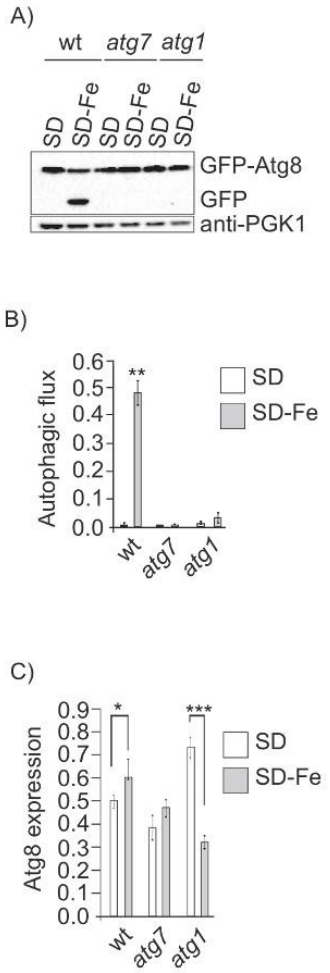
A)
wt
atg7
atg1
SD
SD-Fe
SD
SD-Fe
SD
SD-Fe
GFP-Atg8
GFP
anti-PGK1
B)
Autophagic flux
0.6
0.5
0.4
0.3
0.2
0.1
0.0
**
SD
SD-Fe
wt
atg7
atg1
C)
Atg8 expression
0.9
0.8
0.7
0.6
0.5
0.4
0.3
0.2
0.1
0.0
*
***
SD
SD-Fe
wt
atg7
atg1

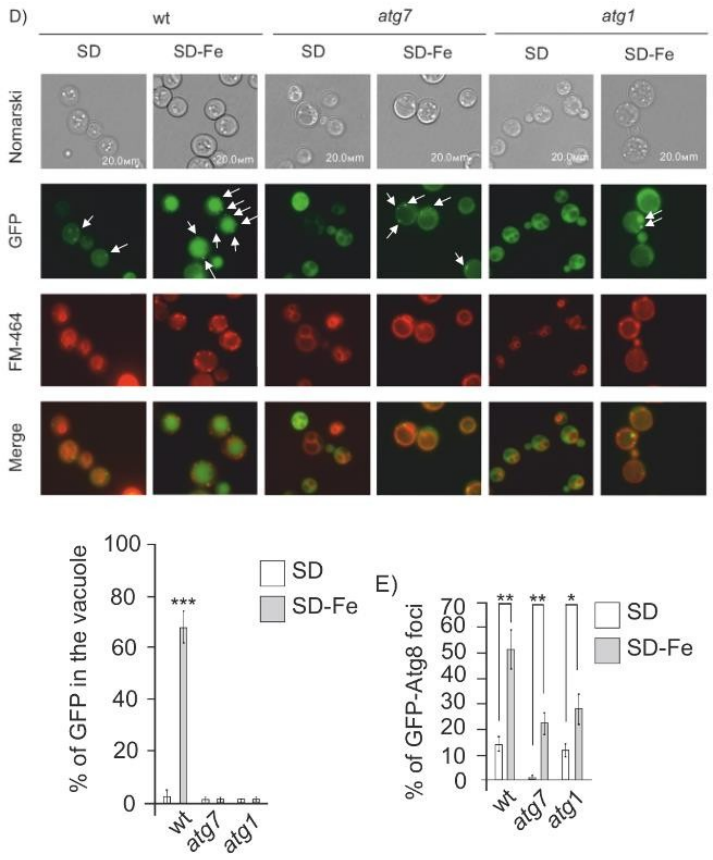
D)
wt
atg7
atg1
SD
SD-Fe
SD
SD-Fe
SD
SD-Fe
Nomarski
GFP
FM-464
Merge
20.0µm
% of GFP in the vacuole
100
80
60
40
20
0
***
SD
SD-Fe
wt
atg7
atg1
E)
% of GFP-Atg8 foci
70
60
50
40
30
20
10
0
**
**
*
SD
SD-Fe
wt
atg7
atg1

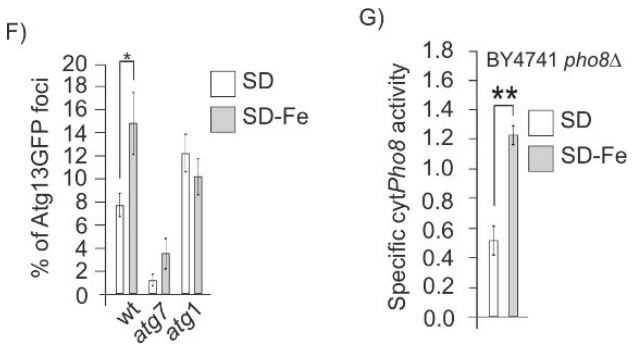
F)
% of Atg13GFP foci
20
18
16
14
12
10
8
6
4
2
0
*
SD
SD-Fe
wt
atg7
atg1
G)
Specific cytPho8 activity
1.8
1.6
1.4
1.2
1.0
0.8
0.6
0.4
0.2
0.0
BY4741 pho8Δ
**
SD
SD-Fe

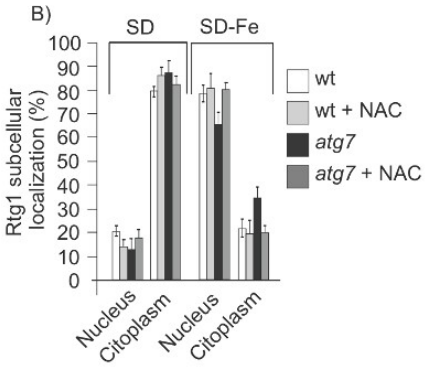
B)
SD
SD-Fe
Rtg1 subcellular localization (%)
100
90
80
70
60
50
40
30
20
10
0
wt
wt + NAC
atg7
atg7 + NAC
Nucleus
Citoplasm
Nucleus
Citoplasm

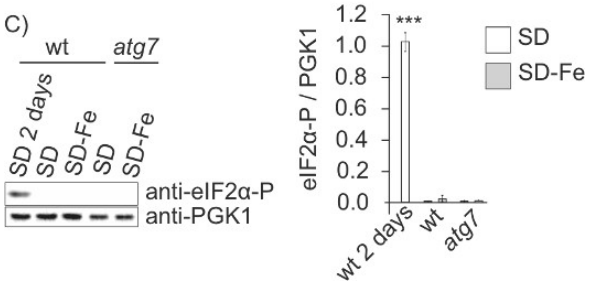
C)
wt
atg7
SD 2 days
SD
SD-Fe
SD
SD-Fe
anti-eIF2α-P
anti-PGK1
eIF2α-P / PGK1
1.2
1.0
0.8
0.6
0.4
0.2
0.0
***
SD
SD-Fe
wt 2 days
wt
atg7

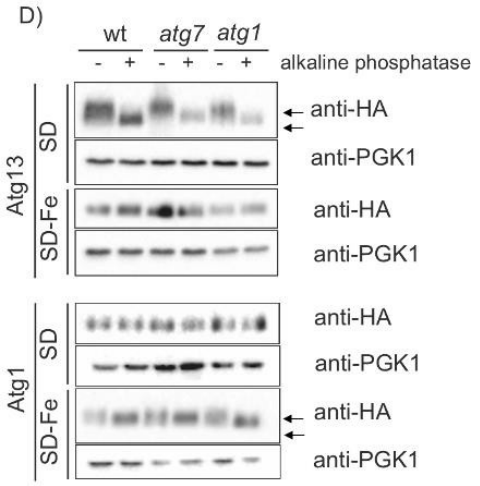
D)
wt
atg7
atg1
- + - + - +
alkaline phosphatase
Atg13
SD
SD-Fe
anti-HA
anti-PGK1
anti-HA
anti-PGK1
Atg1
SD
SD-Fe
anti-HA
anti-PGK1
anti-HA
anti-PGK1

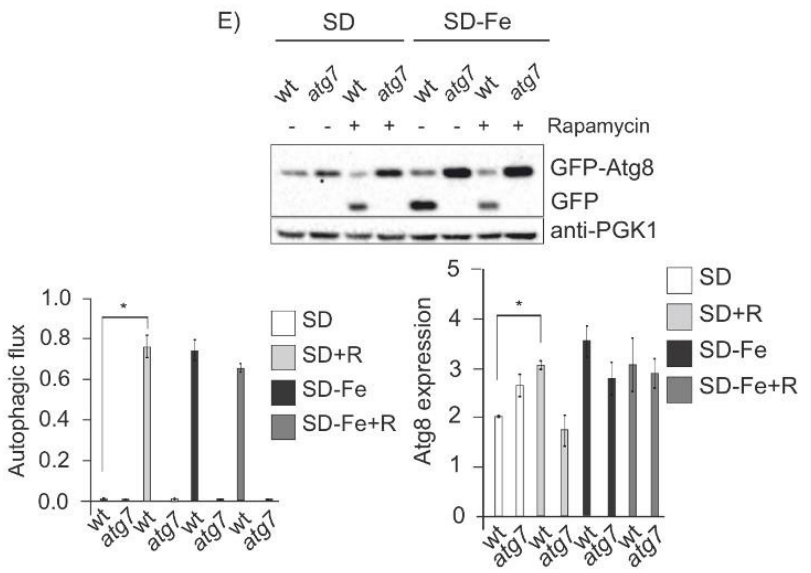
E)
SD
SD-Fe
wt
atg7
Rapamycin
GFP-Atg8
GFP
anti-PGK1
Autophagic flux
Atg8 expression
SD
SD+R
SD-Fe
SD-Fe+R

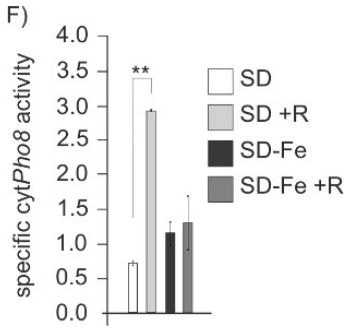
F)
specific cytPho8 activity
SD
SD +R
SD-Fe
SD-Fe +R

Figure 3

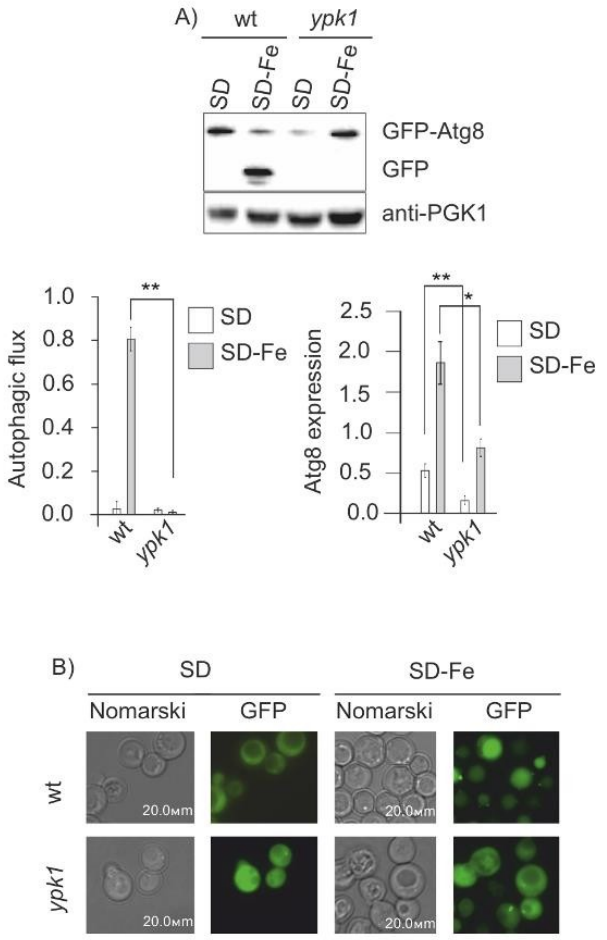
A)
wt
ypk1
SD
SD-Fe
SD
SD-Fe
GFP-Atg8
GFP
anti-PGK1
Autophagic flux
1.0
0.8
0.6
0.4
0.2
0.0
**
SD
SD-Fe
wt
ypk1
Atg8 expression
2.5
2.0
1.5
1.0
0.5
0.0
**
*
SD
SD-Fe
wt
ypk1

B)
SD
SD-Fe
Nomarski
GFP
Nomarski
GFP
wt
ypk1
20.0мм
20.0мм
20.0мм
20.0мм

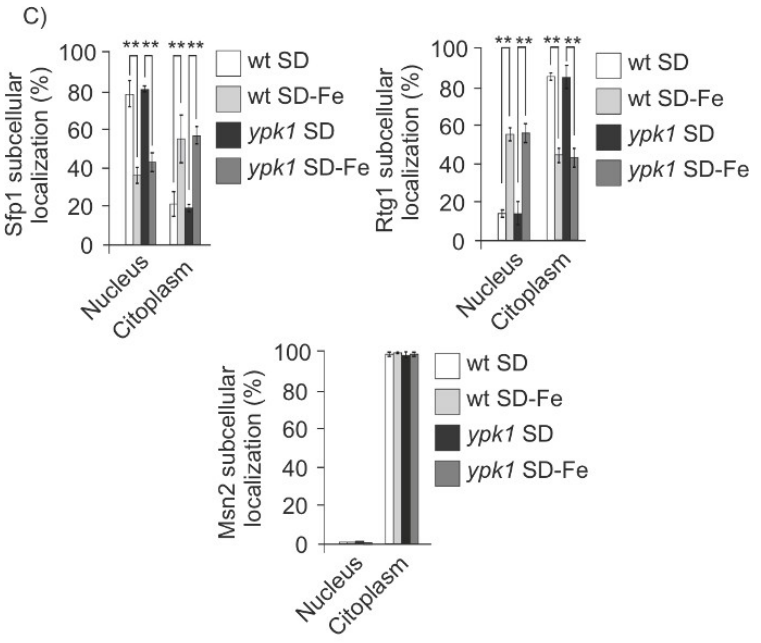
C)
Sfp1 subcellular localization (%)
100
80
60
40
20
0
****
****
wt SD
wt SD-Fe
ypk1 SD
ypk1 SD-Fe
Nucleus
Citoplasm
Rtg1 subcellular localization (%)
**
**
**
**
Msn2 subcellular localization (%)

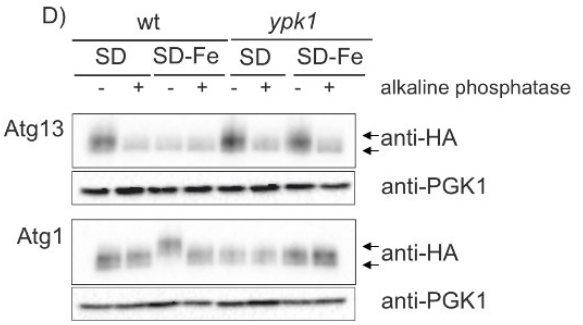
D)
wt
ypk1
SD
SD-Fe
SD
SD-Fe
- + - + - + - +
alkaline phosphatase
Atg13
anti-HA
anti-PGK1
Atg1
anti-HA
anti-PGK1

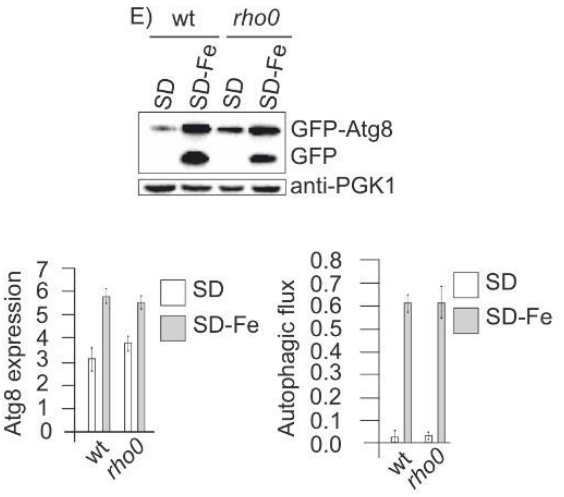
E)
wt
rho0
SD
SD-Fe
SD
SD-Fe
GFP-Atg8
GFP
anti-PGK1
Atg8 expression
7
6
5
4
3
2
1
0
SD
SD-Fe
wt
rho0
Autophagic flux
0.8
0.7
0.6
0.5
0.4
0.3
0.2
0.1
0.0
SD
SD-Fe
wt
rho0

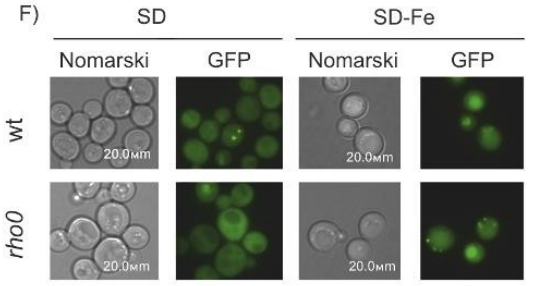
F)
SD
SD-Fe
Nomarski
GFP
Nomarski
GFP
wt
rho0
20.0мм
20.0мм
20.0мм
20.0мм

Figure 4

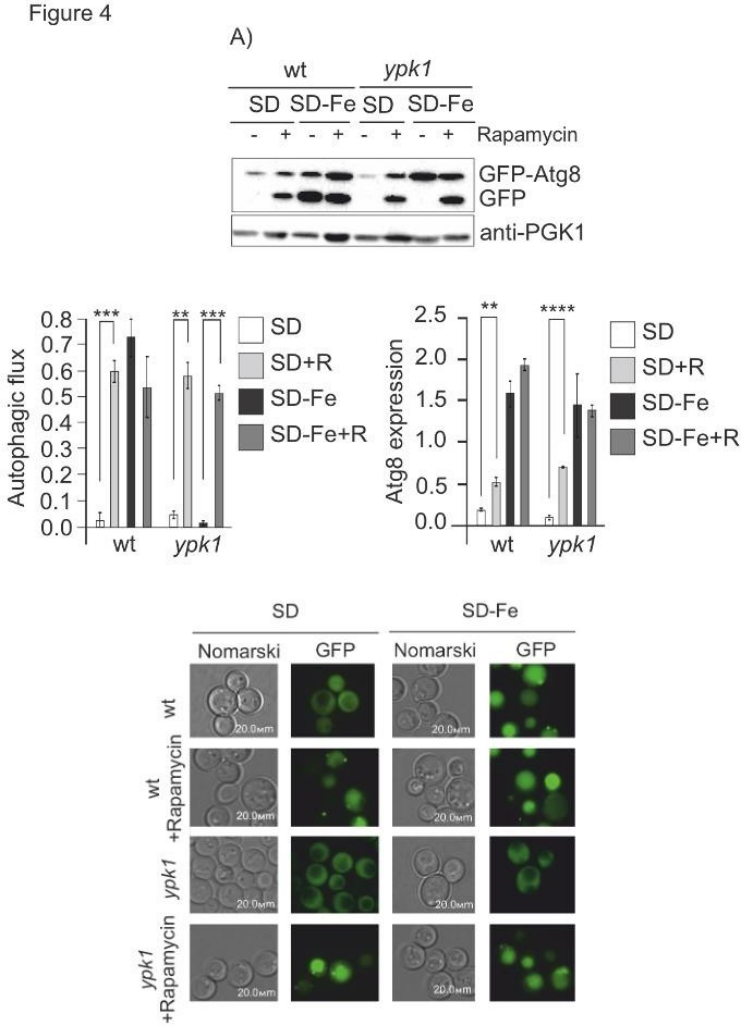
A)
wt
ypk1
SD
SD-Fe
SD
SD-Fe
- + - + - + - +
Rapamycin
GFP-Atg8
GFP
anti-PGK1
Autophagic flux
0.8
0.7
0.6
0.5
0.4
0.3
0.2
0.1
0.0
***
**
***
wt
ypk1
SD
SD+R
SD-Fe
SD-Fe+R
Atg8 expression
2.5
2.0
1.5
1.0
0.5
0.0
**
****
wt
ypk1
SD
SD+R
SD-Fe
SD-Fe+R
SD
SD-Fe
Nomarski
GFP
Nomarski
GFP
wt
wt +Rapamycin
ypk1
ypk1 +Rapamycin
20.0µm

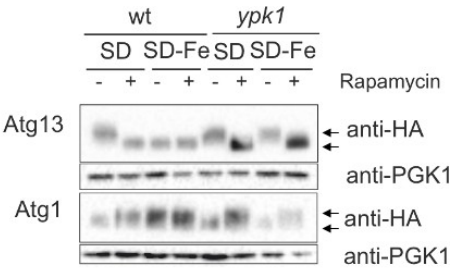
wt
ypk1
SD
SD-Fe
SD
SD-Fe
- + - + - + - +
Rapamycin
Atg13
anti-HA
anti-PGK1
Atg1
anti-HA
anti-PGK1

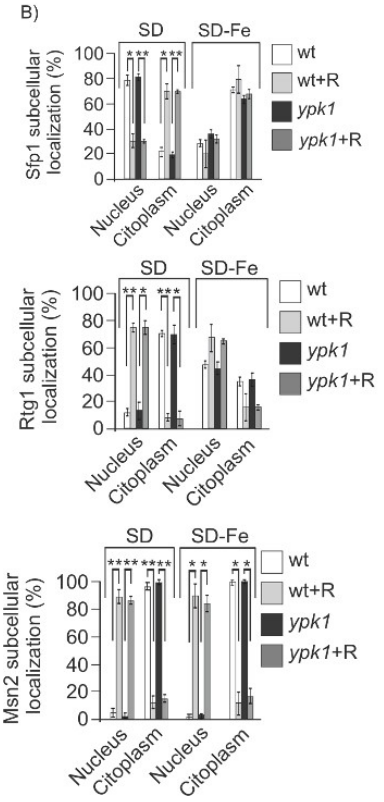
B)
SD
SD-Fe
Sfp1 subcellular localization (%)
Rtg1 subcellular localization (%)
Msn2 subcellular localization (%)
0
20
40
60
80
100
wt
wt+R
ypk1
ypk1+R
Nucleus
Citoplasm
Nucleus
Citoplasm

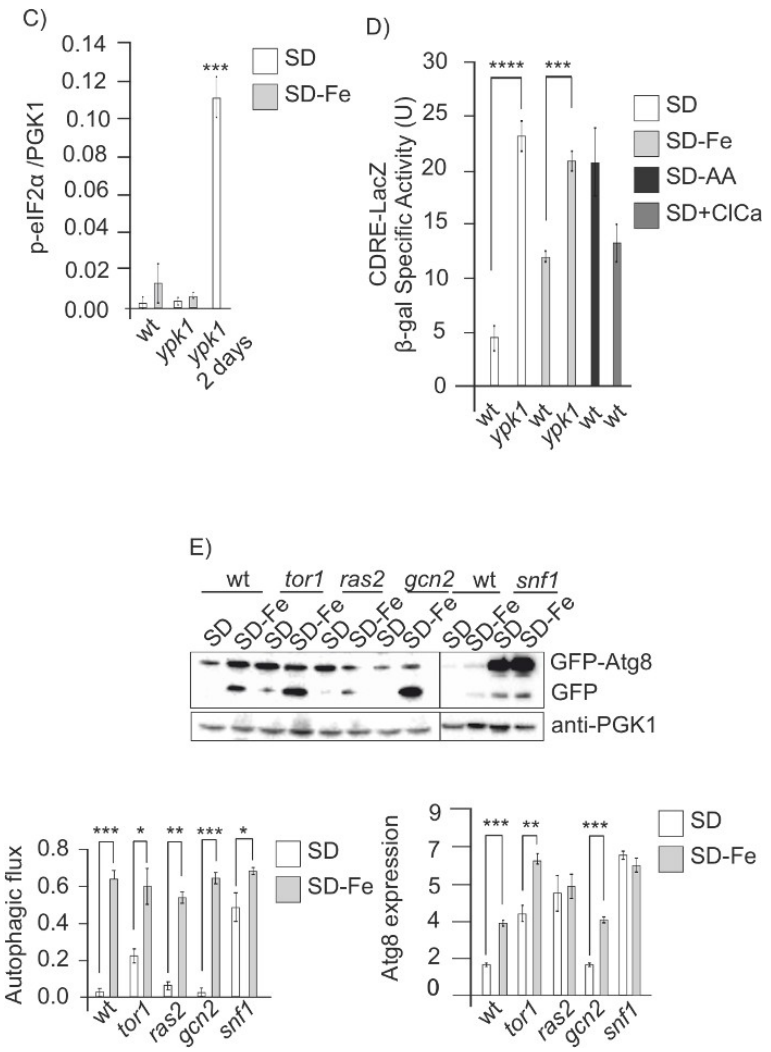
C)
p-eIF2α /PGK1
0.14
0.12
0.10
0.08
0.06
0.04
0.02
0.00
***
SD
SD-Fe
wt
ypk1
ypk1 2 days
D)
CDRE-LacZ β-gal Specific Activity (U)
30
25
20
15
10
5
0
****
***
SD
SD-Fe
SD-AA
SD+ClCa
wt
ypk1
wt
ypk1
wt
wt
E)
wt
tor1
ras2
gcn2
wt
snf1
SD
SD-Fe
GFP-Atg8
GFP
anti-PGK1
Autophagic flux
0.8
0.6
0.4
0.2
0.0
***
*
**
***
*
SD
SD-Fe
wt
tor1
ras2
gcn2
snf1
Atg8 expression
9
7
5
4
2
0
***
**
***
SD
SD-Fe
wt
tor1
ras2
gcn2
snf1

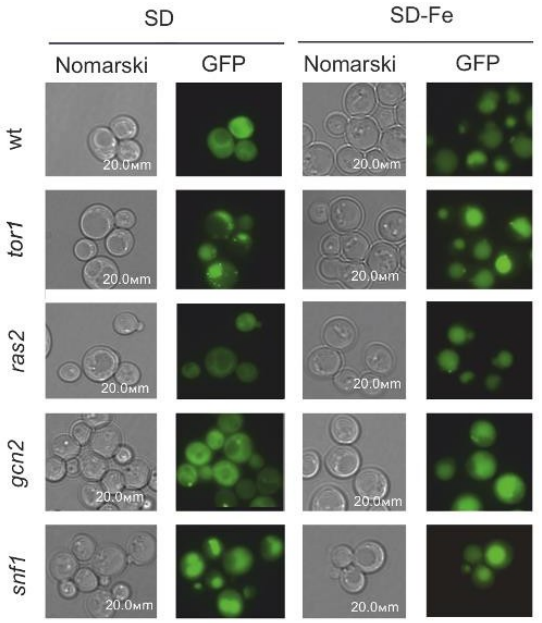
SD
SD-Fe
Nomarski
GFP
Nomarski
GFP
wt
tor1
ras2
gcn2
snf1
20.0μm

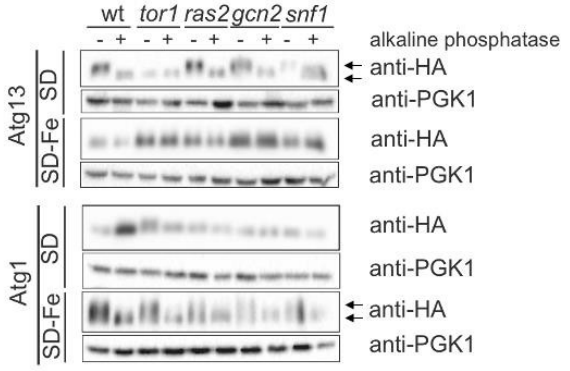
wt
tor1
ras2
gcn2
snf1
- + - + - + - + - +
alkaline phosphatase
Atg13
SD
SD-Fe
anti-HA
anti-PGK1
anti-HA
anti-PGK1
Atg1
SD
SD-Fe
anti-HA
anti-PGK1
anti-HA
anti-PGK1

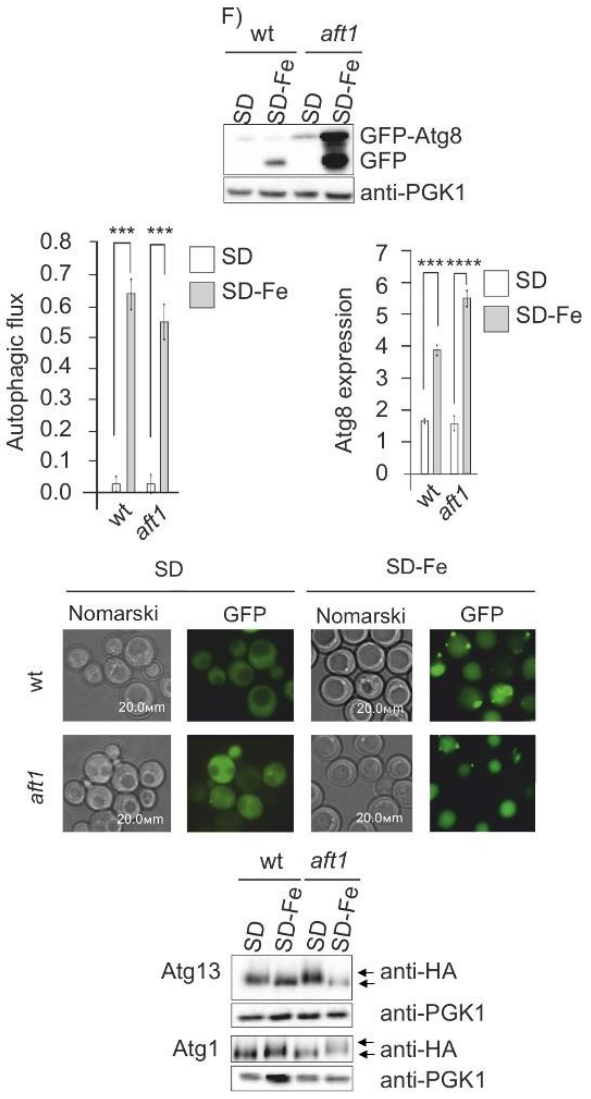
F)
wt
aft1
SD
SD-Fe
SD
SD-Fe
GFP-Atg8
GFP
anti-PGK1
Autophagic flux
0.8
0.7
0.6
0.5
0.4
0.3
0.2
0.1
0.0
***
***
SD
SD-Fe
wt
aft1
Atg8 expression
7
6
5
4
3
2
1
0
****
SD
SD-Fe
wt
aft1
SD
SD-Fe
Nomarski
GFP
Nomarski
GFP
wt
aft1
20.0мм
20.0мм
20.0мм
20.0мм
wt
aft1
SD
SD-Fe
SD
SD-Fe
Atg13
anti-HA
anti-PGK1
Atg1
anti-HA
anti-PGK1

Figure 5

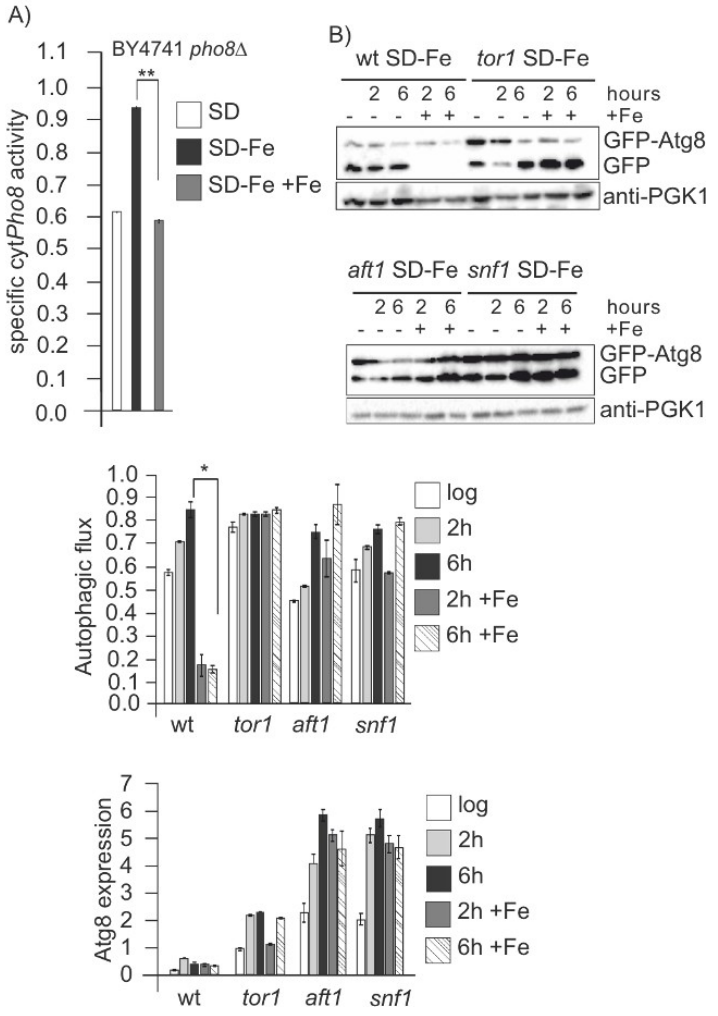
A)
BY4741 pho8Δ
specific cytPho8 activity
SD
SD-Fe
SD-Fe +Fe
B)
wt SD-Fe
tor1 SD-Fe
hours
+Fe
GFP-Atg8
GFP
anti-PGK1
aft1 SD-Fe
snf1 SD-Fe
Autophagic flux
log
2h
6h
2h +Fe
6h +Fe
wt
tor1
aft1
snf1
Atg8 expression

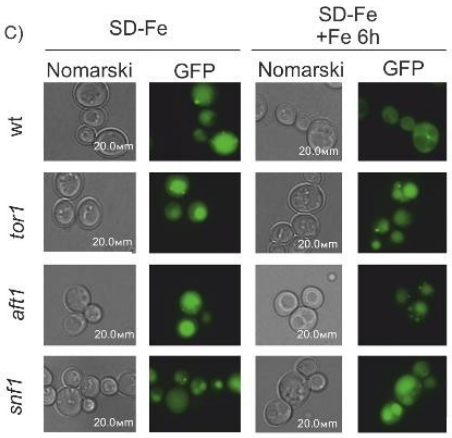
C)
SD-Fe
SD-Fe
+Fe 6h
Nomarski
GFP
Nomarski
GFP
wt
tor1
aft1
snf1
20.0мм

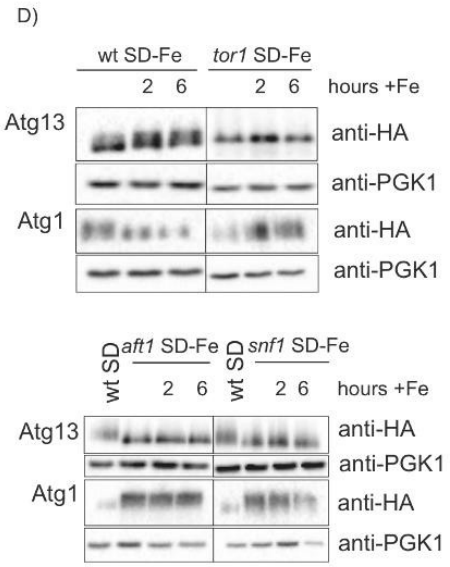
D)
wt SD-Fe
tor1 SD-Fe
2 6
2 6
hours +Fe
Atg13
anti-HA
anti-PGK1
Atg1
anti-HA
anti-PGK1
wt SD
aft1 SD-Fe
wt SD
snf1 SD-Fe
2 6
2 6
hours +Fe
Atg13
anti-HA
anti-PGK1
Atg1
anti-HA
anti-PGK1

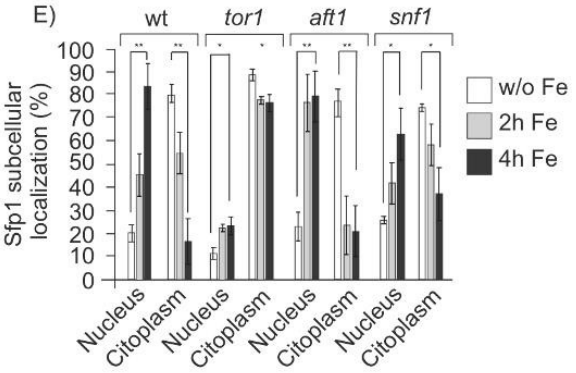
E)
wt
tor1
aft1
snf1
Sfp1 subcellular localization (%)
100
90
80
70
60
50
40
30
20
10
0
w/o Fe
2h Fe
4h Fe
Nucleus
Citoplasm

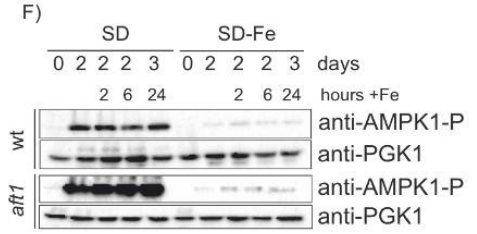
F)
SD
SD-Fe
0 2 2 2 3 0 2 2 2 3 days
2 6 24 2 6 24 hours +Fe
wt
aft1
anti-AMPK1-P
anti-PGK1
anti-AMPK1-P
anti-PGK1

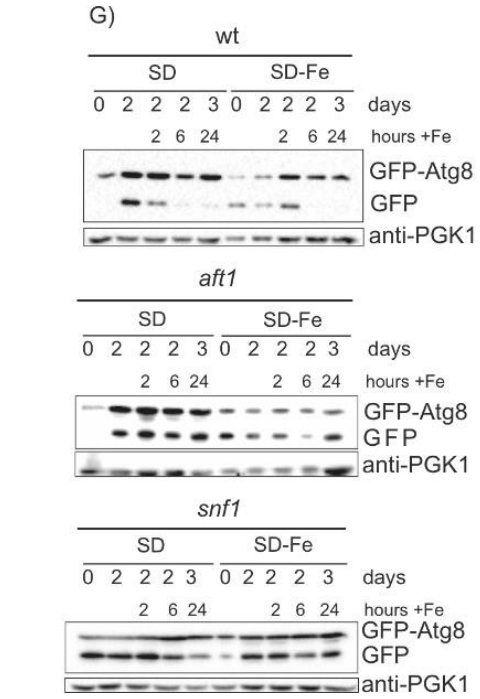
G)
wt
SD
SD-Fe
0 2 2 2 3 0 2 2 2 3 days
2 6 24 2 6 24 hours +Fe
GFP-Atg8
GFP
anti-PGK1
aft1
SD
SD-Fe
0 2 2 2 3 0 2 2 2 3 days
2 6 24 2 6 24 hours +Fe
GFP-Atg8
GFP
anti-PGK1
snf1
SD
SD-Fe
0 2 2 2 3 0 2 2 2 3 days
2 6 24 2 6 24 hours +Fe
GFP-Atg8
GFP
anti-PGK1

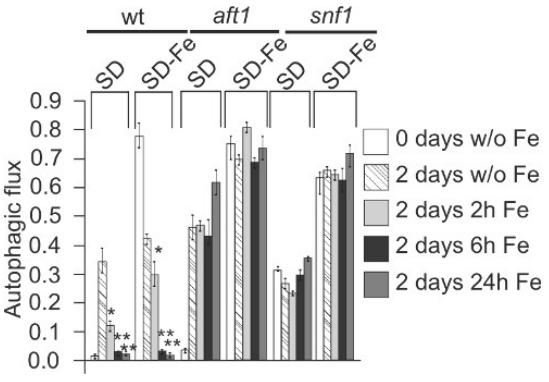
wt
aft1
snf1
SD
SD-Fe
SD
SD-Fe
SD
SD-Fe
Autophagic flux
0.9
0.8
0.7
0.6
0.5
0.4
0.3
0.2
0.1
0.0
0 days w/o Fe
2 days w/o Fe
2 days 2h Fe
2 days 6h Fe
2 days 24h Fe

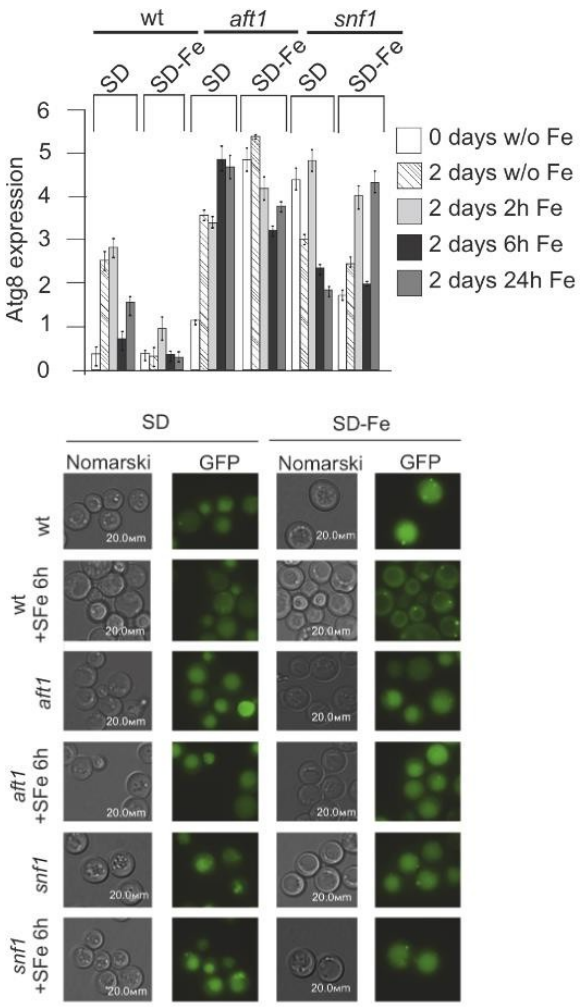
wt
aft1
snf1
SD
SD-Fe
SD
SD-Fe
SD
SD-Fe
Atg8 expression
0
1
2
3
4
5
6
0 days w/o Fe
2 days w/o Fe
2 days 2h Fe
2 days 6h Fe
2 days 24h Fe
SD
SD-Fe
Nomarski
GFP
Nomarski
GFP
wt
wt +SFe 6h
aft1
aft1 +SFe 6h
snf1
snf1 +SFe 6h
20.0мм

Figure 6

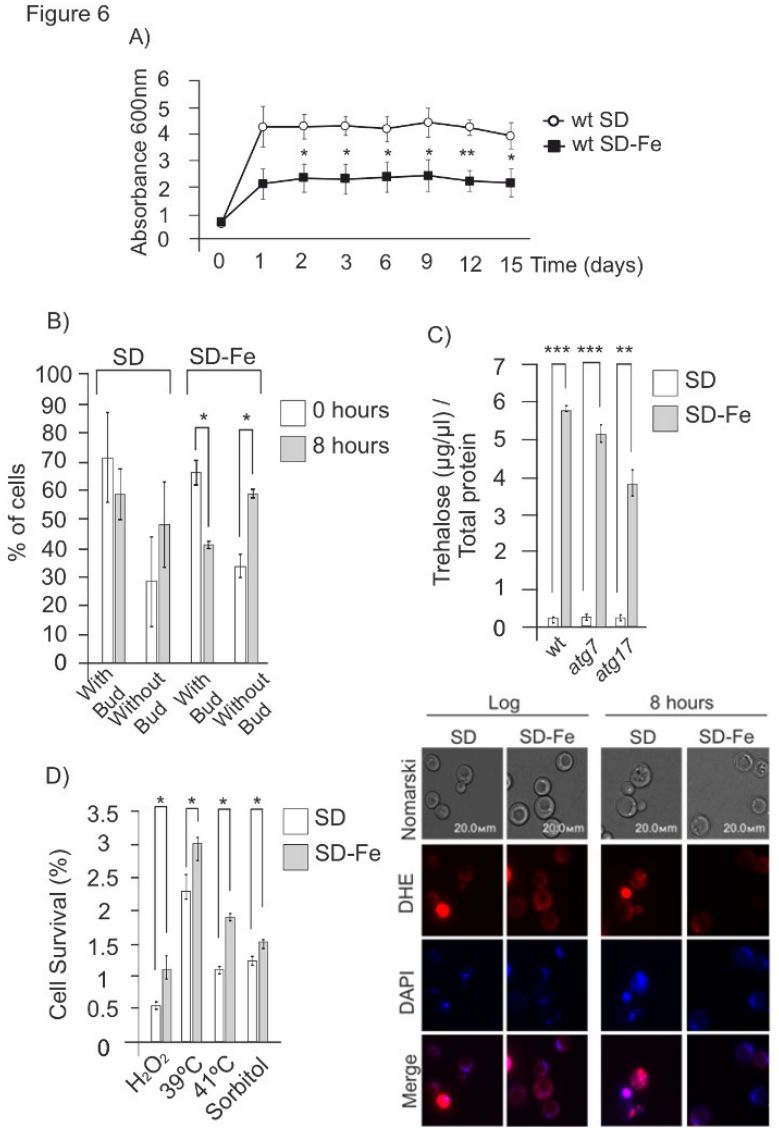
A)
Absorbance 600nm
wt SD
wt SD-Fe
Time (days)
B)
SD
SD-Fe
0 hours
8 hours
% of cells
With Bud
Without Bud
C)
Trehalose (µg/µl) / Total protein
wt
atg7
atg17
D)
Cell Survival (%)
H2O2
39°C
41°C
Sorbitol
Log
8 hours
Nomarski
DHE
DAPI
Merge

E)

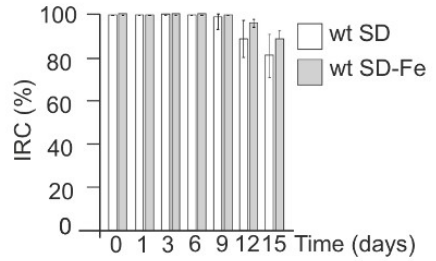
100
80
60
40
20
0
IRC (%)
0 1 3 6 9 12 15 Time (days)
wt SD
wt SD-Fe

F)

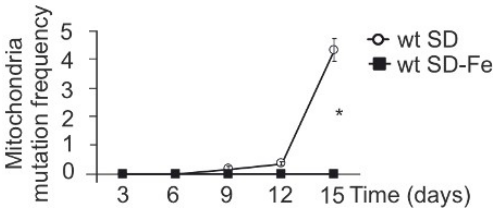
Mitochondria
mutation frequency
5
4
3
2
1
0
3 6 9 12 15 Time (days)
wt SD
wt SD-Fe
*

Figure 7

A)

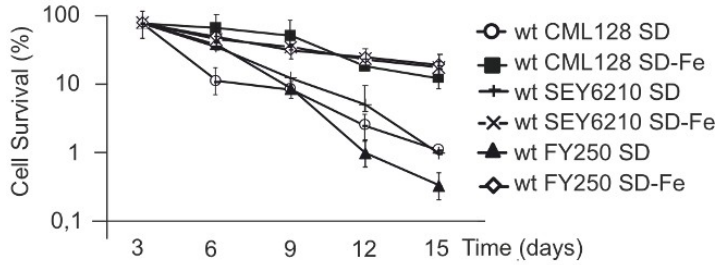

Strains	Maximum lifespan	SD	Average lifespan
wt CML128 SD	18.5	±0,82	9.3
wt SEY6210 SD	19.1	±0,53	9.7
wt FY250 SD	18.1	±0,41	9.1
wt CML128 SD-Fe	23.7	±0,82	10.9
wt SEY6210 SD-Fe	24.1	±0,65	10.7
wt FY250 SD-Fe	24.4	±0,70	10.8

B)

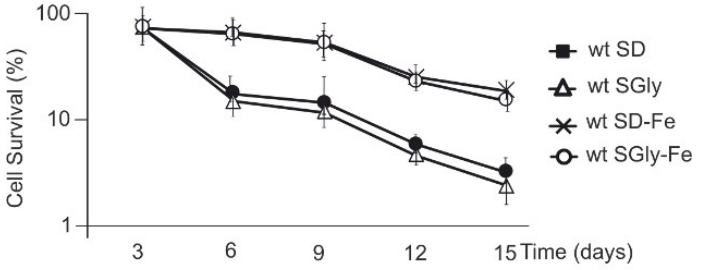

Strains	Maximum lifespan	SD	Average lifespan
wt SD	18.3	±0,24	7.9
wt SGly	18.0	±0,36	7.2
wt SD-Fe	23.0	±0,21	11.2
wt SGly-Fe	22.8	±0,53	10.9

C)

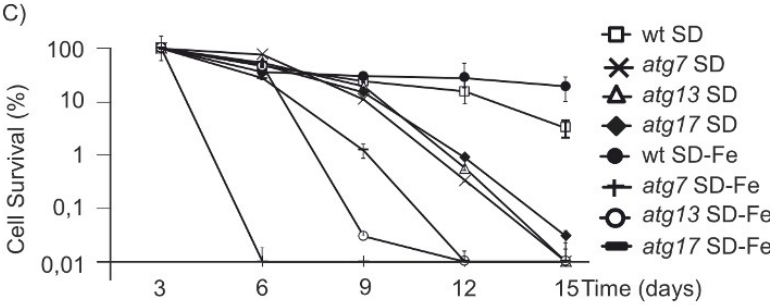

Strains	Maximum lifespan	SD	Average lifespan
wt SD	17.5	±0,21	8.2
atg7 SD	7.0	±0,56	1.5
atg13 SD	10.0	±0,70	1.6
atg17 SD	9.0	±0,14	1.9
wt SD-Fe	22.8	±0,35	11.2
atg7 SD-Fe	5.4	±0,28	0.7
atg13 SD-Fe	6.3	±0,56	1.2
atg17 SD-Fe	7.4	±0,72	1.4

4.3 TERCER ARTICLE

The Cell wall integrity receptor Mtl1 contributes to articulate autophagic responses when glucose availability is compromised

Sandra Montella-Manuel, Nuria Pujol-Carrion and Maria Angeles de la Torre-Ruiz.

Cell Signalling in Yeast Unit, Department of Basic Medical Sciences, Institut de Recerca Biomèdica de Lleida (IRBLleida), University of Lleida, 25198, Lleida, Spain.

Corresponding autor: Maria Angeles de la Torre-Ruiz: mariaangeles.delatorre@udl.cat

Abstract: Mtl1protein is a cell-wall receptor belonging to the CWI pathway. Mtl1 function is related to glucose and oxidative stress signaling. In this report, we show data demonstrating that Mtl1 plays a critical role in the detection of a descent in glucose concentration, in order to activate bulk autophagy machinery as a response to nutrient deprivation and to maintain cell survival in starvation conditions. Autophagy is a tightly regulated mechanism involving several signaling pathways. The data here show that in *Saccharomyces cerevisiae*, Mtl1 signals glucose availability to either Ras2 or Sch9 proteins converging in Atg1 phosphorylation and autophagy induction. TORC1 complex function is not involved in autophagy induction during the diauxic shift when glucose is limited. In this context, *GCN2* gene is required to regulate autophagy activation upon amino acids starvation independently on TORC1 complex. Mtl1 function is also involved in signaling the autophagic degradation of mitochondria during the stationary phase through both Ras2 and Sch9, in a manner dependent on either Atg33 and Atg11 proteins and independent on Atg32 protein, the mitophagy receptor. All of the above suggests a pivotal signaling role for Mtl1 in maintaining correct cell homeostasis function in periods of glucose scarcity in budding yeast.

Key words: Cell wall integrity (CWI); Mtl1; Autophagy; Glucose, Mitophagy; *Saccharomyces cerevisiae*.

1. Introduction

Carbon sources have a major impact on *Saccharomyces cerevisiae* metabolism and also affect longevity. Yeast uses a fermentative metabolism when the preferred carbon source, glucose, is abundant and ethanol, organic acids and ATP are accumulated. Glucose limitation induces a growth slowing down contributing to the switch to a respiratory metabolism, the hallmark of the diauxic shift which along with other metabolic configurations prepare cells for the stationary phase and the process of chronological ageing [1]. Budding yeast chronological life span (CLS) forced by glucose restriction is also dependent on the availability of other nutrients in the culture media such as amino acids or nitrogen among others [2-5]. In a simple way, glucose is a promotor of ageing through the activation of Ras-cAMP-PKA pathway and TORC1-Sch9 [6–8] pathways whereas amino acids operate through Gcn2 protein [9–12] as well as through activation of TORC1 complex, the upstream regulators of Sch9 protein[13].

TORC1 and Ras/PKA pathways are both negative and independent regulators of autophagy [13–16]. Sch9 downregulates autophagy independently and coordinately with Ras/PKA pathway [17].

Ras proteins are essential for growth in fermentable carbon sources such as glucose. In that context, Ras proteins trigger the synthesis of cAMP and the activation of PKA pathway upon binding to the inhibitor Bcy1 protein. The absence of Ras proteins do not allow growth in non-fermentative carbon sources (for reviews [18,19]).

The sucrose non-fermenting protein kinase, Snf1, is the yeast orthologue of mammalian AMPK important for cell adaptation to glucose limitation. Snf1 is the key component of the main glucose repression pathway in yeast and controls genes involved in alternative carbon sources and metabolism. However, regulation of adaptation to glucose limitation is the main role of the SNF1 complex [20, for a review 21]. Snf1 also plays a role in autophagy [22]; its negative regulation is required to downregulate autophagy under certain conditions of nutritional limitation [23].

Mtl1 protein is a transmembrane protein, cell-wall mecano-sensor [24,25] part of the cell wall integrity pathway (CWI) with structural similarity to its paralogue Mid2 protein [26,27]. Mtl1 is also required to activate a stress response towards TORC1 and Ras/PKA signaling pathways under conditions of both oxidative stress and glucose starvation [28]. In addition, this cell-wall receptor plays a role in Cyclin C localization and programmed cell death [29] as well as in the preservation of mitochondrial integrity and life span by regulating TORC1, Sch9, Slt2 and PKA [30].

The CWI is involved in sensing and transducing a wide variety of stimuli, (for reviews [31,32]) including both nutritional and oxidative stresses [27,30,33]. In this pathway, a wide number of

sensors are specialized in the detection of different stresses [25,34] which converge in the GTPase Rho1 to subsequently activate Pkc1 protein (for reviews [31,32]). Pkc1 in its turn, phosphorylates Bck1 protein, the MAPKKK, thus activating the MAPKK module composed of Mkk1/Mkk2 proteins leading to the dual phosphorylation and activation of the last member of the pathway, the MAPK Slt2 protein, whose double phosphorylation is impaired in the mutant *mtl1* [30].

Nutrient limitation strongly induces macroautophagy [23,35–37] to accomplish two main objectives, one is to detoxify and the second is to recycle components to build newly synthetized molecules.

Macroautophagy is a process in which several components (damaged or superfluous organelles, cytoplasmic elements, microorganisms…) are engulfed within cytosolic double-membrane vesicles named autophagosomes. The outer membrane of the phagosome fuses to the vacuolar membrane releasing a spherical body termed autophagic body, that is digested by hydrolases releasing the breakdown products back to the cytosol to be recycled by cells [38]. Morphological and structural characteristics of autophagy are highly conserved from yeast to humans.

The signaling network governing life span usually converges in the autophagic machinery [17,23,39]. In general, nutrient deprivation impinges on Atg13 dephosphorylation that triggers Atg1 kinase activity then leading to the formation of the complex Atg13/Atg1/Atg17/Atg29/Atg31 activating the autophagy process [40,41]. Atg7 is an E1-like enzyme essential for macroautophagy since it is part of the Atg8-Ibl conjugation system [42,43]. Mutants defective in autophagy display a shorter life span [44,45].

Autophagy entails non selective engulfment of cytoplasmic components but there are also other types of autophagy that selectively degrade specific cellular elements (for a review [46]) such is the case of mitophagy. Mitophagy clearances dysfunctional mitochondria and impinges on cellular function by promoting respiration proficiency during the process of ageing (for a review [47]). Selective mitophagy requires the function of Atg32 protein as a mitochondrial receptor and its binding to the adaptor Atg11 which interacts with Atg8 protein in the phagophore inner surface (for a review [48]). Atg33 is a yeast protein located at the outer mitochondrial membrane, its absence suppressed mitophagy in post-log cultures, however, its precise role in mitophagy is still controversial [49].

In this report, we show that bulk autophagy is highly induced during the transition to diauxic shift in a manner totally dependent on glucose and amino acids availability. Mtl1 cell-wall receptor is essential to sense glucose concentration and to transmit the signal to both Ras2 and

Sch9 to phosphorylate Atg1 and to activate the macroautophagic machinery. Gcn2 is the amino acids sensor. Both Mtl1 and Gcn2 operate independently of TORC1 in the signaling process leading to the activation of bulk autophagy. Moreover, Mtl1 is also relevant for the mitochondria clearance dependent on Atg33 and the inactivation of either Ras2 or Sch9, in response to glucose exhaustion.

2. Materials and Methods

2.1 Yeast strains and plasmids

Saccharomyces cerevisiae strains are listed in Table 1. All the strains named GSL are derivatives of the CML128 background. New null mutants described in this study were obtained by a one-step disruption method that uses the *Nat*Mx4 or *Kan*Mx4 cassettes [50]. Strains GSL197, 198, 199, 200, 201, 202, 226, 265, 279, 297, 352, 370, 382, 414 and 415 were constructed upon integration of plasmid pGFP-Atg8 (original name: pHab142), previously digested with Stu1, in the *URA3* gene. Strains GSL372 and 416 were constructed upon integration of plasmid pAtg1-HA previously digested with BstEII. The plasmid pAtg1-HA was obtained upon Atg1 cloning into the Pme1 and PstI sites of the integrative vector pMM351 [51].

Plasmid descriptions are listed in Table 2. Each particular ORF was amplified by PCR from genomic DNA to be directionally cloned in the specific plasmid.

Table 1. Yeast strains.

Strain	Genotype	Source
CML128	*MAT**a** leu2D3,112, ura3D52, trp1D0, his4D0*	[52]
GSL011	*MAT**a** mtl1::NatMx4*	[53]
GSL053	*MAT**a** ras2::Leu2MX5*	[53]
GSL054	*MAT**a** mtl1::KanMx4 ras2::LEU2Mx5*	[53]
GSL197	*MAT**a** leu2D3,112, ura3D52, trp1D0, his4D0 URA3::GFP-ATG8*	[23]
GSL198	*MAT**a** mtl1::KanMx4 URA3::GFP-ATG8*	This work
GSL199	*MAT**a** tor1::KanMx4 URA3::GFP-ATG8*	[23]
GSL200	*MAT**a** mtl1::KanMx4 tor1::LEU2 URA3::GFP-ATG8*	This work
GSL201	*MAT**a** ras2::Leu2MX5 URA3::GFP-ATG8*	[23]
GSL202	*MAT**a** mtl1::KanMx4 ras2::LEU2 URA3::GFP-ATG8*	This work
GSL205	*MAT**a** sch9::NatMx4*	[30]

GSL206	*MAT**a** sch9::NatMx4 mtl1::KanMx4*	[30]
GSL218	*MAT**a** atg7::NatMx4*	[23]
GSL226	*MAT**a** atg7::NatMx4 URA3::GFP-ATG8*	[23]
GSL265	*MAT**a** slt2::NatMx4 URA3::GFP-ATG8*	This work
GSL279	*MAT**a** sch9::NatMx4 URA3::GFP-ATG8*	This work
GSL293	*MAT**a** atg11::NatMx4*	[23]
GSL296	*MAT**a** atg33::NatMX4*	This work
GSL297	*MAT**a** atg11::NatMx4 URA3::GFP-ATG8*	[23]
GSL324	*MAT**a** atg1::NatMx4*	[23]
GSL352	*MAT**a** gcn2::KanMx4 URA3::GFP-ATG8*	[23]
GSL364	*MAT**a** atg32::KanMx4*	[23]
GSL370	*MAT**a** rho0 URA3::GFP-ATG8*	[23]
GSL372	*MAT**a** leu2D3,112, uras3D52, trp1D0, his4D0 ATG1-HA::LEU2*	[23]
GSL382	*MAT**a** snf1:KanMx4 URA3::GFP-ATG8*	[23]
GSL414	*MAT**a** mtl1::KanMX4 sch9::NatMx4 URA3::GFP-ATG8*	This work
GSL415	*MAT**a** mtl1::KanMx4 slt2::NatMx4 URA3::GFP-ATG8*	This work
GSL416	*MAT**a** mtl1:NatMx4 ATG1-HA::LEU2*	This work
BY4741 pho8Δ	*MAT**a** pho8 his3D1, leu2D0, met15D0, ura3D0*	[54]

Table 2. Plasmids employed.

Plasmid	**Restriction sites to clone the ORF**	**Marker**	**Promoter**	**Epitope**	**Source**
pGFP-Atg8	EcoRI, XhoI	*URA3*	ATG8	GFP	[55]
pSfp1-GFP	SalI, SmaI	*URA3*	MET25	GFP	[23]
pAdh1-Msn2-GFP	KspI, SalI	*LEU2*	ADH1	GFP	[56]
pRtg1-GFP	XhoI, EcoRI	*URA3*	RTG1	GFP	[57]
pIdp1-GFP	HindIII, XhoI	*URA3*	IDP1	GFP	[58]
pAtg13-HA	NotI, PstI	*URA3*	ADH1	HA	[23]
pAtg1-HA	NotI, PstI	*LEU2*	ADH1	HA	[23]
pMM351	PstI, HindIII	*LEU2*	ADH1	HA	[51]
pBcy1HA	SmaI, XhoI	*HIS3*	ADH1	HA	[30]
pPkc1*	PmeI, NotI	*LEU2*	ADH1	HA	This work
p*BCK1-20*	HindIII, PstI	*TRP1*	LAC		[28]
pYX242-cytPho8	AvrII, MluI	*LEU2*	PHO8		[54]

2.2 Media, growth conditions and reagents

Yeasts were grown at 30ºC in SD medium (2% glucose, 0.67% yeast nitrogen base that lacked

the corresponding amino acids for plasmid maintenance) plus amino acids [59].
Glucose depletion consisted on SD medium without glucose plus amino acids. Nitrogen depletion consisted on SD medium whose nitrogen base component was free of amino acids and ammonium sulphate plus amino acids. Amino acids depletion consisted in SD medium without adding amino acids. Glycerol medium (3% glycerol, 0.67% yeast nitrogen base that lacked the corresponding amino acids) plus amino acids. Sucrose medium (2% sucrose, 0.67% yeast nitrogen base that lacked the corresponding amino acids) plus amino acids. Fructose medium (2% fructose, 0.67% yeast nitrogen base that lacked the corresponding amino acids) plus amino acids.
Glucose was added as α-D-glucose monohydrate (Serva, 22720.01) at a final concentration of 2%; Amino acids were added at concentrations: 60 mg/ml Leucine, 20 mg/ml Histidine and 20 mg/ml Tryptophan. Nitrogen was added as Yeast Nitrogen Base w/o Amino Acids (Difco, 291940) at a final concentration of 0.67%. Sucrose was added as Sucrose (Sigma, S0389) at a final concentration of 2% and Fructose was added as D-Fructose (Sigma, 47740) at a final concentration of 2%.

We present a list of reagents detailing final concentrations in culture media and from which company they were purchased: N-Acetyl cysteine (NAC) 5 mM (Sigma, A9165); FM4-64 30 μg/μL (Invitrogen, T-3166); Rapamycin 200 ng/ml (Sigma, R0395); ATP 200 mM (Sigma, A1852) and Dihydroethidium (DHE) 50 μM (Sigma, D7008). Cell cultures were exponentially grown at 600 nm [$O.D_{600}$] of 0.6. Iron was added as ammonium iron (III) sulphate hexahydrate [$NH_4Fe(SO_4)_2 \bullet 6H_2O$] (+Fe; Sigma, F1543) at a final concentration of 10 mM.

2.3 Vacuole and dihydroethidium staining
For vacuole visualization, cells were stained with the fluorescent styryl dye FM4-64 (N-(3-triethylammoniumpropyl)-4-(p-diethylaminophenylhexatrienyl) pyridinium
Dibromide. To determine cellular oxidation, we used dihydroethidium (DHE. Both protocols were previously described by our group in [60].

2.4 Cell survival and chronological life span
To assay cell viability cells were grown to mid-log phase OD_{600}:0.6 in SD medium supplemented with the required amino acids. Viability was registered through serial dilutions and plated by triplicate onto YPD plates.

We measured the chronological life span (CLS) in the different strains based on the survival of populations of non-dividing yeast cells according to [61]. The viability was scored by counting the number of cells able to form colonies, CFU (colony-forming units). Cultures were started at an OD_{600}:0.6. The same number of cells collected from each culture were plated in triplicated into YPD plates and allowed to grow at 30ºC for 3-4 days. CLS curves were plotted with the corresponding averages and standard deviations from three independent experiments**.**

2.5 Protein extraction and immunoblot analyses

We follow identical procedure as described in [23]. Total yeast protein extracts were prepared as previously described in [61]. The antibodies for western blotting were as follows: anti-HA 3F10 (no. 12158167001; Roche Applied Science), was used at a dilution of 1: 2,000 in 0.25% non-fat milk and the corresponding secondary was goat anti-Rat IgG horseradish peroxidase conjugate (no. AP136P, Millipore). Anti-GFP (no. 632381; Living Colors) was used at a dilution of 1:2,000 and anti-Phospho-glycerate kinase 1 (anti-PGK1) (459250, Invitrogen) was used at a dilution 1:1,200, both with the secondary antibody anti-Mouse horseradish peroxidase conjugate (LNA931v/AG, GE Healthcare) and anti- Phospho-AMPKα (Thr172) (167253S, Cell Signalling) at a dilution of 1:1,000 with the secondary antibody anti-Rabbit horseradish peroxidase conjugate (LNA934v/AG, GE Healthcare). They were used as indicated by the manufacturers.

The protein-antibody complexes were visualized by enhanced chemiluminescence, using the Supersignal substrate (Pierce) in a Chemidoc (Roche Applied Science).

For all the figures: We used anti-PGK1 to detect PGK1, selected as a loading control in all the western blots shown in this study. For western blot in this paper, we have selected representative samples.

2.6 Autophagy detection

Autophagy progression is monitored through several complementary approaches, such as the immunological detection of GFP accumulation from GFP-Atg8 genomic fusion which is delivered to the vacuole to be degraded once autophagy is induced. The GFP moiety is very resistant to proteolysis compared to Atg8 which is rapidly degraded in the vacuole. Therefore, detection of free GFP processed from GFP-Atg8 is a very reliable tool to measure levels of

complete autophagy through the autophagic flux [62], that is delivery and turnover of the cargo in the vacuole. Autophagic flux is the ratio: free GFP/ GFP-Atg8+free GFP quantified upon western blot detection by using anti-GFP antibody [23]. Another complementary approach is the microscopic observation of GFP accumulation in vacuoles. For all the microscope panels, we have used a representative image of either log or one day samples in order to identify GFP-Atg8 localization. In general, both assays are sufficient as evidences of autophagy activity.
In some particular occasion we also use an alternative approach consisting on measuring the *pho8*Δ60 enzymatic activity to determine nonspecific autophagy, as described by Noda and Klionsky [63] and modified by Guedes et al. [54].

2.7 Glucose determination

We followed the directions detailed in [64].

2.8 Statistical analysis

We followed the same procedure as described in Montella et al. [23]. Error bars in the histograms represent the standard deviation (SD) calculated from three independent experiments. Significance of the data was determinate by *P*-values from a Student's unpaired t-test denoted as follows: *=0.05>P>0.01; **=0.01>P>0.001; ***=0.001>P>0.0001;****=P>0.0001.

3. Results

3.1 Glucose, amino acids, nitrogen and iron deprivation determine the induction of bulk autophagy during diauxic transition

In a previous paper we show that autophagy is required for normal life span extension [23]. We wanted to determine which pathways are involved in autophagy regulation in the process of ageing. To start our analysis, we took daily samples from log phase (day 0) till day 15, following a standard CLS analysis. We used SD medium to avoid the addition of excess of amino acids and thus do not affect the metabolism of the yeast cells. In Figure 1A we can observe that there is a big induction of autophagy and autophagic flux when cell reach the diauxic shift upon one day of growth which is maintained and gradually descents until day 6. The induction of autophagic flux is related with the phosphorylation of Atg1 protein, hence, Atg1 receives the starvation signal in order to induce autophagy during diauxic and posdiauxic shift and also with the enzymatic activity determined by using the *pho8*Δ60 assay. Microscopic

observation of the cultures confirmed the former results, since free GFP derived from GFP-Atg8 fusion protein was accumulated inside vacuoles which appear colored in green and surrounded by a red membrane stained by the fluorescent styryl dye FM4-64. In order to ascertain whether our results were compatible with bulk or selective autophagy we repeated this experiment in the mutants *atg7* (involved in general autophagy) and *atg11* (representing of selective autophagy) (Figure 1B and Figure S1B). Our results demonstrate that free GFP liberated from GFP-Atg8 fusion protein and detected both in western blot and in the fluorescence microscopy indicated bulk autophagy and was independent of any type of selective autophagy.

One day of culture in SD media is the transition between a fermentative to respiratory metabolism, the diauxic shift, a metabolic regulatory checkpoint determinant in the process of ageing. At this point we could observe that glucose is nearly exhausted in the culture media (Figure 1C). Consequently, we performed refeeding experiments upon one day of culture and observed that only upon 6 hours of glucose addition autophagy (determined upon the *pho8Δ*60 specific activity, identification of free GFP by western blot and *in vivo* fluorescence identification of vacuolar accumulation of GFP) significantly decreased, concluding that a severe descent in glucose concentration provoked the induction of autophagy and there is an increase in autophagy (Figure 1D and Figure S1C). We carried out the same strategy with other nutrients which could also be limiting: amino acids, nitrogen and iron. Upon refeeding of iron, nitrogen and amino acids we observed that upon one-day refeeding did not provoke changes in the autophagy (Figure 1D and Figure S1C), however upon two days of culture we observed a clear descent in GFP accumulation caused by amino acids replenishment (Figure 1E and Figure 1D). Both nitrogen and iron replenishment provoked a descent in autophagy upon two days of culture.

Figure 1

A)

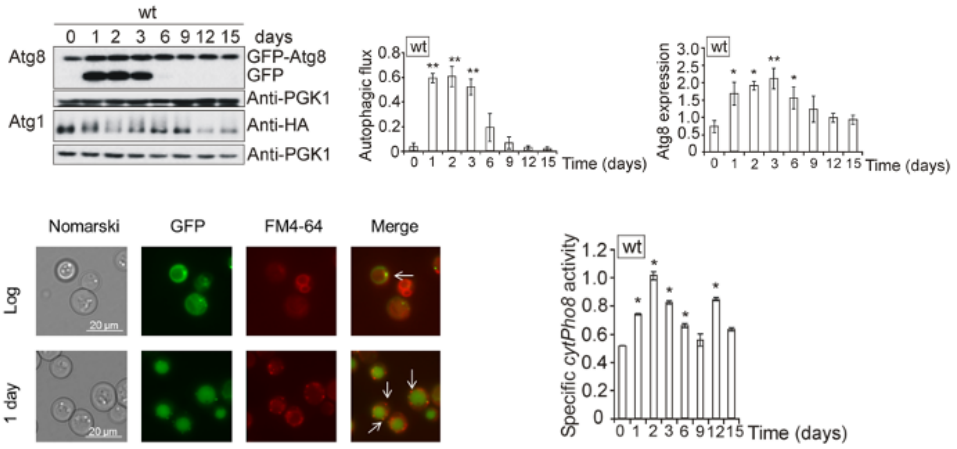
wt
0 1 2 3 6 9 12 15 days
Atg8
GFP-Atg8
GFP
Anti-PGK1
Atg1
Anti-HA
Anti-PGK1
Autophagic flux
Time (days)
Atg8 expression
Time (days)
Nomarski
GFP
FM4-64
Merge
Log
1 day
20 µm
Specific cytPho8 activity
Time (days)

B)

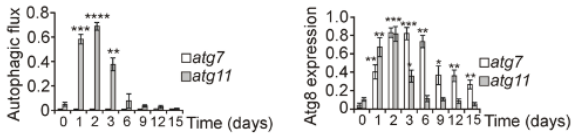

C)

Time	Glucose(%)	SD
SD medium	100.00	±0.56
Log	68.64	±1.90
8 hours	32.23	±1.45
1 day	6.44	±0.22
30 hours	5.02	±0.99
2 days	0.00	±0.00
3 days	0.00	±0.00
6 days	0.00	±0.00
9 days	0.00	±0.00
12 days	0.00	±0.00
15 days	0.00	±0.00

D)

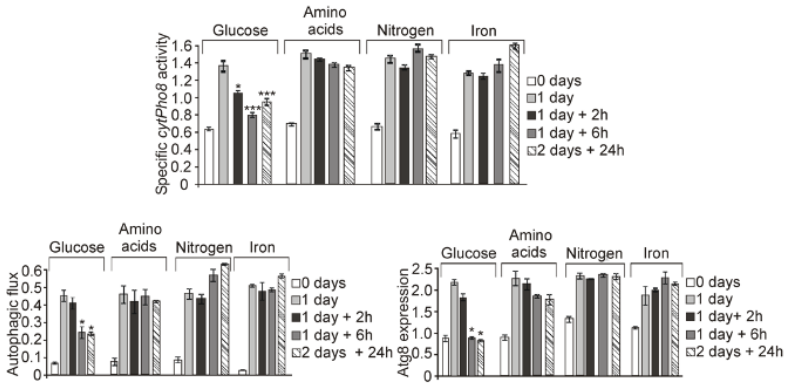

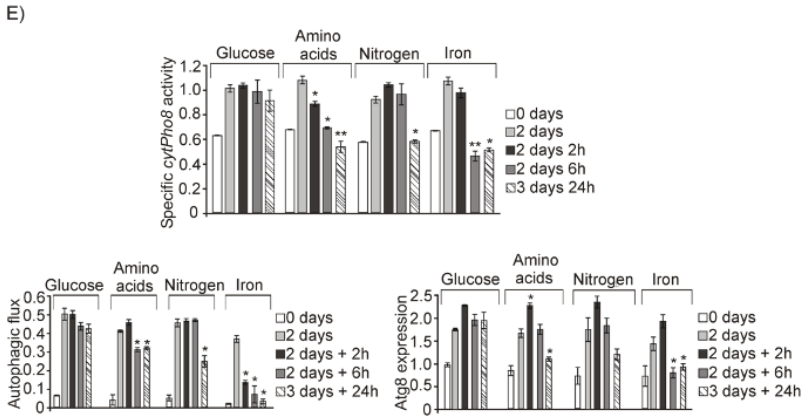

Figure 1. Sequential descent of glucose and amino acids activates bulk autophagy during the diauxic shift in *Saccharomyces cerevisiae*. A) wt cultures in which the fusion protein GFP-Atg8 or Atg1HA were integrated, were grown to log phase (OD_{600}: 0.6) in SD medium at 30ºC. Aliquots were collected at the indicated times for total protein extraction and western blot analysis. GFP-Atg8 was monitored using an anti-GFP antibody. We used anti-PGK1 to detect Pgk1 as loading control. Microscopic observation of GFP-Atg8 was carried out by using a fluorescence microscope. GFP vacuolar accumulation was also determined upon the used of the fluorescent dye FM4-64. Autophagic flux was calculated as the ratio between free GFP and total GFP-Atg8 in the samples. Total GFP-Atg8 was determined as the addition of the form GFP-Atg8 and the band corresponding to free GFP, as a result of Atg8 vacuolar degradation, both detected by western blot. Enzymatic autophagy activity was measured by using the alkaline phosphatase assay in the strain BY4741*pho8*Δ expressing a plasmid with the inactive Pho8 proenzyme targeted to the cytosol. Values of Atg1 proteins were determined upon western blot analysis by using anti-HA antibody. B) *atg7* and *atg11* strains expressing the fusion protein GFP-Atg8, were grown in the same conditions as described in A. Autophagic flux and total Atg8 expression were determined as in A. C) Glucose content in the culture medium (%) was determined in wt cultures growing in SD media at 30ºC at the days indicated in the table for a total period of 15 days. Glucose in the sterile media, SD, at a final concentration of 2%, is the equivalent of 100% in the table. D) wt cells bearing GFP-Atg8 in the genome was exponentially grown at OD_{600}: 0.6 at 30ºC in SD media and a sample was collected for analysis. Upon one day of culture, 2% glucose, amino acids (60 mg/ml Leucine, 20 mg/ml Histidine and 20 mg/ml Tryptophan), 0.67% nitrogen or 10 mM iron, were respectively added to the cultures

and samples were collected upon 2, 6 and 24 hours to perform *pho8Δ*60 enzymatic assay. Autophagic flux and GFP-Atg8 total expression were determined as previously detailed in A. Enzymatic autophagic activity was determined as in A. E) As in D but results correspond to two days of growth.

3.2 Both Mtl1 and Gcn2 control autophagy induction during diauxic transition

In this context, we decided to explore the signaling pathways that could be involved in signaling autophagy when cells age:

We consider the possibility that amino acids and nitrogen depletion would provoke TORC1 inactivation at least partly. We analyzed TOR function by means of the readouts Rtg1, Sfp1, Msn2. Under TORC1 inactivation, Rtg1 and Msn2 are localized into the nucleus, whereas Sfp1 is located in the cytoplasm confirming that Tor1 is not inactivated in our model (Figure 2A). In addition we added rapamycin, a drug that specifically inactivates TORC1, to the previous cultures as a control, and we observed that Rtg1 and Msn2 are localized into the nucleus and Sfp1 is located in the cytoplasm (Figure 2B). Moreover, rapamycin treatment caused a decrease in Atg13 phosphorylation and autophagy values calculated upon Pho8 assay did not increase supporting the conclusion that TORC1 is not completely inactivated upon diauxic shift in the conditions of our study (Figure 2C).

Figure 2

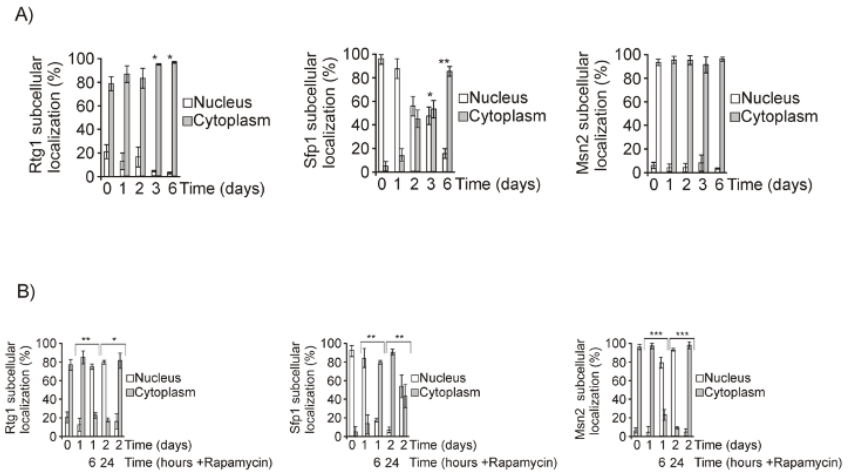

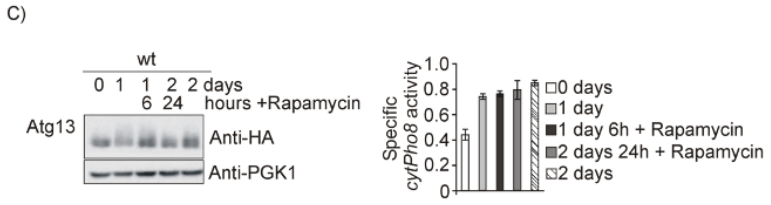

Figure 2. TORC1 is not inactivated during diauxic and posdiauxic shift. A) wt strain transformed with the plasmids Rtg1GFP, Sfp1GFP or Msn2GFP respectively, was grown at 30ºC in SD media for the times indicated in the figures. Aliquots were collected for *in vivo* observation in the fluorescence microscope. Histograms represent the percentages of *in vivo* nuclear or cytoplasmic localization out of more than 1000 cells. B) Cultures in A were treated with rapamycin (200 ng/ml) on day one of culture for 6 hours and aliquots were collected for *in vivo* observation in the fluorescence microscope. Histograms are performed as in A. C) wt strain expressing Atg13HA was exponentially grown at 30ºC in SD media. Rapamycin was added to the culture upon one day of growth at 200 ng/ml and samples were collected upon 6 and 24 hours of exposure to the drug for total protein extraction and western blot analysis and identification of Atg13HA by using anti-HA antibody. Autophagic enzymatic activity was determined through the alkaline phosphatase assay as in (Figure 1A).

However, when *TOR1* is deleted we observed that autophagy (free GFP detected in the western blot and fluorescence microscope accumulated in vacuoles) is extended longer times (Figure 3A and Figure S2A) concomitantly with longer life extension as described in [54]. Taken altogether these results we conclude that TORC1 is not inactivated in our system during the transition between fermentative and respiratory metabolism, therefore it is not the main pathway responsible for the bulk autophagy induction.

We also explored *ras2* mutant since Ras2 is active in exponentially growing cells and becomes inactive as long as cells enter in a respiratory metabolism and glucose becomes exhausted. *RAS2* deletion partially affect autophagy progression as compared to wt cultures (Figure 3B and Figure S2B). Since other nutrients become depleted upon diauxic shift we took into consideration the Gcn2/eIF2alpha pathway which becomes activated under amino acids and other nutrient starvation [65]. Gcn2 pathway is activated upon diauxic shift, indicating the moment in which amino acids concentration significantly decreased in the culture media.

According to our results and coincident with the above mentioned replenishment results, day 2 of growth should be the moment in which cells become starved for amino acids. We observed that upon the second day, autophagy disappears when Gcn2 is deleted, however the absence of Gcn2 did not affect the burst in autophagy observed upon 1 day of growth (Figure 3C and Figure S2C). This result suggests that Gcn2 is required to induce macroautophagy upon two days of growth in SD medium, after the diauxic shift, probably due to a descent in the amino acids concentration one day after the glucose starvation and suggest that Gcn2 is not involved in autophagy signaling in response to carbon source. Following this observation, we wanted to ascertain whether the regulatory function mediated by Gcn2 was dependent on TORC1. We treated *gcn2* mutant cultures upon 1 day with rapamycin and we observed induction of autophagy suggesting that in the transition from fermentative to respiratory metabolism TORC1 and *GCN2* are independent (Figure 3D and Figure S2D). As expected, this conclusion is consistent with the previous observation that TORC1 function is not inactivated during the CLS experiment, as a consequence of that, this pathway is not relevant for autophagy induction during ageing in our experimental conditions.

Our results suggest that glucose is the principal nutrient in the culture medium we use, whose descent causes autophagy induction during the diauxic shift (1 day of growth) therefore, we decided to analyses more in depth the role that could be playing Mtl1 in this process. Mtl1 is a cell wall receptor belonging to the CWI pathway and involved in glucose signaling during diauxic shift and stationary phase [28,30]. Interestingly, in the absence of Mtl1, autophagy is undetectable by western blot, Atg1HA phosphorylation or *in vivo* GFP-Atg8 microscopic accumulation through all the experiment, from day 1 to 15 (Figure 3E and Figure S2E). In yeast, autophagy is initiated when the pre-autophagosome (PAS) structure is formed [66]. PAS can be detected in the fluorescence microscope as dotted like accumulations of Atg proteins next to the vacuole. In *mtl1* diauxic cultures PAS can be detected as also observed in wt strain and they are significantly higher than in *atg1* mutant (Figure 3F) suggesting that Mtl1 does not block the initiation of the autophagy complex. This result suggests that Mtl1 is essential to receive the signal of glucose concentration during the diauxic shift and to transmit this signal to the autophagy machinery. We have also detected similar results when we use alternative and fermentative carbon sources such as sucrose or fructose (Figure S2F)

Figure 3

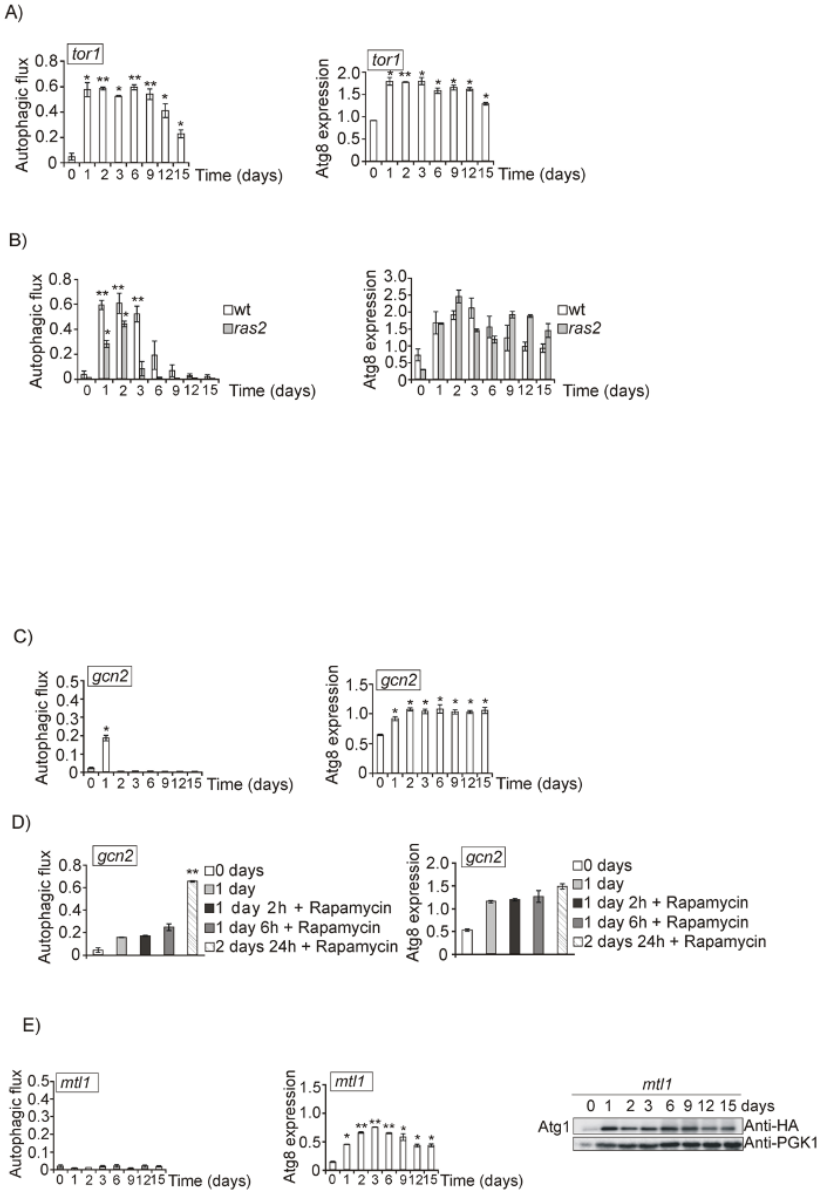
A)
tor1
Autophagic flux
Time (days)
tor1
Atg8 expression
Time (days)
B)
Autophagic flux
wt
ras2
Time (days)
Atg8 expression
wt
ras2
Time (days)
C)
gcn2
Autophagic flux
Time (days)
gcn2
Atg8 expression
Time (days)
D)
gcn2
Autophagic flux
0 days
1 day
1 day 2h + Rapamycin
1 day 6h + Rapamycin
2 days 24h + Rapamycin
gcn2
Atg8 expression
0 days
1 day
1 day 2h + Rapamycin
1 day 6h + Rapamycin
2 days 24h + Rapamycin
E)
mtl1
Autophagic flux
Time (days)
mtl1
Atg8 expression
Time (days)
mtl1
0 1 2 3 6 9 12 15 days
Atg1
Anti-HA
Anti-PGK1

F)

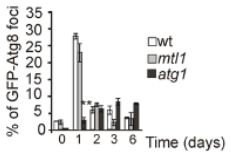

Figure 3. Mtl1 and Gcn2 control autophagy induction during glucose and amino acids starvation. Growth conditions, total Atg8 determination and autophagic flux determined in: A) *tor1* mutant expressing GFP-Atg8; B) wt strain and *ras2* mutant expressing GFP-Atg8 and C) *gcn2* mutant expressing GFP-Atg8, was performed as described in (Figure 1B). D) *gcn2* bearing GFP-Atg8 was exponentially grown at 30ºC in SD plus amino acids. Rapamycin (200 ng/ml) was added to the cultures upon 1 day of growth and samples were subsequently collected upon 2, 6 and 24 hours of exposure to the drug. Aliquots were treated as in (Figure 1B). E) Growth conditions, total Atg8 and autophagic flux determinations in *mtl1* culture expressing the fusion protein GFP-Atg8 was performed as in (Figure 1B). Identification of Atg1 protein in *mtl1* cultures transformed with the plasmid Atg1HA was performed upon western blot analysis by using the anti-HA antibody as in (Figure 1A). F) Percentage of Atg8 foci quantified in the experiments described in (Figure 1A, and Figure 3E) was calculated upon microscopic observation of more than 1000 cells. The axis label "% of GFP-Atg8 foci" is referred at the percentage of cells with GFP-Atg8 foci.

3.3 Mtl1 CWI cell-wall receptor signals glucose concentration to the autophagy machinery in a manner partly dependent on ATP intracellular levels

In previous reports it has been demonstrated that several nutritional stresses (nitrogen, amino acids, iron…) cause the induction of autophagy. In order to analyze the specificity that Mtl1 could play in macroautophagy regulation we used different nutrient concentrations: (glucose: 0.5%, 0.1%, 0.05% and 0%; amino acids: 0.1% and 0%; nitrogen: 0.06%, 0.01% and 0%; and iron: 0%). The descent of each of the nutrients, glucose, amino acids, iron or nitrogen concentrations induced the activation of macroautophagy in wt cells (Figure 4A and Figure S3A) along with the corresponding Atg1 phosphorylation (Figure 4D). In addition, the absence of Gcn2 precluded autophagy in a manner only dependent of amino acids availability (Figure

4B and Figure S3B), whereas the absence of Mtl1 specifically abolished the glucose deprivation dependent autophagy (Figure 4C and Figure S3C) supported by the lack of Atg1 phosphorylation (Figure 4D). We demonstrated that glucose concentration below 0.5% caused a clear induction of autophagy specifically mediated by Mtl1 since in *mtl1* mutant autophagy is not induced.

Figure 4

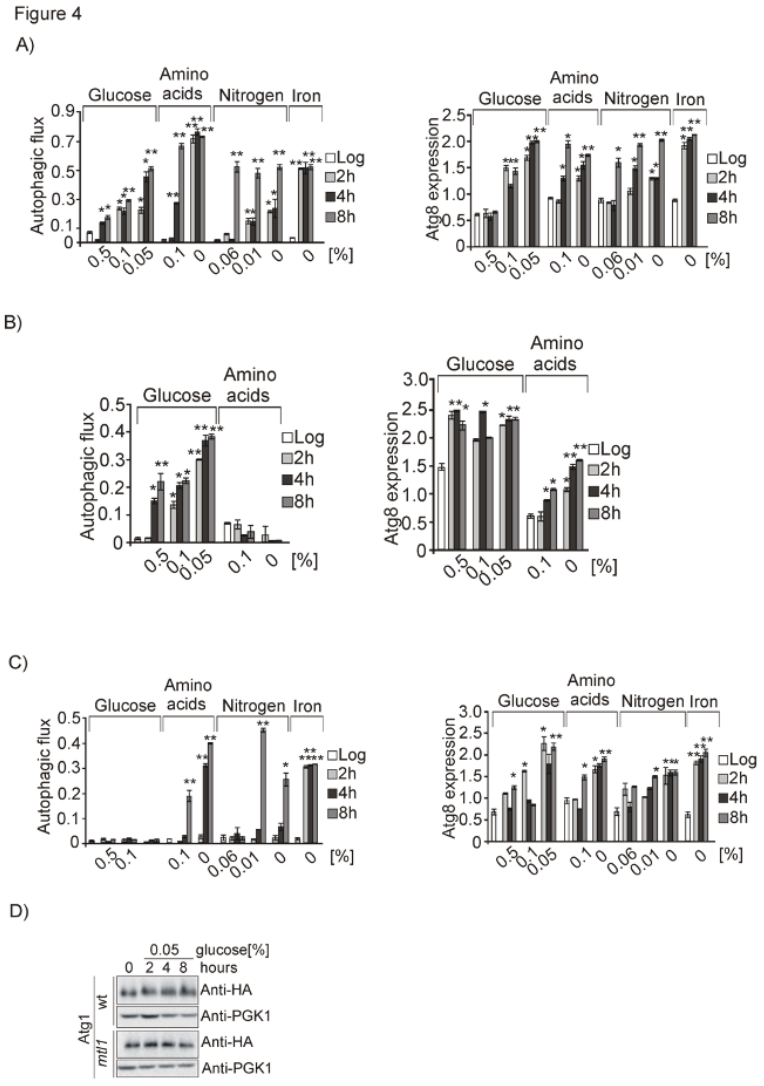

Figure 4. Mtl1 signals glucose limitation to the autophagy machinery. A) wt cells expressing

GFP-Atg8 were exponentially grown in SD media. Aliquots were taken, washed and transferred to different minimum media containing: 0.5, 0.1 or 0.05% glucose; 0.1 or 0% amino acids; 0.06, 0.01 or 0% nitrogen or medium without iron (0%). Autophagic flux and Atg8 expression were determined as in (Figure 1B). The same experiments as in A were carried out in B) *gcn2* mutant cultures expressing GFP-Atg8 and in C) *mtl1* strain expressing GFP-Atg8. D) Atg1HA protein was identified by western blot using anti-HA antibody, as in (Figure 1A).

However, placing cells at 0% glucose, we did not observe free GFP neither in western blot nor accumulated in vacuoles. Hence, bulk autophagy was not induced in wt or *mtl1* strains, as previously described by [67] (Figure 5A and Figure S4A). These authors attributed the result to the sudden lack of ATP required for the autophagy machinery. We added ATP to wt and *mtl1* cultures completely depleted of glucose and observed that whereas in wt cultures the autophagy induction was high, in *mtl1* mutant only part of the autophagy response was restored (Figure 5B and Figure S4B). Identical results were obtained during the diauxic shift in *mtl1* cultures when ATP was added to exponentially growing cells (Figure 5C and Figure S4C). These results led us to the conclusion that the absence of *MTL1* provoked ATP starvation when glucose concentration descent below a threshold. In the former experiment we can observe that autophagy induction occurs when glucose concentration descends from 2% to 0.5% in wt cultures (Figure 4A and Figure S3A). However, in *mtl1*cultures any descent from 2% aborted autophagy (Figure 4C and Figure S3C).

In order to ascertain the contribution of the mitochondrial ATP to the autophagy response during diauxic shift and the reduction in glucose concentrations in exponentially growing cultures, we analyzed a *rho0* mutant with lack mitochondrial DNA. We observed that the absence of mitochondrial DNA did not preclude the induction of bulk autophagy upon one day of culture (Figure 5D and Figure S4D) and upon glucose concentration reduction (Figure 5E and Figure S5E). These results suggest that the functional role that Mtl1 plays in the autophagy response to glucose availability is not only linked to ATP accumulation.

Figure 5

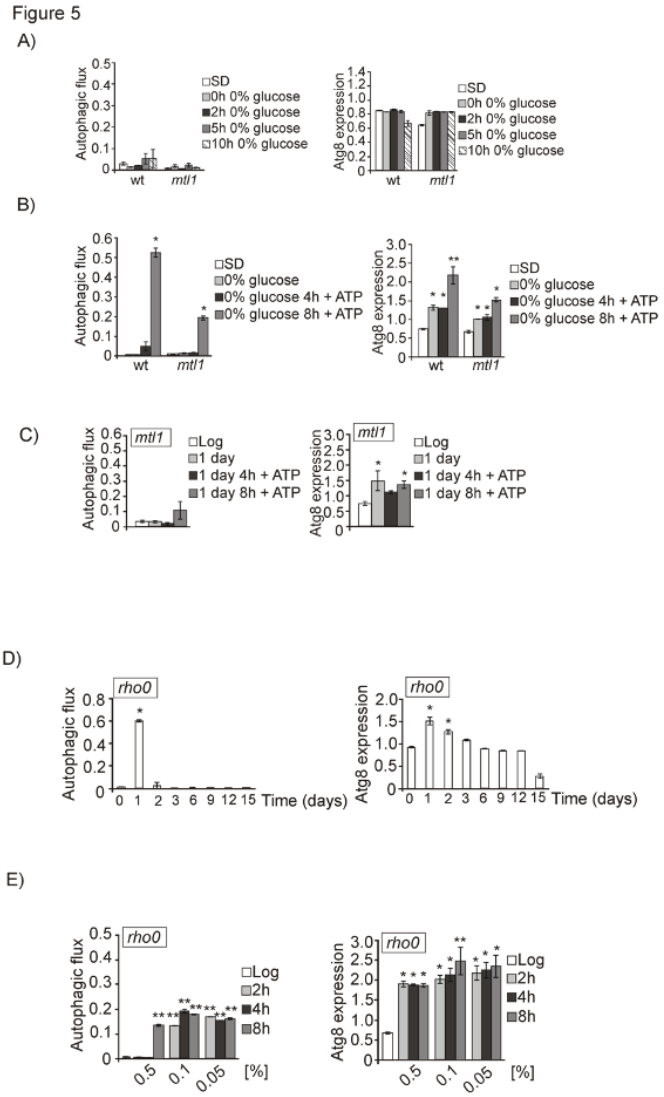

Figure 5. Mtl1 signals the decrease in glucose concentration to the autophagy machinery in a manner not fully dependent on ATP production by mitochondria. A) wt and *mtl1* cells expressing GFP-Atg8 grown in SD media were transferred to minimum media devoid of glucose (0% glucose) to determine autophagic flux and Atg8 expression as in (Figure 1B). B) Upon transference to minimum media without glucose, ATP (at 200 mM final concentration) was added to the cultures described in A and samples were collected at the indicated times for

determination of autophagy as in A. C) ATP (200 mM) was added to *mtl1* cultures growing in SD minimum medium for one day, at the diauxic shift, and samples were collected at 4 and 8 hours for autophagic flux and Atg8 expression determination as in (Figure 1B). D) *rho0* mutant expressing GFP-Atg8 was grown as in (Figure 1B) for autophagy determination. E) *rho0* cells exponentially growing in SD were washed and transferred to several media containing different glucose concentrations to analyze autophagy as in (Figure 4A).

3.4 Both Ras2 or Sch9 suppress mtl1 deficiency in bulk autophagy activation in all the metabolic conditions that imply glucose reduction levels

We next tried to identify the pathway or pathways with which Mtl1 is connected in the signaling process converging in the autophagy machinery. In a previous study we found that Mtl1 is negatively related to both Tor1 and Ras2 in response to oxidative stress and glucose starvation [53]. In addition, Mtl1 is also negatively related to each Sch9, Slt2 and PKA, during the diauxic shift or upon glucose depletion [30].

We demonstrated that Mtl1 mediates Bcy1 activating phosphorylation through TORC1 downregulation thus leading to PKA activation [30]. Therefore, and taking into consideration the hypothesis that *mtl1* mutant could cause the impairment of the glucose signal through PKA, we also analyzed the overexpression of Bcy1, the PKA inhibitor, in both wt and *mtl1* strains. Overexpression of Bcy1 prolonged the autophagy induction in wt cultures for longer times (Figure 6A and Figure S5A) as compared to wt empty strain (Figure 1A and Figure S1A). However, Bcy1 overexpression did not restore autophagy in *mtl1* mutant (Figure 3E, Figure S2E, Figure 6A and Figure S5A). In previous papers we observed a clear impairment in Slt2 phosphorylation upon both oxidative stress and glucose deprivation in *mtl1* mutant [30]. Consistently with this information, we used a plasmid overexpressing the Pkc1 protein and a second plasmid bearing the *BCK1-20* allele which maintains Slt2 kinase constitutively activated, since Bck1 is the MAPKKK of the CWI pathway. Results depicted in (Figures 3E, Figure S2E, Figure 6A and Figure S5A) demonstrate that the lack of bulk autophagy activation observed in *mtl1* mutant, as a result of a descent in glucose concentration during diauxic transition, is not caused by the lack of Slt2 kinase activity, since neither Pkc1 overexpression nor *BCK1-20* allele did not restore the lack of autophagy induction in *mtl1* mutant. We next decided to check Ras2 deletion in *mtl1* since the GTPase is activated in the presence of glucose and is responsible for the synthesis of cAMP when glucose is the carbon source. Ras2 deletion in *mtl1* mutant provoked the activation of bulk autophagy during the diauxic shift, in fact, the

distribution levels of autophagy were equivalent between *ras2* and *mtl1ras2* (Figures 3B, S2B, 6A and S5A respectively) strains, suggesting that Mtl1 signals to Ras2 inactivation upon glucose starvation and diauxic transition signaling to activate bulk autophagy. Lastly and given the association between Mtl1 and Sch9 kinase [30], we also analyzed whether both proteins were also related to the autophagy signaling. Deletion of *SCH9* also restored the autophagy in *mtl1* mutant during the diauxic shift (Figure 6A and Figure S5A). This result suggests a connection of Mtl1 with Sch9 towards autophagy. In order to corroborate the glucose specificity of these responses, exponentially grown cultures of *mtl1ras2* and *mtl1sch9* along with the corresponding controls were assayed for bulk autophagy response upon glucose starvation (Figure 6B and Figure S5B). As expected, deletion of *RAS2* or *SCH9* suppressed the lack of autophagy induction in the absence of *MTL1*.

Snf1 is an AMPK family member which is highly conserved in eukaryotes. When glucose is exhausted, at the beginning of the diauxic shift, Snf1 becomes activated to trigger a wide response regulating activators and repressor to trigger respiratory metabolism (for a review [21]). In order to detect in *mtl1* mutant a possible defect in Snf1 activation, we analyzed Snf1 phosphorylation in Thr20 residue on the activation loop of the catalytic subunit in samples of wt*, mtl1, ras2, ras2mtl1, sch9* and *mtl1sch9*. In (Figure 6C) it can be observed that the Snf1 is correctly and similarly phosphorylated in all the strains, concluding that *mtl1* defects in autophagy during the transition to stationary phase and upon glucose depletion are not a principal consequence of the lack of Snf1 activation as a response to glucose limitation.

In summary, our results suggest that either *RAS2* or *SCH9* deletion reverted the lack of autophagy in the *mtl1* mutant, suggesting that Mtl1 receives the signal of the descent in glucose concentration and connects to both Ras2 and Sch9 inactivation, mechanism that converges in macroautophagy induction. We have also observed similar results when the carbon source is either sucrose or fructose (Figure S2F).

Figure 6

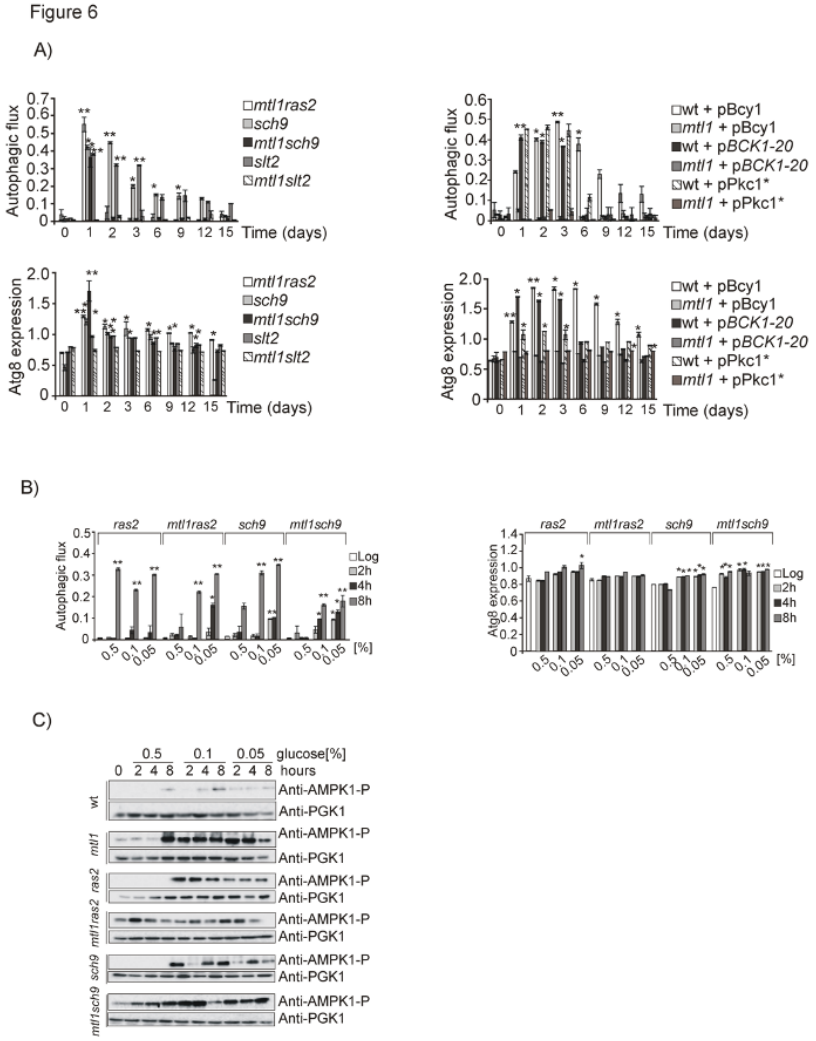

Figure 6. Both Ras2 and Sch9 suppress *mtl1* deficiency in autophagy signaling upon glucose concentration descent. A) *mtl1ras2, sch9, mtl1sch9, slt2, mtl1slt2,* wt+pBcy1, *mtl1*+pBcy1, wt+p*BCK1-20*, *mtl1*+p*BCK1-20*, wt+pPkc1* and *mtl1*+pPkc1* strains expressing GFP-Atg8 were grown at 30ºC in SD media during 15 days. Samples were taken to determine autophagic flux and total Atg8 expression as described in (Figure 1B). B) Strains *ras2, mtl1ras2, sch9* and *mtl1sch9* expressing GFP-Atg8 were exponentially grown in SD media to be subsequently

transferred to minimum medium containing the indicated concentrations of glucose. Samples were taken to determine autophagy as in (Figure 4A). C) wt samples from (Figure 4A) and *mtl1* samples from (Figure 4C) along with *mtl1, ras2, mtl1ras2, sch9* and *mtl1sch9* samples from (Figure 6B) were used for western blot analysis and AMPK1 detection by using anti-AMPK1-P antibody.

3.5 Mtl1 is required for mitochondrial degradation dependently on Atg33 and independently on Atg32 during chronological ageing

We wondered whether Mtl1 involvement in autophagy regulation would be related to any carbon source, not only to glucose availability. To answer this question we decided to analyze a non-fermentative carbon source, glycerol, that forces cells to directly enter into a respiratory metabolism. Mtl1 was clearly not involved in the detection of glycerol concentration linked to autophagy activity since in both wt and *mtl1* cells we detected similar levels and patterns of autophagy (Figure 7A and Figure S6A). In a previous paper, we described that Mtl1 presented uncoupled respiration that provoked mitochondrial dysfunction and ROS accumulation [30]. In order to ascertain whether oxidative stress would be the cause of the autophagy problem, we added the antioxidant NAC to both wt and *mtl1* diauxic cultures (Figures 7B and S6B). In order to demonstrate that NAC was exerting its antioxidant function, samples were collected and stained with dihydroethidium (DHE) for *in vivo* visualization of cellular oxidation in the fluorescent microscope (Fig S6C). Our results indicate that oxidative stress is not the cause of autophagy impairment during diauxic shift in *mtl1* mutant (Figure 7B and Figures S6B and S6C).

Figure 7

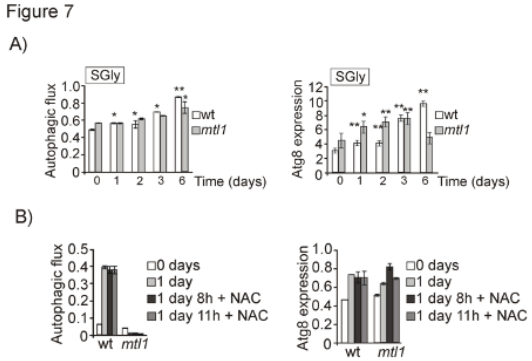

Figure 7. Mtl1 is not deficient in bulk autophagy in respiratory conditions. A) wt and *mtl1* cultures were grown in minimum medium SGly (containing glycerol as unique carbon source)

plus amino acids at 30°C to stationary phase for 6 days. Samples were collected at the indicated times to identify macroautophagy as described in (Figure 1B). B) wt and *mtl1* cultures in SD medium growing to 1 day were treated with N-Acetyl cysteine (NAC) 5 mM for 8 and 11 hours. Samples were collected for autophagy determinations as in A.

There is an alternative possibility, that if the problem of *mtl1* is the mitochondrial function we would expect to detect severe deficiencies in mitophagy. For this purpose, we analyzed mitophagy in cells expressing the fusion of mitochondrial matrix protein to GFP, Idp1-GFP, transformed in either wt or *mtl1* strains [68]. We monitored the vacuole clipping of the fusion protein Idp1-GFP. The identification of free GFP with anti-GFP antibody in a western blot would reveal the existence of mitophagy since GFP is very resistant to degradation [69]. Mitophagy studies are usually carried out in respiratory carbon sources or alternatively in stationary cultures. When wt and *mtl1* cells were grown in SGly to stationary phase, we observed mitophagy in both strains (Figure 8A and Figure S7A) as opposed to *atg32* and *atg11* mutants in which mitophagy was undetectable (Figure 8B and Figure S7B). Atg32 is a mitochondrial outer protein required to initiate mitophagy as a selective type of autophagy (for a review [70]). Atg11 is a critical protein for selective autophagy, it is essential in selective and non-selective autophagy processes (for a review [71]). From the results shown in (Figure 8B and Figure S7B) we conclude that *mtl1* mutant does not present any defect regarding mitophagy dependent on Atg32.

We also checked mitophagy during diauxic shift and stationary phase in cultures growing in SD, with glucose as the only carbon source. We observed mitochondrial degradation as free GFP derived from Idp1-GFP accumulated in vacuoles in wt cultures (Figure 8C and Figure S7C). However, this particular mitochondrial degradation was undetected in each of *atg1*, *atg7* or *atg11* strains (Figure 8C and Figure S7C). This particular mitophagy-like was not dependent on Atg32 since we observed similar results in both wt and *atg32* strains (Figure 8C and Figure S7C). We discarded the possibility that our results reflected bulk autophagy since *atg11* cultures did not present defects in bulk autophagy during diauxic shift nor stationary phase (Figure 8C and Figure S7C). It has been reported in yeast that Atg33, is a mitophagy mitochondrial outer membrane protein [68] required for stationary-phase. We observed a deficiency in mitophagy when we analyzed *atg33* mutant (Figure 8C and Figure S7C). More interesting was the finding that *mtl1* mutant was as deficient as *atg11* and *atg33* in Idp1 mitophagy during diauxic shift and stationary phase (Figure 8C and Figure S7C). The three mutants turned out to have shorter chronological life span than the corresponding wt (Figure 8D). Our results suggest that yeast

cultures in SD present mitochondrial degradation in the vacuole upon diauxic shift and during stationary phase through a selective autophagy process independent of Atg32 but dependent on Atg1, Atg7, Atg11 and Atg33 proteins. We also demonstrate that Mtl1 plays a relevant role in initiating this mechanism, one potential target would be Atg33 that will have to be further investigated.

We decided to check whether *mtl1* absence of mitochondrial degradation during the chronological life span was also alleviated by either *RAS2* or *SCH9* deletion and obtained equivalent results to those described for bulk autophagy, inactivation of *RAS2* or *SCH9* restored mitophagy-like degradation during the diauxic shift to *mtl1* mutants (Figures 8C, S7C, 8E and S7D).

Figure 8

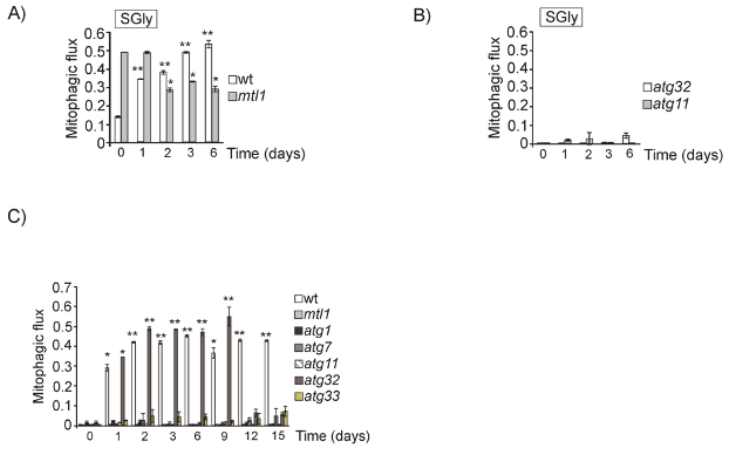

D)

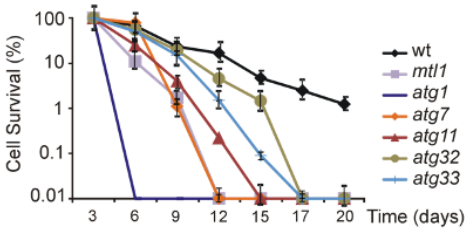

Strains	Maximum lifespan	SD	Average lifespan
wt	17.6	± 0.41	8.2
mtl1	9.9	± 0.21	4.5
atg1	5.2	± 0.63	1.6
atg7	6.8	± 0.14	2.3
atg11	10.2	± 0.70	5.3
atg32	12.5	± 0.53	7.2
atg33	11.4	± 0.17	6.0

E)

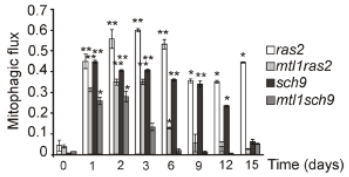

Figure 8. Mtl1 is needed for specific mitochondrial degradation during stationary phase. A) wt and *mtl1* cultures transformed with plasmid Idp1-GFP were grown in SGly media plus amino acids at 30°C. Samples were taken at the indicated times to determine mitophagic flux. Mitophagic flux was calculated as the ratio between free GFP and total Idp1-GFP detected in the western blot. B) *atg32* and *atg11* cultures transformed with Idp1-GFP were grown in SGly medium plus amino acids at 30°C. Samples were collected at the indicated times to determine mitophagic flux as in A. C) wt, *mtl1, atg1, atg7, atg11, atg32* and *atg33* strains bearing the plasmid Idp1-GFP were grown in SD media at 30ºC for 15 days in continuous shacking. Mitophagic flux was determined as in A. D) Chronological life span curves for wt, *mtl1, atg1, atg7, atg11, atg32* and *atg33* strains cultured in SD media plus amino acids at 30°C. Samples were taken at the indicated times to determine CLS, as described in Materials and Methods.

Numerical data regarding maximum life span (the day when cultures reach 10% survival) and average life span (the day at which 50% survival was recorded) for each strain is depicted. E) *ras2, mtl1ras2, sch9* and *mtl1sch9* mutants, transformed with Idp1-GFP were treated as in C and mitophagic flux was determined as in A.

4. Discussion:

Our results point to a situation by which gradual glucose depletion activates bulk autophagy and for this response Mtl1 activity is essential. Unlike in wt cells, in the single mutant *mtl1* there is no a detectable response towards autophagy unless either *RAS2* or *SCH9* are deleted. Deletion of *RAS2* reverts the *mtl1* phenotype regarding bulk autophagy what points to the importance of glucose availability and the switch from a respiratory to a fermentative metabolism suggesting that during that transition Ras2 pathway must be not active and is Mtl1 the connector between glucose and Ras2 activity. This is supported by the observation that these results are also extended to other fermentative sugars (Figure S2F). Interestingly, the signal to autophagy in the models of glucose deprivation does not flow to TORC1, nor to the PKC1 pathway or PKA, but directly to the autophagy machinery to phosphorylate Atg1 protein. Accordingly, some authors [2] already observed that TORC1 does not seem to play a principal function in glucose starvation.

According to former studies [67], the abrupt transition from 2% glucose to 0% glucose does not activate macroautophagy, because for this mechanism, ATP is essential and the mentioned transition leads cells suddenly exhausted for ATP. This is understandable when cells are transferred from a culture containing high glucose concentrations to a culture without glucose nor other carbon source. However, during the transition from fermentative to respiratory metabolism the descent in glucose concentration occurs gradually. In wt cells autophagy is activated already when glucose concentration reaches values of 0.5% (27.77 mM) and reaches maximum values when glucose levels descend to 0.05% (0.13 mM), whereas in *mtl1* mutant autophagy is never induced. We hypothesized that this could occur because there might be a threshold for cells to sense glucose levels (or other alternative fermentable sugars), that would activate autophagy to obtain energy and nutrients probably linked to the induction of a respiratory metabolism. Mtl1 could be the sensor for this threshold unable to switch properly and consequently unable to induce autophagy. In a previous study we observed that *mtl1* mutant accumulates higher cAMP levels than wt cells. We believe that since *mtl1* mutant has a high cyclic AMP accumulation both in exponential or stationary cultures [28], this fact would

deplete cells for ATP, consequently Ras2 deletion might compensate for that depletion avoiding the accumulation of cyclic AMP in *mtl1*. Noneless, this hypothesis is not sustained since other nutrient stresses were capable to activate bulk autophagy in *mtl1* exponential cells (Figure 4C). It could be argued that during the diauxic shift glucose reduction forces the switch from fermentative to respiratory metabolism and in these circumstances the main ATP source should be mitochondrial. Since in the absence of Mtl1 the ratio cAMP/ATP would be higher than in wt cells this would generate a signal of glucose starvation leading to the blockade of autophagy. However, our results demonstrate that the absence of mitochondrial DNA, and consequently the absence of ATP production through respiration metabolism (*rho0* mutant) did not preclude autophagy induction in glucose reduction conditions. Consequently, we also discarded this second hypothesis.

In humans, ATP increases autophagic flux in some cell lines but not in others [72]. Moreover, the addition of ATP to *mtl1* cultures only partly restored at a low degree both autophagy in the diauxic transition and upon partial glucose depletion. This supports the model by which Mtl1 function couples glucose starvation to Ras activity and autophagy induction.

In agreement with the studies of [67] we have observed that after a full reduction of glucose, no nutritional stress can provoke bulk autophagy induction (rapamycin, amino acids, nitrogen or iron).

In this study, we also present a nutritional model by which Gcn2 detects the signal of amino acids deprivation connecting to bulk autophagy in a manner independent of TORC1 activity. Hence, our data demonstrate that both Mtl1 and Gcn2 are key factors to induce bulk autophagy during the starvation process involving first glucose and secondly amino acids deprivation that occurs during the transition from fermentative to respiratory metabolism.

The observation that *mtl1* mutant grows in the presence of glycerol as the only carbon source at similar rates as wt cells, indicates that mitochondrial function is sufficient to support the ATP requirements in this condition. Moreover, we also observed that Mtl1 does not participate in the induction of mitophagy in glycerol cultures dependent of Atg32 (Figure 8A and B).

We observed that either Mtl1 or Atg11 (involved in selective autophagy), are required to degrade mitochondria during the transition to stationary phase in synthetic media containing glucose as the only carbon source. This degradation process depends on the autophagy machinery since in the absence of Atg7 or Atg1 it does not take place. Our data are consistent with a previous paper in which the authors showed that autophagy in response to carbon starvation requires Atg11 as a scaffold protein for the PAS [67]. Nevertheless, the mitophagy-like process that occurred in media containing glucose is independent of Atg32 but dependent

of Atg33 (Figure 8C). This is not unexpected since Atg33 was characterized as an autophagy protein, specific of *Saccharomyces cerevisiae* whose role was linked to the induction of mitophagy during stationary phase [68]. Whether or not the mitochondria degradation that we observe during stationary phase is a type of mitophagy dependent of Atg11 and Atg33 but independent of Atg32, it should be further analyzed in future studies. Consequently, the availability of glucose as a carbon source has specific responses regarding autophagy in which Mtl1 is directly involved.

Snf1 is an AMPK orthologous to the mammalian AMP-kinase (reviewed in [73]) whose activity has been reported to be required in response to glucose starvation [21,74], to downregulate autophagy in stationary phase [23] and it is also required to induce autophagy in that context [67]. Snf1p is a catabolic regulator that is activated by the increase in the ADP/ATP ratio [75]. Nonetheless, in our studies Snf1 activation, both in *mtl1* mutant or in wt cells, is highly activated during diauxic shift when glucose levels are reduced and this activity is high during the stationary phase, therefore we cannot attribute to Snf1 lack of activity the defects observed in *mtl1* mutant.

The conclusion to our data is that the transition from high concentrations to low levels of glucose triggers the connection between Mtl1 and autophagy and is not fully dependent on mitochondrial function and ATP accumulation. Another argument to support our hypothesis is that in *mtl1* mutant it is clearly detectable the presence of PAS in the diauxic transition and in the presence of low glucose concentrations (Figure 3F), as opposed to that observed by previous authors [67] in the absence of ATP.

The linkage between Mtl1 and Ras2 is not the first time that is described [28]. Our data suggest that Ras2 is the key regulator of bulk autophagy and the autophagy of mitochondria during stationary phase. Whether or not this connection is related to mitochondria is at this moment unknown since direct evidence for a regulation of mitochondria by Ras via cAMP–PKA is absent. Moreover, it is not unlikely that the Ras protein acts independently of adenylate cyclase and cAMP according to [76]. PKA is one of the effectors of Ras2 [77,78], also involved in autophagy regulation. However, and concerning Mtl1 signaling to autophagy, PKA does not appear to be required as an intermediary molecule. Moreover, constitutive activation of the RAS-cAMP signaling pathway confers resistance to rapamycin [79–81]. This would explain why in an *mtl1* mutant, rapamycin does not provoke the induction of autophagy in diauxic shift (not shown), taking into consideration the hypothesis that Mtl1 helps to switch from fermentative to respiratory metabolism through Ras/cAMP pathway.

Sch9 is a kinase effector of TORC1 pathway [82]. In addition, Sch9 has been described to act

in a different pathway than PKA in the glucose response, this is in agreement with our observations that Bcy1 overexpression or *SLT2* deletion did not suppress the lack of autophagy observed in *mtl1* mutant. Our results are in line with the conclusion that TORC1, PKA and Sch9 independently regulate autophagy during growth [17,83]. Deletion of Sch9 is sufficient to activate autophagy [17]. Here we observe that *sch9* mutant suppresses the lack of both bulk autophagy and mitophagy of *mtl1* during the diauxic shift and in conditions of low glucose, this restricts the signal to glucose availability. Sch9 is also implicated in the selective autophagic degradation of ribosomes, mitochondria and peroxisomes [84,85]. Although we still do not have a certain interpretation of the fact that Sch9 regulates ribosomal genes transcription, and that ribosomal biogenesis is one of the mechanisms that need more ATP consumption, one interpretation would be that diminishing the level of ribosomal biogenesis also diminishes the ATP consumption perhaps favoring the induction of autophagy. The molecular mechanisms underlying the involvement of cAMP in the induction of autophagy related to nutritional starvation conditions deserves future investigation.

Our findings suggest that Mtl1 cell wall receptor of the CWI pathway is a glucose sensor required to activate both bulk autophagy and Atg33-Atg11 mitophagy in response to glucose concentration decrease. The activation occurs through either Ras2 or Sch9 inactivation converging in Atg1 phosphorylation.

Supplementary Materials:

Figure S1. Sequential descent of glucose and amino acids activates bulk autophagy during the diauxic shift in *Saccharomyces cerevisiae*. Figure S2**.** Mtl1 and Gcn2 control autophagy induction during glucose and amino acids starvation. Figure S3. Mtl1 signals glucose limitation to the autophagy machinery. Figure S4**.** Mtl1 signals the decrease in glucose concentration to the autophagy machinery in a manner not fully dependent on ATP production by mitochondria. Figure S5. Both Ras2 and Sch9 suppress *mtl1* deficiency in autophagy signaling upon glucose concentration descent. Figure S6. Mtl1 is not deficient in bulk autophagy in respiratory conditions. Figure S7. Mtl1 is needed for specific mitochondrial degradation during stationary phase.

Author contributions: Conceptualization, MA.T.; Methodology, MA.T, N.P, S.M; Software, MA.T, N.P, S.M; Validation MA.T, N.P, S.M; Formal Analysis N.P, S.M, MA.T; Investigation, MA.T, N.P, S.M; Resources, MA.T; Data Curation, S.M, N.P, MA.T; Writing-

Original Draft Preparation, MA.T; Writing-Review & Editing, S.M, N.P, MA.T; Visualization, MA.T, N.P, S.M; Supervision, MA.T; Project Administration, MA.T; Funding Acquisition, MA.T.

Acknowledgements: We want to thank Dr. D. Abeliovitch (The Hebrew University of Jerusalem Cell Biology, Freiburg, Germany) for kindly sending us the plasmids pGFP-Atg8 and pIdp1-GFP. We want to acknowledge Ms. Inmaculada Montoliu and Ms. Roser Pané for their technical support. The research described in this publication was partly supported by the Plan Nacional de I+D+I of the Spanish Ministry of Economy, Industry and Competitiveness (BIO2017-87828-C2-2-P). Sandra Montella is funded by a fellowship from the Catalan Government (Spain).

Conflicts of Interest: The authors declare no conflict of interest.

References

1. de Virgilio C. The essence of yeast quiescence. FEMS Microbiol Rev. **2012**;36(2):306–39, doi:10.1111/j.1574-6976.2011.00287.x.
2. Hughes Hallett JE, Luo X, Capaldi AP. State transitions in the TORC1 signaling pathway and information processing in *Saccharomyces cerevisiae*. Genetics. **2014**;198(2):773–86, doi:10.1534/genetics.114.168369.
3. Picazo C, Orozco H, Matallana E, Aranda A. Interplay among Gcn5, Sch9 and mitochondria during chronological aging of wine yeast is dependent on growth conditions. PLoS One. **2015**;10(2):1–17, doi:10.1371/journal.pone.0117267.
4. Santos J, Leão C, Sousa MJ. Ammonium-dependent shortening of CLS in yeast cells starved for essential amino acids is determined by the specific amino acid deprived, through different signaling pathways. Oxid Med Cell Longev. **2013**;2013(1)1-10, doi:10.1155/2013/161986.
5. Liu Z, Wu J, Huang D. New arahypins isolated from fungal-challenged peanut seeds and their glucose uptake-stimulatory activity in 3T3-L1 adipocytes. Phytochem Lett. **2013**;6(1):123–7, doi:10.1016/j.phytol.2012.1104.
6. Fabrizio P, Pozza F, Pletcher SD, Gendron CM, Longo VD. Regulation of longevity and stress resistance by Sch9 in yeast. Science. **2001**;292(5515):288–90, doi:101126/science.1059497.
7. Longo VD. Outline Cited by Turn off PDF reader Previous PDF The Ras and Sch9

pathways regulate stress resistance and longevity. **2003**;38(7):807-811, doi:10.1016/S0531-5565(03)001113-X.

8. Kaeberlein M, Westman E, Dang N, Kerr E, Powers III R, Steffen K, et al. Regulation of Yeast Replicative Life Span by TOR and Sch9 in Response to Nutrients. Science. **2005**;310(5751):1193–6, doi:10.1126/science.1115535.
9. Yan G, Lai Y, Jiang Y. The TOR Complex 1 Is a Direct Target of Rho1 GTPase. Mol Cell. **2012**;45(6):743–53, doi:10.1016/j.molcel.2012.01.028.
10. Thomas JD, Zhang YJ, Wei YH, Cho JH, Morris LE, Wang HY, et al. Rab1A Is an mTORC1 Activator and a Colorectal Oncogene. Cancer Cell. **2014**;26(5):754–69, doi:10.1016/j.ccell.2014.09.008.
11. Yuan W, Guo S, Gao J, Zhong M, Yan G, Wu W, et al. General control nonderepressible 2 (GCN2) kinase inhibits target of rapamycin complex 1 in response to amino acid starvation in *Saccharomyces cerevisiae*. J Biol Chem. **2017**;292(7):2660–9, doi:10.1074/jbc.M116.772194.
12. Postnikoff SDL, Johnson JE, Tyler JK. The integrated stress response in budding yeast lifespan extension. Microb Cell. **2017**;4(11):368–75, doi:10.15698/mic2017.11.597.
13. Stephan JS, Yeh Y-Y, Ramachandran V, Deminoff SJ, Herman PK. The Tor and PKA signaling pathways independently target the Atg1/Atg13 protein kinase complex to control autophagy. Proc Natl Acad Sci. **2009**;106(40):17049–54, doi:10.1073/pnas.0903316106.
14. Kamada Y, Funakoshi T, Shintani T, Nagano K, Ohsumi M, Ohsumi Y. Tor-mediated induction of autophagy via an Apg1 protein kinase complex. J Cell Biol. **2000**;150(6):1507–13, doi:10.1083/jcb.150.6.1507.
15. Kim YC, Guan K. mTOR: a pharmacologic target for autophagy regulation. J Clin Invest. **2015**;2(1):25–32, doi: 10.1172/JCI73939.
16. Budovskaya Y V, Stephan JS, Reggiori F, Klionsky DJ, Herman PK. The Ras/cAMP-dependent Protein Kinase Signaling Pathway Regulates an Early Step of the Autophagy Process in *Saccharomyces cerevisiae*. J Biol Chem. **2004**;279(20):20663–71, doi: 10.1074/jcb.M400272200.
17. Yorimitsu T, Zaman S, Broach JR, Klionsky DJ. Protein Kinase A and Sch9 Cooperatively Regulate Induction of Autophagy in *Saccharomyces cerevisiae*. Mol Biol Cell. **2007**;18(10):4180–9, doi:10.1091/mbc.e07-05-0485.
18. Conrad M, Schothorst J, Kankipati HN, Van Zeebroeck G, Rubio-Texeira M, Thevelein JM. Nutrient sensing and signaling in the yeast *Saccharomyces cerevisiae*. FEMS

Microbiol Rev. **2014**;38(2):254–99, doi:10.1111/1574-6976.12065.

19. Cazzanelli G, Pereira F, Alves S, Francisco R, Azevedo L, Dias Carvalho P, Almeida A, Côte-Real M, Oliveira MJ, Lucas C, Sousa MJ Preto A. The Yeast *Saccharomyces cerevisiae* as a Model for Understanding RAS Proteins and their Role in Human Tumorigenesis. 2018: 7(2):14, doi:10.3390/cells7020014.
20. Celenza JL, Carlson M. A yeast gene that is essential for release from glucose repression encodes a protein kinase. Science. **1986**;233(4769):1175–80, doi:10.1126/science.3526554.
21. Shashkova S, Welkenhuysen N, Hohmann S. Molecular communication: Crosstalk between the Snf1 and other signaling pathways. FEMS Yeast Res. **2015**;15(4):1–10, doi:10.1093/femsyr/fov026.
22. Wang Z, Wilson W a, Fujino M a, Roach PJ. Antagonistic controls of autophagy and glycogen accumulation by Snf1p, the yeast homolog of AMP-activated protein kinase, and the cyclin-dependent kinase Pho85p. Mol Cell Biol. **2001**;21(17):5742–52 ,doi:10.1128/MCB.21.17.5742-5752.2001.
23. Montella-Manuel S, Pujol-Carrion N, Mechoud MA, de la Torre-Ruiz MA. Bulk autophagy induction and life extension is achieved when iron is the only limited nutrient in *Saccharomyces cerevisiae*. Biochem J. **2021**;478(4):811–37, doi:10.1042/BCJ20200849.
24. Petkova MI, Pujol-Carrion N, de la Torre-Ruiz MA. Mtl1 O-mannosylation mediated by both Pmt1 and Pmt2 is important for cell survival under oxidative conditions and TOR blockade. Fungal Genet Biol. **2012**;49(11):903–14, doi:10.1016/j.fgb.2012.08.005.
25. Kock C, Dufrêne YF, Heinisch JJ. Up against the wall: Is yeast cell wall integrity ensured by mechanosensing in plasma membrane microdomains? Appl Environ Microbiol. **2015**;81(3):806–11, doi:10.1128/AEM.03273-14.
26. Rajavel M, Philip B, Buehrer BM, Errede B, Levin DE. Mid2 Is a Putative Sensor for Cell Integrity Signaling in. Mol Cell Biol. **1999**;19(6):3969–76, doi:10.1128/mcb.19.6.3969.
27. Vilella F, Herrero E, Torres J, De La Torre-Ruiz MA. Pkc1 and the upstream elements of the cell integrity pathway in *Saccharomyces cerevisiae*, Rom2 and Mtl1, are required for cellular responses to oxidative stress. J Biol Chem. **2005**;280(10):9149–59, doi:10.1074/jbc.M411062200.
28. Petkova MI, Pujol-Carrion N, Arroyo J, García-Cantalejo J, De La Torre-Ruiz MA. Mtl1 is required to activate general stress response through TOR1 and RAS2 inhibition under

conditions of glucose starvation and oxidative stress. J Biol Chem. **2010**;285(25):19521–31, doi:10.1074/jbc.M109.085282.

29. Jin C, Parshin A V., Daly I, Strich R, Cooper KF. The cell wall sensors Mtl1, Wsc1, and Mid2 are required for stress-induced nuclear to cytoplasmic translocation of cyclin C and programmed cell death in yeast. Oxid Med Cell Longev. **2013**;2013:320823, doi:10.1155/2013/320823.
30. Sundaram V, Petkova MI, Pujol-Carrion N, Boada J, de la Torre-Ruiz MA. Tor1, Sch9 and PKA downregulation in quiescence rely on Mtl1 to preserve mitochondrial integrity and cell survival. Mol Microbiol. **2015**;97(1):93–109, doi:10.1111/mmi.13013.
31. Levin DE. Regulation of cell wall biogenesis in *Saccharomyces cerevisiae*: The cell wall integrity signaling pathway. Genetics. **2011**;189(4):1145–75, doi:10.1534/genetics.111.128264.
32. de la Torre-Ruiz MA, Pujol N, Sundaram V. Coping with oxidative stress. Curr Drug Targets. **2015**;16(1):2-12, doi:10.2174/1389450115666141020160105.
33. Staleva L, Hall A, Orlow SJ. Oxidative Stress Activates FUS1 and RLM1 Transcription in the Yeast *Saccharomyces cerevisiae* in an Oxidant-dependent Manner. Mol Biol Cell. **2004**;15(12):5574-5582, doi:10.1091/mbc.E04-02-0142.
34. Jendretzki A, Wittland J, Wilk S, Straede A, Heinisch JJ. How do I begin? Sensing extracellular stress to maintain yeast cell wall integrity. Eur J Cell Biol. **2011**;90(9):740–4, doi: 10.1016/j.ejcb.2011.04.006.
35. Yang Z, Klionsky DJ. An overview of the molecular mechanism of autophagy. Curr Top Microbiol Immunol. **2009**;335:1–32 doi:10. 1007/978-3-642-00302-8_1.
36. Kawamata T, Horie T, Matsunami M, Sasaki M, Ohsumi Y. Zinc starvation induces autophagy in yeast. J Biol Chem. **2017**;292(20):8520–30, doi:10.1074/jcb.M116.762948.
37. Yokota H, Gomi K, Shintani T. Induction of autophagy by phosphate starvation in an Atg11-dependent manner in *Saccharomyces cerevisiae*. Biochem Biophys Res Commun. 2017;483(1):522–7, doi:10.1016/j.bbrc.2016.12.112.
38. Nakatogawa H, Suzuki K, Kamada Y, Ohsumi Y. Dynamics and diversity in autophagy mechanisms: Lessons from yeast. Nat Rev Mol Cell Biol. **2009**;10(7):458–67, doi:10.1038/nrm2708.
39. Yorimitsu T, Ke Wang CH, Klionsky DJ. Tap42-associated protein phosphatase type 2A negatively regulates induction of autophagy. Autophagy. **2009**;5(5):616–24, doi:10.4161/auto.5.5.8091.

40. Fujioka Y, Suzuki SW, Yamamoto H, Kondo-Kakuta C, Kimura Y, Hirano H, et al. Structural basis of starvation-induced assembly of the autophagy initiation complex. Nat Struct Mol Biol. **2014**;21(6):513–21, doi:10.1038/nsmb.2822.
41. Yamamoto H, Fujioka Y, Suzuki SW, Noshiro D, Suzuki H, Kondo-Kakuta C, et al. The Intrinsically Disordered Protein Atg13 Mediates Supramolecular Assembly of Autophagy Initiation Complexes. Dev Cell. **2016**;38(1):86–99, doi:10.1016/j.devcel.2016.06.015.
42. Ohsumi Y. Historical landmarks of autophagy research. Cell Res. **2014**;24(1):9–23, doi:10.1038/cr.2013.169.
43. Feng Y, He D, Yao Z, Klionsky DJ. The machinery of macroautophagy. Cell Res. **2014**;24(1):24–41, doi:10.1038/cr.2013.168.
44. Powers RW, Kaeberlein M, Caldwell SD, Kennedy BK, Fields S. Extension of chronological life span in yeast by decreased TOR pathway signaling. Genes Dev. **2006**;20(2):174–84, doi:10.1101/gad.1381406.
45. Fabrizio P, Hoon S, Shamalnasab M, Galbani A, Wei M, Giaever G, et al. Genome-wide screen in *Saccharomyces cerevisiae* identifies vacuolar protein sorting, autophagy, biosynthetic, and tRNA methylation genes involved in life span regulation. PLoS Genet. **2010**;6(7):1–14, doi:10.1371/journal.pgen.1001024.
46. Gatica D, Lahiri V, Klionsky DJ. Cargo Recognition and Degradation by Selective Autophagy. Nat Cell Biomol. **2018**;20(3):233–42, doi:10.1038/s41556-018-0037-z.
47. Mamaev D V., Zvyagilskaya RA. Mitophagy in Yeast. Biochem. **2019**;84:225–32, doi: 10.1134/S000629791914013X.
48. Fukuda T, Kanki T. Mechanisms and physiological roles of mitophagy in yeast. Mol Cells. **2018**;41(1):35–44, doi:10.14348/molcells.2018.2214.
49. Welter E, Montino M, Reinhold R, Schlotterhose P, Krick R, Dudek J, Rehling P, Thumm M. Uth1 is a mitochondrial inner membrane protein dispensable for post-log-phase and rapamycin-induced mitophagy. FEBS J. **2013**;280(20):4970–82, doi:10.1111/febs.12468.
50. Wach A, Brachat A, Pöhlmann R, Philippsen P. New heterologous modules for classical or PCR-based gene disruptions in *Saccharomyces cerevisiae*. Yeast. **1994**;10(13):1793–808, doi:10.1002/yea.320101310.
51. Pujol-Carrion N, Belli G, Herrero E, Nogues A, de la Torre-Ruiz MA. Glutaredoxins Grx3 and Grx4 regulate nuclear localisation of Aft1 and the oxidative stress response in *Saccharomyces cerevisiae*. J Cell Sci. **2006**;119(21):4554–64, doi:10.1242/jcs.03229.

52. Gallego C, Eloi G, Colomina N, Enrique H, Aldea M. The Cln3 cyclin is down-regulated by translational repression and degradation during the G1 arrest caused by nitrogen deprivation in budding yeast. EMBO J. **1997**;16(23):7196–206, doi:10.1093/emboj/16.23.7196.
53. Petkova MI, Pujol-Carrion N, de la Torre-Ruiz MA. Signal flow between CWI/TOR and CWI/RAS in budding yeast under conditions of oxidative stress and glucose starvation. Commun Integr Biol. **2010**;3(6):555–7, doi:10.4161/cib.3.6.12974.
54. Guedes A, Ludovico P, Sampaio-Marques B. Caloric restriction alleviates alpha-synuclein toxicity in aged yeast cells by controlling the opposite roles of Tor1 and Sir2 on autophagy. Mech Ageing Dev. **2016**;161(16):270-276, doi: 10.1016/j.mad.2016.04.006.
55. Ecker N, Mor A, Journo D, Abeliovich H, Ecker N, Mor A, et al. Deprivation is distinct from nitrogen starvation- induced macroautophagy Induction of autophagic flux by amino acid deprivation is distinct from nitrogen starvation-induced macroautophagy. Autophagy. **2010**;6(7):870-890, doi:10.4161/auto.6.7.12753.
56. Görner W, Durchschlag E, Martinez-pastor MT, Estruch F, Ammerer G, Hamilton B, et al. Nuclear localization of the C2H2 zinc finger protein Msn2p is regulated by stress and protein kinase A activity. Genes Dev. **1998**;12(4)586–97, doi:10.1101/gad.12.4.863.
57. Komeili A, Wedaman KP, O'Shea EK, Powers T. Mechanism of metabolic control: Target of rapamycin signaling links nitrogen quality to the activity of the Rtg1 and Rtg3 transcription factors. J Cell Biol. **2000**;151(4):863–78, doi:10.1083/jcb.151.4.863.
58. Hagai A, Zareic M, Kristoffer TGR, Richard JY, Joern D. Involvement of mitochondrial dynamics in the segregation of mitochondrial matrix proteins during stationary phase mitophagy. Physiol Behav. **2017**;176(1):100–106, doi:10.1038/ncomms3789.
59. Kaiser C, Michaelis S, Mitchell A. Methods in Yeast Genetics. Cold Spring Harbour Laboratory Press Ltd. NewYork, NY, USA, **1994**; pp. 107–121, ISBN 0-87969-451-3.
60. Pujol-Carrion N, Petkova MI, Serrano L, de la Torre-Ruiz MA. The MAP kinase Slt2 is involved in vacuolar function and actin remodeling in *Saccharomyces cerevisiae* mutants affected by endogenous oxidative stress. Appl Environ Microbiol. **2013**;79(20):6459–71, doi:10.1128/AEM.01692-13.
61. Mechoud MA,, Pujol-Carrion N, Montella-Manuel S, De La Torre-Ruiz MA. Interactions of GMP with Human Glrx3 and with Saccharomyces cerevisiae Grx3 and Grx4 Converge in the Regulation of the Gcn2 Pathway. Am Soc Microbiol. **2020**;86(4) 00221-20, doi:10.1128/AEM.00221-20.

62. Shintani T and Klionsky DJ. Cargo Proteins Facilitate the Formation of Transport Vesicles in the Cytoplasm to Vacuole Targeting Pathway. J Biol Chem. **2004**;279(29):29889–94, doi:10.1074/jbc.M404399200.
63. Noda T, Klionsky DJ. The quantitative Pho8Delta60 assay of nonspecific autophagy. Methods in enzymology. **2008**;6879(08):03203-5, doi:10.1016/S0076-6879(08)03203-5.
64. Hernandez-Lopez M, Prieto J and Randez-Gil F. Osmotolerance and leavening ability in sweet dough. Comparative analysis between *Torulaspora delbrueckii* and *Saccharomyces cerevisiae* baker's yeast strains. Antonie Leeuwenhoek. **2003**;84(2):125-134, doi:10.1023/A:1025413520192.
65. Dever TE, Feng L, Wek RC, Cigan AM, Donahue TF, Hinnebusch AG. Phosphorylation of initiation factor 2α by protein kinase GCN2 mediates gene-specific translational control of GCN4 in yeast. Cell. **1992**;68(3):585–96, doi:10.1016/0092-8674(92)90193-G.
66. Suzuki K, Kirisako T, Kamada Y, Mizushima N, Noda T, Ohsumi Y. The pre-autophagosomal structure organized by concerted functions of APG genes is essential for autophagosome formation. EMBO J. **2001**;20(21):5971–81, doi:10.1093/emboj/20.21.5971.
67. Adachi A, Koizumi M, Ohsumi Y. Autophagy induction under carbon starvation conditions is negatively regulated by carbon catabolite repression. J Biol Chem. **2017**;292(48):19905–18, doi:10.1074/jbc.M117.817510.
68. Tomotake K, Daniel JK. Mitophagy in yeast occurs through a selective mechanism. J Biol Chem. **2008**;283(47):32386-93, doi:10.1074/jbc.M802403200.
69. Kolitsida P, Abeliovich H. Methods for Studying Mitophagy in Yeast. Methods Mol Biol. **2019**;1880:669–78, doi:10.1007/978-1-4939-8873-0_44.
70. Liu Y, Okamoto K. Regulatory mechanisms of mitophagy in yeast. Biochim Biophys Acta-Gen Subj. **2021**;1865(5):129858, doi:10.1016/j.bbagen.2021.129858.
71. Zientara-Rytter K, Subramani S. Mechanistic insights into the role of Atg11 in selecetive autophagy. J Mol Biol. **2020**;432(1):104-122, doi:10.1016/j.jmb.2019.06.017.
72. Grisan F, Iannucci LF, Surdo NC, Gerbino A, Zanin S, Di Benedetto G, Pozzan T, Lefkimmiatis K. PKA compartmentalization links cAMP signaling and autophagy. Cell Death Differ. **2021**;28(8):2436–49, doi:10.1038/s41418-021-00761-8.
73. Coccetti P, Nicastro R, Tripodi F. Conventional and emerging roles of the energy sensor snf1/AMPK in *Saccharomyces cerevisiae*. Microb Cell. **2018**;5(11):482–94,

doi:10.15698/mic2018.11655.

74. Hedbacker K. SNF1/AMPK pathways in yeast. Front Biosci. **2008**;13(13):2408, doi:10.2741/2854.
75. Mayer F V., Heath R, Underwood E, Sanders MJ, Carmena D, McCartney RR, et al. ADP regulates SNF1, the *Saccharomyces cerevisiae* homolog of AMP-activated protein kinase. Cell Metab. **2011**;14(5):707–14, doi:10.1016/j.cmet.2011.09.009.
76. Hlavatá L, Nyström T. Ras Proteins Control Mitochondrial Biogenesis and Function in *Saccharomyces cerevisiae*. Folia Microbiol. **2003**;48(6):725–30, doi: 10.1007/BF02931505.
77. Cebollero E, Reggiori F. Regulation of autophagy in yeast *Saccharomyces cerevisiae*. Biochim Biophys Acta - Mol Cell Res. **2009**;1793(9):1413–21, doi:10.1016/j.bbamcr.2009.01.008.
78. Chen Y, Klionsky DJ. The regulation of autophagy - Unanswered questions. J Cell Sci. **2011**;124(2):161–70, doi: 10.1242/jcs.064576.
79. Pedruzzi I, Bürckert N, Egger P, De Virgilio C. *Saccharomyces cerevisiae* Ras/cAMP pathway controls post-diauxic shift element-dependent transcription through the zinc finger protein Gis1. EMBO J. **2000**;19(11):2569–79, doi:10.1093/emboj/19.11.2569.
80. Pedruzzi I, Dubouloz F, Cameroni E, Wanke V, Roosen J, Winderickx J, et al. TOR and PKA Signaling Pathways Converge on the Protein Kinase Rim15 to Control Entry into G0. Mol Cell. **2003**;12(6):1607–13, doi:10.1016/S1097-2765(03)00485-4.
81. Schmelzle T, Beck T, Martin DE, Hall MN. Activation of the RAS/Cyclic AMP Pathway Suppresses a TOR Deficiency in Yeast. Mol Cell Biol. **2004**;24(1):338–51, doi:10.1128/MCB.24.1.338-351.2004.
82. Urban J, Soulard A, Huber A, Lippman S, Mukhopadhyay D, Deloche O, et al. Sch9 Is a Major Target of TORC1 in Saccharomyces cerevisiae. Mol Cell. **2007**;26(5):663–74, doi: 10.1016/j.molcel.2007.04.020.
83. Deprez MA, Eskes E, Winderickx J, Wilms T. The TORC1-Sch9 pathway as a crucial mediator of chronological lifespan in the yeast *Saccharomyces cerevisiae*. FEMS Yeast Res. **2018**;18(5):1–15, doi:10.1093/femsyr/foy048.
84. Lakhani R, Vogel KR, Till A, Liu J, Burnett SF, Gibson KM, et al. Defects in GABA metabolism affect selective autophagy pathways and are alleviated by mTOR inhibition. EMBO Mol Med. **2014**;6(4):551–66, doi:10.1002/emmm.201303356.
85. Waliullah TM, Yeasmin AMST, Kaneko A, Koike N, Terasawa M, Totsuka T, et al. Rim15 and Sch9 kinases are involved in induction of autophagic degradation of

ribosomes in budding yeast. Biosci Biotechnol Biochem. **2017**;81(2):307–10, doi:10.1080/09168451.2016.1234928.

Figure S1

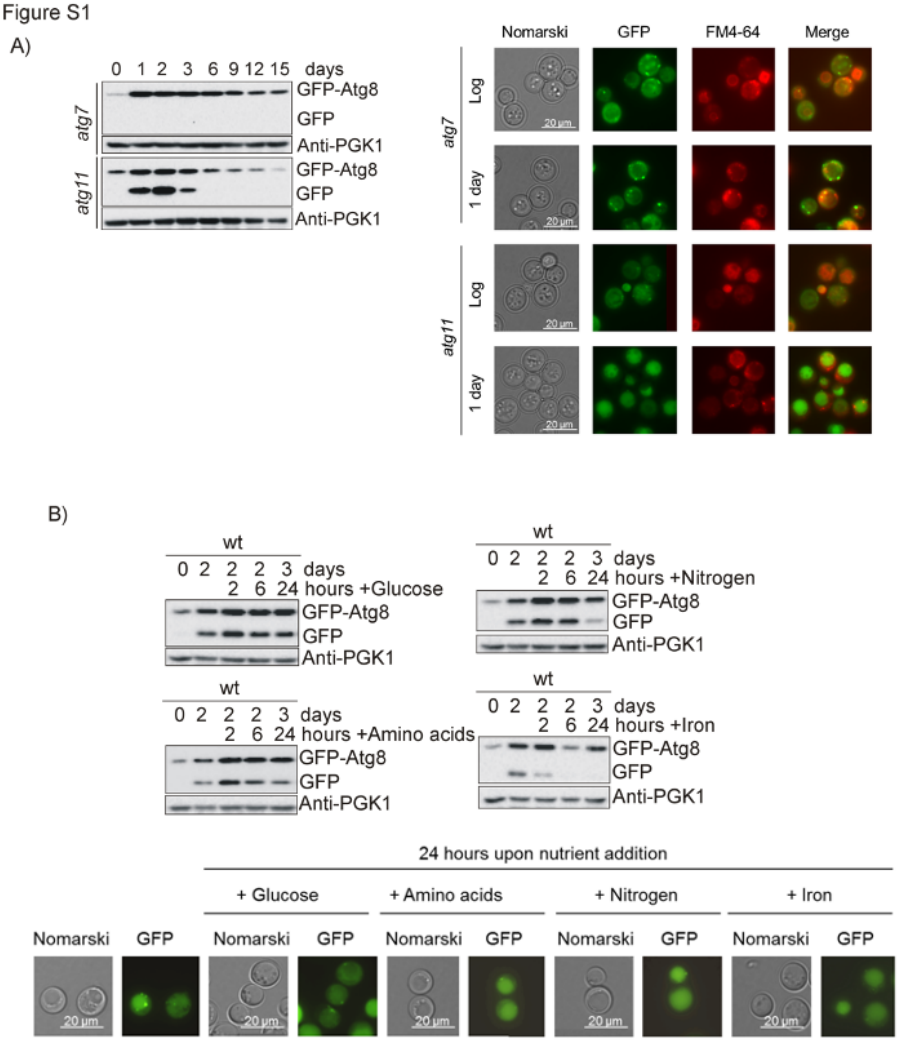

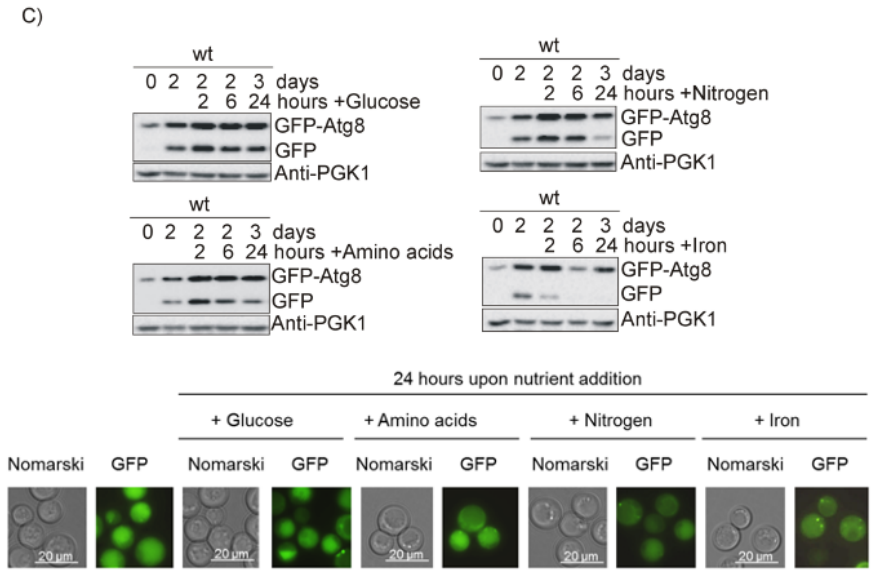

Figure S1. Sequential descent of glucose and amino acids activates bulk autophagy during the diauxic shift in *Saccharomyces cerevisiae*. A) *atg7* and *atg11* strains expressing the fusion protein GFP-Atg8, were grown to log phase (OD_{600}: 0.6) in SD medium at 30ºC. Aliquots were collected for total protein extraction, western blot and for *in vivo* observation of GFP-Atg8 in the fluorescence microscope as in A. B) wt cells bearing GFP-Atg8 in the genome was exponentially grown at OD_{600}: 0.6 at 30ºC in SD media and a sample was collected for analysis. Upon one day of culture, 2% glucose, amino acids (60 mg/ml Leucine, 20 mg/ml Histidine and 20 mg/ml Tryptophan), 0.67% nitrogen or 10 mM iron, were respectively added to the cultures and samples were collected upon 2, 6 and 24 hours to detect GFP-Atg8 by western blot and *in vivo* cellular localization through the fluorescence microscope as in A. Microscopic images represent GFP-Atg8 intracellular localization 24 hours upon re-feeding with each specific nutrient. C) As in D but results correspond to two days of growth.

Figure S2

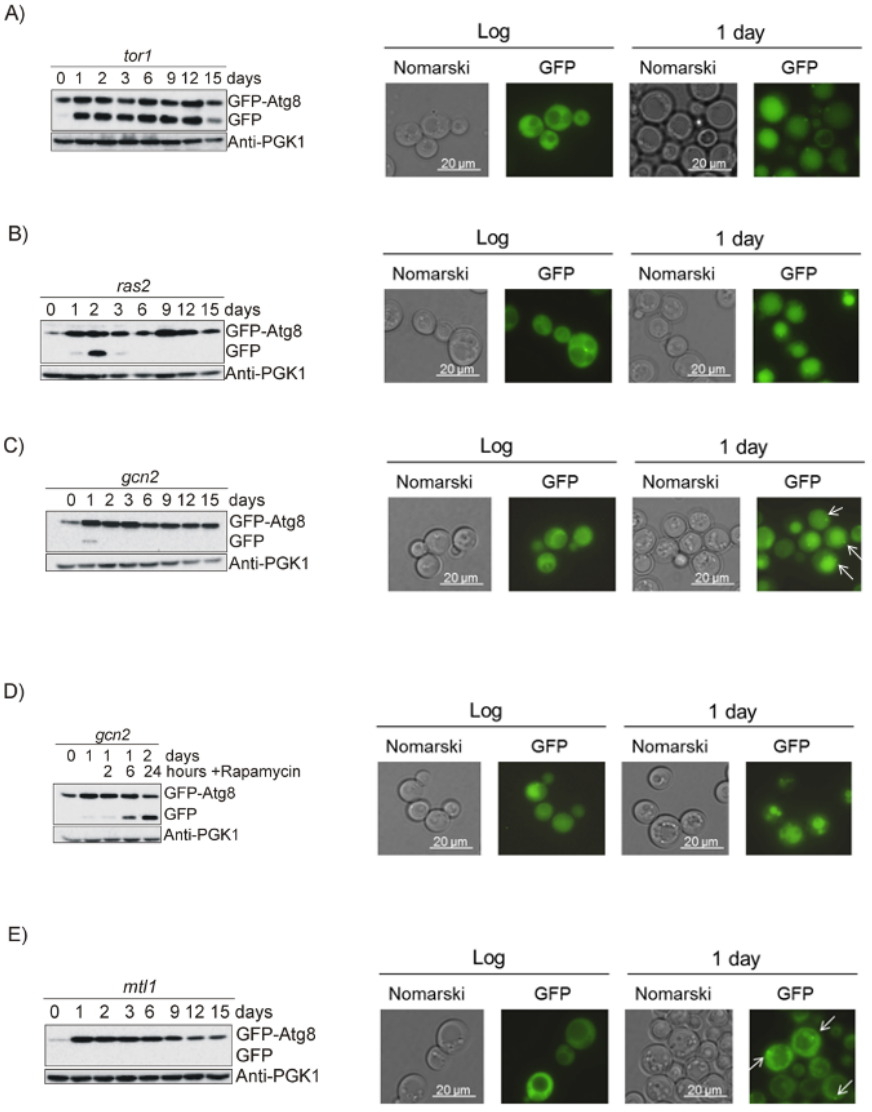
A)
tor1
0 1 2 3 6 9 12 15 days
GFP-Atg8
GFP
Anti-PGK1
Log
1 day
Nomarski
GFP
Nomarski
GFP
20 µm
B)
ras2
0 1 2 3 6 9 12 15 days
GFP-Atg8
GFP
Anti-PGK1
Log
1 day
Nomarski
GFP
Nomarski
GFP
20 µm
C)
gcn2
0 1 2 3 6 9 12 15 days
GFP-Atg8
GFP
Anti-PGK1
Log
1 day
Nomarski
GFP
Nomarski
GFP
20 µm
D)
gcn2
0 1 1 1 2 days
2 6 24 hours +Rapamycin
GFP-Atg8
GFP
Anti-PGK1
Log
1 day
Nomarski
GFP
Nomarski
GFP
20 µm
E)
mtl1
0 1 2 3 6 9 12 15 days
GFP-Atg8
GFP
Anti-PGK1
Log
1 day
Nomarski
GFP
Nomarski
GFP
20 µm

F)

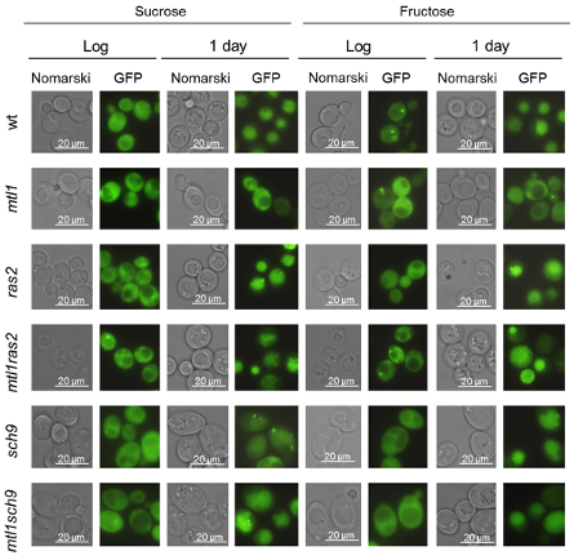

Figure S2. Mtl1 and Gcn2 control autophagy induction during glucose and amino acids starvation. Growth conditions, western blot and in vivo microscope observation determined in: A) *tor1* mutant expressing GFP-Atg8; B) *ras2* mutant expressing GFP-Atg8 and C) *gcn2* mutant expressing GFP-Atg8, was performed as described in (Figure S1A). D) *gcn2* bearing GFP-Atg8 was exponentially grown at 30ºC in SD plus amino acids. Rapamycin (200 ng/ml) was added to the cultures upon 1 day of growth and samples were subsequently collected upon 2, 6 and 24 hours of exposure to the drug. Aliquots were treated as in (Figure S1A). E) Growth conditions, GFP-Atg8 *in vivo* intracellular localization and western blot in *mtl1* culture expressing the fusion protein GFP-Atg8 was performed as in (Figure S1A). F) wt, *mtl1*, *ras2*, *mtl1ras2*, *sch9* and *mtl1sch9* cultures in which the GFP-Atg8 fusion protein was integrated, were grown to log phase and 1 day in Sucrose or Fructose medium at 30º. Aliquots were collected for in vivo microscopic observation by using a fluorescence microscope.

Figure S3

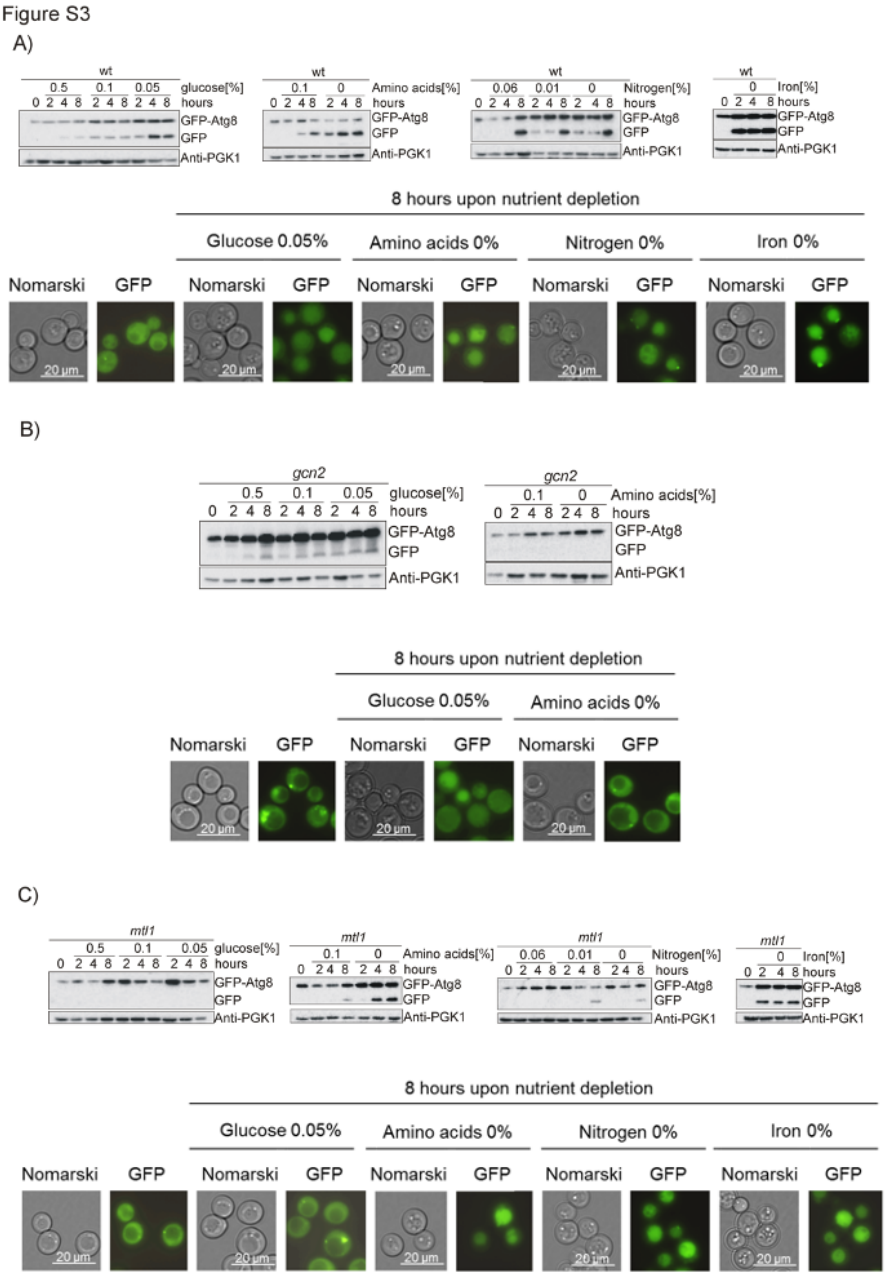

Figure S3. Mtl1 signals glucose limitation to the autophagy machinery. A) wt cells expressing GFP-Atg8 were exponentially grown in SD media. Aliquots were taken, washed and

transferred to different minimum media containing: 0.5, 0.1 or 0.05% glucose; 0.1 or 0% amino acids; 0.06, 0.01 or 0% nitrogen or medium without iron (0%). Autophagy was determined upon western blot analysis or *in vivo* identification of GFP-Atg8 in the fluorescence microscope as in (Figure S1A). The same experiments as in A were carried out in B) *gcn2* mutant cultures expressing GFP-Atg8 and in C) *mtl1* strain expressing GFP-Atg8.

Figure S4

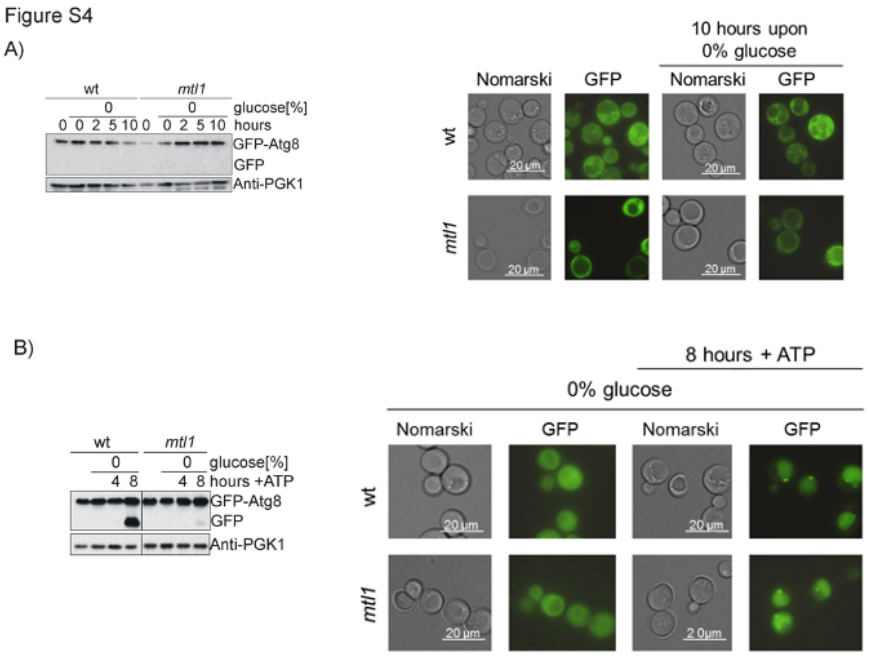

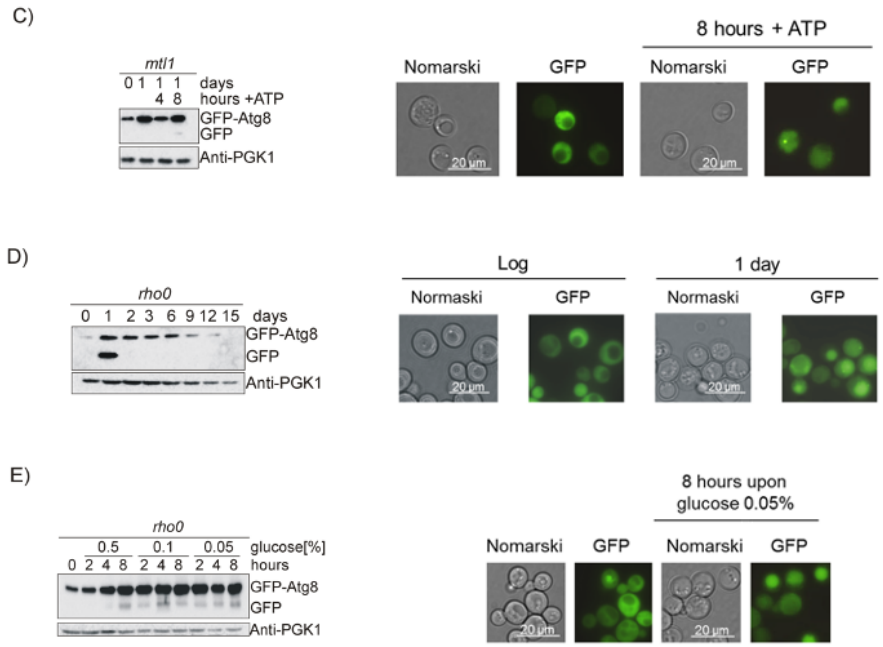

Figure S4. Mtl1 signals the decrease in glucose concentration to the autophagy machinery in a manner not fully dependent on ATP production by mitochondria. A) wt and *mtl1* cells expressing GFP-Atg8 grown in SD media were transferred to minimum media devoid of glucose (0% glucose) to determine autophagy upon detection of GFP-Atg8 vacuolar cleavage by western blot analyses and also *in vivo* through fluorescence microscopy as in (Figure S1A). B) Upon transference to minimum media without glucose, ATP (at 200 mM final concentration) was added to the cultures described in A and samples were collected at the indicated times for western blot and microscopic determination of autophagy as in A. C) ATP (200 mM) was added to *mtl1* cultures growing in SD minimum medium for one day, at the diauxic shift, and samples were collected at 4 and 8 hours for western blot analysis and *in vivo* observation in the fluorescence microscope. D) *rho0* mutant expressing GFP-Atg8 was grown as in (Figure S1A) for autophagy determination. E) *rho0* cells exponentially growing in SD were washed and transferred to several media containing different glucose concentrations to analyse autophagy as in (Figure S3A).

Figure S5

A)

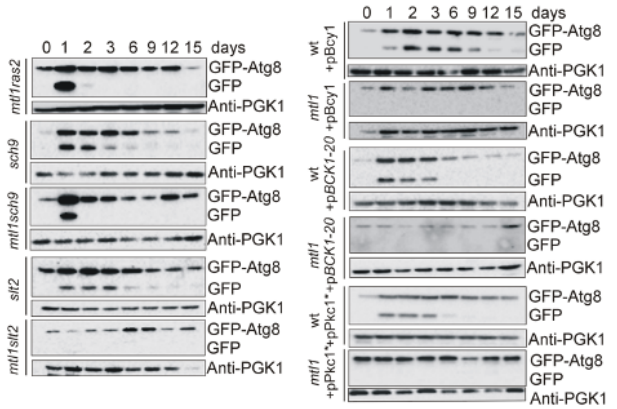
0 1 2 3 6 9 12 15 days
mtl1ras2
sch9
mtl1sch9
slt2
mtl1slt2
GFP-Atg8
GFP
Anti-PGK1
wt +pBcy1
mtl1 +pBcy1
wt +pBCK1-20
mtl1 +pBCK1-20
wt +pPkc1*
mtl1 +pPkc1*

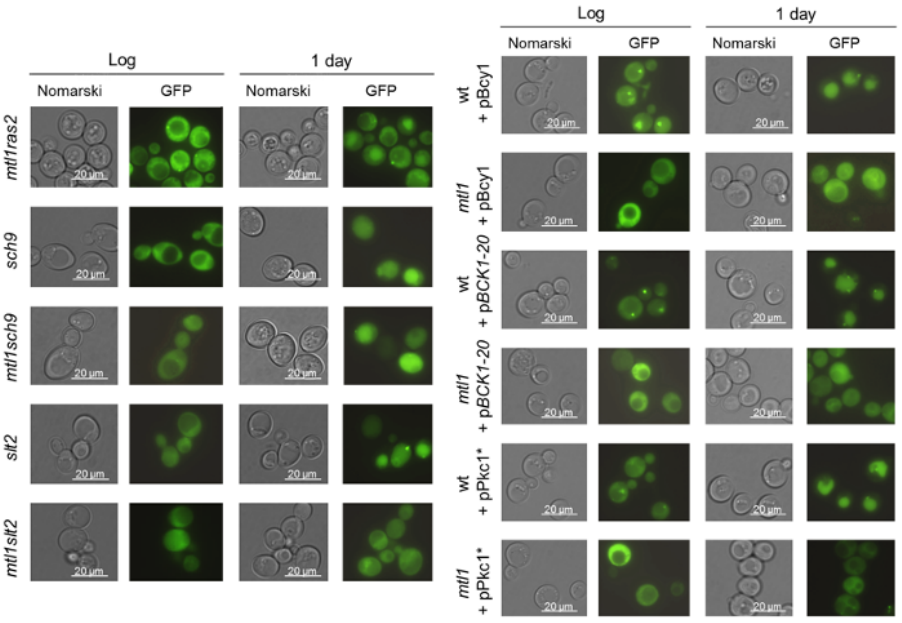
Log
1 day
Nomarski
GFP
mtl1ras2
sch9
mtl1sch9
slt2
mtl1slt2
wt + pBcy1
mtl1 + pBcy1
wt + pBCK1-20
mtl1 + pBCK1-20
wt + pPkc1*
mtl1 + pPkc1*
20 µm

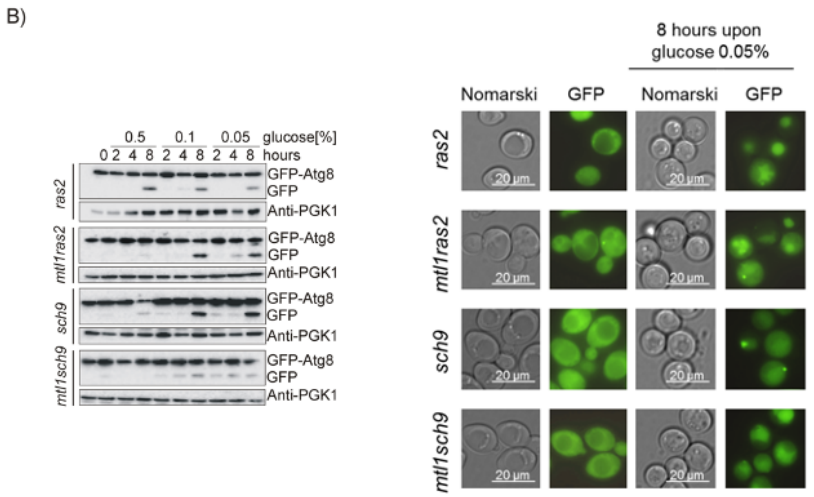

Figure S5. Both Ras2 and Sch9 suppress *mtl1* deficiency in autophagy signaling upon glucose concentration descent. A) *mtl1ras2, sch9, mtl1sch9, slt2, mtl1slt2,* wt+pBcy1, *mtl1*+pBcy1, wt+p*BCK1-20*, *mtl1*+p*BCK1-20*, wt+pPkc1* and *mtl1*+pPkc1* strains expressing GFP-Atg8 were grown at 30ºC in SD media during 15 days. Samples were taken for western blot analysis and *in vivo* observation in the fluorescence microscope of GFP cleavage from GFP-Atg8 were all performed as described in (Figure S1A). B) Strains *ras2, mtl1ras2, sch9* and *mtl1sch9* expressing GFP-Atg8 were exponentially grown in SD media to be subsequently transferred to minimum medium containing the indicated concentrations of glucose. Samples were taken to determine autophagy as in (Figure S3A).

Figure S6

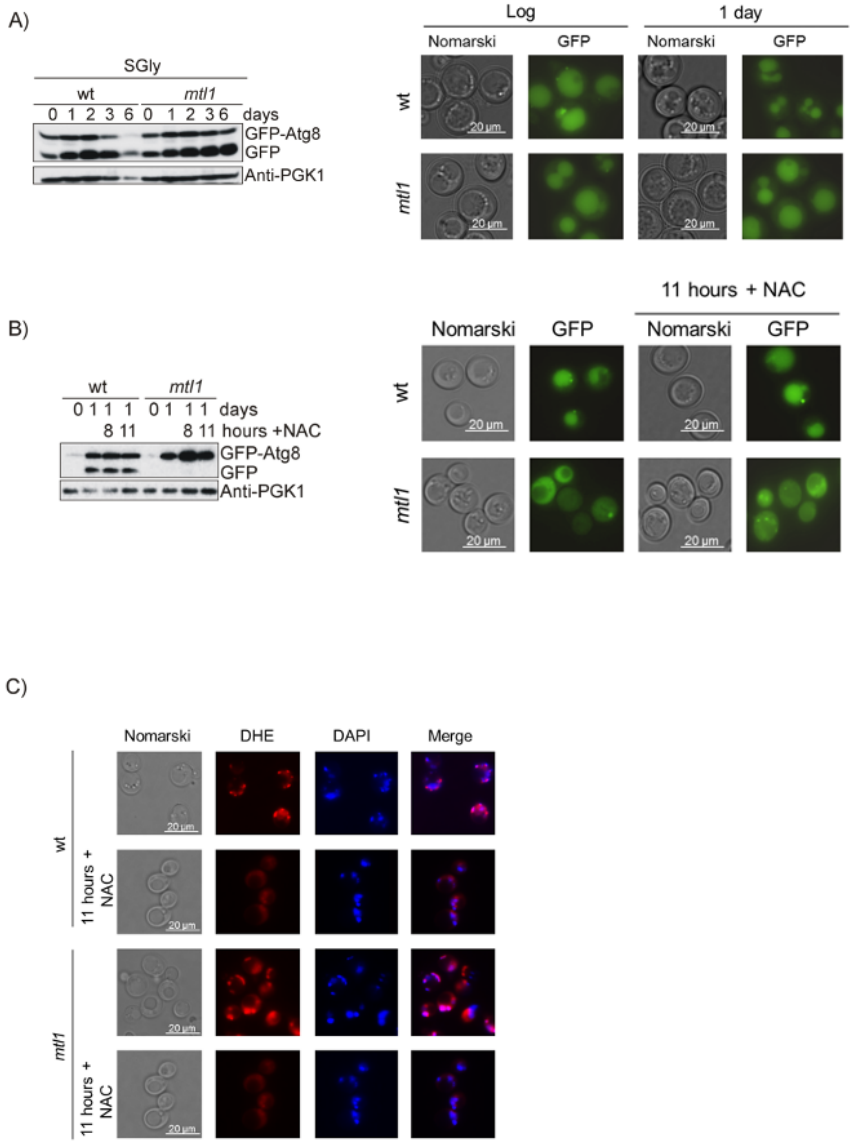

Figure S6. Mtl1 is not deficient in bulk autophagy in respiratory conditions. A) wt and *mtl1* cultures were grown in minimum medium SGly (containing glycerol as unique carbon source) plus amino acids at 30°C to stationary phase for 6 days. Samples were collected at the indicated

times to perfor western blot analysis and *in vivo* microscopic determination as described in (Figure S1A). B) wt and *mtl1* cultures in SD medium growing to 1 day were treated with N-Acetyl cysteine (NAC) 5 mM for 8 and 11 hours. Samples were collected for autophagy determinations as in A. C) wt and *mtl1* cultures were grown in SD medium. At one day of growth, 5mM of NAC was added for 11 hours. Samples were collected and stained with dihydroethidium (DHE) for in vivo visualization of cellular oxidation in the fluorescent microscope.

Figure S7

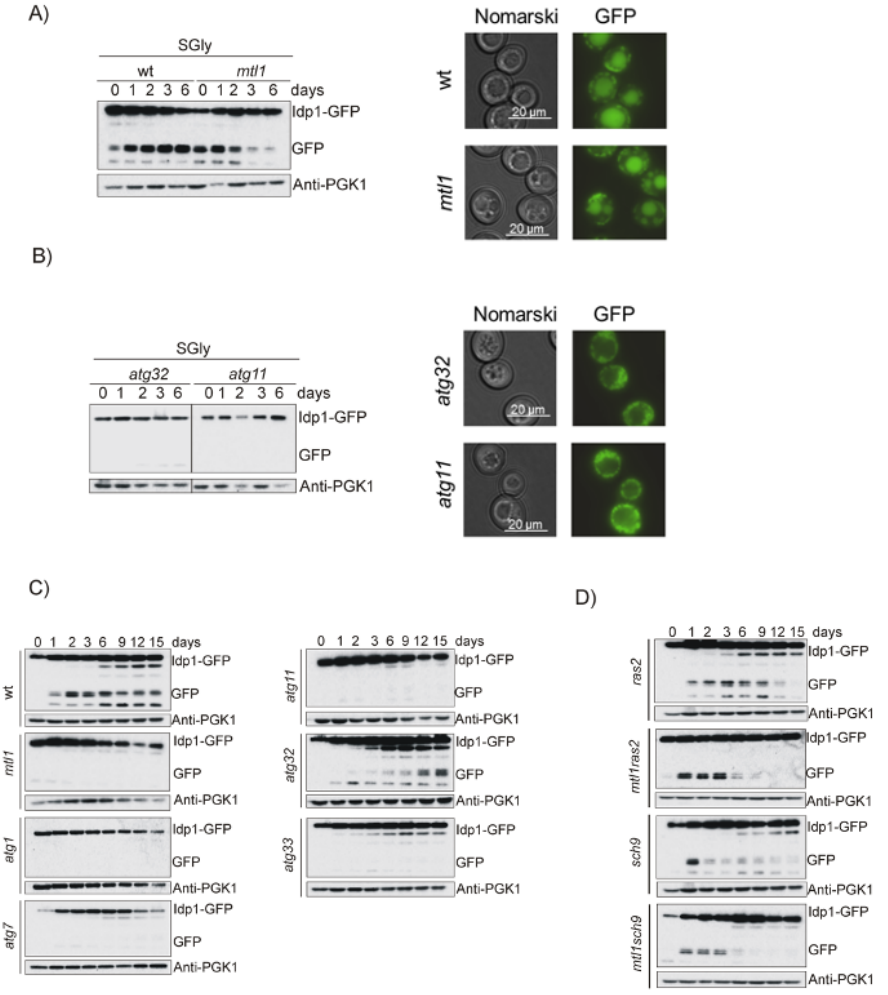

Figure S7. Mtl1 is needed for specific mitochondrial degradation during stationary phase. A) wt and *mtl1* cultures transformed with plasmid Idp1-GFP were grown in SGly media plus amino acids at 30°C. Samples were taken at the indicated times for *in vivo* observation in the fluorescence microscope and western blot analysis. B) *atg32* and *atg11* cultures transformed with Idp1-GFP were grown in SGly medium plus amino acids at 30°C. Samples were collected at the indicated times for *in vivo* observation in the fluorescence microscope and perform western blot as in A. C) wt, *mtl1, atg1, atg7, atg11, atg32* and *atg33* strains bearing the plasmid Idp1-GFP were grown in SD media at 30ºC for 15 days in continuous shacking. Samples were taken at indicated times to monitor Idp1-GFP cleavage. D) *ras2, mtl1ras2, sch9* and *mtl1sch9* mutants, transformed with Idp1-GFP were treated as in C.

4.4 QUART ARTICLE

Aft1 nuclear localization and transcriptional response to iron starvation relies upon TORC2/Ypk1 signaling and sphingolipid biosynthesis

Sandra Montellà-Manuel[1]; Nuria Pujol-Carrion[1]; ~~Ted Powers~~[2] and Maria Angeles de la Torre-Ruiz[1]

[1] Cell Signalling in Yeast Unit, Department of Basic Medical Sciences, Institut de Recerca Biomèdica de Lleida (IRBLleida), University of Lleida, 25198 Lleida, Spain.
[2] ~~Department of Molecular and Cellular Biology, College of Biological Sciences, University of California, Davis, Davis, CA 95616.~~

Abstract

Iron scarcity provokes a cellular response consisting of strong expression of high-affinity systems to optimize iron uptake and mobilization. Aft1 is a primary transcription factor involved in iron homeostasis and controls expression of high-affinity iron uptake genes in *Saccharomyces cerevisiae*. Aft1 responds to iron deprivation by translocating from the cytoplasm to the nucleus. Here, we demonstrate that the AGC kinase Ypk1, as well as its upstream regulator TOR Complex 2 (TORC2), are required for proper Aft1 nuclear localization following iron deprivation. We exclude a role for TOR Complex 1 (TORC1) and its downstream effector Sch9, suggesting this response is specific for the TORC2 arm of the TOR pathway. Remarkably, we demonstrate that Aft1 nuclear localization and a robust transcriptional response to iron starvation also requires biosynthesis of sphingolipids, including complex sphingolipids such as inositol phosphorylceramide (IPC) and upstream precursors, including long chain bases (LCBs) and ceramides. Furthermore, we observe the deficiency of Aft1 nuclear localization and impaired transcriptional response in the absence of iron when TORC2-Ypk1 is impaired is partially suppressed by exogenous addition of the LCB dihydrosphingosine (DHS). This later result is consistent with prior studies linking sphingolipid biosynthesis to TORC2-Ypk1 signaling. Taken together, these results reveal a novel role for sphingolipids, controlled by TORC2-Ypk1, for proper localization and activity of Aft1 in response to iron scarcity.

Key words: TORC2, Ypk1, iron deprivation, Aft1, iron homeostasis, sphingolipids,

LCBs, CK2, survival, inositol phosphorylceramide (IPC)

1. Introduction

Iron is indispensable for life in every organism and plays an essential role in cellular processes such as respiration, DNA synthesis and repair, and diverse metabolic reactions as an essential cofactor [1,2]. Iron levels must also be tightly regulated as elevated levels have toxic effects, including contributing to production of reactive oxygen species (ROS) [3,4]. However insufficient iron levels also cause detrimental effects within cells [5]. Indeed, iron deficiency is the most prevalent nutritional disorder in the world whose consequences on human health are well established [6]. Iron trafficking and metabolism require tight regulation, where studies in budding yeast, *Saccharomyces cerevisiae,* have yielded insights into the metabolism of this metal in humans. In yeast, iron can be captured and internalized within the cytoplasm through the multicopper oxidase Fet3 [7] and transmembrane permease Ftr1 [8,9]. The genes encoding these components, in addition to others involved in iron metabolism, constitute a regulon under the control of the transcription factor Aft1 (and its paralogue Aft2) [10,11]. The intracellular localization of Aft1 is regulated by iron availability, whereby it is localized within the nucleus when iron is scarce and translocates into the cytoplasm when iron becomes replenished [12]. The karyopherin/importin Pse1 mediates nuclear import of Aft1 in response to iron starvation [13]. Remarkably, cellular components that link iron scarcity to Aft1 nuclear localization remain poorly understood.

The TOR (target of rapamycin) is a universal sensor and integrator of nutritional signals in eukaryotes and exists in two proteins complexes, TORC1 and TORC2, where TORC1 is sensitive to the antibiotic rapamycin [14–16]. In yeast, TORC2 is localized at or adjacent to the plasma membrane where it phosphorylates and activates Ypk1 (or its paralogue Ypk2) [17] or Pkc1 [18]. TORC2 phosphorylates Ypk1 at two sites within a C-terminal regulatory domain [16]. Ypk1 is also phosphorylated within its kinase domain by Pkh1/Pkh2, which are homologous of mammalian PDK1 [19]. Ypk1 has a wide variety of cellular activities, including direct involvement in the biosynthesis of sphingolipids. Upon sphingolipid depletion, Ypk1 phosphorylates and inhibits both Orm1 and Orm2, which are themselves inhibitors of serine

palmitoyltransferase (SPT), the enzyme that catalyzes the initial step of sphingolipid biosynthesis [20]. Treatment with Myriocin, a small molecule inhibitor of SPT, signals to Ypk1 via TORC2 through a complex feedback activation loop [21]. Independently, Ypk1 phosphorylates Lac1 and Lag1, the two catalytic subunits of the enzyme ceramide synthase (CerS), thereby stimulating ceramide biosynthesis [22]. CerS activity also requires Casein Kinase 2 (CK2), which independently phosphorylates Lac1 and Lag1 and contributes to the stability of CerS and its localization within the ER [23]. Ceramides are subsequently converted in the Golgi to complex sphingolipids: inositol phosphorylceramide (IPC), mannosylinositol phosphorylceramide (MIPC), and mannosyl-diinositol phosphorylceramide [M(IP)2C] (see review, [24]).

In addition to TORC2-Ypk1 and CK2, other signaling kinases have been linked to sphingolipids. For example, Sch9 kinase is a TORC1 target and has been implicated in the regulation of related of *LAG1* and *LAC1*, as well as the ceramidase genes *YPC1* and *YDC1*. Consequently, deletion of *SCH9* causes impairment of LCB levels [25]. Decreased levels of sphingolipids upon impaired TORC2/Ypk1 signaling is also associated with increased levels of reactive oxygen species (ROS) [27], which impacts mitochondrial activity and, potentially, iron homeostasis. Additional studies have reported connections between iron and sphingolipids, including a role for sphingolipids in iron toxicity [28], as well as influencing survival in stationary phase [29].

We demonstrated previously that TORC2-Ypk1 is required as a positive regulator of autophagy that is induced when iron is limiting. In this context, the autophagy machinery is only induced when TOR2/YPK1 is active, suggesting that these proteins are required for the transmission of a signal for iron scarcity. We also demonstrated this response contributes to extend the chronological lifespan [30].

In mammals, it has been described that TOR regulates iron homeostasis through the modulation of iron transporters and cellular iron flux [31].

In this study, we show that TORC2/Ypk1 mediates the signal for iron deprivation to Aft1. This signal is independent of ROS accumulation, mitochondrial function or changes in Pse1 localization, the nuclear transporter of Aft1. We also present evidence that nuclear accumulation of Aft1 in response to iron deprivation requires appropriate levels of sphingolipids and that this is mediated by TORC2-Ypk1.

2. Material and Methods

2.1 Yeast strains and plasmids

Saccharomyces cerevisiae strains used in this study are listed in Table 1. New mutants described in this work were obtained by one-step disruption method that uses the NatMx4 or KanMx4 cassettes [30]. Strain GSL421 was constructed upon the integration of plasmid pAft1C291F-HA previously digested with EcoRV. GSL451 strain, was constructed upon the integration of pYpk1$^{S644A/T662A}$ plasmid previously digested by BstEII. Strains, GSL454 and GSL455 were constructed upon the integration of plasmid pYpk1-HA previously digested with BstEII. The plasmid pYpk1-HA was obtained upon Ypk1 cloning into the PmeI and NotI sites of the integrative vector pMM351. The plasmid pPse1GFP was obtained through Pse1 cloning into the BamHI and SalI sites of the pUG35 plasmid.

Table 1. Yeast strains.

Strain	Genotype	Source
CML128	*MAT**a** leu2-3,112, ura3-52, trp1, his4*	[32]
GSL034	CML128 background, *tor1::KanMx4*	[33]
GSL190	CML128 background, *slt2::KanMx4*	[34]
GSL205	CML128 background, *sch9::NatMx4*	[34]
GSL280	CML128 background, *tetO$_7$AFT1C291F-HA::LEU2*	[35]
GSL308	CML128 background, *tetO$_7$Aft1-HA::LEU2*	[35]
GSL384	CML128 background, *ypk1::KanMx4*	[30]
GSL385	CML128 background, *ypk1::KanMx4 tetO$_7$Aft1-HA::LEU2*	[35]
GSL410	CML128 background, *pkc1::LEU2*	[36]
GSL420	CML128 background, *ypk1::KanMx4 atg7::NatMx4*	This work
GSL421	CML128 background, *ypk1::KanMx4 tetO$_7$AFT1C291F-HA::LEU2*	This work
GSL430	CML128 background, *lac1::KanMx4*	This work
GSL431	CML128 background, *lag1::KanMx4*	This work
GSL435	CML128 background, *fet3::KanMx4*	This work
GSL436	CML128 background, *ccc1::KanMx4*	This work
GSL437	CML128 background, *mrs3::KanMx4*	This work
GSL447	CML128 background, *fet5::KanMx4*	This work
GSL448	CML128 background, *atm1::KanMx4*	This work
GSL451	CML128 background, *ypk1::KanMx4 YPK1S644AT662A-HA::LEU2*	This work
GSL454	CML128 background, *Ypk1-HA::LEU2*	This work
GSL455	CML128 background, *ypk1::KanMx4 Ypk1-HA::LEU2*	This work
R43	CML128 background, *rho0*	This work
BY4741	*MAT**a** his3-1, leu2, met15, ura3*	[37]
GSL404	BY4741 background, *ypk1::KanMx4*	This work
W303	*MAT**a** ade2-1, trp1-1, leu2-3,2-111, his3-11,75, ura3*	[38]
GSL417	W303 background, *tor2ts::LEU2*	[39]
LHY291	*MAT**a** his3, trp1, lys2, ura3, leu2, bar1*	[23]

PLY979	LHY291 background, *cka2::TRP1*	[23]

Plasmid descriptions are listed in Table 2. Each particular ORF was amplified by PCR from genomic DNA and cloned in the specific plasmid.

Table 2. Plasmids employed.

Plasmid	Marker	Promoter	Epitope	Source
pAft1-GFP	URA3	MET25	GFP	[40]
ptetO_7Aft1-HA	LEU2	tetO_7	HA	[40]
pAft1C291F-HA	LEU2	tetO_7	HA	[35]
pFet3-LacZ	URA3	FET3		[41]
pUG35	URA3	MET25	GFP	[42]
pPse1-GFP	URA3	MET25	GFP	This work
pC-terminal3-HA	URA3	MET25	HA	[38]
pMM351	LEU2	ADH1	HA	[30]
pYpk1-HA	LEU2	ADH1	HA	This work
pYpk1$^{S644A/T662A}$	LEU2	ADH1	HA	[38]

2.2. Growth conditions and reagents

Yeasts were grown at 30ºC in SD medium (2% glucose, 0.67% yeast nitrogen base that lacked the corresponding amino acids for plasmid maintenance) plus amino acids [43]. For iron depletion conditions (SD-Fe) SD medium was used whose yeast nitrogen base was free of iron plus the addition of 80 μM of 4,7-diphenyl-1,10-phenanthrolinedisulfonic acid (BPS) (Sigma, 146617).

We present a list of reagents detailing final concentration in culture media and from which company they were purchased: N-Acetyl cysteine (NAC) 5mM (Sigma, A9165); Rapamycin (Rapa) 200 ng/ml (Sigma, R0395); Cycloheximide (CHX) 150 mg/ml (Sigma, C4859); DAPI 2 mg/ml (Sigma, D9541); (N-(3-triethylammoniumpropyl)-4-(p-diethylaminophenylhexatrienyl)) pyridinium dibromide (FM4-64) 30μg/μl (Invitrogen, T-3166); Myriocin (Myr) 2mM (Sigma, M1177); D-erythro-Dihydrosphingosine (DHS) 20 μM (Sigma, D3314); Aureobasidin A (Aur) 250 ng/ml (MedChem Express, HY-P1975). Cell cultures were exponentially grown at 600 nm [OD_{600}] of 0.6 or longer times as indicated. Iron was added as ammonium iron (III) Sulfate hexacahydrate [$NH_4Fe(SO_4)_2 \cdot 6H_2O$] (+Fe) (Sigma, F1543) at a final concentration of 10mM.

2.3. Endogenous iron measurements

Endogenous iron measurements were performed according to the colorimetric assay

described in [42].

2.4. ß-galactosidase activity

ß-galactosidase activity was determined according to [44], with some variations. 1 ml of cell culture at [O.D.$_{600}$] of 0.6 was centrifuged, and the pellets were suspended in 50 µl buffer Z (Na_2HPO_4 60 mM (Serva, 30200.01); NaH_2PO_4 40 mM (Serva, 13472-35-0); KCl 10 mM (Serva, 26868); $MgSO_4$ 1mM (Sigma, M7634-100G); ß-mercaptoethanol 50 mM (BioRad, 161-0710)) plus 2.5 µl sarcosyl 10% (Sigma, T4376) and 0.5 µl toluene (Merck, 244511). After that, 150 µl of buffer Z and 50 µl *o*-nitrophenyl-ß-D-galactopyranoside (ONPG) 4 mg/ml (Sigma, N1127) were added and subsequently incubated at 28ºC for 5 min. Finally, 500 µl Na_2CO_3 1 M (Sigma, S7795-500G) was added to stop the reaction. Absorbance was measured at 420 nm.

2.5. Protein extraction and immunoblot analyses

We follow an identical procedure as described in [45]. Total yeast protein extracts were prepared as previously described in [30]. The antibodies for western blotting were as follows: anti-HA 3F10 (Roche Applied Science, 12158167001), was used at a dilution of 1: 2,000 in 0.25% non-fat milk and the corresponding secondary was goat anti-Rat IgG horseradish peroxidase conjugate (Millipore, AP136P). Anti-Phospho-glycerate kinase 1 (anti-PGK-1) (Invitrogen, 459250) was used at a dilution 1: 1,200, with the secondary antibody anti-Mouse horseradish peroxidase conjugate (GE Healthcare, LNA931v/AG). Anti-phospho-Ypk1 (T662) (from Dr. Ted Powers) at a dilution of 1:20,000, with the secondary antibody anti-Rabbit horseradish peroxidase conjugate (GE Healthcare, LNA934v/AG). They were used as indicated by the manufacturers.

The protein-antibody complexes were visualized by enhanced chemiluminescence, using the Supersignal substrate (Pierce, 34577) in a Chemidoc (Roche Applied Science).

For all the figures: We used anti-PGK1 to detect PGK1, selected as loading control in the western blots shown in this study. For western blot in this paper, we have selected representative samples.

2.6. Fluorescence microscopy

Cells were visualized under the Fluorescence microscope (Olympus BX-51) using 60X magnification. Cellular localizations were registered at the times indicated in the text

under specific described conditions.

2.7. Statistical analysis

We followed the same procedure as described in [30]. Error bars in the histograms represent the standard deviation (SD) calculated from three independent experiments. Significance of the data was determined by *P*-values from a Student's unpaired t-test denoted as follows: *=0.05>P>0.01; **=0.01>P>0.001; ***=0.001>P>0.0001; ****=P>0.0001.

3. Results

3.1. TORC2 and Ypk1 are required for optimal Aft1 activity during iron starvation

In a previous study, we demonstrated a requirement for TORC2-Ypk1 signaling to induce autophagy under conditions of iron deficiency. This observation made us explore the potential connection between TORC2-Ypk1 and Aft1 during iron starvation. We first used a previously characterized temperature sensitive allele of TOR2 (*tor2ts*) an essential and central component of TORC2 [39]. We studied the role of Aft1, a transcription factor that regulates iron homeostasis, by examining its cellular localization, the expression of one of its reporter genes (FET3), and the levels of intracellular iron in response to varying iron concentrations. We found that when iron was deprived, in the *tor2ts* strain, Aft1 was barely present in the nuclei, with most of the protein scattered throughout the cytoplasm or concentrated in vacuoles (Figure 1A and B). This was in contrast to what was observed in the wild type (wt) cell culture, where Aft1 rapidly translocated to the nucleus in response to low iron levels (Figure 1A and B). These findings correlated with expression of FET3 and iron accumulation under iron starvation conditions. In the *tor2ts* strain, both of these parameters were significantly lower than those observed in wt cells due to impaired induction of the iron regulon and internalization of iron (Figure 1C and D). These results suggest that TORC2 plays a role in linking iron deficiency to the function of Aft1.

Figure 1

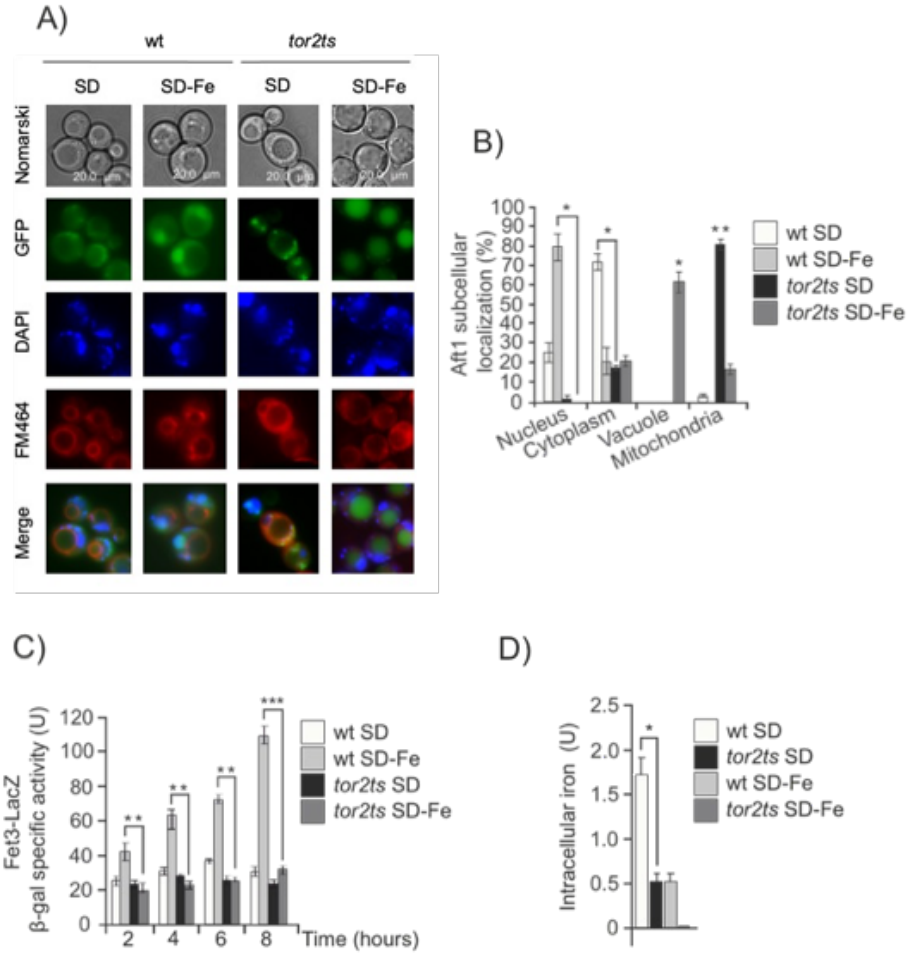

Figure 1. TORC2 regulates iron starvation signal. **(A)** wt and *tor2ts* cultures transformed with pAft1GFP, were grown to log phase in SD and SD-Fe medium at 38ºC. Aliquots were collected for *in vivo* observation in the fluorescence microscope. **(B)** Histogram of Aft1 localization quantified in the experiment described in **(A)** was calculated upon microscopic observation of 1000 cells. **(C)** ß-galactosidase activity content determination in wt and *tor2ts* strains. Cells were grown at 30ºC in SD media to OD_{600}:0.4. Aliquots were taken, washed and transferred to SD or SD-Fe media at 38ºC for 8 hours. Samples were taken every two hours to determine the ß-galactosidase activity reporter construct. **(D)** Intracellular iron content was determined in wt and *tor2ts* exponential cultures grown in SD or SD-Fe media at 38ºC as described under

Material and Methods.

For all the figures: Error bars in the histograms represent the standard deviation (SD) calculated from 3 independent experiments. Significance of the data was determined by P-values from a Student unpaired t-test denoted as follows: *=0,05>P>0,01; **=0,01>P>0,001; ***=0,001>P>0,0001; ****=P>0,0001

TORC2 phosphorylates and activates Ypk1, leading to many downstream signaling events, including crosstalk to Pkc1 and Sch9 kinases [47]. To map the iron starvation signal from TORC2-Ypk1 to Aft1, we analyzed the potential involvement of Pkc1/Slt2 kinases whose activation depends on TORC2. None of them shown any difference in Aft1 behavior as compared to the wt strain in response to iron starvation (Figure 2A). Therefore, the potential role that Pkc1/Slt2 kinases could play in Aft1 nuclear translocation upon iron starvation was ruled out.

Given that in a recent paper, we described a genetic relationship between Tor2/Ypk1 and Tor1, in the context of iron deprivation and induction of autophagy [29]. We decided to rule out the possible role of Tor1 and one of its effectors Sch9 [47] also involved in sphingolipids regulation [25], in Aft1 cellular localization when iron is scarce. Our results indicate that neither Tor1 nor Sch9 are involved in this signaling process since neither the absence of Tor1 nor rapamycin treatment affected Aft1 nuclear localization in response to iron depletion (Figure 2B).

Figure 2

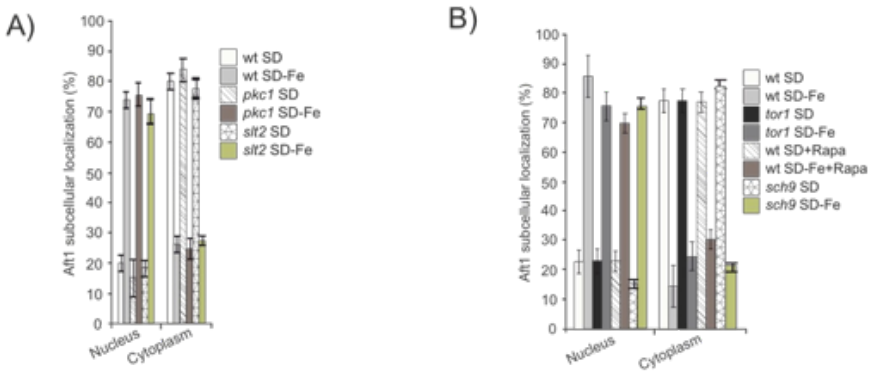

Figure 2. TORC1, Sch9, Pkc1 and Slt2 are not involved in Aft1 nuclear localization. Cultures were grown in SD or SD-Fe to exponential phase at 30ºC. Samples were collected to elucidate Aft1 subcellular localization. **(A)** wt*, pkc1* and *slt2* strains transformed with pAft1GFP. **(B)** wt, *tor1, sch9* and wt treated with Rapamycin for 2 hours (Rapa) bearing pAft1GFP.

3.2. Neither oxidative stress, mitochondrial function, iron compartmentalization nor Pse1 nuclear transporter are signals to drive Aft1 localization in ypk1 cells depleted for iron

In order to check whether the observed aberrant Aft1 localization in *ypk1* mutant was an indirect consequence of either oxidative stress or mitochondrial dysfunction caused by iron deprivation [46] we added the antioxidant N-acetylcisteine (NAC) to both *ypk1* and wt cultures and observed equivalent results as those obtained in the absence of the antioxidant (Figure 3A). We also used a *rho0* strain, deficient in mitochondrial DNA, and upon iron deprivation Aft1 localized to the nuclei as described for wild type cells (Figure 3B). These results lead us to conclude that Aft1 miss-localization in iron starved *ypk1* mutant cells was not a consequence of oxidative stress nor of mitochondrial dysfunction.

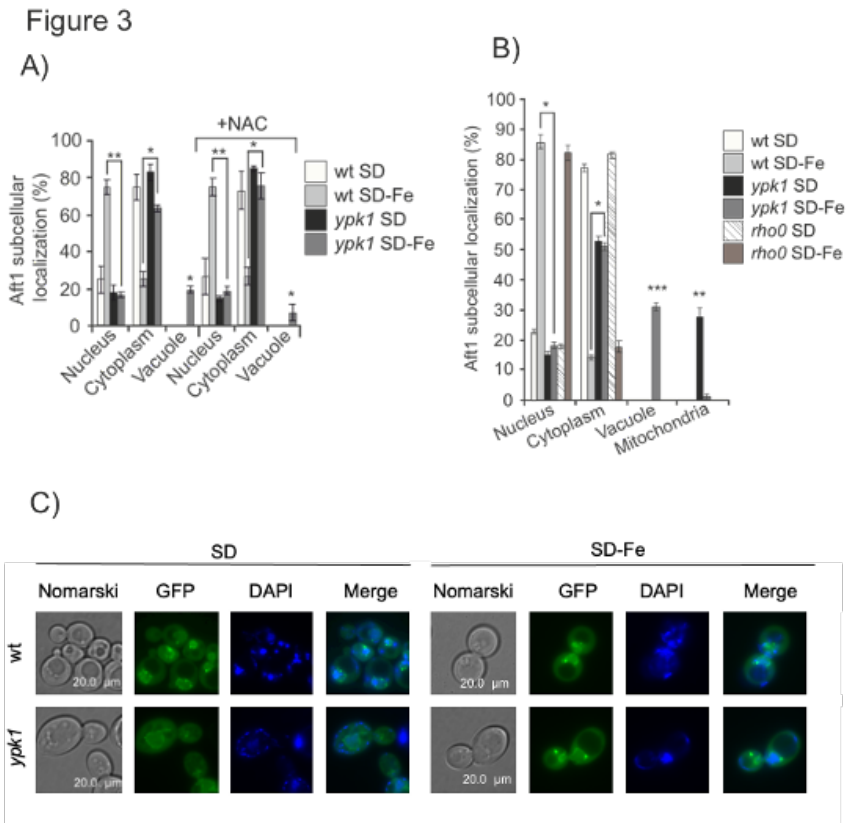

Figure 3. Aft1 miss localization in iron starved *ypk1* mutant cells was not due to oxidative stress or mitochondrial dysfunction**. (A)** wt and *ypk1* cells expressing pAft1GFP were exponentially grown in SD or SD-Fe media with or without NAC overnight. Aliquots were collected for microscopic observation. The histogram represents percentages of *in vivo* Aft1 localization. **(B)** Aft1 subcellular localization in wt, *ypk1* and *rho0* strains grown in the same conditions as Figure 1A. **(C)** wt and *ypk1* mutant expressing pPse1GFP were grown to log phase (OD_{600}:0.6) in SD or SD-Fe medium at 30ºC. Microscopic images represent Pse1 intracellular localization.

Pse1 is the only known transporter for Aft1 which mediates its translocation from the cytoplasm to the nucleus upon iron starvation [13]. We wondered whether in the absence of Ypk1, Pse1 was precluding Aft1 nuclear localization upon iron deprivation. Pse1 was localized to the nuclear envelope (Figure 3C), independently on the presence or absence of Ypk1, both in iron depleted cells or upon iron replenishment.

In conclusion, Pse1 is not involved in Aft1 localization in *ypk1* mutant cells in response to iron starvation.

We also considered the possibility that the signal to Aft1 nuclear localization in response to iron starvation could be originated in one of the cellular compartments where iron is stored. This would imply that one specific iron transporter would be conditioning the cellular signaling to Aft1. In order to analyze this, we made different mutants in each of the known iron transporters: Fet3: plasmatic membrane iron importer; Ccc1: vacuolar iron importer; Fet5: iron exporter from the vacuole; Mrs3: mitochondrial iron importer; Atm1: mitochondrial exporter of iron-sulfur clusters. Aft1 localization in all the mutants tested was equivalent to that determined in wt cells growing in SD-Fe (Figure 4). These observations lead us to conclude that iron accumulation in specific cellular compartments is not the main signal that determines Aft1 translocation to the nucleus when iron is limited.

Figure 4

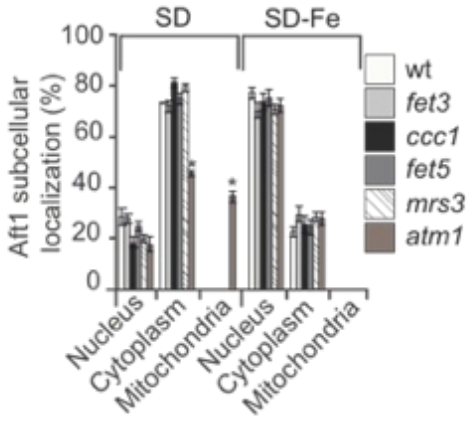

Figure 4. Iron accumulation in organelles do not determine Aft1 localization upon iron depletion. wt, *fet3, ccc1, fet5, mrs3* and *atm1* mutants were transformed with pAft1GFP and grown to log phase in SD or SD-Fe media with amino acids at 30ºC. Samples were collected for *in vivo* observation in the fluorescence microscope.

3.3. Lack of YPK1 prevents Aft1 nuclear translocation in the absence of iron

Ypk1 is phosphorylated and regulated by TORC2 in two specific residues (see review [47]). We wondered whether Ypk1 was involved in the process of sensing iron starvation downstream of Tor2. Upon iron depletion, we could observe a similar but less dramatic phenotype than that shown above for *tor2ts* mutant (Figure 1A-D). Aft1 mostly remained in the cytoplasm or partly in the vacuole, (Figure 5A). This localization correlated to the detection of both a very low iron intracellular content and significantly reduced Fet3 expression in iron deprived *ypk1* cultures, as compared to wt cultures (Figure 5B and C).

Figure 5

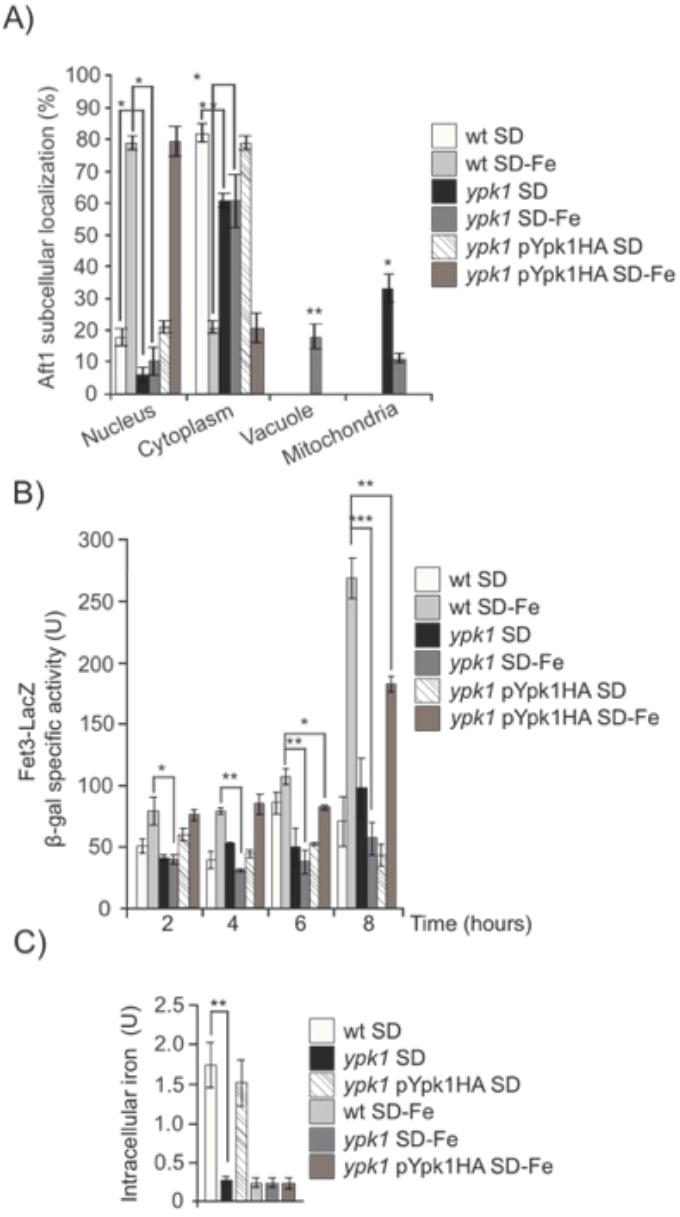
A)
Aft1 subcellular localization (%)
100
90
80
70
60
50
40
30
20
10
0
Nucleus
Cytoplasm
Vacuole
Mitochondria
wt SD
wt SD-Fe
ypk1 SD
ypk1 SD-Fe
ypk1 pYpk1HA SD
ypk1 pYpk1HA SD-Fe
B)
Fet3-LacZ
β-gal specific activity (U)
300
250
200
150
100
50
0
2
4
6
8
Time (hours)
wt SD
wt SD-Fe
ypk1 SD
ypk1 SD-Fe
ypk1 pYpk1HA SD
ypk1 pYpk1HA SD-Fe
C)
Intracellular iron (U)
2.5
2.0
1.5
1.0
0.5
0
wt SD
ypk1 SD
ypk1 pYpk1HA SD
wt SD-Fe
ypk1 SD-Fe
ypk1 pYpk1HA SD-Fe

D)

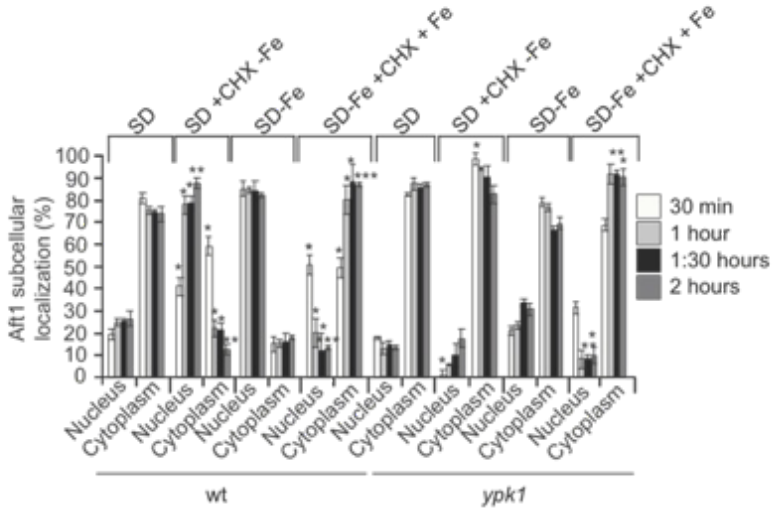

Figure 5. The absence of Ypk1 causes deregulation of the Aft1 dependent iron regulon, during iron starvation. **(A)** wt, *ypk1* and *ypk1* pYpk1HA transformed with the plasmid pAft1GFP, were logarithmically grown in SD medium plus amino acids or in iron-free SD (SD-Fe) to be observed in fluorescence microscopy. The histogram represents percentages of *in vivo* nuclear, cytoplasmic, vacuolar or mitochondrial localization out of 1000 cells. **(B)** Strains wt, *ypk1* and *ypk1*+pYpk1HA were each transformed with plasmid p*FET3*-LacZ. Cells were grown at 30ºC in SD media to OD_{600}:0.4. Aliquots were taken washed and transferred to SD or SD-Fe media for 8 hours. Samples were taken every two hours to determine the ß-galactosidase activity reporter construct. **(C)** Intracellular iron content was determined in wt, *ypk1* and *ypk1*+pYpk1HA exponential cultures grown in SD or SD-Fe media as described under Material and Methods. **(D)** *In vivo* fluorescence observation at indicated times of wt and *ypk1* strains bearing pAft1GFP. Cells were grown in SD or SD-Fe media until exponential phase, cultures were divided, cycloheximide (+CHX) was added before to both of them. The SD ones were washed and transferred to a media without iron with CHX; and iron (+Fe) were added to SD-Fe+CHX cultures.

Commented [LMM1]: Aqui no he puesto el + que dice Nuria porque es integrative y cuando hablamos me dijiste que en los inegrativos no se ponia el + que los quitamos también de la tabla de material y métodos

In order to discard any artifact caused by the mechanical process of *ypk1* construct, we decided to check the specificity of *YPK1 f*unction in the response to iron starvation by means of a complementation assay. We transformed *ypk1* mutant cells with a plasmid overexpressing Ypk1 and observed a clear complementation given that Aft1 both localization and function were equivalent to that observed in wt cells and

confirming the hypothesis that Ypk1 plays a direct role in the cellular response to iron deprivation (Figure 5A-C). In order to observe the actual localization of the recently synthetized protein, we blocked protein synthesis in both wt and *aft1* strains with cycloheximide. This assay reinforced our former hypothesis, since we obtained identical results regarding Aft1 localization in both wt and *ypk1* strains (Figure 5A), and also allowed us to conclude that Ypk1 was not involved in iron replenishment since in this condition Aft1 translocated from the nucleus to the cytoplasm in both wt and *ypk1* cultures (Figure 5D). Given the relevance of our results, we validated them in a different genetic background (Supplemental 1). Therefore, our results suggest that in conditions of iron starvation, the absence of Ypk1 precludes Aft1 translocation to the nucleus and consequently seriously impairs the induction of the iron regulon in response to the low levels of the metal.

Tor2 activates Ypk1 upon phosphorylation in two residues: S644 and T662 [16, 20]. In order to biochemically characterize this function, we made use of an antibody that specifically recognizes both phosphorylated residues and analyzed Ypk1 phosphorylation Tor2 specific in wild type cells starved or not for iron. We did not detect significant differences (Figure 6A) being Ypk1 constitutively phosphorylated by Tor2 during exponential growth in both conditions. Our results strongly suggest that cells actually require a constitutively activated Tor2-Ypk1 pathway in order to signal Aft1 correct response to iron availability. In order to gain further insight into this mechanism, we used a complementation approach by transforming *ypk1* mutant with a plasmid bearing the wild type *YPK1* coding sequence and another plasmid mutated in both S644A/T662A *YPK1* residues specifically phosphorylated by TORC2. Upon analyzing the results, we noted that whereas the plasmid bearing wild type *YPK1* ORF completely complemented *ypk1* strain, regarding Aft1 function in response to iron deprivation, the plasmid carrying pYpk1$^{S644A/T662A}$, was not able to complement a *ypk1* mutant under the above mentioned nutritional conditions (Figure 5A-C and 6B-D). Our results strongly suggest that Tor2 signals iron scarcity through Ypk1 to Aft1 function.

Figure 6

A)

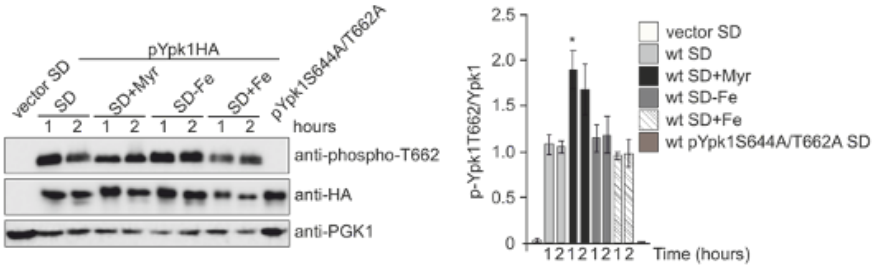
vector SD
pYpk1HA
SD
SD+Myr
SD-Fe
SD+Fe
pYpk1S644A/T662A
1 2 1 2 1 2 1 2
hours
anti-phospho-T662
anti-HA
anti-PGK1
p-Ypk1T662/Ypk1
2.5
2.0
1.5
1.0
0.5
0
1 2 1 2 1 2 1 2
Time (hours)
vector SD
wt SD
wt SD+Myr
wt SD-Fe
wt SD+Fe
wt pYpk1S644A/T662A SD

B)

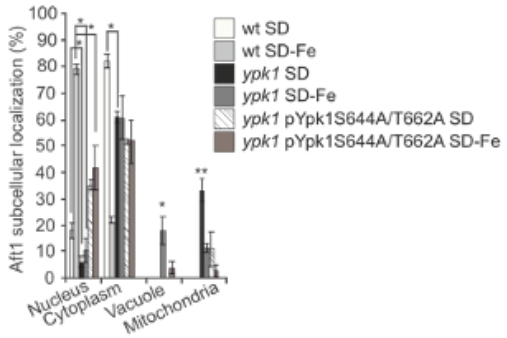
Aft1 subcellular localization (%)
100
90
80
70
60
50
40
30
20
10
0
Nucleus
Cytoplasm
Vacuole
Mitochondria
wt SD
wt SD-Fe
ypk1 SD
ypk1 SD-Fe
ypk1 pYpk1S644A/T662A SD
ypk1 pYpk1S644A/T662A SD-Fe

C)

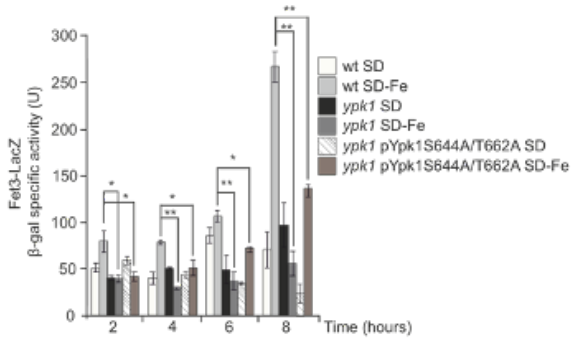
Fet3-LacZ
β-gal specific activity (U)
300
250
200
150
100
50
0
2
4
6
8
Time (hours)
wt SD
wt SD-Fe
ypk1 SD
ypk1 SD-Fe
ypk1 pYpk1S644A/T662A SD
ypk1 pYpk1S644A/T662A SD-Fe

D)

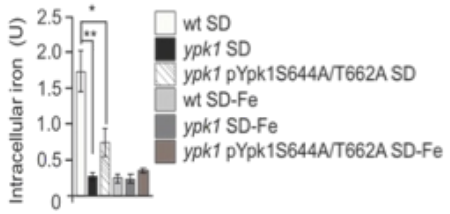

Figure 6. Ypk1 specific phosphorylation by TORC2 regulates the cellular response to iron starvation. **(A)** wt strain was transformed with pC-terminal3-HA (vector), pYpk1HA or pYpk1$^{S644A/T662A}$. Cells were grown in SD to exponential phase, the cultures were washed and transferred to SD, SD+Myr, SD-Fe or SD+Fe. Samples were collected at indicated times for western blot analysis, probing with anti-phospho-T662, anti-HA and anti-PGK1 antibodies. The histogram represents the ratio between Ypk1 phospho-T662 and total Ypk1. **(B)** wt, *ypk1* and *ypk1* pYpk1$^{S644A/T662A}$, strains transformed with the plasmids pAft1GFP were logarithmically grown in SD medium plus amino acids or in iron-free SD (SD-Fe) to be observed in fluorescence microscopy. The histogram represents percentages of *in vivo* nuclear, cytoplasmic, vacuolar or mitochondrial localization out of 1000 cells and **(C)** ß-galactosidase activity of wt, *ypk1* and *ypk1*+pYpk1$^{S644A/T662A}$ strains. Aliquots were collected as described in Figure 5B. **(D)** intracellular iron was assed as in Figure 5C .

3.4. Complex LCBs levels control Aft1 nuclear localization and function when iron is limited

Ypk1 kinase activity controls sphingolipids homeostasis upon TORC2 regulation. We decided to investigate downstream members of the pathway with the aim to identify at which level of the sphingolipid pathway the signal diverges to regulate Aft1 localization in response to iron concentration. Hence, we treated wild type iron depleted cultures with myriocin, which is a very potent inhibitor of serine palmitoyltransferase, that catalyzes the conversion into 3-ketodihydrosphingosine, the first step in sphingosine biosynthesis. We observed a high proportion of Aft1 in the cytoplasm and vacuole correlated to a significant descent both in *FET3* expression and iron content (Figures 7A-C).

Figure 7

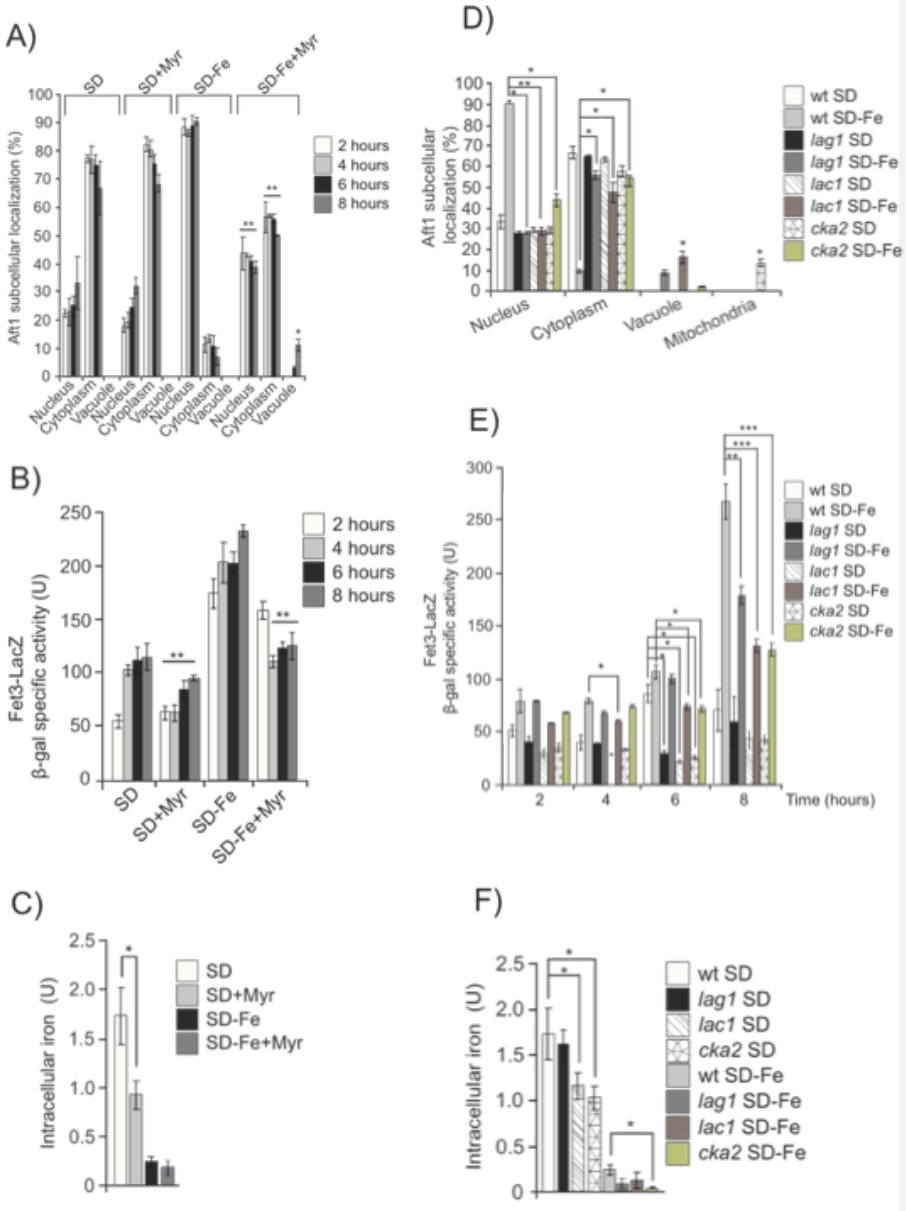
A)
SD
SD+Myr
SD-Fe
SD-Fe+Myr
Aft1 subcellular localization (%)
2 hours
4 hours
6 hours
8 hours
Nucleus
Cytoplasm
Vacuole
D)
Aft1 subcellular localization (%)
wt SD
wt SD-Fe
lag1 SD
lag1 SD-Fe
lac1 SD
lac1 SD-Fe
cka2 SD
cka2 SD-Fe
Nucleus
Cytoplasm
Vacuole
Mitochondria
B)
Fet3-LacZ β-gal specific activity (U)
2 hours
4 hours
6 hours
8 hours
SD
SD+Myr
SD-Fe
SD-Fe+Myr
E)
Fet3-LacZ β-gal specific activity (U)
wt SD
wt SD-Fe
lag1 SD
lag1 SD-Fe
lac1 SD
lac1 SD-Fe
cka2 SD
cka2 SD-Fe
Time (hours)
C)
Intracellular iron (U)
SD
SD+Myr
SD-Fe
SD-Fe+Myr
F)
Intracellular iron (U)
wt SD
lag1 SD
lac1 SD
cka2 SD
wt SD-Fe
lag1 SD-Fe
lac1 SD-Fe
cka2 SD-Fe

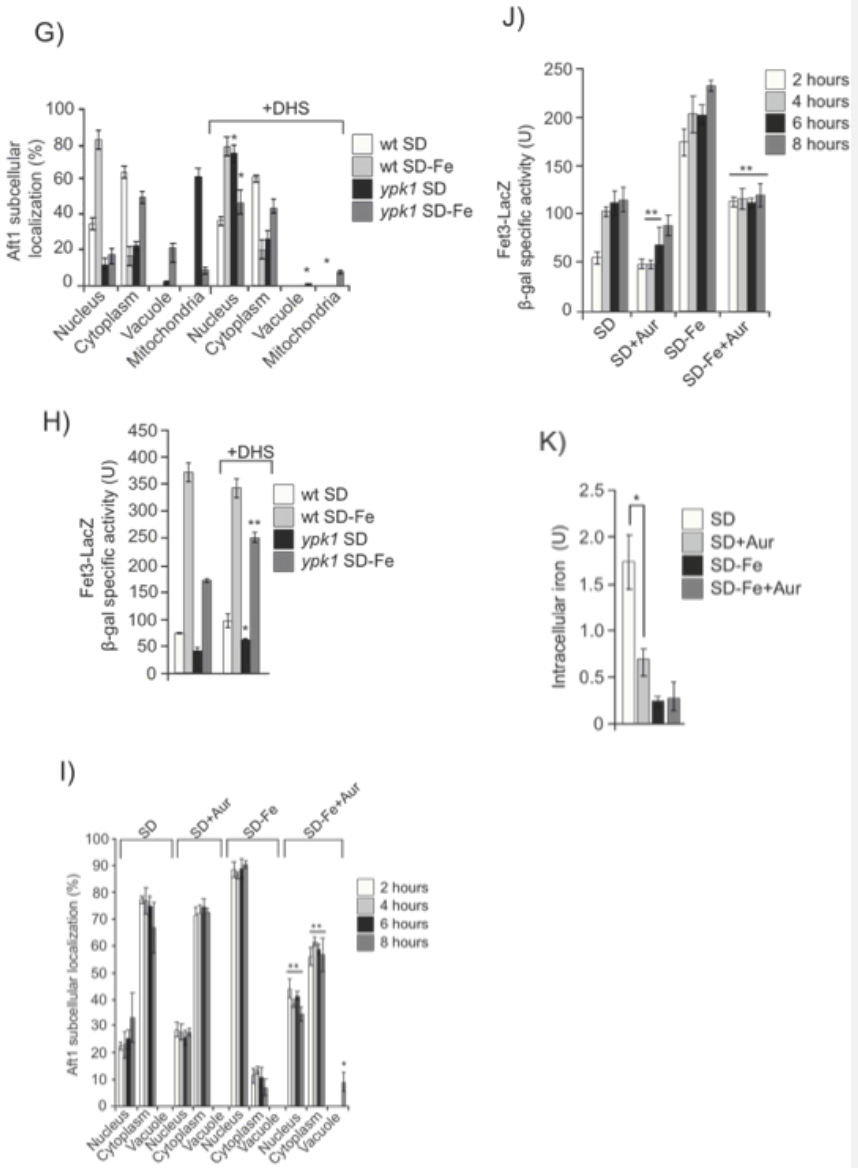

Figure 7. Sphingolipid metabolic pathway regulates Aft1 localization and function in iron starvation conditions. **(A)** wt strain transformed with pAft1GFP was grown either in SD or SD-Fe medium with amino acids and subsequently treated or not with Myriocin (Myr). Samples

were taken at the indicated times to analyze Aft1 subcellular localization **(B)** wt bearing p*FET3*-LacZ was grown in either SD or SD-Fe medium with amino acids and subsequently treated or not with Myriocin. Samples were taken at indicated times. **(C)** Intracellular iron content determined in wt cells exponentially grown either in SD or SD-Fe and treated or not with Myriocin. **D)** Aft1 subcellular localization in wt, *lac1, lag1* and *cka2* strains bearing pAft1GFP plasmid. **(E)** ß-galactosidase activity determined in exponentially growing cultures of each wt, *lac1, lag1* and *cka2* strains bearing p*FET3*-LacZ. **(F)** Intracellular iron content determined in wt, *lac1, lag1* and *cka2* strains. **(G)** Aft1 subcellular localization and **(H)** ß-galactosidase activity were analyzed in both wt or *ypk1* strains bearing each pAft1GFP or p*FET3*-LacZ plasmids. Cultures were exponentially grown either in SD or SD-Fe medium and treated or not with dihydrosphingosine (DHS)**. (I)** Aft1 subcellular localization in exponentially growing wt cells transformed with pAft1GFP, treated or not with Aureobasidin A (Aur). **(J)** wt strain transformed with p*FET3*-LacZ was exponentially grown either in SD or SD-Fe medium and treated or not with Aureobasidin A, samples were taken at the indicated times. **(K)** Intracellular iron content in wt cells exponentially grown either in SD or SD-Fe treated or not with Aureobasidin A.

Downstream in the sphingolipids pathway, dihydrosphingosine (DHS), is a ceramide precursor, since it can be converted to ceramide by ceramide synthase (CerS), which catalyzes the formation of an amide bond between the LCB and a C26 very long-chain fatty acid [24].

CerS activity is regulated by direct phosphorylation of the catalytic subunits, Lac1 and Lag1, through TORC1, TORC2, and casein kinase 2 [22,23]. We observed that blocking CerS activity upon deletion of either *LAC1* or *LAG1* genes, or their regulatory protein CK2, significantly impaired Aft1 function upon iron starvation, since a clear descent in Fet3 expression and in Aft1 nuclear localization were detected as compared to wild type values (Figure 7D-F). These results were similar to those previously described in cells treated with Myriocin (Figs 7A-C).

In order to test the importance of ceramide synthesis in the process of iron deficiency signaling, we added DHS to both wt and *ypk1* iron depleted cultures and allowed them grown over night to exponential phase. Interestingly, we could observe that addition of the precursor of ceramide to *ypk1* cultures partly restored Aft1 wild type response to iron starvation, since 35% of the cells contained Aft1 in the nucleus correlated to a significant increase in both *FET3* expression and cellular iron content, as compared to *ypk1* cultures not added for DHS (Figure 7G). All these results evidence that iron

starvation signal relies in ceramide synthesis.

Aureobasidin A is a cyclic depsipeptide which inhibits the inositolphosphorylceramide synthase, *AUR1,* downstream of ceramide synthesis, thus preventing the accumulation of long chain complex sphingolipids. Addition of Aureobasidin A to cultures depleted for iron also precluded Aft1 translocation into the nucleus and consequently negatively affected both *FET3* induction and iron intracellular accumulation (Figures 7H-K). Next, we also added DHS to wild type cells blocked in sphingolipid synthesis after a previous treatment with Myriocin. In this case and similarly to that described above in *ypk1* cultures, we observed that DHS was able to partly restore Aft1 function in response to iron starvation (Figure 8A). However, and contrary to the results recently described, DHS addition to iron deprived wt cultures treated with Aureobasidin A, did not restore Aft1 wild type function in response to iron starvation (Figure 8B). Taking altogether these results we conclude that the activity of the sphingolipid pathway leaded by TORC2 and *YPK1* to induce the synthesis of long chain sphingolipids, is the main signal converging in Aft1 and induces its nuclear translocation to activate the iron regulon in order to maintain iron homeostasis in response to iron deficiency.

Figure 8

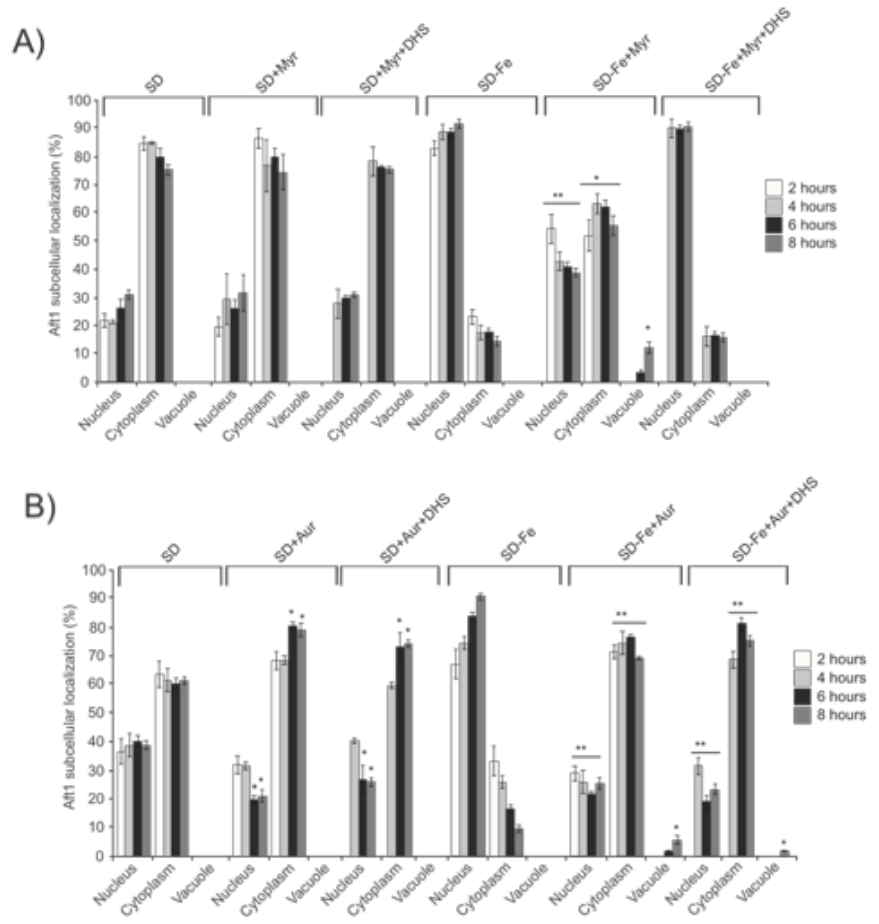

Figure 8. Complex sphingolipids signal Aft1 to localize to the nucleus upon iron depletion. wt cells expressing pAft1GFP were grown to OD_{600}:0.4 in SD medium at 30ºC. **(A)** Aliquots were taken, washed and transferred to either SD, SD+Myr, SD-Fe or SD-Fe+Myr media. After 2 hours, the cultures with myriocin (Myr) were divided in two halves and DHS was only added to one of them, the other half was maintained as a control. Samples were collected for *in vivo* observation in the fluorescence microscope, every two hours for eight hours. **(B)** Aliquots were taken, washed and transferred to SD, SD+Aur, SD-Fe or SD-Fe+Aur media. After 2 hours the cultures with aureobasidin A (Aur) were divided into two halves and DHS was only added to one of them. Samples were collected for *in vivo* observation in the fluorescence microscope at the indicated times.

4. Discussion

Iron is an essential metal for living organisms [48]. However, its excess can cause dramatic damage to cells mainly through oxidative reactions [49], whereas its deficiency is associated to several metabolic disorders [50], consequently, iron homeostasis must be tightly regulated in all living cells, part to hinder the potential damage that its dysregulation can provoke. In *Saccharomyces cerevisiae,* Aft1 is the main responsible for iron utilization and homeostasis. Its function has been associated to its transcriptional regulation correlated to its nuclear localization in order to maintain the correct equilibrium of the iron cellular requirements [11,39,51]. Grx3/Grx4 both regulate the translocation of Aft1 from the nucleus to the cytoplasm when iron is replenished [39]. However, when iron is depleted from the culture medium, Aft1 translocation from the cytoplasm to the nucleus has not been associated with any accompanying protein to date. Recently, we demonstrated that iron deprivation induces bulk autophagy in a manner completely dependent on Ypk1 and Tor1 [29]. Our next interest was to explore the potential connection between the iron homeostasis regulator Aft1 and Tor2/Ypk1 in the cellular response to iron starvation. Here, we show evidence demonstrating that Aft1 translocation to the nucleus in response to iron deprivation is dependent on TORC2/Ypk1 signaling pathway. Interestingly, preliminary and unpublished data from J. Thorner [16] support the conclusion that TORC2-Ypk1 signaling could be related to iron metabolism at least mechanistically. It has been widely demonstrated that TORC2 through Ypk1, positively signals the activation of the sphingolipid pathway in conditions unrestricted of nutrients [47]. Here, we demonstrate that iron deprivation determines Aft1 nuclear localization in a manner dependent on the activity of the sphingolipid synthesis through TORC2/Ypk1 signaling activity.

We also present evidence demonstrating that Aft1 miss-localization upon iron starvation, in a context of sphingolipid synthesis impairment, is not caused by a deficient expression of the nuclear import receptor Pse1, which remains localized in in the nuclear membrane regardless iron availability. Apart from Ypk1, Pkc1 is another target of TORC2 in the response to certain types of stress [18]. Our results clearly show that Pkc1 does not participate in the regulation of Aft1 nuclear translocation and the consequent induction of the iron regulon upon iron deprivation.

Sphingolipids are essential components of the cellular membranes that frequently

participate in several signaling processes in all the eukaryotic cellular systems [28]. In line with this, we explored the possibility that low iron concentration localized in specific cellular compartments could be the signal to direct Aft1 into the nucleus. Our results made us rule out this hypothesis since all the mutants in the various iron-dependent membrane transporters checked in this study presented a wild type Aft1 response upon iron deprivation.

Iron can promote the production of ceramides in humans [52] as previously shown in *Saccharomyces cerevisiae* [28]. The connection between sphingolipids and iron has also been reported [53] upon the demonstration that iron deprivation caused the induction of some sphingolipids. Other authors have described a relationship between ceramides and the modulation of iron levels [54]. In our study, we observe that sphingolipids are constitutively activated in wild type cells growing exponentially in conditions not limited for nutrients, independently of iron availability. As long as the sphingolipid pathway is active, iron depletion signal is correctly transmitted to Aft1 resulting in its translocation to the nucleus and the consequent induction of the iron regulon. A blockade in long-chain sphingolipids synthesis interrupts this signal and provokes a cytoplasmic/vacuolar Aft1 localization when iron is not available. This aberrant localization is detrimental for survival since forcing nuclear localization of Aft1 by using the pAft1C291F allele in a *ypk1* mutant significantly increased cell survival close to wild type levels (Supplemental 2), which clearly remarks the importance that sphingolipids signaling has in the response to iron deprivation.

In humans, the mTOR pathway can regulate expression of CD71, which is responsible for cellular iron uptake [55]. Indeed, it has been recently proposed that inhibition of mTOR could reduce iron accumulation and thus, lessens the neurodegenerative effects induced by this metal [55]. These observations are in accordance with our results in that Tor2 inhibition negatively converges in Aft1 reducing the expression of the iron regulon. Fet3 is the responsible for extracellular iron uptake in budding yeast and because is included in the iron regulon, its expression is drastically diminished upon Tor2 inhibition and the subsequent blockade of the sphingolipid pathway.

We have analyzed the sphingolipid pathway at various levels: i) upstream by blocking the kinase Ypk1, or using myriocin which blocks the activity of the palmitoiltranspherase and consequently the production of sphingosine, and ii) downstream in the signaling cascade, by inhibiting both ceramide and LCBs synthesis. Administration of DHS which promotes ceramides and consequently LCBs synthesis

complements the lack of signaling to Aft1 in iron starved cells when Tor2/Ypk1 are mutated (Figure 7G-H).

In this study we show evidences demonstrating that long-chain sphingolipids play a crucial role in the transmission of the iron starvation signal to Aft1, since addition of the precursor of ceramides (DHS), did not restore Aft1 wild type response to iron deprivation in cells blocked in the production of long-chain sphingolipids, upon Aureobasidin A treatment.

Several studies have demonstrated that Ypk1 is related to ROS production in a manner dependent on sphingolipids [27,~~46~~ 45]. Our findings rule out the possibility that sphingolipid downregulation caused by *YPK1* deletion in iron deprivation conditions, impinges on Aft1 wild type response in a manner dependent on ROS production or mitochondrial function.

Recently, Jordà et. al. [56] have published that sterol synthesis impairment precludes Aft1 function. Although Ypk1 has been suggested to be an ergosterol sensor [57], subsequent studies discarded this connection and demonstrated the independence between ergosterol and Ypk1 activity [20].

In this study we also show the existence of a connection between Ypk1 and Tor2 for bulk autophagy regulation, since in a *tor2ts* mutant the deficiency in autophagy activation is equivalent to that determined in *ypk1* (not shown).

Our results offer a demonstration of the importance of the sphingolipid pathway mediated by TORC2/Ypk1 proteins in the cellular response to iron scarcity in the context of iron homeostasis. In addition, our findings suggest that Aft1 not only regulates the expression of a group of genes needed for iron acquisition, detoxification or storage but also participates in remodeling the metabolism as previously proposed for different metalosensors in the eukaryotic model *Saccharomyces cerevisiae* [58]. Further studies will be required in order to ascertain the molecular mechanism involved in Aft1 regulation by long-chain sphingolipids as well as its potential role in vacuolar function.

Supplementary Materials: Figure S1. The absence of Ypk1 causes iron regulon deregulation during iron starvation. Figure S2. Aft1 nuclear localization is a prosurvival strategy to sphingolipids pathway impairment.

Author Contributions: Conceptualization, MA.T, T.P; Methodology, MA.T, N.P, S.M;

Software, MA.T, N.P, S.M; Validation MA.T, N.P, S.M; Formal Analysis S.M, MA.T; Investigation, MA.T, S.M; Resources, MA.T, T.P; Data Curation, S.M, MA.T; Writing-Original Draft Preparation, MA.T; Writing-Review & Editing, S.M, T.P, MA.T; Visualization, MA.T, N.P, S.M; Supervision, MA.T, T.P; Project Administration, MA.T; Funding Acquisition, MA.T.

Funding: The research described in this publication was partly supported by the Plan Nacional de I+D+I of the Spanish Ministry of Economy, Industry and Competitiveness (BIO2017-87828-C2-2-P) and . Sandra Montellà is currently funded by a fellowship from the Institut de Recerca Biomèdica de Lleida.

Acknowledgments: We thank Dr. T. Powers for discussions and for comments on the manuscript.

Conflicts of Interest: The authors declare no conflict of interest.

References

1. Outten CE, Albetel A-N. Iron Sensing and Regulation in Saccharomyces cerevisiae: Ironing Out the Mechanistic Details. Curr Opin Microbiol. **2013**;16(6):662-8.
2. Bogdan AR, Miyazawa M, Hashimoto K, Tsuji Y. Regulators of Iron Homeostasis: New Players in Metabolism, Cell Death, and Disease. Trends Biochem Sci. **2016**;41(3):274–86.
3. Eid R, Arab NTT, Greenwood MT. Iron mediated toxicity and programmed cell death: A review and a re-examination of existing paradigms. Biochim Biophys Acta - Mol Cell Res. **2017**;1864(2):399–430.
4. Ramos-Alonso L, Romero AM, Martínez-Pastor MT, Puig S. Iron Regulatory Mechanisms in Saccharomyces cerevisiae. Front Microbiol. **2020**;11:2222.
5. Carmona-Gutierrez D, Bauer MA, Zimmermann A, Aguilera A, Austriaco N, Ayscough K, et al. Guidelines and recommendations on yeast cell death nomenclature. Microb Cell. **2018**;5(1):4–31.
6. Percy L, Mansour D, Fraser I. Iron deficiency and iron deficiency anaemia in women. Best Pract Res Clin Obstet Gynaecol. **2017**;40:55–67.
7. Askwith C, Eide D, Van Ho A, Bernard PS, Li L, Davis-Kaplan S, et al. The FET3 gene of S. cerevisiae encodes a multicopper oxidase required for ferrous iron uptake. Cell. **1994**;76(2):403–10.
8. Stearman R, Yuan DS, Yamaguchi-Iwai Y, Klausner RD, Dancis A. A permease-oxidase complex involved in high-affinity iron uptake in yeast. Science. **1996**;271(5255):1552–7.
9. Dancis A. Genetic analysis of iron uptake in the yeast Saccharomyces cerevisiae. J Pediatr. **1998**;132(3 Pt 2):S24-9.
10. Shakoury-Elizeh M, Tiedeman J, Rashford J, Ferea T, Demeter J, Garcia E, et al. Transcriptional Remodeling in Response to Iron Deprivation in

Saccharomyces cerevisiae. Mol Biol Cell. **2004**;15(3):1233–43.
11. Yamaguchi-Iwai Y, Stearman R, Dancis A, Klausner RD. Iron-regulated DNA binding by the AFT1 protein controls the iron regulon in yeast. EMBO J. **1996**;15(13):3377–84.
12. Ueta R, Fujiwara N, Iwai K, Yamaguchi-Iwai Y. Mechanism Underlying the Iron-dependent Nuclear Export of the Iron-responsive Transcription Factor Aft1p in Saccharomyces cerevisiae. Mol Biol Cell. **2007**;18(8):2980.
13. Ueta R, Fukunaka A, Yamaguchi-Iwai Y. Pse1p mediates the nuclear import of the iron-responsive transcription factor Aft1p in Saccharomyces cerevisiae. J Biol Chem. **2003**;278(50):50120–7.
14. Saxton RA, Sabatini DM. mTOR Signaling in Growth, Metabolism, and Disease. Cell. **2017**;168(6):960–76.
15. González A, Hall MN. Nutrient sensing and TOR signaling in yeast and mammals. EMBO J. **2017**;36(4):397–408.
16. Leskoske KL, Roelants FM, Marshall MNM, Hill JM, Thorner J. The Stress-Sensing TORC2 Complex Activates Yeast AGC-Family Protein Kinase Ypk1 at Multiple Novel Sites. Genetics. **2017**;207(1):179–95.
17. Chen P, Lee KS, Levin DE. A pair of putative protein kinase genes (YPK1 and YPK2) is required for cell growth in Saccharomyces cerevisiae. Mol Gen Genet]. **1993**;236(2):443–7.
18. Levin DE, Fields FO, Kunisawa R, Bishop JM, Thorner J. A candidate protein kinase C gene, PKC1, is required for the S. cerevisiae cell cycle. Cell. **1990**;62(2):213–24.
19. Casamayor A, Torrance PD, Kobayashi T, Thorner J, Alessi DR. Functional counterparts of mammalian protein kinases PDK1 and SGK in budding yeast. Curr Biol. **1999**;9(4):186-S4.
20. Roelants FM, Breslow DK, Muir A, Weissman JS, Thorner J. Protein kinase Ypk1 phosphorylates regulatory proteins Orm1 and Orm2 to control sphingolipid homeostasis in Saccharomyces cerevisiae. Proc Natl Acad Sci USA. **2011**;108(48):19222–7.
21. Berchtold D, Piccolis M, Chiaruttini N, Riezman I, Riezman H, Roux A, et al. Plasma membrane stress induces relocalization of Slm proteins and activation of TORC2 to promote sphingolipid synthesis. Nat Cell Biol. **2012**;14(5):542–7.
22. Muir A, Ramachandran S, Roelants FM, Timmons G, Thorner J. TORC2-dependent protein kinase Ypk1 phosphorylates ceramide synthase to stimulate synthesis of complex sphingolipids. Elife. **2014**;3:e03779.
23. Fresques T, Niles B, Aronova S, Mogri H, Rakhshandehroo T, Powers T. Regulation of Ceramide Synthase by Casein Kinase 2-dependent Phosphorylation in Saccharomyces cerevisiae. **2015**;290(3):1395–403.
24. Megyeri M, Riezman H, Schuldiner M, Futerman AH. Making Sense of the Yeast Sphingolipid Pathway. J Mol Biol. **2016**;428(24 Pt A):4765–75.
25. Swinnen E, Wilms T, Idkowiak-Baldys J, Smets B, De Snijder P, Accardo S, et al. The protein kinase Sch9 is a key regulator of sphingolipid metabolism in Saccharomyces cerevisiae. Mol Biol Cell. **2014**;25(1):196–211.
26. Niles BJ, Joslin AC, Fresques T, Powers T. TOR Complex 2-Ypk1 Signaling Maintains Sphingolipid Homeostasis by Sensing and Regulating ROS Accumulation. CellReports. **2014;**6(3):541–52.
27. Lee YJ, Huang X, Kropat J, Henras A, Merchant SS, Dickson RC, et al. Sphingolipid Signaling Mediates Iron Toxicity. Cell Metab. **2012** Jul 3;16(1):90–6.

28. Lester RL, Withers BR, Schultz MA, Dickson RC. Iron, glucose and intrinsic factors alter sphingolipid composition as yeast cells enter stationary phase. Biochim Biophys Acta - Mol Cell Biol Lipids. **2013**;1831(4):726–36.
29. Montella-Manuel S, Pujol-Carrion N, Mechoud MA, de la Torre-Ruiz MA. Bulk autophagy induction and life extension is achieved when iron is the only limited nutrient in Saccharomyces cerevisiae. Biochem J. **2021**;478(4):811–37.
30. Bayeva M, Khechaduri A, Puig S, Chang HC, Patial S, Blackshear PJ, et al. mTOR Regulates Cellular Iron Homeostasis through Tristetraprolin. Cell Metab. **2012**;16(5):645–57.
31. Gallego C, Eloi G, Colomina N, Enrique H, Aldea M. The Cln3 cyclin is down-regulated by translational repression and degradation during the G1 arrest caused by nitrogen deprivation in budding yeast. EMBO J. **1997**;16(23):7196–206.
32. Petkova MI, Pujol-Carrion N, de la Torre-Ruiz MA. Signal flow between CWI/TOR and CWI/RAS in budding yeast under conditions of oxidative stress and glucose starvation. Commun Integr Biol. **2010**;3(6):555–7.
33. Sundaram V, Petkova MI, Pujol-Carrion N, Boada J, de la Torre-Ruiz MA. Tor1, Sch9 and PKA downregulation in quiescence rely on Mtl1 to preserve mitochondrial integrity and cell survival. Mol Microbiol. **2015**;97(1):93–109.
34. Pujol-Carrion N, Pavón-Vergés M, Arroyo J de la Torre-Ruiz MA. BBA - Molecular Cell Research. The MAPK Slt2 / Mpk1 plays a role in iron homeostasis through direct regulation of the transcription factor Aft1. **2021**;1868(5)118974.
35. Mitjana F V, Petkova MI, Pujol-carrion N, de la Torre-Ruiz MA. Pkc1 and actin polymerisation activities play a role in ribosomal gene repression associated with secretion impairment caused by oxidative stress. **2011**;11:(8)656–9.
36. Petkova MI, Pujol-Carrion N, de la Torre-Ruiz MA. Mtl1 O-mannosylation mediated by both Pmt1 and Pmt2 is important for cell survival under oxidative conditions and TOR blockade. Fungal Genet Biol. **2012**;49(11):903–14.
37. Niles BJ, Mogri H, Hill A, Vlahakis A, Powers T. Plasma membrane recruitment and activation of the AGC kinase Ypk1 is mediated by target of rapamycin complex 2 (TORC2) and its effector proteins Slm1 and Slm2. Proc Natl Acad Sci USA. **2012**;109(5):1536-41.
38. Costanzo M, Baryshnikova A, Bellay J, Kim Y, Spear ED, Sevier CS, et al. The Genetic Landscape of a Cell. **2010**;327(1):425–32.
39. Pujol-Carrion N, Belli G, Herrero E, Nogues A, de la Torre-Ruiz MA. Glutaredoxins Grx3 and Grx4 regulate nuclear localisation of Aft1 and the oxidative stress response in Saccharomyces cerevisiae. J Cell Sci. **2006**;119(21):4554–64.
40. ordà T, Rozèz N, Puig S. Sterol Composition Modulates the Response of Saccharomyces cerevisiae to Iron Deficiency. J fungi (Basel) **2021**;7(11):901.
41. Pujol-carrion N, Gonzalez-alfonso A, Puig S, Torre-ruiz MA De. Both human and soya bean ferritins highly improve the accumulation of bioavailable iron and contribute to extend the chronological life in budding yeast. Microb Biotechnol. **2022**;15(5)1525-1541.
42. Kaiser C, Michaelis S, Mitchell A. Methods in Yeast Genetics. Cold Spring Harbour Laboratory Press Ltd.; New York, NY, USA. **1994**; pp107–121. ISBN:0-87969-451-3.
43. Mónica A. Mechoud, Nuria Pujol-Carrion, Sandra Montella-Manuel MA de la T-R. Interactions of GMP with Human Glrx3 and with Saccharomyces cerevisiae Grx3 and Grx4 Converge in the Regulation of the Gcn2 Pathway. Am Soc

Microbiol. **2020**;86(14)e00221-20.
44. Montella-manuel S, Pujol-carrion N, Torre-ruiz MA De. The Cell Wall Integrity Receptor Mtl1 Contributes to Articulate Autophagic Responses When Glucose Availability Is Compromised. J Fungi. **2021**;7(11):903.
45. Niles BJ, Joslin AC, Fresques T, Powers T. TOR complex 2-Ypk1 signaling maintains sphingolipid homeostasis by sensing and regulating ROS accumulation. Cell Rep. **2014**;6(3):541–52.
46. Roelants FM, Leskoske KL, Marshall MNM, Locke MN, Thorner J. The TORC2-Dependent Signaling Network in the Yeast Saccharomyces cerevisiae. Biomolecules. **2017**;7(3):66.
47. Kaeberlein M, Westman E, Dang N, Kerr E, Powers III R, Steffen K, et al. Regulation of Yeast Replicative Life Span by TOR and Sch9 in Response to Nutrients. Science. **2005**;310(5751):1193–6.
48. Milto I V, Suhodolo I V, Prokopieva VD, Klimenteva TK. Molecular and Cellular Bases of Iron Metabolism in Humans. Biochem Biokhimiia. **2016**;81(6):549–64.
49. Toledano MB, Delaunay A, Biteau B, Spector D, Azevedo D. Oxidative stress responses in yeast. Yeast Stress Responses. Berlin, GB. **2003**; pp241–303. ISBN:978-3-540-45611-7.
50. Wallace DF. The Regulation of Iron Absorption and Homeostasis. Clin Biochem Rev. **2016**;37(2):51.
51. Ueta R, Fujiwara N, Iwai K, Yamaguchi-Iwai Y. Iron-induced dissociation of the Aft1p transcriptional regulator from target gene promoters is an initial event in iron-dependent gene suppression. Mol Cell Biol. **2012**;32(24):4998–5008.
52. Lane DJR, Merlot AM, Huang MLH, Bae DH, Jansson PJ, Sahni S, et al. Cellular iron uptake, trafficking and metabolism: Key molecules and mechanisms and their roles in disease. Biochim Biophys Acta - Mol Cell Res. **2015**;1853(5):1130–44.
53. Shakoury-Elizeh M, Protchenko O, Berger A, Cox J, Gable K, Dunn TM, et al. Metabolic response to iron deficiency in Saccharomyces cerevisiae. J Biol Chem. **2010**;285(19):14823–33.
54. Almeida T, Marques M, Mojzita D, Amorim MA, Silva RD, Almeida B, et al. Isc1p Plays a Key Role in Hydrogen Peroxide Resistance and Chronological Lifespan through Modulation of Iron Levels and Apoptosis. Mol Biol Cell. **2008**;19(3):865.
55. Jodeiri Farshbaf M, Ghaedi K. Does any drug to treat cancer target mTOR and iron hemostasis in neurodegenerative disorders? BioMetals. **2016**;30(1):1–16.
56. Jordá T, Rozès N, Puig S. Sterol composition modulates the response of saccharomyces cerevisiae to iron deficiency. J Fungi. **2021**;7(11):901.
57. Li X, Gianoulis TA, Yip KY, Gerstein M, Snyder M. Extensive In Vivo Metabolite-Protein Interactions Revealed by Large-Scale Systematic Analyses. Cell. **2010**;143(4):639–50.
58. Bird AJ. Metallosensors, the ups and downs of gene regulation. Adv Microb Physiol. **2008**;53:231–67.

5. DISCUSSIÓ GLOBAL DELS RESULTATS

5.1 Mecanismes de resposta de *S. cerevisiae* enfront del dèficit de ferro

L'estudi de l'expressió genètica i dels mecanismes de senyalització cel·lular que tenen lloc en les cèl·lules de llevat, exposades a dèficit de ferro, resulta una eina molt potent per entendre i buscar teràpies per poder tractar les malalties relacionades amb el dèficit de ferro. La manca de ferro biodisponible al medi obliga les cèl·lules a consumir el ferro que tenen emmagatzemat als seus reservoris; en el llevat, el vacúol és el principal reservori subcel·lular del ferro juntament amb les mitocòndries, i en mamífers ho són els lisosomes (L. Li and Ward 2018b), exhaurint així el ferro cel·lular, tal com es mostra en la *Figura Suplementària 1E de l'Article 1*. L'esgotament del ferro cel·lular, limita els processos cel·lulars que depenen d'aquest metall, cosa que es tradueix en una disminució de la seva taxa de divisió i creixement i en una davallada en el procés de fermentació de la glucosa en etanol com podem observar en la *Figura Suplementària 1A,C de l'Article 1 i* la *Figura 6A,B de l'Article 2*.

5.2 La limitació de ferro indueix la inhibició del complex 1 de TOR

L'adaptació transcripcional del llevat de gemmació al dèficit de ferro engloba 10 clústers genètics, entre ells s'estimula la transcripció del clústers genètics de l'homeòstasi del ferro i de resposta a estímuls externs (*Figura 2* i *3 de l'Article 1*). L'activació de la transcripció de gens que regulen la resposta a estímuls externs, com és la resposta general a l'estrès a través de Msn2/4 (*Figura 4B de l'Article 2*), demostra que la manca de ferro suposa un estrès cel·lular. Aquest mecanisme també s'activa enfront d'altres estressos com l'estrès tèrmic, estrès osmòtic i altres restriccions nutricionals com la del carboni (Gasch et al. 2000), demostrant la importància de l'homeòstasi del ferro pel funcionament normal de la cèl·lula i la seva supervivència. L'activitat de Msn2/4 és regulada per TORC1 a través de la seva fosforilació, impedint així, la seva localització nuclear i, per tant, l'activació de la transcripció dels gens de resposta general a estrès (Yuhua Wang et al. 2023). TORC1 també fosforila a Sch9, i el dèficit de ferro indueix la defosforilació de Sch9 (*Figura 5H de l'Article 1*), probablement en resposta a la inhibició de TORC1, fet que es tradueix en una menor expressió dels gens RP i RiBi, similar a la que s'obté amb els mutants *stb3* i *dot6tod6* (*Figura 5E,F de l'Article 1).* Sfp1, és

un altre factor transcripcional regulat per TORC1 i Sch9, involucrat en la regulació de l'expressió dels gens RP i RiBi. La inhibició de TORC1 indueix la defosforilació de Sch9, i impedeix que Sfp1 es localitzi al nucli, induint aixi la transcripció dels gens RP i RiBi (Wei and Zheng 2011). La

mancà de ferro, reté a Sfp1 al citoplasma (*Figura 5C,D de l'Article 1*), prova que demostra que la depleció de ferro inhibeix l'activitat de TORC1 i, a més, es correlaciona amb la davallada de l'expressió de gens RP i RiBi.

TORC1 promou la disminució dels nivells de síntesi de noves subunitats ribosomals, causant que alguns dels factors de biogènesi ribosomal quedin atrapats al nucli. Rrp12 és una d'aquestes proteïnes que es queden atrapades dins el nucli (Reiter et al. 2011). En el nostre estudi, la manca de ferro provoca que Rrp12 quedi atrapada dins el nucli (*Figura Suplementària 3 de l'Article 1*), avalant la inactivació de TORC1 en aquestes condicions. Altrament, Rrp12 interacciona físicament amb Pse1. Pse1 forma el canal d'import del factor transcripcional del reguló del ferro, Aft1 al nucli (Dosil 2011). Pse1 es localitza a la membrana nuclear, independentment de la quantitat de ferro cel·lular (*Figura 2C de l'Article 4*). Pse1 no només medià l'import d'Aft1 al nucli sinó també d'altres proteïnes com Yap1, Pdr1, Ste12 (Isoyama et al. 2001; Leslie et al. 2002; Delahodde et al. 2001). Rrp12/Pse1 participen en la internalització de proteïnes al nucli relacionades amb síntesi i reparació de DNA, com és el cas de la ribonucleòtid reductasa (RNR), Rnr4, proteïna limitant en la síntesi de dNTPs en el llevat (Voegtli et al. 2001). Rrn4 s'associa amb la subunitat petita Rnr2, en resposta a dany en el DNA, l'heterodímer Rnr2/Rnr4 surt del nucli de forma dependent de Mec1/Rad53/Dun1, per induir la producció de dNTPs (R. Yao et al. 2003). El ferro té un paper important en la reparació i transcripció del DNA (Puig et al. 2017). El fet que Rrp12 es localitzi al nucli en resposta a la depleció de ferro té un paper dual, bloquejant la formació de noves subunitats ribosomals, per tant, disminuint la ràtio de síntesi de proteïnes; i juntament amb Pse1, promovent la internalització de Rnr4 al nucli per a limitar la síntesi de dNTPs. Les RNR requereixen ferro per a la seva activitat (Sanvisens, de Llanos, and Puig 2013). El segrest de Rnr4 al nucli en absència de ferro impedeix la síntesi de dNTPs. Els baixos nivells de dNTPs, limiten la replicació i traducció del DNA, disminuint l'activitat de les polimerases, tal com passa després de la depleció del ferro, on els nivells de Rpc160, una subunitat de la RNA polimerasa III, disminueixen (resultats mostrats en l'article que es publicat en col·laboració amb els grups del Dr. Puig i Dr. Perez *Figura 6F de l'Article 1*).

La inhibició de TORC1, la disminució de la síntesi de proteïnes i de la transcripció de DNA, es correlacionen amb l'alentiment del creixement del llevat i la parada del cicle cel·lular del llevat que podem veure en la *Figura 6A,B del Article 2*. Característiques que poden indicar que les cèl·lules es troben en quiescència. La *Figura 6 de l'Article 2* demostra, segons els criteris que es recopilen per Sun i Gresham, que les cèl·lules de llevat que creixen en un medi amb dèficit de ferro, entren en fase de quiescència (S. Sun and Gresham 2021). L'entrada en quiescència permet a la cèl·lula adaptar-se a les condicions ambientals adverses per preservar la seva capacitat proliferativa durant llargs períodes de temps, fent front a l'envelliment cel·lular (Sagot and Laporte 2019). L'entrada en quiescència en resposta a la depleció de ferro li permet optimitzar l'ús de les seves reserves, entre altres coses, evitant que l'exhauriment de la glucosa indueixi la respiració cel·lular, un procés que requereix altes concentracions de ferro (X. Jin et al. 2021). Les cèl·lules que creixen sense ferro tenen un major índex de competència respiratòria i no presenten mutacions mitocondrials (*Figura 6E,F de l'Article 2)*, això es pot relacionar amb la parada metabòlica i possible davallada dels nivells respiratoris en resposta a llargues exposicions en un ambient sense ferro. La mancà de ferro, compromet la funció mitocondrial i producció d'ATP, alterant així el potencial de membrana mitocondrial, senyal que provoca l'activació de la ruta de senyalització RTG. En el clúster genètic número 4 s'observa que augmenta l'expressió dels gens *RTG* (*Figura 7A,B de l'Article 1).* La via RTG també es controla a través de TORC1; la inactivació de TORC1 indueix la localització nuclear del complex Rtg1/Rtg3, activant als seus gens diana (Komeili et al. 2000b). Alguns dels gens diana del complex Rtg1/Rtg3 són *CIT1, CIT2, IDH1, IDH2* i *ACO1,* la transcripció d'aquests incrementa en resposta a la depleció de ferro indicant l'activació de la ruta i indirectament la inactivació de TORC1 (*Figura 7 de l'Article 1).* La importància fisiològica de l'activació de la ruta RTG podria ser la de suplir els nivells de glutamat i glutamina, ja que la síntesi de glutamat requereix clústers Fe/S per a l'activitat del seu enzim Gltr1 (Shakoury-Elizeh et al. 2004).

El complex TORC1 és el que més contribueix a la regulació de la disponibilitat nutricional (González and Hall 2017b). Aquest treball demostra que la disminució dels nivells de ferro és censada per TORC1.

5.3 L'escassetat de ferro, com a única restricció nutricional activa l'autofàgia

En el present treball, descrit en l'Article 2, es demostra que en resposta a la depleció de ferro s'indueix l'activació de l'autofàgia a través de les vies de senyalització TORC2/Ypk1 i TORC1 (Figura 14). En cèl·lules de mamífer també s'ha detectat activació de l'autofàgia en resposta a la deficiència de ferro per ajudar a eliminar proteïnes danyades i reciclar els seus components, inclòs el ferro que contenen, però no es coneixen els mecanismes de senyalització que regulen aquest procés (H. Inoue et al. 2015). Tant l'autofàgia com les rutes de senyalització de TOR es troben conservades en els diferents organismes. Per tant, en futurs estudis s'haurà de comprovar si el mecanisme d'activació de l'autofàgia en condicions de depleció de ferro també es troba conservat. El comentari publicat per Kakhlon (Kakhlon 2021), un mes després de la publicació d'aquest mecanisme, avala la seva rellevància (Apèndix 1).

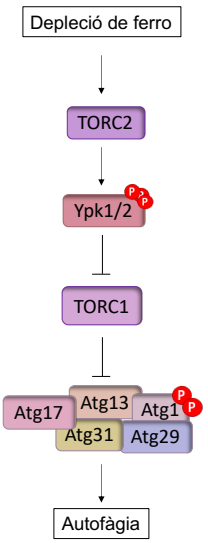

Figura 14. Mecanisme d'activació de l'autofàgia en resposta a la depleció de ferro. El senyal de la manca de ferro es transmet a través de TORC2/Ypk1 per inhibir al complex 1 de TOR. La inhibició de l'activitat de TORC1 permet la defosforilació d'Atg13 i la formació del complex Atg1, estimulant la inducció de l'autofàgia.

TOR2 és un gen essencial, fet que dificulta la seva manipulació. Per això en aquest article, treballem amb el mutant *ypk1* per estudiar aquesta ruta de senyalització. Anteriorment a aquest treball, el grup dirigit pel Dr. Ted Powers de la Universitat de Davis, California, va publicar que l'activitat de TORC2-Ypk1 regula positivament l'autofàgia en resposta a la falta d'aminoàcids (Vlahakis et al. 2014). Aquests resultats, juntament amb els presentats en aquesta tesi, suggereixen una regulació oposada de l'autofàgia pels dos complexos de TOR. Alguns aminoàcids com la leucina, la valina i el glutamat, requereix ferro per a la seva síntesi, mentre que altres aminoàcids com la serina, la metionina i la lisina disminueixen en condicions d'escassetat de ferro (Shakoury-Elizeh et al. 2010b). Aquesta observació podria indicar una relació entre els mecanismes d'inducció de la resposta autofàgica en resposta a l'escassetat d'aminoàcids i la depleció de ferro. La restricció d'aminoàcids indueix l'autofàgia a través de TORC2-Ypk1, els quals regulen negativament la calcineurina, permeten l'activació de Gcn2 i induint l'autofàgia (Vlahakis et al. 2014). En el nostre estudi, demostrem que TORC2 és essencial per a la detecció del senyal del disminució de la concentració de ferro, no obstant, aquest senyal no es transmet a la calcineurina (*Figura 4D de l'Article 2*), ni tampoc a Gcn2 (*Figura 4E de l'Article 2*), atès que demostrem que aquestes proteïnes no participen en aquest senyal. Ara bé, demostrem que el senyal transcor cap a la inhibició de TORC1. Curiosament, no detectem que la depleció de ferro fosforili a eIF-2α (*Figura 2C i 4C de l'Article 2*). Aquesta troballa és rellevant, ja que tant TORC1 com diferents situacions d'estrès causen l'increment de tRNAs no carregats i activació de la quinasa Gcn2, que fosforila a eIF-2α per reduir la síntesi proteica global (Castilho et al. 2014).

De l'anterior observació, vam deduir que TORC1 en aquest procés de senyalització no s'inactivava per tots els seus substrats. Al mutant *ypk1,* es produeix el mateix fenomen, TORC1 només senyalitza a alguns dels seus "*readouts*", avalant la hipòtesi. La inactivació parcial de TORC1 es demostra mitjançant el tractament amb rapamicina, ja que els substrats de TORC1 que no responen a la depleció de ferro, si ho fan a la droga (*Figura 3C,D de l'Article 2*). L'especificitat de TORC1 envers alguns substrats en conseqüència de l'estat nutricional de la cèl·lula ja s'havia observat anteriorment. En un treball publicat l'any 2004, els autors van plantejar la hipòtesi que TOR ha de ser capaç d'activar o reprimir selectivament gens diana específics, en funció de l'estat nutricional de la cèl·lula (T. Powers et al. 2004). Aquest model també és coherent amb les conclusions de Schreiber, segons les quals TOR es presenta com un processador multicanal que integra diferents senyals nutricionals (Shamji, Kuruvilla, and

Schreiber 2000). L'habilitat de la quinasa TORC1 de diferència entre substrats, segons la situació cel·lular permet el control de l'expressió gènica adequada per a cada situació sense haver d'activar totes les possibles respostes, que engloba la via TORC1, evitant gastar energia innecessària activant només la resposta específica en cada moment.

5.4 Snf1, Aft1 i Tor1 son essencials per inhibir l'autofàgia un cop es restauren els nivells de ferro

Si l'activació de l'autofàgia requereix la inactivació de TORC1, es podria considerar que l'activació de TORC1 és necessària per al bloqueig de l'autofàgia. Aquesta tesi es demostra que quan es restaura el ferro cel·lular, el senyal es transmet a TORC1 a través de Snf1 i Aft1 per inhibir el mecanisme autofàgic (Figura 15). El complex SNF1 s'activa durant el "*shift"* diauxic a causa de diversos factors, com l'esgotament de nutrients ,per a regular l'expressió gènica (Palomino, Herrero, and Moreno 2006). L'autor Sagliocco i els seus col·laboradors mostren que l'activació de Snf1 durant el "*shift"* diauxic provoca la inducció del reguló del ferro a través del factor transcripcional Aft1, el qual es desplaça al nucli (Haurie, Boucherie, and Sagliocco 2003). TORC1 rep el senyal del restabliment dels nivells de ferro a través del factor transcripcional Aft1 *(Figura 5D de l'Article 2)*. Snf1 és l'encarregat de senyalitzar a Aft1 que el ferro torna a estar biodisponible (*Figura 5F de l'Article 2)*. L'activació de TORC1 fosforila a Atg13, conseqüentment, Atg1 es defosforila i es dissocia el complex Atg1 inhibint l'autofàgia.

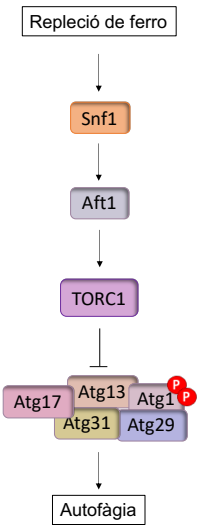

Figura 15. Mecanisme d'inhibició de l'autofàgia en resposta a la repleció de ferro. Quan el ferro torna a estar biodisponible per a la cèl·lula, Snf1 és l'encarregat de transmetre el senyal a Aft1 per activar al complex 1 de TOR, inhibint l'autofàgia.

La connexió entre el metabolisme de la glucosa i l'homeòstasi del ferro es reforça gràcies als resultats descrits en el - 214 -paràgraf anterior. Estudis previs ja suggerien aquesta connexió. Tpk2, una de les subunitats de PKA, és inhibida en resposta a l'exhauriment de la glucosa durant el "*shift"* diauxic. En aquesta situació, Tpk2 es dissocia dels gens que reprimeix, i entre aquests gens es troben els gens diana d'Aft1 (Robertson et al. 2000). Durant la depleció de ferro, hi ha una disminució del procés de fermentació de la glucosa del medi (*Figura Suplementària 1C de l'Article 1*) i una menor activació de la quinasa Snf1 (*Figura 5F de l'Article 2*), resultats que reforcen el nexe d'unió entre els dos metabolismes, el de la glucosa i el del ferro. El sentit biològic que podria tenir aquesta relació, és que després de l'exhauriment de la glucosa, el llevat canvia del metabolisme fermentatiu al respiratori. La respiració és un procés altament dependent del ferro. Quan la cèl·lula censa que ha de fer aquest canvi de metabolisme, Aft1 és translocat al nucli activant els gens involucrats en la captació de ferro, perquè aquest metall sigui utilitzat com a cofactor pels citocroms de la cadena de transport d'electrons, la citrat sintasa i a ferrodoxina (Cheung, Murphy, and Heinrichs 2012).

5.5 La depleció de ferro, l'activació de l'autofàgia i la quiescència contribueixen a l'extensió de la CLS del llevat de gemmació

L'autofàgia és un mecanisme vital per prevenir l'eliminació prematura de les cèl·lules a través de processos com la necrosi i l'apoptosi (Tabibzadeh 2023). La regulació precisa de l'activació de l'autofàgia és essencial, ja que una activació excessiva pot tenir efectes nocius sobre les cèl·lules induint apoptosi o necrosi (Maiuri et al. 2007). Per contra, la pèrdua de l'autofàgia contribueix a l'acumulació de molècules danyades o innecessàries, afavoreix la inflamació i el càncer i accelera l'envelliment (Tabibzadeh 2023). L'activació en els nivells adequats, contribueix positivament en alentir el procés de l'envelliment. Desafortunadament, aquesta protecció proporcionada per l'autofàgia disminueix amb l'edat. El col·lectiu de persones de la tercera edat presenten nivells baixos de BECLIN1, l'homòleg d'Atg6. En canvi, els humans centenaris mostren nivells més alts d'aquesta proteïna, fet que l'autor de l'estudi correlaciona amb una major esperança de vida (Emanuele et al. 2014). Aquests resultats es reflecteixen en els experiments amb llevat. La mutació d'un sol gen autofàgic, provoca disminució de la CLS (*Figura 7C de l'Article 2)*, un fet que es veu accentuat en condicions de manca de ferro.

L'autofàgia és un dels múltiples factors que intervenen en el procés d'envelliment (Barbosa, Grosso, and Fader 2018). La quiescència també contribueix a augmentar la supervivència cel·lular, quan les condicions ambientals no són òptimes (de Virgilio 2012). Les cèl·lules que creixen en un ambient amb escassetat de ferro entren en quiescència, tal com es demostra en la *Figura 6 de l'Article 2*. A partir d'aquests resultats es pot concloure que l'entrada en quiescència, juntament amb la inducció de l'autofàgia a causa de la depleció de ferro, contribueixen a una extensió de la vida cronològica de la cèl·lula. Atès que els mutants autofàgics entren en estat quiescent al créixer en un medi sense ferro, com les cèl·lules salvatges (*Figura 6C de l'Article 2),* però el bloqueig en el procés autofàgic causa la disminució de la seva CLS.

L'estrès oxidatiu és una de les primeres causes d'envelliment (Zahoor et al. 2022). La depleció de ferro provoca un augment de l'estrès oxidatiu durant la fase exponencial, ue posteriorment disminueix, com es mostra a la *Figura 6D de l'Article 2*. La reducció de les ROS després del "*shift"* diauxic suggereix que aquesta disminució també contribueix a l'augment de la CLS. Fins i tot, com es va demostrar en un estudi del 2007, les ROS produïdes durant la fase

exponencial contribueixen positivament a l'extensió de la CLS (Bonawitz et al. 2007). L'efecte positiu de l'increment de les ROS durant la fase exponencial sobre la CLS pot ser explicat pel fenomen conegut com hormesi, definit com l'adaptació a dosis baixes d'un estrès que millora la resposta cel·lular. De manera que, l'exposició a ROS durant la fase exponencial pot contribuir a l'adaptació i millora de la resposta cel·lular a l'estrès oxidatiu, reduint així l'envelliment.

D'altra banda, els nivells més baixos d'estrès oxidatiu durant la fase estacionària en les cèl·lules que creixen sense ferro en comparació amb les que creixen en el medi mínim control, podrien relacionar-se amb el fet que les cèl·lules que creixen en el medi SD, durant la fase estacionària presenten un metabolisme respiratori, a causa de l'exhauriment de la glucosa del medi. La respiració és la font principal de generació de ROS. Per contra, les cèl·lules que creixen en SD-Fe encara tenen alts nivells de glucosa, i la hipòtesi més plausible és que el seu metabolisme no sigui respiratori per dues raons: en primer lloc, continuen tenint glucosa disponible en el medi, i en segon lloc, no posseeixen el ferro necessari per a dur a terme la respiració. Per tant, mitjançant l'efecte Crabtree, es redueix la necessitat de la fosforilació oxidativa a través del cicle de Krebs i la cadena de transport electrònic, disminuint el consum d'oxigen i generació de ROS.

5.6 El desens de la glucosa durant el "*shift diauxic*" determina la inducció de l'autofàgia

La majoria d'estudis d'autofàgia realitzats en *S. cerevisiae* s'han centrat en el creixement exponencial. Treballar amb aquesta fase de creixement en el laboratori permet controlar les restriccions calòriques aplicades als cultius i conèixer les vies de senyalització que s'activen com a resposta. EN canvi, s'ha prestat poca atenció a l'autofàgia durant la fase estacionària. Després d'un dia de cultiu, coincidint amb el "*shift"* diauxic, en les condicions de treball establertes en el tercer article, observem un pic d'inducció d'autofàgia (*Figura 1A de l'Article 3)*. La hipòtesi de partida va ser considerar que l'esgotament d'algun nutrient essencial era la causa d'aquesta inducció. Es va demostrar, que a un dia de cultiu l'esgotament de la glucosa induïa l'autofàgia (*Figura 1D de l'Article 3)*, mentre que després de dos dies de cultiu, era la limitació de la font de nitrogen, d'aminoàcids i ferro la que provocava l'activació de l'autofàgia (*Figura 1E de l'Article 3)*. Aquests resultats concorden amb altres estudis que han demostrat

que la limitació de la glucosa (Adachi, Koizumi, and Ohsumi 2017), de nitrogen (H. Huang et al. 2015) i d'aminoàcids (Vlahakis et al. 2014) causen una clara inducció de l'autofàgia.

La quinasa Gcn2, regula l'autofàgia en resposta a la manca d'aminoàcids (Vlahakis et al. 2014). En les condicions del nostre experiment, transcorreguts dos dies de cultiu, sembla ser el moment en què els aminoàcids s'han exhaurit, ja que en aquest punt el mutant *gcn2* és incapaç d'induir autofàgia (*Figura 3C de l'Article 3*). L'autofàgia que s'activa a un dia de cultiu, a causa de la glucosa, com la que s'indueix als dos dies de cultiu sembla que són independents de TORC1. Atès que, el tractament amb rapamicina en el mutant *gcn2* és capaç d'induir autofàgia (*Figura 3D de l'Article 3*). I els "*readouts*" de TORC1, en l'experiment que es du a terme durant tota la CLS en un wt, mostren que TORC1 roman actiu en tot moment, tant pels "*readouts*" que s'activen en resposta a estrès com Rtg1, Sfp1 i Msn2, (*Figura 2A,B de l'Article 3*), com per la proteïna diana de l'autofàgia de TORC1, Atg13, que es troba fosforilada i es defosforila després del tractament amb rapamicina (*Figura 2C de l'Article 3*). Aquests resultats estan en concordança amb els d'altres autors que han conclòs que TORC1 no sembla que exerceixi una funció predominant durant la restricció de glucosa (Hughes Hallett, Luo, and Capaldi 2014).

5.7 Mtl1 és imprescindible per activar l'autofàgia en resposta a baixos nivells de glucosa

Mtl1, és un receptor transmembrana que forma part de la via CWI. En un altre treball del grup de la Dra. Maria Angeles de la Torre s'estableix que Mtl1 actua de sensor de la depleció de glucosa (Petkova et al. 2010). En la present tesi, es reforça aquesta afirmació i es va més enllà afirmant que Mtl1 és necessari per activar l'autofàgia generalitzada en resposta a l'escassetat de glucosa, com mostra la *Figura 3E de l'Article 3*.

En l'article publicat l'any 2010 pel grup de la Dra. Maria Angeles de la Torre (Petkova et al, 2010), es presenten evidències que demostren el paper de Mtl1 com a regulador negatiu de Tor1 i Ras2 durant les restriccions de glucosa i l'estrès oxidatiu. Aquesta regulació repercuteix positivament en la viabilitat cel·lular (Petkova et al. 2010). Pel que fa a l'activació de l'autofàgia a causa de la falta de glucosa, Tor1 no sembla tenir cap paper.

Mtl1 també està relacionada amb la ruta de senyalització de Ras2 (Petkova et al. 2010). Ras2/PKA s'inactiva durant el canvi de metabolisme de fermentatiu a respiratori (Colombo et al. 2004). La inhibició de Ras2 ja havia estat identificada com a reguladora positiva de l'autofàgia (Boutouja and Platta 2020). Durant el "*shift"* diauxic i l'inici de la fase estacionària, el mutant *ras2,* no presenta problemes en la inducció de l'autofàgia, tot i que sí que té un menor flux autofàgic que un wt (*Figura 3B de l'Article 3*). Addicionalment, la mutació de *RAS2* en *mtl1* rescata l'autofàgia (*Figura 6A de l'Article 3*). Aquests resultats posen en rellevància el paper de Ras2 en la inducció de l'autofàgia en resposta a la restricció de glucosa i estableixen que Mtl1 inhibeix Ras2 durant el canvi de metabolisme fermentatiu a respiratori (Figura 16). Homòlogament, la mutació de *RAS* en humans contribueix a la inducció de l'autofàgia, esdeveniment que ocorre en més del 30% dels càncers (Siegel Mph et al. 2023). L'Article 3 posa en relleu què la funció de Ras2, com a inhibidor de l'autofàgia, està conservada entre espècies. El càncer és una malaltia complexa on conflueixen múltiples senyalitzacions, i l'autofàgia és considerada pro-cancerígena, proporciona a les cèl·lules tumorals una major supervivència, gràcies al fet que els permet obtenir energia durant els períodes de limitació nutricional i preservar la integritat mitocondrial (J. Y. Guo et al. 2011). Paradoxalment, al mateix temps, l'autofàgia bloqueja la iniciació del desenvolupament tumoral impedint el dany crònic dels teixits, la producció d'espècies reactives d'oxigen i la mutagènesi del material genètic (Mathew et al. 2009). Conèixer els mecanismes pels quals s'activa o inhibeix l'autofàgia esdevenen eines molt útils per desenvolupament de teràpies específiques per al tractament de tumors.

Posteriorment, l'any 2015, es va demostrar la connexió entre Mtl1 i Sch9 (Sundaram et al. 2015). La deleció de Sch9 indueix autofàgia (Yorimitsu et al. 2007). A la *Figura 6A de l'Article 3,* es pot observar com el doble mutant *sch9mtl1* suprimeix la falta d'autofàgia del mutant simple *mtl1* en condicions d'escassetat de glucosa durant el "*shift"* diauxic. Resultats que reforcen la connexió entre el receptor Mtl1 i la proteïna Sch9, on la inhibició de Sch9 a través de Mtl1 regula positivament la inducció de l'autofàgia en resposta a l'escassetat de glucosa (Figura 16).

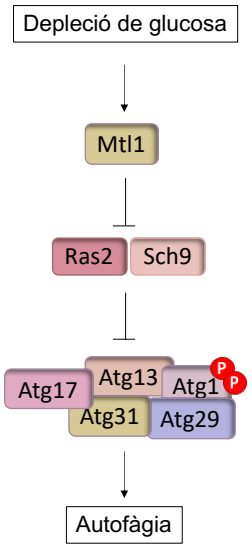

Figura 16. Mecanisme d'inducció de l'autofàgia en resposta a la depleció de glucosa. El desens dels nivells de glucosa en el medi són censats per Mtl1. Mtl1 regula negativament a Ras2 i Sch9 per activar la resposta autofàgica.

Mtl1 censa estímuls que alteren la paret cel·lular induint una cascada de senyalització de la via CWI, a través de Pkc1 per activar a la MAPK Slt2 (A. B. Sanz et al. 2018). Per tant, el mutant *mtl1* és incapaç d'activar Slt2. La disrupció del gen *SCH9* en *mtl1* indueix la fosforilació i activació Slt2 (Sundaram et al. 2015). L'activació de Slt2, s'ha establert com a necessària, per activar l'autofàgia generalitzada en resposta a dany en el DNA (Ueda et al. 2019). Desl resultats d'aquesta tesi, es fa evident que l'autofàgia durant la transició del metabolisme fermentatiu a respiratori no es dona a través de Pkc1/Slt2, demostrant un paper de Mtl1 fora de la via CWI.

Les cèl·lules de *S. cerevisiae* que creixen en condicions no restrictives en un medi amb presència de sucres fermentables com la glucosa utilitzen un metabolisme fermentatiu, impulsat per l'efecte Crabtree, durant la fase exponencial per obtenir ATP. Quan les cèl·lules en cultiu es sotmeten a un xoc brusc on s'elimina tota la glucosa del medi de cop, la producció d'ATP s'atura, deixant la cèl·lula sense energia per dur a terme els seus processos fisiològics. Com a resultat, la cèl·lula és incapaç d'activar l'autofàgia i és necessari subministrar ATP de forma exògena per activar-la (*Figura 5A,B de l'Article 3*). Aquests resultats es correlacionen

amb els pubicats pel grup del Dr. Ohsumi, on es demostra que és necessari mantenir els nivells d'ATP intracel·lulars per induir l'autofàgia en resposta a la inanició de carboni, suggerint una regulació negativa de l'autofàgia a través de la repressió catabòlica del carboni (Adachi, Koizumi, and Ohsumi 2017). A partir de l'ATP se sintetitza cAMP. El mutant *mtl1* presenta nivells més elevats de cAMP (Petkova et al. 2010), el que probablement està directament relacionat amb menors nivells d'ATP. Per afegiment, Mtl1, regula negativament els nivells de cAMP a través de la regulació de Ras2. Quan al mutant *mtl1* durant el "*shift"* diauxic se li aporta ATP, parcialment es restaura l'activació de l'autofàgia. Suggerint que quan no hi ha glucosa en el medi, si no tenim a Mtl1, Ras incrementa la conversió d'ATP en cAMP, bloquejant l'autofàgia. No obstant, la falta d'ATP no explica la totalitat del dèficit d'autofàgia observat en el mutant *mtl1*, ja que l'addició d'ATP només la rescata parcialment. D'altra banda, la reducció gradual de la concentració de glucosa del medi del 2% al 0,5%, 0,1% o 0,05%, per simular el que succeeix durant la transició del metabolisme fermentatiu al respiratori, mostra una activació gradual de l'autofàgia de forma dependent de Mtl1, Ras2 i Sch9 (*Figura 4A,C i 6B de l'Article 3*).

Mtl1 és un sensor de la glucosa, un sucre fermentable. Altres sucres fermentables com la sucrosa i la fructosa també necessiten Mtl1 per activar l'autofàgia (*Figura Suplementària 2F de l'Article 3*). No obstant aixpo, quan s'empra una font de carboni no-fermentable com el glicerol, Mtl1 no és necessari per a induir l'autofàgia (*Figura 7A de l'Article 3*).

L'increment de les ROS generades durant la transició del metabolisme fermentatiu al respiratori, juntament amb la respiració desacoblada de *mtl1* provoca que el mutant presenti disfuncions mitocondrial (Sundaram et al. 2015). Tanmateix, en el nostre estudi, les disfuncions mitocondrials no són inhibitòries de l'autofàgia, ja que el mutant *rho,* el qual no presenta material genètic mitocondrial, no té problemes en la inducció de l'autofàgia durant el "*shift"* diauxic*,* ni en resposta a les diferents concentracions de glucosa (*Figura 5D,E de l'Article 3*). Tampoc l'increment en la producció de ROS, pel fet que el tractament amb NAC, un antioxidant, no restaura l'autofàgia en el mutant *mtl1* (*Figura 7B de l'Article 3*).

5.8 Mtl1 i Atg33 son essencials per a la mitofàgia durant la fase estacionària

La respiració desacoblada i l'increment de ROS en el mutant *mtl1* no influeixen a l'autofàgia generalitzada, però si provoquen dany mitocondrial. La mitofàgia, és l'autofàgia especialitzada de les mitocòndries, a través de la qual s'eliminen les mitocòndries danyades (Bhatia-Kissova and Camougrand 2021). Els estudis de mitofàgia, normalment, es realitzen utilitzant fonts de carboni respiratòries com el lactat o el glicerol (Eiyama and Okamoto 2017). En aquestes condicions, igual que succeeix amb l'autofàgia generalitzada, Mtl1 no impedeix la mitofàgia, la qual depèn d'Atg11 i Atg32 *(Figura 8A,B de l'Article 3*). Antagònicament, la mitofàgia que s'indueix a causa de l'inici de la respiració requereix Mtl1, Ras2 i Sch9, exactament igual que l'autofàgia (*Figura 8C,E de l'Article 3*). Prèviament, ja s'havia descrit el paper de Sch9 en diferents tipus de autofàgies específiques com la ribofàgia, pexofàgia i, com es demostra en aquest estudi, la mitofàgia (Waliullah et al. 2017; Mao and Klionsky 2011; Lakhani et al. 2014), així com el paper de Ras2 en la pexofàgia (Boutouja and Platta 2020).

Durant la fase estacionària, la mitofàgia no depèn d'Atg32, sinó d'Atg33, una proteïna de la membrana mitocondrial que actua com a receptor per la mitofàgia. Atg33 va ser identificat en una recerca genòmica i sembla desenvolupar el seu paper en la fase post-diauxica, però fins ara ha estat escassament estudiat (Kanki, Wang, Baba, et al. 2009). El mecanisme que permet que Atg33 substitueixi Atg32 com a receptor mitofàgic durant la fase estacionaria requerirà investigacions futures més detallades.

Tant l'activació de la mitofàgia com de l'autofàgia són imprescindibles per a l'extensió de la vida cronològica de *S. cerevisiae.* Els mutants amb alteracions en aquests processos, així com el propi *mtl1,* presenten una CLS més reduïda que un wt (*Figura 8D de l'Article 3*). La disminució de CLS, d'*atg32* es corrobora amb anteriors treballs que relacionen la pèrdua d'*ATG32* amb l'acumulació de mitocòndries disfuncionals, causants de la reducció de la CLS (Richard et al. 2013). No obstant això, els mutants mitofàgics, presenten una menor disminució de la CLS. Una hipòtesi per explicar aquesta observació podria ser que, com aquests mutants no tenen dificultats per activar l'autofàgia generalitzada, poden continuar reciclant les mitocòndries danyades a través d'autofàgia no selectiva, però aquest reciclatge de les mitocòndries no sembla ser suficient. La mitofàgia no només és necessària per eliminar

mitocòndries danyades, sinó que també promou la biogènesi mitocondrial i assegura el control de la qualitat mitocondrial, contribuint així a l'homeòstasi cel·lular. L'estudi de la mitofàgia és essencial, ja que alteracions en aquest procés han estat associades a malalties com ara cardiopaties (Billia et al. 2011), Alzheimer i Parkinson (Barbosa, Grosso, and Fader 2018), a més de contribuir al fenotip d'envelliment (N. Sun et al. 2015).

5.9 TORC2 i Ypk1 són necessaris per l'activitat d'Aft1 en resposta a la depleció de ferro

Els resultats mostrats en aquest treball postulen a la ruta de senyalització TORC2-Ypk1 com a sensor dels nivells de ferro cel·lular. La inhibició d'aquesta ruta provoca una localització aberrant d'Aft1, bloquejant la captació i emmagatzematge de ferro (*Figura 1 i 2B de l'Article 4*). Aquest és un mecanisme novell, pel fet que fins al moment es coneix perfectament quina és la resposta que es desencadena davant de la falta de ferro, però no com és censada aquesta escassetat. El mutant *ypk1* té una alta producció de ROS, a causa d'una mala respiració mitocondrial i a defectes en l'acidificació vacuolar provocada per un increment de l'activitat de Fpk1 (Niles et al. 2014). Tot i això, aquesta no és l'explicació de per què Aft1 no es localitza al nucli, tampoc ho és el defecte en l'expressió o localització de Pse1 (*Figura 2A,B de l'Article 4*).

TORC2 té dues dianes de senyalització, Ypk1 i Pkc1 (Thorner 2022). Cada una d'aquestes dianes conforma una branca de senyalització independent, i totes dues actuen per separat en diferents processos, com ara la síntesi d'esfingolípids a través d'Ypk1 i la polarització de l'actina mitjançant Pkc1 (Niles and Powers 2014). En l'homeòstasi del ferro, TORC2 també diferència entre aquestes dues branques de senyalització. És Ypk1 la quinasa imprescindible per regular la localització d'Aft1 i l'activitat del reguló del ferro. Ypk1 no només és fosforilada per TORC2, sinó que també requereix l'acció de les quinases Pkh1 i Pkh2 per fosforilar-la en el seu "*loop*" d'activació, el qual activa la seva funció quinasa. En tots els estudis publicats fins al moment les dues fosforilacions sobre Ypk1 són imprescindibles (Thorner 2022). A través d'un estudi de complementació, demostrem que la fosforilació de TORC2 és imprescindible per activar el reguló del ferro en resposta a l'escassetat del metall (*Figura 4 de l'Article 4*), però no la fosforilació per part de les Pkhs (Apèndix 1). Aquest descobriment és novedós, ja que cap altre autor ha demostrat mai una activació d'Ypk1 que no requereixi l'acció de les

Pkhs, i en un futur requerirà un estudi més profund i detallat.

5. 10 Els esfingolípids complexos controlen la localització nuclear d'Aft1 en resposta a la limitació de ferro

TORC2-Ypk1 governen múltiples processos fisiològics, un d'ells és la biosíntesi d'esfingolípids (Aronova et al. 2008). Els resultats presentats en aquesta tesi (*Figura 5 i 6 de l'Article 4*) mostren que la síntesi d'esfingolípids, concretament la síntesi de LCBs de cadena llarga és imprescindible per transmetre el senyal d'escassetat de ferro al factor transcripcional Aft1 (Figura 17). Aquest no és el primer estudi que destaca l'habilitat dels esfingolípids per actuar com a molècules senyalitzadores (Fernandis and Wenk 2007; Dickson, Nagiec, Skrzypek, et al. 1997).

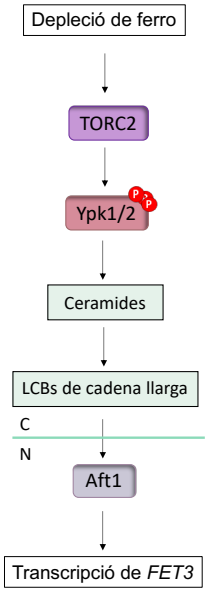

Figura 17. Mecanisme d'activació del reguló del ferro en resposta a la depleció del metall. TORC2 fosforila a Ypk1 en resposta a la davallada dels nivells de ferro. L'activació d'Ypk1 indueix la biosíntesi d'esfingolípids. Els esfingolípids de cadena llarga són els encarregats d'induir la translocació d'Aft1 al nucli (N) activant la transcripció dels gens que formen part del reguló del ferro, entre ells Fet3.

Tanmateix, aquest sí és el primer estudi en demostrar que TORC2 censa la biodisponibilitat de ferro i transmet aquest senyal al reguló del ferro emprant als esfingolípids com a molècules senyalitzadores. Existeixen estudis previs que demostren una relació entre els esfingolípids i la fosforilació d'Aft1. Els mutants *isc1,* els quals no poden reciclar els LCBs de cadena llarga a LCBs, no poden desfosforilar a Aft1, cosa que provoca un augment en els nivells de ferro intracel·lular (Almeida et al. 2008; Martins, Costa, and Pereira 2018). D'altra banda, el mutant *ypk1,* no presenta problemes en la fosforilació d'Aft1 (Pujol-Carrion et al. 2021). La combinació d'aquests dos resultats posa de manifest, un cop més, la rellevància dels esfingolípids de cadena llarga en aquest procés, ja que són necessaris per a activar al reguló del ferro, tot i això, una acumulació excessiva d'aquests impedeix la inhibició del reguló. Addicionalment, la deficiència de ferro incrementa els nivells de l'enzim Sur2, augmentant la síntesi de dihidroesfingosina (Shakoury-Elizeh et al. 2010a; Lester et al. 2013). Aquest resultat és consistent amb els mostrats en el present treball, ja que es confirma que la presència d'esfingolípids és essencial per transmetre el senyal d'escassetat de ferro i així activar la captació del metall.

Les mitocòndries són un dels compartiments on s'emmagatzema el ferro. Aquest metall s'importa a la mitocòndria a través de Mrs3/4. Un cop dins la mitocòndria, el ferro és emprat per a la síntesi de clústers Fe/S, que posteriorment s'exporten cap al citosol a través deel transportador Atm1 (Lill, Srinivasan, and Mühlenhoff 2014). El bloqueig de l'entrada de ferro a la mitocòndria no causa defectes en la localització d'Aft1 (*Figura 3 de l'Article 4*), descartant la possibilitat que la mitocòndria senyalitzi a TORC2 la davallada de ferro. Tot i això, el bloqueig de la sortida dels clústers Fe/S de la mitocòndria, quan les cèl·lules creixen en presència del metall, provoca una localització parcial d'Aft1 en aquest orgànul, efecte que es reprodueix en el mutant *ypk1*, i de manera més severa en el *tor2ts*. Aquesta localització aberrant es podria explicar a través de la disminució de la concentració d'esfingolípids en aquests mutants. Les membranes mitocondrials contenen diversos tipus de lípids, entre ells els esfingolípids (Spincemaille et al. 2014). Les interconnexions dels esfingolípids afecten a les propietats de la membrana com la permeabilitat, fissió i fusió (Megyeri et al. 2016). Les membranes mitocondrials estan enriquides amb fitoceramides hidroxilades, i una davallada en la concentració d'aquests lípids provoca alteracions de la permeabilitat mitocondrial, impedint

el transport de molècules i compostos a través de la membrana (Kitagaki et al. 2007). En el cas del mutant *atm1,* el bloqueig de la sortida dels clústers Fe/S indueix la localització parcial d'Aft1 a la mitocòndria, i aquest fenomen podria estar ocorrent també en els mutants *ypk1* i *tor2ts.* Aquests dos mutants tenen nivells reduïts d'esfingolípids, la qual cosa, segurament afecta la permeabilitat de les membranes mitocondrials, impedint la sortida dels clústers Fe/S cap al citoplasma. Aquesta hipòtesi requerirà una investigació més profunda en futurs estudis per a poder corroborar-la.

El vacúol és l'altre compartiment d'emmagatzematge de ferro, quan el metall es troba en excés (Martínez-Pastor et al. 2013). La restricció de ferro, en els mutants *ypk1* i *tor2ts*, i en les cèl·lules tractades amb drogues que bloquegen la producció d'esfingolípids, situen a Aft1 dins el vacúol. Fins ara, només hi ha un altre treball en què se situa a Aft1 dins el vacúol quan hi ha una desregulació en el metabolisme de l'ergosterol, el qual parcialment també es troba influenciat per la senyalització de TORC2/Ypk1 (Jordá, Rozès, and Puig 2021); tot i això els autors no realitzen cap mena d'experiment ni formulen cap hipòtesi per profunditzar en aquesta observació.

En el nostre estudi hem comprovat que Aft1 dins el vacúol no és degradat per autofàgia, a més la proteïna roman estable durant alts períodes de temps (Apèndix 2). Així mateix, podem descartar que aquesta localització d'Aft1 dins el vacúol sigui el resultat de la mancà de ferro dins l'organul, ja que això no succeeix en el mutant *ccc1*. Curiosament, en les situacions en què Aft1 es localitza a l'interior del vacúol es correlacionen amb el bloqueig en la inducció de l'autofàgia. Això planteja la hipòtesi que Aft1 dins el vacúol podria estar inhibint l'autofàgia, especialment tenint en compte que el mutant *aft1* no pot bloquejar l'autofàgia quan se restableixen els nivells de ferro, com s'ha presentat en l'Article 2. Aquesta hipòtesi requereix més estudi, i actualment està sent explorada al laboratori.

6. CONCLUSIONS

1. In response to iron depletion, the cell activates changes in the transcriptional response, leading to the inactivation of TORC1.

2. Iron deprivation, as the only limiting nutrient, induces bulk autophagy through the inactivation of TORC1 and the subsequent Atg13 dephosphorylation along with the Atg1 phosphorylatory activation.

3. The iron scarcity signal must be transmitted by an active TORC2/Ypk1 to inactivate TORC1 complex and thus to induce non-specific bulk autophagy.

4. Iron replenishment causes the end of the autophagic process initiated upon iron starvation in a manner dependent on Snf1, Aft1, and Tor1 activity.

5. Entry into quiescence or bulk autophagy activation occurring upon iron starvation are mechanisms that favour chronological life extension.

6. Transition through diauxic shift and stationary phase in minimum medium is a good model to study the sequential activation of bulk autophagy due to depletion of glucose.

7. Mtl1 is a transmembrane receptor of the CWI pathway required to sense the descent in fermentable carbon sources in order to transmit the signal to the inactivation of both Ras2 or Sch9, to activate Atg1 upon phosphorylation leading to the induction of bulk autophagy required to extend lifespan. This signaling process is independent of both TORC1 or oxidative stress.

8. Mtl1 is independent of mitophagy caused by respiratory carbon sources and Atg32 receptor.

9. Transition through diauxic shift and stationary phase in *S. cerevisiae* activates Atg33-dependent and Atg32 independent mitophagy mainly due to glucose depletion. This mechanism requires Mtl1 function to inactivate both Ras2 and Sch9 leading to the induction of Atg33-dependent mitophagy.

10. TORC2 regulates both the transcriptional function and subcellular localization of Aft1, the transcription factor that controls the expression of the iron regulon, in response to iron deprivation.

11. TORC2 specifically transmits the signal of iron depletion through Ypk1 and subsequently the sphingolipids pathway, leading to complex LCBs. The signal converges in Aft1 and determines both the localization and the activity of the transcription factor to regulate iron uptake.

12. Low levels of sphingolipids during iron scarcity cause Aft1 vacuolar localization. We ruled out the possibility that this subcellular localisation is a reflect of either autophagy or protein degradation.

7. APÈNDIXS

7.1 APÈNDIX 1

Figura 1

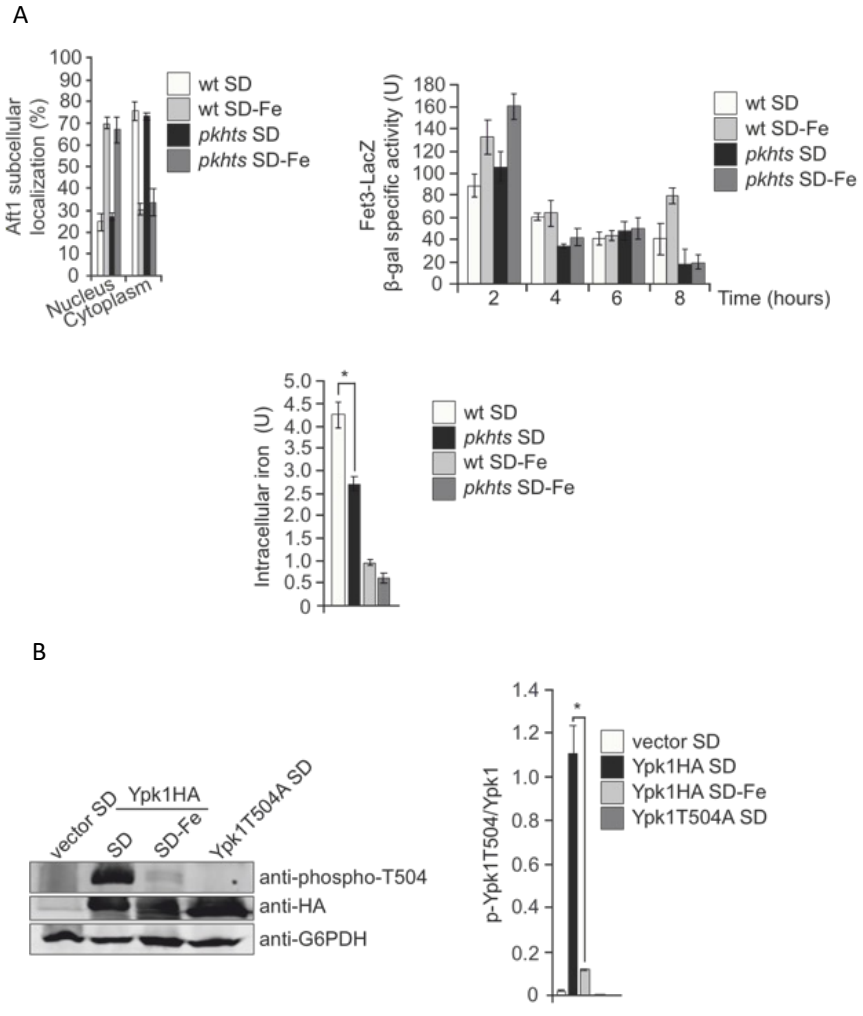
A
Aft1 subcellular localization (%)
Nucleus
Cytoplasm
wt SD
wt SD-Fe
pkhts SD
pkhts SD-Fe
Fet3-LacZ β-gal specific activity (U)
Time (hours)
Intracellular iron (U)
B
vector SD
Ypk1HA
SD
SD-Fe
Ypk1T504A SD
anti-phospho-T504
anti-HA
anti-G6PDH
p-Ypk1T504/Ypk1
vector SD
Ypk1HA SD
Ypk1HA SD-Fe
Ypk1T504A SD

C

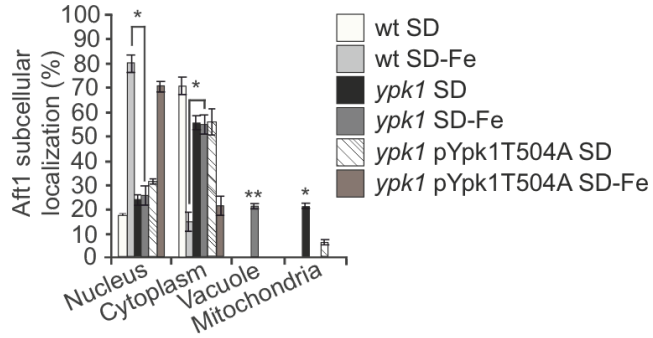
Aft1 subcellular localization (%)
100
90
80
70
60
50
40
30
20
10
0
Nucleus
Cytoplasm
Vacuole
Mitochondria
wt SD
wt SD-Fe
ypk1 SD
ypk1 SD-Fe
ypk1 pYpk1T504A SD
ypk1 pYpk1T504A SD-Fe

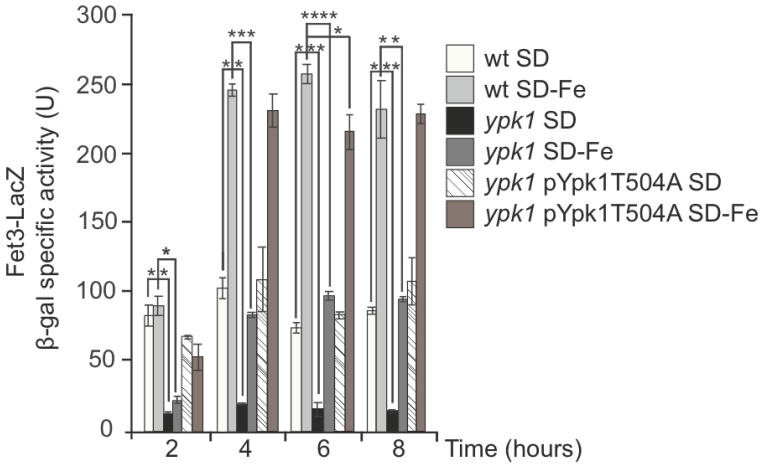
Fet3-LacZ
β-gal specific activity (U)
300
250
200
150
100
50
0
2
4
6
8
Time (hours)
wt SD
wt SD-Fe
ypk1 SD
ypk1 SD-Fe
ypk1 pYpk1T504A SD
ypk1 pYpk1T504A SD-Fe

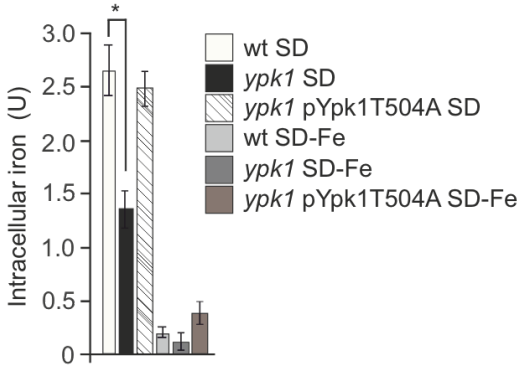
Intracellular iron (U)
3.0
2.5
2.0
1.5
1.0
0.5
0
wt SD
ypk1 SD
ypk1 pYpk1T504A SD
wt SD-Fe
ypk1 SD-Fe
ypk1 pYpk1T504A SD-Fe

Figura 1. TORC2 regula el senyal de depleció de ferro a través d'Ypk1 i independentment de les Pkhs. A) Cultius de soques wt i *pkhts* van ser transformats amb el plasmid pAft1GFP o p*FET3*-LacZ i crescuts exponencialment en medi SD o SD-Fe a 38ºC. Es van recollir mostres per analitzar-les al microscopi, determinar l'activitat β-galactosidasa i els nivells de ferro intracel·lulars. B) Cèl·lules wt es van transformar amb els plasmids pC-terminal3-HA, pYpk1HA o pYpk1^{T504A}. Les cèl·lules es van créixer fins a arribar a fase exponencial i es van recollir mostres per analitzar-les mitjançant western blot. Els anticossos emprats per la detecció van ser anti-phospho-T504, anti-HA i anti-G6PDH. L'histograma representa la ràtio entre phospho-T504 Ypk1 i Ypk1 total. C) Mostres de cultius de les soques wt, *ypk1* i *ypk1*+pYpk1^{T504A} transformades amb els plasmids pAft1GFP o p*FET3*-LacZ van ser recollides per analitzar la localització subcel·lular d'Aft1, l'activitat β-galactosidasa i els nivells de ferro intracel·lulars.

7.2 APÈNDIX 2

Figura 1

A

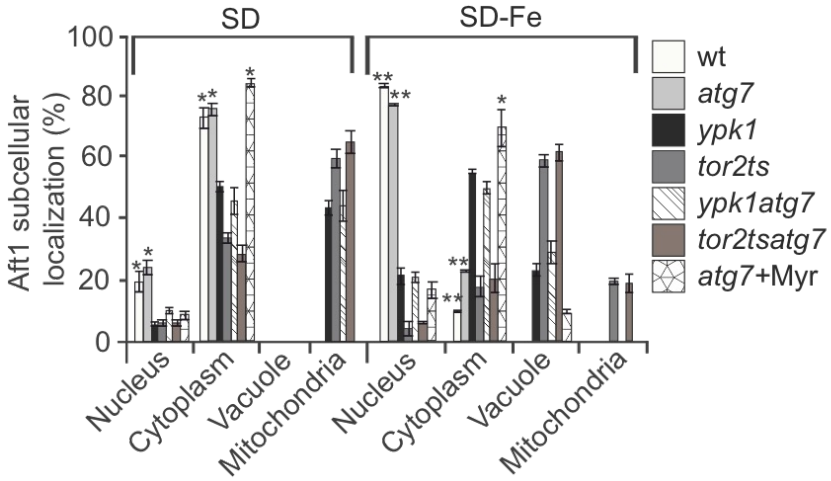
SD
SD-Fe
100
80
60
40
20
0
Aft1 subcellular localization (%)
Nucleus
Cytoplasm
Vacuole
Mitochondria
wt
atg7
ypk1
tor2ts
ypk1atg7
tor2tsatg7
atg7+Myr

B

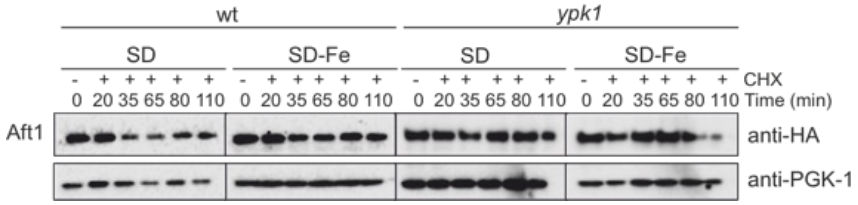
wt
ypk1
SD
SD-Fe
CHX
0 20 35 65 80 110 Time (min)
Aft1
anti-HA
anti-PGK-1

C

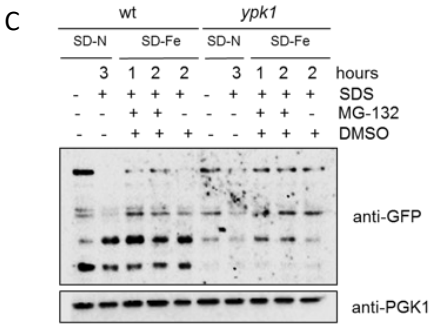
wt
ypk1
SD-N
SD-Fe
hours
SDS
MG-132
DMSO
anti-GFP
anti-PGK1

Figura 1. La localització vacuolar d'Aft1 no es deu a la seva degradació. A) Cultius de soques wt, *atg7, ypk1, tor2ts, ypk1atg7, tor2tsatg7* i *atg7* tractat amb Miriocina (Myr) que expressen pAft1GFP, es van créixer exponencialment en medi SD o SD-Fe a 30ºC o 38ºC. Es van recollir mostres per analitzar-les *in vivo* al microscopi de fluorescència. B) Les soques wtAft1HA i *ypk1*Aft1HA es van créixer exponencialment en SD o SD-Fe i es va recollir una mostra. El volum de cultiu restant es va tractar amb Cicloheximida (CHX). Es van recollir mostres als temps indicats per extreure'n la proteïna i analitzar-la per western blot. La proteïna Aft1 es va detectar utilitzant l'anticòs anti-HA. Per la detecció de Pgk1 com a control de càrrega, es va emprar l'anticòs anti-PGK-1. C) Cèl·lules wt i *ypk1* transformades amb el plasmid pAft1-GFP es van créixer en medi SD-Nitrogen exponencialment i es va recollir una mostra, la resta de cultiu va ser tractat amb el detergent SDS durant tres hores i es va agafar una altra mostra. Finalment, el cultiu restant es transfereix a medi nou sense ferro que conté SDS, MG-132 i DMSO. Es va procedir a recollir mostres als temps indicats per a la seva anàlisi per western blot. La proteïna Aft1 es va detectar mitjançant l'anticòs anti-GFP. Com a control de càrrega es va fer ús de la proteïna Pgk1, la qual es va detectar amb l'anticòs anti-Pgk1.

BIBLIOGRAFIA

Abate, Georgia, Emanuela Bastonini, Katherine A. Braun, Loredana Verdone, Elton T. Young, and Micaela Caserta. 2012. 'Snf1/AMPK Regulates Gcn5 Occupancy, H3 Acetylation and Chromatin Remodelling at S. Cerevisiae ADY2 Promoter'. *Biochimica et Biophysica Acta* 1819 (5): 419. https://doi.org/10.1016/J.BBAGRM.2012.01.009.

Abeliovich, Hagai. 2015. 'Regulation of Autophagy by Amino Acid Availability in S. Cerevisiae and Mammalian Cells'. *Amino Acids* 47 (10): 2165–75. https://doi.org/10.1007/s00726-014-1787-y.

Adachi, Atsuhiro, Michiko Koizumi, and Yoshinori Ohsumi. 2017. 'Autophagy Induction under Carbon Starvation Conditions Is Negatively Regulated by Carbon Catabolite Repression'. *Journal of Biological Chemistry* 292 (48): 19905–18. https://doi.org/10.1074/jbc.M117.817510.

Ahuatzi, Deifilia, Alberto Riera, Rafael Peláez, Pilar Herrero, and Fernando Moreno. 2007. 'Hxk2 Regulates the Phosphorylation State of Mig1 and Therefore Its Nucleocytoplasmic Distribution'. *Journal of Biological Chemistry* 282 (7): 4485–93. https://doi.org/10.1074/JBC.M606854200.

Alepuz, Paula M., Kyle W. Cunningham, and Francisco Estruch. 1997. 'Glucose Repression Affects Ion Homeostasis in Yeast through the Regulation of the Stress-Activated ENA1 Gene'. *Molecular Microbiology* 26 (1): 91–98. https://doi.org/10.1046/J.1365-2958.1997.5531917.X.

Almeida, Teresa, Marta Marques, Dominik Mojzita, Maria A. Amorim, Rui D. Silva, Bruno Almeida, Pedro Rodrigues, et al. 2008. 'Isc1p Plays a Key Role in Hydrogen Peroxide Resistance and Chronological Lifespan through Modulation of Iron Levels and Apoptosis'. *Molecular Biology of the Cell* 19 (3): 865. https://doi.org/10.1091/MBC.E07-06-0604.

Alonso-Rodríguez, Esmeralda, Pablo Fernández-Piñar, Almudena Sacristán-Reviriego, María Molina, and Humberto Martín. 2016. 'An Analog-Sensitive Version of the Protein Kinase Slt2 Allows Identification of Novel Targets of the Yeast Cell Wall Integrity Pathway'. *Journal of Biological Chemistry* 291 (11): 5461–72. https://doi.org/10.1074/JBC.M115.683680.

Alvers, Ashley L., Laura K. Fishwick, Michael S. Wood, Doreen Hu, Hye S. Chung, William A. Dunn, and John P. Aris. 2009. 'Autophagy and Amino Acid Homeostasis Are Required for Chronological Longevity in Saccharomyces Cerevisiae'. *Aging Cell* 8 (4): 353–69. https://doi.org/10.1111/j.1474-9726.2009.00469.x.

Aman, Yahyah, Tomas Schmauck-Medina, Malene Hansen, Richard I. Morimoto, Anna Katharina Simon, Ivana Bjedov, Konstantinos Palikaras, et al. 2021. 'Autophagy in Healthy Aging and Disease'. *Nature Aging* 1 (8): 634–50. https://doi.org/10.1038/S43587-021-00098-4.

Andrews, Brenda J., and Lynda A. Moore. 1992. 'Interaction of the Yeast Swi4 and Swi6 Cell Cycle Regulatory Proteins in Vitro'. *Proceedings of the National Academy of Sciences of the United States of America* 89 (24): 11852–56. https://doi.org/10.1073/PNAS.89.24.11852.

Angajala, Anusha, Sangbin Lim, Joshua B. Phillips, Jin Hwan Kim, Clayton Yates, Zongbing You, and Ming Tan. 2018. 'Diverse Roles of Mitochondria in Immune Responses: Novel Insights Into Immuno-Metabolism'. *Frontiers in Immunology* 9 (JUL). https://doi.org/10.3389/FIMMU.2018.01605.

Aoki, Yoshimasa, Tomotake Kanki, Yuko Hirota, Yusuke Kurihara, Tetsu Saigusa, Takeshi Uchiumi, and Dongchon Kang. 2011. 'Phosphorylation of Serine 114 on Atg32 Mediates Mitophagy'. *Molecular Biology of the Cell* 22 (17): 3206–17. https://doi.org/10.1091/MBC.E11-02-0145/ASSET/IMAGES/LARGE/3206FIG6.JPEG.

Ariño, Joaquín. 2011. 'ELS LLEVATS COM A ORGANISME MODEL DE RECERCA EN

BIOLOGIA'. *Organismes Model En Biologia* 62 (June). https://doi.org/10.2436/20.1501.02.103.

Aronova, Sofia, Karen Wedaman, Pavel A Aronov, Kristin Fontes, Karmela Ramos, Bruce D Hammock, and Ted Powers. 2008. 'Regulation of Ceramide Biosynthesis by TOR Complex 2'. *Cell Metabolism* 7: 148–58. https://doi.org/10.1016/j.cmet.2007.11.015.

Ashrafi, K., S. S. Lin, J. K. Manchester, and J. I. Gordon. 2000. 'Sip2p and Its Partner Snf1p Kinase Affect Aging in S. Cerevisiae'. *Genes & Development* 14 (15): 1872. https://doi.org/10.1101/gad.14.15.1872.

Aubert, Geraldine, and Peter M. Lansdorp. 2008. 'Telomeres and Aging'. *Physiological Reviews* 88 (2): 557–79. https://doi.org/10.1152/PHYSREV.00026.2007.

Babele, Piyoosh Kumar, Pilendra Kumar Thakre, Ramesh Kumawat, and Raghuvir Singh Tomar. 2018. 'Zinc Oxide Nanoparticles Induce Toxicity by Affecting Cell Wall Integrity Pathway, Mitochondrial Function and Lipid Homeostasis in Saccharomyces Cerevisiae'. *Chemosphere* 213 (December): 65–75. https://doi.org/10.1016/J.CHEMOSPHERE.2018.09.028.

Bankov, Katrin, Falko Schulze, Steffen Gretser, Henning Reis, Nada Abedin, Fabian Finkelmeier, Jörg Trojan, et al. 2023. 'Active Autophagy Is Associated with Favorable Outcome in Patients with Surgically Resected Cholangiocarcinoma'. *Cancers* 15 (17). https://doi.org/10.3390/CANCERS15174322.

Baranwal, Shivani, Gajendra Kumar Azad, Vikash Singh, and Raghuvir S. Tomar. 2014. 'Signaling of Chloroquine-Induced Stress in the Yeast Saccharomyces Cerevisiae Requires the Hog1 and Slt2 Mitogen-Activated Protein Kinase Pathways'. *Antimicrobial Agents and Chemotherapy* 58 (9): 5552. https://doi.org/10.1128/AAC.02393-13.

Barbosa, María Carolina, Rubén Adrián Grosso, and Claudio Marcelo Fader. 2018. 'Hallmarks of Aging: An Autophagic Perspective'. *Frontiers in Endocrinology* 9 (JAN). https://doi.org/10.3389/FENDO.2018.00790.

Barnett, James A. 2003. 'Beginnings of Microbiology and Biochemistry: The Contribution of Yeast Research'. *Microbiology* 149 (3): 557–67. https://doi.org/10.1099/mic.0.26089-0.

Barrett, Lakisha, Marianna Orlova, Marcin Maziarz, and Sergei Kuchin. 2012. 'Protein Kinase a Contributes to the Negative Control of SNF1 Protein Kinase in Saccharomyces Cerevisiae'. *Eukaryotic Cell* 11 (2): 119–28. https://doi.org/10.1128/EC.05061-11.

Beeler, Troy, Dagmar Bacikova, Ken Gable, Lisa Hopkins, Courtney Johnson, Harry Slife, and Teresa Dunn. 1998. 'The Saccharomyces Cerevisiae TSC10/YBR265W Gene Encoding 3- Ketosphinganine Reductase Is Identified in a Screen for Temperature-Sensitive Suppressors of the Ca2+-Sensitive Csg2Δ Mutant'. *Journal of Biological Chemistry* 273 (46): 30688–94. https://doi.org/10.1074/jbc.273.46.30688.

Berchtold, Doris, Manuele Piccolis, Nicolas Chiaruttini, Isabelle Riezman, Howard Riezman, Aurélien Roux, Tobias C. Walther, and Robbie Loewith. 2012. 'Plasma Membrane Stress Induces Relocalization of Slm Proteins and Activation of TORC2 to Promote Sphingolipid Synthesis'. *Nature Cell Biology 2012 14:5* 14 (5): 542–47. https://doi.org/10.1038/ncb2480.

Bermejo, Clara, Raúl García, Andrea Straede, José M. Rodríguez-Peña, César Nombela, Jürgen J. Heinisch, and Javier Arroyo. 2010. 'Characterization of Sensor-Specific Stress Response by Transcriptional Profiling of Wsc1 and Mid2 Deletion Strains and Chimeric Sensors in Saccharomyces Cerevisiae'. *Omics : A Journal of Integrative Biology* 14 (6): 679–88. https://doi.org/10.1089/OMI.2010.0060.

Bhatia-Kissova, Ingrid, and Nadine Camougrand. 2021. 'Mitophagy in Yeast: Decades of Research'. *Cells* 10 (12): 1–22. https://doi.org/10.3390/cells10123541.

Billia, Filio, Ludger Hauck, Filip Konecny, Vivek Rao, Jie Shen, and Tak Wah Mak. 2011. 'PTEN-Inducible Kinase 1 (PINK1)/Park6 Is Indispensable for Normal Heart Function'.

Proceedings of the National Academy of Sciences of the United States of America 108 (23): 9572–77. https://doi.org/10.1073/PNAS.1106291108.

Binda, Matteo, Marie Pierre Péli-Gulli, Grégory Bonfils, Nicolas Panchaud, Jörg Urban, Thomas W. Sturgill, Robbie Loewith, and Claudio De Virgilio. 2009. 'The Vam6 GEF Controls TORC1 by Activating the EGO Complex'. *Molecular Cell* 35 (5): 563–73. https://doi.org/10.1016/J.MOLCEL.2009.06.033.

Bonawitz, Nicholas D., Marc Chatenay-Lapointe, Yong Pan, and Gerald S. Shadel. 2007. 'Reduced TOR Signaling Extends Chronological Life Span via Increased Respiration and Upregulation of Mitochondrial Gene Expression'. *Cell Metabolism* 5 (4): 265–77. https://doi.org/10.1016/j.cmet.2007.02.009.

Bonilla, Myriam, and Kyle W. Cunningham. 2003. 'Mitogen-Activated Protein Kinase Stimulation of Ca2+ Signaling Is Required for Survival of Endoplasmic Reticulum Stress in Yeast'. *Molecular Biology of the Cell* 14 (10): 4296. https://doi.org/10.1091/MBC.E03-02-0113.

Boutouja, Fahd, and Harald W. Platta. 2020. 'Autophagy Stimulus-Dependent Role of the Small GTPase Ras2 in Peroxisome Degradation'. *Biomolecules* 10 (11): 1–14. https://doi.org/10.3390/BIOM10111553.

Breitenbach, Michael, S. Michal Jazwinski, and Peter Laun. 2012. *Aging Research in Yeast*. Springer Dordrecht Heidelberf. https://doi.org/10.1007/978-94-007-2561-4.

Brejning, Jeanette, and Lene Jespersen. 2002. 'Protein Expression during Lag Phase and Growth Initiation in Saccharomyces Cerevisiae'. *International Journal of Food Microbiology* 75 (1–2): 27–38. https://doi.org/10.1016/S0168-1605(01)00726-7.

Breslow, David K., Sean R. Collins, Bernd Bodenmiller, Ruedi Aebersold, Kai Simons, Andrej Shevchenko, Christer S. Ejsing, and Jonathan S. Weissman. 2010. 'Orm Family Proteins Mediate Sphingolipid Homeostasis'. *Nature* 463 (7284): 1048. https://doi.org/10.1038/NATURE08787.

Budovskaya, Yelena V, Joseph S Stephan, Fulvio Reggiori, Daniel J Klionsky, and Paul K Herman. 2004. 'The Ras/CAMP-Dependent Protein Kinase Signaling Pathway Regulates an Early Step of the Autophagy Process in Saccharomyces Cerevisiae'. *J Biol Chem.* 279 (20): 20663–71.

Busti, Stefano, Paola Coccetti, Lilia Alberghina, and Marco Vanoni. 2010. 'Glucose Signaling-Mediated Coordination of Cell Growth and Cell Cycle in Saccharomyces Cerevisiae'. *Sensors* 10 (6): 6195–6240. https://doi.org/10.3390/s100606195.

Caligaris, Marco, Raffaele Nicastro, Zehan Hu, Farida Tripodi, Johannes Erwin Hummel, Benjamin Pillet, Marie Anne Deprez, et al. 2023. 'Snf1/AMPK Fine-Tunes TORC1 Signaling in Response to Glucose Starvation'. *ELife* 12: 1–29. https://doi.org/10.7554/eLife.84319.

Camiolo, Giuseppina, Alessandro Barbato, Cesarina Giallongo, Nunzio Vicario, Alessandra Romano, Nunziatina L. Parrinello, Rosalba Parenti, et al. 2020. 'Iron Regulates Myeloma Cell/Macrophage Interaction and Drives Resistance to Bortezomib'. *Redox Biology* 36 (September). https://doi.org/10.1016/J.REDOX.2020.101611.

Camonis, J. H., M. Kalékine, B. Gondré, H. Garreau, E. Boy-Marcotte, and M. Jacquet. 1986. 'Characterization, Cloning and Sequence Analysis of the CDC25 Gene Which Controls the Cyclic AMP Level of Saccharomyces Cerevisiae.' *The EMBO Journal* 5 (2): 375. https://doi.org/10.1002/J.1460-2075.1986.TB04222.X.

Capon, Daniel J., Peter H. Seeburg, John P. McGrath, Joel S. Hayflick, Ursula Edman, Arthur D. Levinson, and David V. Goeddel. 1983. 'Activation of Ki-Ras2 Gene in Human Colon and Lung Carcinomas by Two Different Point Mutations'. *Nature 1983 304:5926* 304 (5926): 507–13. https://doi.org/10.1038/304507a0.

Carvelli, Tiziana, and Alvaro Galli. 2021. 'Yeast as a Tool to Understand the Significance of

Human Disease-Associated Gene VAriants'. *Genes* 12 (9). https://doi.org/10.3390/genes12091303.

Caspani, Giorgio, Paolo Tortora, Giorgio M. Hanozet, and Andrea Guerritore. 1985. 'Glucose-Stimulated CAMP Increase May Be Mediated by Intracellular Acidification in Saccharomyces Cerevisiae'. *FEBS Letters* 186 (1): 75–79. https://doi.org/10.1016/0014-5793(85)81342-9.

Castell, Carmen, Encarnación Díaz-Santos, Luis G. Heredia-Martínez, Luis López-Maury, José M. Ortega, José A. Navarro, Mercedes Roncel, and Manuel Hervás. 2022. 'Iron Deficiency Promotes the Lack of Photosynthetic Cytochrome C550 and Affects the Binding of the Luminal Extrinsic Subunits to Photosystem II in the Diatom Phaeodactylum Tricornutum'. *International Journal of Molecular Sciences* 23 (20). https://doi.org/10.3390/IJMS232012138.

Castells-Roca, Laia, Ulrich Mühlenhoff, Roland Lill, Enrique Herrero, and Gemma Bellí. 2011. 'The Oxidative Stress Response in Yeast Cells Involves Changes in the Stability of Aft1 Regulon MRNA'. *Molecular Microbiology* 8 (1): 232–48. https://doi.org/10.1111/j.1365-2958.2011.07689.x.

Castilho, Beatriz A., Renuka Shanmugam, Richard C. Silva, Rashmi Ramesh, Benjamin M. Himme, and Evelyn Sattlegger. 2014. 'Keeping the EIF2 Alpha Kinase Gcn2 in Check'. *Biochimica et Biophysica Acta - Molecular Cell Research* 1843 (9): 1948–68. https://doi.org/10.1016/j.bbamcr.2014.04.006.

Celenza, J L, and M Carlson. 1984. 'Structure and Expression of the SNF1 Gene of Saccharomyces Cerevisiae'. *Molecular and Cellular Biology* 4 (1): 54–60. https://doi.org/10.1128/MCB.4.1.54-60.1984.

Chen, Yijun, Douglas E Feldman, Changchun Deng, James A Brown, Anthony F De Giacomo, Allison F Gaw, Gongyi Shi, Quynh T Le, J Martin Brown, and Albert C Koong. 2005. 'Identification of Mitogen-Activated Protein Kinase Signaling Pathways That Confer Resistance to Endoplasmic Reticulum Stress in Saccharomyces Cerevisiae Developing Novel Treatments for Lymphoma View Project Identification of Mitogen-Activated Protein Kina'. https://doi.org/10.1158/1541-7786.MCR-05-0181.

Cheung, Johnson, Michael E.P. Murphy, and David E. Heinrichs. 2012. 'Discovery of an Iron-Regulated Citrate Synthase in Staphylococcus Aureus'. *Chemistry & Biology* 19 (12): 1568–78. https://doi.org/10.1016/J.CHEMBIOL.2012.10.003.

Chua, Jason P., Hortense De Calbiac, Edor Kabashi, and Sami J. Barmada. 2022. 'Autophagy and ALS: Mechanistic Insights and Therapeutic Implications'. *Autophagy* 18 (2). https://doi.org/10.1080/15548627.2021.1926656.

Claret, Sandra, Xavier Gatti, François Doignon, Didier Thoraval, and Marc Crouzet. 2005. 'The Rgd1p Rho GTPase-Activating Protein and the Mid2p Cell Wall Sensor Are Required at Low PH for Protein Kinase C Pathway Activation and Cell Survival in Saccharomyces Cerevisiae'. *EUKARYOTIC CELL* 4 (8): 1375–86. https://doi.org/10.1128/EC.4.8.1375-1386.2005.

Colombo, Sonia, Pingsheng Ma, Liesbet Cauwenberg, Joris Winderickx, Marion Crauwels, Aloys Teunissen, David Nauwelaers, et al. 1998. 'Involvement of Distinct G-Proteins, Gpa2 and Ras, in Glucose- and Intracellular Acidification-Induced CAMP Signalling in the Yeast Saccharomyces Cerevisiae'. *The EMBO Journal* 17 (12): 3326–41. https://doi.org/10.1093/EMBOJ/17.12.3326.

Colombo, Sonia, Daniela Ronchetti, Johan M. Thevelein, Joris Winderickx, and Enzo Martegani. 2004. 'Activation State of the Ras2 Protein and Glucose-Induced Signaling in Saccharomyces Cerevisiae'. *Journal of Biological Chemistry* 279 (45): 46715–22. https://doi.org/10.1074/JBC.M405136200.

Conrad, Michaela, Joep Schothorst, Harish Nag Kankipati, Griet Van Zeebroeck, Marta Rubio-

Texeira, and Johan M. Thevelein. 2014. 'Nutrient Sensing and Signaling in the Yeast Saccharomyces Cerevisiae'. *FEMS Microbiology Reviews* 38 (2): 254–99. https://doi.org/10.1111/1574-6976.12065.

Cook, A., and P. Giunti. 2017. 'Friedreich's Ataxia: Clinical Features, Pathogenesis and Management'. *British Medical Bulletin* 124 (1): 19. https://doi.org/10.1093/BMB/LDX034.

Córcoles-Sáez, Isaac, Lídia Ballester-Tomas, Maria A. De La Torre-Ruiz, Jose A. Prieto, and Francisca Randez-Gil. 2012. 'Low Temperature Highlights the Functional Role of the Cell Wall Integrity Pathway in the Regulation of Growth in Saccharomyces Cerevisiae'. *Biochemical Journal* 446 (3): 477–88. https://doi.org/10.1042/BJ20120634.

Costanzo, Michael, Anastasia Baryshnikova, Jeremy Bellay, Yungil Kim, Eric D Spear, Carolyn S Sevier, Huiming Ding, et al. 2010. 'The Genetic Landscape of a Cell' 327 (January): 425–32.

Crane, Matthew M., Kenneth L. Chen, Ben W. Blue, and Matt Kaeberlein. 2020. 'Trajectories of Aging: How Systems Biology in Yeast Can Illuminate Mechanisms of Personalized Aging'. *Proteomics* 20 (5–6). https://doi.org/10.1002/pmic.201800420.

Crespo, José L., and Michael N. Hall. 2002. 'Elucidating TOR Signaling and Rapamycin Action: Lessons from Saccharomyces Cerevisiae'. *Microbiology and Molecular Biology Reviews* 66 (4): 579. https://doi.org/10.1128/MMBR.66.4.579-591.2002.

Czubowicz, Kinga, Henryk Jęśko, Przemysław Wencel, Walter J. Lukiw, and Robert P. Strosznajder. 2019. 'The Role of Ceramide and Sphingosine-1-Phosphate in Alzheimer's Disease and Other Neurodegenerative Disorders'. *Molecular Neurobiology* 56 (8): 5436–55. https://doi.org/10.1007/S12035-018-1448-3.

Dardalhon, Michèle, Bernadette Agoutin, Malene Watzinger, and Dietrich Averbeck. 2009. 'Slt2 (Mpk1) MAP Kinase Is Involved in the Response of Saccharomyces Cerevisiae to 8-Methoxypsoralen plus UVA'. *Journal of Photochemistry and Photobiology. B, Biology* 95 (3): 148–55. https://doi.org/10.1016/J.JPHOTOBIOL.2009.02.001.

Dashko, Sofia, Nerve Zhou, Concetta Compagno, and Jure Piškur. 2014. 'Why, When, and How Did Yeast Evolve Alcoholic Fermentation?' *FEMS Yeast Research* 14 (6): 826–32. https://doi.org/10.1111/1567-1364.12161.

Davenport, Kenneth R., Michael Sohaskey, Yoshiaki Kamada, David E. Levin, and Michael C. Gustin. 1995. 'A Second Osmosensing Signal Transduction Pathway in Yeast: HYPOTONIC SHOCK ACTIVATES THE PKC1 PROTEIN KINASE-REGULATED CELL INTEGRITY PATHWAY'. *Journal of Biological Chemistry* 270 (50): 30157–61. https://doi.org/10.1074/JBC.270.50.30157.

Delahodde, Agnès, Rudy Pandjaitan, Marisol Corral-Debrinski, and Claude Jacq. 2001. 'Pse1/Kap121-Dependent Nuclear Localization of the Major Yeast Multidrug Resistance (MDR) Transcription Factor Pdr1'. *Molecular Microbiology* 39 (2): 304–13. https://doi.org/10.1046/J.1365-2958.2001.02182.X.

Delley, Pierre Alain, and Michael N. Hall. 1999. 'Cell Wall Stress Depolarizes Cell Growth via Hyperactivation of Rho1'. *The Journal of Cell Biology* 147 (1): 163. https://doi.org/10.1083/JCB.147.1.163.

Delorme-Axford, Elizabeth, and Daniel J. Klionsky. 2018. 'Transcriptional and Post-Transcriptional Regulation of Autophagy in the Yeast Saccharomyces Cerevisiae'. *Journal of Biological Chemistry* 293 (15): 5396–5403. https://doi.org/10.1074/jbc.R117.804641.

Deng, Rong, Hai Liang Zhang, Jun Hao Huang, Rui Zhao Cai, Yan Wang, Yu Hong Chen, Bing Xin Hu, et al. 2021. 'MAPK1/3 Kinase-Dependent ULK1 Degradation Attenuates Mitophagy and Promotes Breast Cancer Bone Metastasis'. *Autophagy* 17 (10): 3011–29. https://doi.org/10.1080/15548627.2020.1850609.

Deprez, Marie Anne, Elja Eskes, Joris Winderickx, and Tobias Wilms. 2018. 'The TORC1-Sch9 Pathway as a Crucial Mediator of Chronological Lifespan in the Yeast Saccharomyces Cerevisiae'. *FEMS Yeast Research* 18 (5): 1–15. https://doi.org/10.1093/femsyr/foy048.

Deretic, Vojo. 2021. 'Autophagy in Inflammation, Infection, and Immunometabolism'. *Immunity* 54 (3): 437–53. https://doi.org/10.1016/J.IMMUNI.2021.01.018.

Dever, Thomas E., Lan Feng, Ronald C. Wek, A. Mark Cigan, Thomas F. Donahue, and Alan G. Hinnebusch. 1992. 'Phosphorylation of Initiation Factor 2α by Protein Kinase GCN2 Mediates Gene-Specific Translational Control of GCN4 in Yeast'. *Cell* 68 (3): 585–96. https://doi.org/10.1016/0092-8674(92)90193-G.

Dever, Thomas E, Weimin Yang, Stefan Åstro¨m, Åstro¨ Åstro¨m, Anders S Bystro¨mbystro¨bystro¨m, and Alan G Hinnebusch. 1995. 'Modulation of TRNA i Met , EIF-2, and EIF-2B Expression Shows That GCN4 Translation Is Inversely Coupled to the Level of EIF-2 GTP Met-TRNA i Met Ternary Complexes'. *MOLECULAR AND CELLULAR BIOLOGY* 15 (11): 6351–63.

Dickson, Robert C. 2008. 'New Insights into Sphingolipid Metabolism and Function in Budding Yeast'. *Journal of Lipid Research* 49 (5): 909–21. https://doi.org/10.1194/jlr.R800003-JLR200. 2010. 'Roles for Sphingolipids in Saccharomyces Cerevisiae'. *Advances in Experimental Medicine and Biology* 688: 217–31. https://doi.org/10.1007/978-1-4419-6741-1_15.

Dickson, Robert C., Elzbieta E. Nagiec, Marek Skrzypek, Philip Tillman, Gerald B. Wells, and Robert L. Lester. 1997. 'Sphingolipids Are Potential Heat Stress Signals in Saccharomyces'. *The Journal of Biological Chemistry* 272 (48): 30196–200. https://doi.org/10.1074/JBC.272.48.30196.

Dickson, Robert C., Elzbieta E. Nagiec, Gerald B. Wells, M. Marek Nagiec, and Robert L. Lester. 1997. 'Synthesis of Mannose-(Inositol-P)2-Ceramide, the Major Sphingolipid in Saccharomyces Cerevisiae, Requires the IPT1 (YDR072c) Gene'. *The Journal of Biological Chemistry* 272 (47): 29620–25. https://doi.org/10.1074/JBC.272.47.29620.

Dix, David R, Jamie T Bridgham, Margaret A Broderius, Craig A Byersdorfer, and David J Eide. 1994. 'The FET4 Gene Encodes the Low Affinity Fe(II) Transport Protein of Saccharomyces Cerevisiae'. *The Journal of Biological Chemistry* 269 (21): 26092–99.

Dong, Yan, Hengwen Chen, Jialiang Gao, Yongmei Liu, Jun Li, and Jie Wang. 2019. 'Molecular Machinery and Interplay of Apoptosis and Autophagy in Coronary Heart Disease'. *Journal of Molecular and Cellular Cardiology* 136 (November): 27–41. https://doi.org/10.1016/J.YJMCC.2019.09.001.

Dosil, Mercedes. 2011. 'Ribosome Synthesis-Unrelated Functions of the Preribosomal Factor Rrp12 in Cell Cycle Progression and the DNA Damage Response'. *Molecular and Cellular Biology* 31 (12): 2422. https://doi.org/10.1128/MCB.05343-11.

Du, Jie, Yulin Li, and Wei Zhao. 2020. 'Autophagy and Myocardial Ischemia'. *Advances in Experimental Medicine and Biology* 1207: 217–22. https://doi.org/10.1007/978-981-15-4272-5_15.

Dubouloz, Frédérique, Olivier Deloche, Valeria Wanke, Elisabetta Cameroni, and Claudio De Virgilio. 2005. 'The TOR and EGO Protein Complexes Orchestrate Microautophagy in Yeast'. *Molecular Cell* 19 (1): 15–26. https://doi.org/10.1016/J.MOLCEL.2005.05.020.

Dunayevich, Paula, Rodrigo Baltanás, José Antonio Clemente, Alicia Couto, Daiana Sapochnik, Gustavo Vasen, and Alejandro Colman-Lerner. 2018. 'Heat-Stress Triggers MAPK Crosstalk to Turn on the Hyperosmotic Response Pathway'. *Scientific Reports* 8 (1): 1–15. https://doi.org/10.1038/s41598-018-33203-6.

Düvel, Katrin, Arti Santhanam, Stephen Garret, Lisa Schneper, and James R. Broach. 2003. 'Multiple Roles of Tap42 in Mediating Rapamycin-Induced Transcriptional Changes in

Yeast'. *Molecular Cell* 11: 1467–78. https://doi.org/10.1007/978-3-642-18930-2_2.

Ecker, Nitai, Angelica Mor, Dikla Journo, Hagai Abeliovich, Nitai Ecker, Angelica Mor, Dikla Journo, and Hagai Abeliovich. 2010. 'Deprivation Is Distinct from Nitrogen Starvation-Induced Macroautophagy Induction of Autophagic Flux by Amino Acid Deprivation Is Distinct from Nitrogen Starvation-Induced Macroautophagy'. *Autophagy* 8627. https://doi.org/10.4161/auto.6.7.12753.

Eiyama, Akinori, and Koji Okamoto. 2017. 'Assays for Mitophagy in Yeast'. *Methods in Molecular Biology* 1567: 337–47. https://doi.org/10.1007/978-1-4939-6824-4_20.

Emanuele, Enzo, Piercarlo Minoretti, Fabian Sanchis-Gomar, Helios Pareja-Galeano, Yusuf Yilmaz, Nuria Garatachea, and Alejandro Lucia. 2014. 'Can Enhanced Autophagy Be Associated with Human Longevity? Serum Levels of the Autophagy Biomarker Beclin-1 Are Increased in Healthy Centenarians'. *Rejuvenation Research* 17 (6): 518–24. https://doi.org/10.1089/REJ.2014.1607.

Fabrizio, Paola, Lee Loung Liou, Vanessa N. Moy, Alberto Diaspro, Joan Selverstone Valentine, Edith Butler Gralla, and Valter D. Longo. 2003. 'SOD2 Functions Downstream of Sch9 to Extend Longevity in Yeast'. *Genetics* 163 (1): 35–46. https://doi.org/10.1093/genetics/163.1.35.

Fabrizio, Paola, and Valter D. Longo. 2008. 'Chronological Aging-Induced Apoptosis in Yeast'. *Biochimica et Biophysica Acta - Molecular Cell Research* 1783 (7): 1280–85. https://doi.org/10.1016/j.bbamcr.2008.03.017.

Fadri, Maria, Alexes Daquinag, Shimei Wang, Tao Xue, and Jeannette Kunz. 2005. 'The Pleckstrin Homology Domain Proteins Slm1 and Slm2 Are Required for Actin Cytoskeleton Organization in Yeast and Bind Phosphatidylinositol-4,5-Bisphosphate and TORC2'. *Molecular Biology of the Cell* 16 (4): 1883. https://doi.org/10.1091/MBC.E04-07-0564.

Fernandis, Aaron Z., and Markus R. Wenk. 2007. 'Membrane Lipids as Signaling Molecules'. *Current Opinion in Lipidology* 18 (2): 121–28. https://doi.org/10.1097/MOL.0B013E328082E4D5.

Freist, Wolfgang, Janko F. Verhey, Andreas Rühlmann, Dieter H. Gauss, and John G. Arnez. 1999. 'Histidyl-TRNA Synthetase'. *Biological Chemistry* 380 (6): 623–46. https://doi.org/10.1515/BC.1999.079.

Fresques, Tara, Brad Niles, Sofia Aronova, Huzefa Mogri, Taha Rakhshandehroo, and Ted Powers. 2015. 'Regulation of Ceramide Synthase by Casein Kinase 2-Dependent Phosphorylation in Saccharomyces Cerevisiae'. *The Journal of Biological Chemistry* 290 (3): 1395. https://doi.org/10.1074/JBC.M114.621086.

Fujioka, Yuko, Nobuo N. Noda, Hitoshi Nakatogawa, Yoshinori Ohsumi, and Fuyuhiko Inagaki. 2010. 'Dimeric Coiled-Coil Structure of Saccharomyces Cerevisiae Atg16 and Its Functional Significance in Autophagy'. *The Journal of Biological Chemistry* 285 (2): 1508–15. https://doi.org/10.1074/JBC.M109.053520.

Fukuda, Tomoyuki, Kentaro Furukawa, Tatsuro Maruyama, Shun ichi Yamashita, Daisuke Noshiro, Chihong Song, Yuta Ogasawara, et al. 2023. 'The Mitochondrial Intermembrane Space Protein Mitofissin Drives Mitochondrial Fission Required for Mitophagy'. *Molecular Cell* 83 (12): 2045-2058.e9. https://doi.org/10.1016/j.molcel.2023.04.022.

Funato, Kouichi, Béatrice Vallée, and Howard Riezman. 2002. 'Biosynthesis and Trafficking of Sphingolipids in the Yeast Saccharomyces Cerevisiae'. *Biochemistry* 41 (51): 15105–14. https://doi.org/10.1021/bi026616d.

Gable, Ken, Harry Slife, Dagmar Bacikova, Erin Monaghan, and Teresa M. Dunn. 2000. 'Tsc3p Is an 80-Amino Acid Protein Associated with Serine Palmitoyltransferase and Required for Optimal Enzyme Activity'. *The Journal of Biological Chemistry* 275 (11): 7597–7603. https://doi.org/10.1074/JBC.275.11.7597.

Galdieri, Luciano, Swati Mehrotra, Sean Yu, and Ales Vancura. 2010. 'Transcriptional Regulation in Yeast during Diauxic Shift and Stationary Phase'. *OMICS A Journal of Integrative Biology* 14 (6): 629–38. https://doi.org/10.1089/omi.2010.0069.

Gallego, Carme, Garí Eloi, Neus Colomina, Herrero Enrique, and Martí Aldea. 1997. 'The Cln3 Cyclin Is Down-Regulated by Translational Repression and Degradation during the G1 Arrest Caused by Nitrogen Deprivation in Budding Yeast'. *The EMBO Journal* 16 (23): 7196–7206. https://doi.org/10.1093/emboj/16.23.7196.

Gao, Weitong, Xueying Wang, Yang Zhou, Xueqian Wang, and Yan Yu. 2022. 'Autophagy, Ferroptosis, Pyroptosis, and Necroptosis in Tumor Immunotherapy'. *Signal Transduction and Targeted Therapy* 7 (1). https://doi.org/10.1038/S41392-022-01046-3.

García-Rodríguez, Luis J., Rosario Valle, Ángel Durán, and César Roncero. 2005. 'Cell Integrity Signaling Activation in Response to Hyperosmotic Shock in Yeast'. *FEBS Letters* 579 (27): 6186–90. https://doi.org/10.1016/J.FEBSLET.2005.10.001.

Gasch, A. P., P. T. Spellman, C. M. Kao, O. Carmel-Harel, M. B. Eisen, G. Storz, D. Botstein, and P. O. Brown. 2000. 'Genomic Expression Programs in the Response of Yeast Cells to Environmental Changes'. *Molecular Biology of the Cell* 11 (12): 4241. https://doi.org/10.1091/MBC.11.12.4241.

Goffeau, A., G. Barrell, H. Bussey, R. W. Davis, B. Dujon, H. Feldmann, F. Galibert, et al. 1996. 'Life with 6000 Genes'. *Science* 274 (5287): 546–67. https://doi.org/10.1126/SCIENCE.274.5287.546.

Goldstein, Alan L, and John H McCusker. 1999. 'Three New Dominant Drug Resistance Cassettes for Gene Disruption in Saccharomyces Cerevisiae'. *Yeast* 15: 1541–53. https://doi.org/10.1002/(SICI)1097-0061(199910)15:14.

González-Rubio, Gema, Ángela Sellers-Moya, Humberto Martín, and María Molina. 2021. 'A Walk-through MAPK Structure and Functionality with the 30-Year-Old Yeast MAPK Slt2'. *International Microbiology* 24 (4): 531–43. https://doi.org/10.1007/s10123-021-00183-z.

González, Asier, and Michael N Hall. 2017a. 'Nutrient Sensing and TOR Signaling in Yeast and Mammals'. *The EMBO Journal* 36 (4): 397–408. https://doi.org/10.15252/EMBJ.201696010.

Görner, Wolfram, Erich Durchschlag, Maria Teresa Martinez-pastor, Francisco Estruch, Gustav Ammerer, Barbara Hamilton, Helmut Ruis, and Christoph Schu. 1998. 'Nuclear Localization of the C2H2 Zinc Finger Protein Msn2p Is Regulated by Stress and Protein Kinase A Activity'. *Genes Development*, 586–97.

Görner, Wolfram, Erich Durchschlag, Maria Teresa Martinez-Pastor, Francisco Estruch, Gustav Ammerer, Barbara Hamilton, Helmut Ruis, and Christoph Schüller. 1998. 'Nuclear Localization of the C2H2 Zinc Finger Protein Msn2p Is Regulated by Stress and Protein Kinase A Activity'. *Genes & Development* 12 (4): 586. https://doi.org/10.1101/GAD.12.4.586.

Gottfried, Susanne, Siaosi M.B.M.J. Koloamatangi, Clement Daube, Anja H. Schiemann, and Evelyn Sattlegger. 2022. 'A Genetic Approach to Identify Amino Acids in Gcn1 Required for Gcn2 Activation'. *PLoS ONE* 17 (11 November): 1–20. https://doi.org/10.1371/journal.pone.0277648.

Gourlay, C. W., and K. R. Ayscough. 2006. 'Actin-Induced Hyperactivation of the Ras Signaling Pathway Leads to Apoptosis in Saccharomyces Cerevisiae'. *Molecular and Cellular Biology* 26 (17): 6487–6501. https://doi.org/10.1128/MCB.00117-06.

Grahame, D, David Carling, and Marian Carlson. 1998. 'THE AMP-ACTIVATED/SNF1 PROTEIN KINASE SUBFAMILY: Metabolic Sensors of the Eukaryotic Cell?' www.annualreviews.org.

Gray, Joseph V., Gregory A. Petsko, Gerald C. Johnston, Dagmar Ringe, Richard A. Singer,

and Margaret Werner-Washburne. 2004. ‘ “Sleeping Beauty”: Quiescence in Saccharomyces Cerevisiae ’. *Microbiology and Molecular Biology Reviews* 68 (2): 187–206. https://doi.org/10.1128/mmbr.68.2.187-206.2004.

Gubas, Andrea, and Ivan Dikic. 2022. ‘ER Remodeling via ER-Phagy’. *Molecular Cell* 82 (8): 1492–1500. https://doi.org/10.1016/J.MOLCEL.2022.02.018.

Guedes, Ana, Paula Ludovico, and Belém Sampaio-Marques. 2016. ‘Caloric Restriction Alleviates Alpha-Synuclein Toxicity in Aged Yeast Cells by Controlling the Opposite Roles of Tor1 and Sir2 on Autophagy’. *Mechanisms of Ageing and Development*. https://doi.org/10.1016/j.mad.2016.04.006.

Guerreiro, Joana F., Alexander Muir, Subramaniam Ramachandran, Jeremy Thorner, and Sá Correia Isabel. 2016. ‘Sphingolipid Biosynthesis Upregulation by TOR Complex 2-Ypk1 Signaling during Yeast Adaptive Response to Acetic Acid Stress’. *The Biochemical Journal* 473 (23): 4311. https://doi.org/10.1042/BCJ20160565.

Guillas, Isabelle, Paul A. Kirchman, Rachel Chuard, Martine Pfefferli, James C. Jiang, S. Michal Jazwinski, and Andreas Conzelmann. 2001. ‘C26-CoA-Dependent Ceramide Synthesis of Saccharomyces Cerevisiae Is Operated by Lag1p and Lac1p’. *The EMBO Journal* 20 (11): 2655. https://doi.org/10.1093/EMBOJ/20.11.2655.

Guo, Jessie Yanxiang, Hsin Yi Chen, Robin Mathew, Jing Fan, Anne M. Strohecker, Gizem Karsli-Uzunbas, Jurre J. Kamphorst, et al. 2011. ‘Activated Ras Requires Autophagy to Maintain Oxidative Metabolism and Tumorigenesis’. *Genes & Development* 25 (5): 460–70. https://doi.org/10.1101/GAD.2016311.

Guo, Jing, and Wei Chung Chiang. 2022. ‘Mitophagy in Aging and Longevity’. *IUBMB Life* 74 (4): 296–316. https://doi.org/10.1002/IUB.2585.

Haak, Dale, Ken Gable, Troy Beeler, and Teresa Dunn. 1997. ‘Hydroxylation of Saccharomyces Cerevisiae Ceramides Requires Sur2p and Scs7p’. *The Journal of Biological Chemistry* 272 (47): 29704–10. https://doi.org/10.1074/JBC.272.47.29704.

Hagai, Abeliovich, Mostafa Zareic, T.G. Rigboltc Kristoffer, J. Youleb Richard, and Dengjelc Joern. 2017. ‘Involvement of Mitochondrial Dynamics in the Segregation of Mitochondrial Matrix Proteins during Stationary Phase Mitophagy’. *Physiology & Behavior* 176 (1): 100–106. https://doi.org/10.1038/ncomms3789.Involvement.

Hahn, Ji Sook, and Dennis J. Thiele. 2002. ‘Regulation of the Saccharomyces Cerevisiae Slt2 Kinase Pathway by the Stress-Inducible Sdp1 Dual Specificity Phosphatase’. *The Journal of Biological Chemistry* 277 (24): 21278–84. https://doi.org/10.1074/JBC.M202557200.

Harari, Yaniv, Lihi Gershon, Elisa Alonso-Perez, Shir Klein, Yael Berneman, Karan Choudhari, Pragyan Singh, Soumitra Sau, Batia Liefshitz, and Martin Kupiec. 2020. ‘Telomeres and Stress in Yeast Cells: When Genes and Environment Interact’. *Fungal Biology* 124 (5): 311–15. https://doi.org/10.1016/j.funbio.2019.09.003.

Haurie, Valérie, Hélian Boucherie, and Francis Sagliocco. 2003. ‘The Snf1 Protein Kinase Controls the Induction of Genes of the Iron Uptake Pathway at the Diauxic Shift in Saccharomyces Cerevisiae’. *Journal of Biological Chemistry* 278 (46): 45391–96. https://doi.org/10.1074/JBC.M307447200.

He, Congcong, and Daniel J. Klionsky. 2006. ‘Autophagy and Neurodegeneration’. *ACS Chemical Biology* 1 (4): 211–13. https://doi.org/10.1021/CB600182H.

Hechtberger, Petra, and Günther Daum. 1995. ‘Intracellular Transport of Inositol-Containing Sphingolipids in the Yeast, Saccharomyces Cerevisiae’. *FEBS Letters* 367 (2): 201–4. https://doi.org/10.1016/0014-5793(95)00567-S.

Hedbacker, Kristina, Robert Townley, and Marian Carlson. 2004. ‘Cyclic AMP-Dependent Protein Kinase Regulates the Subcellular Localization of Snf1-Sip1 Protein Kinase’. *Molecular and Cellular Biology* 24 (5): 1836. https://doi.org/10.1128/MCB.24.5.1836-1843.2004.

Heitman, Joseph, N. Rao Movva, and Michael N. Hall. 1991. 'Targets for Cell Cycle Arrest by the Immunosuppressant Rapamycin in Yeast'. *Science (New York, N.Y.)* 253 (5022): 905–9. https://doi.org/10.1126/SCIENCE.1715094.

Helliwell, Stephen B, Philipp Wagner, Jeannette Kunz, Maja Deuter-Reinhard, Ruben Henriquez, and Michael N Hall. 1994. 'TOR1 and TOR2 Are Structurally and Functionally Similar but Not Identical Phosphatidylinositol Kinase Homologues in Yeast'. *Molecular Biology of the Cell* 5: 105–18.

Herman, Paul K. 2002. 'Stationary Phase in Yeast'. *Current Opinion in Microbiology* 5 (6): 602–7. https://doi.org/10.1016/S1369-5274(02)00377-6.

Hernandez-Lopez, M.J, J.A Prieto, and F Randez-Gil. 2003. 'Osmotolerance and Leavening Ability in Sweet and Frozen Sweet Dough. Comparative Analysis between Torulaspora Delbrueckii and Saccharomyces Cerevisiae Baker's Yeast Strains', no. Evans 1990: 125–34.

Hinnebusch, A. G. 1984. 'Evidence for Translational Regulation of the Activator of General Amino Acid Control in Yeast'. *Proceedings of the National Academy of Sciences of the United States of America* 81 (20): 6442–46. https://doi.org/10.1073/PNAS.81.20.6442.

Hinnebusch, Alan G. 1986. 'The General Control of Amino Acid Biosynthetic Genes in the Yeast Saccharomyces Cerevisiae'. *CRC Critical Reviews in Biochemistry* 21 (3): 277–317. https://doi.org/10.3109/10409238609113614.

Hong, Seung Pyo, and Marian Carlson. 2007. 'Regulation of Snf1 Protein Kinase in Response to Environmental Stress'. *Journal of Biological Chemistry* 282 (23): 16838–45. https://doi.org/10.1074/jbc.M700146200.

Hong, Seung Pyo, Fiona C. Leiper, Angela Woods, David Carling, and Marian Carlson. 2003. 'Activation of Yeast Snf1 and Mammalian AMP-Activated Protein Kinase by Upstream Kinases'. *Proceedings of the National Academy of Sciences of the United States of America* 100 (15): 8839. https://doi.org/10.1073/PNAS.1533136100.

Honigberg, Saul M., and Rita H. Lee. 1998. 'Snf1 Kinase Connects Nutritional Pathways Controlling Meiosis in Saccharomyces Cerevisiae'. *Molecular and Cellular Biology* 18 (8): 4548–55. https://doi.org/10.1128/MCB.18.8.4548.

Hu, Yun, Enkai Liu, Xiaojia Bai, and Aili Zhang. 2010. 'The Localization and Concentration of the PDE2-Encoded High-Affinity CAMP Phosphodiesterase Is Regulated by CAMP-Dependent Protein Kinase A in the Yeast Saccharomyces Cerevisiae'. *FEMS Yeast Research* 10 (2): 177–87. https://doi.org/10.1111/j.1567-1364.2009.00598.x.

Huang, Hanghang, Tomoko Kawamata, Tetsuro Horie, Hiroshi Tsugawa, Yasumune Nakayama, Yoshinori Ohsumi, and Eiichiro Fukusaki. 2015. 'Bulk RNA Degradation by Nitrogen Starvation-Induced Autophagy in Yeast'. *The EMBO Journal* 34 (2): 154. https://doi.org/10.15252/EMBJ.201489083.

Huang, Yuxiang J, and Daniel J Klionsky. 2022. 'Yeast Mitophagy: Unanswered Questions', 1–18. https://doi.org/10.1016/j.bbagen.2021.129932.Yeast.

Huber, Alexandre, Sarah L. French, Hille Tekotte, Seda Yerlikaya, Michael Stahl, Mariya P. Perepelkina, Mike Tyers, Jacques Rougemont, Ann L. Beyer, and Robbie Loewith. 2011. 'Sch9 Regulates Ribosome Biogenesis via Stb3, Dot6 and Tod6 and the Histone Deacetylase Complex RPD3L'. *The EMBO Journal* 30 (15): 3052. https://doi.org/10.1038/EMBOJ.2011.221.

Hughes Hallett, James E., Xiangxia Luo, and Andrew P. Capaldi. 2014. 'State Transitions in the TORC1 Signaling Pathway and Information Processing in Saccharomyces Cerevisiae'. *Genetics* 198 (2): 773–86. https://doi.org/10.1534/genetics.114.168369.

Igual, J Carlos, Anthony L Johnson, and Leland H Johnston. 1996. 'Coordinated Regulation of Gene Expression by the Cell Cycle Transcription Factor SWI4 and the Protein Kinase C MAP Kinase Pathway for Yeast Cell Integrity'. *The EMBO Journal* 15 (18): 5001–13.

Innokentev, Aleksei, and Tomotake Kanki. 2021. 'Mitophagy in Yeast: Molecular Mechanism and Regulation'. *Cells* 10 (12). https://doi.org/10.3390/cells10123569.

Inoue, Hirofumi, Ken Ichi Kobayashi, Moussa Ndong, Yuji Yamamoto, Shin Ichi Katsumata, Kazuharu Suzuki, and Mariko Uehara. 2015. 'Activation of Nrf2/Keap1 Signaling and Autophagy Induction against Oxidative Stress in Heart in Iron Deficiency'. *Bioscience, Biotechnology, and Biochemistry* 79 (8): 1366–68. https://doi.org/10.1080/09168451.2015.1018125.

Inoue, Yuko, and Daniel J. Klionsky. 2010. 'Regulation of Macroautophagy in Saccharomyces Cerevisiae'. *Semin Cell Dev Biol* 21 (7): 664–70. https://doi.org/10.1016/j.semcdb.2010.03.009.

Irie, Kenji, Masanori Takase, Kyung S Lee, David E Levin, Hiroyuki Araki, Kunihiro Matsumoto,', and Yasuji Oshima2. 1993. 'MKK1 and MKK2, Which Encode Saccharomyces Cerevisiae Mitogen-Activated Protein Kinase-Kinase Homologs, Function in the Pathway Mediated by Protein Kinase C'. *Molecular and Cellular Biology* 13 (5): 3076–83. https://doi.org/10.1128/MCB.13.5.3076-3083.1993.

Isoyama, Takeshi, Asako Murayama, Akio Nomoto, and Shusuke Kuge. 2001. 'Nuclear Import of the Yeast AP-1-like Transcription Factor Yap1p Is Mediated by Transport Receptor Pse1p, and This Import Step Is Not Affected by Oxidative Stress'. *Journal of Biological Chemistry* 276 (24): 21863–69. https://doi.org/10.1074/jbc.M009258200.

Jacoby, J. J., S. M. Nilius, and J. J. Heinisch. 1998. 'A Screen for Upstream Components of the Yeast Protein Kinase C Signal Transduction Pathway Identifies the Product of the SLG1 Gene'. *Molecular and General Genetics* 258 (1–2): 148–55. https://doi.org/10.1007/S004380050717/METRICS.

Jendretzki, Arne, Janina Wittland, Sabrina Wilk, Andrea Straede, and Jürgen J. Heinisch. 2011. 'How Do I Begin? Sensing Extracellular Stress to Maintain Yeast Cell Wall Integrity'. *European Journal of Cell Biology* 90 (9): 740–44. https://doi.org/10.1016/j.ejcb.2011.04.006.

Jęśko, Henryk, Adam Stępień, Walter J. Lukiw, and Robert P. Strosznajder. 2019. 'The Cross-Talk Between Sphingolipids and Insulin-Like Growth Factor Signaling: Significance for Aging and Neurodegeneration'. *Molecular Neurobiology* 56 (5): 3501–21. https://doi.org/10.1007/S12035-018-1286-3.

Jiang, Rong, and Marian Carlson. 1996. 'Glucose Regulates Protein Interactions within the Yeast SNF1 Protein Kinase Complex'. *Genes & Development* 10 (24): 3105–15. https://doi.org/10.1101/GAD.10.24.3105.

Jiménez-Gutiérrez, Elena, Estíbaliz Alegría-Carrasco, Esmeralda Alonso-Rodríguez, Teresa Fernández-Acero, María Molina, and Humberto Martín. 2020. 'Rewiring the Yeast Cell Wall Integrity (CWI) Pathway through a Synthetic Positive Feedback Circuit Unveils a Novel Role for the MAPKKK Ssk2 in CWI Pathway Activation'. *FEBS Journal* 287 (22): 4881–4901. https://doi.org/10.1111/febs.15288.

Jiménez-Gutiérrez, Elena, Estíbaliz Alegría-Carrasco, Ángela Sellers-Moya, María Molina, and Humberto Martín. 2020. 'Not Just the Wall: The Other Ways to Turn the Yeast CWI Pathway On'. *International Microbiology* 23 (1): 107–19. https://doi.org/10.1007/s10123-019-00092-2.

Jin, Chunyan, Randy Strich, and Katrina F. Cooper. 2014. 'Slt2p Phosphorylation Induces Cyclin C Nuclear-to-Cytoplasmic Translocation in Response to Oxidative Stress'. *Molecular Biology of the Cell* 25 (8): 1396–1407. https://doi.org/10.1091/MBC.E13-09-0550/ASSET/IMAGES/LARGE/1396FIG9.JPEG.

Jin, Min, and Yanyun Zhang. 2020. 'Autophagy and Immune-Related Diseases'. *Advances in Experimental Medicine and Biology* 1207: 401–3. https://doi.org/10.1007/978-981-15-4272-5_27.

Jin, Xueyang, Ming Zhang, Jinghui Lu, Ximeng Duan, Jinyao Chen, Yue Liu, Wenqiang Chang, and Hongxiang Lou. 2021. 'Hinokitiol Chelates Intracellular Iron to Retard Fungal Growth by Disturbing Mitochondrial Respiration'. *Journal of Advanced Research* 34 (December): 65–77. https://doi.org/10.1016/J.JARE.2021.06.016.

Jin, Yui, and Lois S. Weisman. 2015. 'The Vacuole/Lysosome Is Required for Cell-Cycle Progression'. *ELife* 4 (AUGUST2015). https://doi.org/10.7554/ELIFE.08160.

Jing, Jovian Lin, Trishia Cheng Yi Ning, Federica Natali, Frank Eisenhaber, and Mohammad Alfatah. 2022. 'Iron Supplementation Delays Aging and Extends Cellular Lifespan through Potentiation of Mitochondrial Function'. *Cells* 11 (5): 1–14. https://doi.org/10.3390/cells11050862.

Jordá, Tania, Nicolas Rozès, and Sergi Puig. 2021. 'Sterol Composition Modulates the Response of Saccharomyces Cerevisiae to Iron Deficiency'. *Journal of Fungi* 7 (11): 901. https://doi.org/10.3390/JOF7110901/S1.

Jorgensen, Paul, Ivan Rupeš, Jeffrey R. Sharom, Lisa Schneper, James R. Broach, and Mike Tyers. 2004. 'A Dynamic Transcriptional Network Communicates Growth Potential to Ribosome Synthesis and Critical Cell Size'. *Genes and Development* 18 (20): 2491–2505. https://doi.org/10.1101/gad.1228804.

Jung, Un Sung, Andrew K. Sobering, Martin J. Romeo, and David E. Levin. 2002. 'Regulation of the Yeast Rlm1 Transcription Factor by the Mpk1 Cell Wall Integrity MAP Kinase'. *Molecular Microbiology* 46 (3): 781–89. https://doi.org/10.1046/J.1365-2958.2002.03198.X.

Kabeya, Yukiko, Yoshiaki Kamada, Misuzu Baba, Hirosato Takikawa, Mitsuru Sasaki, and Yoshinori Ohsumi. 2005. 'Atg17 Functions in Cooperation with Atg1 and Atg13 in Yeast Autophagy'. *Mol Biol Cell* 16: 2533–53.

Kachroo, Aashiq H., Michelle Vandeloo, Brittany M. Greco, and Mudabir Abdullah. 2022. 'Humanized Yeast to Model Human Biology, Disease and Evolution'. *Disease Models & Mechanisms* 15 (6). https://doi.org/10.1242/DMM.049309.

Kaibuchi, K., A. Miyajima, K. I. Arai, and K. Matsumoto. 1986. 'Possible Involvement of RAS-Encoded Proteins in Glucose-Induced Inositolphospholipid Turnover in Saccharomyces Cerevisiae'. *Proceedings of the National Academy of Sciences of the United States of America* 83 (21): 8172–76. https://doi.org/10.1073/pnas.83.21.8172.

Kakhlon, Or. 2021. 'Casting Iron into the Cell Fate Mold'. *The Biochemical Journal* 478 (10): 1879–83. https://doi.org/10.1042/BCJ20210108.

Kamada, Yoshiaki, Un Sung Jung, Julia Piotrowski, and David E Levin. 1995. 'The Protein Kinase C-Activated MAP Kinase Pathway of Saccharomyces Cerevisiae Mediates a Novel Aspect of the Heat Shock Response'. *Genes Development* 9: 1559–71. https://doi.org/10.1101/gad.9.13.1559.

Kamada, Yoshiaki, Hiroshi Qadota, Christophe P. Python, Yasuhiro Anraku, Yoshikazu Ohya, and David E. Levin. 1996. 'Activation of Yeast Protein Kinase C by Rho1 GTPase'. *The Journal of Biological Chemistry* 271 (16): 9193–96. https://doi.org/10.1074/JBC.271.16.9193.

Kaminska, Joanna, Piotr Soczewka, Weronika Rzepnikowska, and Teresa Zoladek. 2022. 'Yeast as a Model to Find New Drugs and Drug Targets for VPS13 -Dependent Neurodegenerative Diseases'. *International Journal of Molecular Sciences* 23 (9). https://www.mdpi.com/1422-0067/23/9/5106.

Kanki, Tomotake, Ke Wang, Misuzu Baba, Clinton R. Bartholomew, Melinda A. Lynch-Day, Zhou Du, Jiefei Geng, et al. 2009. 'A Genomic Screen for Yeast Mutants Defective in Selective Mitochondria Autophagy'. *Molecular Biology of the Cell* 20 (22): 4730. https://doi.org/10.1091/MBC.E09-03-0225.

Kanki, Tomotake, Ke Wang, Yang Cao, Misuzu Baba, and Daniel J Klionsky. 2009. 'Atg32 Is

a Mitochondrial Protein That Confers Selectivity during Mitophagy'. *Developmental Cell* 17: 98–109. https://doi.org/10.1016/j.devcel.2009.06.014.

Kaplan, Craig D., and Jerry Kaplan. 2009. 'Iron Acquisition and Transcriptional Regulation'. *Chemical Reviews* 109 (10): 4536–52. https://doi.org/10.1021/CR9001676/ASSET/IMAGES/LARGE/CR-2009-001676_0005.JPEG.

Kataoka, Tohru, Daniel Broek, and Michael Wigler. 1985. 'DNA Sequence and Characterization of the S. Cerevisiae Gene Encoding Adenylate Cyclase'. *Cell* 43 (2): 493–505. https://doi.org/10.1016/0092-8674(85)90179-5.

Kenyon, Cynthia, Jean Chang, Erin Gensch, Adam Rudner, and Ramon Tabtiang. 1993. 'A C. Elegans Mutant That Lives Twice as Long as Wild Type'. *Nature 1993 366:6454* 366 (6454): 461–64. https://doi.org/10.1038/366461a0.

Ketela, Troy, Robin Green, and Howard Bussey. 1999. 'Saccharomyces Cerevisiae Mid2p Is a Potential Cell Wall Stress Sensor and Upstream Activator of the PKC1-MPK1 Cell Integrity Pathway'. *Journal of Bacteriology* 181 (11): 3330. https://doi.org/10.1128/JB.181.11.3330-3340.1999.

Kim, John, and Daniel J Klionsky. 2000. 'A UTOPHAGY , C YTOPLASM - TO -V ACUOLE T ARGETING P ATHWAY , AND P EXOPHAGY'.

Kim, Ki-Young, Andrew W. Truman, and David E. Levin. 2008. 'Yeast Mpk1 Mitogen-Activated Protein Kinase Activates Transcription through Swi4/Swi6 by a Noncatalytic Mechanism That Requires Upstream Signal'. *Molecular and Cellular Biology* 28 (8): 2579–89. https://doi.org/10.1128/MCB.01795-07/SUPPL_FILE/PRIMER_SEQUENCES.ZIP.

Kimball, Scot R. 1999. 'Eukaryotic Initiation Factor EIF2'. *The International Journal of Biochemistry & Cell Biology* 31 (1): 25–29. https://doi.org/10.1016/S1357-2725(98)00128-9.

Kirchner, Philipp, Mathieu Bourdenx, Julio Madrigal-Matute, Simoni Tiano, Antonio Diaz, Boris A. Bartholdy, Britta Will, and Ana Maria Cuervo. 2019. 'Proteome-Wide Analysis of Chaperone-Mediated Autophagy Targeting Motifs'. *PLoS Biology* 17 (5): 1–27. https://doi.org/10.1371/JOURNAL.PBIO.3000301.

Kirisako, Takayoshi, Yoshinobu Ichimura, Hisashi Okada, Yukiko Kabeya, Noboru Mizushima, Tamotsu Yoshimori, Mariko Ohsumi, Toshifumi Takao, Takeshi Noda, and Yoshinori Ohsumi. 2000. 'The Reversible Modification Regulates the Membrane-Binding State of Apg8/Aut7 Essential for Autophagy and the Cytoplasm to Vacuole Targeting Pathway'. *Journal of Cell Biology* 151 (2): 263–76. https://doi.org/10.1083/JCB.151.2.263.

Kirkin, Vladimir. 2020. 'History of the Selective Autophagy Research: How Did It Begin and Where Does It Stand Today?' *Journal of Molecular Biology* 432 (1): 3–27. https://doi.org/10.1016/j.jmb.2019.05.010.

Kiššova, Ingrid, Bénédicte Salin, Jacques Schaeffer, Sapan Bhatia, Stéphen Manon, and Nadine Camougrand. 2007. 'Selective and Non-Selective Autophagic Degradation of Mitochondria in Yeast'. *Autophagy* 3 (4): 329–36. https://doi.org/10.4161/auto.4034.

Kitagaki, Hiroshi, L. Ashley Cowart, Nabil Matmati, Silvia Vaena de Avalos, Sergei A. Novgorodov, Youssef H. Zeidan, Jacek Bielawski, Lina M. Obeid, and Yusuf A. Hannun. 2007. 'Isc1 Regulates Sphingolipid Metabolism in Yeast Mitochondria'. *Biochimica et Biophysica Acta (BBA) - Biomembranes* 1768 (11): 2849–61. https://doi.org/10.1016/J.BBAMEM.2007.07.019.

Klein, C, and K Struhl. 1994. 'Protein Kinase A Mediates Growth-Regulated Expression of Yeast Ribosomal Protein Genes by Modulating RAP1 Transcriptional Activity.' *Molecular and Cellular Biology* 14 (3): 1920. https://doi.org/10.1128/MCB.14.3.1920.

Klis, Frans M., Andre Boorsma, and Piet W.J. De Groot. 2006. 'Cell Wall Construction in Saccharomyces Cerevisiae'. *Yeast (Chichester, England)* 23 (3): 185–202. https://doi.org/10.1002/YEA.1349.

Komeili, A., K. P. Wedaman, E. K. O'Shea, and T. Powers. 2000a. 'Mechanism of Metabolic Control: Target of Rapamycin Signaling Links Nitrogen Quality to the Activity of the Rtg1 and Rtg3 Transcription Factors'. *Journal of Cell Biology* 151 (4): 863–78. https://doi.org/10.1083/jcb.151.4.863.

Kraft, Claudine, Anna Deplazes, Marc Sohrmann, and Matthias Peter. 2008. 'Mature Ribosomes Are Selectively Degraded upon Starvation by an Autophagy Pathway Requiring the Ubp3p/Bre5p Ubiquitin Protease'. *Nature Cell Biology* 10 (5): 602–10. https://doi.org/10.1038/ncb1723.

Kuchin, Sergei, Valmik K. Vyas, and Marian Carlson. 2002. 'Snf1 Protein Kinase and the Repressors Nrg1 and Nrg2 Regulate FLO11, Haploid Invasive Growth, and Diploid Pseudohyphal Differentiation'. *Molecular and Cellular Biology* 22 (12): 3994. https://doi.org/10.1128/MCB.22.12.3994-4000.2002.

Kuroda, M., T. Hashida-Okado, R. Yasumoto, K. Gomi, I. Kato, and K. Takesako. 1999. 'An Aureobasidin A Resistance Gene Isolated from Aspergillus Is a Homolog of Yeast AUR1, a Gene Responsible for Inositol Phosphorylceramide (IPC) Synthase Activity'. *Molecular and General Genetics* 261 (2): 290–96. https://doi.org/10.1007/S004380050969/METRICS.

Lakhani, Ronak, Kara R. Vogel, Andreas Till, Jingjing Liu, Sarah F. Burnett, K. Michael Gibson, and Suresh Subramani. 2014. 'Defects in GABA Metabolism Affect Selective Autophagy Pathways and Are Alleviated by MTOR Inhibition'. *EMBO Molecular Medicine* 6 (4): 551–66. https://doi.org/10.1002/emmm.201303356.

Lastauskiene, Egle, Aukse Zinkevičiene, and Donaldas Čitavičius. 2014. 'Ras/PKA Signal Transduction Pathway Participates in the Regulation of Saccharomyces Cerevisiae Cell Apoptosis in an Acidic Environment'. *Biotechnology and Applied Biochemistry* 61 (1): 3–10. https://doi.org/10.1002/bab.1183.

Lee, K S, K Irie, Y Gotoh, Y Watanabe, H Araki, E Nishida, K Matsumoto, and D E Levin. 1993. 'A Yeast Mitogen-Activated Protein Kinase Homolog (Mpk1p) Mediates Signalling by Protein Kinase C'. *Molecular and Cellular Biology* 13 (5): 3067–75. https://doi.org/10.1128/MCB.13.5.3067-3075.1993.

Lee, Kyung S, and David E Levin. 1992. 'Dominant Mutations in a Gene Encoding a Putative Protein Kinase (BCK1) Bypass the Requirement for a Saccharomyces Cerevisiae Protein Kinase C Homolog.' *Molecular and Cellular Biology* 12 (1): 172. https://doi.org/10.1128/MCB.12.1.172.

Lee, Yueh Jung, Xinhe Huang, Janette Kropat, Anthony Henras, Sabeeha S. Merchant, Robert C. Dickson, and Guillaume F. Chanfreau. 2012. 'Sphingolipid Signaling Mediates Iron Toxicity'. *Cell Metabolism* 16 (1): 90–96. https://doi.org/10.1016/J.CMET.2012.06.004.

Leslie, Deena M., Brock Grill, Michael P. Rout, Richard W. Wozniak, and John D. Aitchison. 2002. 'Kap121p-Mediated Nuclear Import Is Required for Mating and Cellular Differentiation in Yeast'. *Molecular and Cellular Biology* 22 (8): 2544–55. https://doi.org/10.1128/MCB.22.8.2544-2555.2002.

Lester, Robert L., Bradley R. Withers, Megan A. Schultz, and Robert C. Dickson. 2013. 'Iron, Glucose and Intrinsic Factors Alter Sphingolipid Composition as Yeast Cells Enter Stationary Phase'. *Biochimica et Biophysica Acta (BBA) - Molecular and Cell Biology of Lipids* 1831 (4): 726–36. https://doi.org/10.1016/J.BBALIP.2012.12.012.

Lesuisse, Emmanuel, Monique Simon-Casteras, and Pierre Labbe. 1999. 'Siderophore-Mediated Iron Uptake in Saccharomyces Cerevisiae: The SIT1 Gene Encodes a Ferrioxamine B Permease That Belongs to the Major Facilitator Superfamily

Transcriptionnal Regulation of Iron Metabolism View Project Siderophore-Mediated Iron Uptake in Saccharomyces Cerevisiae : The S/Tl Gene Encodes a Ferrioxamine B Permease That Belongs to the Major Facilitator Superfamily'. https://doi.org/10.1099/00221287-144-12-3455.

Levade, Thierry, Nathalie Augé, Robert Jan Veldman, Olivier Cuvillier, Anne Négre-Salvayre, and Robert Salvayre. 2001. 'Sphingolipid Mediators in Cardiovascular Cell Biology and Pathology'. *Circulation Research* 89 (11): 957–68. https://doi.org/10.1161/HH2301.100350.

Levin, David E. 2011. 'Regulation of Cell Wall Biogenesis in Saccharomyces Cerevisiae: The Cell Wall Integrity Signaling Pathway'. *Genetics* 189 (4): 1145–75. https://doi.org/10.1534/genetics.111.128264.

Li, Angtao, Xuan Jia, Diane M. Ward, and Jerry Kaplan. 2011. 'Yap5 Protein-Regulated Transcription of the TYW1 Gene Protects Yeast from High Iron Toxicity'. *The Journal of Biological Chemistry* 286 (44): 38488–97. https://doi.org/10.1074/JBC.M111.286666.

Li, Haoran, Daphne T. Mapolelo, Nin N. Dingra, Sunil G. Naik, Nicholas S. Lees, Brian M. Hoffman, Pamela J. Riggs-Gelasco, Hanh Huynh Boi, Michael K. Johnson, and Caryn E. Outten. 2009. 'The Yeast Iron Regulatory Proteins Grx3/4 and Fra2 Form Heterodimeric Complexes Containing a [2Fe-2S] Cluster with Cysteinyl and Histidyl Ligation'. *Biochemistry* 48 (40): 9569–81. https://doi.org/10.1021/BI901182W/SUPPL_FILE/BI901182W_SI_001.PDF.

Li, Jianhui, and Mark Hochstrasser. 2020. 'Microautophagy Regulates Proteasome Homeostasis'. *Current Genetics* 66 (4): 683–87. https://doi.org/10.1007/s00294-020-01059-x.

Li, Liangtao, Dustin Bagley, Diane M. Ward, and Jerry Kaplan. 2008. 'Yap5 Is an Iron-Responsive Transcriptional Activator That Regulates Vacuolar Iron Storage in Yeast'. *Molecular and Cellular Biology* 28 (4): 1326–37. https://doi.org/10.1128/MCB.01219-07.

Li, Liangtao, Ren Miao, Sophie Bertram, Xuan Jia, Diane M. Ward, and Jerry Kaplan. 2012. 'A Role for Iron-Sulfur Clusters in the Regulation of Transcription Factor Yap5-Dependent High Iron Transcriptional Responses in Yeast'. *The Journal of Biological Chemistry* 287 (42): 35709. https://doi.org/10.1074/JBC.M112.395533.

Li, Liangtao, and Diane M. Ward. 2018a. 'Iron Toxicity in Yeast: Transcriptional Regulation of the Vacuolar Iron Importer Ccc1'. *Current Genetics* 64 (2): 413–16. https://doi.org/10.1007/s00294-017-0767-7.

———. 2018b. 'Iron Toxicity in Yeast: Transcriptional Regulation of the Vacuolar Iron Importer Ccc1'. *Current Genetics* 64 (2): 413. https://doi.org/10.1007/S00294-017-0767-7.

Li, Shuangxi, Aiguo Tian, Shuang Li, Yuhong Han, Bing Wang, and Jin Jiang. 2020. 'Gilgamesh (Gish)/CK1γ Regulates Tissue Homeostasis and Aging in Adult Drosophila Midgut'. *The Journal of Cell Biology* 219 (4). https://doi.org/10.1083/JCB.201909103.

Li, Wen, Pengcheng He, Yuge Huang, Yi Fang Li, Jiahong Lu, Min Li, Hiroshi Kurihara, et al. 2020. 'Selective Autophagy of Intracellular Organelles: Recent Research Advances'. *Theranostics* 11 (1): 222–56. https://doi.org/10.7150/THNO.49860.

Lill, Roland, Vasundara Srinivasan, and Ulrich Mühlenhoff. 2014. 'The Role of Mitochondria in Cytosolic-Nuclear Iron–Sulfur Protein Biogenesis and in Cellular Iron Regulation'. *Current Opinion in Microbiology* 22 (December): 111–19. https://doi.org/10.1016/J.MIB.2014.09.015.

Lin, Stephen S., Jill K. Manchester, and Jeffrey I. Gordon. 2003. 'Sip2, an N-Myristoylated Beta Subunit of Snf1 Kinase, Regulates Aging in Saccharomyces Cerevisiae by Affecting Cellular Histone Kinase Activity, Recombination at RDNA Loci, and Silencing'. *The Journal of Biological Chemistry* 278 (15): 13390–97.

https://doi.org/10.1074/JBC.M212818200.

Lin, Xue. 2021. 'The Regulation of Saccharomyces Cerevisiae Snf1 Protein Kinase on Glucose Utilization Is in a Glucose-Dependent Manner'. *Current Genetics* 67 (2): 245–48. https://doi.org/10.1007/s00294-020-01137-0.

Lin, Yu yi, Jin ying Lu, Junmei Zhang, Wendy Walter, Weiwei Dang, Jun Wan, Sheng Ce Tao, et al. 2009. 'Protein Acetylation Microarray Reveals NuA4 Controls Key Metabolic Target Regulating Gluconeogenesis'. *Cell* 136 (6): 1073. https://doi.org/10.1016/J.CELL.2009.01.033.

Liu, Jun, Lihui Wang, Zhiguo Wang, and Jun-Ping Liu. 2019. 'Roles of Telomere Biology in Cell Senescence, Replicative and Chronological Ageing'. *Cells*, 1–10.

Liu, Li, and David E. Levin. 2018. 'Intracellular Mechanism by Which Genotoxic Stress Activates Yeast SAPK Mpk1'. *Molecular Biology of the Cell* 29 (23): 2898. https://doi.org/10.1091/MBC.E18-07-0441.

Liu, Shiyan, Mutian Chen, Yichang Wang, Huihui Li, Shiqian Qi, Jia Geng, and Kefeng Lu. 2023. 'Autophagy Is Regulated by Endoplasmic Reticulum Calcium Homeostasis and Sphingolipid Metabolism'. *Autophagy*. https://doi.org/10.1080/15548627.2023.2249761.

Liu, Xiao Dong, and Dennis J. Thiele. 1996. 'Oxidative Stress Induced Heat Shock Factor Phosphorylation and HSF-Dependent Activation of Yeast Metallothionein Gene Transcription'. *Genes & Development* 10 (5): 592–603. https://doi.org/10.1101/GAD.10.5.592.

Liu, Zhengchang, and Ronald A. Butow. 1999. 'A Transcriptional Switch in the Expression of Yeast Tricarboxylic Acid Cycle Genes in Response to a Reduction or Loss of Respiratory Function'. *Molecular and Cellular Biology* 19 (10): 6720. https://doi.org/10.1128/MCB.19.10.6720.

Locke, Melissa N., and Jeremy Thorner. 2019. 'Regulation of TORC2 Function and Localization by Rab5 GTPases in Saccharomyces Cerevisiae'. *Cell Cycle* 18 (10): 1084–94. https://doi.org/10.1080/15384101.2019.1616999.

Loewith, Robbie, and Michael N. Hall. 2011. 'Target of Rapamycin (TOR) in Nutrient Signaling and Growth Control'. *Genetics* 189 (4): 1177–1201. https://doi.org/10.1534/GENETICS.111.133363.

Loewith, Robbie, Estela Jacinto, Stephan Wullschleger, Anja Lorberg, José L. Crespo, Débora Bonenfant, Wolfgang Oppliger, Paul Jenoe, and Michael N. Hall. 2002. 'Two TOR Complexes, Only One of Which Is Rapamycin Sensitive, Have Distinct Roles in Cell Growth Control'. *Molecular Cell* 10 (3): 457–68. https://doi.org/10.1016/S1097-2765(02)00636-6.

Longo, Valter D. 2003. 'The Ras and Sch9 Pathways Regulate Stress Resistance and Longevity'. *Experimental Gerontology* 38 (7): 807–11. https://doi.org/10.1016/S0531-5565(03)00113-X.

Longo, Valter D., Edith Butler Gralla, and Joan Selverstone Valentine. 1996. 'Superoxide Dismutase Activity Is Essential for Stationary Phase Survival in Saccharomyces Cerevisiae: Mitochondrial Production of Toxic Oxygen Species in Vivo'. *Journal of Biological Chemistry* 271 (21): 12275–80. https://doi.org/10.1074/jbc.271.21.12275.

Longo, Valter D., Gerald S. Shadel, Matt Kaeberlein, and Brian Kennedy. 2012. 'Replicative and Chronological Aging in Saccharomyces Cerevisiae'. *Cell Metabolism* 16 (1): 18–31. https://doi.org/10.1016/j.cmet.2012.06.002.

Lu, Jin Ying, Yu Yi Lin, Jin Chuan Sheu, June Tai Wu, Fang Jen Lee, Yue Chen, Min I. Lin, et al. 2011. 'Acetylation of Yeast AMPK Controls Intrinsic Aging Independently of Caloric Restriction'. *Cell* 146 (6): 969–79. https://doi.org/10.1016/j.cell.2011.07.044.

Ludin, Katja, Rong Jiang, and Marian Carlson. 1998. 'Glucose-Regulated Interaction of a Regulatory Subunit of Protein Phosphatase 1 with the Snf1 Protein Kinase in

Saccharomyces Cerevisiae'. *Proceedings of the National Academy of Sciences of the United States of America* 95 (11): 6245–50. https://doi.org/10.1073/PNAS.95.11.6245/ASSET/3922E5DA-CC60-4756-B73A-A05344183E87/ASSETS/GRAPHIC/PQ1180388004.JPEG.

Lynch-Day, Melinda A., and Daniel J. Klionsky. 2010. 'The Cvt Pathway as a Model for Selective Autophagy'. *FEBS Letters* 584 (7): 1359–66. https://doi.org/10.1016/j.febslet.2010.02.013.

Ma, Pingsheng, Stefaan Wera, Patrick Van Dijck, and Johan M. Thevelein. 1999. 'The PDE1-Encoded Low-Affinity Phosphodiesterase in the Yeast Saccharomyces Cerevisiae Has a Specific Function in Controlling Agonist-Induced CAMP Signaling'. *Molecular Biology of the Cell* 10 (1): 91–104. https://doi.org/10.1091/MBC.10.1.91.

Magazinnik, Tanya, Monika Anand, Evelyn Sattlegger, Alan G. Hinnebusch, and Terri Goss Kinzy. 2005. 'Interplay between GCN2 and GCN4 Expression, Translation Elongation Factor 1 Mutations and Translational Fidelity in Yeast'. *Nucleic Acids Research* 33 (14): 4584–92. https://doi.org/10.1093/nar/gki765.

Maiuri, M. Chiara, Einat Zalckvar, Adi Kimchi, and Guido Kroemer. 2007. 'Self-Eating and Self-Killing: Crosstalk between Autophagy and Apoptosis'. *Nature Reviews Molecular Cell Biology 2007 8:9* 8 (9): 741–52. https://doi.org/10.1038/nrm2239.

Malpartida, Ana Belen, Matthew Williamson, Derek P. Narendra, Richard Wade-Martins, and Brent J. Ryan. 2021. 'Mitochondrial Dysfunction and Mitophagy in Parkinson's Disease: From Mechanism to Therapy'. *Trends in Biochemical Sciences* 46 (4): 329–43. https://doi.org/10.1016/J.TIBS.2020.11.007.

Mao, Kai, and Daniel J. Klionsky. 2011. 'MAPKs Regulate Mitophagy in Saccharomyces Cerevisiae'. *Autophagy* 7 (12): 1564. https://doi.org/10.4161/AUTO.7.12.17971.

Marbach, Irit, Ruth Licht, Hanns Frohnmeyer, and David Engelberg. 2001. 'Gcn2 Mediates Gcn4 Activation in Response to Glucose Stimulation or UV Radiation Not via GCN4 Translation'. *Journal of Biological Chemistry* 276 (20): 16944–51. https://doi.org/10.1074/jbc.M100383200.

Marín, María José, Marta Flández, Clara Bermejo, Javier Arroyo, Humberto Martín, and María Molina. 2009. 'Different Modulation of the Outputs of Yeast MAPK-Mediated Pathways by Distinct Stimuli and Isoforms of the Dual-Specificity Phosphatase Msg5'. *Molecular Genetics and Genomics : MGG* 281 (3): 345–59. https://doi.org/10.1007/S00438-008-0415-5.

Martín, Humberto, Jose M. Rodríguez-Pachón, Cristina Ruiz, César Nombela, and María Molina. 2000. 'Regulatory Mechanisms for Modulation of Signaling through the Cell Integrity Slt2-Mediated Pathway in Saccharomyces Cerevisiae'. *The Journal of Biological Chemistry* 275 (2): 1511–19. https://doi.org/10.1074/JBC.275.2.1511.

Martínez-Pastor, María Teresa, Rosa de Llanos, Antonia María Romero, and Sergi Puig. 2013. 'Post-Transcriptional Regulation of Iron Homeostasis in Saccharomyces Cerevisiae'. *International Journal of Molecular Sciences* 14 (8): 15785–809. https://doi.org/10.3390/ijms140815785.

Martínez-Pastor, María Teresa, Ana Perea-García, and Sergi Puig. 2017. 'Mechanisms of Iron Sensing and Regulation in the Yeast Saccharomyces Cerevisiae'. *World Journal of Microbiology and Biotechnology* 33 (4): 0. https://doi.org/10.1007/s11274-017-2215-8.

Martins, Telma S., Vítor Costa, and Clara Pereira. 2018. 'Signaling Pathways Governing Iron Homeostasis in Budding Yeast'. *Molecular Microbiology* 109 (4): 422–32. https://doi.org/10.1111/mmi.14009.

Matecic, Mirela, Daniel L. Smith, Xuewen Pan, Nazif Maqani, Stefan Bekiranov, Jef D. Boeke, and Jeffrey S. Smith. 2010. 'A Microarray-Based Genetic Screen for Yeast Chronological Aging Factors'. *PLoS Genetics* 6 (4). https://doi.org/10.1371/journal.pgen.1000921.

Mathew, Robin, Cristina M. Karp, Brian Beaudoin, Nhan Vuong, Guanghua Chen, Hsin Yi Chen, Kevin Bray, et al. 2009. 'Autophagy Suppresses Tumorigenesis Through Elimination of P62'. *Cell* 137 (6): 1062. https://doi.org/10.1016/J.CELL.2009.03.048.

Matmati, Nabil, Bachar H. Hassan, Jihui Ren, Ashraf A. Shamssedine, Eunmi Jeong, Baasil Shariff, Justin Snider, et al. 2020. 'Yeast Sphingolipid Phospholipase Gene ISC1 Regulates the Spindle Checkpoint by a CDC55-Dependent Mechanism'. *Molecular and Cellular Biology* 40 (12). https://doi.org/10.1128/MCB.00340-19.

Matoba, Kazuaki, Tetsuya Kotani, Akihisa Tsutsumi, Takuma Tsuji, Takaharu Mori, Daisuke Noshiro, Yuji Sugita, et al. 2020. 'Atg9 Is a Lipid Scramblase That Mediates Autophagosomal Membrane Expansion'. *Nature Structural and Molecular Biology* 27 (12): 1185–93. https://doi.org/10.1038/s41594-020-00518-w.

Mattison, Christopher P., Scott S. Spencer, Kurt A. Kresge, Ji Lee, and Irene M. Ota. 1999. 'Differential Regulation of the Cell Wall Integrity Mitogen-Activated Protein Kinase Pathway in Budding Yeast by the Protein Tyrosine Phosphatases Ptp2 and Ptp3'. *Molecular and Cellular Biology* 19 (11): 7651–60. https://doi.org/10.1128/MCB.19.11.7651.

Mayordomo, Isabel, Francisco Estruch, and Pascual Sanz. 2002. 'Convergence of the Target of Rapamycin and the Snf1 Protein Kinase Pathways in the Regulation of the Subcellular Localization of Msn2, a Transcriptional Activator of STRE (Stress Response Element)-Regulated Genes'. *Journal of Biological Chemistry* 277 (38): 35650–56. https://doi.org/10.1074/jbc.M204198200.

McCartney, Rhonda R., Leopold Garnar-Wortzel, Dakshayini G. Chandrashekarappa, and Martin C. Schmidt. 2016. 'Activation and Inhibition of Snf1 Kinase Activity by Phosphorylation within the Activation Loop'. *Biochimica et Biophysica Acta - Proteins and Proteomics* 1864 (11): 1518–28. https://doi.org/10.1016/j.bbapap.2016.08.007.

McQuiston, Travis, Charles Haller, and Maurizio Poeta. 2006. 'Sphingolipids as Targets for Microbial Infections'. *Mini Reviews in Medicinal Chemistry* 6 (6): 671–80. https://doi.org/10.2174/138955706777435634.

Mechoud, Mónica A., Nuria Pujol-Carrion, Sandra Montella-Manuel, and Maria Angeles de la Torre-Ruiz. 2020. 'Interactions of GMP with Human Glrx3 and with Saccharomyces Cerevisiae Grx3 and Grx4 Converge in the Regulation of the Gcn2 Pathway'. *Applied and Environmentall Microbiology* 86 (14): 00221–20. https://journals.asm.org/doi/epub/10.1128/AEM.00221-20.

Megyeri, Márton, Howard Riezman, Maya Schuldiner, and Anthony H. Futerman. 2016. 'Making Sense of the Yeast Sphingolipid Pathway'. *Journal of Molecular Biology* 428 (24 Pt A): 4765–75. https://doi.org/10.1016/J.JMB.2016.09.010.

Meijer, Wiebe H., Ida J. Van Der Klei, Marien Veenhuis, and Jan A.K.W. Kiel. 2007. 'ATG Genes Involved in Non-Selective Autophagy Are Conserved from Yeast to Man, but the Selective Cvt and Pexophagy Pathways Also Require Organism-Specific Genes'. *Autophagy* 3 (2): 106–16. https://doi.org/10.4161/auto.3595.

Mijaljica, Dalibor, and Rodney J Devenish. 2013. 'Nucleophagy at a Glance.' *Journal of Cell Science* 126 (Pt 19): 4325–30. https://doi.org/10.1242/jcs.133090.

Mishra, Ranjan, Frank Van Drogen, Reinhard Dechant, Soojung Oh, Noo Li Jeon, Sung Sik Lee, Matthias Peter, and David A. Weitz. 2017. 'Protein Kinase C and Calcineurin Cooperatively Mediate Cell Survival under Compressive Mechanical Stress'. *Proceedings of the National Academy of Sciences of the United States of America* 114 (51): 13471–76. https://doi.org/10.1073/PNAS.1709079114/-/DCSUPPLEMENTAL.

Mitjana, Felipe V, Mima I Petkova, and Nuria Pujol-carrion. 2011. 'Pkc1 and Actin Polymerisation Activities Play a Role in Ribosomal Gene Repression Associated with Secretion Impairment Caused by Oxidative Stress' 11: 656–59.

https://doi.org/10.1111/j.1567-1364.2011.00754.x.

Miyake, Yurika, Yasunori Kozutsumi, Sachiko Nakamura, Tetsuro Fujita, and Toshisuke Kawasaki. 1995. 'Serine Palmitoyltransferase Is the Primary Target of a Sphingosine-like Immunosuppressant, ISP-1/Myriocin'. *Biochemical and Biophysical Research Communications* 211 (2): 396–403. https://doi.org/10.1006/BBRC.1995.1827.

Miyata, Non, Takanori Ito, Miyu Nakashima, Satoru Fujii, and Osamu Kuge. 2022. 'Mitochondrial Phosphatidylethanolamine Synthesis Affects Mitochondrial Energy Metabolism and Quiescence Entry through Attenuation of Snf1/AMPK Signaling in Yeast'. *FASEB Journal* 36 (7): 1–19. https://doi.org/10.1096/fj.202101600RR.

Mizuno, Tomoaki, Kei Muroi, and Kenji Irie. 2020. 'Snf1 AMPK Positively Regulates ER-Phagy via Expression Control of Atg39 Autophagy Receptor in Yeast ER Stress Response'. *PLoS Genetics* 16 (9): 1–28. https://doi.org/10.1371/journal.pgen.1009053.

Mizunuma, Masaki, Ryohei Tsubakiyama, Takafumi Ogawa, Atsunori Shitamukai, Yoshifumi Kobayashi, Tomomi Inai, Kazunori Kume, and Dai Hirata. 2013. 'Ras/CAMP-Dependent Protein Kinase (PKA) Regulates Multiple Aspects of Cellular Events by Phosphorylating the Whi3 Cell Cycle Regulator in Budding Yeast'. *Journal of Biological Chemistry* 288 (15): 10558–66. https://doi.org/10.1074/jbc.M112.402214.

Mizushima, N, T Noda, T Yoshimori, Y Tanaka, T Ishii, M D George, D J Klionsky, M Ohsumi, and Y Ohsumi. 1998. 'A Protein Conjugation System Essential for Autophagy'. *Nature* 395 (6700): 395–98. https://doi.org/10.1038/26506.

Mizushima, Noboru, Takeshi Noda, and Yoshinori Ohsumi. 1999. 'Apg16p Is Required for the Function of the Apg12p-Apg5p Conjugate in the Yeast Autophagy Pathway'. *The EMBO Journal* 18 (14): 3888–96. http://www.isrec.isb-sib.ch/.

Mohammad, Karamat, Paméla Dakik, Younes Medkour, Mélissa McAuley, Darya Mitrofanova, and Vladimir I. Titorenko. 2018. 'Some Metabolites Act as Second Messengers in Yeast Chronological Aging'. *International Journal of Molecular Sciences* 19 (3). https://doi.org/10.3390/ijms19030860.

Mohammad, Karamat, Jennifer Anne Baratang Junio, Tala Tafakori, Emmanuel Orfanos, and Vladimir I. Titorenko. 2020. 'Mechanisms That Link Chronological Aging to Cellular Quiescence in Budding Yeast'. *International Journal of Molecular Sciences* 21 (13): 1–14. https://doi.org/10.3390/ijms21134717.

Mónica A. Mechoud, Nuria Pujol-Carrion, Sandra Montella-Manuel, Maria Angeles de la Torre-Ruiz. 2020. 'Interactions of GMP with Human Glrx3 and with Saccharomyces Cerevisiae Grx3 and Grx4 Converge in the Regulation of the Gcn2 Pathway'. *American Society For Microbiology* 86 (May). https://doi.org/10.1128/AEM.00221-20.

Montefusco, David J., Nabil Matmati, and Yusuf A. Hannun. 2014. 'The Yeast Sphingolipid Signaling Landscape'. *Chemical Physiological Lipids* 177: 26–40. https://doi.org/doi:10.1016/j.chemphyslip.2013.10.006.

Montefusco, David J., Benjamin Newcomb, Jason L. Gandy, Sarah E. Brice, Nabil Matmati, L. Ashley Cowart, and Yusuf A. Hannun. 2012. 'Sphingoid Bases and the Serine Catabolic Enzyme CHA1 Define a Novel Feedforward/Feedback Mechanism in the Response to Serine Availability'. *Journal of Biological Chemistry* 287 (12): 9280–89. https://doi.org/10.1074/jbc.M111.313445.

Mühlenhoff, Ulrich, Sabine Molik, José R Godoy, Marta A Uzarska, Nadine Richter, Andreas Seubert, Yan Zhang, et al. 2010. 'Cytosolic Monothiol Glutaredoxins Function in Intracellular Iron Sensing and Trafficking via Their Bound Iron-Sulfur Cluster'. *Cell Metabolism* 12: 373–85. https://doi.org/10.1016/j.cmet.2010.08.001.

Muir, Alexander, Subramaniam Ramachandran, Françoise M. Roelants, Garrett Timmons, and Jeremy Thorner. 2014. 'TORC2-Dependent Protein Kinase Ypk1 Phosphorylates Ceramide Synthase to Stimulate Synthesis of Complex Sphingolipids'. *ELife* 3.

https://doi.org/10.7554/ELIFE.03779.

Murphree, Catherine R., Nga N. Nguyen, Vikram Raghunathan, Sven R. Olson, Thomas DeLoughery, and Joseph J. Shatzel. 2020. 'Diagnosis and Management of Hereditary Haemochromatosis'. *Vox Sanguinis* 115 (4): 255–62. https://doi.org/10.1111/VOX.12896.

Muthusamy, Thangaselvam, Thekla Cordes, Michal K. Handzlik, Le You, Esther W. Lim, Jivani Gengatharan, Antonio F.M. Pinto, et al. 2020. 'Serine Restriction Alters Sphingolipid Diversity to Constrain Tumour Growth'. *Nature* 586 (7831): 790–95. https://doi.org/10.1038/S41586-020-2609-X.

Nagiec, M. Marek, Elzbieta E. Nagiec, Julie A. Baltisberger, Gerald B. Wells, Robert L. Lester, and Robert C. Dickson. 1997. 'Sphingolipid Synthesis as a Target for Antifungal Drugs. Complementation of the Inositol Phosphorylceramide Synthase Defect in a Mutant Strain of Saccharomyces Cerevisiae by the AUR1 Gene'. *The Journal of Biological Chemistry* 272 (15): 9809–17. https://doi.org/10.1074/JBC.272.15.9809.

Nakatogawa, Hitoshi. 2020. 'Mechanisms Governing Autophagosome Biogenesis'. *Nature Reviews Molecular Cell Biology* 21 (8): 439–58. https://doi.org/10.1038/s41580-020-0241-0.

Nakhaei-Rad, Saeideh, Zahra Soleimani, Saeedeh Vahedi, and Zahra Gorjinia. 2023. 'Testicular Germ Cell Tumors: Genomic Alternations and RAS-Dependent Signaling'. *Critical Reviews in Oncology/Hematology* 183 (March). https://doi.org/10.1016/J.CRITREVONC.2023.103928.

Nath, Nandita, Rhonda R. McCartney, and Martin C. Schmidt. 2002. 'Purification and Characterization of Snf1 Kinase Complexes Containing a Defined Beta Subunit Composition'. *The Journal of Biological Chemistry* 277 (52): 50403–8. https://doi.org/10.1074/JBC.M207058200.

Neuman-Silberberg, F S, S Bhattacharya, and J R Broach. 1995. 'Nutrient Availability and the RAS/Cyclic AMP Pathway Both Induce Expression of Ribosomal Protein Genes in Saccharomyces Cerevisiae but by Different Mechanisms.' *Molecular and Cellular Biology* 15 (6): 3187. https://doi.org/10.1128/MCB.15.6.3187.

Newhall, D A, R Oliver, and S Lugthart. 2020. 'Anaemia: A Disease or Symptom?' *The Netherlands Journal of Medicine* 78 (3): 104–100.

Nicastro, Raffaele, Farida Tripodi, Marco Gaggini, Andrea Castoldi, Veronica Reghellin, Simona Nonnis, Gabriella Tedeschi, and Paola Coccetti. 2015. 'Snf1 Phosphorylates Adenylate Cyclase and Negatively Regulates Protein Kinase A-Dependent Transcription in Saccharomyces Cerevisiae'. *Journal of Biological Chemistry* 290 (41): 24715–26. https://doi.org/10.1074/jbc.M115.658005.

Nikawa, Jun-Ichi, Philip Sass, and Michael Wigler. 1987. 'Cloning and Characterization of the Low-Affinity Cyclic AMP Phosphodiesterase Gene of Saccharomyces Cerevisiae.' *Molecular and Cellular Biology* 7 (10): 3629. https://doi.org/10.1128/MCB.7.10.3629.

Niles, Brad J., Amelia C. Joslin, Tara Fresques, and Ted Powers. 2014. 'TOR Complex 2-Ypk1 Signaling Maintains Sphingolipid Homeostasis by Sensing and Regulating ROS Accumulation'. *Cell Reports* 6 (3): 541–52. https://doi.org/10.1016/J.CELREP.2013.12.040.

Niles, Brad J., and Ted Powers. 2014. 'TOR Complex 2–Ypk1 Signaling Regulates Actin Polarization via Reactive Oxygen Species'. *Molecular Biology of the Cell* 25 (24): 3962. https://doi.org/10.1091/MBC.E14-06-1122.

Niles, Brad J, Huzefa Mogri, Andrew Hill, Ariadne Vlahakis, and Ted Powers. 2011. 'Plasma Membrane Recruitment and Activation of the AGC Kinase Ypk1 Is Mediated by Target of Rapamycin Complex 2 (TORC2) and Its Effector Proteins Slm1 and Slm2' 2. https://doi.org/10.1073/pnas.1117563109.

Noda, Takeshi, and Daniel J. Klionsky. 2009. *The Quantitative Pho8Delta60 Assay of*

Nonspecific Autophagy. Methods in Enzymology. 1st ed. Vol. 451. Elsevier Inc. https://doi.org/10.1016/S0076-6879(08)03203-5.

Noda, Takeshi, and Yoshinori Ohsumi. 1998. 'Tor, a Phosphatidylinositol Kinase Homologue, Controls Autophagy in Yeast'. *The Journal of Biological Chemistry* 273 (7): 3963–66. https://doi.org/10.1074/JBC.273.7.3963.

Obeid, Lina M., Yasuo Okamoto, and Cungui Mao. 2002. 'Yeast Sphingolipids: Metabolism and Biology'. *Biochimica et Biophysica Acta - Molecular and Cell Biology of Lipids* 1585 (2–3): 163–71. https://doi.org/10.1016/S1388-1981(02)00337-2.

Okamoto, Koji, Noriko Kondo-Okamoto, and Yoshinori Ohsumi. 2009. 'Mitochondria-Anchored Receptor Atg32 Mediates Degradation of Mitochondria via Selective Autophagy'. *Developmental Cell* 17 (1): 87–97. https://doi.org/10.1016/J.DEVCEL.2009.06.013.

Orlova, Marianna, Ellen Kanter, David Krakovich, and Sergei Kuchin. 2006. 'Nitrogen Availability and TOR Regulate the Snf1 Protein Kinase in Saccharomyces Cerevisiae'. *Eukaryotic Cell* 5 (11): 1831–37. https://doi.org/10.1128/EC.00110-06.

Östling, Jonas, and Hans Ronne. 1998. 'Negative Control of the Mig1p Repressor by Snf1p-Dependent Phosphorylation in the Absence of Glucose'. *European Journal of Biochemistry* 252 (1): 162–68. https://doi.org/10.1046/J.1432-1327.1998.2520162.X.

Ozaki, Kumi, Kazuma Tanaka, Hiroshi Imamura, Taro Hihara, Takaaki Kameyama, Hidetaro Nonaka, Hisanobu Hirano, Yoshiharu Matsuura, and Yoshimi Takai. 1996. 'Rom1p and Rom2p Are GDP/GTP Exchange Proteins (GEPs) for the Rho1p Small GTP Binding Protein in Saccharomyces Cerevisiae.' *The EMBO Journal* 15 (9): 2196. https://doi.org/10.1002/j.1460-2075.1996.tb00573.x.

Palomino, A., P. Herrero, and F. Moreno. 2006. 'Tpk3 and Snf1 Protein Kinases Regulate Rgt1 Association with Saccharomyces Cerevisiae HXK2 Promoter'. *Nucleic Acids Research* 34 (5): 1427–38. https://doi.org/10.1093/nar/gkl028.

Papamichos-Chronakis, Manolis, Thomas Gligoris, and Dimitris Tzamarias. 2004. 'The Snf1 Kinase Controls Glucose Repression in Yeast by Modulating Interactions between the Mig1 Repressor and the Cyc8-Tup1 Co-Repressor'. *EMBO Reports* 5 (4): 368. https://doi.org/10.1038/SJ.EMBOR.7400120.

Park, Jong In, Chris M. Grant, and Ian W. Dawes. 2005. 'The High-Affinity CAMP Phosphodiesterase of Saccharomyces Cerevisiae Is the Major Determinant of CAMP Levels in Stationary Phase: Involvement of Different Branches of the Ras-Cyclic AMP Pathway in Stress Responses'. *Biochemical and Biophysical Research Communications* 327 (1): 311–19. https://doi.org/10.1016/j.bbrc.2004.12.019.

Parrella, Edoardo, and Valter D. Longo. 2008. 'The Chronological Life Span of Saccharomyces Cerevisiae to Study Mitochondrial Dysfunction and Disease'. *Methods* 46 (4): 256–62. https://doi.org/10.1016/j.ymeth.2008.10.004.

Pedruzzi, Ivo, Frédérique Dubouloz, Elisabetta Cameroni, Valeria Wanke, Johnny Roosen, Joris Winderickx, and Claudio De Virgilio. 2003. 'TOR and PKA Signaling Pathways Converge on the Protein Kinase Rim15 to Control Entry into G0'. *Molecular Cell* 12 (6): 1607–13. https://doi.org/10.1016/S1097-2765(03)00485-4.

Peterson, J., Y. Zheng, L. Bender, A. Myers, R. Cerione, and A. Bender. 1994. 'Interactions between the Bud Emergence Proteins Bem1p and Bem2p and Rho-Type GTPases in Yeast'. *The Journal of Cell Biology* 127 (5): 1395–1406. https://doi.org/10.1083/JCB.127.5.1395.

Petkova, Mima Ivanova, Nuria Pujol-Carrion, Javier Arroyo, Jesús García-Cantalejo, and Maria Angeles De La Torre-Ruiz. 2010. 'Mtl1 Is Required to Activate General Stress Response through TOR1 and RAS2 Inhibition under Conditions of Glucose Starvation and Oxidative Stress'. *Journal of Biological Chemistry* 285 (25): 19521–31.

https://doi.org/10.1074/jbc.M109.085282.

Petkova, Mima Ivanova, Nuria Pujol-Carrion, and Maria Angeles de la Torre-Ruiz. 2010. 'Signal Flow between CWI/TOR and CWI/RAS in Budding Yeast under Conditions of Oxidative Stress and Glucose Starvation'. *Communicative & Integrative Biology* 3 (6): 555–57. https://doi.org/10.4161/cib.3.6.12974.

———. 2012. 'Mtl1 O-Mannosylation Mediated by Both Pmt1 and Pmt2 Is Important for Cell Survival under Oxidative Conditions and TOR Blockade'. *Fungal Genetics and Biology* 49 (11): 903–14. https://doi.org/10.1016/j.fgb.2012.08.005.

Petkova, Mima Ivanova, Nuria Pujol-carrion, and Maria Angeles De Torre-ruiz. 2012. 'Mtl1 O-Mannosylation Mediated by Both Pmt1 and Pmt2 Is Important for Cell Survival under Oxidative Conditions and TOR Blockade'. *Fungal Genetics and Biology* 49 (11): 903–14. https://doi.org/10.1016/j.fgb.2012.08.005.

Philpott, Caroline C., Sébastien Leidgens, and Avery G. Frey. 2012. 'Metabolic Remodeling in Iron-Deficient Fungi'. *Biochimica et Biophysica Acta* 1823 (9): 1509. https://doi.org/10.1016/J.BBAMCR.2012.01.012.

Pimentel, Catarina, Cristina Vicente, Regina Andrade Menezes, Soraia Caetano, Laura Carreto, and Claudina Rodrigues-Pousada. 2012. 'The Role of the Yap5 Transcription Factor in Remodeling Gene Expression in Response to Fe Bioavailability'. *PLOS ONE* 7 (5): e37434. https://doi.org/10.1371/JOURNAL.PONE.0037434.

Pinto, William J, Bharath Srinivasan, Sherri Shepherd, Ann Schmidt, Robert C Dickson, and Robert L Lester. 1992. 'Sphingolipid Long-Chain-Base Auxotrophs of Saccharomyces Cerevisiae: Genetics, Physiology, and a Method for Their Selection'. *JOURNAL OF BACTERIOLOGY* 174 (8): 2565–74.

Piškur, Jure, and Concetta Compagno. 2014. *Molecular Mechanisms in Yeast Carbon Metabolism*. *Molecular Mechanisms in Yeast Carbon Metabolism*. https://doi.org/10.1007/978-3-642-55013-3.

Portillo, Francisco, José M. Mulet, and Ramón Serrano. 2005. 'A Role for the Non-Phosphorylated Form of Yeast Snf1: Tolerance to Toxic Cations and Activation of Potassium Transport'. *FEBS Letters* 579 (2): 512–16. https://doi.org/10.1016/J.FEBSLET.2004.12.019.

Powers, S., T. Kataoka, O. Fasano, M. Goldfarb, J. Strathem, J. Broach, and M. Wigler. 1984. 'Genes in S. Cerevisiae Encoding Proteins with Domains Homologous to the Mammalian Ras Proteins'. *Cell* 36 (3): 607–12. https://doi.org/10.1016/0092-8674(84)90340-4.

Powers, T., I. Dilanova, C.-Y. Chen, and K. Wedaman. 2004. 'Yeast TOR Signaling: A Mechanism for Metabolic Regulation'. In *TOR Target of Rapamycin*, edited by G Thomas, 39–51. Springer-Verlag Berlin Heidelberg.

Powers, Ted. 2022. 'The Origin Story of Rapamycin: Systemic Bias in Biomedical Research and Cold War Politics'. *Molecular Biology of the Cell* 33 (13). https://doi.org/10.1091/MBC.E22-08-0377.

Prize, Nobel. n.d. 'NobelPrize.Org'. Accessed 29 November 2022. https://www.nobelprize.org/prizes/medicine/.

Protchenko, Olga, Tracy Ferea, Jared Rashford, John Tiedeman, Patrick O. Brown, David Botstein, and Caroline C. Philpott. 2001. 'Three Cell Wall Mannoproteins Facilitate the Uptake of Iron in Saccharomyces Cerevisiae'. *The Journal of Biological Chemistry* 276 (52): 49244–50. https://doi.org/10.1074/JBC.M109220200.

Puig, Sergi, Eric Askeland, and Dennis J. Thiele. 2005. 'Coordinated Remodeling of Cellular Metabolism during Iron Deficiency through Targeted MRNA Degradation'. *Cell* 120 (1): 99–110. https://doi.org/10.1016/j.cell.2004.11.032.

Puig, Sergi, Lucía Ramos-Alonso, Antonia María Romero, and María Teresa Martínez-Pastor. 2017. 'The Elemental Role of Iron in DNA Synthesis and Repair'. *Metallomics* 9 (11):

1483–1500. https://doi.org/10.1039/C7MT00116A.

Pujol-Carrion, Nuria, Gemma Belli, Enrique Herrero, Antoni Nogues, and Maria Angeles de la Torre-Ruiz. 2006. 'Glutaredoxins Grx3 and Grx4 Regulate Nuclear Localisation of Aft1 and the Oxidative Stress Response in Saccharomyces Cerevisiae'. *Journal of Cell Science* 119 (Pt 21): 4554–64. https://doi.org/10.1242/JCS.03229.

Pujol-carrion, Nuria, Alma Gomez-alfonso, Sergi Puig, and Maria Angeles De Torre-ruiz. 2022. 'Both Human and Soya Bean Ferritins Highly Improve the Accumulation of Bioavailable Iron and Contribute to Extend the Chronological Life in Budding Yeast'. *Microbial Biotechnology* 15 (5): 1525–41. https://doi.org/10.1111/1751-7915.13939.

Pujol-Carrion, Nuria, Mónica Pavón-Vergés, Javier Arroyo, and Maria Angeles de la Torre-Ruiz. 2021. 'The MAPK Slt2 / Mpk1 Plays a Role in Iron Homeostasis through Direct Regulation of the Transcription Factor Aft1'. *Biochimica et Biophysica Acta (BBA)* 1868 (January). https://doi.org/10.1016/j.bbamcr.2021.118974.

Pujol-Carrion, Nuria, Mima I. Petkova, Luis Serrano, and Maria Angeles de la Torre-Ruiz. 2013. 'The MAP Kinase Slt2 Is Involved in Vacuolar Function and Actin Remodeling in Saccharomyces Cerevisiae Mutants Affected by Endogenous Oxidative Stress'. *Applied and Environmental Microbiology* 79 (20): 6459–71. https://doi.org/10.1128/AEM.01692-13.

Qadota, Hiroshi, Christophe P. Python, Shunsuke B. Inoue, Mikio Arisawa, Yasuhiro Anraku, Yi Zheng, Takahide Watanabe, David E. Levin, and Yoshikazu Ohya. 1996. 'Identification of Yeast Rho1p GTPase as a Regulatory Subunit of 1,3-β-Glucan Synthase'. *Science* 272 (5259): 279–81. https://doi.org/10.1126/SCIENCE.272.5259.279.

Qian, Bo, Shaowei Chen, Ting Wang, Xinhao Zhang, and Hongli Bao. 2017. 'Iron-Catalyzed Carboamination of Olefins: Synthesis of Amines and Disubstituted β-Amino Acids'. *Journal of the American Chemical Society* 139 (37): 13076–82. https://doi.org/10.1021/JACS.7B06590.

Qin, Zheng-Hong. 2019. *Autophagy: Biology and Diseases*. Edited by Zheng-Hong Qin. *International Journal of Radiation Biology*. Vol. 44. Singapore: Science Press. https://doi.org/10.1007/978-981-15-0602-4.

Queralt, Ethel, and J. Carlos Igual. 2005. 'Functional Connection between the Clb5 Cyclin, the Protein Kinase C Pathway and the Swi4 Transcription Factor in Saccharomyces Cerevisiae'. *Genetics* 171 (4): 1485–98. https://doi.org/10.1534/GENETICS.105.045005.

Quilis, Inma, Mercè Gomar-Alba, and Juan Carlos Igual. 2021. 'The Cwi Pathway: A Versatile Toolbox to Arrest Cell-Cycle Progression'. *Journal of Fungi* 7 (12). https://doi.org/10.3390/jof7121041.

Rajavel, Mathumathi, Bevin Philip, Benjamin M. Buehrer, Beverly Errede, and David E. Levin. 1999. 'Mid2 Is a Putative Sensor for Cell Integrity Signaling in Saccharomyces Cerevisiae'. *Molecular and Cellular Biology* 19 (6): 3969–76. https://doi.org/10.1128/MCB.19.6.3969.

Ray, Alo, Ronald E. Hector, Nilanjan Roy, Jee Hyeon Song, Kathleen L. Berkner, and Kurt W. Runge. 2003. 'Sir3p Phosphorylation by the Slt2p Pathway Effects Redistribution of Silencing Function and Shortened Lifespan'. *Nature Genetics 2003 33:4* 33 (4): 522–26. https://doi.org/10.1038/ng1132.

Reinke, Aaron, Scott Anderson, J. Michael McCaffery, John Yates, Sofia Aronova, Stephanie Chu, Stephen Fairclough, Cory Iverson, Karen P. Wedaman, and Ted Powers. 2004. 'TOR Complex 1 Includes a Novel Component, Tco89p (YPL180w), and Cooperates with Ssd1p to Maintain Cellular Integrity in Saccharomyces Cerevisiae'. *Journal of Biological Chemistry* 279 (15): 14752–62. https://doi.org/10.1074/jbc.M313062200.

Reiter, Alarich, Robert Steinbauer, Anja Philippi, Jochen Gerber, Herbert Tschochner, Philipp Milkereit, and Joachim Griesenbeck. 2011. ' Reduction in Ribosomal Protein Synthesis

Is Sufficient To Explain Major Effects on Ribosome Production after Short-Term TOR Inactivation in Saccharomyces Cerevisiae '. *Molecular and Cellular Biology* 31 (4): 803–17. https://doi.org/10.1128/MCB.01227-10.

Ren, Jun, and Yingmei Zhang. 2018. 'Targeting Autophagy in Aging and Aging-Related Cardiovascular Diseases'. *Trends in Pharmacological Sciences* 39 (12): 1064–76. https://doi.org/10.1016/J.TIPS.2018.10.005.

Richard, Vincent R., Anna Leonov, Adam Beach, Michelle T. Burstein, Olivia Koupaki, Alejandra Gomez-Perez, Sean Levy, et al. 2013. 'Macromitophagy Is a Longevity Assurance Process That in Chronologically Aging Yeast Limited in Calorie Supply Sustains Functional Mitochondria and Maintains Cellular Lipid Homeostasis'. *Aging (Albany NY)* 5 (4): 234. https://doi.org/10.18632/AGING.100547.

Rietzschel, Nicole, Antonio J. Pierik, Eckhard Bill, Roland Lill, and Ulrich Mühlenhoff. 2015. 'The Basic Leucine Zipper Stress Response Regulator Yap5 Senses High-Iron Conditions by Coordination of [2Fe-2S] Clusters'. *Molecular and Cellular Biology* 35 (2): 370–78. https://doi.org/10.1128/MCB.01033-14.

Riley, Ronald T., and Alfred H. Merrill. 2019. 'Ceramide Synthase Inhibition by Fumonisins: A Perfect Storm of Perturbed Sphingolipid Metabolism, Signaling, and Disease'. *Journal of Lipid Research* 60 (7): 1183–89. https://doi.org/10.1194/jlr.S093815.

Rittenhouse, Judith, Lorraine Moberly, and Frank Marcus. 1987. 'THE JOURNAL OF BIOLOGICAL CHEMISTRY Phosphorylation in Vivo of Yeast (Saccharomyces Cereuisiae) Fructose-1,6-Bisphosphatase at the Cyclic AMP-Dependent Site*'. *Journal of Biological Chemistry* 262 (21): 10114–19. https://doi.org/10.1016/S0021-9258(18)61085-3.

Robertson, Laura S., Helen C. Causton, Richard A. Young, and Gerald R. Fink. 2000. 'The Yeast A Kinases Differentially Regulate Iron Uptake and Respiratory Function'. *Proceedings of the National Academy of Sciences of the United States of America* 97 (11): 5984–88. https://doi.org/10.1073/PNAS.100113397.

Roelants, Françoise M., David K. Breslow, Alexander Muir, Jonathan S. Weissman, and Jeremy Thorner. 2011a. 'Protein Kinase Ypk1 Phosphorylates Regulatory Proteins Orm1 and Orm2 to Control Sphingolipid Homeostasis in Saccharomyces Cerevisiae'. *Proceedings of the National Academy of Sciences of the United States of America* 108 (48): 19222–27. https://doi.org/10.1073/PNAS.1116948108.

———. 2011b. 'Protein Kinase Ypk1 Phosphorylates Regulatory Proteins Orm1 and Orm2 to Control Sphingolipid Homeostasis in Saccharomyces Cerevisiae'. *Proceedings of the National Academy of Sciences of the United States of America* 108 (48): 19222–27. https://doi.org/10.1073/PNAS.1116948108/SUPPL_FILE/SAPP.PDF.

Roelants, Françoise M., Pamela D. Torrance, and Jeremy Thorner. 2004. 'Differential Roles of PDK1- and PDK2-Phosphorylation Sites in the Yeast AGC Kinases Ypk1, Pkc1 and Sch9'. *Microbiology (Reading, England)* 150 (Pt 10): 3289–3304. https://doi.org/10.1099/MIC.0.27286-0.

Rohde, John R., Robert Bastidas, Rekha Puria, and Maria E Cardenas. 2008. 'Nutritional Control via Tor Signaling in Saccharomyces Cerevisiae'. *Current Opinion in Microbiology* 11 (2): 153–60. https://www.ncbi.nlm.nih.gov/pmc/articles/PMC3624763/pdf/nihms412728.pdf.

Rolfes, R J, and A G Hinnebusch. 1993. 'Translation of the Yeast Transcriptional Activator GCN4 Is Stimulated by Purine Limitation: Implications for Activation of the Protein Kinase GCN2'. *Molecular and Cellular Biology* 13 (8): 5099–5111. https://doi.org/10.1128/mcb.13.8.5099-5111.1993.

Rolland, Filip, Johannes H. De Winde, Katleen Lemaire, Eckhard Boles, Johan M. Thevelein, and Joris Winderickx. 2000. 'Glucose-Induced CAMP Signalling in Yeast Requires Both

a G-Protein Coupled Receptor System for Extracellular Glucose Detection and a Separable Hexose Kinase-Dependent Sensing Process'. *Molecular Microbiology* 38 (2): 348–58. https://doi.org/10.1046/J.1365-2958.2000.02125.X.

Rolland, Filip, Joris Winderickx, and Johan M. Thevelein. 2002. 'Glucose-Sensing and -Signalling Mechanisms in Yeast'. *FEMS Yeast Research* 2 (2): 183–201. https://doi.org/10.1016/S1567-1356(02)00046-6.

Roosen, Johnny, Kristof Engelen, Kathleen Marchal, Janick Mathys, Gerard Griffioen, Elisabetta Cameroni, Johan M. Thevelein, Claudio De Virgilio, Bart De Moor, and Joris Winderickx. 2005. 'PKA and Sch9 Control a Molecular Switch Important for the Proper Adaptation to Nutrient Availability'. *Molecular Microbiology* 55 (3): 862–80. https://doi.org/10.1111/j.1365-2958.2004.04429.x.

Roszczyc-Owsiejczuk, Kamila, and Piotr Zabielski. 2021. 'Sphingolipids as a Culprit of Mitochondrial Dysfunction in Insulin Resistance and Type 2 Diabetes'. *Frontiers in Endocrinology* 12 (March). https://doi.org/10.3389/FENDO.2021.635175.

Roumanie, Olivier, Caroline Weinachter, Isabelle Larrieu, Marc Crouzet, and François Doignon. 2001. 'Functional Characterization of the Bag7, Lrg1 and Rgd2 RhoGAP Proteins from Saccharomyces Cerevisiae'. *FEBS Letters* 506 (2): 149–56. https://doi.org/10.1016/S0014-5793(01)02906-4.

Ruiz, Amparo, Xinjing Xu, and Marian Carlson. 2011. 'INAUGURAL ARTICLE by a Recently Elected Academy Member:Roles of Two Protein Phosphatases, Reg1-Glc7 and Sit4, and Glycogen Synthesis in Regulation of SNF1 Protein Kinase'. *Proceedings of the National Academy of Sciences of the United States of America* 108 (16): 6349. https://doi.org/10.1073/PNAS.1102758108.

———. 2013. 'Ptc1 Protein Phosphatase 2C Contributes to Glucose Regulation of SNF1/AMP-Activated Protein Kinase (AMPK) in Saccharomyces Cerevisiae'. *The Journal of Biological Chemistry* 288 (43): 31052. https://doi.org/10.1074/JBC.M113.503763.

Sagot, Isabelle, and Damien Laporte. 2019. 'The Cell Biology of Quiescent Yeast – a Diversity of Individual Scenarios'. *Journal of Cell Science* 132 (1). https://doi.org/10.1242/jcs.213025.

Sakai, Yasuyoshi, Masahide Oku, Ida J. van der Klei, and Jan a K W Kiel. 2006. 'Pexophagy: Autophagic Degradation of Peroxisomes'. *Biochimica et Biophysica Acta - Molecular Cell Research* 1763 (12): 1767–75. https://doi.org/10.1016/j.bbamcr.2006.08.023.

Sampaio-Marques, Belém, Carolina Felgueiras, Alexandra Silva, Fernando Rodrigues, and Paula Ludovico. 2011. 'Yeast Chronological Lifespan and Proteotoxic Stress: Is Autophagy Good or Bad?' *Biochemical Society Transactions* 39 (5): 1466–70. https://doi.org/10.1042/BST0391466.

Sanders-Loehr, J. 1988. 'Involvement of Oxo-Bridged Binuclear Iron Centers in Oxygen Transport, Oxygen Reduction, and Oxygenation.' *Progress in Clinical and Biological Research* 274 (January): 193–209. https://europepmc.org/article/med/3043460.

Santangelo, George M. 2006. 'Glucose Signaling in Saccharomyces Cerevisiae Glucose Signaling in Saccharomyces Cerevisiae'. *Microbiology and Molecular Biology Reviews* 70 (1): 253–82. https://doi.org/10.1128/MMBR.70.1.253.

Sanvisens, Nerea, Rosa de Llanos, and Sergi Puig. 2013. 'Function and Regulation of Yeast Ribonucleotide Reductase: Cell Cycle, Genotoxic Stress, and Iron Bioavailability'. *Biomedical Journal* 36 (2): 51–58. https://doi.org/10.4103/2319-4170.110398.

Sanz, Ana Belén, Raúl García, Mónica Pavón-Vergés, José Manuel Rodríguez-Peña, and Javier Arroyo. 2022. 'Control of Gene Expression via the Yeast CWI Pathway'. *International Journal of Molecular Sciences* 23 (3). https://doi.org/10.3390/ijms23031791.

Sanz, Ana Belén, Raúl García, José M. Rodríguez-Peña, and Javier Arroyo. 2018. 'The CWI

Pathway: Regulation of the Transcriptional Adaptive Response to Cell Wall Stress in Yeast'. *Journal of Fungi* 4 (1): 1–12. https://doi.org/10.3390/jof4010001.

Sanz, Pascual, Geoffrey R Alms, Timothy A.J. Haystead, and Marian Carlson. 2000. 'Regulatory Interactions between the Reg1-Glc7 Protein Phosphatase and the Snf1 Protein Kinase'. *Molecular and Cellular Biology* 20 (4): 1321–28. https://doi.org/10.1128/MCB.20.4.1321-1328.2000.

Sanz, Pascual, Rosa Viana, and Maria Adelaida Garcia-Gimeno. 2016. 'AMPK in Yeast: The SNF1 (Sucrose Non-Fermenting 1) Protein Kinase Complex'. *Exs* 107: 353–74. https://doi.org/10.1007/978-3-319-43589-3_14.

Sarbassov, Dos D., Siraj M. Ali, Shomit Sengupta, Joon Ho Sheen, Peggy P. Hsu, Alex F. Bagley, Andrew L. Markhard, and David M. Sabatini. 2006. 'Prolonged Rapamycin Treatment Inhibits MTORC2 Assembly and Akt/PKB'. *Molecular Cell* 22 (2): 159–68. https://doi.org/10.1016/J.MOLCEL.2006.03.029.

Sarkar, Chinmoy, Jace W. Jones, Nivedita Hegdekar, Julia A. Thayer, Alok Kumar, Alan I. Faden, Maureen A. Kane, and Marta M. Lipinski. 2020. 'PLA2G4A/CPLA2-Mediated Lysosomal Membrane Damage Leads to Inhibition of Autophagy and Neurodegeneration after Brain Trauma'. *Autophagy* 16 (3): 466–85. https://doi.org/10.1080/15548627.2019.1628538.

Sass, P., J. Field, J. Nikawa, T. Toda, and M. Wigler. 1986. 'Cloning and Characterization of the High-Affinity CAMP Phosphodiesterase of Saccharomyces Cerevisiae'. *Proceedings of the National Academy of Sciences of the United States of America* 83 (24): 9303–7. https://doi.org/10.1073/PNAS.83.24.9303.

Sato, Keisuke, Yoichi Noda, and Koji Yoda. 2009. 'Kei1: A Novel Subunit of Inositolphosphorylceramide Synthase, Essential for Its Enzyme Activity and Golgi Localization'. *Molecular Biology of the Cell* 20 (20): 4444. https://doi.org/10.1091/MBC.E09-03-0235.

Sawai, Hirofumi, Yasuo Okamoto, Chiara Luberto, Cungui Mao, Alicja Bielawska, Naochika Domae, and Yusuf A. Hannun. 2000. 'Identification of ISC1 (YER019w) as Inositol Phosphosphingolipid Phospholipase C in Saccharomyces Cerevisiae'. *The Journal of Biological Chemistry* 275 (50): 39793–98. https://doi.org/10.1074/JBC.M007721200.

Schepers, Jana, and Christian Behl. 2021. 'Lipid Droplets and Autophagy—Links and Regulations from Yeast to Humans'. *Journal of Cellular Biochemistry* 122 (6): 602–11. https://doi.org/10.1002/jcb.29889.

Schepers, Wim, Griet Van Zeebroeck, Martijn Pinkse, Peter Verhaert, and Johan M. Thevelein. 2012. 'In Vivo Phosphorylation of Ser21 and Ser83 during Nutrient-Induced Activation of the Yeast Protein Kinase A (PKA) Target Trehalase'. *The Journal of Biological Chemistry* 287 (53): 44130. https://doi.org/10.1074/JBC.M112.421503.

Schirmer, Melanie, Ashley Garner, Hera Vlamakis, and Ramnik J. Xavier. 2019. 'Microbial Genes and Pathways in Inflammatory Bowel Disease'. *Nature Reviews. Microbiology* 17 (8): 497–511. https://doi.org/10.1038/S41579-019-0213-6.

Schmelzle, Tobias, Thomas Beck, Dietmar E. Martin, and Michael N. Hall. 2004. 'Activation of the RAS/Cyclic AMP Pathway Suppresses a TOR Deficiency in Yeast'. *Molecular and Cellular Biology* 24 (1): 338–51. https://doi.org/10.1128/mcb.24.1.338-351.2004.

Schmelzle, Tobias, and Michael N. Hall. 2000. 'TOR, a Central Controller of Cell Growth'. *Cell* 103 (2): 253–62. https://doi.org/10.1016/S0092-8674(00)00117-3.

Schmelzle, Tobias, Stephen B. Helliwell, and Michael N. Hall. 2002. 'Yeast Protein Kinases and the RHO1 Exchange Factor TUS1 Are Novel Components of the Cell Integrity Pathway in Yeast'. *Molecular and Cellular Biology* 22 (5): 1329–39. https://doi.org/10.1128/MCB.22.5.1329-1339.2002.

Schmidt, Anja, Tobias Schmelzle, and Michael N. Hall. 2002. 'The RHO1-GAPs SAC7, BEM2

and BAG7 Control Distinct RHO1 Functions in Saccharomyces Cerevisiae'. *Molecular Microbiology* 45 (5): 1433–41. https://doi.org/10.1046/J.1365-2958.2002.03110.X.

Schmidt, Oliver, Yannick Weyer, Simon Sprenger, Michael A. Widerin, Sebastian Eising, Verena Baumann, Mihaela Angelova, et al. 2020. 'TOR Complex 2 (TORC2) Signaling and the ESCRT Machinery Cooperate in the Protection of Plasma Membrane Integrity in Yeast'. *Journal of Biological Chemistry* 295 (34): 12028–44. https://doi.org/10.1074/jbc.RA120.013222.

Scrimale, Thomas, Louis Didone, Karen L. De Mesy Bentley, and Damian J. Krysan. 2009. 'The Unfolded Protein Response Is Induced by the Cell Wall Integrity Mitogen-Activated Protein Kinase Signaling Cascade and Is Required for Cell Wall Integrity in Saccharomyces Cerevisiae'. *Molecular Biology of the Cell* 20 (1): 164. https://doi.org/10.1091/MBC.E08-08-0809.

Serrano, Raquel, Humberto Martín, Antonio Casamayor, and Joaquín Ariño. 2006. 'Signaling Alkaline PH Stress in the Yeast Saccharomyces Cerevisiae through the Wsc1 Cell Surface Sensor and the Slt2 MAPK Pathway'. *Journal of Biological Chemistry* 281 (52): 39785–95. https://doi.org/10.1074/jbc.M604497200.

Shakoury-Elizeh, Minoo, Olga Protchenko, Alvin Berger, James Cox, Kenneth Gable, Teresa M. Dunn, William A. Prinz, Martin Bard, and Caroline C. Philpott. 2010a. 'Metabolic Response to Iron Deficiency in Saccharomyces Cerevisiae'. *The Journal of Biological Chemistry* 285 (19): 14823. https://doi.org/10.1074/JBC.M109.091710.

———. 2010b. 'Metabolic Response to Iron Deficiency in Saccharomyces Cerevisiae'. *The Journal of Biological Chemistry* 285 (19): 14823–33. https://doi.org/10.1074/JBC.M109.091710.

Shakoury-Elizeh, Minoo, John Tiedeman, Jared Rashford, Tracey Ferea, Janos Demeter, Emily Garcia, Ronda Rolfes, Patrick O. Brown, David Botstein, and Caroline C. Philpott. 2004. 'Transcriptional Remodeling in Response to Iron Deprivation in Saccharomyces Cerevisiae'. *Molecular Biology of the Cell* 15 (3): 1233–43. https://doi.org/10.1091/MBC.E03-09-0642/ASSET/IMAGES/LARGE/ZMK0030425410008.JPEG.

Shamji, Alykhan F, Finny G Kuruvilla, and Stuart L Schreiber. 2000. 'Partitioning the Transcriptional Program Induced by Rapamycin among the Effectors of the Tor Proteins'. http://www-schreiber.chem.harvard.edu.

Shetty, Sunil, Jon Hofstetter, Stefania Battaglioni, Danilo Ritz, and Michael N Hall. 2023. ' TORC1 Phosphorylates and Inhibits the Ribosome Preservation Factor Stm1 to Activate Dormant Ribosomes '. *The EMBO Journal* 42 (5): 1–15. https://doi.org/10.15252/embj.2022112344.

Shin, Dong Wook. 2020. 'Lipophagy: Molecular Mechanisms and Implications in Metabolic Disorders'. *Molecules and Cells* 43 (8): 686–93. https://doi.org/10.14348/MOLCELLS.2020.0046.

Shirra, Margaret K., Rhonda R. McCartney, Chao Zhang, Kevan M. Shokat, Martin C. Schmidt, and Karen M. Arndt. 2008. 'A Chemical Genomics Study Identifies Snf1 as a Repressor of GCN4 Translation'. *Journal of Biological Chemistry* 283 (51): 35889–98. https://doi.org/10.1074/jbc.M805325200.

Siegel Mph, Rebecca L, Kimberly D Miller, Nikita Sandeep, Wagle Mbbs, | Ahmedin, Jemal Dvm, and Rebecca L Siegel. 2023. 'Cancer Statistics, 2023'. *CA: A Cancer Journal for Clinicians* 73 (1): 17–48. https://doi.org/10.3322/CAAC.21763.

Simpson-Lavy, Kobi J., and Mark Johnston. 2013. 'SUMOylation Regulates the SNF1 Protein Kinase'. *Proceedings of the National Academy of Sciences of the United States of America* 110 (43): 17432–37. https://doi.org/10.1073/PNAS.1304839110/-/DCSUPPLEMENTAL.

Smith, Angela, Mary P. Ward, and Stephen Garrett. 1998. 'Yeast PKA Represses Msn2p/Msn4p-Dependent Gene Expression to Regulate Growth, Stress Response and Glycogen Accumulation'. *The EMBO Journal* 17 (13): 3556–64. https://doi.org/10.1093/EMBOJ/17.13.3556.

Soontorngun, Nitnipa, Marc Larochelle, Simon Drouin, François Robert, and Bernard Turcotte. 2007. 'Regulation of Gluconeogenesis in Saccharomyces Cerevisiae Is Mediated by Activator and Repressor Functions of Rds2'. *Molecular and Cellular Biology* 27 (22): 7895. https://doi.org/10.1128/MCB.01055-07.

Sorrentino, Vincenzo, Mario Romani, Laurent Mouchiroud, John S. Beck, Hongbo Zhang, Davide D'Amico, Norman Moullan, et al. 2017. 'Enhancing Mitochondrial Proteostasis Reduces Amyloid-β Proteotoxicity'. *Nature* 552 (7684): 187–93. https://doi.org/10.1038/NATURE25143.

Soulard, Alexandre, Alessio Cremonesi, Suzette Moes, Frédéric Schütz, Paul Jenö, and Michael N. Hall. 2010. 'The Rapamycin-Sensitive Phosphoproteome Reveals That TOR Controls Protein Kinase A toward Some but Not All Substrates'. *Molecular Biology of the Cell* 21 (19): 3475–86. https://doi.org/10.1091/MBC.E10-03-0182/ASSET/IMAGES/LARGE/ZMK0191095960006.JPEG.

Spiegel, Sarah, Olivier Cuvillier, Lisa C. Edsall, Takafumi Kohama, Ramil Menzeleev, Zoltan Olah, Ana Olivera, et al. 1998. 'Sphingosine-1-Phosphate in Cell Growth and Cell Death'. *Annals of the New York Academy of Sciences* 845: 11–18. https://doi.org/10.1111/J.1749-6632.1998.TB09658.X.

Spiegel, Sarah, and Alfred H. Merrill. 1996. 'Sphingolipid Metabolism and Cell Growth Regulation'. *FASEB Journal : Official Publication of the Federation of American Societies for Experimental Biology* 10 (12): 1388–97. https://doi.org/10.1096/FASEBJ.10.12.8903509.

Spincemaille, Pieter, Bruno P.A. Cammue, and Karin Thevissen. 2014. 'Sphingolipids and Mitochondrial Function, Lessons Learned from Yeast'. *Microbial Cell* 1 (7): 210–24. https://doi.org/10.15698/mic2014.07.156.

Spincemaille, Pieter, Nabil Matmati, Yusuf A. Hannun, Bruno P.A. Cammue, and Karin Thevissen. 2014. 'Sphingolipids and Mitochondrial Function in Budding Yeast'. *Biochimica et Biophysica Acta Biophys Acta* 1814 (10): 3131–37. https://doi.org/doi:10.1016/j.bbagen.2014.06.015.

Stahl, Guillaume, Samia N.Ben Salem, Lifeng Chen, Bing Zhao, and Philip J. Farabaugh. 2004. 'Translational Accuracy during Exponential, Postdiauxic, and Stationary Growth Phases in Saccharomyces Cerevisiae'. *Eukaryotic Cell* 3 (2): 331–38. https://doi.org/10.1128/EC.3.2.331-338.2004.

Staschke, Kirk A., Souvik Dey, John M. Zaborske, Lakshmi Reddy Palam, Jeanette N. McClintick, Tao Pan, Howard J. Edenberg, and Ronald C. Wek. 2010. 'Integration of General Amino Acid Control and Target of Rapamycin (TOR) Regulatory Pathways in Nitrogen Assimilation in Yeast'. *The Journal of Biological Chemistry* 285 (22): 16893–911. https://doi.org/10.1074/JBC.M110.121947.

Stathopoulos, Angelike M., and Martha S. Cyert. 1997. 'Calcineurin Acts through the CRZ1/TCN1-Encoded Transcription Factor to Regulate Gene Expression in Yeast'. *Genes & Development* 11 (24): 3432. https://doi.org/10.1101/GAD.11.24.3432.

Stearman, Robert, Daniel S. Yuan, Yuko Yamaguchi-Iwai, Richard D. Klausner, and Andrew Dancis. 1996. 'A Permease-Oxidase Complex Involved in High-Affinity Iron Uptake in Yeast'. *Science (New York, N.Y.)* 271 (5255): 1552–57. https://doi.org/10.1126/SCIENCE.271.5255.1552.

Steinkraus, K. A., M. Kaeberlein, and B. K. Kennedy. 2008. 'Replicative Aging in Yeast: The Means to the End'. *Annual Review of Cell and Developmental Biology* 24: 29–54.

https://doi.org/10.1146/annurev.cellbio.23.090506.123509.

Sukegawa, Yuko, Takahiro Negishi, Yo Kikuchi, Keiko Ishii, Miyuki Imanari, Farzan Ghanegolmohammadi, Satoru Nogami, and Yoshikazu Ohya. 2018. 'Genetic Dissection of the Signaling Pathway Required for the Cell Wall Integrity Checkpoint'. *Journal of Cell Science* 131 (13). https://doi.org/10.1242/jcs.219063.

Sun, Nuo, Jeanho Yun, Jie Liu, Daniela Malide, Chengyu Liu, Ilsa I. Rovira, Kira M. Holmström, et al. 2015. 'Measuring In Vivo Mitophagy'. *Molecular Cell* 60 (4): 685–96. https://doi.org/10.1016/J.MOLCEL.2015.10.009.

Sun, Siyu, and David Gresham. 2021. 'Cellular Quiescence in Budding Yeast'. *Yeast (Chichester, England)* 38 (1): 12. https://doi.org/10.1002/YEA.3545.

Sun, Yidi, Yansong Miao, Yukari Yamane, Chao Zhang, Kevan M Shokat, Hiromu Takematsu, Yasunori Kozutsumi, and David G Drubin. 2012. 'Orm Protein Phosphoregulation Mediates Transient Sphingolipid Biosynthesis Response to Heat Stress via the Pkh-Ypk and Cdc55-PP2A Pathways'. https://doi.org/10.1091/mbc.E12-03-0209.

Sundaram, Venkatraghavan, Mima I. Petkova, Nuria Pujol-Carrion, Jordi Boada, and Maria Angeles de la Torre-Ruiz. 2015. 'Tor1, Sch9 and PKA Downregulation in Quiescence Rely on Mtl1 to Preserve Mitochondrial Integrity and Cell Survival'. *Molecular Microbiology* 97 (1): 93–109. https://doi.org/10.1111/mmi.13013.

Swinnen, Erwin, Tobias Wilms, Jolanta Idkowiak-Baldys, Bart Smets, Pepijn De Snijder, Sabina Accardo, Ruben Ghillebert, et al. 2014a. 'The Protein Kinase Sch9 Is a Key Regulator of Sphingolipid Metabolism in Saccharomyces Cerevisiae'. *Molecular Biology of the Cell* 25 (1): 196. https://doi.org/10.1091/MBC.E13-06-0340.

———. 2014b. 'The Protein Kinase Sch9 Is a Key Regulator of Sphingolipid Metabolism in Saccharomyces Cerevisiae'. *Molecular Biology of the Cell* 25 (1): 196–211. https://doi.org/10.1091/MBC.E13-06-0340.

Tabibzadeh, Siamak. 2023. 'Role of Autophagy in Aging: The Good, the Bad, and the Ugly'. *Aging Cell* 22 (1). https://doi.org/10.1111/ACEL.13753.

Takahiro Shintani and Daniel J. Klionsky. 2004. 'Cargo Proteins Facilitate the Formation of Transport Vesicles in the Cytoplasm to Vacuole Targeting Pathway'. *J Biol Chem.* 279 (29): 29889–94.

Tamanoi, Fuyuhiko. 1988. 'Yeast RAS Genes'. *Biochimica et Biophysica Acta* 948: 1–15.

Tamarit, Jordi, Verónica Irazusta, Armando Moreno-Cermeño, and Joaquim Ros. 2006. 'Colorimetric Assay for the Quantitation of Iron in Yeast'. *Analytical Biochemistry* 351 (1): 149–51. https://doi.org/10.1016/J.AB.2005.12.001.

Tanaka, Kazuma, Masato Nakafuku, Takaya Satoh, Mark S. Marshall, Jackson B. Gibbs, Kunihiro Matsumoto, Yoshito Kaziro, and Akio Toh-e. 1990. 'S. Cerevisiae Genes IRA1 and IRA2 Encode Proteins That May Be Functionally Equivalent to Mammalian Ras GTPase Activating Protein'. *Cell* 60 (5): 803–7. https://doi.org/10.1016/0092-8674(90)90094-U.

Tani, Motohiro, and Kouichi Funato. 2018. 'Protection Mechanisms against Aberrant Metabolism of Sphingolipids in Budding Yeast'. *Current Genetics* 64 (5): 1021–28. https://doi.org/10.1007/s00294-018-0826-8.

Tatjer, Laura, Almudena Sacristán-Reviriego, Carlos Casado, Asier González, Boris Rodríguez-Porrata, Lorena Palacios, David Canadell, et al. 2016. 'Wide-Ranging Effects of the Yeast Ptc1 Protein Phosphatase Acting through the MAPK Kinase Mkk1'. *Genetics* 202 (1): 141–56. https://doi.org/10.1534/GENETICS.115.183202/-/DC1.

Taylor, Ian A., Pauline B. McIntosh, Preshna Pala, Monika K. Treiber, Steven Howell, Andrew N. Lane, and Stephen J. Smerdon. 2000. 'Characterization of the DNA-Binding Domains from the Yeast Cell-Cycle Transcription Factors Mbp1 and Swi4'. *Biochemistry* 39 (14): 3943–54. https://doi.org/10.1021/BI992212I.

Thevelein, J. M. 1991. 'Fermentable Sugars and Intracellular Acidification as Specific Activators of the RAS-adenylate Cyclase Signalling Pathway in Yeast: The Relationship to Nutrient-induced Cell Cycle Control'. *Molecular Microbiology* 5 (6): 1301–7. https://doi.org/10.1111/j.1365-2958.1991.tb00776.x.

Thevelein, Johan M., and Johannes H. De Winde. 1999. 'Novel Sensing Mechanisms and Targets for the CAMP-Protein Kinase A Pathway in the Yeast Saccharomyces Cerevisiae'. *Molecular Microbiology* 33 (5): 904–18. https://doi.org/10.1046/J.1365-2958.1999.01538.X.

Thorner, Jeremy. 2022. 'TOR Complex 2 Is a Master Regulator of Plasma Membrane Homeostasis'. *Biochemical Journal* 479 (18): 1917–40. https://doi.org/10.1042/BCJ20220388.

Tisi, Renata, Fiorella Belotti, and Enzo Martegani. 2014. *Yeast as a Model for Ras Signalling*. *Methods in Molecular Biology*. Vol. 1120. https://doi.org/10.1007/978-1-62703-791-4_23.

Toda, Takashi, Scott Cameron, Philip Sass, Mark Zoller, J D Scott, B McMULLEN, M Hurwitz, E G Krebs, and Michael Wigler. 1987. 'Cloning and Characterization of BCY1, a Locus Encoding a Regulatory Subunit of the Cyclic AMP-Dependent Protein Kinase in Saccharomyces Cerevisiae'. *MOLECULAR AND CELLULAR BIOLOGY* 7 (4): 1371–77.

Toda, Takashi, Scott Cameron, Philip Sass, Mark Zoller, and Michael Wigler. 1987. 'Three Different Genes in S. Cerevisiae Encode the Catalytic Subunits of the CAMP-Dependent Protein Kinase'. *Cell* 50 (2): 277–87. https://doi.org/10.1016/0092-8674(87)90223-6.

Toda, Takashi, Isao Uno, Tatsuo Ishikawa, Scott Powers, Tohru Kataoka, Daniel Broek, Scott Cameron, James Broach, Kunihiro Matsumoto, and Michael Wigler. 1985. 'In Yeast, RAS Proteins Are Controlling Elements of Adenylate Cyclase'. *Cell* 40 (1): 27–36. https://doi.org/10.1016/0092-8674(85)90305-8.

Tomotake, Kanki, and J. Klionsky Daniel. 2008. 'MITOPHAGY IN YEAST OCCURS THROUGH A SELECTIVE MECHANISM'. *JBC*, no. 6. https://doi.org/10.1074/jbc.M802403200.

Torres, Jordi, Charles J. Di Como, Enrique Herrero, and Maria Angeles De La Torre-Ruiz. 2002. 'Regulation of the Cell Integrity Pathway by Rapamycin-Sensitive TOR Function in Budding Yeast'. *Journal of Biological Chemistry* 277 (45): 43495–504. https://doi.org/10.1074/jbc.M205408200.

Tripodi, Farida, Roberta Fraschini, Monica Zocchi, Veronica Reghellin, and Paola Coccetti. 2018. 'Snf1/AMPK Is Involved in the Mitotic Spindle Alignment in Saccharomyces Cerevisiae'. *Scientific Reports* 8 (1): 1–12. https://doi.org/10.1038/s41598-018-24252-y.

Tyler, Jessica K., and Jay E. Johnson. 2018a. 'The Role of Autophagy in the Regulation of Yeast Life Span'. *Annals of the New York Academy of Sciences*, 31–43. https://doi.org/10.1111/nyas.13549.

———. 2018b. 'The Role of Autophagy in the Regulation of Yeast Life Span'. *Annals of the New York Academy of Sciences* 1418 (1): 31–43. https://doi.org/10.1111/nyas.13549.

Udom, Nisarut, Pakkanan Chansongkrow, Varodom Charoensawan, and Choowong Auesukaree. 2019. 'Coordination of the Cell Wall Integrity and Highosmolarity Glycerol Pathways in Response to Ethanol Stress in Saccharomyces Cerevisiae'. *Applied and Environmental Microbiology* 85 (15). https://doi.org/10.1128/AEM.00551-19.

Ueda, Sayuri, Ryota Ozaki, Atsuki Kaneko, Ryoma Akizuki, Haruko Katsuta, Atsuhiro Miura, Akira Matsuura, and Takashi Ushimaru. 2019. 'TORC1, Tel1/Mec1, and Mpk1 Regulate Autophagy Induction after DNA Damage in Budding Yeast'. *Cellular Signalling* 62 (October): 109344. https://doi.org/10.1016/J.CELLSIG.2019.109344.

Uemura, Satoshi, Akio Kihara, Jin Ichi Inokuchi, and Yasuyuki Igarashi. 2003. 'Csg1p and Newly Identified Csh1p Function in Mannosylinositol Phosphorylceramide Synthesis by

Interacting with Csg2p'. *Journal of Biological Chemistry* 278 (46): 45049–55. https://doi.org/10.1074/JBC.M305498200.

Ueta, Ryo, Naoko Fujiwara, Kazuhiro Iwai, and Yuko Yamaguchi-Iwai. 2007. 'Mechanism Underlying the Iron-Dependent Nuclear Export of the Iron-Responsive Transcription Factor Aft1p in Saccharomyces Cerevisiae'. *Molecular Biology of the Cell* 18 (8): 2980. https://doi.org/10.1091/MBC.E06-11-1054.

———. 2012. 'Iron-Induced Dissociation of the Aft1p Transcriptional Regulator from Target Gene Promoters Is an Initial Event in Iron-Dependent Gene Suppression'. *Molecular and Cellular Biology* 32 (24): 4998–5008. https://doi.org/10.1128/MCB.00726-12.

Ueta, Ryo, Ayako Fukunaka, and Yuko Yamaguchi-Iwai. 2003. 'Pse1p Mediates the Nuclear Import of the Iron-Responsive Transcription Factor Aft1p in Saccharomyces Cerevisiae'. *The Journal of Biological Chemistry* 278 (50): 50120–27. https://doi.org/10.1074/JBC.M305046200.

Urban, Jörg, Alexandre Soulard, Alexandre Huber, Soyeon Lippman, Debdyuti Mukhopadhyay, Olivier Deloche, Valeria Wanke, et al. 2007. 'Sch9 Is a Major Target of TORC1 in Saccharomyces Cerevisiae'. *Molecular Cell* 26 (5): 663–74. https://doi.org/10.1016/j.molcel.2007.04.020.

Urita, Atsuya, Yohei Ishibashi, Ryotaro Kawaguchi, Yukimi Yanase, and Motohiro Tani. 2022. 'Crosstalk between Protein Kinase A and the HOG Pathway under Impaired Biosynthesis of Complex Sphingolipids in Budding Yeast'. *FEBS Journal* 289 (3): 766–86. https://doi.org/10.1111/febs.16188.

Vallée, Béatrice, and Howard Riezman. 2005. 'Lip1p: A Novel Subunit of Acyl-CoA Ceramide Synthase'. *The EMBO Journal* 24 (4): 730. https://doi.org/10.1038/SJ.EMBOJ.7600562.

Vazquez de Aldana, C R, R C Wek, P S Segundo, A G Truesdell, and A G Hinnebusch. 1994. 'Multicopy TRNA Genes Functionally Suppress Mutations in Yeast EIF-2 Alpha Kinase GCN2: Evidence for Separate Pathways Coupling GCN4 Expression to Unchanged TRNA'. *Molecular and Cellular Biology* 14 (12): 7920–32. https://doi.org/10.1128/mcb.14.12.7920-7932.1994.

Venkataramani, Vivek. 2021. 'Iron Homeostasis and Metabolism: Two Sides of a Coin'. *Advances in Experimental Medicine and Biology* 1301: 25–40. https://doi.org/10.1007/978-3-030-62026-4_3/COVER.

Verna, James, Adriana Lodder, Kyunghee Lee, Alicia Vagts, and Roymarie Ballester. 1997. 'A Family of Genes Required for Maintenance of Cell Wall Integrity and for the Stress Response in Saccharomyces Cerevisiae'. *Proceedings of the National Academy of Sciences of the United States of America* 94 (25): 13804. https://doi.org/10.1073/PNAS.94.25.13804.

Versele, Matthias, Johannes H De Winde, and Johan M Thevelein. 1999. 'A Novel Regulator of G Protein Signalling in Yeast, Rgs2, Downregulates Glucose-Activation of the CAMP Pathway through Direct Inhibition of Gpa2'. *The EMBO Journal* 18 (20): 5577–91.

Vilella, Felipe, Enrique Herrero, Jordi Torres, and Maria Angeles De La Torre-Ruiz. 2005. 'Pkc1 and the Upstream Elements of the Cell Integrity Pathway in Saccharomyces Cerevisiae, Rom2 and Mtl1, Are Required for Cellular Responses to Oxidative Stress'. *Journal of Biological Chemistry* 280 (10): 9149–59. https://doi.org/10.1074/jbc.M411062200.

Vincent, Olivier, Robert Townley, Sergei Kuchin, and Marian Carlson. 2001. 'Subcellular Localization of the Snf1 Kinase Is Regulated by Specific β Subunits and a Novel Glucose Signaling Mechanism'. *Genes & Development* 15 (9): 1104. https://doi.org/10.1101/GAD.879301.

Virgilio, Claudio de. 2012. 'The Essence of Yeast Quiescence'. *FEMS Microbiology Reviews* 36 (2): 306–39. https://doi.org/10.1111/j.1574-6976.2011.00287.x.

Vlahakis, Ariadne, Martin Graef, Jodi Nunnari, and Ted Powers. 2014. 'TOR Complex 2-Ypk1 Signaling Is an Essential Positive Regulator of the General Amino Acid Control Response and Autophagy'. https://doi.org/10.1073/pnas.1406305111.

Voegtli, Walter C., Jie Ge, Deborah L. Perlstein, Joanne Stubbe, and Amy C. Rosenzweig. 2001. 'Structure of the Yeast Ribonucleotide Reductase Y2Y4 Heterodimer'. *Proceedings of the National Academy of Sciences of the United States of America* 98 (18): 10073. https://doi.org/10.1073/PNAS.181336398.

Vroegindeweij, Lena H.P., Lucia Bossoni, Agnita J.W. Boon, J. H.Paul Wilson, Marjolein Bulk, Jacqueline Labra-Muñoz, Martina Huber, Andrew Webb, Louise van der Weerd, and Janneke G. Langendonk. 2021. 'Quantification of Different Iron Forms in the Aceruloplasminemia Brain to Explore Iron-Related Neurodegeneration'. *NeuroImage : Clinical* 30 (January): 102657. https://doi.org/10.1016/J.NICL.2021.102657.

Waite, Kenrick A., Alicia Burris, Gabrielle Vontz, Angelica Lang, and Jeroen Roelofs. 2022. 'Proteaphagy Is Specifically Regulated and Requires Factors Dispensable for General Autophagy'. *The Journal of Biological Chemistry* 298 (1). https://doi.org/10.1016/J.JBC.2021.101494.

Waite, Kenrick A., and Jeroen Roelofs. 2022. 'Proteasome Granule Formation Is Regulated through Mitochondrial Respiration and Kinase Signaling'. *Journal of Cell Science* 135 (17). https://doi.org/10.1242/jcs.259778.

Waliullah, Talukdar Muhammad, Akter M.S.T. Yeasmin, Atsuki Kaneko, Naoki Koike, Mashu Terasawa, Takaya Totsuka, and Takashi Ushimaru. 2017. 'Rim15 and Sch9 Kinases Are Involved in Induction of Autophagic Degradation of Ribosomes in Budding Yeast'. *Bioscience, Biotechnology and Biochemistry* 81 (2): 307–10. https://doi.org/10.1080/09168451.2016.1234928.

Wang, Ke, Meiyan Jin, Xu Liu, and Daniel J. Klionsky. 2013. 'Proteolytic Processing of Atg32 by the Mitochondrial I-AAA Protease Yme1 Regulates Mitophagy'. *Autophagy* 9 (11): 1828–36. https://doi.org/10.4161/AUTO.26281.

Wang, Shuai, Zhantao Deng, Yuanchen Ma, Jiewen Jin, Fangjie Qi, Shuxian Li, Chang Liu, Feng Juan Lyu, and Qiujian Zheng. 2020. 'The Role of Autophagy and Mitophagy in Bone Metabolic Disorders'. *International Journal of Biological Sciences* 16 (14): 2675–91. https://doi.org/10.7150/IJBS.46627.

Wang, Ying, Michael Pierce, Lisa Schneper, C. Gökçe Güldal, Xiuying Zhang, Saeed Tavazoie, and James R. Broach. 2004. 'Ras and Gpa2 Mediate One Branch of a Redundant Glucose Signaling Pathway in Yeast'. *PLOS Biology* 2 (5): e128. https://doi.org/10.1371/JOURNAL.PBIO.0020128.

Wang, Yuhua, Xi Zheng, Guohong Li, and Xin Wang. 2023. 'TORC1 Signaling in Fungi: From Yeasts to Filamentous Fungi'. *Microorganisms* 11 (1): 1–15. https://doi.org/10.3390/microorganisms11010218.

Wang, Z, W a Wilson, M a Fujino, and P J Roach. 2001. 'Antagonistic Controls of Autophagy and Glycogen Accumulation by Snf1p, the Yeast Homolog of AMP-Activated Protein Kinase, and the Cyclin-Dependent Kinase Pho85p.' *Molecular and Cellular Biology* 21 (17): 5742–52. https://doi.org/10.1128/MCB.21.17.5742-5752.2001.

Watanabe, Daisuke, Mitsuhiro Abe, and Yoshikazu Ohya. 2001. 'Yeast Lrg1p Acts as a Specialized RhoGAP Regulating 1,3-Beta-Glucan Synthesis'. *Yeast (Chichester, England)* 18 (10): 943–51. https://doi.org/10.1002/YEA.742.

Wei, Yuehua, and X. F.Steven Zheng. 2011. 'Nutritional Control of Cell Growth via TOR Signaling in Budding Yeast'. *Methods in Molecular Biology* 759 (3): 307–19. https://doi.org/10.1007/978-1-61779-173-4_18.

Weisman, Ronit. 2016. 'Target of Rapamycin (TOR) Regulates Growth in Response to Nutritional Signals'. *Microbiology Spectrum* 4 (5): 535–48.

https://doi.org/10.1128/9781555819583.ch25.

Welter, Evelyn, Marco Montino, Robert Reinhold, Petra Schlotterhose, Roswitha Krick, Jan Dudek, Peter Rehling, and Michael Thumm. 2013. 'Uth1 Is a Mitochondrial Inner Membrane Protein Dispensable for Post-Log-Phase and Rapamycin-Induced Mitophagy'. *FEBS Journal* 280 (20): 4970–82. https://doi.org/10.1111/febs.12468.

Werner-Washburne, Margaret, Edward Braun, Gerald C. Johnston, and Richard A. Singer. 1993. 'Stationary Phase in the Yeast Saccharomyces Cerevisiae'. *American Society For Microbiology* 57 (2): 383–401. https://doi.org/0146-0749/93/020383-19$02.00/0.

Willis, Stephen D., David C. Stieg, Kai Li Ong, Ravina Shah, Alexandra K. Strich, Julianne H. Grose, and Katrina F. Cooper. 2018. 'Snf1 Cooperates with the CWI MAPK Pathway to Mediate the Degradation of Med13 Following Oxidative Stress'. *Microbial Cell* 5 (8): 357–70. https://doi.org/10.15698/mic2018.08.641.

Wilson, Wayne A., Simon A. Hawley, and D. Grahame Hardie. 1996. 'Glucose Repression/Derepression in Budding Yeast: SNF1 Protein Kinase Is Activated by Phosphorylation under Derepressing Conditions, and This Correlates with a High AMP:ATP Ratio'. *Current Biology : CB* 6 (11): 1426–34. https://doi.org/10.1016/S0960-9822(96)00747-6.

Woodbury, Maya E., and Tsuneya Ikezu. 2014. 'Fibroblast Growth Factor-2 Signaling in Neurogenesis and Neurodegeneration'. *Journal of Neuroimmune Pharmacology : The Official Journal of the Society on NeuroImmune Pharmacology* 9 (2): 92–101. https://doi.org/10.1007/S11481-013-9501-5.

Woods, A., M.R. Munday, J. Scott, X. Yang, M. Carlson, and D. Carling. 1994. 'Yeast SNF1 Is Functionally Related to Mammalian AMP-Activated Protein Kinase and Regulates Acetyl-CoA Carboxylase in Vivo.' *Journal of Biological Chemistry* 269 (30): 19509–15. https://doi.org/10.1016/S0021-9258(17)32198-1.

Wu, Fanglong, Jin Yang, Junjiang Liu, Ye Wang, Jingtian Mu, Qingxiang Zeng, Shuzhi Deng, and Hongmei Zhou. 2021. 'Signaling Pathways in Cancer-Associated Fibroblasts and Targeted Therapy for Cancer'. *Signal Transduction and Targeted Therapy* 6 (1). https://doi.org/10.1038/S41392-021-00641-0.

Wullschleger, Stephan, Robbie Loewith, and Michael N. Hall. 2006. 'TOR Signaling in Growth and Metabolism'. *Cell* 124 (3): 471–84. https://doi.org/10.1016/j.cell.2006.01.016.

Wullschleger, Stephan, Robbie Loewith, Wolfgang Oppliger, and Michael N. Hall. 2005. 'Molecular Organization of Target of Rapamycin Complex 2'. *Journal of Biological Chemistry* 280 (35): 30697–704. https://doi.org/10.1074/jbc.M505553200.

Xie, Zhiping, Usha Nair, and Daniel J. Klionsky. 2008. 'Dissecting Autophagosome Formation: The Missing Pieces'. *Autophagy* 4 (7): 920–22. https://doi.org/10.4161/AUTO.6692.

Yamaguchi-Iwai, Yuko, Ryo Ueta, Ayako Fukunaka, and Ryuzo Sasaki. 2002. 'Subcellular Localization of Aft1 Transcription Factor Responds to Iron Status in Saccharomyces Cerevisiae'. *Journal of Biological Chemistry* 277 (21): 18914–18. https://doi.org/10.1074/jbc.M200949200.

Yang, Ruojing, Sheree A. Wek, and Ronald C. Wek. 2000. ' Glucose Limitation Induces GCN4 Translation by Activation of Gcn2 Protein Kinase '. *Molecular and Cellular Biology* 20 (8): 2706–17. https://doi.org/10.1128/mcb.20.8.2706-2717.2000.

Yao, Ruojin, Zhen Zhang, Xiuxiang An, Brigid Bucci, Deborah L. Perlstein, Jo Anne Stubbe, and Mingxia Huang. 2003. 'Subcellular Localization of Yeast Ribonucleotide Reductase Regulated by the DNA Replication and Damage Checkpoint Pathways'. *Proceedings of the National Academy of Sciences of the United States of America* 100 (11): 6628. https://doi.org/10.1073/PNAS.1131932100.

Yao, Yanhua, Scott Tsuchiyama, Ciyu Yang, Anne Laure Bulteau, Chong He, Brett Robison, Mitsuhiro Tsuchiya, et al. 2015. 'Proteasomes, Sir2, and Hxk2 Form an Interconnected

Aging Network That Impinges on the AMPK/Snf1-Regulated Transcriptional Repressor Mig1'. *PLOS Genetics* 11 (1): e1004968. https://doi.org/10.1371/JOURNAL.PGEN.1004968.

Ye, Tian, Karin Elbing, and Stefan Hohmann. 2008. 'The Pathway by Which the Yeast Protein Kinase Snf1p Controls Acquisition of Sodium Tolerance Is Different from That Mediating Glucose Regulation'. *Microbiology (Reading, England)* 154 (Pt 9): 2814–26. https://doi.org/10.1099/MIC.0.2008/020149-0.

Yeasmin, Akter M.S.T., Talukdar Muhammad Waliullah, Akihiro Kondo, Atsuki Kaneko, Naoki Koike, and Takashi Ushimaru. 2016. 'Orchestrated Action of PP2A Antagonizes Atg13 Phosphorylation and Promotes Autophagy after the Inactivation of TORC1'. *PLoS ONE* 11 (12). https://doi.org/10.1371/JOURNAL.PONE.0166636.

Yorimitsu, Tomohiro, Congcong He Ke Wang, and Daniel J Klionsky. 2009. 'Tap42-Associated Protein Phosphatase Type 2A Negatively Regulates Induction of Autophagy'. *Autophagy* 5 (5): 616–24. https://www.ncbi.nlm.nih.gov/pmc/articles/PMC3624763/pdf/nihms412728.pdf.

Yorimitsu, Tomohiro, Shadia Zaman, James R Broach, and Daniel J Klionsky. 2007. 'Protein Kinase A and Sch9 Cooperatively Regulate Induction of Autophagy in Saccharomyces Cerevisiae'. *Molecular Biology of the Cell* 18 (October): 4180–89. https://doi.org/10.1091/mbc.E07.

Yu, Guang Hui, Yakov Kuzyakov, Yu Luo, Bernard A. Goodman, Andreas Kappler, Fei Fei Liu, and Fu Sheng Sun. 2021. 'Molybdenum Bioavailability and Asymbiotic Nitrogen Fixation in Soils Are Raised by Iron (Oxyhydr)Oxide-Mediated Free Radical Production'. *Environmental Science & Technology* 55 (21): 14979–89. https://doi.org/10.1021/ACS.EST.1C04240.

Zahoor, Hira, Kwanrutai Watchaputi, Janejira Hata, Wachirachai Pabuprapap, Apichart Suksamrarn, Lee Suan Chua, and Nitnipa Soontorngun. 2022. 'Model Yeast as a Versatile Tool to Examine the Antioxidant and Anti-Ageing Potential of Flavonoids, Extracted from Medicinal Plants'. *Frontiers in Pharmacologyfile:///Users/Sandra/Desktop/Articles Intro/Glrx.Pdf*, no. Ethnopharmacology: 1–14. https://doi.org/10.3389/fphar.2022.980066.

Zhang, Aili, Yubao Shen, Wenxuan Gao, and Jian Dong. 2011. 'Role of Sch9 in Regulating Ras-CAMP Signal Pathway in Saccharomyces Cerevisiae'. *FEBS Letters* 585 (19): 3026–32. https://doi.org/10.1016/j.febslet.2011.08.023.

Zhang, Caiguo. 2014. 'Essential Functions of Iron-Requiring Proteins in DNA Replication, Repair and Cell Cycle Control'. *Protein & Cell* 5 (10): 750–60. https://doi.org/10.1007/S13238-014-0083-7.

Zhang, Jie, Stefania Vaga, Pramote Chumnanpuen, Rahul Kumar, Goutham N. Vemuri, Ruedi Aebersold, and Jens Nielsen. 2011. 'Mapping the Interaction of Snf1 with TORC1 in Saccharomyces Cerevisiae'. *Molecular Systems Biology* 7 (545): 1–11. https://doi.org/10.1038/msb.2011.80.

Zhang, Xiao Jie, Sheng Chen, Kai Xing Huang, and Wei Dong Le. 2013. 'Why Should Autophagic Flux Be Assessed?' *Acta Pharmacologica Sinica* 34 (5): 595–99. https://doi.org/10.1038/aps.2012.184.

Zhou, Tao, Ling Chang, Yi Luo, Ying Zhou, and Jianjun Zhang. 2019. 'Mst1 Inhibition Attenuates Non-Alcoholic Fatty Liver Disease via Reversing Parkin-Related Mitophagy'. *Redox Biology* 21 (February). https://doi.org/10.1016/J.REDOX.2019.101120.